P.679

LR 28384

FINAL REPORT– DRAFT

STUDY OF FUEL SYSTEMS FOR LH_2-FUELED SUBSONIC TRANSPORT AIRCRAFT

by G. D. Brewer
R. E. Morris
G. W. Davis
E. F. Versaw
G. R. Cunnington, Jr.
J. C. Riple
C. F. Baerst
G. Garmong

December, 1977
Prepared under Contract NAS 1-14614

for

Langley Research Center
National Aeronautics and Space Administration

by

Lockheed – California Company
Burbank, California

(NASA-CR-185900) STUDY OF FUEL SYSTEMS FOR LH2-FUELED SUBSONIC TRANSPORT AIRCRAFT Final Report, Sep. 1976 - Dec. 1977 (Lockheed-California Co.) 679 p

N90-70111

Unclas
00/05 0234041

supported by

Lockheed Missiles and Space Company, Inc.
AiResearch Divisions of the Garrett Corporation
Rocketdyne Division of Rockwell International

#234041

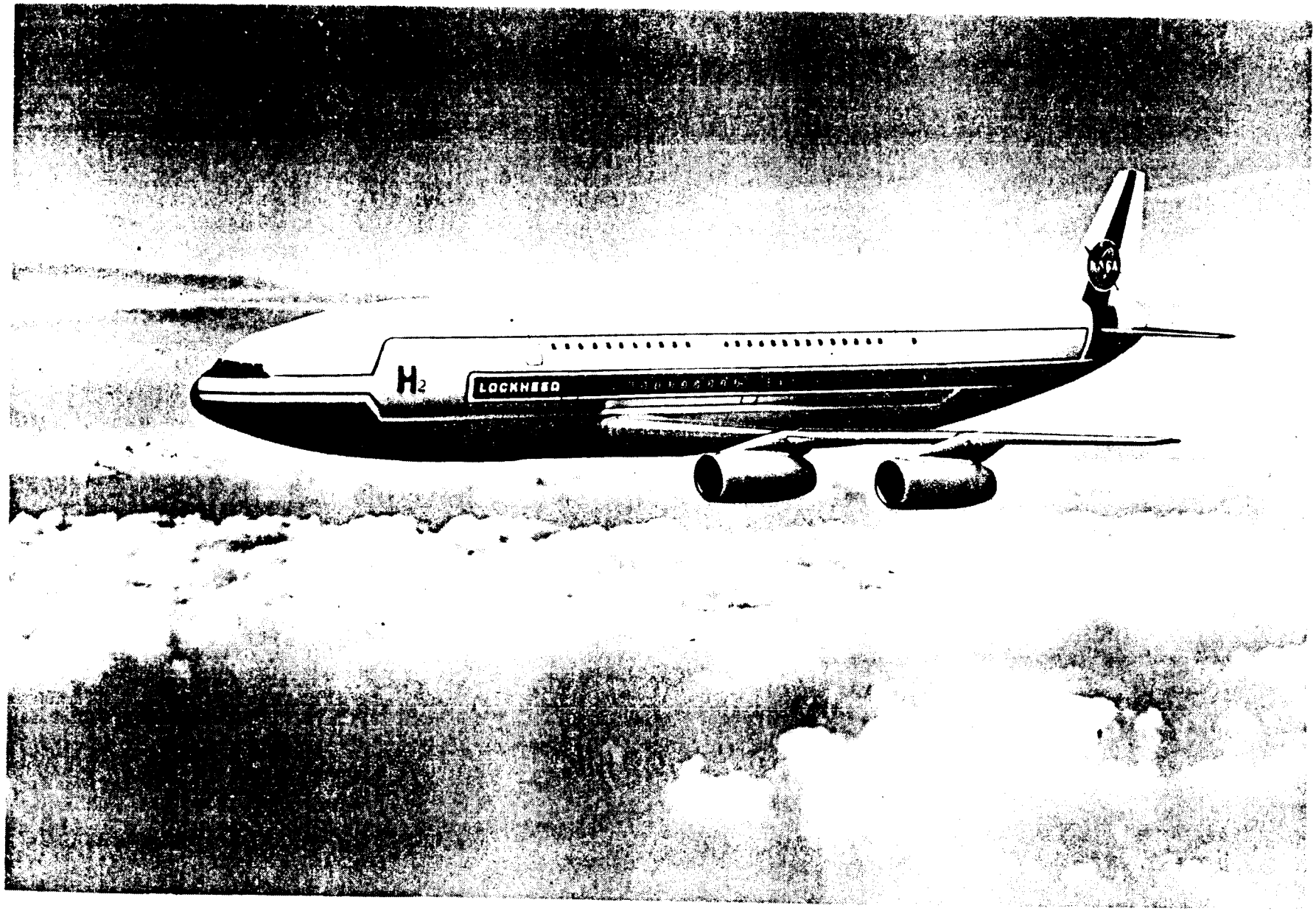

Frontispiece Subsonic LH_2 Fueled Transport

FOREWORD

This is the final report of a study made under Contract NAS 1-141614 for NASA-Langley Research Center, Hampton, Virginia. The report presents results of work performed during the 14 month period, October 1976 through November 1977.

The Lockheed-California Company was the prime contractor to NASA and the work was performed in the Commercial Advanced Design Division at Burbank, California. In addition, important segments of the work which required special expertise were subcontracted to the following organizations. The individuals named were principal contributors.

LOCKHEED-CALIFORNIA COMPANY

G. Daniel Brewer, Study Manager

Robert E. Morris, Project Engineer

George Davis, Structures

Edward Versaw, Fuel Systems

Roger Jensen, Weights

Roy Adamson, Propulsion

Dalen Horning, DOC Analysis

LOCKHEED MISSILES AND SPACE COMPANY, INC.

George Cunnington, Jr., Tank Insulation

Richard Parmley, Tank Insulation

Jorgen Skogh, Tank Stress Analysis

Richard Cima, Heat Transfer Analysis

AIRESEARCH DIVISION OF THE GARRETT CORP.

James C. Riple, Engine Pump and Fuel Control System

Carl F. Baerst, LH_2 Engine Design

ROCKETDYNE DIVISION OF ROCKWELL INTERNATIONAL

Greg Garmong, Engine Fuel Supply System

William R. Bissell, Boost Pump

Ron Tobin, Fuel Feed Lines

Mr. Robert D. Witcofski of the Aeronautical Systems Division at NASA-Langley Research Center was technical monitor for the study.

iv

TABLE OF CONTENTS

Section		Page
	FOREWORD	iii
	LIST OF ILLUSTRATIONS	x
	LIST OF TABLES	xviii
	SUMMARY	1
	LIST OF SYMBOLS	5
1	INTRODUCTION	7
2	TECHNICAL APPROACH	8
2.1	Team Organization	8
2.2	Work Plan	8
3	STUDY GUIDELINES AND INITIAL DATA	11
3.1	Guidelines and Requirements	11
3.2	Basic Data	11
3.3	Sensitivity Factors	14
3.3.1	Sensitivity of DOC to engine weight, SFC, and maintenance cost	18
3.3.2	Sensitivity of DOC to fuel pumping system power and weight	19
3.3.3	Sensitivity of DOC to volume and weight of fuel containment system	21
3.3.4	Sensitivity of DOC to aircraft ground losses	24
3.4	Calculation of Direct Operating Cost	25
3.4.1	Background	25
3.4.2	Parameters required for DOC evaluation	27
4	LH_2 ENGINE DEFINITION	31
4.1	Feasibility Studies - Hydrogen Exploitation	31
4.1.1	Approach	32
4.1.2	Compressor air precooling	35
4.1.3	Compressor intercooling	36
4.1.4	Hydrogen cooling of turbine cooling air	38
4.1.5	Fuel heating with exhaust gas	41

TABLE OF CONTENTS (Continued)

Section		Page
4.1.6	H_2 expander cycle	49
4.1.7	Selection of preferred concepts	50
4.2	Cycle Definition and Configuration Definition	50
4.2.1	Review of previous studies	53
4.2.2	Initial LH_2 engine cycle selection	54
4.2.3	High temperature investigation	59
4.3	Selected Engine Concept	82
4.3.1	Description and performance	82
4.3.2	Weight, geometry, and scaling relationships	83
4.3.3	Engine cost	84
4.3.4	Noise and emissions	84
4.3.5	Operational characteristics	87
4.3.6	Description of engine mounted heat exchangers	91
4.4	Technology Development Required	95
4.4.1	Combustor	95
4.4.2	H_2 cooling of turbine cooling air	95
5	ENGINE FUEL SUPPLY SYSTEM	100
5.1	Candidate System Concepts	100
5.1.1	Concept descriptions	100
5.1.2	Results of evaluation	100
5.1.3	Characteristics of selected systems	104
5.2	Engine Feed Supply Lines	104
5.2.1	Size Selection	104
5.2.2	Insulation system comparison	105
5.2.3	Design description	112
5.3	Boost Pump	115
5.3.1	Design requirements	116
5.3.2	Candidate pump types	119
5.3.3	Candidate pump drive systems	120
5.3.4	Boost pump and drive candidate evaluation	125
5.3.5	Selected boost pump and drive system	133
5.3.6	Boost pump mounting and changing tool	133

TABLE OF CONTENTS (Continued)

Section		Page
5.4	Engine Fuel Pump	134
5.4.1	Design requirements	139
5.4.2	Candidate pump types and selection of preferred concept	139
5.4.3	Candidate pump drive systems	142
5.4.4	Engine pump and drive candidate evaluation	142
5.4.5	Pump bearing considerations	143
5.4.6	Selected pump and drive system	148
5.5	Fuel Control System	152
5.5.1	Design requirements	152
5.5.2	Candidate concepts	155
5.5.3	Selected system	155
5.6	Engine Fuel Supply System Final Design and Performance	158
5.6.1	Head added to hydrogen	160
5.6.2	Final system selection	161
5.6.3	Final system configuration	165
5.6.4	Engine operational procedures	165
5.7	Technology Development Required	172
5.7.1	Engine fuel pump	173
5.7.2	Engine fuel control system	173
5.7.3	Overall system	173
6	FUEL SUBSYSTEMS	174
6.1	Fuel Tank Arrangement	174
6.2	Fueling and Defueling	174
6.3	Engine Fuel Supply	185
6.4	Auxiliary Power Unit Fuel Supply	186
6.5	Fuel Transfer	186
6.6	Fuel Jettison	186
6.7	Tank Vent and Pressurization System	186
6.8	Nitrogen Inerting System	187
6.9	Technology Developments Required	191
6.9.1	Negative "g" operation	191
6.9.2	Engine starting without boost pumps operating	191
6.9.3	Float-operated valve development	191

TABLE OF CONTENTS (Continued)

Section		Page
6.9.4	Fuel quantity gauging	191
7	FUEL CONTAINMENT SYSTEM	192
7.1	Tank Insulation	192
7.1.1	Design requirements and evaluation criteria	193
7.1.2	Candidate insulation concepts	194
7.1.3	Concept screening procedure	195
7.1.4	Screening results	221
7.1.5	Selection of preferred candidates	228
7.1.6	Analysis of preferred candidates	229
7.2	Tank Structure	264
7.2.1	Structural design criteria and loads	264
7.2.2	Structural design concepts and materials	274
7.2.3	Concept screening	277
7.2.4	Parametric studies	332
7.3	Evaluation of Preferred FCS Candidates	346
7.3.1	Weight considerations	346
7.3.2	Cost consideration	368
7.3.3	Evaluation results	369
8	LH_2 FUELED AIRCRAFT CHARACTERISTICS	373
8.1	LH_2 Aircraft Description	373
8.2	Weight Estimating Relationships	375
8.3	Operational Requirements of LH_2 Fuel System	377
8.3.1	Fueling and defueling	377
8.3.2	Flight engineer's panel	380
8.3.3	Fuel management	382
8.3.4	Maintenance	382
8.4	Fuel System Malfunction Analysis	384
8.5	Reliability Analysis	384
8.5.1	Pumping and distribution system	384
8.5.2	Fuel venting regulation and control system	393
8.6	Safety and Fire Protection	395

TABLE OF CONTENTS (Continued)

Section		Page
8.6.1	Compartment purging	395
8.6.2	Nitrogen inerting	396
8.6.3	Preparation for repair of insulation leaks	396
8.7	Adjustments Required in FAR or Industry Standards	396
9	EQUIVALENT JET A-FUELED AIRCRAFT	401
9.1	Jet A Engine Definition	401
9.2	Comparison: LH_2 vs Jet A Equivalent Aircraft	403
10	TECHNOLOGY DEVELOPMENT	407
10.1	First Priority	407
10.2	Second Priority	409
10.3	Third Priority	411
10.4	Fourth Priority	414
10.5	Fifth Priority	415
REFERENCES		417
APPENDIX A	PRELIMINARY MISSION FUEL FLOW SCHEDULE	421
APPENDIX B	DESIGN CONCEPTS OF SELECTED LH_2 FUEL SYSTEM COMPONENTS	429
APPENDIX C	CONCEPT SCREENING ANALYSIS THERMAL MODEL DEVELOPMENT	440
APPENDIX D	"THERM" PROGRAM	450
APPENDIX E	SAFETY ANALYSIS	453
APPENDIX F	INSULATION CONCEPT PRODUCIBILITY AND OPERATIONAL ANALYSIS	465
APPENDIX G	ENGINE PERFORMANCE CHARTS	478

LIST OF ILLUSTRATIONS

Figure		Page
1	Study work plan	9
2	Baseline LH_2-fueled passenger transport	13
3	Sensitivity of CL 1317-1 aircraft to changes in specific fuel consumption	16
4	Sensitivity of CL 1317-1 aircraft to inert weight variation	17
5	Fuselage length vs fuel containment system thickness and tank volume	23
6	Schematic of engine cycle with compressor precooling with H_2 fuel	35
7	Engine performance with precooling	37
8	Schematic of engine cycle with compressor intercooling with H_2 fuel	38
9	Engine performance with intercooling	39
10	Schematic of cooled turbine cooling air cycle	40
11	Effect of cooling turbine cooling air with fuel at max. cruise, (35 000 ft) Mach 0.85	42
12	Effect of cooling turbine cooling air with fuel at max. cruise 10.67 km (35 000 ft), Mach 0.85	43
13	HP turbine efficiency and cooling air schedules used in study of fuel cooling of turbine cooling air	44
14	Schematic of engine cycle with exhaust gas heating of H_2 fuel	45
15	Effect of exhaust heating on fuel at max. cruise ($\Delta P/P = 0$)	46
16	Effect of exhaust heating of fuel at max. cruise ($\Delta P/P = 0.04$)	47
17	Effect of exhaust heating of fuel at max. cruise ($\Delta P/P = 0.08$)	48
18	Schematic of expander cycle	49
19	Net hydrogen turbine horsepower	51
20	Engine performance - expander cycle	52
21	Selection of cycle overall pressure ratio	58
22	Effect of fan pressure ratio and nozzle velocity ratio on engine performance	60
23	Effect of fan pressure ratio and nozzle velocity ratio on bypass ratio	61

LIST OF ILLUSTRATIONS (Continued)

Figure		Page
24	Effect of fan pressure ratio and bypass ratio on engine weight	62
25	Effect of fan pressure ratio and bypass ratio on direct operating cost	63
26	Effect of fan pressure ratio on direct operating cost	64
27	Related bypass ratio	65
28	Engine station designations	67
29	Effect of core energy extraction and fan pressure ratio on SFC and bypass ratio (CPR = 40)	72
30	Effect of fan pressure ratio and bypass ratio on engine weight (CPR = 40)	73
31	Effect of core energy extraction and fan pressure ratio on SFC and BPR (CPR = 50)	74
32	Effect of fan pressure ratio and bypass ratio on engine weight (CPR = 50)	75
33	Effect of core energy extraction and fan pressure ratio on SFC and BPR (CPR = 60)	76
34	Effect of fan pressure ratio and bypass ratio on engine weight (CPR = 60)	77
35	Effect of bypass ratio and FPR on DOC for CPR = 40	78
36	Effect of bypass ratio and FPR on DOC for CPR = 50	79
37	Effect of bypass ratio and FPR on DOC for CPR = 60	80
38	Effect of fan pressure ratio and cycle pressure ratio on DOC and bypass ratio	81
39	Envelope drawing - selected LH_2 engine	85
40	LH_2 engine flight operating envelope	89
41	LH_2 engine operating load limits	90
42	LH_2 engine ambient flight and starting temperature envelope	92
4.3.6a	Turbine cooling air to hydrogen heat exchanger	94
4.3.6b	Engine oil to hydrogen heat exchanger	96
4.3.6c	ECS bleed air to hydrogen heat exchanger	97
4.3.6d	Engine exhaust fuel heater	98
43	Boost pump pressure rise effects	103
44	Concept I schematic (tank mounted low-pressure pump-engine mounted high-pressure pump)	103

LIST OF ILLUSTRATIONS (Continued)

Figure		Page
45	LH_2 fuel feed line pressure loss	105
46	Size optimization for energy fuel supply line	107
47	Effect of insulation on heat leak rate	107
48	Foam insulation requirements	108
49	Fuel feed line weight requirements	109
50	Selected fuel-line configuration	115
51	Deleted	
52	Design point performance for centrifugal pumps designed for maximum efficiency	121
53	Off design performance for centrifugal pumps designed for maximum efficiency	122
54	270 V brushless dc motor weight breakdown	123
55	270 V brushless dc motor weights - includes weight of electronic assembly	124
56	400 cycle AC motor weights - 24 000 rpm, 2 pole	126
57	Electrical motor efficiencies at full load	127
58	Zero NPSH pumping capability requirement for hydrogen	128
59	Boost pump inlet diameter requirements	129
60	Boost pump assembly and installation	135
61	Boost pump replacement concept	137
62	Alternative pump drive concepts	138
63	Engine high pressure LH_2 pump	150
64	Performance maps for two stage centrifugal pump	153
65	Bleed air driven turbopump system	156
66	270 Vdc motor driven pump system	156
67	Engine shaft driven pump system, fixed speed ratio	157
68	Engine shaft driven pump system, variable speed ratio	157
69	LH_2 engine fuel delivery and control system	159
70	Selected LH_2 boost pump	162
71	Three stage pump characteristics	163
72	Pump characteristics (transient)	164
73	Engine pump inlet conditions	166
74	Engine fuel supply system	167

LIST OF ILLUSTRATIONS (Continued)

Figure		Page
75	Aircraft fuel system schematic	175
76	Layout-fueling/defuel system	177
77	Layout-vent and pressurization system	181
6.8a	N_2 purge system schematic	189
78	Tank insulation analysis procedure	193
79	Plumbing schematic for system 1	203
80	Plumbing schematic for system 2	204
81	Plumbing schematic for system 9	205
82	Plumbing schematic for systems 10, 11, and 12	206
83	General configuration of aft tank	209
84	Tank diameter D_1 vs tank length "ℓ"	210
85	Tank length ℓ vs volume & t	211
86	Thermal model used for concept screening	212
87	Correlation of tank top surface temperature with Nusselt number for various liquid levels	215
88	Comparison of measured and computed liquid heat rate ratio as a function of tank liquid fraction	216
89	Thermal conductivity of foams, rigidized silica and microsphere insulations	220
90	Candidate no. 1, nonintegral tank - external foam	231
91	Candidate no. 2, nonintegral tank - hard shell vacuum	232
92	Candidate no. 3, integral tank - external foam	233
93	Candidate no. 4, integral tank - external microspheres	234
94	Tank insulation and vent model for analysis of preferred candidates	235
95	Fuel losses as a function of insulation thickness for candidate no. 1, aft tank	238
96	Fuel losses as a function of insulation thickness (primary and open cell foam) for candidate no. 3, aft tank	239
97	Fuel losses as a function of insulation thickness (microspheres and open cell foam) for candidate no. 4, aft tank	240
98	Tank pressure during flight as a function of vacuum level, candidate no. 2 - aluminum core HC	243

LIST OF ILLUSTRATIONS (Continued)

Figure		Page
99	Tank pressure variation during flight for candidate no. 4	245
100	Liquid temperature differences for three vent pressure settings for candidate no. 3	246
101	Tank pressure variation during flight for vent pressure settings of 21, 30 and 40 psia	247
102	Liquid temperature differences as a functional of flight time for candidate no. 1	248
103	Liquid temperature differences as a function of flight time for candidate no. 4	248
104	Candidate no. 1 circumferential temperature distributions for liquid fractions of 0.90, 0.50 and 0.15	250
105	Candidate no. 2, aluminum core, circumferential temperature distributions in tank wall and vapor barrier for liquid fractions of 0.80, 0.50 and 0.15, vacuum = 1×10^{-4} torr	251
106	Candidate no. 2, aluminum core, circumferential temperature distributions in tank wall and vapor barrier for liquid fractions of 0.90, 0.50 and 0.15 with vacuum space at atmospheric pressure	252
107	Candidate no. 2, composite core, circumferential temperature distributions in tank wall and vapor barrier for liquid fractions of 0.90, 0.50 and 0.15 with vacuum space at atmospheric pressure	253
108	Candidate no. 3 circumferential temperature distributions for liquid fraction = 0.90	254
109	Candidate no. 4, circumferential temperature distributions for tank wall and vacuum jacket	257
110	Change in DOC with overall fuel containment system thickness (t)	263
111	Design speeds vs altitude	265
112	Maneuver envelope - 400 000 lb gross weight, 26 000 ft altitude	267
113	LH_2 subsonic transport fuselage aftbody limit loads, fuselage tank configuration	267
114	LH_2 subsonic transport fuselage aftbody limit loads (-1.0 g max, P_{z_t} = 16 000 lb)	269
115	LH_2 subsonic transport fuselage aftbody limit loads (1.0 g max. weight start of cruise, P_{z_t} = 50 000 lb)	269

LIST OF ILLUSTRATIONS (Continued)

Figure		Page
116	Variation in circumferential design stress with fatigue quality for 10 000 flights including a life reduction factor of four on number of flights	272
117	Fail-safe analysis of circumferential damage conditions	281
118	Fail-safe analysis of longitudinal damage condition	282
119	Fuselage and tank dimensions used for the nonintegral tank structural model	285
120	Applied loads and structural model for the nonintegral tank design	286
121	Normal displacements of the nonintegral tank structural model	288
122	Inplane stress resultants for the internal pressurization condition, nonintegral tank design	289
123	Bending moments for the internal pressurization condition, nonintegral tank design	290
124	Inplane stress resultants for the inertia and air load condition, nonintegral tank design	291
125	Bending moments for the inertia and air load condition, nonintegral tank design	292
126	Inplane stress resultants for the temperature condition, nonintegral tank design	293
127	Bending moments for the temperature condition, nonintegral tank design	294
128	Fuselage and tank dimensions used for the integral tank structural model	295
129	Applied loads and structural model for the integral tank design	297
130	Normal displacements of the integral tank structural model	298
131	Inplane stress resultants for the internal pressurization condition, integral tank design	299
132	Bending moments for the internal pressurization condition, integral tank design	300
133	Inplane stress resultants for the inertia and air load condition, integral tank design	301
134	Bending moments for the inertia and air load condition, integral tank design	302
135	Inplane stress resultants for the temperature condition, integral tank design	303

LIST OF ILLUSTRATIONS (Continued)

Figure		Page
136	Bending moments for the temperature condition, integral tank design	304
137	Point design regions	306
138	Point design structure	309
139	Fuselage shell equivalent thickness, nonintegral design	310
140	Fuselage frame loads, nonintegral design	313
141	Fuselage unit weight at the quarter-length location, nonintegral design	318
142	Unit weights vs strap spacing for nonintegral tank (quarter-length point design region)	324
143	Tank equivalent thickness, integral design	325
144	Frame equivalent thickness as a function of spacing, integral design	326
145	Total unit weight comparison of structural candidates, integral tank design	331
146	Average circumferential weight comparison of structural candidates, integral tank design	331
147	Integral LH_2 tank wall, optimum weight including fail-safe straps and weld lands	333
148	Nonintegral LH_2 tank wall, optimum weight including fail-safe straps and weld lands	335
149	Fuselage shell and tank configuration, nonintegral design	336
150	Candidate configurations for dome shape study	336
151	Elliptical dome design data	339
152	Torispherical dome design data	339
153	Tank weight comparison dome shape study	340
154	Cost comparison date, dome shape study	340
155	Elliptic dome-nonlinear stress initial undeformed structure	342
156	Torispherical dome-nonlinear stress initial undeformed structure	343
157	Elliptical dome stresses	344
158	Candidate no. 1, nonintegral tank - external foam	347
159	Candidate no. 2, nonintegral tank - hard shell vacuum	348
160	Candidate no. 3, integral tank - external foam	349

LIST OF ILLUSTRATIONS (Continued)

Figure		Page
161	Candidate no. 4, integral tank - microsphere insulation	350
7.3.1a	Candidate no. 1 nonintegral tank - external foam	351
7.3.1b	Candidate no. 2 nonintegral tank - hard shell vacuum	355
7.3.1c	Candidate no. 3 integral tank - external foam	359
7.3.1d	Candidate no. 4 integral tank - external microsphere insulation	363
162	View C-C - refuel panel	379
163	Fuel system control panel - flight engineer	381
164	C.G. travel with blocked feet line	383
165	Sensitivity of DOC to fuel price for both LH_2 and Jet A aircraft	405
B-1	Liquid hydrogen fuel level control shutoff valve	431
B-2	Ground fueling quick disconnect	433
B-3	Vapor recovery quick disconnect	435
B-4	Absolute tank pressure regulator (relief valve and vent valve)	437
B-5	Absolute tank pressure regulator	439
C-1	Tank wall model	440
G-1	AiResearch LH_2 engine takeoff power - thrust	479
G-2	AiResearch LH_2 engine takeoff power - fuel flow	480
G-3	AiResearch LH_2 engine maximum climb - thrust	481
G-4	AiResearch LH_2 engine maximum climb - fuel flow	482
G-5	AiResearch LH_2 engine part power - cruise	483
G-6	Jet A engine takeoff power - thrust	484
G-7	Jet A engine takeoff power - fuel flow	485
G-8	Jet A engine maximum climb - thrust	486
G-9	Jet A engine maximum climb - fuel flow	487
G-10	Jet A engine part power - cruise	488

LIST OF TABLES

Table		Page
1	Guidelines and Requirements	12
2	Effect of Change in Specific Fuel Consumption	15
3	Effect of Change in Inert Weight Variation	15
4	Cost Elements and Variables in 1967 ATA Formulas	26
5	Maintenance Factors for DOC Calculation	30
6	Baseline Engine	32
7	Baseline Engine Characteristics	33
8	Hydrogen Exploitation Summary	53
9	Baseline Engine Cycle, Initial Cycle Selection	66
10	Internal Cycle Temperatures (^{o}R) (Sea Level, Hot Day, Takeoff Thrust)	68
11	Allowable Metal Temperature Limits	68
12	LH_2 Combustor Pattern Factors	69
13	Turbine Cooling Air Flow Requirements (%) 1760° (3200°F) Rotor Inlet Temperature	70
14	Cycle and Performance Characteristics - Selected LH_2 Fueled Engine	84
15	Performance Ratings at U.S. Standard Atmosphere Sea-Level Static Conditions	88
16	Performance Ratings at 93.6^{o}F (34.2^{o}C) Sea-Level Static Conditions	88
17	Performance Ratings at U.S. Standard Atmosphere 35 000 Feet, 0.85 Mach	88
4.3.6	Liquid Hydrogen Fueled Engine Heat Exchanger Design Conditions	93
18	LH_2 Turbofan Engine Net Thrust, Fuel Flow, and Fuel Pressure Schedule for Initial Design Considerations	95
19	Candidate Materials for Liquid Hydrogen Application (-423°F)	113
20	Line Weight Summary	114
21	Functional Requirements	117
22	Electric Driven Boost Pump Candidate Summary	131
23	Effect of Pressure Rise Requirement at Minimum Flow on Pump Design and Minimum Flow Performance	132
24	Summary of Baseline Engine Operating Conditions	140
25	Variable Speed Pump, Summary of Operating Conditions	144

LIST OF TABLES (Continued)

Table		Page
26	Fixed Ratio Shaft Driven Pump, Summary of Operating Conditions	145
27	Comparison of Alternative Pump Drives	146
28	Liquid Hydrogen Pump	149
29	Tank Insulation System Concepts	197
30	Status of Development Applicable to the Candidate Insulation Systems	195
31	Safety Ranking Criteria	207
32	Effect of Vapor Nusselt Number on Heat Input to Liquid	213
33	Mission Fuel Schedule - Aft Tank	217
34	Data Sources for Properties of Insulation Concepts	218
35	Ranking of Candidate Insulation Systems Based on Safety Criteria	222
36	Summary of Safety Ranking	223
37	Concept Screening Performance Analysis Summary	225
38	DOC, - Weight and Volume Summary for Concept Screening	226
39	Impact of Ground Boiloff (Recovered) on DOC	227
40	Summary of Thickness Parameters and Fuel Losses for the Four Preferred Candidate Insulation Systems (Aft Tank Only)	241
41	Maximum Computed Circumferential Temperature Gradients in Tank Wall and Insulation System for Normal Operating Conditions	258
42	Effects of GH_2 and Air Leakage Into Evacuated Insulation Candidates	259
43	Initial Values, Design Weight Summary	265
44	Combined Loads and Thermal Criteria	272
45	Fuselage Allowable Gross Area Tension Stresses for Ultimate Design and Operating Conditions	273
46	Structural Design Concepts	275
47	Materials Data Pertinent to LH_2 Fueled Subsonic Transport Fuel Containment Tankage/Fuselage Structures	276
48	Concepts and Dimensions of Baseline Integral and Nonintegral Tanks	283
49	Tank Pressure Schedule	305
50	Point Design Load Environment, PLA Flight Condition	307

LIST OF TABLES (Continued)

Table		Page
51	Point Design Load Environment, Negative Maneuver Condition	307
52	Point Design Load Environment, Cruise Condition	308
53	Fuselage Frame Stability Requirements, Nonintegral Tank Design	312
54	Fuselage Frame Strength Requirements, Nonintegral Design	314
55	Summary of Fuselage Frame Requirements, Nonintegral Design	315
56	Summary of Fuselage Weight Data for the Hat-Stiffened Design, Nonintegral Tank	316
57	Summary of Fuselage Weight Data for the Zee-Stiffened Design, Nonintegral Tank	317
58	Tank Fatigue and Fail-Safe Requirements, Nonintegral Tank Design	320
59	Tank Fail-Safe Strap and Weld Land Requirements, Nonintegral Tank Design	321
60	Summary of Upper Fiber Unit Weights at the Quarter-Length Location, Nonintegral Tank Design	322
61	Summary of Lower Fiber Unit Weights at the Quarter-Length Location, Nonintegral Tank Design	323
62	Frame and Strap Fail-Safe Requirements for 30.0 Frame Spacing Design, Integral Tank	327
63	Frame and Strap Requirements for a 30.0 Inch Frame Spacing Design, Integral Design	328
64	Summary of Minimum-Weight Strap Designs, Integral Tank	328
65	Summary of Upper Fiber Unit Weights at the Quarter-Length Location, Integral Design	329
66	Summary of Lower Fiber Unit Weights at the Quarter-Length Location, Integral Design	330
67	Summary of Unit Weights for Integral Tank Design	332
68	Aft Tank Weight	334
69	Summary of Unit Weights for the Nonintegral Tank Design	334
70	Radii of Curvature of Candidate Dome Configurations	338
71	Comparison of Data for Minimum DOC Domes Configuration	341
72		341
73	System Weight Comparison of Fuel Containment System Candidates	366

LIST OF TABLES (Continued)

Table		Page
74	Characteristics of Aircraft Designed for Four Preferred Fuel Containment Systems	370
75	Evaluation of Preferred FCS Candidates	372
76	Characteristics of Final Design, LH_2- Fueled Transport Aircraft [400 Pax; 10 190 km (5500 n.mi.); Mach 0.85	374
77	Advanced Technology Weight Reduction Factors and Estimated Materials Distribution	377
78	Deleted	
79	Fuel System Malfunction Analysis	385
80	Allowable Failure Rates for LH_2 Pumping and Venging System Components	389
81	Thermodynamic Design Parameters	402
82	Comparison: LH_2 vs Jet A Subsonic Transport Aircraft	404
A-1	Design Mission Fuel Flow Schedule	
E-1	Potential Malfunction Screening Analysis	454
F-1	Preliminary Producibility Analysis	466
F-2	Example of Inspection, Maintenance and Operational Requirements	470
F-3	Factors Influencing the Candidate Insulation System's Life Expectancy	475

STUDY OF FUEL SYSTEMS FOR LH_2-FUELED SUBSONIC TRANSPORT AIRCRAFT

G. D. Brewer, R. E. Morris, G. W. Davis, E. F. Versaw
G. R. Cunnington, Jr.,* J. C. Riple,** C. F. Baerst,** G. Garmong,***

Lockheed-California Company
Burbank, California

SUMMARY

Concern for the potential short supply of petroleum-base fuels has led to a series of studies sponsored by NASA which have explored the technological aspects and established the potential of using liquid hydrogen (LH_2) for fuel in advanced commercial transport aircraft. Previous studies have investigated most promising methods of producing hydrogen, processes for liquefying the gas, aircraft configurations, and air terminal design and operations as they would be affected by introduction of LH_2-fueled aircraft.

The present study was directed at exploring the design problems presented by the fuel system of a representative LH_2-fueled transport. This encompasses everything required in the aircraft to contain, control, or handle the fuel. Although hydrogen fuel systems have been developed for space mission applications, the requirements for aircraft are so different in regard to mission duration, system life, operating cycles, and safety aspects that entirely different design problems are presented. The experience with LH_2 systems in the U.S. Space Program did, however, provide valuable reference data and serve as a point of departure in establishing designs for some of the aircraft components.

An aircraft design from a previous study performed by Lockheed for NASA (Reference 1) was used as basis for developing the fuel system design. The aircraft is shown in the frontispiece. It carries 400 passengers 10 190 km (5500 n.mi.) at a cruise speed of Mach 0.85. A design guideline was that the technology should represent initial operational capability in 1990-1995.

In order to provide maximum competence in all aspects of the study Lockheed-California Company was supported by Lockheed Missiles and Space Company, Inc., the California and Arizona AiResearch Divisions of the Garrett Corporation, and the Rocketdyne Division of Rockwell International in the performance of the work.

An initial task in the study was to define an efficient engine cycle, one which would take best advantage of the unique properties of hydrogen. Five ideas for exploiting the advantages offered by the large heat capacity and the low temperature of hydrogen were explored. These included precompressor cooling, compressor interstage cooling, cooling of the turbine cooling air, regenerative

---

*Lockheed Missiles and Space Company

**AiResearch Divisions of the Garrett Corporation

***Rocketdyne Division of Rockwell International

heating of the hydrogen fuel by the core exhaust, and use of an expansion cycle in connection with exhaust heat regeneration to provide power for engine accessories. In addition, two levels of turbine rotor inlet temperatures, 1756 and 2033 K (2700 and 3200°F), were evaluated, each in conjunction with an appropriate range of values of cycle pressure ratios and fan pressure ratios to permit selection of a preferred set of those parameters. All of this work was based on a definition of engine component performance and efficiencies agreed upon as representative of technology which can be developed for operational use by 1990.

The selected engine cycle was based on the following characteristics at sea level static, standard day conditions.

Rotor Inlet Temperature	1756 K (2700°F)
Cycle Pressure Ratio	35
Fan Pressure Ratio (tip)	1.594
Bypass Ratio	10.25

The design uses hydrogen to cool the turbine cooling air and also adds heat to the fuel in an exhaust regenerator.

The engine fuel supply system and the engine delivery and control system received significant attention. The engine fuel supply system takes the LH_2 out of the tanks and delivers it to the inlet of the engine high pressure pump. It consists, in main, of the boost pumps, valves, and fuel delivery lines. For reasons of reliability, each of the four tank compartments in the airplane is provided with a cluster of three boost pumps. The pumps are 3-stage, variable speed, centrifugal designs which are driven by 270 Vdc motors. They are designed to be line replaceable units (LRU's) for ready removal from the airplane in case they malfunction.

Fuel delivery lines are stainless steel, 2.54 cm dia x 0.406 mm wall (1.0 in. x 0.016 in.). The lines are enclosed in 3.81 cm (1.5 in.) of closed cell foam insulation, which is itself contained in a 10.16 cm dia. x 0.406 mm wall (4 in. x 0.016 in.) aluminum tube which serves as a vapor barrier and provides mechanical protection.

The engine delivery and control system consists of the engine-mounted high pressure pump, heat exchangers, and the fuel control system, all mounted in the engine nacelle. The engine pump is a two-stage centrifugal design, shaft driven at a fixed speed ratio. It is designed to take saturated liquid hydrogen (0 NPSH) at 345 Pa (50 psia) and provide a flow of 0.386 m^3/min (102 gpm) at a pressure rise of 4813 k Pa (698 psi). Its design rotational speed is 50000 rpm.

Four heat exchangers were designed to serve the following purposes:

- cool compressor bleed air which is then used to cool high pressure turbine vanes and blades
- cool engine lubricating oil
- cool compressor bleed air used in the aircraft environmental control system

- warm the hydrogen fuel to 677 K (1219 R) before entry into the combustor.

The engine fuel control system employs electronic control circuitry and has a flowmeter and a flow modulating and shut-off valve located just ahead of the engine combustor to control fuel flow to the engine. These units are located downstream of the heat exchangers to avoid lag in response which would otherwise result from the capacitance of the heat exchangers.

Fuel subsystems which were designed include the following: Fueling/Defuel, Vent and Pressurization, Fuel Transfer, and Fuel Jettison. The design requirements of each of these subsystems was established, then the designs were created so weights and costs could be estimated and operational requirements assessed.

An extensive analytical study was carried out to determine the best design for the fuel containment system. This consisted of investigation of various tank structural concepts and 15 different tank insulation systems. The structural investigation included analysis of both integral and nonintegral tank designs, plus several parametric studies involving consideration of

- dome shape
- pressure stabilization
- pressure level
- design life
- tank suspension methods

The tank insulation study was conducted in a concept screening phase in which 15 designs were investigated, followed by selection and more detailed examination of four preferred candidates, two each for integral and nonintegral tank structural designs. These four candidates were each treated as a basis for a separate airplane design so the comparison and final choice could be made in terms of parameters of primary interest to the aircraft operators.

Tank insulation concepts which originally entered the concept screening phase included representatives of all conceivable types including active systems dependent on reasonably hard vacuum [0.0133 Pa (1×10^{-4} torr)] ; some which were self evacuating by a process of cryopumping an included gas; and those which were completely passive, represented by closed cell plastic foam systems.

The fuel containment system which ranked highest in the overall rating scheme was a design which used an integral tank and an insulation system consisting of tiny, hollow borosilicate spheres (microspheres) contained in an annulus enclosing the tank which is pumped to a soft vacuum. The design pressure in the annular space is 13.33 Pa (0.1 torr). A very close second choice in the final evaluation was a design which also used an integral tank but the insulation system was a wrap of closed cell plastic foam around the tank, with a vapor barrier then wrapped around that to prevent air from penetrating the foam. These two insulation systems were so close in the ratings it is recommended both be further developed. The nonintegral tank designs were eliminated because of their inherent tendency to be both heavier and thicker.

Following the design of all elements of the aircraft LH_2 fuel system it was required that a comparison be made between the LH_2 and a corresponding Jet A-fueled aircraft. However, since some of the component efficiencies of the LH_2 engine were revised from those used in the original study (Reference 1), and since in the original study the LH_2 and Jet A-fueled engines had equal component performance, except as they may have been affected by the use of LH_2, a one-to-one correlation was no longer possible between the aircraft. Therefore, it was necessary to generate a new Jet A engine design which would match the component performance used in the LH_2 engine derived in the present work. This was accomplished and LH_2-fueled and Jet A-fueled aircraft designs were then established so the comparison of their characteristics could be made. A summary of some of the significant parameters is presented in the following table.

		LH_2	Jet A	Ratio $\frac{\text{Jet A}}{LH_2}$
Gross weight	kg (lb)	377,800	532,420	1.41
Operating empty wt	kg (lb)	230,000	243,400	1.06
Block fuel weight	kg (lb)	50,710	172,720	3.41
Thrust per engine	N (lb)	24,080	35,940	1.49
Wing area	m^2 (ft^2)	3242.9	4259	1.31
Span	m (ft)	170.84	195.8	1.17
Body length	m (ft)	215.64	197.0	0.91
Aircraft price	$\$10^6$	38.09	40.94	1.07
DOC*	¢/seat km ¢/seat n.mi.	1.599	1.699	1.07
Energy utilization	kJ/seat km Btu/seat n.mi.	1189	1445	1.22

*Calculated for baseline prices of each fuel

The LH_2-fueled design is superior in nearly every parameter. In fact, the advantages are greater than those calculated originally as presented in Reference 1. This is due primarily to the reduction in some engine component efficiencies, reflected in engines using both fuels, but through exploitation of the properties of hydrogen, the specific fuel consumption of the LH_2 design was nearly restored to its original value.

The baseline prices of each fuel used in calculating DOC, viz., \$5.69 per GJ for LH_2 and \$4.74 per GJ for Jet A, were established in previous studies made for NASA (References 41 and 4). Coal and water were the basic resources for the production processes for both fuels. At the baseline price for synthetic Jet A, a price differential amounting to an additional \$1.71 per GJ (\$1.80/10^6 Btu) can be paid for LH_2 fuel and still provide equal DOC.

NOMENCLATURE

NOTE: Computations in this analysis were performed in U.S. Customary units and then converted to S.I. units.

AR	=	Aspect Ratio
ATA	=	Air Transport Association
BPR	=	Bypass Ratio
CPR	=	Cycle Pressure Ratio
DOC	=	Direct Operating Cost
DTAM	=	Deviation from std. ambient Temperature
E_c	=	Young's Modules of Elasticity (compression)
E_t	=	Young's Modules of Elasticity (tension)
FAR	=	Federal Air Regulation
FCS	=	Full Containment System
fg	=	Fiberglass
F_N	=	Net Thrust
FPR	=	Fan Pressure Ratio
F_{t_u}	=	Ultimate fiber stress, tension
HC	=	Honeycomb
HP	=	High Pressure
H.P.EXT	=	Horsepower Extraction
I	=	Integral
IGV	=	Inlet Guide Vanes
IOC	=	Initial Operational Capability
Jet A	=	Conventional Hydrocarbon fuel
KEAS	=	Knots Equivalent airspeed
L/D	=	Lift-to-Drag ratio
LH_2	=	Liquid Hydrogen
LHV	=	Fuel Lower Heating Value
LP	=	Low Pressure
M	=	Mach Number
M_D	=	Design Mach Number
NI	=	Nonintegral
NPSH	=	Net Positive Suction Head
OPR	=	Overall Pressure Ratio

NOMENCLATURE (Continued)

OEW	=	Operating Empty Weight
P	=	Pressure
PLA	=	Positive Low Angle of Attack
P_{T_2}	=	Average Fan Face Total Pressure
P_{T_0}	=	Freestream Total Pressure
Q	=	Heating rate or Flow rate
QEC	=	Quick Engine Change Nacelle
RIT	=	Rotor Inlet Temperature
S	=	Wing Reference Area
SLS	=	Sea Level Static
TOGW	=	Takeoff Gross Weight
T/W	=	Thrust to Weight Ratio
TCA	=	Turbine Cooling Air
TIT	=	Turbine Inlet Temperature
VjP	=	Primary exhaust jet velocity
VjD	=	Fan Duct exhaust jet velocity
Vo	=	Flight velocity
Vr	=	Takeoff rotate Velocity
Vs	=	stall Velocity
$\dot{w}$	=	Flow rate
$W_a \frac{\sqrt{\theta_{T_2}}}{\delta_{P_2}}$	=	Engine corrected airflow
W_{pod}	=	Engine pod weight
W/S	=	Wing Loading = $\frac{\text{Aircraft weight}}{\text{wing area}}$
ZFW	=	Zero Fuel Weight
α	=	Angle of Attack
δ_{P_2}	=	Delta $P_2 = P_{T_2}$ (PSIA/14.7)
θ_{T_2}	=	Theta $T_2 = T_{T_2}$ (^{o}K/288.2)
η	=	efficiency
ρ	=	density
ϵ_6	=	heat exchanger effectiveness

1. INTRODUCTION

As a result of serious concern regarding the potential short supply of petroleum-base fuels, in 1973 the National Aeronautics and Space Administration instigated a program to investigate alternate fuels for commercial transport aircraft.

Liquid hydrogen (LH_2), liquid methane (LCH_4), and synthetic Jet A (synjet), all manufactured from coal and water, are leading alternate fuel candidates. To date, attention has been focused primarily on liquid hydrogen and on synjet, assuming the synthetic jet fuel would have the same properties as the present fuel for commercial airliners, Jet A or Jet A-1. Aircraft designs based on use of both of these alternate fuels have been created and compared (Reference 1), and the facilities, equipment, and operations needed at representative major air terminals to service liquid hydrogen-fueled aircraft have been studied (References 2 and 3).

The LH_2-fueled aircraft design from the previous study (Reference 1) was a conceptual design in which advanced technology features were incorporated representing an initial operational capability in the 1990 decade. The aircraft was sized to carry 400 passengers 10 190 km (5500 n.mi.) at a cruise speed of Mach 0.85. Necessarily, many assumptions were made concerning the characteristics of the LH_2-fueled engine, the fuel containment system, the engine fuel supply system, and other elements of the complete aircraft fuel system.

In the present work, attention was focused on precisely those items so that a more realistic evaluation of the potential of a hydrogen fueled transport aircraft could be obtained. The objectives of this study were as follows:

- Define the characteristics of a preferred design of fuel system for the specified LH_2-fueled transport aircraft.
- Establish the size, weight, cost and performance of the LH_2-fueled aircraft using the final fuel system design.
- Compare the LH_2-fueled aircraft with an equivalent technology Jet A-fueled design.
- Identify related research and technology development requirements for the LH_2 fuel system.

An outline of the approach taken in performing this study is described in Section 2.

2. TECHNICAL APPROACH

2.1 Team Organization

The wide scope of technical expertise required to define adequately a practical fuel system for a liquid hydrogen-fueled aircraft led to formation of a team, the members of which were selected for their competence in specified technical areas. Lockheed-California Company reached agreement with the following companies to participate in the study on a subcontract basis to provide special skills and innovative thinking in the areas indicated:

- Lockheed Missiles and Space Company, Inc. - For analysis, design, and evaluation of cryogenic insulation systems, and for specialized tank structural analysis

- Airesearch Divisions of the Garrett Corporation - For analysis and design of an advanced design LH_2-fueled turbofan engine, a fuel control system, pumps and other specific components

- Rocketdyne Division of Rockwell International - For analysis and design of the LH_2 engine fuel supply system, and for boost pump design

This team provided an ideal combination of basic knowledge and familiarity with the reference aircraft design, plus experience with technology developed in the U.S. Space Program on cryogenic fuel systems in general, and use of LH_2 in particular.

2.2 Work Plan

A schematic representation of the study work plan is shown in Figure 1. The work was performed in four phases. Phase I involved compilation of input data needed in the remainder of the study. These items are described in Section 3.

Phase II, System Studies, was the focus of the principal effort of the study. In this phase, the designs of the LH_2-fueled turbofan engine, the engine fuel supply system, the fuel subsystems, and the fuel containment system were established. In essence, these tasks involved examining the requirements, originating design concepts for evaluation, and choosing preferred designs for each of these elements of the fuel system of an LH_2-fueled aircraft. In addition, a comparable design of Jet A-fueled turbofan engine was also established to provide a basis for equivalent comparison of aircraft operated with the respective fuels.

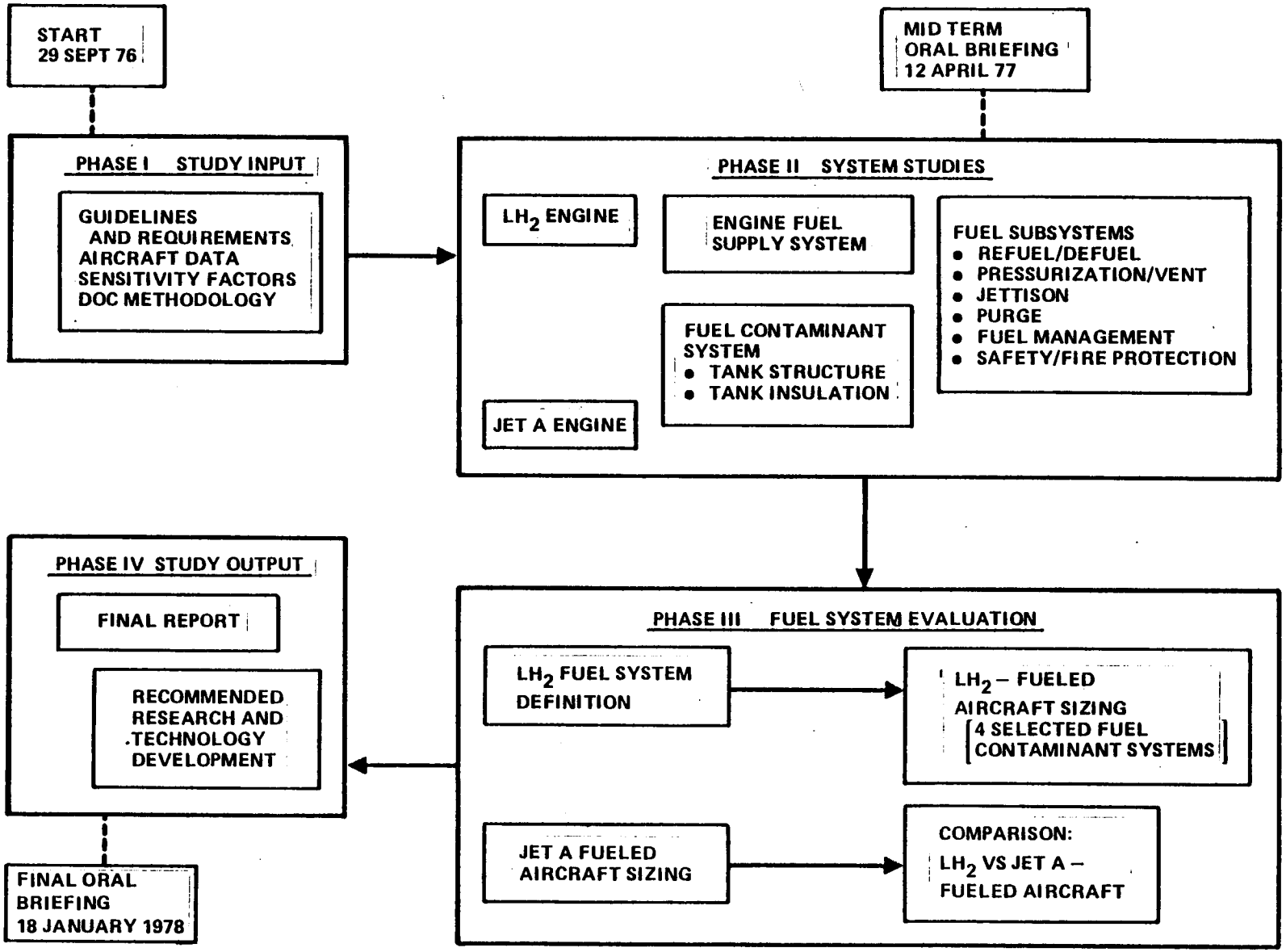

Figure 1. – Study work plan.

Phase III was an evaluation of the fuel system design which resulted from the work of Phase II. Drawings of the engine fuel supply system, the pressurization/vent system, and the fueling/defuel system, plus principal components of each of these, were prepared so weight, reliability, maintenance, and operational requirements could be assessed.

Four designs of fuel containment systems (tank structure, insulation system, and support structure) were selected from 15 candidates originally conceived and studied. These four selected designs were evaluated using the Lockheed Aircraft System Synthesis Evaluation Technique (ASSET) computer program to establish the potential of each in terms of aircraft size, weight, performance, and cost. Direct operating cost (DOC) was the principal measure of merit used in selecting the final preferred design.

The characteristics of the aircraft with the preferred fuel containment system, which also used the LH_2 engine and fuel system designs from Phase II, were compared with those of an equivalent technology Jet A-fueled aircraft. The Jet A design was subjected to the same optimization procedure using ASSET as the LH_2-fueled design so that the comparison would be on an equitable basis.

Phase IV consisted of summarizing the results of the work and preparing the final report. A recommended research and technology development program for critical LH_2 fuel system elements was formulated as a part of this effort.

3. STUDY GUIDELINES AND INITIAL DATA

Information required to perform analyses of the LH_2-fueled engine and fuel system components was generated or assembled as an initial step in the program. This work included reaching agreement with NASA on specific guidelines and requirements to be met; compiling basic data from Reference 1 on the baseline aircraft into a convenient package; generating sensitivity factors so that the benefit or liability of changes in key aircraft parameters could be assessed, and thus provide help in guiding design decisions; and finally, formulating a procedure for calculating direct operation cost (DOC) for the subject aircraft which would reflect a reasonable approximation of current airline practices, and which would also account for differences between LH_2-fueled and conventionally-fueled aircraft.

3.1 Guidelines and Requirements

The guidelines and requirements which were established for use during the study are listed in Table 1. These items were either originally specified by NASA as a basis for the study, or were perceived during the early stages of the program as being necessary for validity and consistency of results.

3.2 Basic Data

Basic information on the reference LH_2-fueled aircraft, and its design mission, which was needed to establish a starting point for the fuel system design requirements and analysis was derived, for the most part, from Reference 1. Some additional information was generated by making special runs of the ASSET computer program, and by separate analyses. In all, the following items were assembled and transmitted to all study team members and to the NASA Technical Monitor as preliminary data:

- Drawing CL 1317-1-1, General Arrangement - LH_2 M 0.85, 400 PAX, 5500 n.mi.
- Drawing CL 1317-1-4, Engine Feed System - LH_2 Subsonic Transport (preliminary draft)
- Drawing CL 1317-1-5, Fueling/Vent System - LH_2 Subsonic Transport (preliminary draft)
- Design Mission Fuel Flow Schedule (shown in Appendix A).

TABLE 1. - GUIDELINES AND REQUIREMENTS

Baseline aircraft: Final design in Reference 1: 400 passengers, 10 190 km (5500 n.mi.) range, Mach 0.85 cruise speed. See Figure 2.

Initial Operational Capability: 1990 - 1995

Baseline fuel costs:

LH_2 = \$5.69 per GJ (\$6 per 10^6 Btu = 31¢/lb)

Synjet = \$4.74 per GJ (\$5 per 10^6 Btu = 9.2¢/lb = 62.2¢/gal)

DOC basis:

1967 ATA equations updated to 1976 cost experience and modified to more accurately reflect airline practice, as well as differences resulting from use of alternate fuels. Assume production of 350 aircraft and 3600 engines.

Evaluation criteria:

DOC to be final measure of merit. All concepts must meet safety, reliability, maintainability, and operational requirements.

Safety:

Equal to or better than conventionally fueled commercial transport.

Design criteria:

Meet all applicable or anticipated regulatory requirements including FAR 25.

- LH_2 Turbofan Engine Thrust and Fuel Flow
- Fuel Flow Envelope - LH_2 Turbofan
- Design mission flight profile
- Lockheed LH_2 engine characteristics, component efficiencies, and installation factors (inlet recovery, installation drag, bleed air requirements, power extraction requirements).

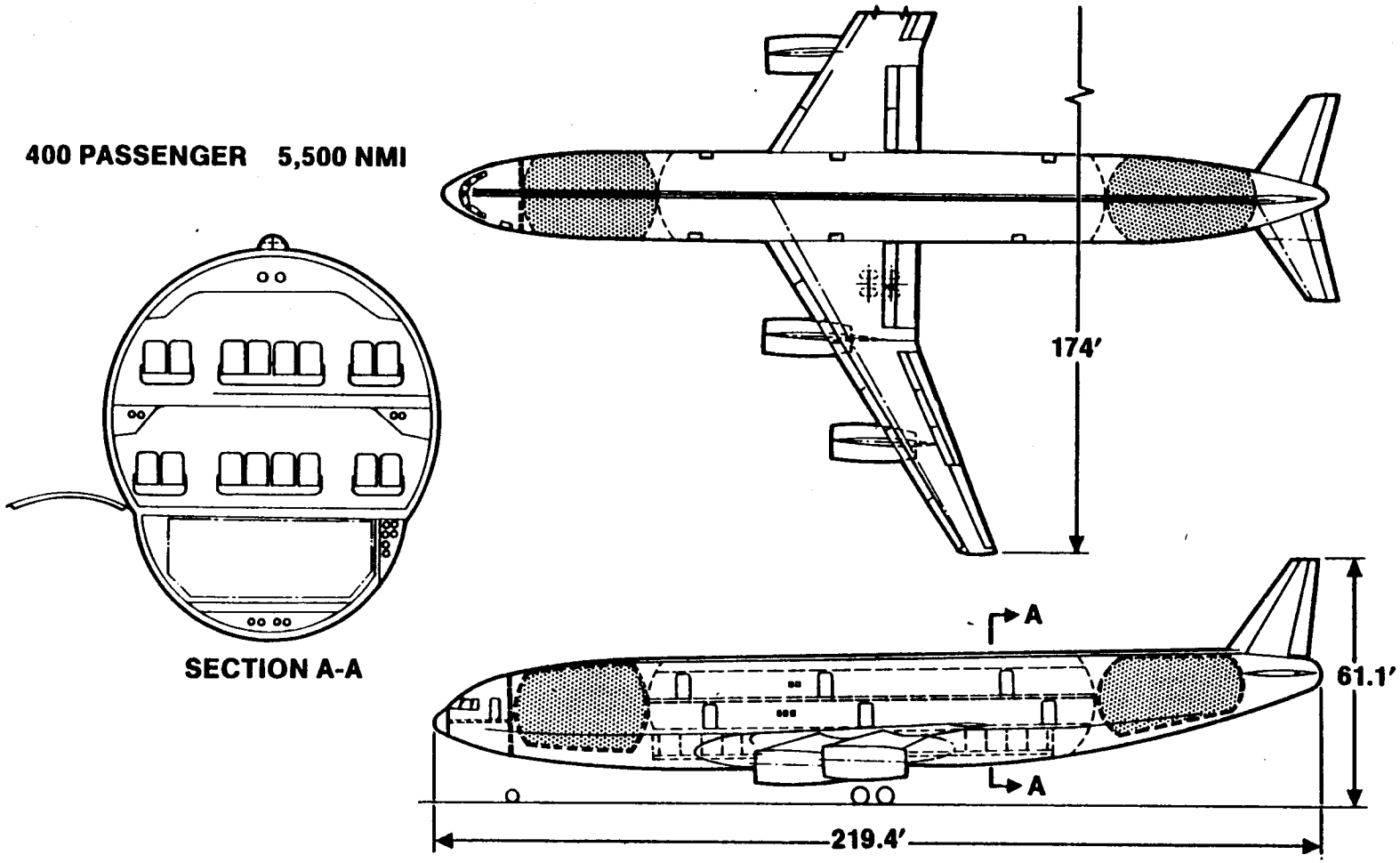

Figure 2. Baseline LH_2-fueled passenger transport.

3.3 Sensitivity Factors

Sensitivity factors were generated for the reference LH_2-fueled airplane to provide a basis for evaluation of the effect of changes from the baseline design. For example, in the study of the LH_2 engine design, a given option may have offered a few percent reduction in specific fuel consumption (SFC), but at the expense of an increase in inert weight. Sensitivity factors were a means of evaluating the net benefit which might be realized by incorporating that option in the design of the engine. Note that the sensitivity factors were used merely as an evaluation procedure to assist in screening attractive candidates. Evaluation of final design concepts was made by incorporating appropriate data in the ASSET aircraft synthesis program.

The sensitivity factors, or exchange ratios as they are sometimes called, were established by using the ASSET computer program to define optimized vehicles for each of a series of derivations from the nominal value of items like specific fuel consumption (SFC), vehicle inert weight (W_i), and thickness of fuel tank insulation system. The results were then plotted vs various airplane characteristics so the slope of the curve through the design point represented the sensitivity of those characteristics to small changes in the parameter being studied.

An example of this process is presented in Table 2 and Figure 3. The effect of 10 percent and 20 percent changes in SFC, both above and below the nominal value, on takeoff gross weight (TOGW), fuel weight (W_f), operating empty weight (OEW), manufacturer's empty weight (MEW), engine size, airplane cost, and direct operating cost (DOC) were all evaluated. The aircraft represented by each column in Table 2 are real in the sense that they have been sized using the ASSET program so that they represent a minimum gross weight design to perform the required mission, and that they meet all the specified design constraints.

The results as plotted in Figure 3 illustrate the effect changes in SFC would have on TOGW, OEW, W_f, and DOC. The slope of the curves at the design point, shown for each case, is the sensitivity factor. It is accurate in representing the effect on the various airplane characteristics of small derivations in the subject parameter. If large derivations are contemplated, their effect must be read from the curves, or a separate evaluation must be performed.

Similar data are tabulated and plotted in Table 3 and Figure 4 to illustrate the effect changes in inert weight of the aircraft would have on certain characteristics assuming the design has not been frozen. This assumption allows design characteristics of the aircraft such as wing loading and thrust-to-weight ratio to be changed to accommodate the inert weight variations in the most efficient manner.

TABLE 2. - EFFECT OF CHANGE IN SPECIFIC FUEL CONSUMPTION

(Reference SFC_{cruise} = 0.199 $\frac{lb}{hr}$/lb)

SFC Basis	80%	90%	Reference	110%	120%
TOGW (lb)	358 120	373 610	391 700	411 640	433 230
Fuel wt. (lb)	46 930	53 880	61 610	70 090	79 210
OEW (lb)	223 200	231 730	242 090	253 550	266 010
MEW (lb)	203 060	211 410	221 560	232 790	245 010
Thrust per Engine (lb)	26 230	27 370	28 690	30 150	31 730
Cost/aircraft ($\$10^6$)	38.96	40.25	41.81	43.53	45.39
DOC (¢/S n.mi.)	1.597	1.707	1.833	1.969	2.116
(% of ref.)	87.1	93.1	100	1.07	1.15

TABLE 3. - EFFECT OF CHANGE IN INERT WEIGHT VARIATION

Inert Wt. (lb)	-20 000	-10 000	Reference	+10 000	+20 000
TOGW (lb)	351 210	372 400	391 700	413 070	434 980
Fuel wt. (lb)	57 650	60 050	61 610	64 020	66 620
OEW (lb)	205 560	224 350	242 090	261 050	280 360
MEW (lb)	185 150	203 870	221 560	240 440	259 680
Thrust per Engine (lb)	25 730	27 280	28 690	30 260	31 860
Cost/Aircraft ($\$10^6$)	35.77	38.88	41.81	44.90	48.02
DOC (¢/S n.mi.)	1.681	1.763	1.833	1.914	1.998
(% of ref.)	91.7	96.2	100	104	109

Sensitivity factors for these two parameters, SFC and W_i, in addition to the effect of variation in thickness of fuselage tank insulation systems and the resulting influence this would have an fuselage length, were the primary tools needed to evaluate design or concept tradeoffs throughout Phase II. The following are some of the specific tradeoff relationships which were developed for application during this part of the program.

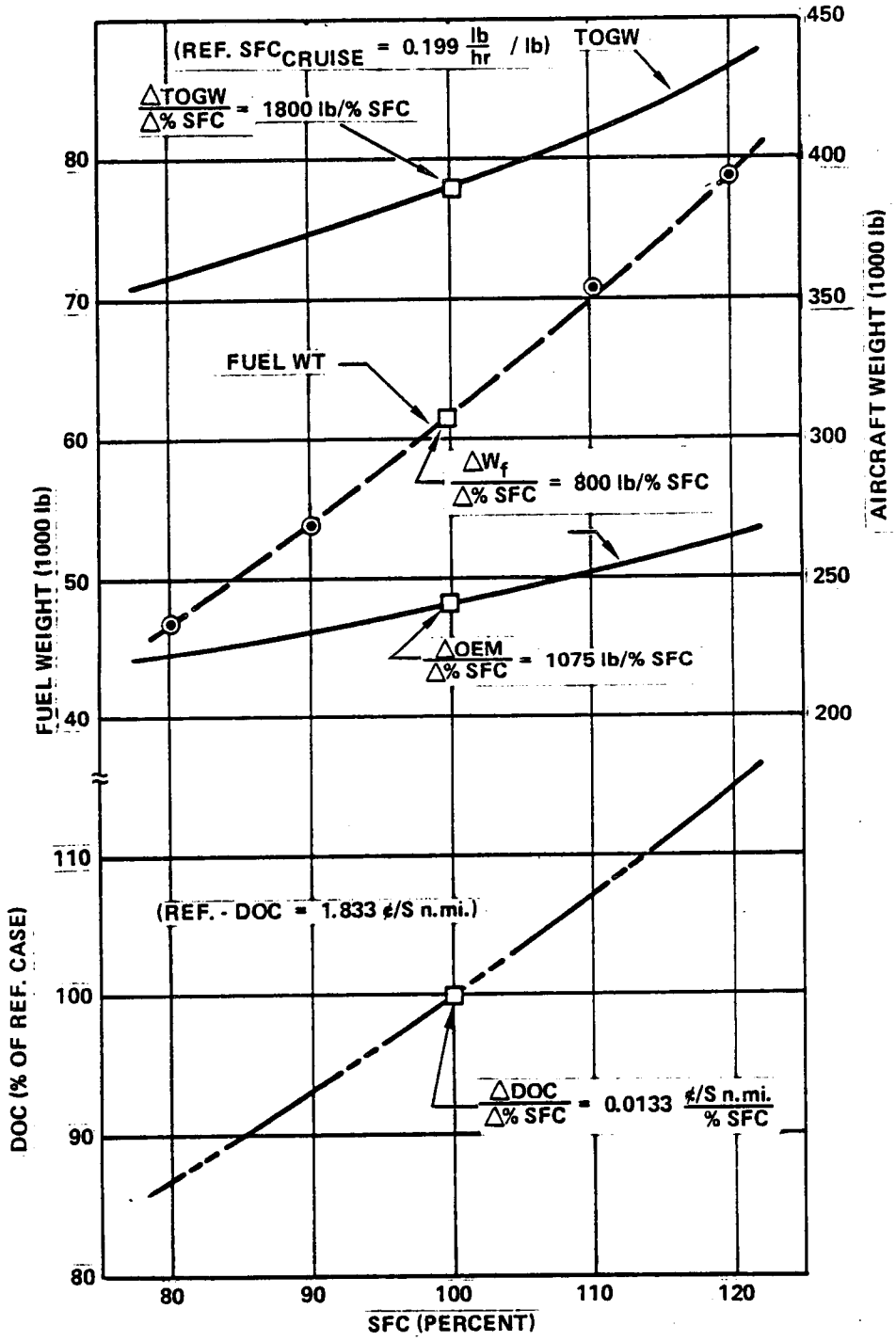

Figure 3. - Sensitivity of CL 1317-1 aircraft to changes in specific fuel consumption.

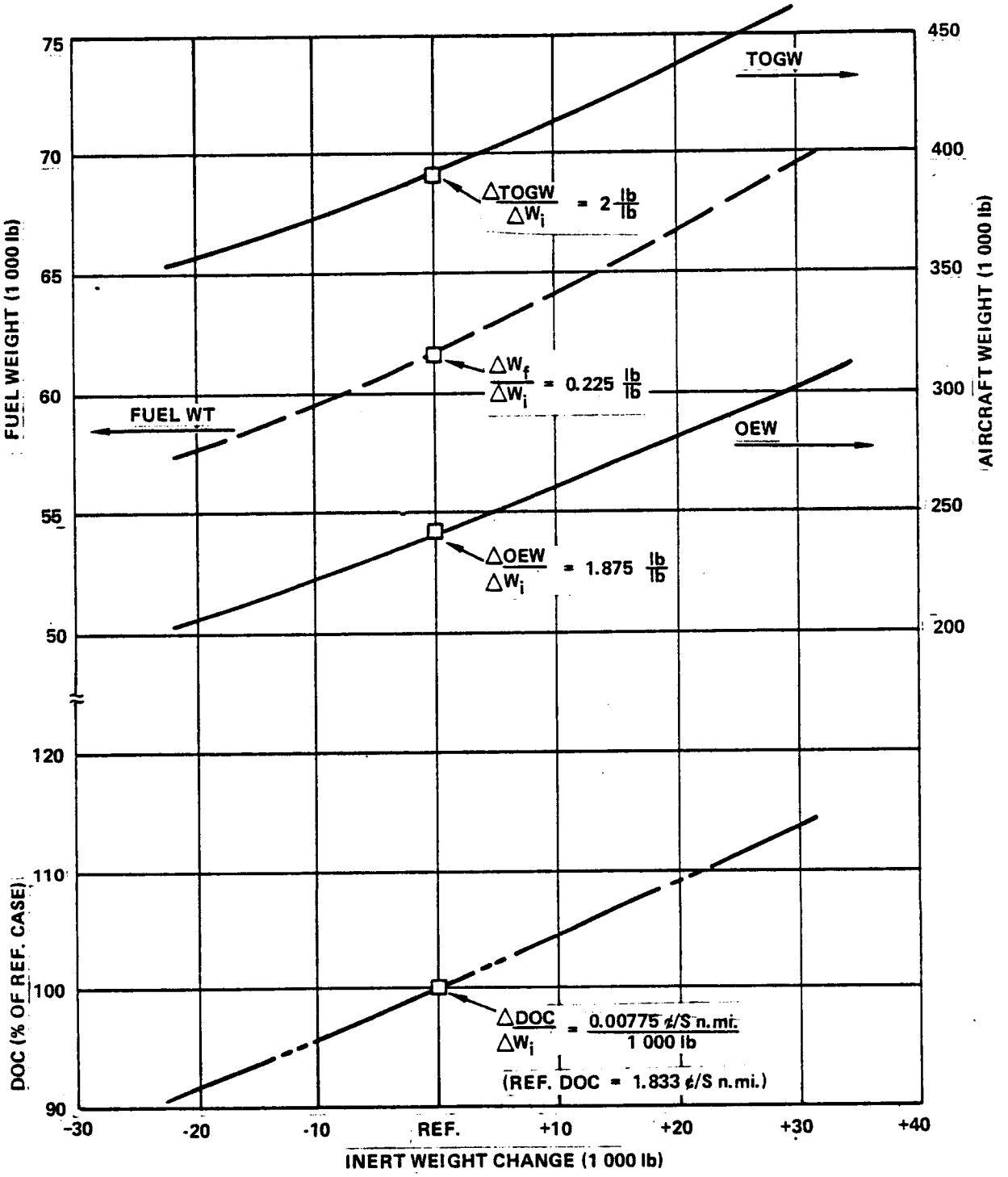

Figure 4. - Sensitivity of CL 1317-1 aircraft to inert weight variation.

3.3.1 Sensitivity of DOC to engine weight, SFC, and maintenance cost. - The following procedure permitted trade-offs to be made of engine cycles or concepts in which, for example, a more complex, heavier engine might deliver a reduced SFC. To use this evaluation method, it was necessary that preliminary estimates be made of the installed SFC, weight and maintenance requirements of the proposed engine relative to equivalent values for the baseline engine.

$$DOC = K \left(0.89 + 0.11 \frac{Maint}{Maint_{bl}}\right)$$

where:

DOC is evaluated in $\frac{¢}{Sn.mi.}$

$$K = 1.8334 + \frac{7.75}{10^6}\left[W_{prop} - W_{prop_{bl}}\right] + 1.332 \left[\frac{\overline{SFC}}{\overline{SFC}_{bl}} - 1\right]$$

$\frac{Maint}{Maint_{bl}}$ = Estimated maintenance manhours and material relative to the baseline engine based on complexity, operating temperatures, pressures, etc.

$W_{prop} - W_{prop_{bl}}$ = Change in weight of the proposed engine(s) or propulsion system compared to the following baseline values:

$F_{SLS\ (installed)}$ = 28 694 lb per engine

Weight (For 4 engines):

Engines	22 141 lb
Exhaust (including thrust rev.)	2 006
Inlets	2 558
Nacelles	6 599
Start system	382
	33 686 lb

Installed $\frac{thrust}{weight} = \frac{4 \times 28694}{33686} = 3.41$

(Note that the proposed engine thrust level must be the same as the baseline engine for a valid comparison.)

$\frac{\overline{SFC}}{SFC_{bl}}$ = Estimated SFC of the proposed engine relative to values for the baseline engine.

The scaling limits of this method are: $\pm$15% SFC

$\pm$10 000 lb weight

3.3.2 Sensitivity of DOC to fuel pumping system power and weight. - This trade-off was for purposes of assessing the relative benefit (or liability) of weight vs power requirements of candidate pumping systems. ASSET vehicle synthesis data were used, together with the baseline engine characteristics, to obtain an approximation of the horsepower-weight trade-off of tank mounted aircraft fuel pumping systems. It was assumed that the pumps were driven by electric, hydraulic, or other suitable power source extracted from the engine accessory drive. The approach used was to compare systems on the basis of the incremental change in direct operating cost (DOC) as shown:

$$DOC = \frac{3.22}{10^5} \Sigma hp_{cruise} + \frac{7.75}{10^6} \left[W_{system} + 6 \Sigma hp_{max} \right]$$

where:

DOC is expressed in $\frac{¢}{Sn.mi.}$

Σhp_{cruise} = total input horsepower to all tank mounted pumps running during cruise flight

W_{system} = total weight of pumping system including pumps, drives, installation, plumbing, etc.

$6 \Sigma hp_{max}$ = factor to account for the aircraft system installed weight penalty to provide the necessary input power. This is based on the total maximum horsepower of all pumps

EXAMPLE:

	System	
Drive type	No. 1 Electric	No. 2 Hydraulic
Σ hp max	80	70
Σ hp cruise	50	40
Wt. pumps - lb	40	40
Wt. drives	58	90
Wt. installation	20	30
Wt. lines	100	120
W_{system}	218	280

$$DOC_{Sys\ No.\ 1} = 0.0000322 \times 50 + \frac{7.75}{10^6}(218 + 6 \times 80)$$

$$= 0.0016 + 0.00541$$

$$= 0.00702 \ \frac{¢}{Sn.mi.}$$

$$DOC_{Sys\ No.\ 2} = 0.000322 \times 40 + \frac{7.75}{10^6}(280 + 6 \times 70)$$

$$= 0.00129 + 0.00543$$

$$= 0.00672 \ \frac{¢}{Sn.mi.}$$

System No. 2 has the lowest increment of DOC and would be favored over No. 1. However, since this evaluation does not address the important aspects of reliability and maintenance, it can only be considered as a screening

means to eliminate the least likely candidates or to measure the relative impact of power consumption and weight tradeoffs on the aircraft.

3.3.3 Sensitivity of DOC to volume and weight of fuel containment system. - The various candidate tank insulation systems and tank structural concepts offer trade-offs of thickness "t" (measured from inside surface of tank to exterior surface of aircraft) and weight. As thickness varies, the aircraft fuselage length must change to provide the required fuel volume within the fixed fuselage cross section. The following procedure, and associated values of influence coefficients, was derived from a matrix of ASSET cases which were run to simulate all reasonable combinations of fuel containment system thicknesses and weights. As noted earlier, all aircraft represented by the combinations of thickness and weight in the matrix are real in that they are sized to perform the design mission while meeting necessary design constraints.

1. Determine total fuel boiloff for the 5500 n.mi. mission for the insulation concept and thickness being evaluated.

2. Calculate the fuel tank volume required using the following allowances:

	Integral Baseline Case	New Case
• Ullage	2.00%	2.00%
• Net tank contraction due to cooling*, plus expansion due to pressurization	0.90	0.90
• Structure and equipment	0.64	0.64
• Trapped and unusable fuel	1.60	1.60
Subtotal	5.14	5.14
• Boiloff:		
Pressurant gas	1.00	As Calculated
Vented gas	2.56	
Total Allowance (percent)	8.70	5.14 + % Boiloff

*where insulation is on outside of tank

$$\text{Total Vol}/_{\text{tank}} = \frac{61\ 630}{2} \times \frac{\dfrac{1}{\rho_{H_2}\ \text{(Sat. liq. at 21 psia)}}}{1 + \dfrac{\text{Total allowance (\%)}}{100}}$$

For baseline case:

$$\text{(Ref.)} = \frac{61\ 630}{2} \times \frac{\dfrac{1}{4.325}}{1.087} = 7746\ \text{ft}^3/_{\text{tank}}$$

3. From Figure 5, find the aircraft fuselage length (L_{fus}) knowing "t".

4. Calculate the installed weight of the total fuel containment system (ΣW_{fcs}). Assume weight of forward tank is same as aft tank.

   NOTE: Installed weight includes tank, tank supports, shell structure (nonintegral), insulation, adhesive, vapor barrier protective cover, etc. For nonintegral tanks add the weight of the fuselage shell structure in the tank region and the tank removal provisions. Assume forward tank shell specific weight is the same.

5. Calculate DOC using the following equation:

$$\text{DOC} = 1.8334 + \frac{7.75}{10^6}\left(\Sigma\ W_{fcs} + \Sigma W_{H_2} - 82{,}294\right)$$

$$+ \frac{3540}{10^6}\ (L_{fus} - 224.3)$$

where:

1.8334 = Baseline aircraft DOC - ¢/Sn.mi. (fuel cost = $\$6/10^6$ BTU)

$\frac{7.75}{10^6}$ = Wt. influence coefficient

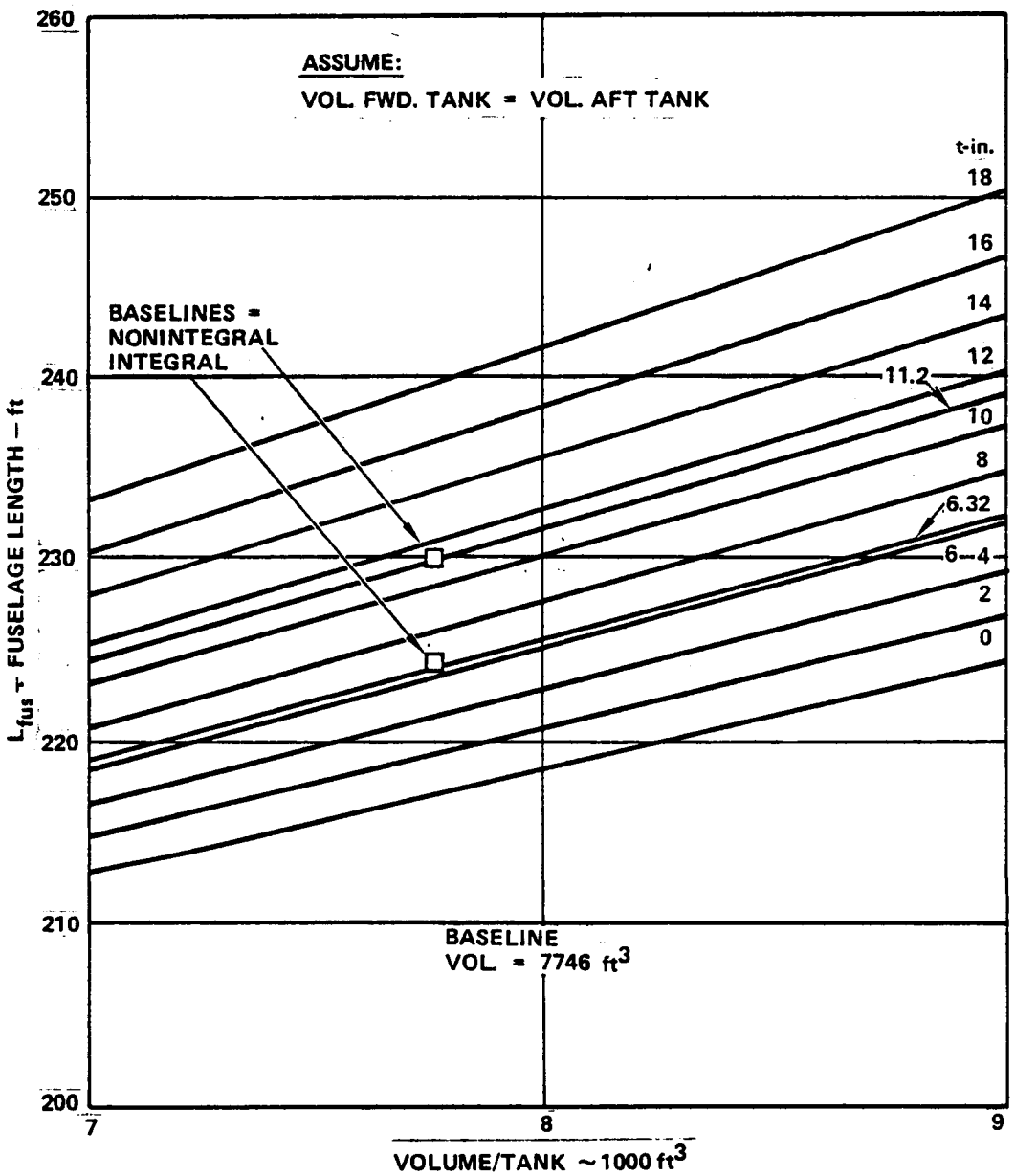

Figure 5. - Fuselage length vs fuel containment system thickness and tank volume.

$\frac{3540}{10^6}$ = Length influence coefficient

224.3 = Fuselage length (feet) for baseline integral tank (with t = 6.32 in.)

82 294 = $\Sigma W_{fcs} + \Sigma W_{H_2}$ for the baseline integral tank design

ΣWH_2 = Weight of tanked liquid plus both pressurization and vented gas.

3.3.4 Sensitivity of DOC to aircraft ground losses. - The choice of fuel containment concept is influenced by the fuel boiloff losses during tank refueling and by the boiloff during the daily out-of-service periods. In the LH_2 Airport Requirements Study (Reference 2) the economic desirability of collecting this vent gas for reliquefaction was established. The following method of analyzing the worth of capturing and reliquefying this ground boiloff hydrogen was derived to provide a basis for comparing competitive fuel containment system concepts. The assessment is in terms of DOC.

Assumptions:

1. The vapor is returned via a vacuum jacketed collection header and insulated surge tank to the hydrogen liquefier at a point just upstream of heat exchanger X-8 (stream No. 56) as shown in Figure 7 of the report "Survey Study of the Efficiency and Economics of Hydrogen Liquefaction" (Reference 4). It enters at a pressure of 15 to 16 psia and a temperature of approximately 70 K (126°R). It then passes through the heat exchanger and, in turn, through the H_2 flash and recycle compressors.

2. The cost of reliquefaction is assumed to consist of the cost of the electric power at 2¢/kWh used in recompression, and a prorated share of the storage, distribution and plant costs using the discounted cash flow (DCF) method of accounting described on page 45 of Reference 2.

   On this basis the estimated cost of reliquefaction is:

	($/lb)
Electric power	0.05
Share of plant costs	0.027
Total	0.077

The cost of the original GH_2 feedstock was, of course, included in the cost of the liquid hydrogen.

The effect of hydrogen boiloff losses on DOC of the baseline aircraft with a utilization of 4000 hours/year is:

$$\Delta DOC_{grnd.} = \frac{\Sigma W_{H_2\ grnd.}}{day} \times 3.75 \times 10^{-6} \left(\frac{¢}{Sn.mi.}\right)$$

where:

$\Sigma W_{H_2\ grnd.}$ = total of all daily ground boiloff losses

3.4 Calculation of Direct Operating Cost

Direct Operating Cost (DOC) was used as a primary selection criteria in evaluation of design options for the LH_2 transport aircraft, and as a basis for comparing the economic performance of liquid hydrogen fueled aircraft of advanced design with that of conventionally fueled counterparts.

The 1967 ATA DOC equations (Reference 35) were used as a starting point in the derivation of an improved method for calculating LH_2 and Jet A aircraft DOC. The 1967 ATA equations do not accurately reflect operation of either current or advanced technology aircraft and therefore required considerable modification. To provide a basis for reasonable evaluation of DOC for the subject LH_2 and Jet A aircraft, an extensive survey of airline operational practices was made, actual CAB data analyzed, and Lockheed and engine manufacturer's specialists consulted regarding probable maintenance requirements of the LH_2 aircraft. The information derived as a result of this work was used to formulate modifications to the 1967 ATA formulas in terms of January 1976 dollars for international trunk operation.

3.4.1 Background. - The DOC elements, and variables which affect their evaluation as reflected in the standard ATA formula, are listed in Table 4.

The airline surveys involved a series of meetings with four major U.S. air carriers to determine the elements which are of significance to them and the parameters and methods which they conventionally use in determining DOC. The following airline representatives cooperated in the investigation and contributed valuable data and advice:

TABLE 4. - COST ELEMENTS AND VARIABLES IN 1967 ATA FORMULAS

Element	Evaluated as Functions of the Following Variables
Crew cost	GTOW
Fuel and oil	Lbs fuel, fuel cost, non-revenue flying
Maintenance	
Airframe	
Labor	Airframe weight, speed, labor rate
Material	Airplane cost
Engine	
Labor	Thrust, labor rate
Material	Engine cost
Burden	Ratio of maintenance labor cost
Insurance	% of airplane cost
Depreciation	Cost of airplane, life, residual

American Airlines	-	Mr. Jack Graef
	-	Mr. Keith Grayson
Pan American World Airways	-	Mr. William Hibbs
Trans World Airlines	-	Mr. Walt Sherwood
United Airlines	-	Mr. John Curry

The participation of these airlines was solicited to provide representation of a spectrum of route structures, operational procedures, and financial practices.*

*It should be noted that each of the airlines consulted has its own methodology for determining DOC according to its individual requirements. The method and procedure described herein should not be construed as representing that of any one of the cooperating airlines. Rather, the method presented in this report is the result of an attempt by Lockheed to represent nominal industry values.

Statistical analyses of 1973, 1975, and 1976 CAB airline operating data were made in order to provide realistic parameters in addition to those provided by the airlines. Various statistical techniques, including multiple regression, were used to identify trends in the data. The CAB data were also used to identify and quantify variations between domestic and international trunk operation, variations between airlines, and variations between types of airframes and engines. The variations between 1973, 1975, and 1976 data were used to evaluate and define trends and to provide escalation factors. Consultations with both airframe and engine specialists were used to determine relative engine life, spares requirements, and maintenance values for LH_2 operation.

Evaluation of DOC for the subject aircraft study was performed within the Lockheed ASSET computer program which was used to develop aircraft configurations and mission performance, as well as cost data. Airframe and engine costs were derived from detail parametric formulas within ASSET using values for aircraft and engine parameters which were developed for the subject aircraft.

3.4.2 Parameters required for DOC evaluation. - The following paragraphs present the basis for evaluation of the parameters involved in determination of DOC for the subject study.

3.4.2.1 Weight: Weight is a primary factor in developing aircraft cost and DOC. Formulas containing weight as a parameter are based upon weight-cost relationships resulting from current technology aircraft. When advanced materials such as composites are introduced, the historical weight-cost relationships are no longer valid and must be modified. These modifications were made by using weights equivalent to current technology aircraft rather than calculated weights. Equivalent weights were used for weight related parameters such as density.

3.4.2.2 Aircraft cost: Airframe cost and schedule were based upon a five aircraft development program and a 345 aircraft production for a total of 350 aircraft. A maximum production rate of four aircraft per month was used. Most labor costs were estimated in terms of hours with applicable Lockheed-California Company January 1976 direct and overhead rates applied. Warranty costs and a profit of 15% were added.

Engine costs were based upon use of the engine in two separate aircraft production programs requiring a total of 3600 engines.

Airframe and engine spare costs were estimated as a percent of the engine or airframe cost. These percentages were derived from curves provided by TWA which relate percent of spares to fleet size. A fleet size of 20 was selected. Twelve percent was used for airframe; 29 percent was used for the conventional

engine, and 21 percent used for the LH_2 engine. The reduction for the LH_2 engines is considered appropriate because of an expected 30 percent increase in life for engines using that fuel. This stems from considerations such as 1) gaseous hydrogen and air mix very rapidly and thoroughly in the combustion chamber, which results in a very uniform temperature profile, thereby minimizing thermal stresses; 2) the very low emissivity of H_2/air combustion gases minimizes metal temperatures for a given temperature of the working fluid; 3) there are no carbon compounds to form coke or lacquer in the fuel lines, on the combustor walls, or in the turbine section; and 4) there is no sulfur or any other impurity in the fuel to cause either erosion or corrosion.

3.4.2.3 Mission characteristics: An average stage length (ASL) of 2187 nautical miles was selected from prior route studies. This agrees very closely with Lockheed formulas for deriving ASL for an international route. Block and flight times were calculated in ASSET based upon the mission profile for the ASL. Block time equals flight time plus ground time. A utilization of 3993 block hours/year (10.9 block hours/day) is estimated from Lockheed developed formula:

$$U = 2942.75 \times (\text{block time})^{0.191}$$

3.4.2.4 DOC elements:

- Crew Cost. - An international crew cost of $450/block hour was estimated from Lockheed-developed formula for 1973 domestic crew cost times a percentage for international bonus and adjusted for inflation from 1973 to January 1976. The formula and adjustment factors were derived from CAB data.

$$\text{DCC (1976)} = 38.38 \times \text{ASL}^{0.12} \times \text{OEW}^{0.202}$$

$$\text{ICC (1973)} = \text{DCC (1973)} \times 1.10$$

$$\text{ICC (JAN 1976)} = \text{ICC (1973) escalated at 12.7\%/year}$$

Where

DCC = Domestic Crew Cost

ICC = International Crew Cost

OEW = Operating Empty Weight

- Fuel Cost. - Fuel costs were given by NASA (see Table I, Guidelines and Requirements), assuming both fuels are produced from coal and water in the 1990's.

$$LH_2 = \$5.69 \text{ per GJ } (\$6/10^6 \text{ Btu} = 31¢/\text{lb} = 18.3¢/\text{gal})$$

$$\text{JET A} = \$4.74 \text{ per GJ } (\$5/10^6 \text{ Btu} = 9.2¢/\text{lb} = 62.2¢/\text{gal})$$

Block fuel usage is calculated by ASSET.

A factor of 1.23 percent for nonrevenue flying was applied, based upon average airline operations from CAB data.

- Maintenance Cost. - A maintenance labor rate of $9.00/hour was used as representative of the rates reported by the airlines from the airline survey. A maintenance burden factor of 2.27 was applied to maintenance labor. The burden factor was developed from a selected average for 1975 escalated at 3 percent per year to January 1976.

  The correction factors for the various elements of maintenance are summarized in Table 5.

- Insurance. - An average insurance rate over the life of the aircraft of 0.304 is estimated from an LCC developed formula.

$$\text{Avg. Rate} = (-1357.9 + 1359 \times \text{Years}^{0.001})/\text{LIFE}$$

- Depreciation. - Estimated average aircraft cost, including spares less residual value, is divided by the estimated life of the aircraft. A 4 percent residual value for wide body was derived from the airline survey. The 16 year life is normal for current large aircraft.

TABLE 5. - MAINTENANCE FACTORS FOR DOC CALCULATION

Maintenance Element	Maintenance Correction Factors				
	① Equiv. Weight	x ② ATA-to-Actual	x ③ LH_2 Cmplxty	x ④ Intntl DMSTC	= Total Factor Applied to ATA Formula
Airframe Labor					
Jet A	1.408	0.52	1.0	1.07	0.783
LH_2	1.388	0.52	1.02	1.07	0.788
Airframe Material	(Uses cost)		(Incl. in cost)		
Jet A	-	0.68	-	1.07	0.728
LH_2	-	0.68	-	1.07	0.717
Engine Labor	(Uses thrust)				
Jet A	-	0.62	1.0	1.07	0.663
LH_2	-	0.62	0.7532	1.07	0.50
Engine Material	(Uses cost)				
Jet A	-	1.31	1.0	1.07	1.402
LH_2	-	1.31	0.7382	1.07	1.035

① - Airframe weight is used in airframe labor only. The equivalent weight factor adjusts the weight of advanced technology materials to an equivalent current technology weight.

② - The ATA-to-actual ratio reflects a factor which must be applied to the ATA formulas to adjust to actual experience on wide body airframes and high bypass engines.

③ - The LH_2 complexity factor accounts for variations between a Jet A-fueled aircraft and an LH_2-fueled aircraft. A detailed maintenance analysis of each subsystem indicated a net 2 percent increase in airframe labor for the LH_2-airframe. Engine maintenance for the LH_2 is reduced 30 percent from the Jet A-engine maintenance for the same reasons discussed previously to account for longer life with LH_2 engines.

④ - The international/domestic adjustment is required because ATA-to-actual factors were developed on domestic trunk operation only and CAB data indicates a relatively higher cost for international maintenance.

4. LH_2 ENGINE DEFINITION

The objective of the engine definition task was to determine the optimum engine for a liquid hydrogen-fueled transport considering the requirements of the aircraft, i.e., mission profile and performance requirements, and the unique properties of the liquid hydrogen fuel. The work was performed as follows:

- The first element of this task addressed a feasibility investigation of various schemes to exploit the properties of hydrogen.
- The second element consisted of parametric engine investigations oriented toward selecting cycle variables and the engine configuration which minimized direct operating cost. The factors considered in evaluating direct operating cost were specific fuel consumption and engine weight.
- The third element of the engine definition task was the detailed definition of the selected engine design. The definition included determining engine performance throughout the flight envelope; weight and geometry; scaling laws; engine estimated cost; noise and emission levels; and operating limits and capabilities.
- The final element consisted of formulating a list of technology development requirements.

It is appropriate to point out that this task was not originally identified as a major activity in the study. Although definition of an optimum design of a LH_2-fueled engine is a topic deserving of serious effort, it served the purposes of the present study to limit the work to a preliminary investigation. Accordingly, the results are presented with the reservation that many of the design choices were made, necessarily, with less than adequate technical justification. A much more comprehensive design study is recommended to fully explore the potential of LH_2 as a fuel for advanced turbofan engines.

4.1 Feasibility Studies - Hydrogen Exploitation

The objective of this task was to determine if the unique properties of hydrogen could be capitalized on to provide engine performance and/or weight benefits. The concepts which were selected for evaluation included:

- Compressor air precooling
- Compressor air intercooling

- Cooling of turbine cooling air
- Regenerative fuel heating
- Expander cycle

4.1.1 Approach. - The approach used in the feasibility studies was to select a turbofan cycle compatible with the requirements of the liquid hydrogen-fueled transport and to investigate the effects of the selected concepts on this baseline. Previous Lockheed work (Reference 1) resulted in the definition of a turbofan cycle for a liquid hydrogen-fueled transport. Characteristics of this cycle are shown in Table 6. The data shown in Table 6 were derived using AiResearch analysis and modeling techniques and therefore differ slightly from Lockheed results as reported in Reference 1. AiResearch reviewed this cycle and found it to be generally consistent with technology projections for 1990. The bypass ratio and fan pressure ratio selected appeared to be high and low respectively, but the detailed parametrics required to select optimum values were not completed until later in the study. Therefore, this cycle was used as a baseline for the hydrogen exploitation feasibility studies. The high bypass ratio and low fan pressure ratio had little or no effect on the results of the feasibility studies.

TABLE 6. - BASELINE ENGINE

(From Reference 1, NASA CR 132559)

Parameter	Takeoff SLS, Std	Maximum Climb 35 000 feet M = 0.85
Rotor inlet temperature, °F	2 580	2 514
Cycle pressure ratio	35.2:1	41.13
Fan pressure ratio	1.51:1	1.634
Core pressure ratio	23.3:1	25.17
Nozzle-to-core-velocity ratio	1.022	1.17
Bypass ratio	12.95:1	13.0:1
Net thrust, lb	28 700	6 000
Specific fuel consumption, (lb/hr)/lb	0.094	0.1983
Specific thrust, lb/(lb/sec)	26.10	12.14

Two notable changes were made to the cycle shown in Table 6 during the course of the feasibility studies. The first change adjusted the cycle for the low temperature of the hydrogen fuel as it entered the combustor. The second change debited the cycle for the effects of turbine cooling air. Cycle and performance characteristics associated with these changes are shown in Table 7.

The effects of turbine cooling air were incorporated only for the investigation of the concept where compressor discharge air was cooled by the hydrogen fuel before it entered the turbine blades. Since the analysis method required evaluation of differential effects only, for all other concepts, zero turbine cooling air was assumed. The Lockheed defined cycle assumed the use of sodium-potassium (NaK) fluid to cool the turbine. The NaK was cooled by the hydrogen fuel.

TABLE 7. - BASELINE ENGINE CHARACTERISTICS

(Maximum Climb, 35 000 ft, M = 0.85)

Cycle and Performance Characteristics	Adjusted for Fuel Temperature	Adjusted for Turbine Cooling
Rotor inlet temperature, °F	2 514	2 514
Bypass ratio	13:1	13:1
Fan pressure ratio	1.634:1	1.634:1
Core pressure ratio	25.17:1	25.17:1
Nozzle-to-core velocity ratio	1.19	1.10
Fuel temperature to combustor, °R	90	90
Net thrust, lb.	6 000	6 000
Specific fuel consumption, (lb/hr)/lb	0.2042	0.2088
Specific thrust, lb/(lb/sec)	12.20	11.47
Horsepower extraction	125	125
Aircraft systems bleed extraction, %	4.1	4.1
Inlet total pressure recovery	0.991	0.991
Nozzle thrust coefficients	0.995	0.995

All concepts were evaluated at the initial cruise flight conditions of 35 000 feet, Mach 0.85. This flight condition determined engine sizing and was also typical of the cruise condition where the majority of fuel is consumed.

The criteria used for evaluation of the concepts was direct operating cost. The sensitivity of direct operating cost to changes in specific fuel consumption and engine weight was based on a relationship presented in Section 3.3. The relationship used in the engine study was

$$\Delta DOC\ (\%) = \frac{\frac{7.75}{10^6}\ (\Delta \text{engine weight}) + 1.332\ \left(\frac{SFC}{SFC_{base}} - 1\right)}{DOC_{base}} \times 100$$

The change in specific fuel consumption was evaluated using a design point thermodynamic routine which allowed the various concepts to be modeled. Engine weight for the various concepts was determined by adding the weight of the components associated with each concept to the baseline weight and adjusting the baseline weight for changes in airflow, bypass ratio and turbine design considerations.

For all cycle investigations, thrust, cycle pressure ratio, turbine inlet temperature, and fan pressure ratio were held constant. Specific thrust (F_N/W_a) was held nearly constant by fixing the energy extraction of the low pressure turbine. This was accomplished by specifying a constant jet nozzle velocity ratio (V_{core}/V_{fan}) in addition to the other constant parameters. Holding specific thrust approximately constant allows the effects of the various concepts to be observed independently of propulsive efficiency changes. It should be noted that holding the jet nozzle velocity ratio and fan pressure ratio constant does not hold specific thrust exactly constant but it results in only very minor changes in specific thrust and the analytical procedure is greatly simplified. The jet nozzle velocity ratio selected was 1.19 which was based on the original Lockheed cycle.

Installation effects that were included in the analysis were bleed and horsepower extraction for aircraft systems, inlet total pressure recovery, and exhaust system losses including fan scrubbing drag. Freestream cowl drag and inlet spillage drag were not included. To a first approximation, freestream cowl drag is a function of specific thrust and therefore, for this analysis, is a constant. Spillage drag at the design point condition is insignificant.

Other important assumptions included the temperature of the liquid hydrogen fuel at the fuel pump outlet, the specific heat of hydrogen, and the temperature of the fuel into the combustor. The fuel pump outlet temperature of 90°R was calculated based on an assumed temperature rise through fuel

system lines and the temperature rise across the engine high pressure fuel pump. Over the range of temperatures encountered, the specific heat of LH_2 is not constant but can be approximated by a constant 3.5 Btu/lb/°R. The fuel temperature into the compustor was assumed equal to the temperature out of the last engine heat exchanger for all concepts except the expander cycle. For that concept it was assumed equal to the temperature out of the hydrogen expansion turbine.

4.1.2 Compressor air precooling. - The concept incorporating compressor air precooling is shown in Figure 6. An annular heat exchanger is required in the core stream in front of the compressor. Fuel would be routed to the heat exchanger, entering at a temperature of approximately 90°R and, after passing through the heat exchanger, to the burner at an increased temperature. Precooling the compressor inlet air results in less compression work required and the benefit is a reduced gas generator size. A second benefit is the fuel heating effect. As discussed, LH_2 would typically enter the combustor at 90°R and part of the heat of combustion is required to heat the fuel to compressor discharge temperature. The elevated temperature of the fuel at the heat exchanger outlet minimizes this penalty. The benefit achieved is limited by the effectiveness and the air side pressure drop of the heat exchanger.

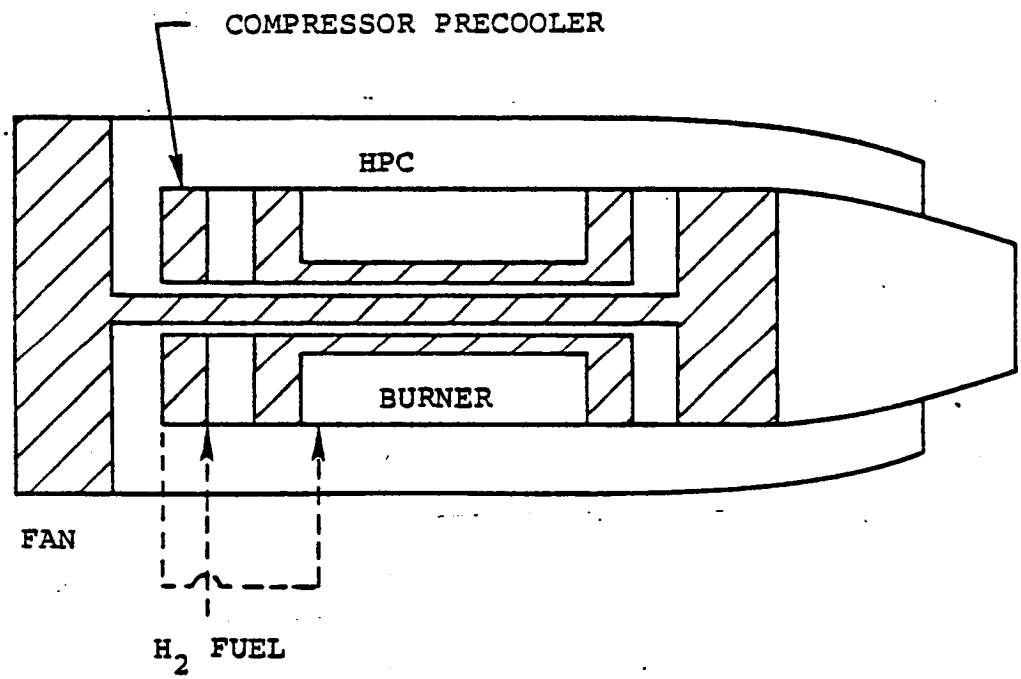

Figure 6. - Schematic of engine cycle with compressor precooling with H_2 fuel.

The results of this investigation are shown in Figure 7 in terms of specific fuel consumption versus precooler heat exchanger effectiveness and precooler air side pressure drop, all for an exhaust nozzle velocity ratio of 1.19.

Preliminary heat exchanger design analysis indicated that an effectiveness (H_2 side) of 0.8 and air side pressure drop of six percent was feasible. This combination results in a 1.86 percent improvement in specific fuel consumption. Basic engine weight decreased 63 pounds but the heat exchanger added 75 pounds. The net effect was an improvement in DOC of 1.33 percent.

Detailed heat exchanger design conducted later in the study indicated a severe air side freezing problem. Recirculation of warm fuel was investigated but did not solve the problem. Potential damage due to foreign object injestion was also identified as a serious problem associated with this concept.

4.1.3 Compressor intercooling. - The potential performance improvement due to intercooling the compressor air at an intermediate point in its compression process with the H_2 fuel was evaluated. The benefit to the cycle was expected to result from a reduction in core size due to compressor horsepower reduction per pound of core airflow and decrease in fuel flow due to heating of the fuel. An offsetting effect, as with compressor precooling, is the pressure drop on the air side of the intercooling heat exchanger.

The cycle with compressor intercooling is illustrated in Figure 8. The point in the compression process selected for the heat exchanger was chosen as one giving approximately equal enthalpy rise in the compression process prior to and following intercooling.

The results of this study are presented in Figure 9 in terms of specific fuel consumption versus intercooling effectiveness and pressure drop, all for an exhaust nozzle velocity ratio of 1.19.

Preliminary heat exchanger design indicated that an effectiveness (H_2 side) of 0.8 and an air side pressure drop of 4 percent was feasible. This combination results in a 1.0 percent improvement in SFC relative to the baseline cycle. Basic engine weight decreased 40 pounds but the heat exchanger added 100 pounds. The net effect was an improvement in DOC of 0.57 percent.

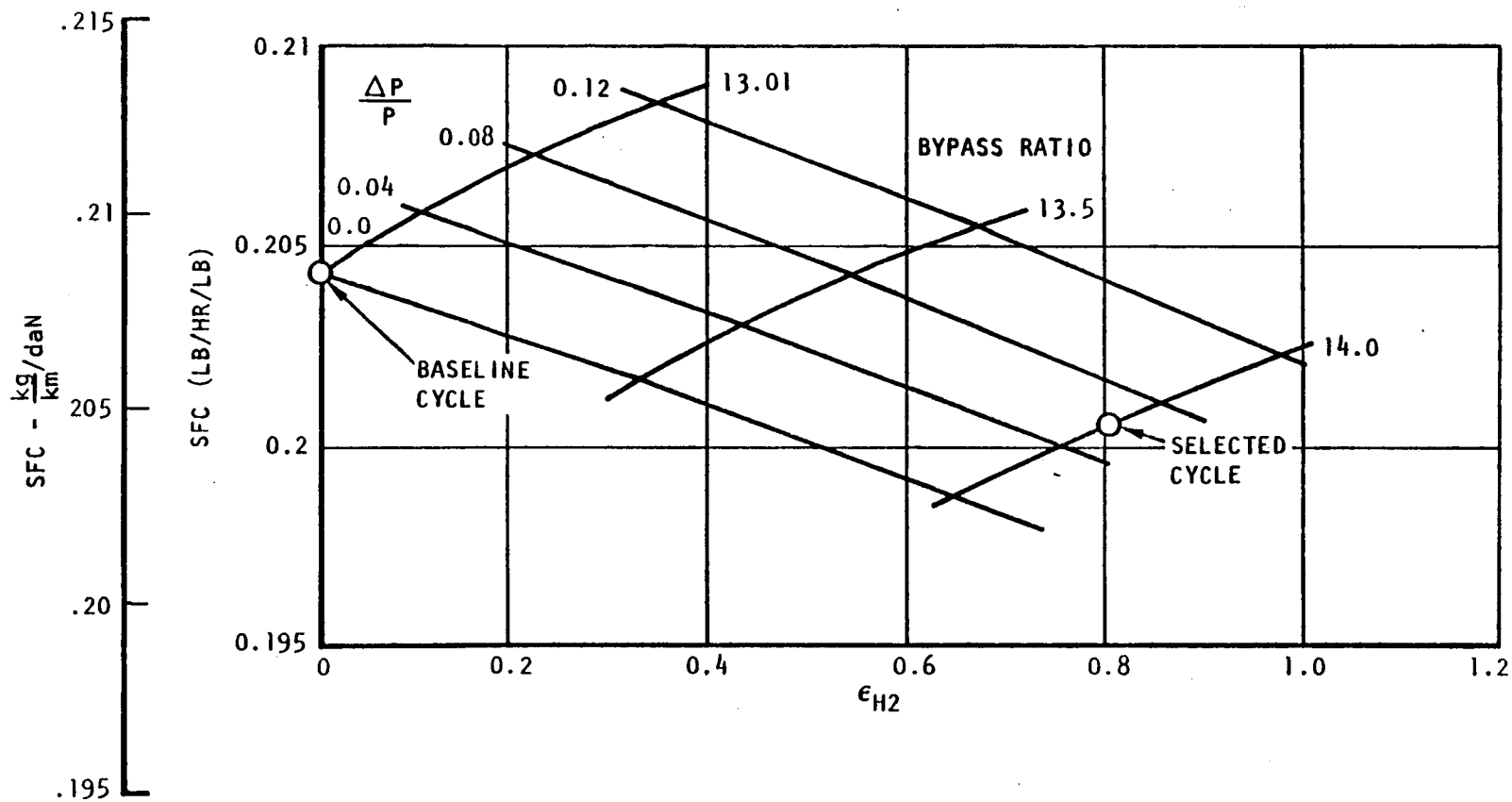

Figure 7. - Engine performance with precooling.

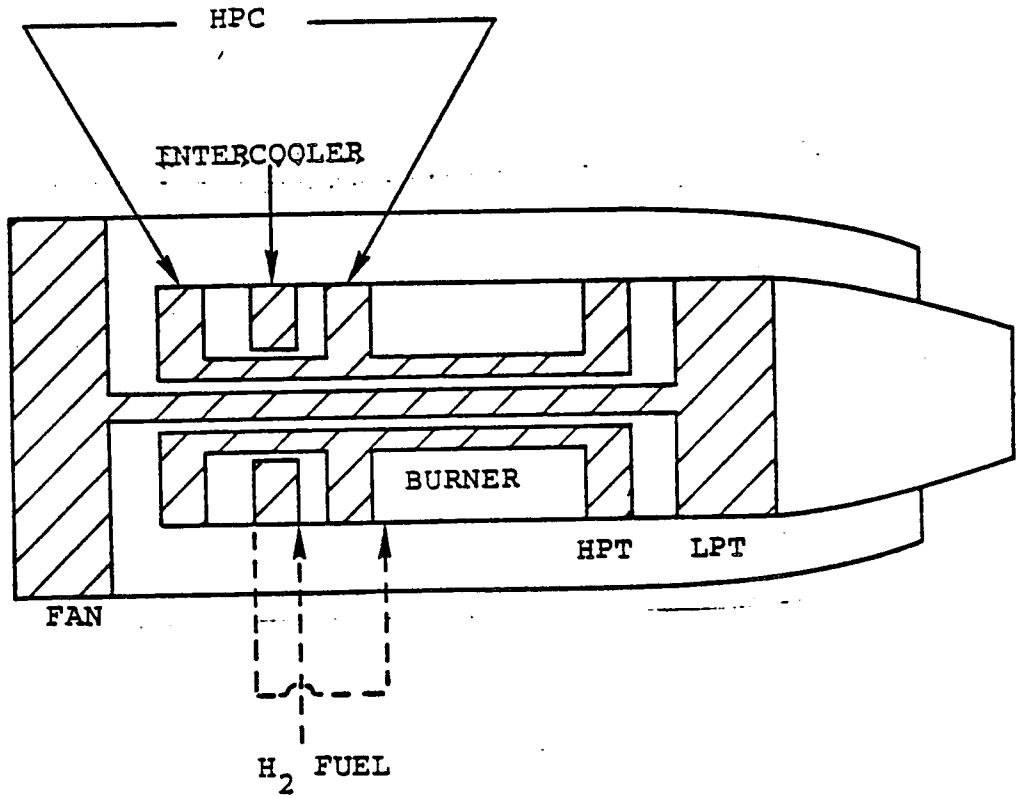

Figure 8. - Schematic of engine cycle with compressor intercooling with H_2 fuel.

4.1.4 Hydrogen cooling of turbine cooling air. - An evaluation was made of the potential benefit which might be derived from cooling the HP turbine blade cooling air with the hydrogen fuel. Hydrogen cooling of the turbine cooling air would reduce the quantity of turbine cooling air extracted from the compressor and, simultaneously, would heat the hydrogen fuel.

A schematic of this concept is illustrated in Figure 10. Air for cooling the turbine hub is extracted from the compressor and routed to the turbine by conventional means. Hub cooling air is not cooled by the hydrogen as the flow requirements are set by the pumping characteristics of the turbine disks and not by heat transfer requirements. If there was no flow of cool air through the cavities in front of or behind a disk, the air in the cavity would quickly reach the temperature of the main stream. This is due to a significant recirculation between the cavity air that is pumped in a toroidal flow pattern by the rotating disk and the high velocity main stream air. To maintain the cavity air at an acceptable level, cool air must be introduced into the cavity to avoid recirculation, or at least limit it. The quantity required is set by the rotating flow process more than by the temperature of the air. If some recirculation were allowed, cooling the cavity purge

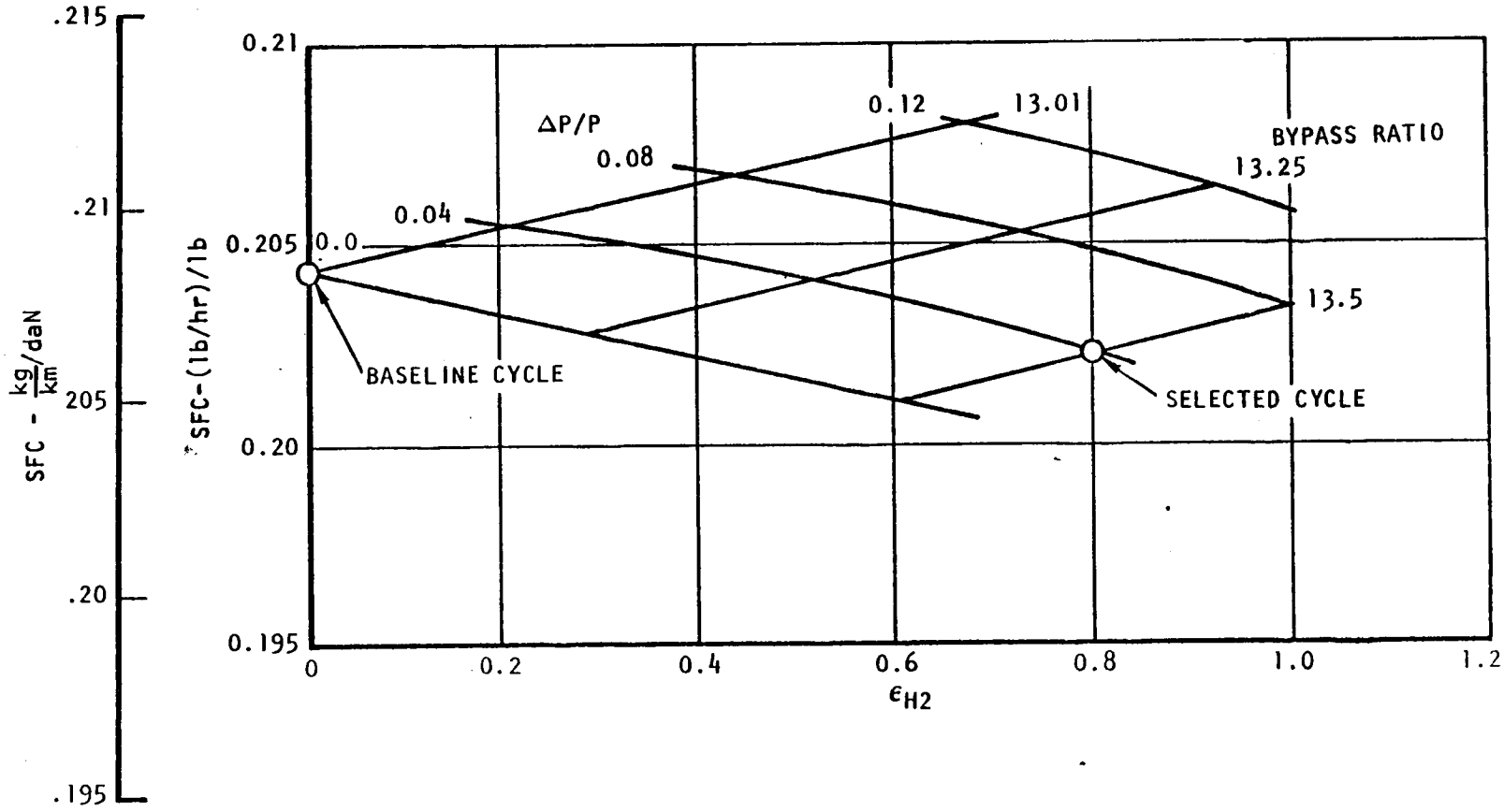

Figure 9. - Engine performance with intercooling.

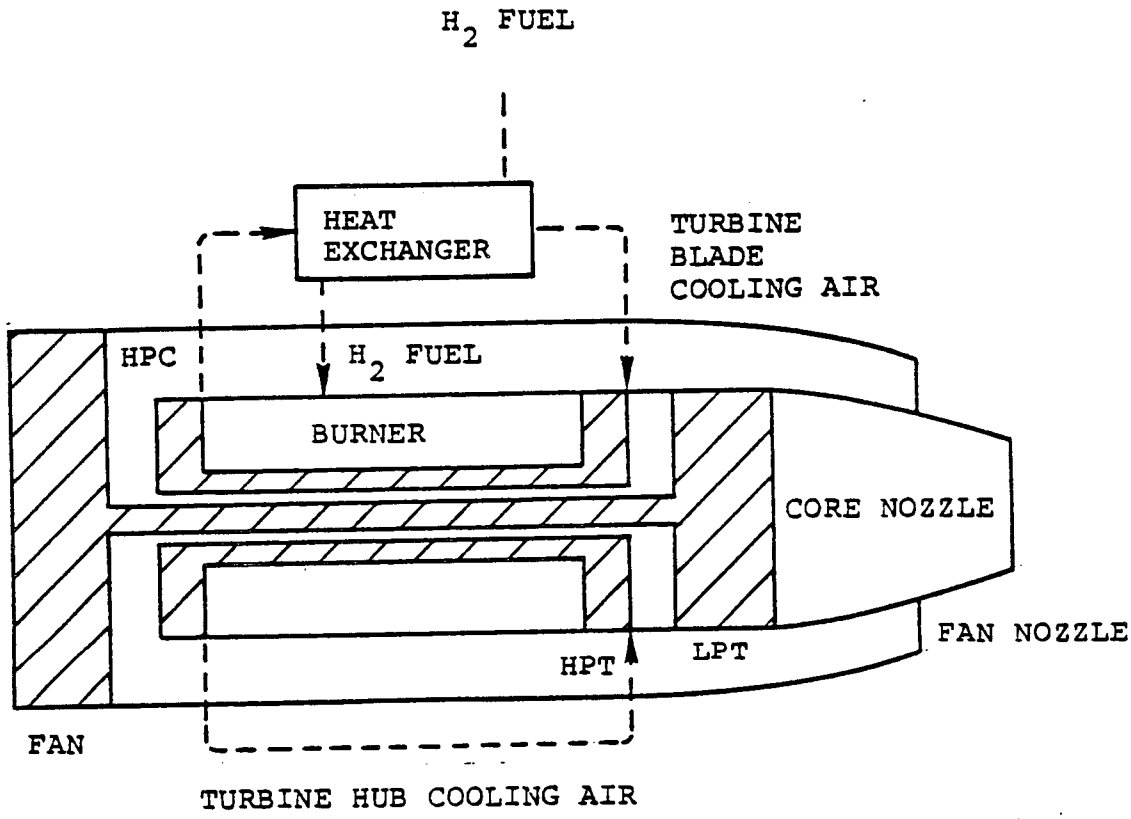

Figure 10. - Schematic of cooled turbine cooling air cycle.

air could reduce the flow. However, design standards which account for worn seals, varying engine power levels, and allowable disk temperature environment would need to be established. Furthermore, different approaches to routing of the air to the disks would have to be established.

Turbine blade cooling air is extracted from the compressor and directed to a heat exchanger and from there to the HP turbine at a temperature lower than compressor discharge temperature. The air used to cool the HP turbine vanes does not bypass any work producing stages and therefore is considered nonchargeable provided that the turbine inlet temperature is quoted at the rotor inlet rather than the combustor outlet. (For an explanation of the terms chargeable and nonchargeable, see Paragraph 3.2.3.1.4.) Cooling of the vane cooling air would reduce the amount of air required but it would not impact the cycle. Another reason for cooling the cooling air would be to reduce the vane flow in order to diminish the effect of cooling flow on

turbine efficiency. As the vane cooling flow exits, it disrupts the vane flow field. At high flows, this effect can be significant. However, for the time period specified and at the turbine inlet temperature level assumed, the vane cooling flow is low enough to preclude significant efficiency penalties.

The analytical method used to evaluate the effects of cooling was to penalize the turbine efficiency for pumping losses, etc., and to assume that the blade and hub cooling air do no work in the turbine being cooled and re-enter the cycle behind the HP turbine. This assumption is valid only in the case of a single stage turbine. For a multi-stage turbine, cooling air bypasses only the stage being cooled and re-enters the cycle behind that stage. Turbine vanes in multi-stage turbines also require different handling. The cooling air to a second stage vane bypasses the first turbine stage and therefore must be considered as chargeable cooling air.

Turbine efficiency was penalized for the amount of cooling air required. In other words, turbine efficiency increased as required blade cooling decreased. The efficiency penalty schedule used was 0.2 points of efficiency for each percent cooling air.

The results of this study are summarized in Figures 11, 12, and 13. Presented in Figures 11 and 12, are curves of specific fuel consumption, bypass ratio, and specific net thrust as functions of jet nozzle velocity ratio and heat exchanger effectiveness. Figure 13 presents curves of HP turbine efficiency, and HP turbine cooling airflow versus heat exchanger effectiveness.

At a jet nozzle velocity ratio of 1.19 and a heat exchanger effectiveness of 0.8, the maximum benefit to the cycle was approximately 0.53 percent improvement in specific fuel consumption. This improvement was relative to the baseline cycle with cooling air (see earlier discussion of baselines). Basic engine weight decreased 27 pounds per engine but the heat exchangers added 10 pounds per engine. The net improvement in DOC was 0.41 percent. The benefit to the cycle was small because the projected blade cooling air requirement for the 1985-1990 time frame is small.

Although the benefit to the cycle was small, hydrogen cooling of the blade cooling air seemed promising from other aspects. It suggested that the combined benefit of higher turbine inlet temperature plus inexpensive cooling might be attractive. Accordingly a more detailed study was conducted at 3200°F turbine inlet temperature. The results of this study will be discussed in a subsequent section.

4.1.5 Fuel heating with exhaust gas. - The concept of regenerative fuel heating was suggested because of the effect of the low temperature fuel at the combustor inlet. As noted earlier, the introduction of low temperature

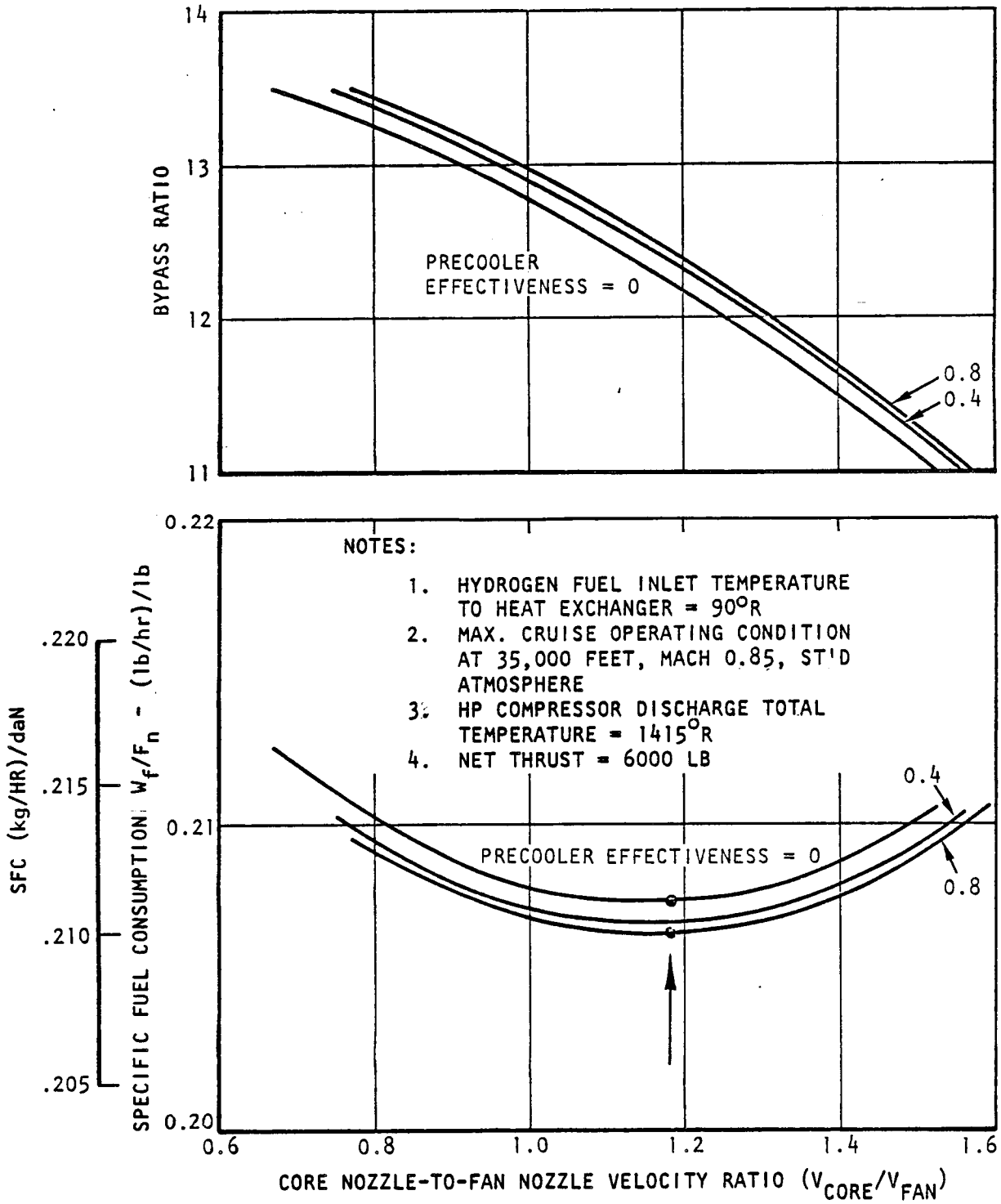

Figure 11. - Effect of cooling turbine cooling air with fuel at max. cruise, (35 000 ft) Mach 0.85.

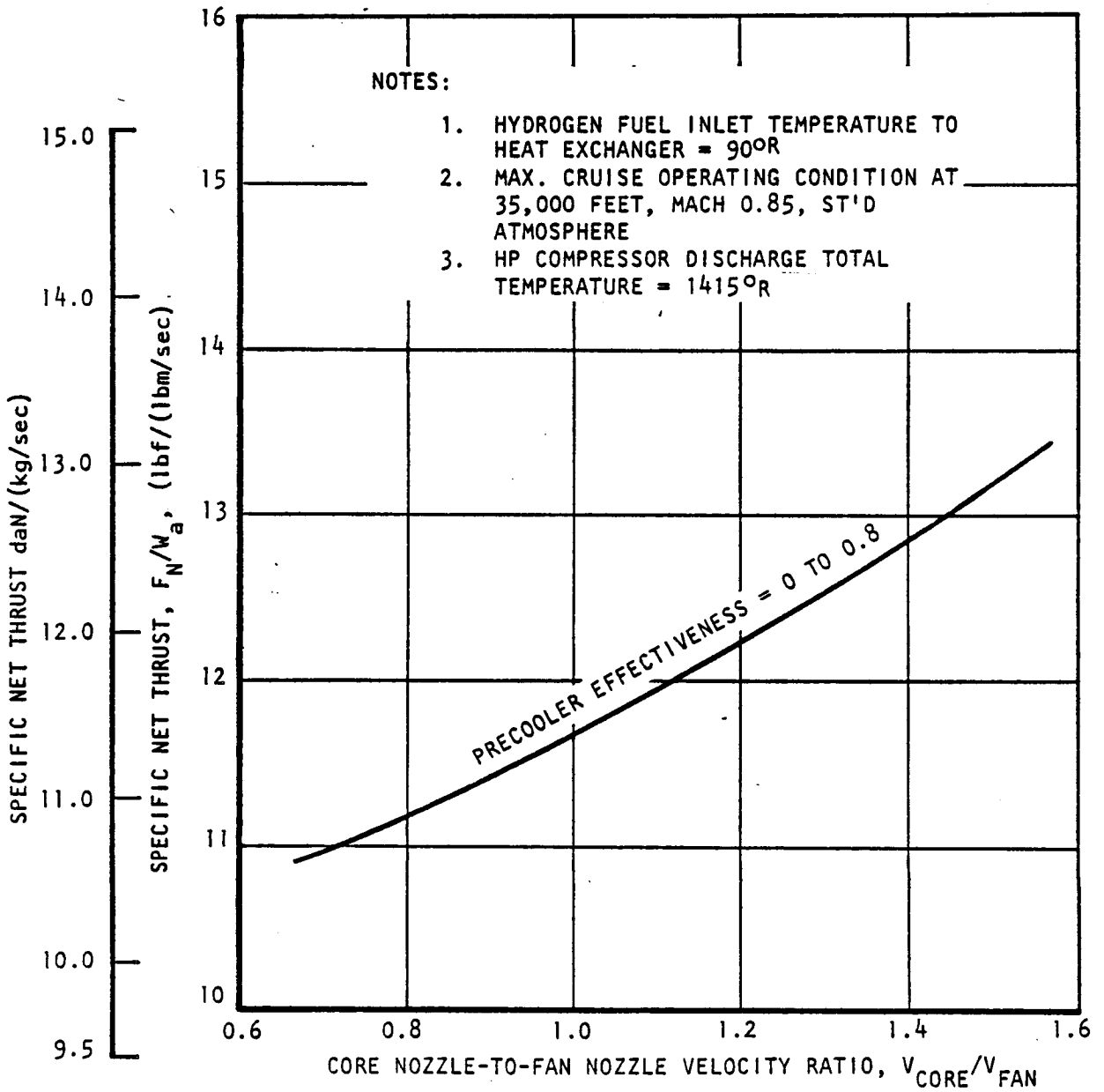

Figure 12. - Effect of cooling turbine cooling air with fuel at max. cruise 10.67 km (35 000 ft), Mach 0.85.

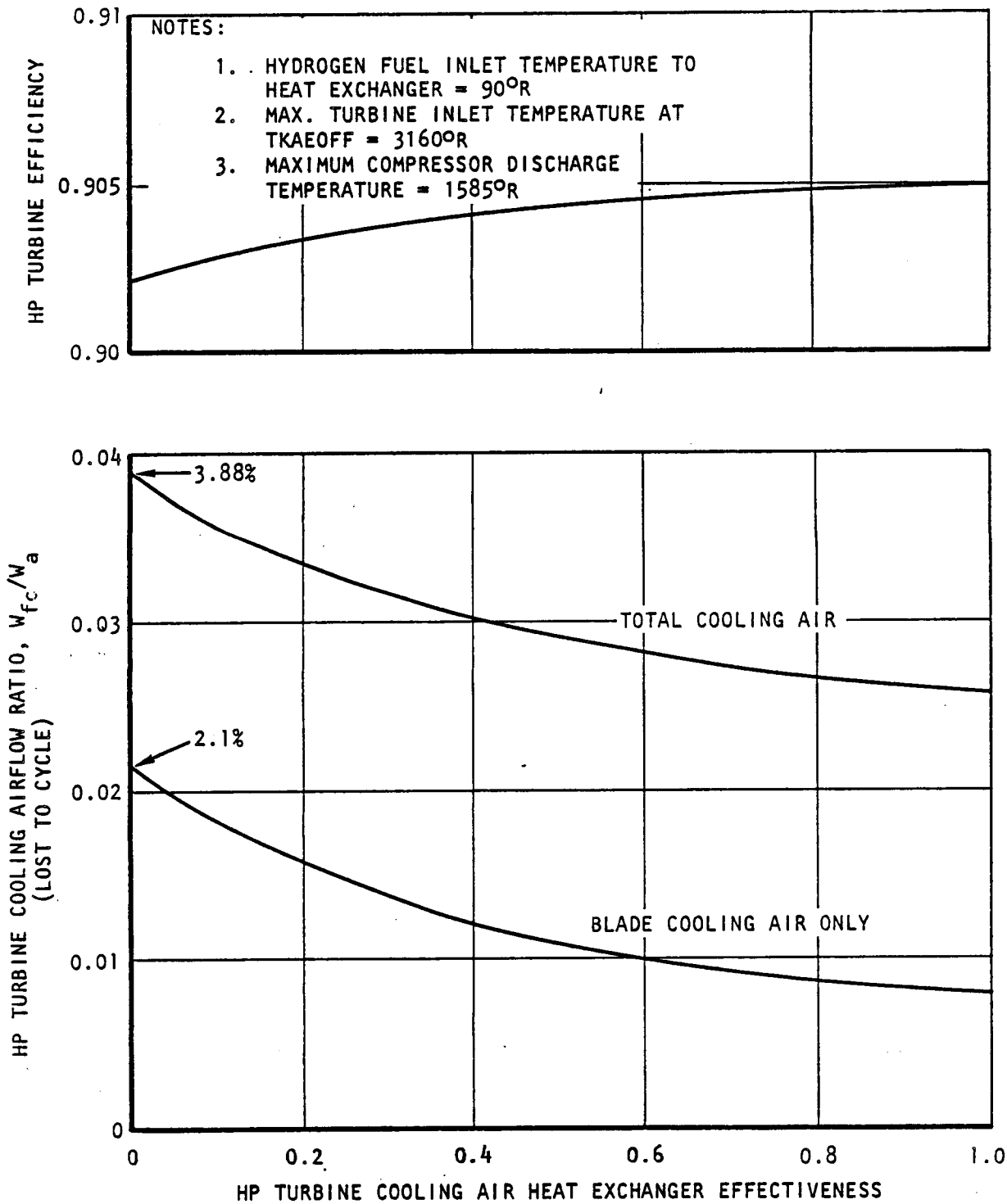

Figure 13. - HP turbine efficiency and cooling air schedules used in study of fuel cooling of turbine cooling air.

fuel into the combustor results in a performance penalty when compared with the fuel temperatures typical of conventional kerosene type fuels. The scheme is essentially a regenerative gas turbine cycle except that the energy is added to the fuel rather than the air. It is illustrated in Figure 14. It is interesting to note that, with the high pressure ratio cycles being evaluated, regeneration of the compressor discharge air would not be feasible because its temperature is higher than that of the exhaust gas.

The results of this study are presented in Figures 15, 16, and 17. Presented are curves of specific net thrust, and specific fuel consumption as functions of exhaust heat exchanger effectiveness (H_2 side) and exhaust nozzle velocity ratio. Figure 15 is for the case where the exhaust gas side pressure drop is zero, Figure 16 shows 4 percent, and Figure 17 shows 8 percent.

The results indicate that this scheme offers the maximum benefit of any of the concepts evaluated. The improvement in specific fuel consumption at a combination of 0.80 effectiveness and 4 percent pressure drop at a 1.19 jet nozzle velocity ratio is 4.31 percent, relative to the reference value as shown on Figure 16. Engine weight increased 27 pounds and the heat exchanger added an additional 112 pounds. The net improvement in DOC was 2.9 percent.

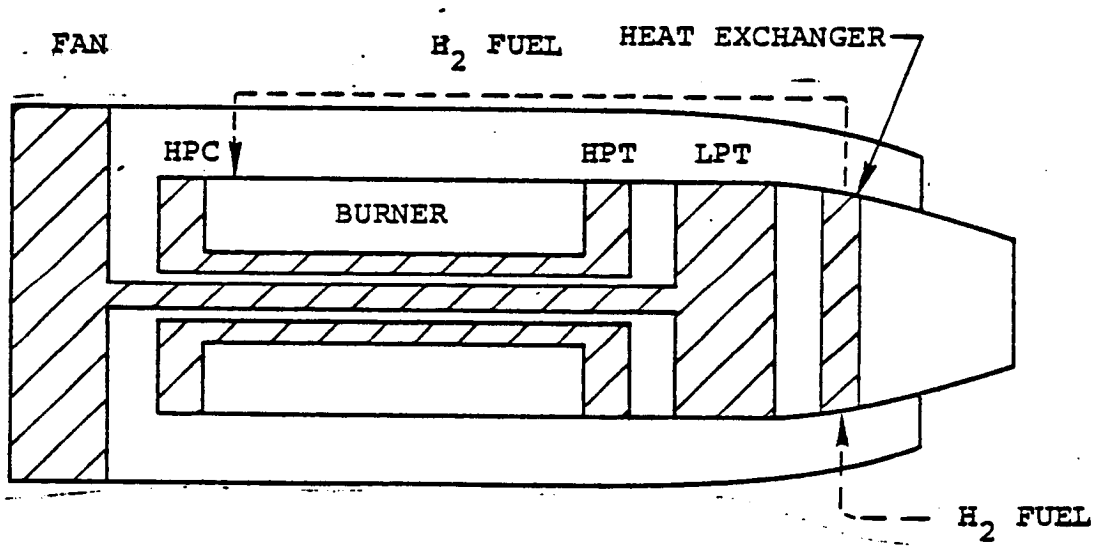

Figure 14. - Schematic of engine cycle with exhaust gas heating of H_2 fuel.

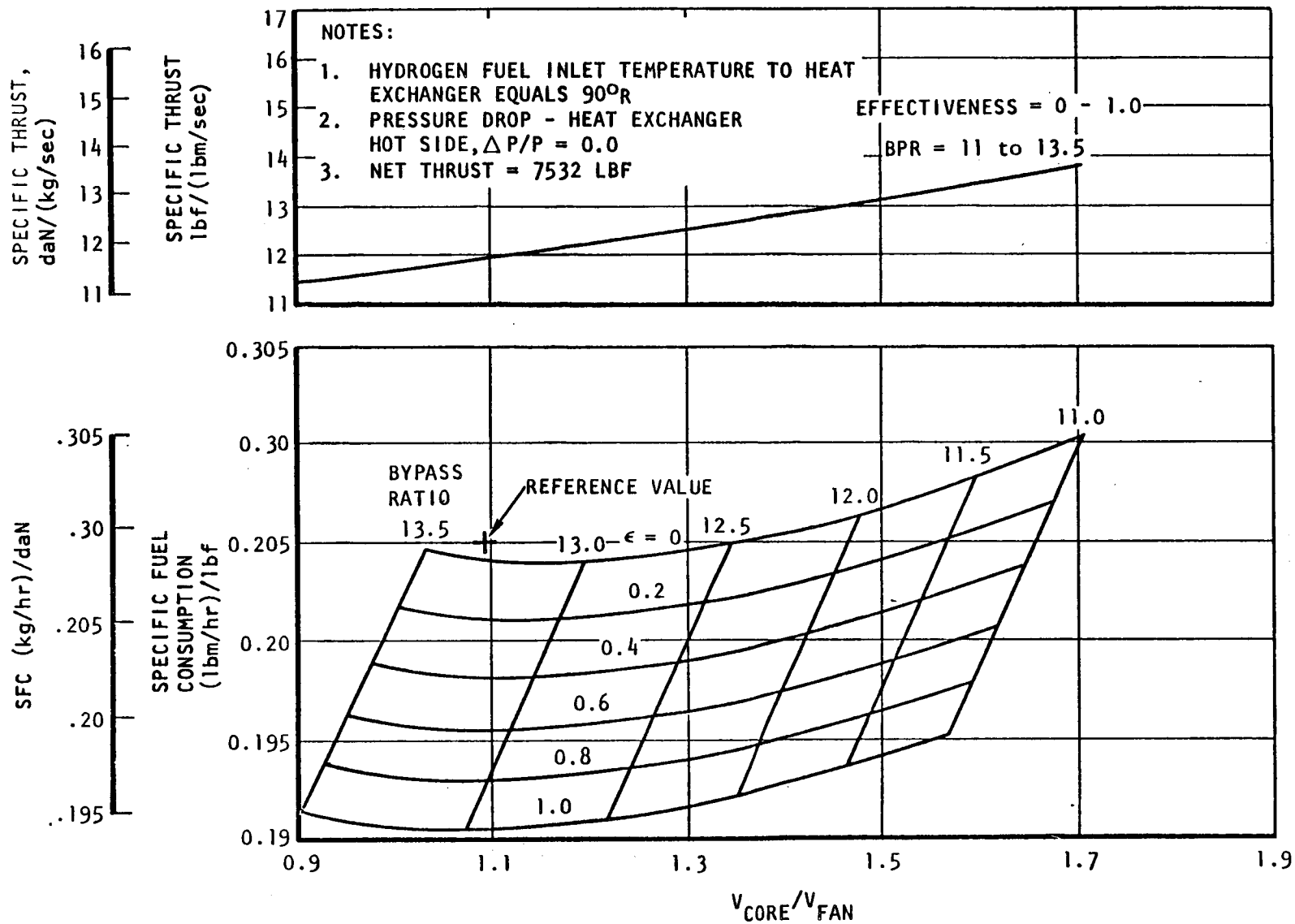

Figure 15. - Effect of exhaust heating on fuel at max. cruise (ΔP/P = 0).

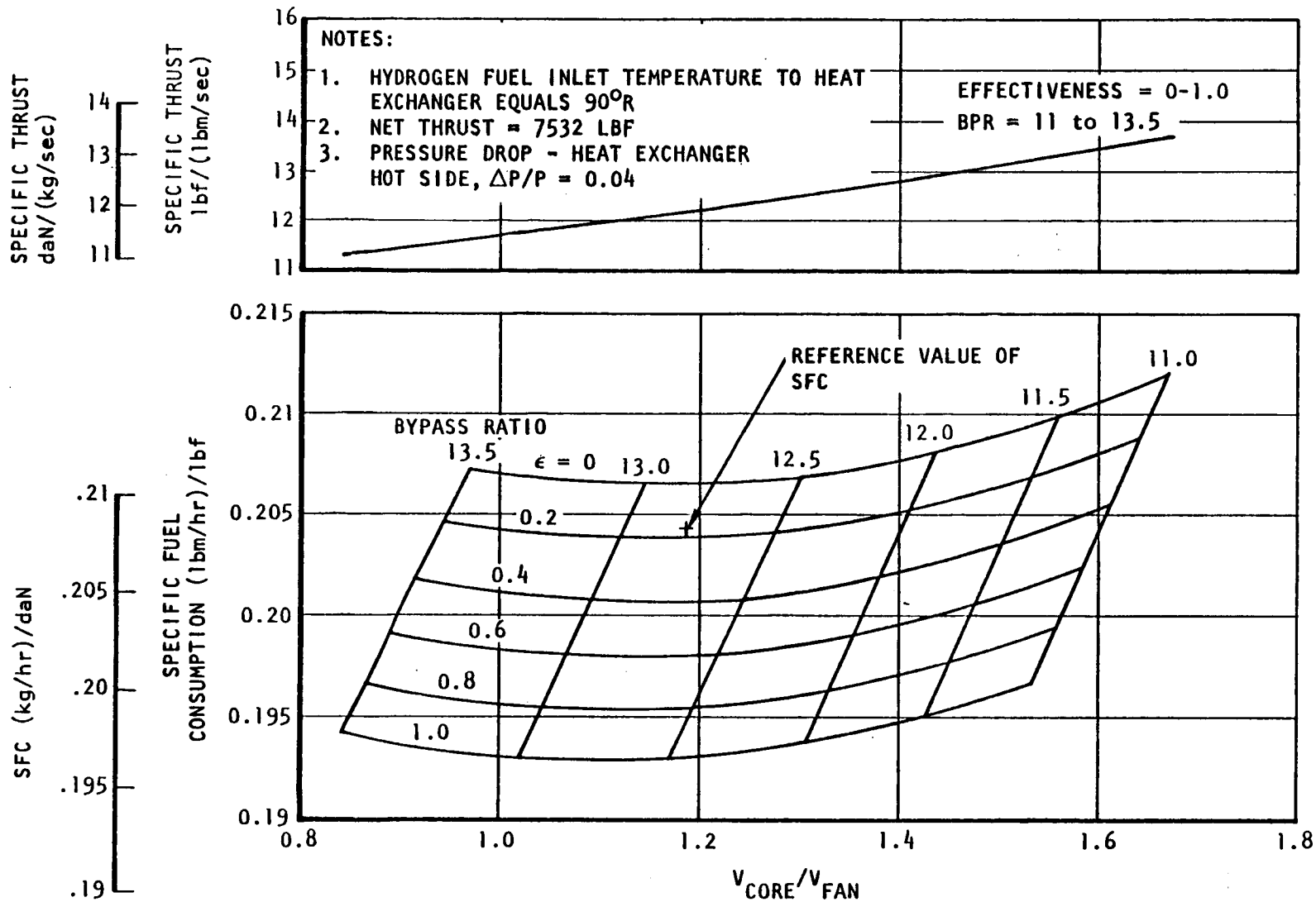

Figure 16. - Effect of exhaust heating of fuel at max. cruise (ΔP/P = 0.04).

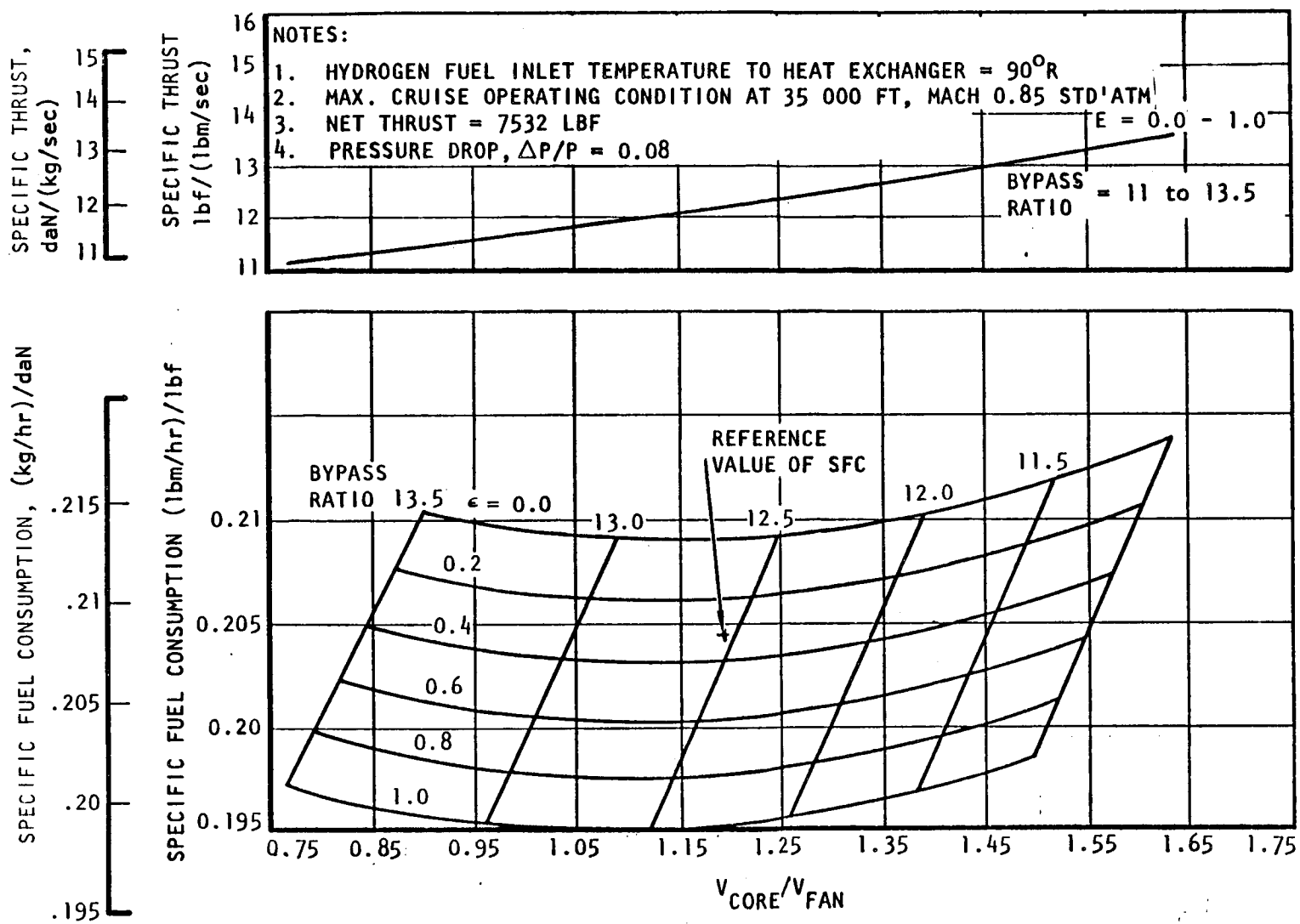

Figure 17. - Effect of exhaust heating of fuel at max. cruise (ΔP/P = 0.08).

4.1.6 H_2 expander cycle. - A study was completed to evaluate the performance improvement which might be obtained by providing aircraft accessory horsepower using a hydrogen expansion turbine rather than extracting it from the engine through a gearbox. Originally it was hoped that the expander cycle could provide some of the fan or compressor horsepower requirements. However, preliminary calculations showed that the fuel would have to be pumped to very high pressures to provide significant amounts of power relative to the requirements of the fan and compressor. For example, 2000 psi is required to obtain 580 hp, which is only five percent of the compressor horsepower. Further increases in power would require higher hydrogen pressures since the turbine flow rate which is the engine fuel flow rate, and the heat addition from the exhaust stream is constant. It is believed that the increase in engine complexity required to use the hydrogen expansion turbine to provide only a small amount of the compression horsepower requirements is unwarranted.

The emphasis shifted to the investigation of providing aircraft accessory horsepower requirements. The expander cycle is illustrated in Figure 18. This scheme consists of pumping the hydrogen fuel to a pressure level above that required for delivery to the engine, heating it in an exhaust gas heat exchanger, and expanding it through a turbine. The benefit to the cycle was

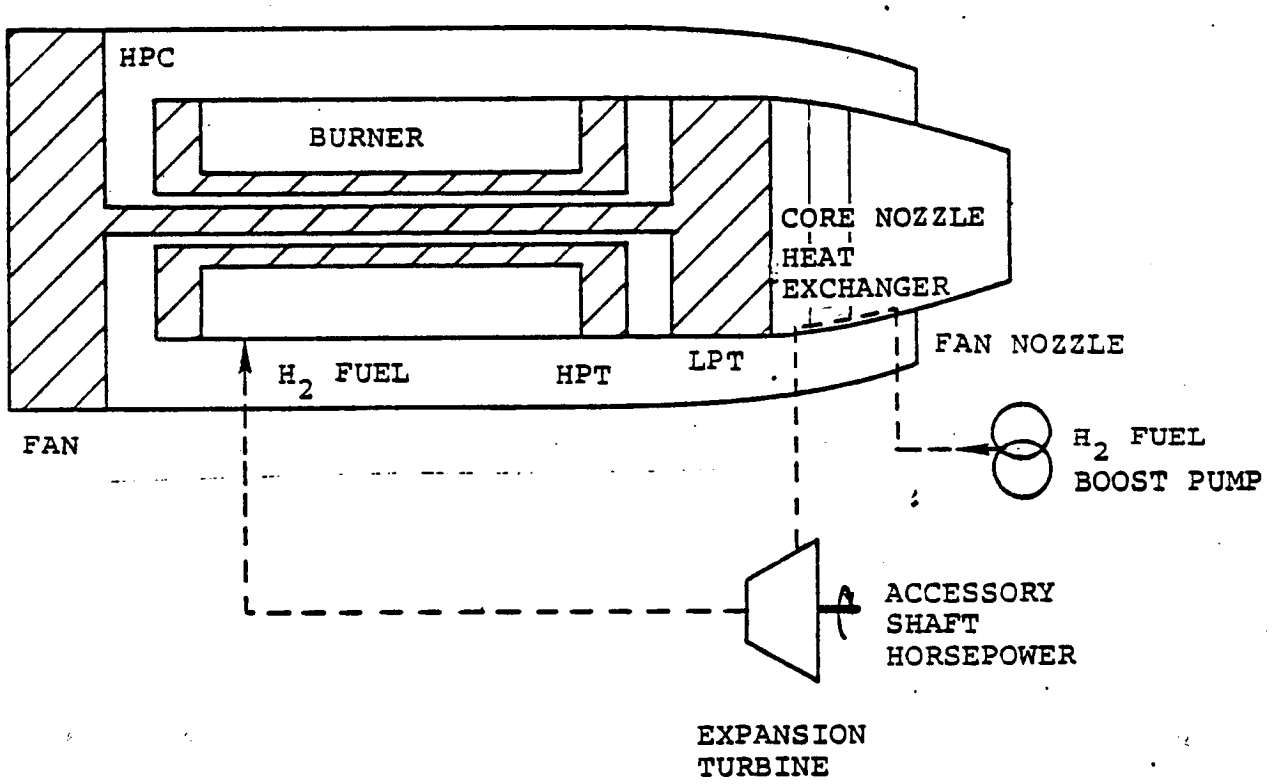

Figure 18. - Schematic of expander cycle.

expected to result from the elimination of the accessory power load and the decrease in fuel flow due to fuel heating. There would also be a decrease in engine weight associated with a smaller engine gearbox, but it was assumed that was offset by the increased weight of the fuel pump and the additional weight of the hydrogen turbine and the associated gearing.

The heat exchanger effectiveness and pressure drop ($\Delta P/P$) selected were 0.8 and 0.04 respectively. The pressure to which the fuel must be pumped to yield a net output of 125 hp for the aircraft accessories was calculated. Only the power required to pump the hydrogen to pressures above 360 psia was charged to the expander cycle.

The relationship of net horsepower available to the aircraft accessories and the hydrogen turbine inlet pressure is shown in Figure 19. The fuel pump efficiency was selected as 65 percent and hydrogen turbine efficiency including mechanical losses was assumed to be 80 percent. The fuel temperature out of the fuel pump was calculated as a function of fuel pressure rise. The hydrogen temperature into the H_2 turbine was calculated using all the engine exhaust flow and the effectiveness of 0.8. The hydrogen was expanded across the turbine to the required combustor inlet pressure of 360 psia. The H_2 temperature at the outlet of the turbine was calculated based on a 90 percent adiabatic efficiency. Engine performance was based on the fuel temperature at the turbine outlet and includes the effects of exhaust gas pressure drop and cooling in the heat exchanger. Specific fuel consumption and core jet-to-fan duct velocity ratio are shown versus bypass ratio in Figure 20. The specific fuel consumption at a core-to-fan nozzle velocity ratio of 1.19 is 0.1954 (lb/hr)/lb. The regenerator weight is 112 pounds/engine and the decrease in engine weight is 27 pounds/engine. The improvement in DOC is 2.9 percent.

4.1.7 Selection of preferred concepts. - A summary of the feasibility studies is included as Table 8. The concepts which yield the largest reduction in DOC are fuel heating and the expander cycle. The fuel heating concept was recommended for use in the study as it is less complex and provides an equal DOC benefit. As noted earlier, however, hydrogen cooling of the turbine cooling air is attractive in many respects and offers advantages if higher turbine inlet temperatures were selected. This concept is further discussed in section 4.2.3.1.

4.2 Cycle Definition and Configuration Definition

The cycle definition and configuration work was accomplished in three parts. The first part was a review of prior studies of advanced turbofan engines. The second part was selection of the initial cycle for a LH_2-fueled engine. It relied heavily on these prior studies and cycle variables were

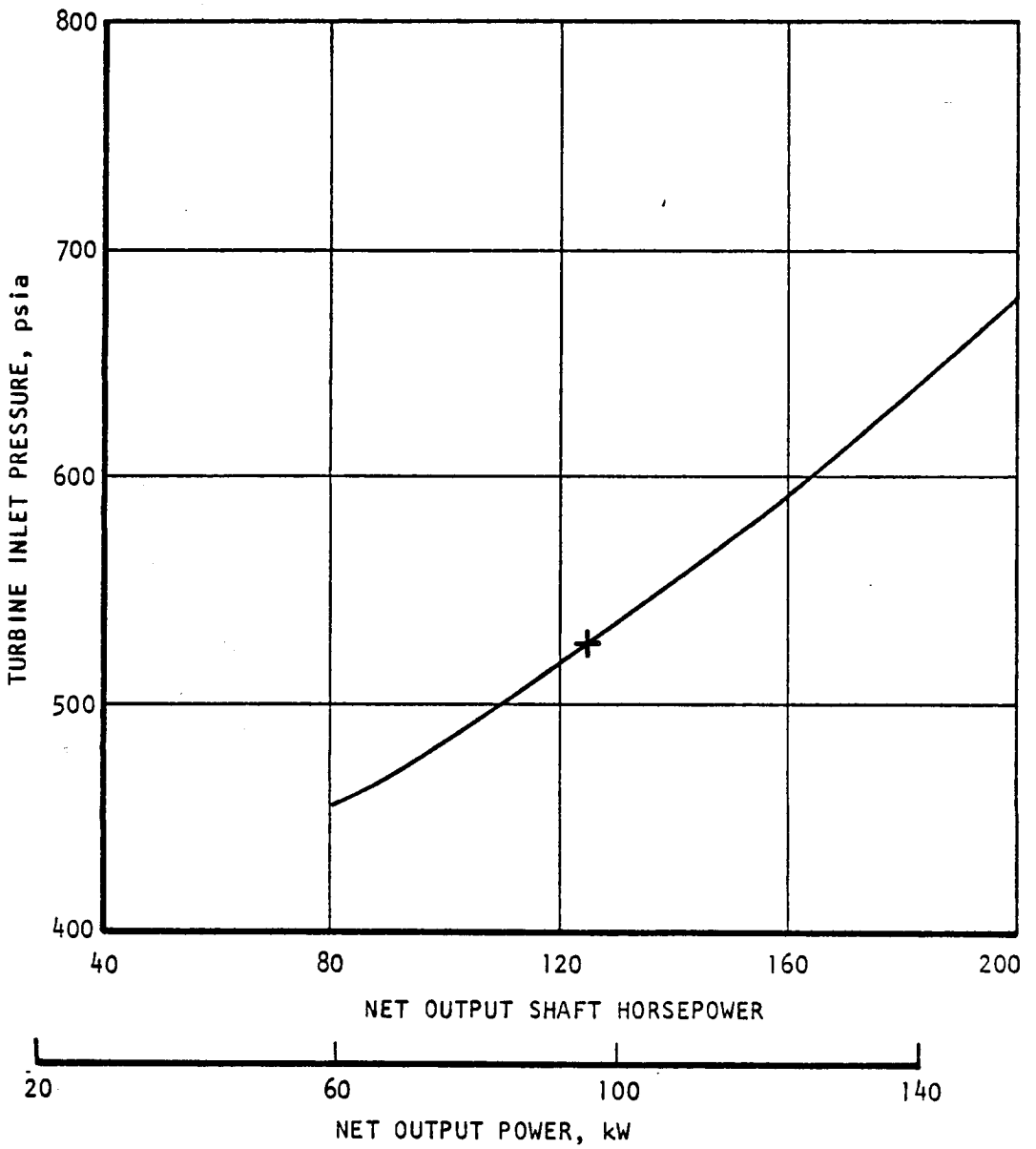

Figure 19. - Net hydrogen turbine horsepower.

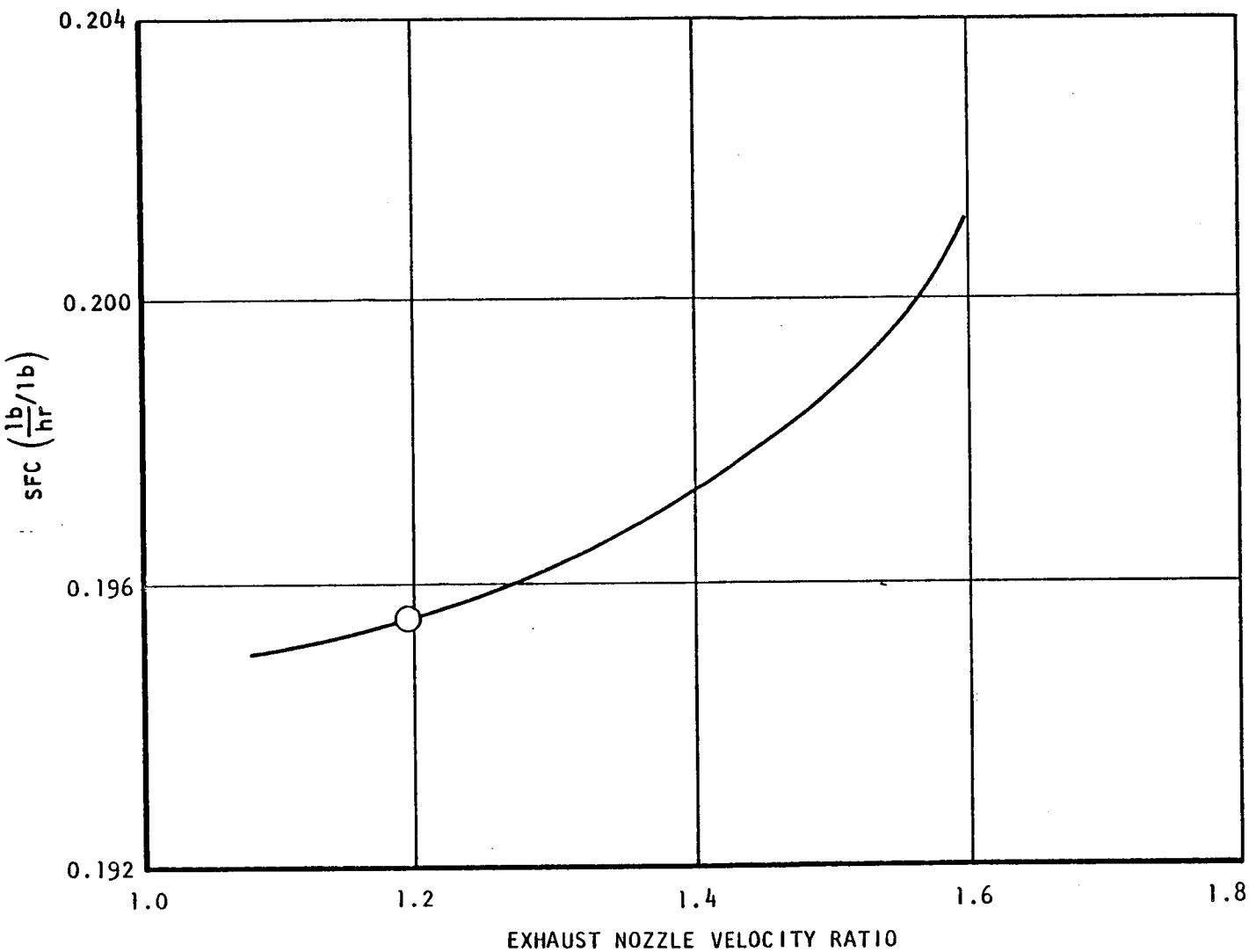

Figure 20. - Engine performance - expander cycle.

TABLE 8. - HYDROGEN EXPLOITATION SUMMARY

	ϵ_{H2}	$\frac{\Delta P}{P_{air}}$	ΔSFC %	Engine Δwt	HX Δwt	ΔDOC* %
Precooling	0.8	0.06	-1.86	-63	+ 75	-1.33
Inter cooling	0.8	0.04	-0.93	-40	+100	-0.57
Cooled turbine cooling air	0.8	N/A	-0.53	-27	+ 10	-0.41
Fuel heating	0.8	0.04	-4.31	+27	+112	-2.90
H_2 Expander cycle	0.8	0.04	-4.31	+27	+112	-2.90

$$*\Delta DOC(\%) = \frac{\frac{7.75}{10^6}(\Delta wt) + 1.332\frac{SFC}{SFC_{bl}} - 1}{DOC_{base}} \times 100$$

selected consistent with them. In the third part, a more detailed study was made of a high temperature, high pressure ratio cycle. Work completed in the second part was updated and compared to the results of the high temperature study.

4.2.1 Review of previous studies. - In a previous LH_2 transport Study (Ref. 1), Lockheed established a baseline engine cycle which is defined in Table 6. The General Electric Company and Pratt and Whitney Aircraft have studied turbofan engines designed for low fuel consumption under contract to NASA Lewis. The work is reported in References 36, 37, and 38. A brief summary of the results of the General Electric and Pratt and Whitney Studies is given in the following sections.

4.2.1.1 Turbine temperature and cycle pressure ratio: General Electric found that low-pressure turbine (LPT) cooling requirements became the overriding factor at rotor inlet temperatures greater than 2800°F. Minimum SFC occured at 2600°F for cycle pressure ratios from 32:1 to 45:1. Minimum engine weight occured at approximately 2800°F for cycle pressure ratios from 32:1 to 45:1. Minimum DOC occured between 2700 and 2750°F for cycle pressure ratios from 32:1 to 45:1. GE selected a 2600°F takeoff rotor inlet temperature and a cycle pressure ratio of 38:1.

Following similar logic, Pratt and Whitney selected a 2600°F maximum combustor outlet temperature and a cycle pressure ratio of 45:1.

4.2.1.2 Fan pressure ratio and bypass ratio: General Electric's results showed that higher fan pressure ratios (up to 1.8:1) yielded improved direct operating cost (DOC). GE selected a fan pressure ratio of 1.7:1 for initial rating with possible growth to 1.8:1. For a separate flow exhaust system, an exhaust nozzle velocity ratio of approximately 1.5 yielded minimum DOC.

Pratt and Whitney found that the lower SFC possible at low fan pressure ratio and higher bypass ratios was offset completely by increased propulsion system weight. Nacelle drag drives high bypass ratio engines to more compact, high fan pressure ratio levels. A fan pressure ratio of 1.7:1 and a bypass ratio of 8.0:1 was selected.

4.2.1.3 Engine configuration: The General Electric Energy Efficient Engine is comprised of a single stage fan driven by a 4-1/2 stage low pressure turbine; a three stage low pressure ratio compressor providing a pressure ratio of 1.7 driven by the LPT; a nine stage high pressure compressor providing a pressure ratio of approximately 14:1 driven by a single stage cooled axial turbine; a double-annular combustor; and a mixed flow exhaust system.

The selected P&W engine consists of a high-speed, single-stage 1.7 pressure ratio fan, a three-stage low pressure compressor with a pressure ratio of 1.53, and a two-stage, 18.2:1 pressure ratio high-pressure compressor. A low emission, two-stage vortex combustor with aerating pilot nozzles is included to provide a 2600°F maximum average combustor exit temperature. The compression system is powered by a two-stage, cooled high-pressure turbine and a five-stage low-pressure turine. The exhaust system consists of a fan nozzle and a core nozzle.

4.2.2 Initial LH_2 engine cycle selection. - The initial LH_2 engine cycle selection proceeded on the basis that a rotor inlet temperature of 2600° to 2800°F was optimum. The assumption was based on findings that show temperatures above this level require cooling for the low pressure turbine vanes and blades. Cooling the low pressure turbine results in significant performance penalties and is expensive. This assumption was tested later in the study through the investigation of a 3200°F engine that used hydrogen to cool the turbine cooling air and thereby minimize the performance penalty. The results of this investigation are covered in a subsequent section.

4.2.2.1 Baseline engine description: The baseline engine chosen for the initial cycle selection study is a two spool, separately exhausted turbofan consisting of the following components:

- Single stage fan
- Two-stage low-pressure compressor (booster stages)

- Ten-stage high-pressure compressor
- Annular combustor
- Axial cooled HP turbine (single stage)
- Axial uncooled fan turbine (4-6 stages)
- Exhaust regenerator (for fuel heating)
- Separate fan and core convergent exhaust nozzles

The cycle characteristics of the baseline engine were selected to approximate the cycle used in the feasibility studies discussed in 4.1. Additional intercomponent pressure drops, cooling flows and leakage were added, however. A definition of the baseline cycle for the cycle selection studies is provided in Table 9. Also shown in Table 9 are three other cycles which provide a summary of how the cycle was changed from the initial Lockheed cycle to the baseline cycle derived for the cycle selection studies. The cycle labeled 4 is the baseline cycle used in the hydrogen exploitation feasibility, studies and is quite close to the original Lockheed cycle (see 4.1.1). Cycle number 3 resulted when the exhaust regenerator was added for fuel heating. A 4.3 percent improvement in specific fuel consumption resulted when the exhaust regenerator was added.

There was some optimism in cycle 3, however, and cycle number 2 incorporated the following changes:

- HP turbine efficiency was reduced 1 point to 0.90 to allow for losses due to cooling.
- LP turbine efficiency was reduced 3 points to 0.88 as a result of turbine preliminary design.
- 21 horsepower allowed for bearing losses, etc., and to drive engine accessories.
- Fan duct and intercompressor pressure drops were modified.
- 3.5 percent turbine cooling air was added.

The net effect of these changes was to increase specific fuel consumption 7.8 percent with respect to the cycle number 3.

The baseline cycle for cycle selection studies resulted from flow path and component analysis. The core compressor ratio of 25.17 postulated for cycles 2, 3, 4 was considered too high. Extensive variable geometry (all stages) would be required and the turbine work levels for a single stage high

TABLE 9. - BASELINE ENGINE CYCLE, INITIAL CYCLE SELECTION

	1 Baseline	2 Adjusted Cycle	3 Exhaust Heating Study	4 Baseline Feasibility Studies
FAN				
Inlet Corrected Flow, lb/sec	1507	1453	1362	1364
Pressure Ratio	1.6	1.6	1.634	1.634
Adiabatic Efficiency	0.892	0.892	0.889	0.889
Bypass Ratio	12.0:1	12.0:1	12.5:1	13.0:1
LP Compressor (Booster)				
Pressure Ratio	1.3	-	-	-
Adiabatic Efficiency	0.865	-	-	-
HP Compressor				
Pressure Ratio	19.5	25.17	25.17	25.17
Adiabatic Efficiency	0.862	0.862	0.862	0.862
Combustor				
Efficiency	1.0	1.0	1.0	1.0
Pressure Drop, $\Delta P/P$	0.045	0.045	0.045	0.045
Hp Turbine				
Rotor Inlet Total Temperature ^{o}F	2514	2514	2514	2514
Adiabatic Efficiency	0.90	0.90	0.91	0.91
Horsepower Extraction	125	125	125	125
LP Turbine				
Inlet Total Temperature, ^{o}F	1758	1738	1787	1793
Adiabatic Efficiency	0.88	0.88	0.91	0.91
Horsepower Extraction	21	21	0	0
Exhaust Regenerator				
Effectiveness	0.8	0.8	0.8	-
Gas Side Pressure Drop ($\Delta P/P$)	0.04	0.04	0.04	-
Core Nozzle Thrust Coefficient	0.988	0.988	0.995	0.995
Fan Nozzle Thrust Coefficient	0.98	0.98	0.995	0.995
Fan Duct Pressure Loss, $\Delta P/P$	0.015	0.015	0.03	0.03
LPC-HPC Pressure Loss $\Delta P/P$	0.015	0.015	0	0
LPT-Nozzle Pressure Loss, $\Delta P/P$	0.005	0.005	0.005	0.005
Aircraft Bleed Extraction, Percent	4.1	4.1	4.1	4.1
Turbine Cooling Air, Percent	3.5	3.5	0	0
Leakage, Percent	1.0	0	0	0
Net Thrust, lb	6674	6649	6674	6674
Specific Fuel Consumption, (lb/hr)/lb	0.2141	0.2106	0.1954	0.2042
Net Thrust, lb (Includes Nacelle Drag)	6000	6000	6000	6000
SFC, (lb/hr)/lb (Includes Nacelle Drag)	0.2381	0.2333	0.2174	0.2272

pressure turbine were considered excessive. To maintain cycle pressure ratio at 40:1 with a lower core pressure ratio, booster stages were added to the fan spool. Provisions for seal leakage (1 percent) were also incorporated. This resulted in a 1.7 percent increase in specific fuel consumption with respect to cycle number 2.

With respect to the cycle defined by Lockheed in the previous study, specific fuel consumption was higher by 7.7 percent, including the effect of the exhaust regenerator.

The flight condition chosen for the cycle selection studies was initial cruise of 35 000 feet, M = 0.85, maximum climb power. The studies were made on the basis of installed performance and included the effects of cowl drag but not inlet spillage drag.

The selection criteria for all investigations was minimum DOC. DOC was evaluated using the equation given in 4.1.1.

4.2.2.2 Selection of rotor inlet temperature and cycle pressure ratio: As stated earlier, turbine inlet temperature was limited to a restricted range (2600-2800°F). The G.E. Energy Efficient Engine study showed minimum DOC occurring between 2700-2750°F. A maximum rotor inlet temperature of 2700°F was selected on the basis of the prior studies.

Cycle pressure ratio was selected primarily on the basis of utilizing a single stage high pressure turbine. Although extensive tradeoff studies could be made addressing single and two stage HP turbines, AiResearch experience has shown that a single stage turbine minimizes turbine cooling required and that minimizing the number of cooled stages results in lower engine cost.

The actual maximum turbine work level is based on tip speed, flow path, cooling and stresses, but for cycle selection a value of 210 Btu/lb at the temperature selected is a reasonable maximum. Likewise, the maximum core compressor ratio is rightfully the subject of a detailed study but for this program, the selection of a 20:1 maximum core pressure ratio is reasonable and avoids consideration of mismatch and stability problems.

Shown in Figure 21 is the relationship of high pressure turbine work, fan pressure ratio and high pressure compressor pressure ratio. A maximum turbine inlet temperature of 2700°F and a booster pressure ratio of 1.30:1 was assumed. Within the constraints of 210 Btu/lb turbine work and core compressor ratio, an overall pressure ratio of 45:1 is reached only with high fan pressure ratios. At an overall pressure ratio of 40:1, fan pressure ratio can be approximately 1.55 to 2.0:1. Furthermore, a cycle pressure ratio of 40:1 achieves most of the benefit of high cycle pressure ratio. Based on these considerations, cycle pressure ratio was selected at 40:1.

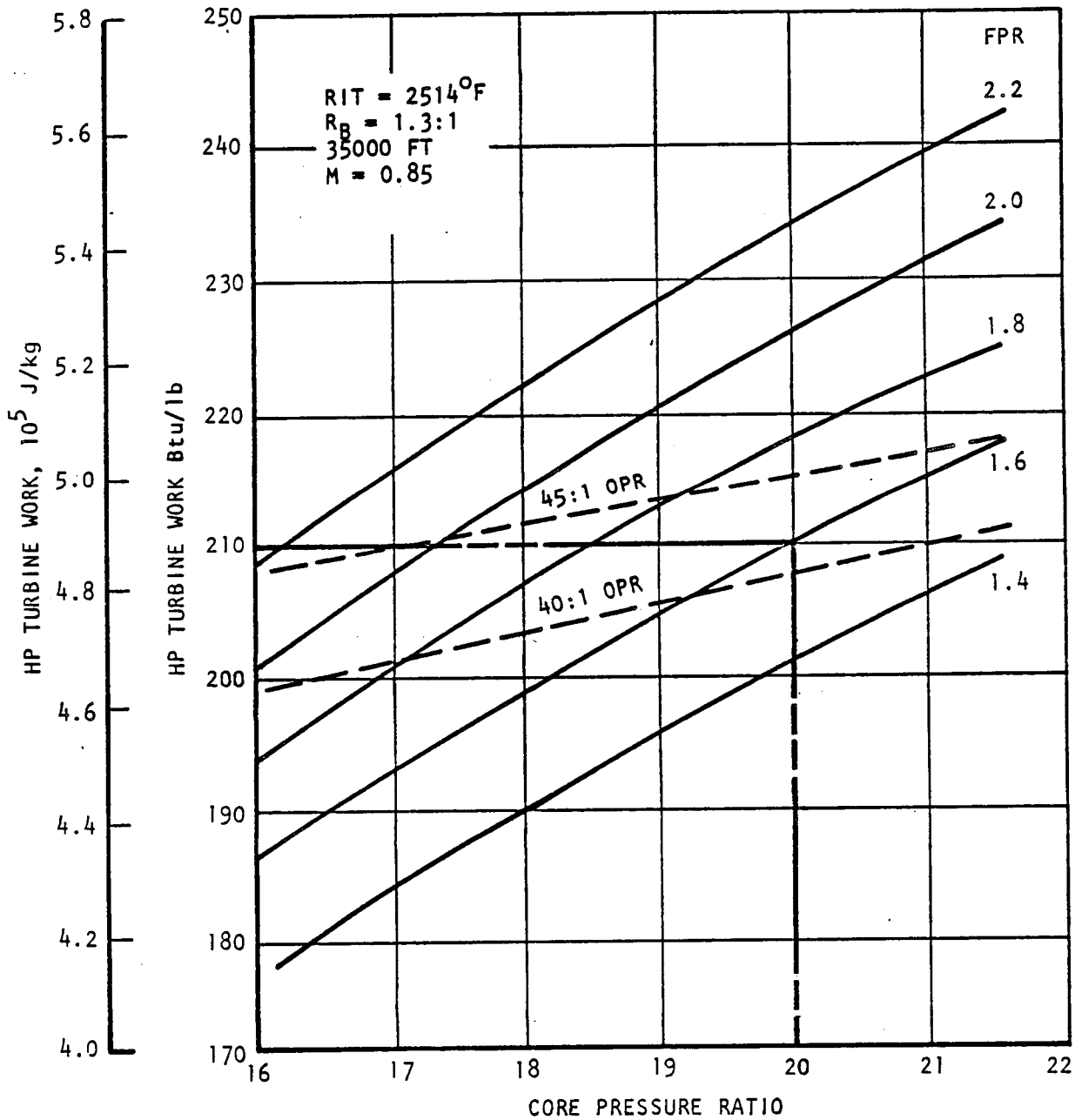

Figure 21. - Selection of cycle overall pressure ratio.

4.2.2.3 Fan pressure ratio and bypass ratio selection: Fan pressure ratios from 1.4 to 2.2 were studied. The turbine inlet temperature of 2700°F maximum (2514°F cruise) and the maximum cruise cycle pressure ratio of 40:1 were held constant in this portion of the study. Primary stream energy extraction was varied by considering a range of bypass ratios.

Fan pressure ratio was selected on the basis of minimum DOC which includes the effects of specific fuel consumption and engine weight. Maintenance was not included.

The baseline engine is as described in 4.2.2.1. Figure 22 shows specific fuel consumption versus exhaust nozzle velocity ratio for the range of fan pressure ratios considered. Figure 23 shows bypass ratio versus fan pressure ratio and exhaust nozzle velocity ratio. Figure 24 shows estimated engine relative weight versus fan pressure ratio and bypass ratio.

The trends in DOC are shown in Figure 25. Each fan pressure ratio has a minimum DOC. The curve of minimum DOC and fan pressure ratio is shown in Figure 26. Based on this curve, the fan pressure ratio for minimum DOC is 1.7:1. The related bypass ratio is 9.3:1 as shown in Figure 27.

4.2.3 High temperature investigation. - As the results of the hydrogen exploitation studies and the initial cycle selection work became available, it was apparent that some benefit might accrue to a high temperature cycle which used hydrogen to cool the cooling air and thereby minimize the cooling penalty for both the high and low pressure turbines. In order to take full advantage of the higher turbine inlet temperatures, higher cycle pressure ratios are required and a two stage high pressure turbine becomes necessary. At a fan pressure ratio of 1.6, for example, high pressure compressor pressure ratio would be between 21.5:1 and 26:1 at cycle pressure ratios between 50:1 and 60:1 respectively. Attaining these pressure ratios in a reasonable number of stages and avoiding mismatch and stability problems is quite a formidable task without even considering weight, complexity and cost penalties.

The introduction of a two stage high pressure turbine and a cooled fan turbine required a more detailed turbine cooling flow analysis.

Turbine inlet temperature was held constant at 3200°F. This temperature was arbitrarily selected but is representative of the maximum turbine inlet temperature feasible in the study time period. Cycle pressure ratios of 40, 50, and 60 were investigated. Fan pressure ratio was also varied although it was believed that changes from the fan pressure ratio selected in the earlier investigation would be second order.

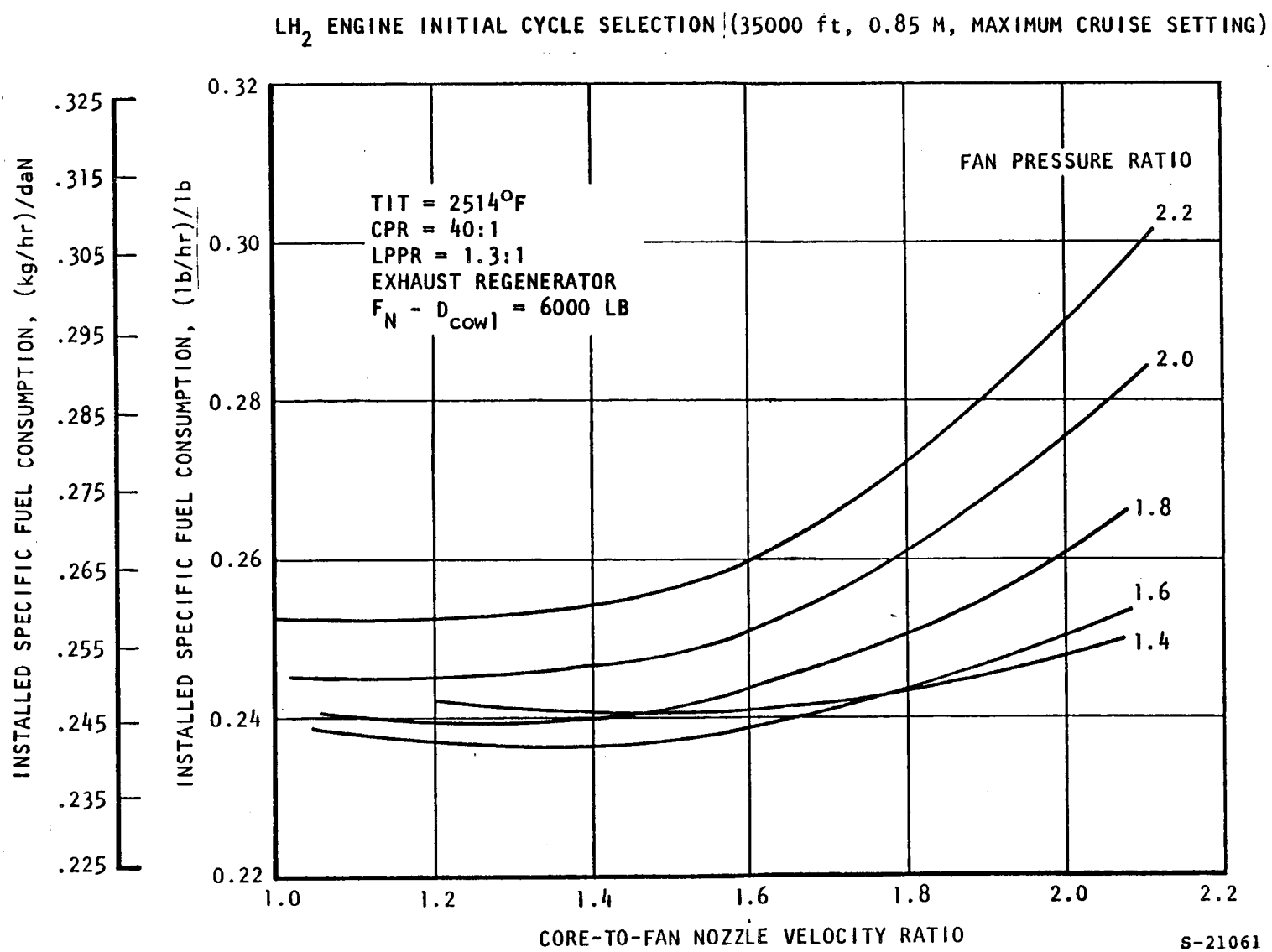

Figure 22. - Effect of fan pressure ratio and nozzle velocity ratio on engine performance.

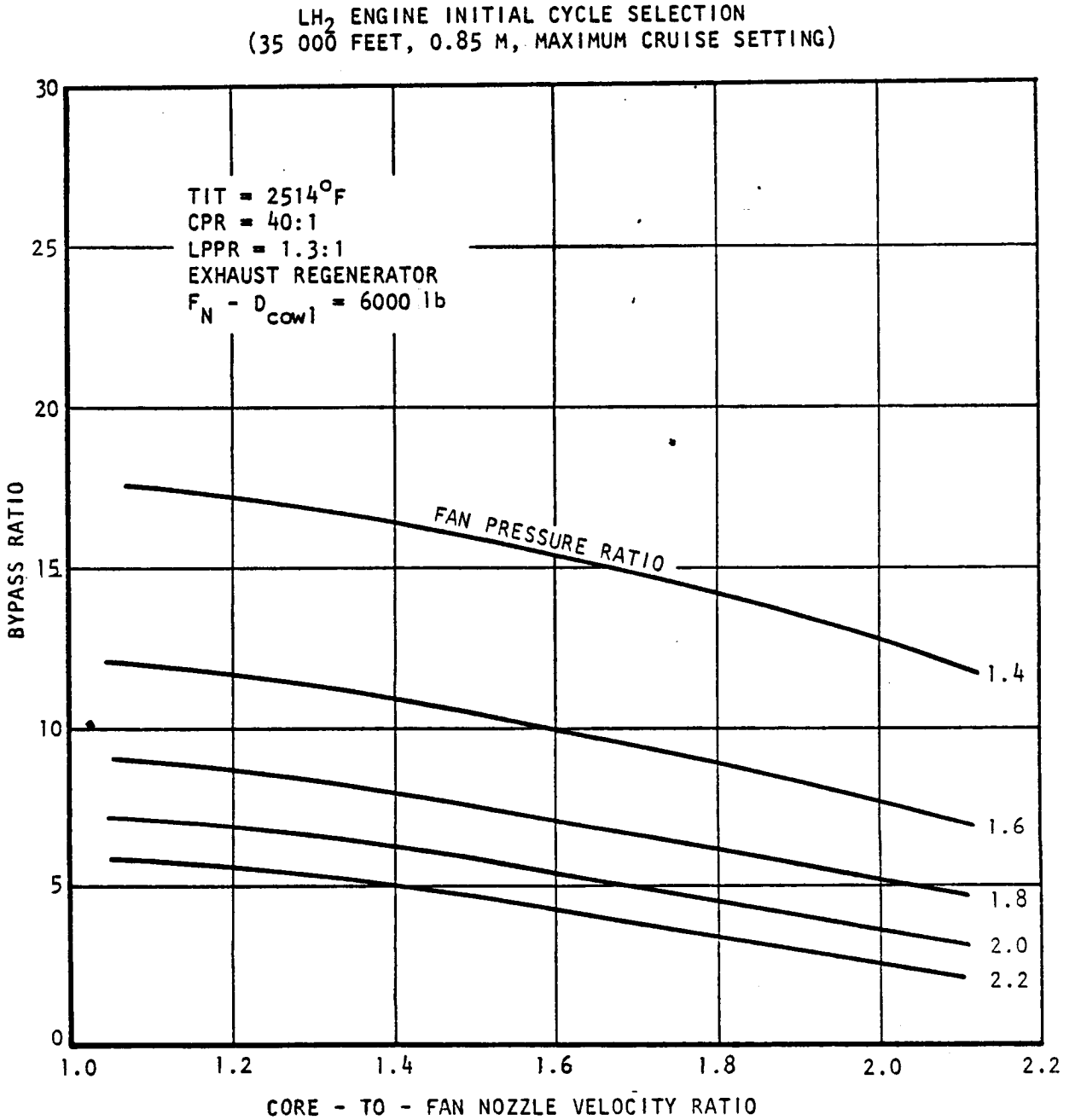

Figure 23. - Effect of fan pressure ratio and nozzle velocity ratio on bypass ratio

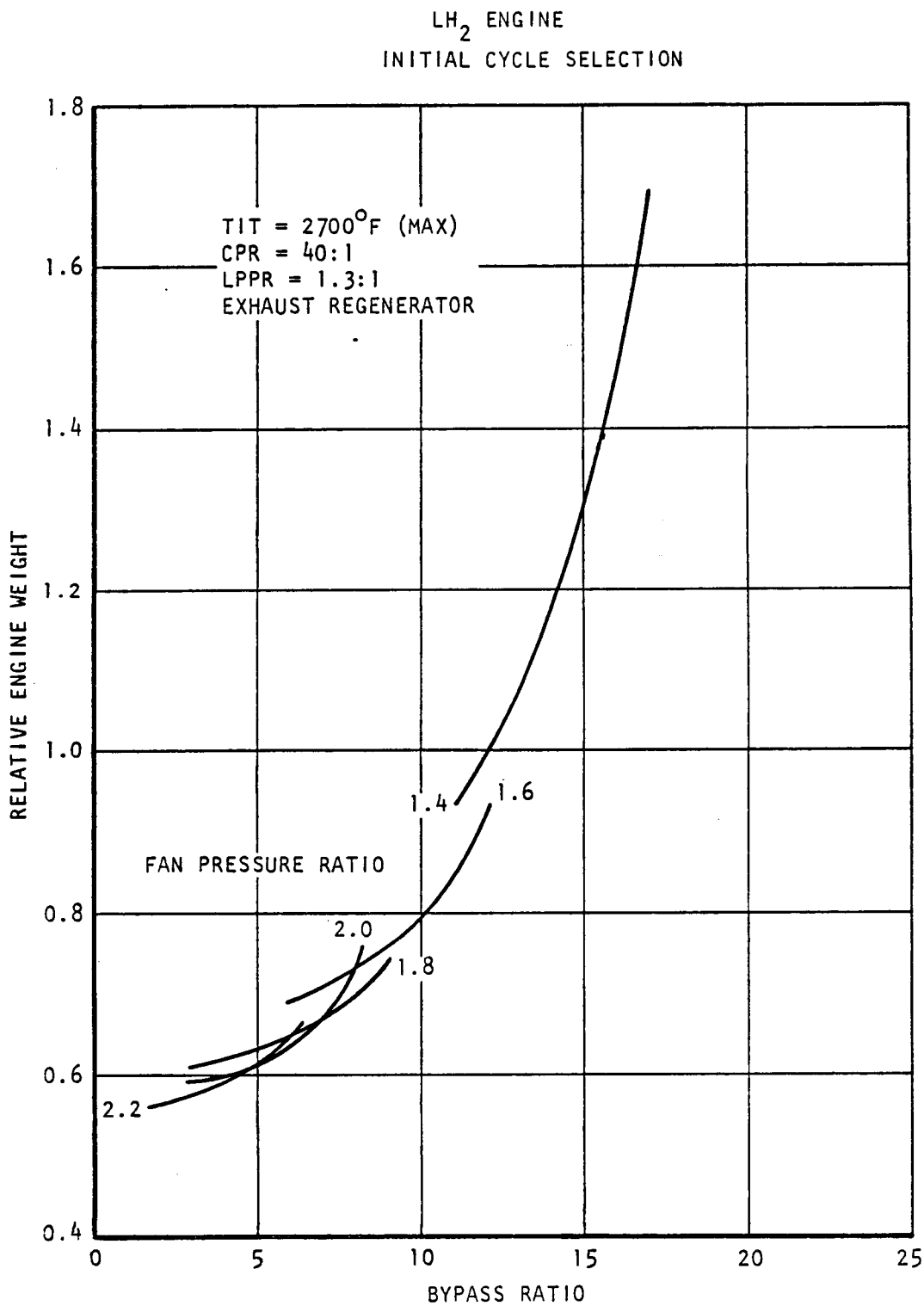

Figure 24. - Effect of fan pressure ratio and bypass ratio on engine weight.

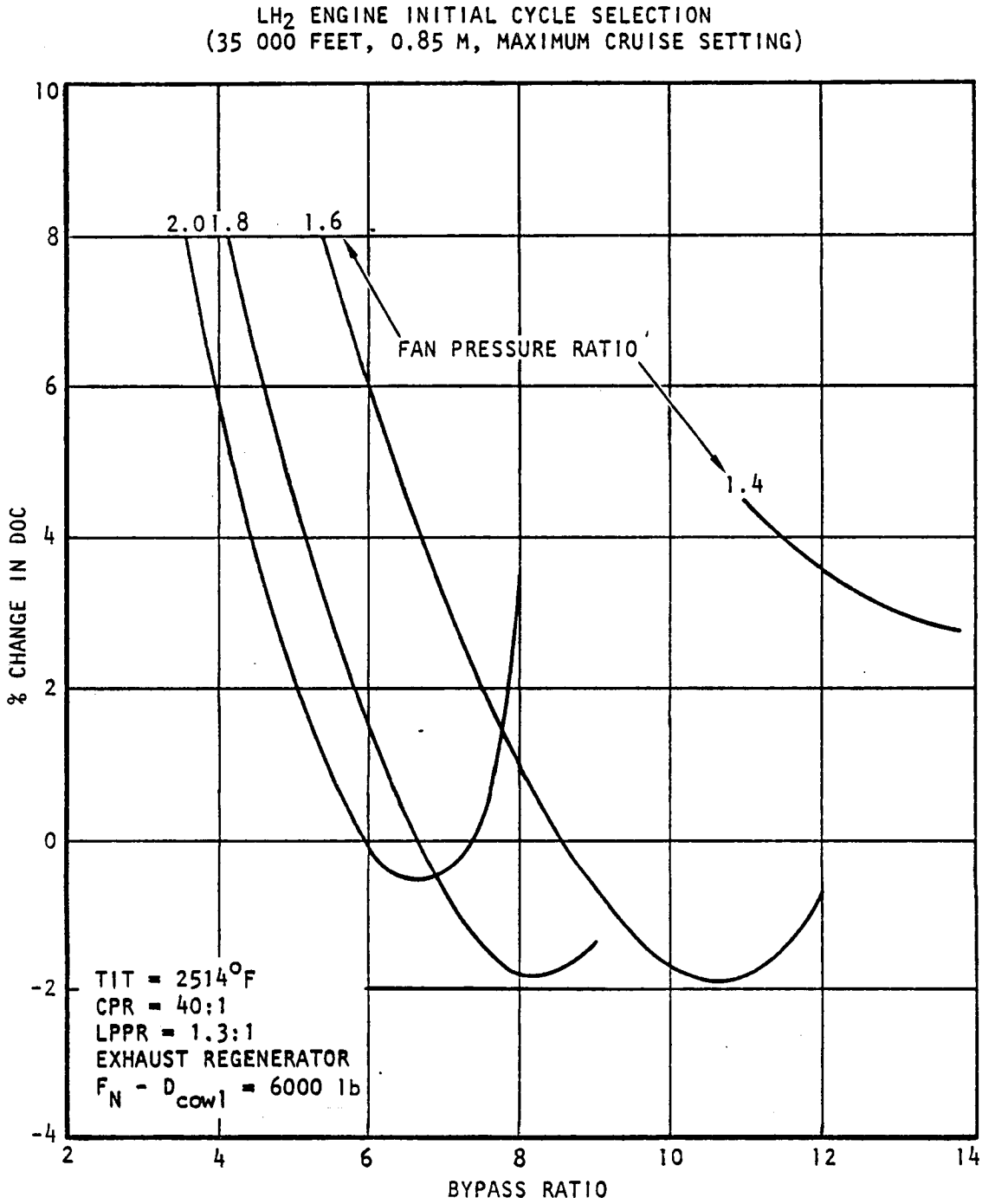

Figure 25. - Effect of fan pressure ratio and bypass ratio on direct operating cost.

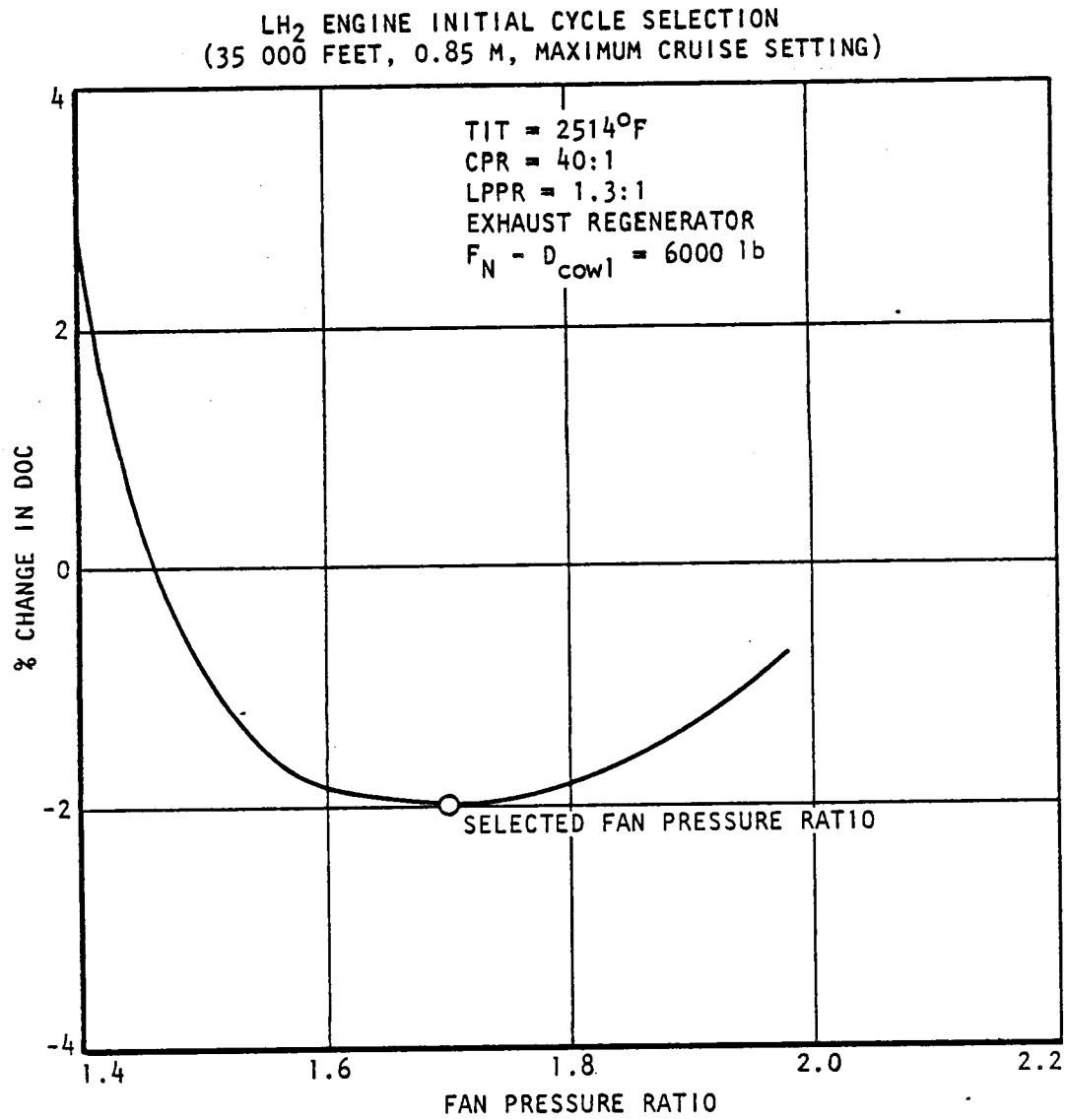

Figure 26. - Effect of fan pressure ratio on direct operating cost.

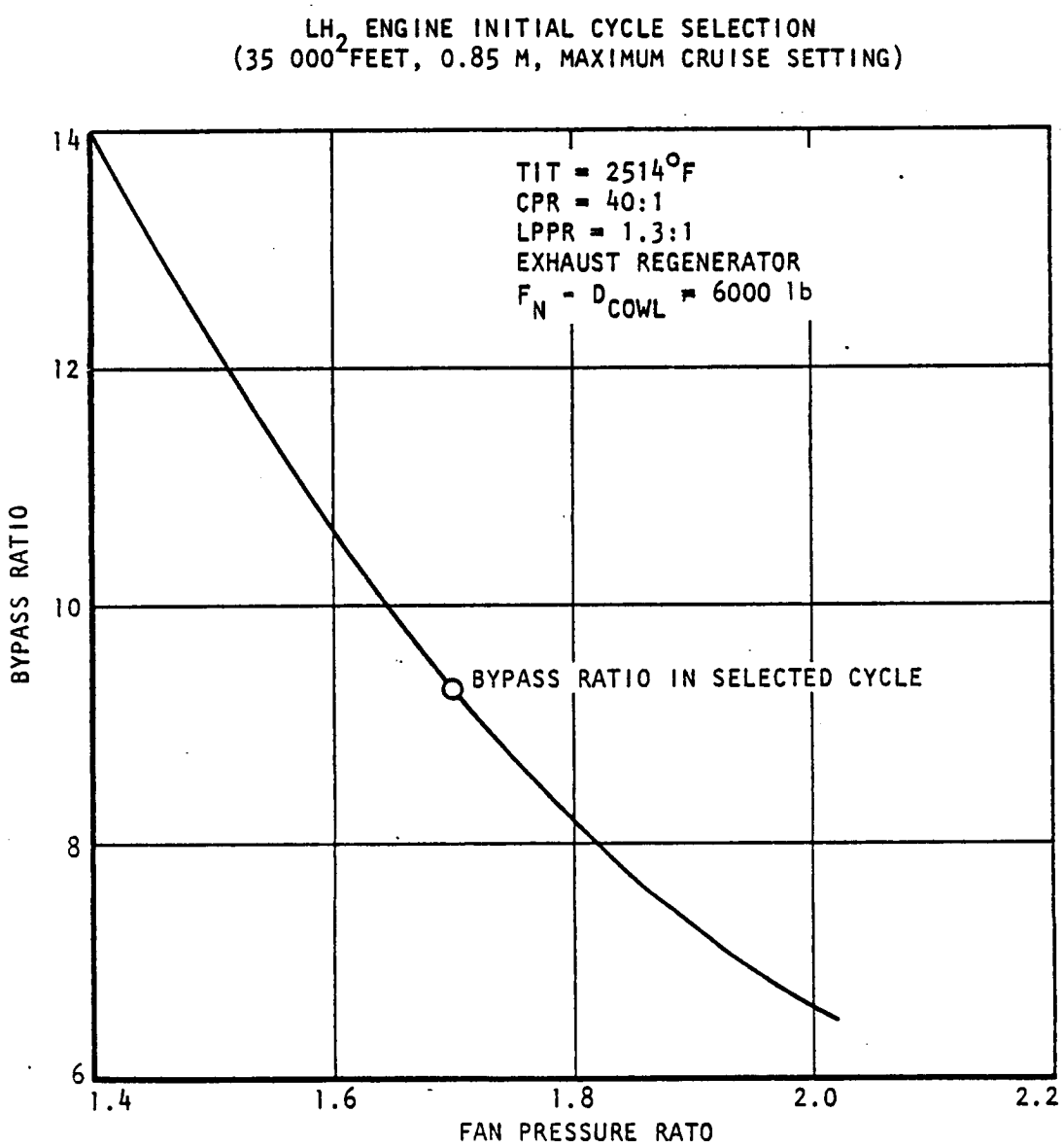

Figure 27. - Related bypass ratio.

The flight condition, installation factors, and other related assumptions were identical to those assumed earlier. The baseline engine is identical to that described in 3.2.2.1.

Cooling flow requirements were defined at maximum power, hot day, sea level. An engine having a fan pressure ratio of 1.7:1 and a bypass ratio of 9.3:1 was assumed in computing the cooling flow requirements. A schematic representation of the hydrogen cooling of the turbine cooling air was shown previously in Figure 10.

4.2.3.1 Turbine cooling requirements:

4.2.3.1.1 Engine operating conditions: Turbine cooling requirements were established for hot day, sea level, maximum power conditions. Cycle temperatures are related to temperatures at the cruise conditions using ratios established in prior studies. The temperatures that are important are compressor discharge temperature, combustor outlet temperature, high pressure rotor inlet temperature, and low pressure turbine inlet temperature. These locations are shown schematically in Figure 28. The temperatures used in this study are shown in Table 10.

Temperatures at turbine stations other than those listed in Table 10 were calculated based on equal temperature drop across each turbine stage. For example, if the ΔT across the low pressure turbine is 1000° and there are four stages, the temperature drop across each stage is assumed to be 250°. The temperatures between each blade or vane row are based on the mass averaged temperatures of the gas stream and the cooling flows. Also, combustor outlet temperature is that required to provide the rated rotor inlet temperature after mixing of the first high pressure turbine vane cooling air.

TABLE 10. - INTERNAL CYCLE TEMPERATURES ($^{\circ}$R) (SEA LEVEL, HOT DAY, TAKEOFF THRUST).

	Cycle Pressure Ratio		
Station	40:1	50:1	60:1
Compressor Discharge T_3	1546	1648	1742
Combustor Outlet $T_{3.9}$	3756	3756	3756
HP Rotor Inlet T_4	3660	3660	3660
LP Turbine Inlet $T_{4.2}$	2910	2838	2766

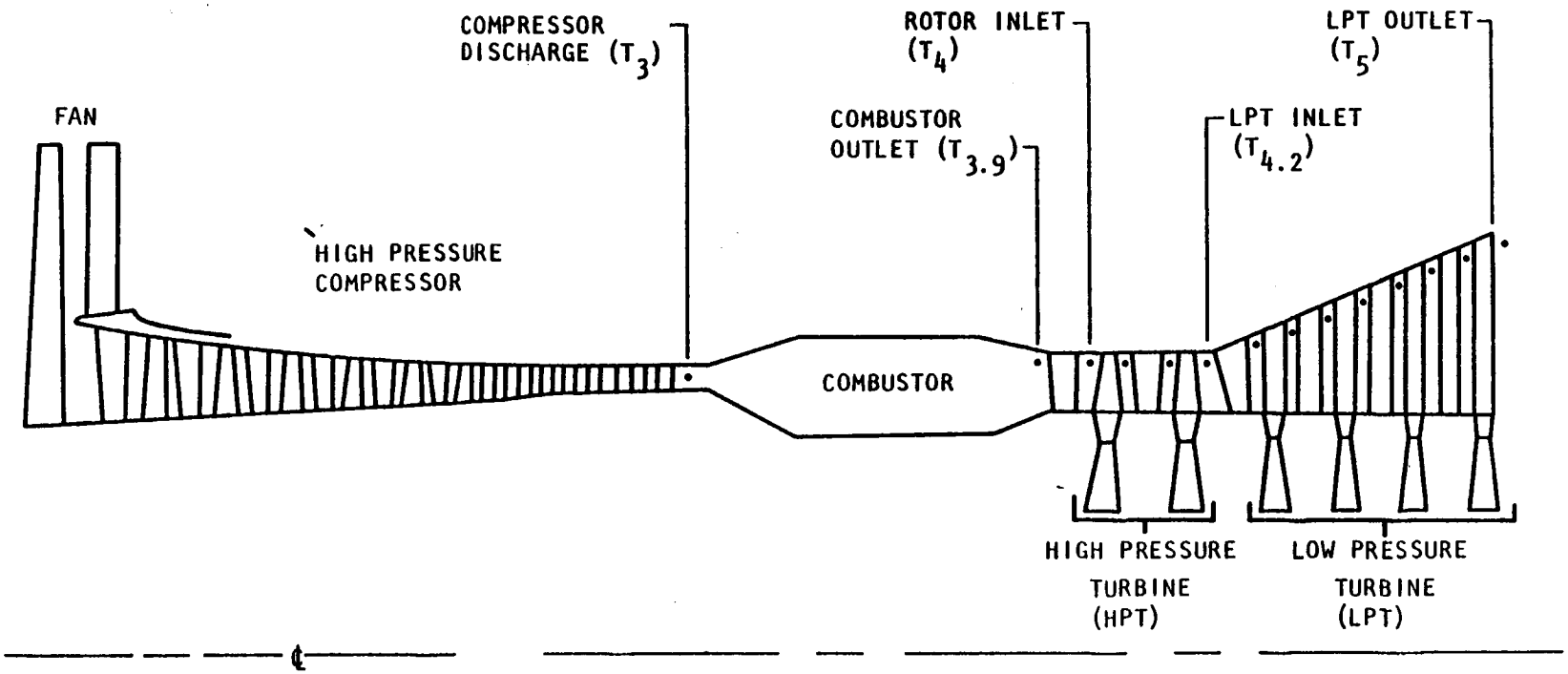

Figure 28. - Engine station designations.

4.2.3.1.2 Turbine cooling air heat exchanger: The turbine cooling air heat exchanger is similar to those used in prior work which has been discussed earlier. At first, it was assumed that the heat exchanger had an effectiveness of 0.8. Further study indicated that the resulting cooling air outlet temperature was approximately 380°R. Heat exchanger freezing would be a problem at this temperature and cooling air outlet temperature was limited to 560°R to avoid this problem. A bypass arrangement or a lower effectiveness heat exchanger is required. (Refer to heat exchanger design, Section 4.3.6.)

4.2.3.1.3 Turbine design criteria: Minimum design criteria were established to allow the determination of turbine cooling requirements. The criteria established included the following:

- Allowable metal temperatures
- Combustor pattern factor
- Blade and vane heat transfer effectiveness
- Blade relative gas temperature
- Turbine work limits
- Turbine cooling efficiency penalties

AiResearch is conducting extensive company-sponsored and Government-funded programs to develop turbine materials and processes for high temperature applications. The allowable metal temperatures assumed for this study are shown in Table 11 and are based on the results and projections of these programs and are applicable to long-life transport engines.

TABLE 11. - ALLOWABLE METAL TEMPERATURE LIMITS

	Temperature Limit
High Pressure Turbine Vanes	2200°F
High Pressure Turbine Blades	2000°F
Low Pressure Turbine Vanes	2100°F
Low Pressure Turbine Blades	2000°F

The combustor pattern factor $(T_{3.9max} - T_{3.9avg})/T_{3.9avg} - T_3)$ determines the peak temperature that the turbine vanes feel. Blades are not influenced by the pattern factor as their rotation tends to average the temperatures to which they are exposed. The combustor pattern factor persists throughout the turbine, although it is attenuated and tends to shift both radially and circumferentially. Hydrogen-fueled engines will have lower pattern factors than Jet A fueled engines. However, the inherent lower pattern factor can be traded to some extent for smaller combustor volumes. The pattern factors assumed for the study are shown in Table 12.

Blade and vane cooling requirements were calculated on the basis of simple effectiveness correlations, a simplified approach. To establish cooling flows precisely requires consideration of a number of factors not included in the simple effectiveness correlations and is beyond the scope of this study. Two levels of effectiveness versus cooling flow were used. One, used for the higher pressure turbine, reflects a sophisticated, high effectiveness, high cost approach. The second is a lower effectiveness, lower cost approach which was used for the low pressure turbine.

The temperature environment of the rotating blade is a function of the stage work, mean blade speed and the gas temperature. For this study, it was assumed that the temperature felt by the blade was 90 percent of the gas temperature for high pressure turbine blades and 93 percent of the gas temperature for the low pressure turbine.

An analysis of the turbine work required to drive the high pressure compressor in the 40:1, 50:1 and 60:1 cycle pressure ratio engines indicated that the 40:1 engine required a single-stage turbine and the 50:1 and 60:1 cycles required two-stage high pressure turbines.

TABLE 12. - LH_2 COMBUSTOR PATTERN FACTORS.

Turbine Vane	Pattern Factor
First High Pressure Vane	0.15
Second High Pressure Vane	0.15
First Low Pressure Vane	0.125
Second Low Pressure Vane	0.10

Turbine cooling flow leaving the turbine blades or vanes disrupts the flow field and causes losses. These losses are small when trailing edge discharge is feasible. However, to achieve the high effectiveness cooling schemes required, film cooling is required and efficiency penalties are incurred. Baseline turbine efficiencies were, therefore, adjusted to reflect the type of cooling air discharge and the quantity of cooling air.

4.2.3.1.4 Turbine cooling flow quantities: Turbine cooling flow requirements are shown in Table 13 for the three pressure ratios being investigated. As just stated, a single-stage high pressure turbine is satisfactory for the 40:1 pressure ratio cycle, but a two-stage high pressure turbine is required for the 50:1 and 60:1 pressure ratio cycles.

The flow requirements are separated into cooled chargeable, uncooled chargeable, and, in the case of the high pressure turbine, nonchargeable cooling air. Cooled chargeable air is cooling flow that is cooled by hydrogen and which bypasses one or more work producing stages of the turbines. It therefore reduces horsepower produced by the turbine. Uncooled chargeable air is cooling flow that is not cooled by the hydrogen and which bypasses one or more work producing stages. Nonchargeable air is the air used to cool the first high-pressure vane. First high-pressure vane cooling air does not bypass any work producing stage and, therefore, does not diminish horsepower produced by the turbine. First vane cooling air does have an

TABLE 13. - TURBINE COOLING AIR FLOW REQUIREMENTS (%)
1760° (3200°F) ROTOR INLET TEMPERATURE.

Cycle Pressure Ratio	HP Turbine*			LP Turbine*	
	Cooled Chargeable	Uncooled Chargeable	Nonchargeable (1st Vane	Cooled Chargeable	Uncooled Chargeable
40:1 (1 STG HPT)	3.0	1.8	3.0	5.0	2.4
50:1 (2 STG HPT)	6.2	2.3	3.0	4.1	2.4
60:1 (2 STG HPT)	5.0**	2.3	3.0	2.7	2.4

*Cooling flow includes blades, vanes, shroud, discs and leakage

**Note that cooling flow requirements are lower for the 60:1 pressure ratio design due to the lower inlet temperature at the second stage of the high pressure turbine and at the inlet of the low pressure turbine. These lower temperatures result from the greater work extraction at higher pressure ratios.

effect on the temperature of the gas entering the first turbine rotor. However, all cycle calculations are based on the mixed temperature at the first rotor inlet. Therefore, the gas temperature at the first vane inlet (combustor outlet) is higher than the temperature at the first rotor inlet. The amount of cooling flow to the vane is only important in determining the temperature environment of the vane and the efficiency of the turbine. High vane cooling can effect the efficiency of the turbine as discussed earlier. To minimize the amount of vane cooling and the efficiency penalty, hydrogen cooling of the vane cooling air is utilized. Cooling air for the second high pressure turbine vane and the low pressure turbine vane is chargeable as it bypasses one or more work producing stages.

As described in Paragraph 4.1.4, disc cooling air is not cooled by the hydrogen.

4.2.3.1.5 Thermodynamic accountability of turbine cooling air: Turbine cooling air results in two penalties to the cycle. The first is a reduction in turbine efficiency due to disturbing the blade and vane flow fields. This has been covered in earlier discussion. The penalty assessed was 0.2 points in efficiency for every percent cooling air used. The second penalty results from bypassing one or more work producing stages of the turbine. In the thermodynamic model of the engine, flow to any of the blade or vane rows, other than the first vane, is assumed to completely bypass the high pressure turbine. This is also true for all air going to the low pressure turbine. This approach simplifies the model considerably but results in a more severe penalty than is actually incurred. For example, vane cooling to the second vane of the HPT bypasses only one stage of the HPT. To account for this, the actual cooling air to any cascade row was reduced by the ratio of the number of work producing stages it bypasses and the total number of stages in the turbine. This is a simplification which is considered satisfactory for this investigation.

4.2.3.2 Cycle selection: The cooling flows listed in Table 13 were used in the cycle selection studies for the high temperature investigation. Rotor inlet temperature was held constant at 3200°F and cycle pressure ratio, fan pressure ratio and bypass ratio were varied. Booster pressure ratio was held constant at 1.45:1. All engine cycles were evaluated at 35000 feet, Mach 0.85. Engine thrust minus cowl drag was held constant at 6000 pounds. The exhaust regenerator was included in the cycle. Figures 29 through 34 show the results of the investigation for the range of cycle pressure ratios and fan pressure ratios investigated. The weight and performance data shown in Figures 29 through 34 were used to determine ΔDOC relative to the baseline. Trends of DOC versus fan pressure ratio and bypass ratio are shown in Figures 35, 36, and 37 for the three selected values of cycle pressure ratio. The minimum DOC at each fan pressure ratio and cycle pressure ratio is shown in Figure 38. Figure 38 also shows the bypass ratios as a function of fan pressure ratio and cycle pressure ratio.

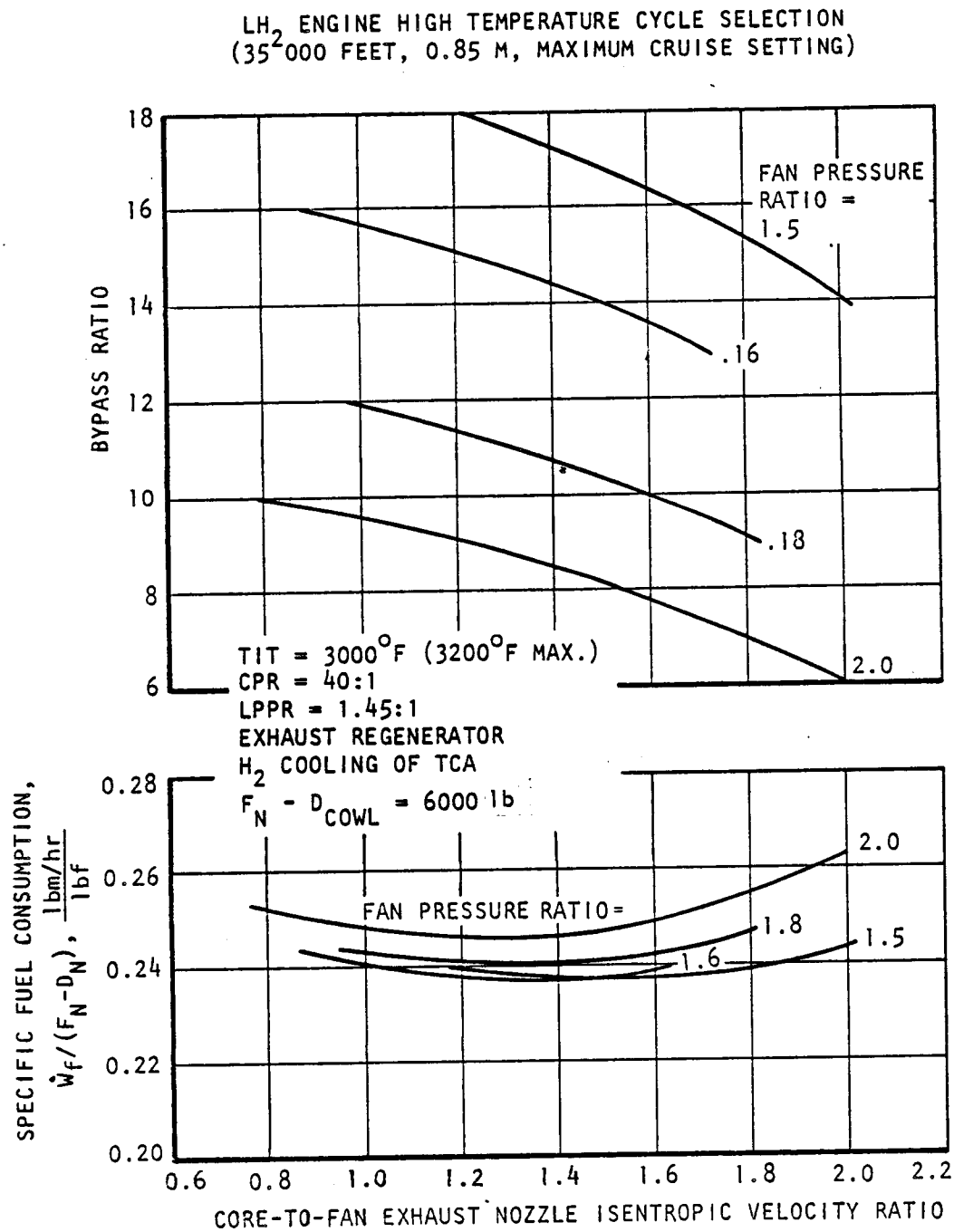

Figure 29. - Effect of core energy extraction and fan pressure ratio on SFC and bypass ratio (CPR = 40)

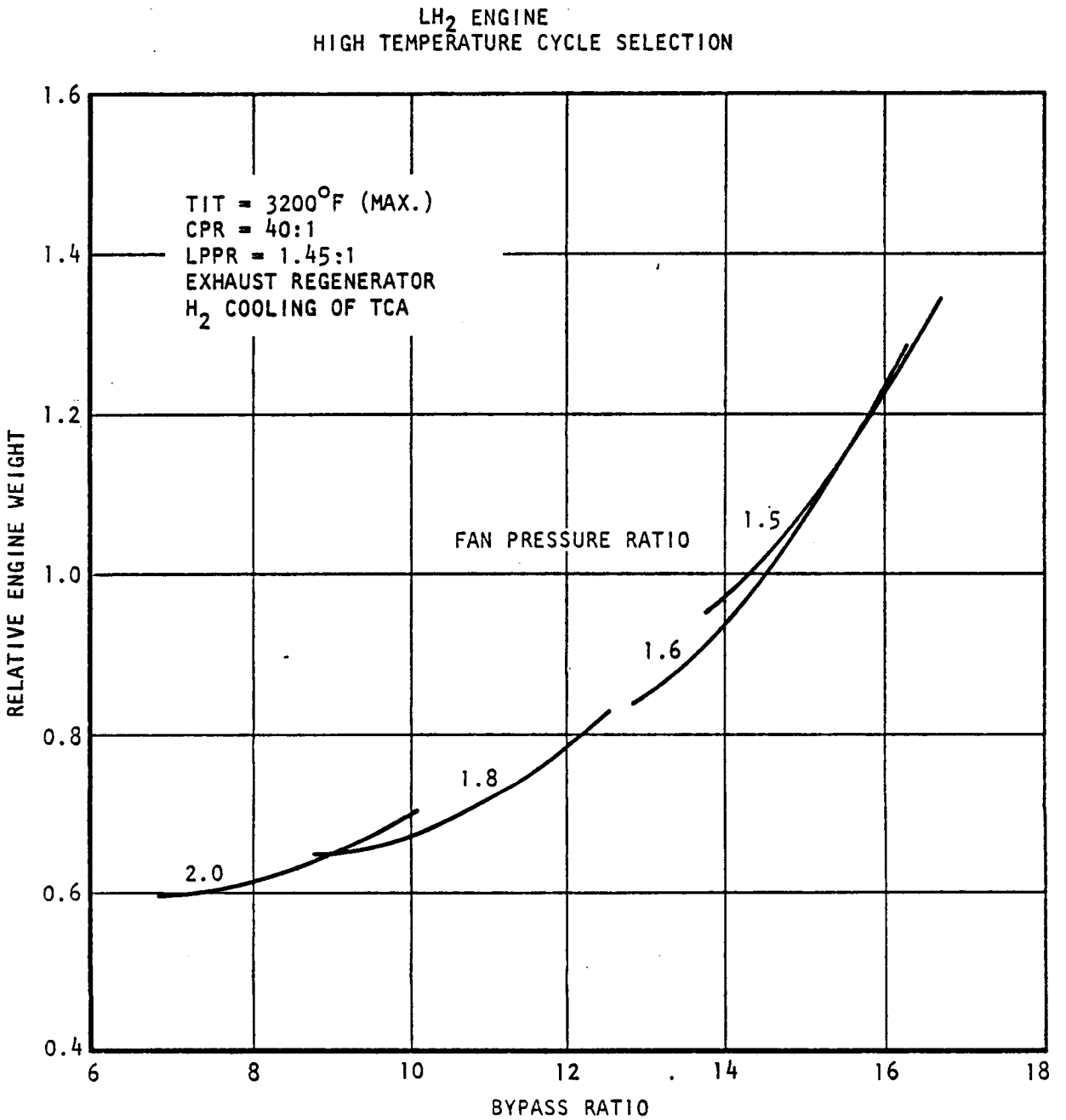

Figure 30. - Effect of fan pressure ratio and bypass ratio on engine weight (CPR = 40).

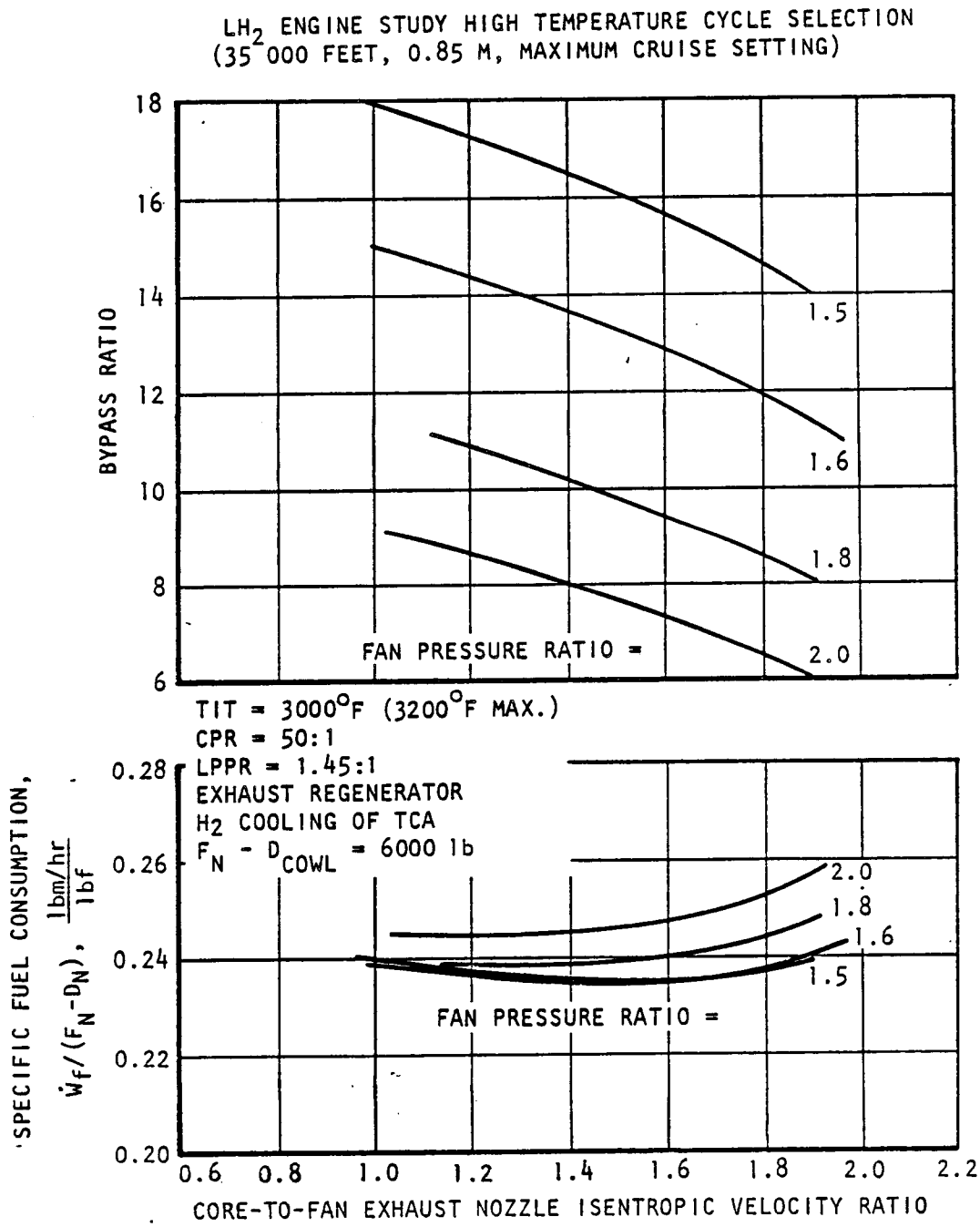

Figure 31. - Effect of core energy extraction and fan pressure ratio on SFC and BPR (CPR = 50).

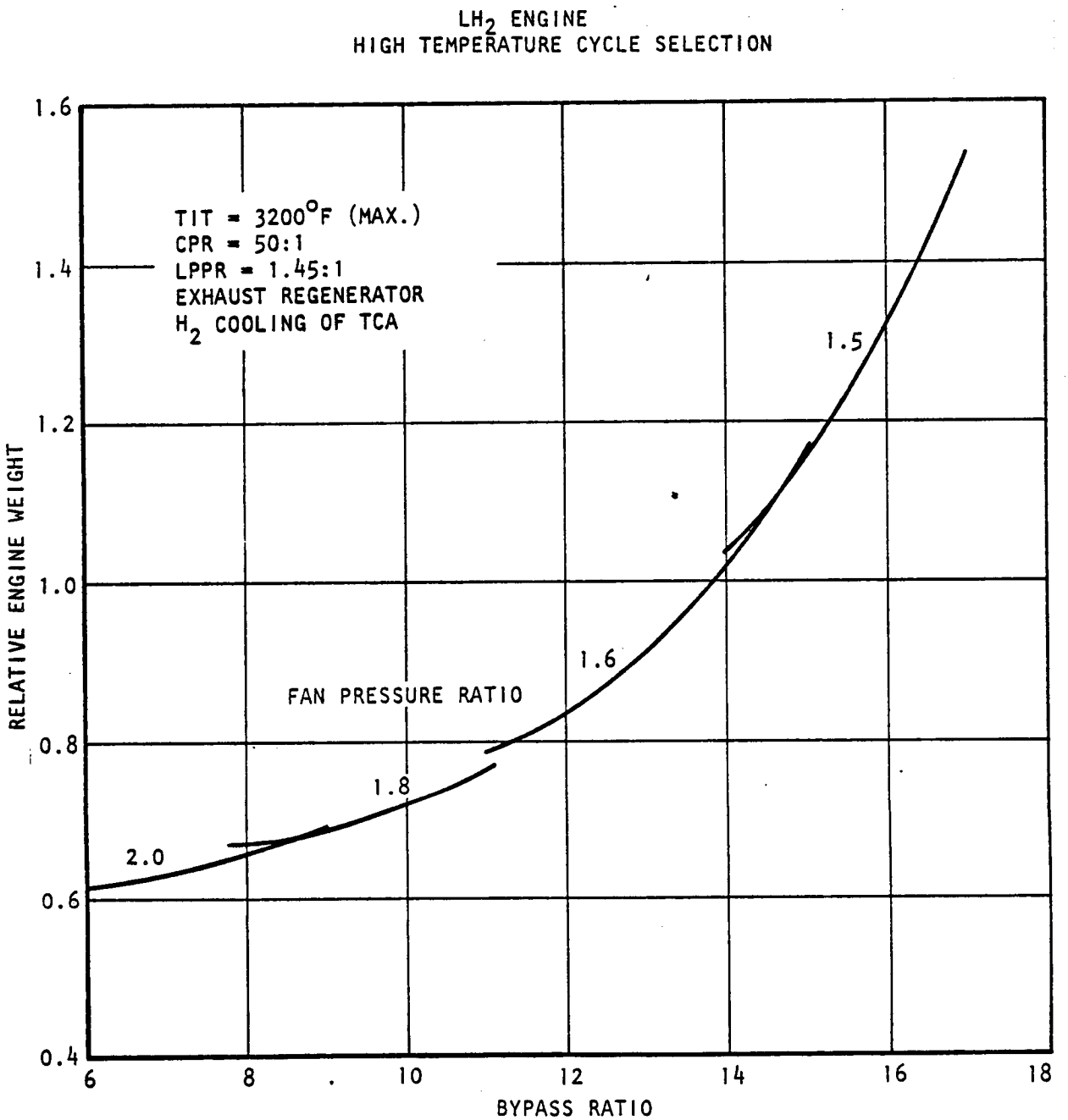

Figure 32. - Effect of fan pressure ratio and bypass ratio on engine weight (CPR = 50)

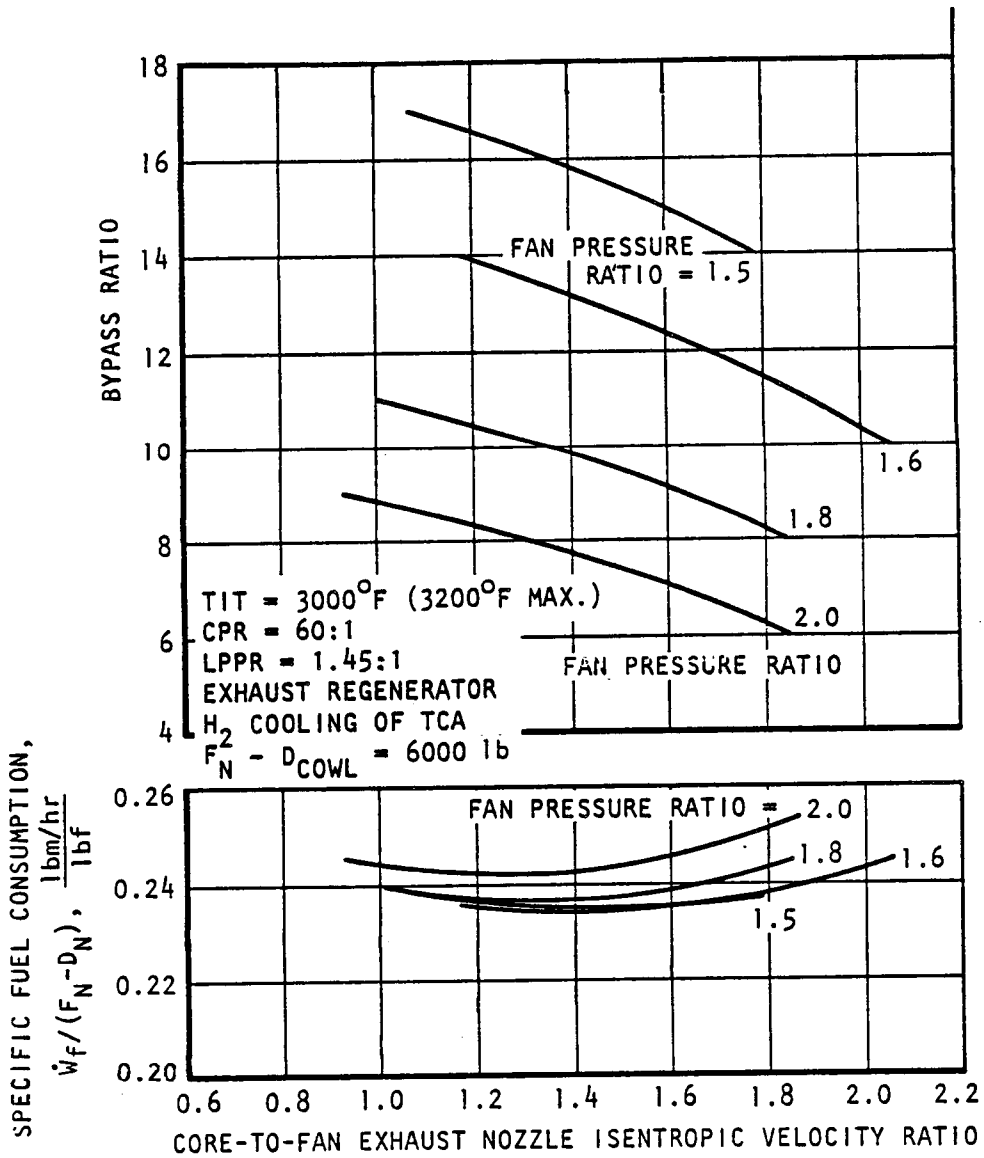

Figure 33. - Effect of core energy extraction and fan pressure ratio on SFC and BPR (CPR = 60)

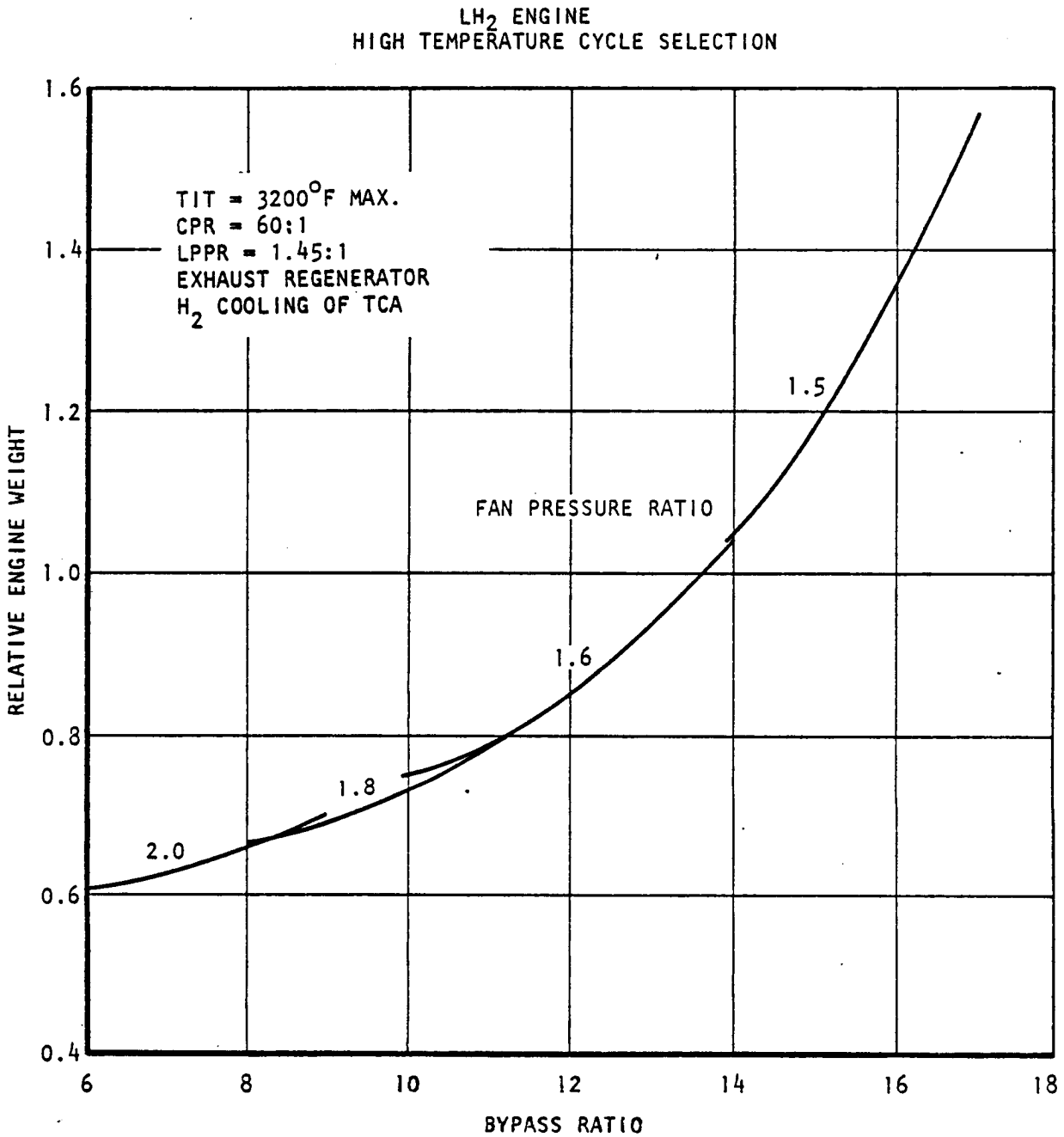

Figure 34. - Effect of fan pressure ratio and bypass ratio on engine weight (CPR = 60)

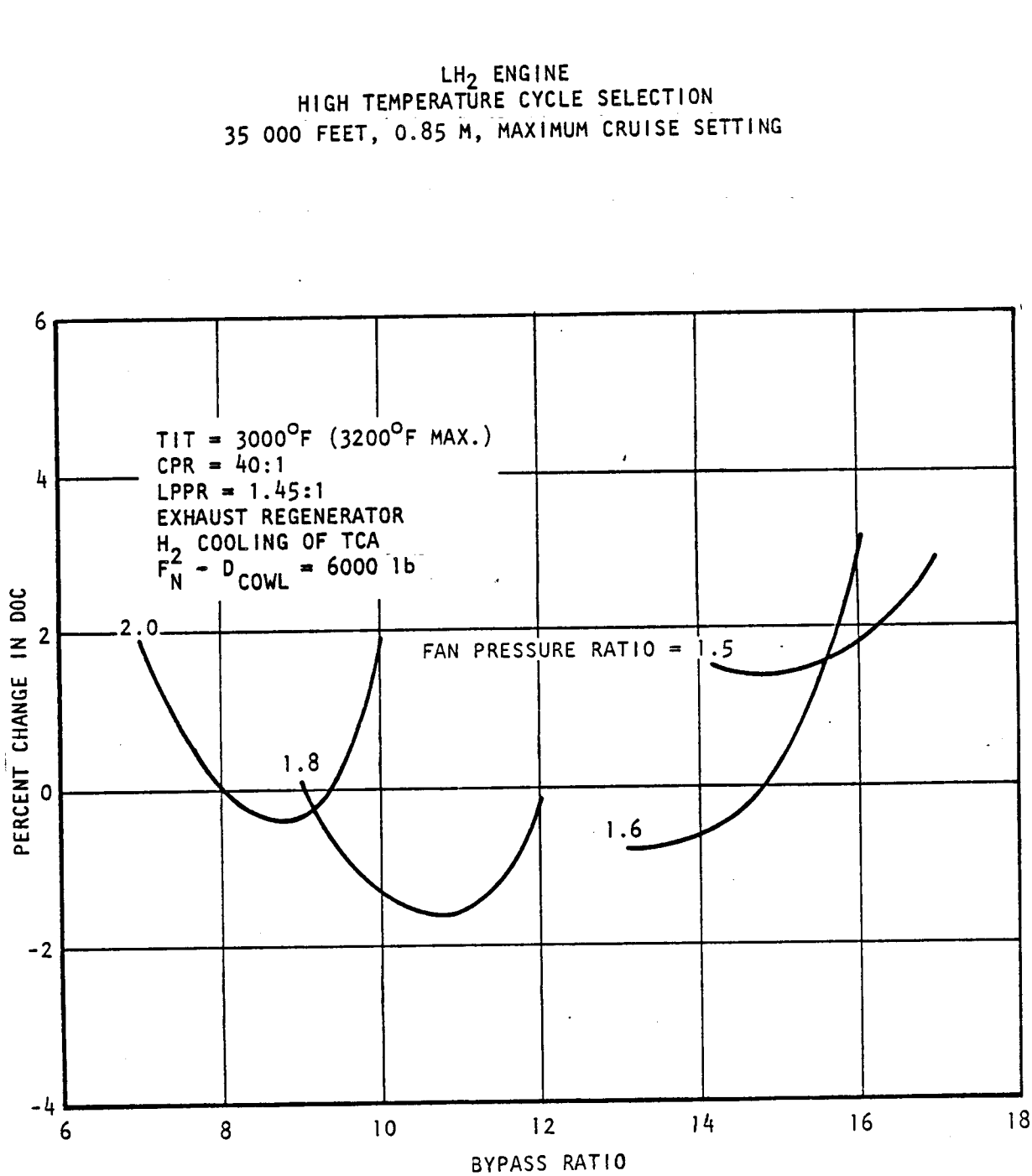

Figure 35. - Effect of bypass ratio and FPR on DOC for CPR = 40.

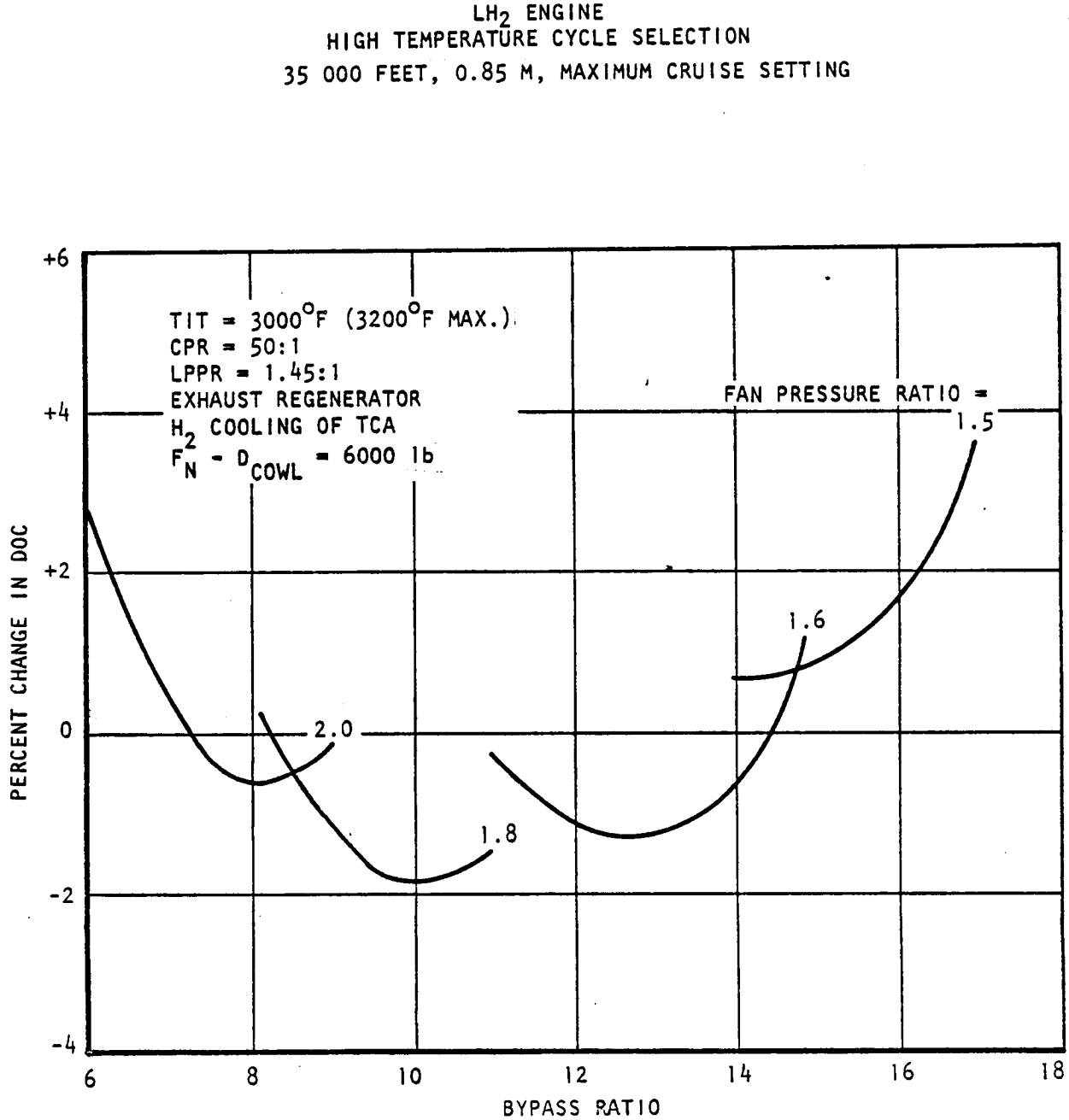

Figure 36. - Effect of bypass ratio and FPR on DOC for CPR = 50.

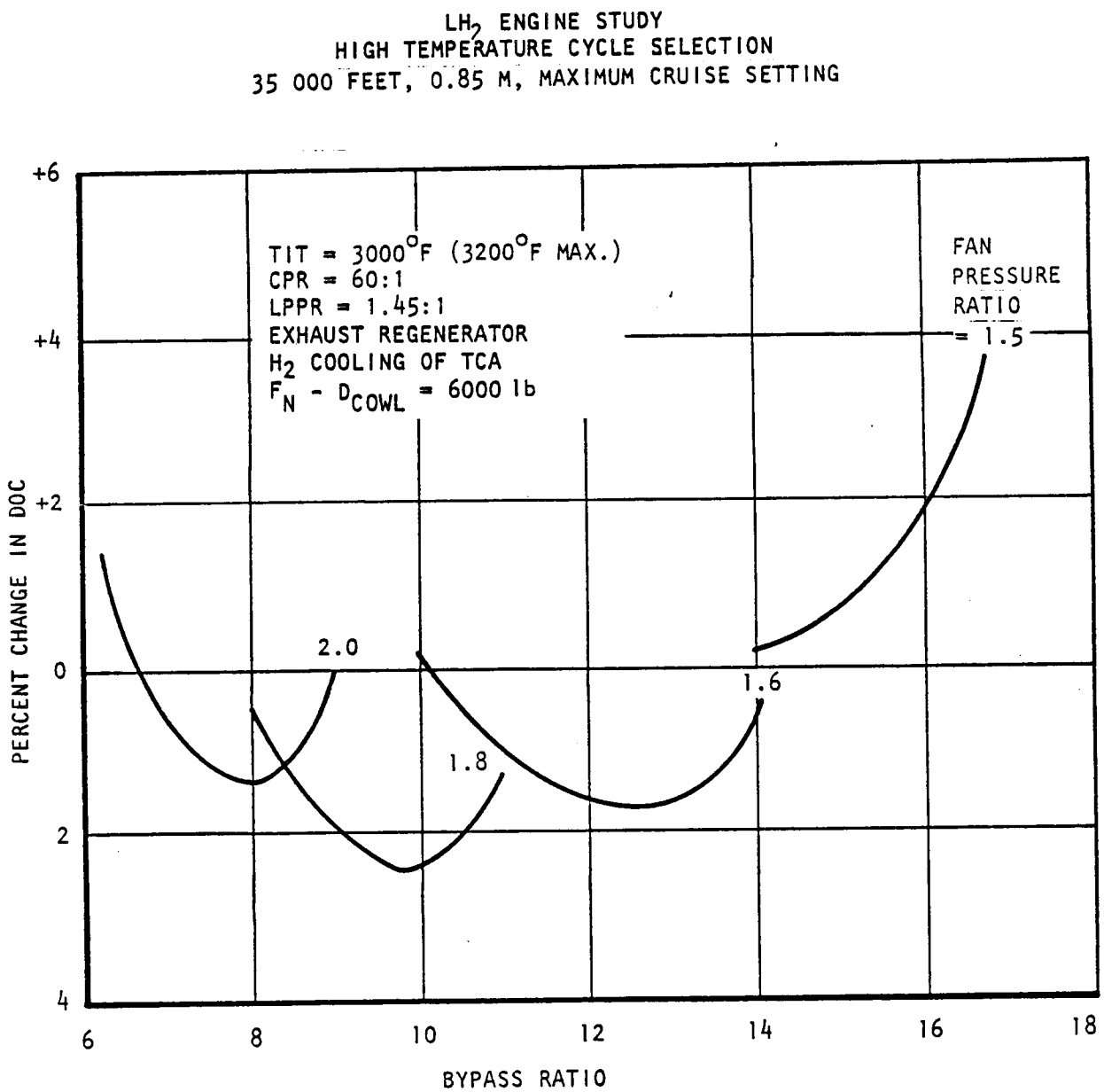

Figure 37. - Effect of bypass ratio and FPR on DOC for CPR = 60.

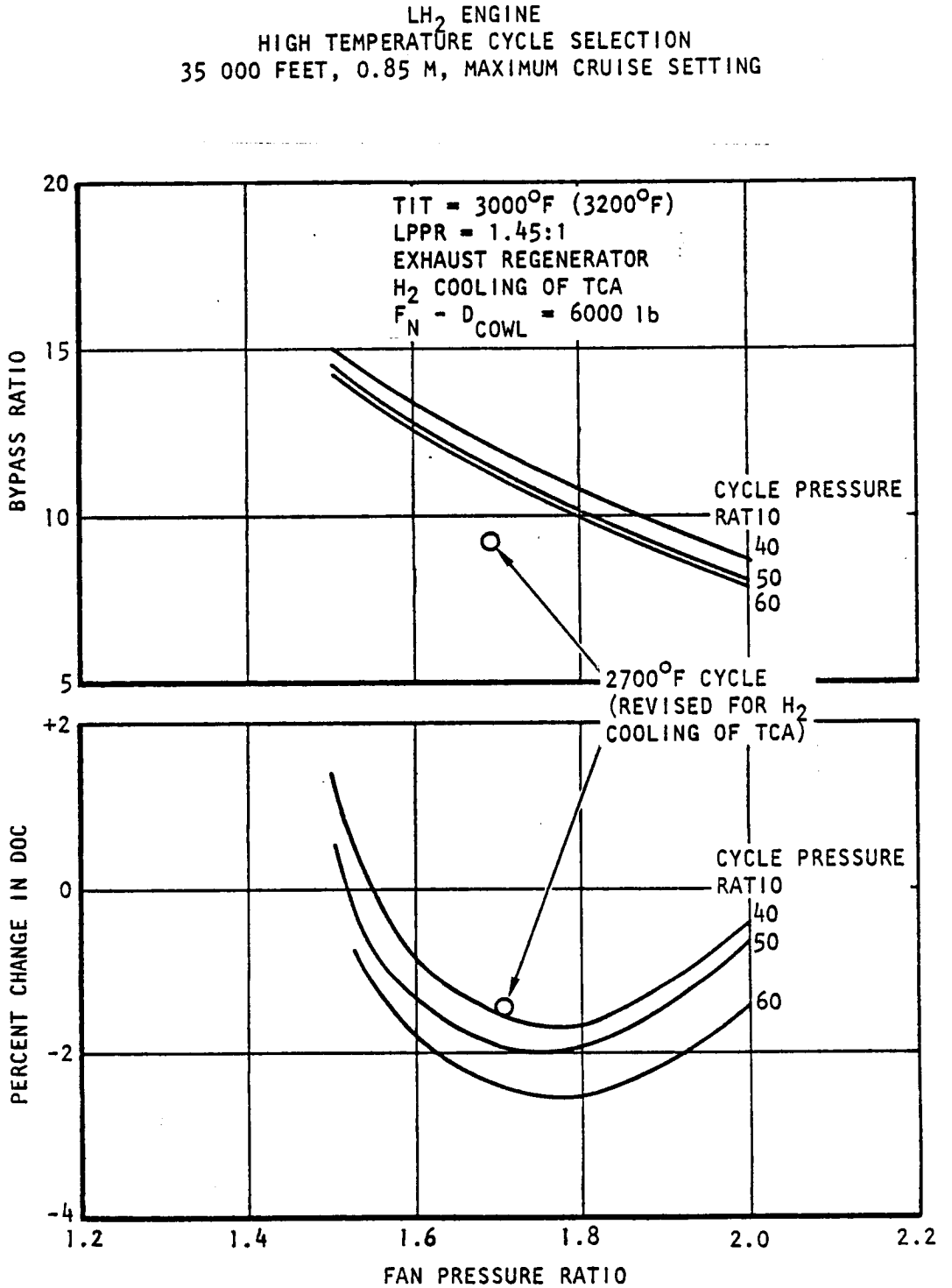

Figure 38. - Effect of fan pressure ratio and cycle pressure ratio on DOC and bypass ratio.

Minimum DOC occurs at a fan pressure ratio of approximately 1.75:1 for all three cycle pressure ratios and a 60:1 cycle pressure ratio yields the most improvement. There is approximately 0.8 percent difference in DOC between a cycle pressure ratio of 40:1 and 60:1. This small difference in DOC was not believed to be high enough to justify the significant complexity and cost penalties associated with the very high pressure ratio engine.

The 2700°F cycle initially selected offered a ΔDOC of 2 percent. However, cooling flows were calculated on a different basis and hydrogen cooling was not utilized. Accordingly, cooling flows were calculated on the basis of the revised methodology (4.2.3.1) and weight and SFC recalculated. The ΔDOC for this cycle is shown in Figure 38.

The 2700°F, 40:1 cycle pressure ratio engine incorporating hydrogen cooling of the turbine cooling air and the exhaust regenerator was selected as the cycle to represent technology and performance appropriate for the subject LH_2 fuel system study. This selection results in a DOC approximately 1 percent higher than the 60:1, 3200°F cycle. The high temperature, high pressure ratio engine would be significantly higher in cost than the selected engine. If the cost were more than 6 percent higher, which is very likely, the DOC advantage would be negated.

4.3 Selected Engine Concept

The final cycle selected as a result of the hydrogen exploitation studies and cycle selection investigations has the following significant features at the engine design point (Maximum cruise power, 35 000 feet, M 0.85):

- Fan pressure ratio of 1.7:1 and a bypass ratio of 10:1
- A booster pressure ratio of 1.45:1
- A compressor pressure ratio of 16.5:1
- A rotor inlet temperature of 2514°F (2700°F maximum rotor inlet temperature)
- A cycle pressure ratio of 40:1

4.3.1 Description and performance. - The selected engine is a twin spool, direct drive, separately exhausted turbofan. A single stage fan and two booster stages are driven by a multistage, uncooled, axial turbine. The gas generator consists of a 10-stage axial compressor, a through-flow circular combustor and a single-stage cooled axial turbine. The spool shafts are concentric and the low pressure spool shaft passes through the high pressure shaft.

Four heat exchangers are included as part of the engine to provide (a) hydrogen cooling of the turbine cooling air, (b) engine oil cooling, (c) hydrogen cooling of the aircraft environmental control system air and (d) fuel heating.

Basic cycle and performance data are listed in Table 14 at the engine design point and at sea level static takeoff conditions. The performance includes the effects of inlet pressure recovery, horsepower extraction, aircraft bleed extraction and fan stream scrubbing drag. Freestream cowl drag and inlet spillage drag is not included. The cycle and performance characteristics shown in Table 14 are the final results of cycle optimization. They reflect final estimates of component performance, pressure losses, cooling flows, etc. The primary refinements included increases in low pressure turbine efficiency and nozzle thrust coefficients, compared to those used in the early part of the study.

4.3.2 Weight, geometry, and scaling relationships. - An envelope drawing of the selected engine is included as Figure 39. Dimensions, mount locations, accessory gearbox and thrust reverser details are shown.

The estimated dry weight of the bare engine is 3780 pounds. This weight includes engine accessories, i.e., fuel control, fuel pump, lubrication pumps, heat exchangers and accessory gearbox. Aircraft accessories, inlet, nozzles, fan thrust reverser and noise suppression are not included. The estimated weight of the inner and outer fan ducts, fan and core nozzles, and fan thrust reverser is 809 pounds. The total dry weight of the engine exclusive of inlet, aircraft accessories and noise suppression is 4589 pounds.

The engine may be scaled within ± 25 percent of its base size according to the following relationships:

$$\text{Scaled Weight} = W_{bl} \left(\frac{\text{Scaled Thrust}}{\text{Base Thrust}} \right)^{1.0}$$

$$\text{Scaled Length} = L_{bl} \left(\frac{\text{Scaled Thrust}}{\text{Base Thrust}} \right)^{0.25}$$

$$\text{Scaled Diameter} = D_{bl} \left(\frac{\text{Scaled Thrust}}{\text{Base Thrust}} \right)^{0.5}$$

TABLE 14. - CYCLE AND PERFORMANCE CHARACTERISTICS - SELECTED LH_2 FUELED ENGINE.

	SLS, Std Day	M 0.85 35 000 ft
Power setting	Takeoff	Max. cruise
Net thrust, lb	30 706	6542
SFC, (lb/hr)/lb	0.1025	0.2014
Bypass ratio	10.25	10.0
Fan airflow, lb/sec	1066.4	478.8
Fan pressure ratio (tip)	1.594	1.7
Fan pressure ratio (hub)*	2.26	2.466
Compressor pressure ratio	15.5	16.5
Rotor inlet temperature, ^{o}F	2700	2514

*Hub pressure ratio includes booster stages

4.3.3 Engine cost. - Engine cost was established using techniques developed for estimating the cost of Jet A fueled engines, with suitable allowances made for the differences between Jet A fueled engine technology and H_2 fueled engine technology. Costs were developed for the base engine, and also for the installation of nozzles and thrust reverser. The cost data were in 1976 dollars, and were transmitted to Lockheed for use as inputs in the ASSET computer program.

4.3.4 Noise and emissions. -

4.3.4.1 Noise: It is estimated that the engine selected for the LH_2 transport will allow the requirements of FAR36 minus 10 EPNdB to be met. The penalty to specific fuel consumption to meet these requirements is estimated to be negligible. The penalty to engine weight and cost is estimated to be less than two percent.

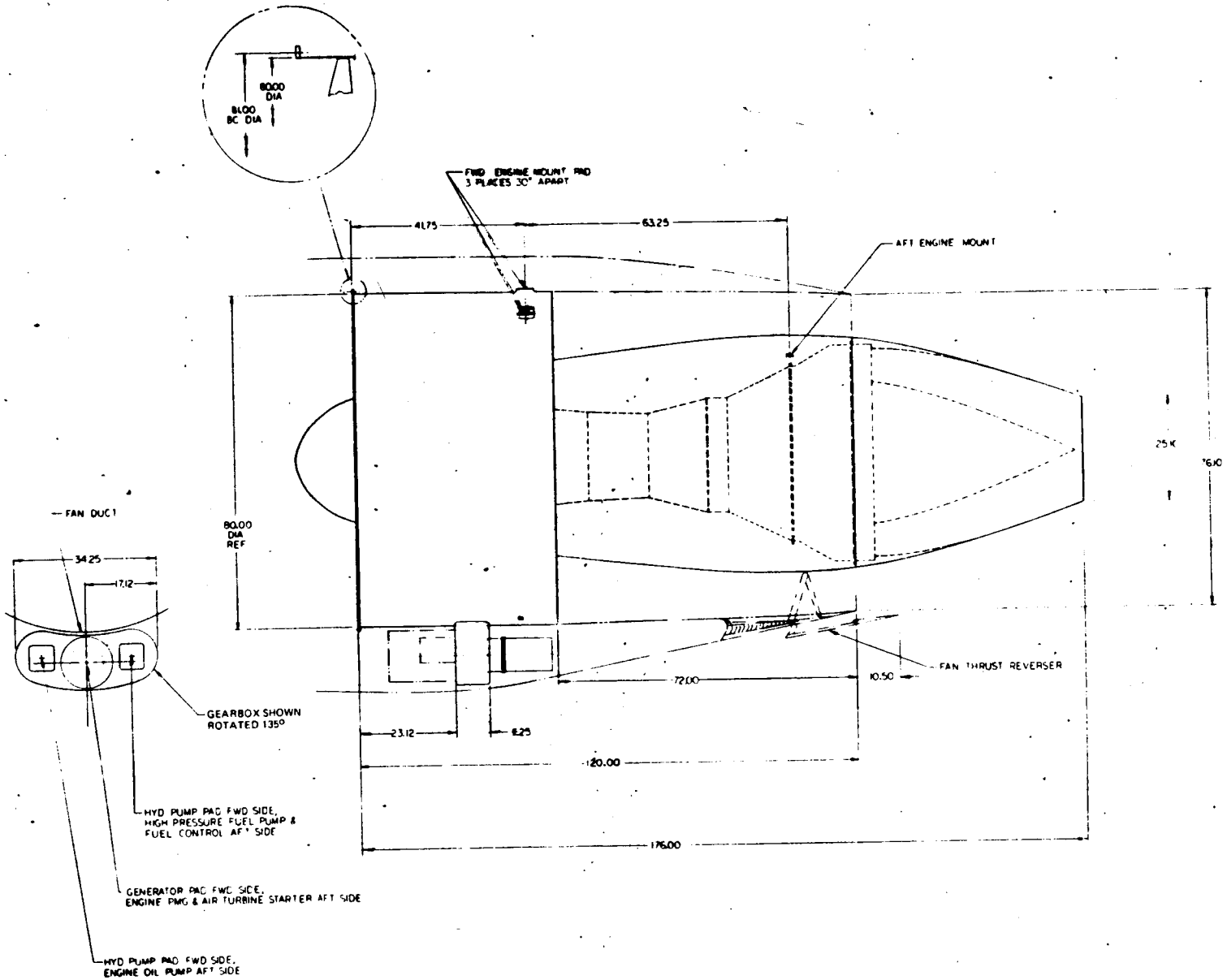

Figure 39. - Envelope drawing - selected baseline LH_2 engine.

Noise reduction in the following areas will be necessary:

- Fan source noise through improved airfoil design and proper blade-to-stator spacing
- Combustor noise
- Turbine source noise through optimization of blade and vane numbers and spacing

It is anticipated that the technology for achieving the reduction in the areas listed above will be available by the 1990 time period. The acoustical treatment of the inlet, fan duct and turbine exhaust will continue to be a requirement. With respect to noise, there is no difference between Jet A and LH_2 fueled engines.

4.3.4.2 Emissions: The use of liquid hydrogen as a fuel simplifies the emissions problem as products of combustion do not include hydrocarbons, carbon monoxide, or impurities such as sulfur or carbon. The exhaust from a LH_2-fueled engine is basically water vapor. The only pollutant that will be produced are some oxides of nitrogen (NO_x) as a result of nitrogen and oxygen from the air combining at the high combustion temperatures encountered in aircraft jet engines. The NO_x output is an exponential function of temperature and residence time in the combustor.

Hydrogen, injected in gaseous form into the combustor, has the characteristic of diffusing rapidly into the air so that mixing occurs thoroughly and very quickly. Combustion of H_2/air also occurs at a high rate so the result is smooth, complete burning with a much more uniform temperature profile than is characteristic with Jet A fuel. Elimination of the high temperature peaks, which occur with Jet A, can significantly reduce the production of NO_x from a LH_2-fueled engine, even though the average temperature in the combustion chambers of comparable engines is the same.

4.3.5 Operational characteristics. -

4.3.5.1 Rated performance: Performance ratings for the engine are shown in Tables 15, 16, and 17. The performance shown includes the effects of 125 horsepower extraction and 3.2 percent bleed air extraction. It also includes the effects of internal nozzle performance, inlet recovery, and fan stream scrubbing drag.

TABLE 15. - PERFORMANCE RATINGS AT U.S. STANDARD ATMOSPHERE SEA-LEVEL STATIC CONDITIONS

Power Setting	Net Thrust daN (Pounds)	Specific Fuel Consumption kg/hr/daN (LB/HR/LB)	Turbine Inlet Temperature °C (°F)	Low Pressure Spool Speed RPM	High Pressure Spool Speed RPM
Takeoff (5 minutes)	13659, (30706)	.1045 (.1025)	1482 (2700)	4059	17297
Maximum Climb	13045, (29327)	.1032 (.1012)	1454 (2650)	3984	17094

TABLE 16. - PERFORMANCE RATINGS AT 93.6°F (34.2°C) SEA-LEVEL STATIC CONDITIONS.

Power Setting	Net Thrust daN (Pounds)	Specific Fuel Consumption kg/hr/daN (LB/HR/LB)	Turbine Inlet Temperature °C (°F)	Low Pressure Spool Speed RPM	High Pressure Spool Speed RPM
Takeoff (5 minutes)	11443, (25724)	.1048 (.1028)	1482 (2700)	3902	17104

TABLE 17. - PERFORMANCE RATINGS AT U.S. STANDARD ATMOSPHERE 35 000 FEET, 0.85 MACH

Power Setting	Net Thrust daN (Pounds)	Specific Fuel Consumption kg/hr/daN (LB/HR/LB)	Turbine Inlet Temperature °C (°F)	Low Pressure Spool Speed RPM	High Pressure Spool Speed RPM
Maximum Climb	3236, (7275)	.2096 (.2055)	1454 (2650)	4300	17341
Maximum Cruise	2910, (6542)	.2054 (.2014)	1379 (2514)	4127	16886

4.3.5.2 Capabilities and limits:

4.3.5.2.1 Engine flight envelope: The engine flight operating envelope is shown in Figure 40.

4.3.5.2.2 Flight-maneuver loads: The flight maneuver operating load diagrams are shown in Figure 41.

4.3.5.2.3 Starting: The engine shall be capable of groundstarts at altitudes from sea level to 15 000 feet. The air start envelope in terms of altitude and Mach number is shown on Figure 37. The ambient temperature range for ground starting is from -40°F (-40°C) to 125°F (51°C).

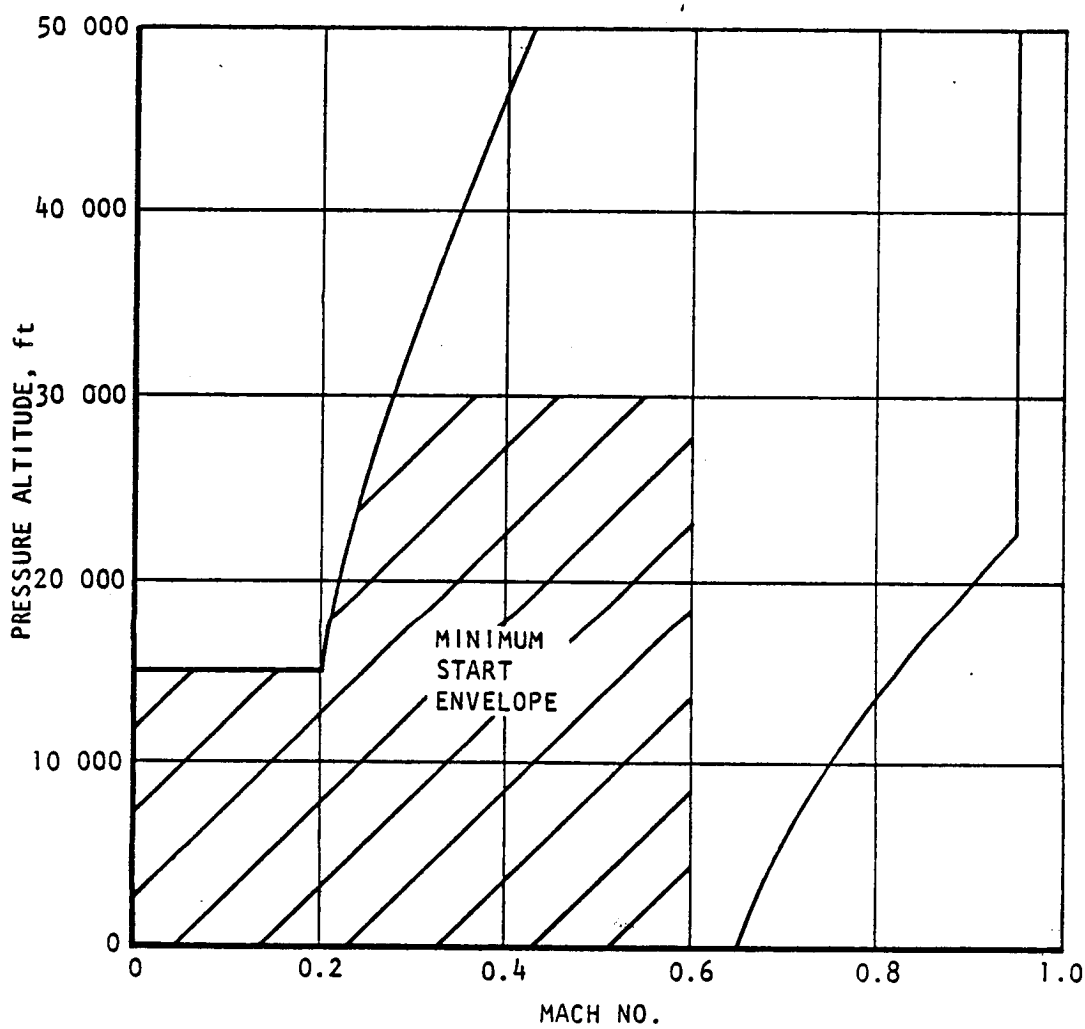

Figure 40. - LH_2 engine flight operating envelope.

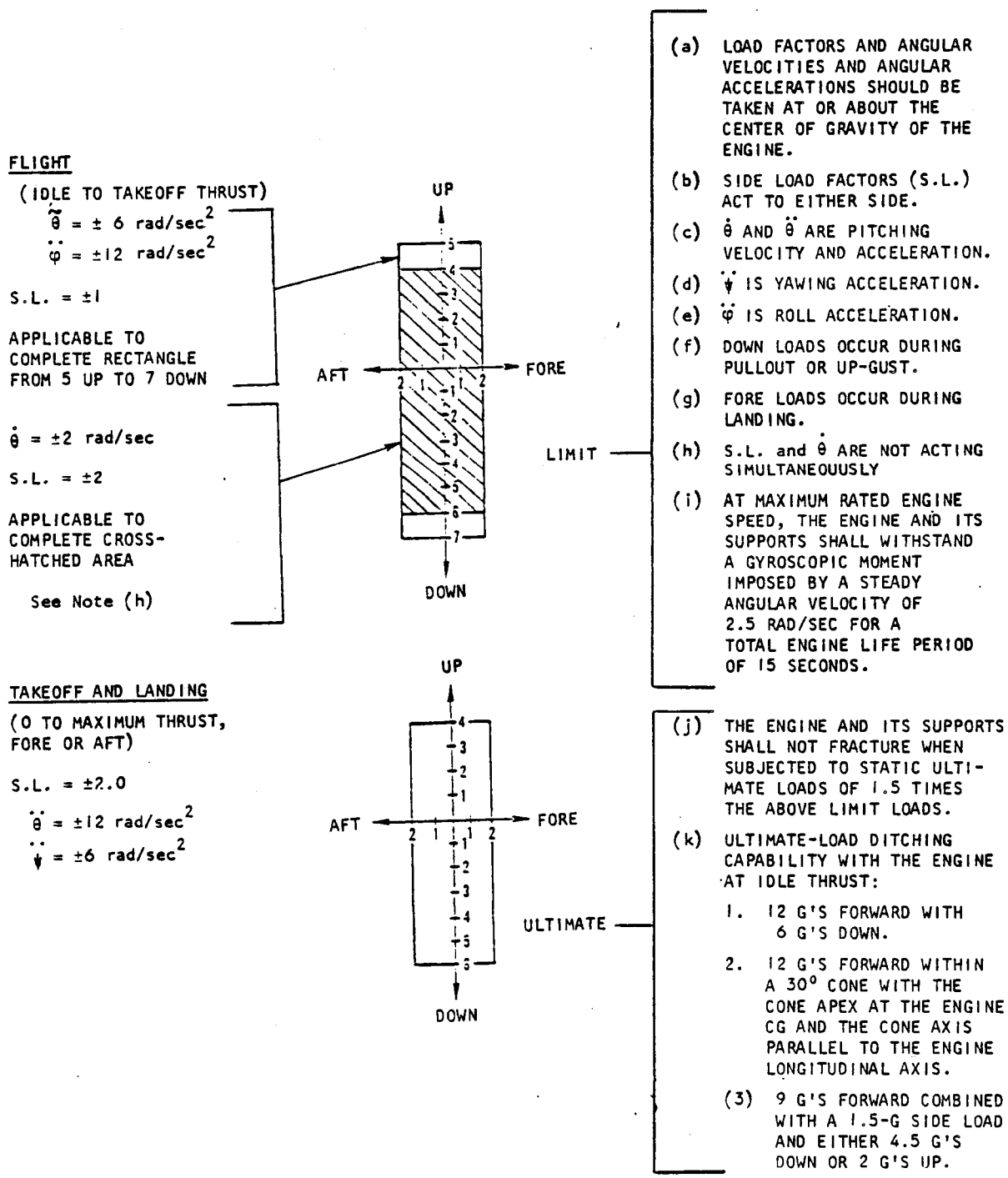

Figure 41. - LH_2 engine operating load limits.

4.3.5.2.4 Ambient temperature limits: The engine ambient temperature flight envelope is as shown on Figure 42.

4.3.5.2.5 Engine speed limits: Maximum low pressure spool (fan) speed is 4430 rpm and maximum high pressure spool (compressor) speed is 17 860 rpm.

4.3.6 Description of Engine Mounted Heat Exchangers. - Based upon the engine analysis, problem statements for the four engine mounted heat exchangers were prepared, and heat exchanger preliminary designs were established to meet these requirements. Engine mounted heat exchangers are required to perform the following functions:

- An air to hydrogen heat exchanger to cool compressor bleed air for use in cooling the HP turbine vanes and rotor blades.
- An oil to hydrogen heat exchanger to cool the engine oil.
- An air to hydrogen heat exchanger to cool compressor bleed air for use in the aircraft environmental control system.
- An exhaust gas to hydrogen heat exchanger, located in the engine flow path downstream of the low pressure turbine and upstream of the exhaust nozzle, to transfer heat from the engine exhaust gas to the hydrogen fuel.

Design point data for the four heat exchangers are presented in Table 4.3.6.

Because of the high hydrogen inlet pressure 2758 kPa (400 psia), only tubular heat exchangers were considered for these applications. The heat exchangers were designed to eliminate freezing problems which can occur when moisture is condensed out of the air as it is cooled and is then exposed to tube wall temperatures below $0^{\circ}C$ ($32^{\circ}F$).

To provide compact heat exchanger designs and eliminate freezing problems, the turbine cooling air heat exchanger and the aircraft ECS heat exchanger both utilize finned tubes and hydrogen recirculation. The fins provide high thermal conductance to the air and the recirculation preheats the hydrogen to raise the tube wall temperature above the freezing point.

The engine lubrication oil heat exchanger is also in the recirculation loop and was designed as a shell and tube heat exchanger. An ejector (jet pump) is used to produce the hydrogen recirculation flow with only a small additional pressure drop in the hydrogen. The turbine cooling air heat exchanger, the engine lubrication oil cooler, and the aircraft ECS air heat exchanger heat the hydrogen in series from $50^{\circ}K$ ($90^{\circ}R$) to a temperature of $264.1^{\circ}K$ ($475.4^{\circ}R$) to eliminate freezing problems in the engine exhaust gas heat exchanger. The turbine cooling air heat exchanger was arranged in a pattern as shown in Figure 4.3.6a. The engine lubrication oil cooler was

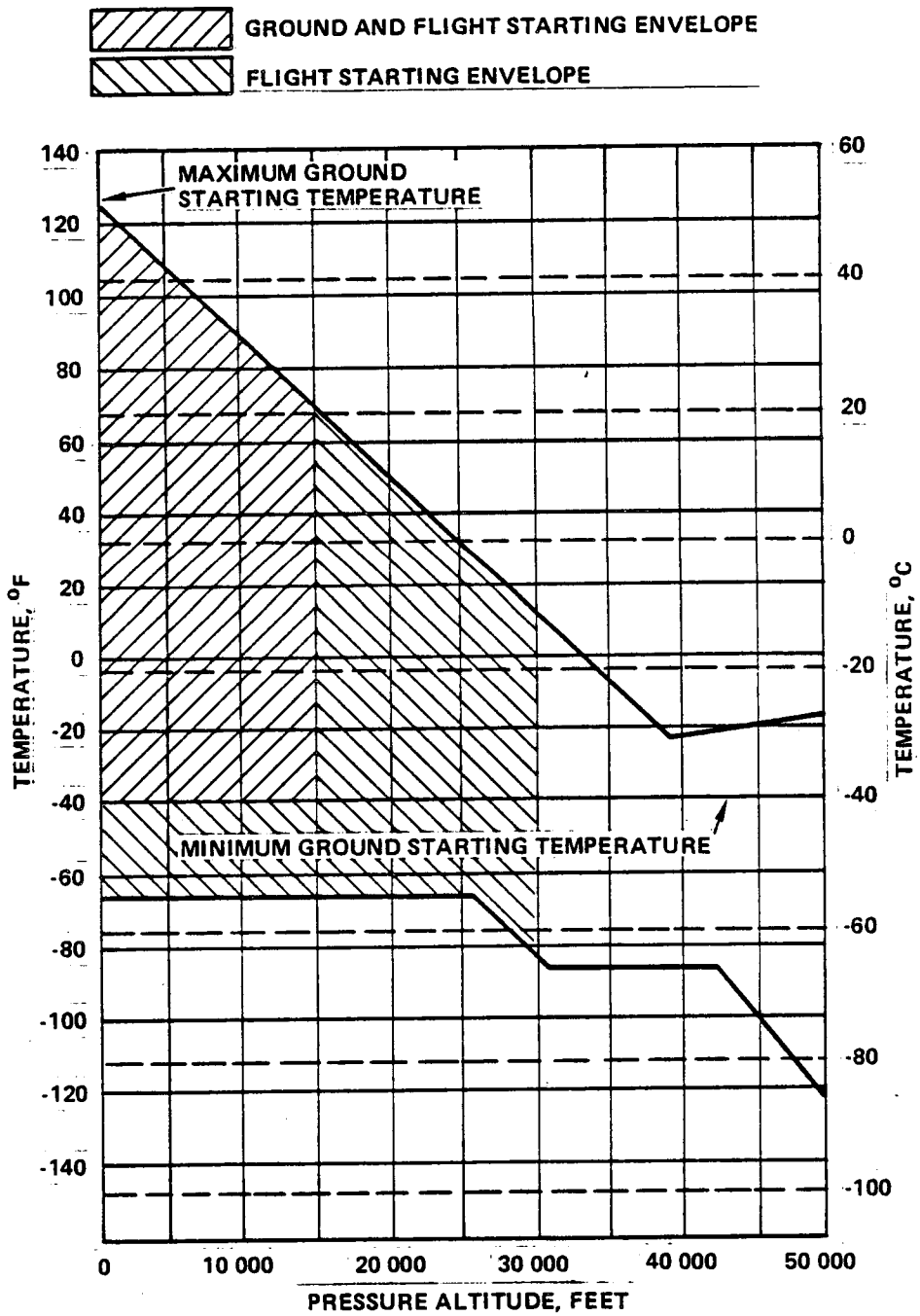

Figure 42. - LH_2 engine ambient flight and starting temperature envelope.

TABLE 4.3.6. LIQUID HYDROGEN FUELED ENGINE HEAT EXCHANGER DESIGN CONDITIONS

	Turbine Cooling Air HX	Oil Cooler	ECS Bleed HX	Engine Exhaust HX
Total Heat Transferred, kJ/min (Btu/min)	26628 (25219)	4012 (3800)	1921 (1819)	60422 (57225)
Shell Side Air (Oil) Flow, kg/min (lb/min	49.9 (110)	57.6 (127)	48.4 (106.7)	1144 (2523)
Air (Oil) Inlet Temp., ^{o}K (^{o}R)	791 (1423)	378 (680)	336 (604)	778 (1400)
Air (Oil) Outlet Temp., ^{o}K (^{o}R)	303 (546)	343 (617.3)	297 (535)	733 (1319)
Air Inlet Pressure, kPa (psia)	1515.5 (219.8)		92.05 (13.35)	40.04 (5.81)
Air Pressure Drop $\Delta P/P$ inlet	0.04		0.074	0.032
Oil Pressure Drop, kPa (psi)		83 (12)		
Shell Side Effectiveness	0.825	0.276	0.502	0.0873
Tube Side Hydrogen Flow, kg/min (lb/min)	32.59 (71.85)*	32.59 (71.85)*	32.59 (71.85)*	9.95 (21.94)
Hydrogen Inlet Temperature, ^{o}K (^{o}R)	200 (360)	251 (452)	260 (468)	264 (475)
Hydrogen Outlet Temperature, ^{o}K (^{o}R)	251 (452)	260 (468)	264 (475)	677 (1219)
Hydrogen Pressure Drop, kPa (psi)	2.76 (0.4)	26.2 (3.8)	2.14 (0.31)	45.5 (6.6)
Tube Side Effectiveness	0.0873	0.0686	0.0509	0.8043

*Recirculation flow of 22.637 kg (49.905 lb/min) hydrogen required to prevent water condensate freezing. Hydrogen temperature before mixing recirculation flow is 50°K (90°R).

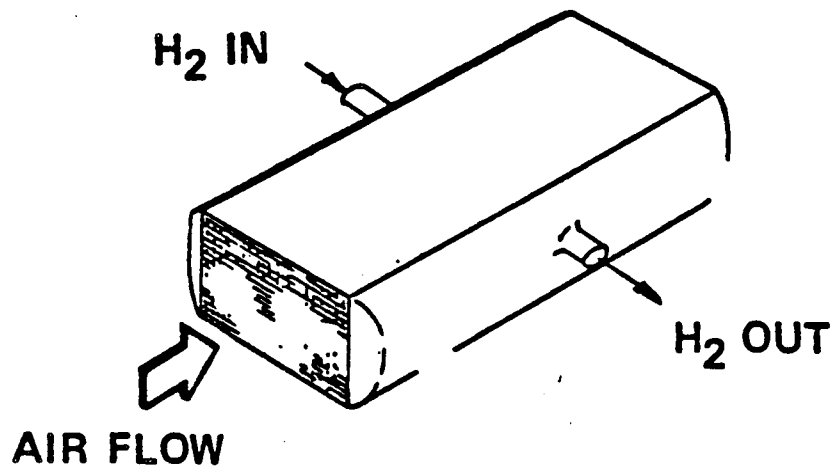

AIRFLOW LENGTH	48.59 cm (19.13 in.)
WIDTH	12.7 cm (5.0 in.)
HEIGHT	9.42 cm (3.71 in.)
FINNED TUBES	
TUBE O.D.	0.64 cm (0.25 in.)
TUBE WALL	0.04 cm (0.016 in.)
TUBE MATERIAL	304 CRES
FIN O.D.	1.27 cm (0.50 in.)
FIN SPACING	0.06 cm (0.025 in.)
FIN THICKNESS	0.010 cm (0.004 in.)
FIN MATERIAL	OFHC COPPER
FIN AND TUBE COATING	NiCr
TOTAL NUMBER TUBES	308
NUMBER HYDROGEN PASSES	1
TUBE WEIGHT	7.4 kg (16.3 lb)
TOTAL HEAT EXCHANGER WT	18 kg (40 lb)

Figure 4.3.6a. Turbine cooling air to hydrogen heat exchanger

designed as shown in Figure 4.3.6b. The aircraft ECS air cooler was arranged as shown in Figure 4.3.6c.

The engine exhaust gas heat exchanger heated the hydrogen for entry to the combustor. This heat exchanger is exposed to a large flow rate of air (exhaust gas) and had to be designed with low air pressure drop in a location with limited air flow area. To satisfy these requirements, an inline tubular heat exchanger such as used by Pratt and Whitney in the 304 engine was selected. The proposed design has involute curved tubes running from a 56.4 cm (22.2 in.) inner diameter to a 126.5 cm (49.8 in.) outer diameter air passage. The involute tubes are arranged in a pattern as shown in Figure 4.3.6d.

4.4 Technology Development Required

The technology postulated for the LH_2-fueled engine is representative of that which would be incorporated in an engine entering service in the 1990 time period. Much of the technology is not, however, unique to use of LH_2 fuel. Much of the aerodynamics, materials, mechanical design and manufacturing processes, while advanced, are equally applicable to future kerosene-fueled advanced transport engines.

Elements which are unique to the LH_2 fueled engine are:

- Combustor
- H_2 cooling of the turbine cooling air
- Heat exchangers
- Fuel control

The fuel control system is discussed in section 5.5 of this report.

4.4.1 Combustor. - Technology development is required to take advantage of the properties of hydrogen and to execute a combustor design which is smaller, provides an improved pattern factor, and is low in oxides of nitrogen emissions.

The design of hydrogen combustion systems is particularly amenable to analysis relative to conventional kerosene combustion systems. The kinetic schemes and reaction rates are well established except for turbulent flow. Therefore, a technology program to develop a hydrogen combustion system could consist of analytical design augmented by an experimental program to provide turbulent flow kinetics and to verify the analytical design.

4.4.2 H_2 cooling of turbine cooling air. - There are two problems introduced when hydrogen cooling of turbine cooling air is incorporated in an engine.

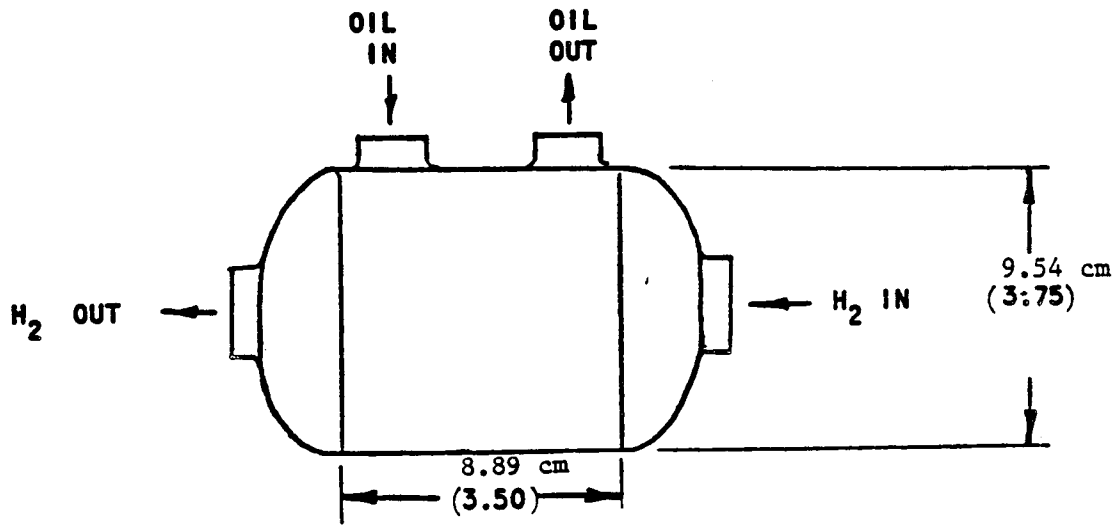

TUBES	
TUBE O.D.	0.32 cm (0.125 in.)
TUBE WALL	0.030 cm (0.012 in.)
TUBE MATERIAL	304 CRES
TOTAL NUMBER OF TUBES	600
NUMBER OF HYDROGEN PASSES	1
NUMBER OF OIL PASSES	2
TUBE WEIGHT	1.2 kg (2.6 lb)
TOTAL HEAT EXCHANGER WEIGHT	2.6 kg (5.75 lb)

Figure 4.3.6b. Engine oil to hydrogen heat exchanger

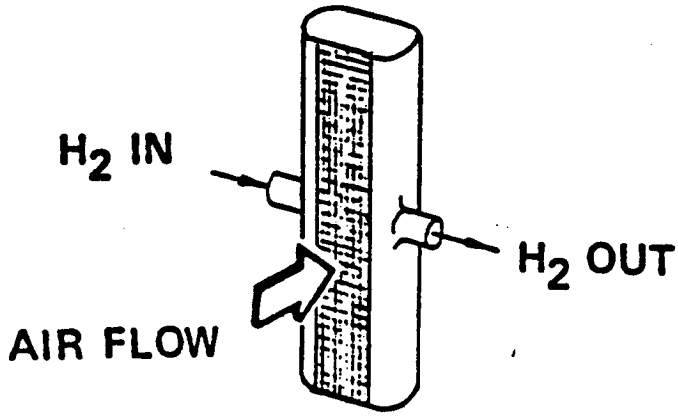

AIR FLOW LENGTH	7.9 cm (3.1 in.)
WIDTH	7.6 cm (3.0 in.)
HEIGHT	60.7 cm (23.9 in.)
FINNED TUBE	
TUBE O.D.	0.64 cm (0.25 in.)
TUBE WALL	0.041 in. (0.016 in.)
TUBE MATERIAL	304 CRES
FIN O.D.	1.27 cm (0.50 in.)
FIN SPACING	0.064 cm (0.025 in.)
FIN THICKNESS	0.010 cm (0.004 in.)
FIN MATERIAL	OFHC COPPER
FIN AND TUBE COATING	NiCr
TOTAL NUMBER TUBES	315
NUMBER HDYROGEN PASSES	1
TUBE WEIGHT	4.5 kg (10.0 lb)
TOTAL HEAT EXCHANGER WEIGHT	11.3 kg (25.0 lb)

Figure 4.3.6c. ECS bleed air to hydrogen heat exchanger

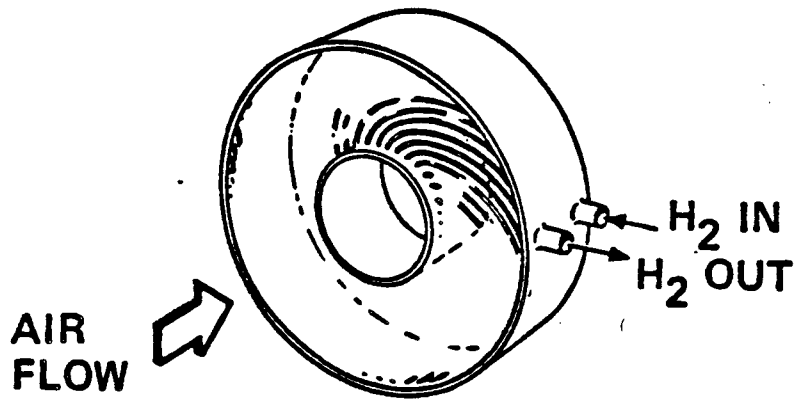

OUTSIDE DIAMETER	126.5 cm (49.8 in.)
INSIDE DIAMETER	56.4 cm (22.2 in.)
AIR FLOW LENGTH	19.1 cm (7.5 in.)
INVOLUTE TUBE LENGTH	56.9 cm (22.4 in.)
CIRCUMFERENTIAL TUBE SPACING	6 DIAMETERS
AXIAL TUBE SPACING	1.25 DIAMETERS
TUBE O.D.	0.478 cm (0.188 in.)
TUBE WALL	0.030 cm (0.012 in.)
TUBE MATERIAL	304 CRES
TOTAL NUMBER OF TUBES	1984
NUMBER OF HYDROGEN PASSES	8
TUBE WEIGHT	38.3 kg (84.5 lb)
TOTAL HEAT EXCHANGER WEIGHT	77.1 kg (170 lb)

Figure 4.3.6d. Engine exhaust fuel heater

The first is a design problem. Normally turbine cooling air is routed internally through the engine from the compressor to the cooled turbine. The routing is different when the turbine cooling air is hydrogen cooled. Complex design problems would have to be addressed but the task could be best undertaken concurrently with engine design.

The second problem is caused by the lower temperatures of the turbine cooling air. Thermal gradients in the blades would be more severe than presently experienced for a similar blade heat transfer system. These high thermal gradients can result in low cycle fatigue damage. In order to realize the advantages of H_2 cooling of the turbine cooling air, it is recommended that parallel technology programs be undertaken to

1. Develop heat transfer systems which produce more uniform temperatures

2. Extend development of single crystal turbine blades which have higher cyclic fatigue strength.

5. ENGINE FUEL SUPPLY SYSTEM

5.1 Candidate System Concepts

5.1.1 Concept descriptions. - The basic fuel system performance requirement is that a pump or combination of pumps must supply fuel according to a specified flow-pressure schedule. The schedule shown in Table 18 was used for initial design considerations. Additionally, a tank-mounted pump must be included in the system, to provide a pressure higher than the vapor pressure to the fuel lines and the engines. The wide range of pumping systems that could achieve these requirements is constrained by cost considerations, as expressed through the ΔDOC equation applied in Section 5.1.2. The objective of the concept selection was to determine the general arrangement of the fuel supply system which could most efficiently meet the basic requirements of the system.

Two concepts for the arrangement of pumps in the engine fuel supply subsystem were considered initially. In Concept 1, a low-pressure-rise (nominally 50 psi rise) boost pump would be in the tank and a high-pressure rise main pump would be on the engine. The boost pump would provide a positive pressure to move LH_2 from the tank to the engine and would meet main pump inlet pressure requirements. In Concept 2, the main pump on the engine would be eliminated, with the total flow-pressure requirements of the engine met by a single tank-mounted pump. The analytical concept selection procedure described below (Section 5.1.2) also included evaluation of a Concept 1-1/2 pump arrangement. Here, an engine-mounted main pump and a tank-mounted boost pump would be performance matched so that the boost pump would supply some intermediate pressure rise (determined as a parameter of the analysis) and the main pump would supply the balance of the pressure rise. In such an arrangement, the performance requirements of the main pump (and hence its weight and power requirements) could be reduced and conceivably provide benefits to the overall system.

5.1.2 Results of evaluation. - The concept selection process utilized a parametric trade-off study approach based upon the ΔDOC sensitivity equation appropriate to the fuel subsystem. With this approach, the entire range of system configurations could be evaluated. In performing this analysis, both the pump concept and the optimum fuel line diameter were selected. Pressure dropline diameter and calculated line diameter-line weight data (see Sec. 5.2.1) were introduced into the analysis at the appropriate points. For example, as the line diameter was decreased, the line weight decreased but the pressure drop necessarily overcome by the tank-mounted pump increased, thus increasing the required size and weight of the boost pump.

TABLE 18. - LH_2 TURBOFAN ENGINE NET THRUST, FUEL FLOW AND FUEL PRESSURE SCHEDULE FOR INITIAL DESIGN CONSIDERATIONS

Condition	Altitude (1000 ft)	Mach	$\dot{w}$/Engine (lb/sec)	Net Thrust/Eng. (lb)	Comp. Discharge Pressure-psia
Max SLS	0	0	0.749	28 700	707
Takeoff	0	0	0.750	28 700	707
Climb	0	0.38	0.774	18 780	735
	2	0.39	0.755	18 040	
	4	0.41	0.732	17 140	
	6	0.42	0.690	16 000	
	8	0.44	0.664	15 090	
	10	0.46	0.635	14 350	604
	10	0.64	0.667	12 750	637
	15	0.71	0.613	11 320	
	20	0.78	0.553	10 050	541
	25	0.85	0.498	8 690	
	30	0.85	0.429	7 380	444
	35	0.85	0.348	6 150	387
Cruise	35	0.85	0.351	6 000	383
	38	0.85	0.292	5 300	355
Flight Idle	35	0.85	0.063	-205	225
	38	0.85	0.051	-164	
	0	0.4	0.171	820	
Ground Idle	0	0	0.085	1 830	271
	5	0	0.071	1 520	
Ground Start	0	0	.024	-	22

Concept selection was translated into a problem of optimization of the tank-mounted boost pump pressure rise. If the optimum rise were small, Concept 1 would be chosen; if large, Concept 2; and if some intermediate pressure rise were found optimum, Concept 1-1/2 would be chosen.

An analysis based on ΔDOC was conducted to determine the optimum design pressure rise (at maximum flow) for the boost pump. If the engine-mounted main pump efficiency (ηm) is assumed to be a constant 45 percent regardless of the boost pump pressure rise, and if the main pump weight is assumed to be

a constant 25 pounds, the minimum direct operating cost occurs at the lowest possible boost-pump pressure rise. The reason for this is shown by an investigation of the ΔDOC sensitivity equation.

$$DOC \times 10^5 = 3.22 \sum hp_c + .775 \left(W_s + 6 \sum hp_{max}\right)$$

where

DOC is expressed in $\frac{¢}{\text{seat nmi}}$

$\sum hp_c$ = horsepower at cruise for all pumps (tank and engine mounted)

W_s = total weight

6 = coefficient approximating the aircraft weight penalty to provide and transmit the required horsepower

$\sum hp_{max}$ = maximum horsepower into pump drives that are tank mounted (not engine mounted)

Parameters on the right-hand side were related to pressure rise ΔP through the relations HP ∝ P and $W_{pump} \propto P^{0.6}$, the latter equation being based on extensive Rocketdyne experience with cryogenic pumps. Results of the analysis are shown in Figure 43. For this case of constant main pump weight, increasing the boost pump pressure rise decreases HP_c slightly because the boost pump is more efficient than the main pump. However, this factor is far outweighed by the increased boost pump weight (which increases W_s) and the $6 \sum hp_{max}$ term, which is directly proportional to boost-pump pressure rise. The net effect is that, for constant main pump weight, the minimum feasible ΔDOC occurs at the minimum boost pump pressure rise that will provide sufficient pressure to the main pump inlet.

If, as is usually the case, the main pump design speed is assumed to be NPSH limited (resulting in a weight that decreases with increasing boost-pump pressure rise), the optimum ΔDOC is shown to occur at a boost pump pressure rise of 46 psi. An investigation of the ΔDOC relation shows the reason for this. At boost pump pressure rises (ΔP_B) below 40 psia, the main pump NPSH is so low that the main pump weight becomes large and consequently dominates the ΔDOC equation. This causes ΔDOC to increase with decreasing ΔP_B. If, on the other hand, ΔP_B is greater than 50 psi, the main pump NPSH is so large that the main pump weight reduction has little effect. However, the boost pump power is directly proportional to ΔP_B and, therefore, the tank-mounted pump power term ($6 \sum hp_{max}$) becomes the dominant factor. As a result, ΔDOC increases with increasing ΔP_B if ΔP_B is greater than 50 psi.

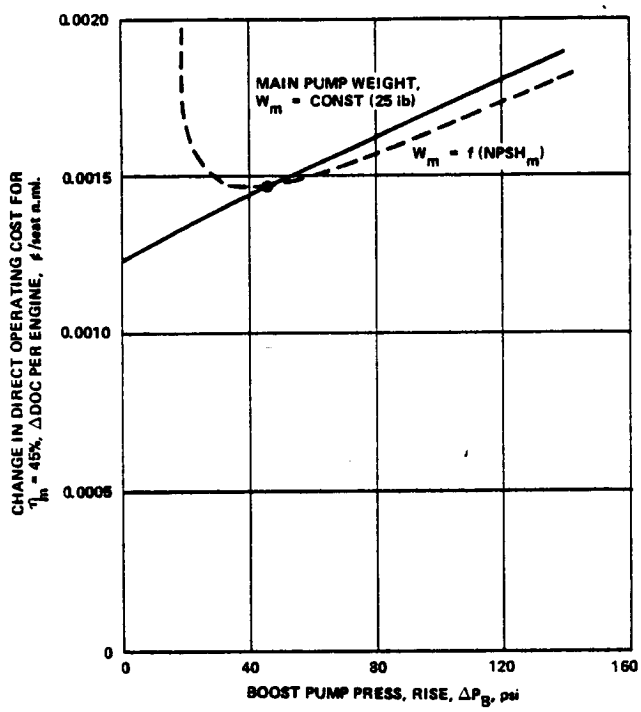

Figure 43. - Boost pump pressure rise effects.

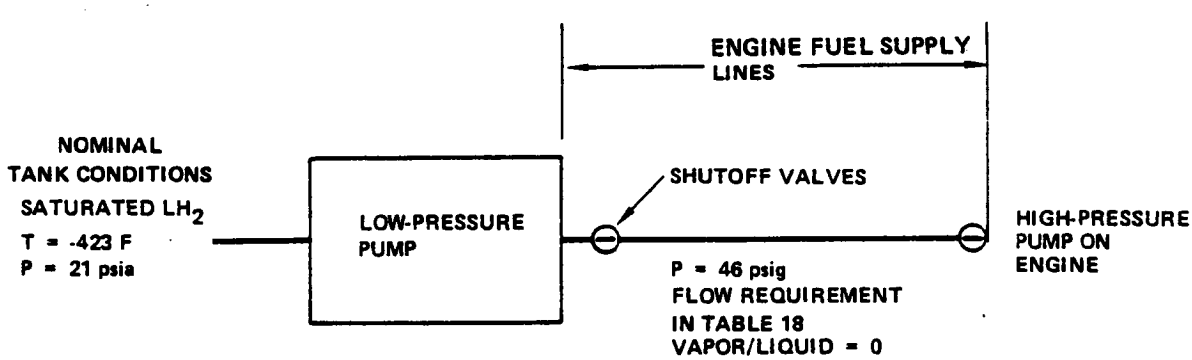

Figure 44. - Concept I schematic (tank mounted low-pressure pump/engine mounted high-pressure pump).

These results show that it is not economical to increase the boost pump design pressure rise much above 46 psi. Therefore, the Concept 1-1/2 approach does not appear to be practical. This, in combination with the even higher ΔDOC for Concept 2 (main pump in the tank) results in the selection of Concept 1, with a minimum boost pump design pressure rise, for the hydrogen-fueled aircraft. These parametric results were verified by preliminary calculations using several system configurations. Again Concept 1 with a pressure rise of 46 psi was found to be favored.

5.1.3 Characteristics of selected systems. - Figure 44 depicts the selected pump concept. This figure, together with the flow-pressure schedule found in Table 18 defined the requirements for the selected boost pump/drive system described in Section 5.3 and the engine-mounted fuel pump described in Section 5.4.

5.2 Engine Fuel Supply Lines

Selection of the configuration of the engine fuel supply lines that carry the fuel from the tank to the engines involves determination of two basic factors. First, the diameter of the lines which contain the fuel must be selected. Second, the appropriate insulation system for the cryogenic lines must be found. Diameter affects system performance in establishing both fuel-line pressure drop that must be overcome by the tank-mounted boost pump, and also line weight. The choice of insulation enters the system calculation in weight and heat leakage. Qualitative insulation effects such as safety and fabricability must also be considered. This section presents the results of the feed-lines portion of this investigation and the methods used.

5.2.1 Size Selection. - The line diameter for the fuel-feed lines was optimized in the concept selection analysis described in Section 5.1.2 above. As a precursor to that calculation, it was first necessary to determine the line pressure loss as a function of line diameter. Feed Line No. 4 (aft tank to right-hand outboard engine), was selected as the most severe configuration in terms of total line length and number of bends. Total line length, including a growth factor of 1.2, was calculated to be 176 feet. Line losses for eight right-angle bends were calculated assuming utilization of optimum line bend radius ratio (Y/d_{tube}) of about three to five. This results in loss coefficients (K_L) of about 0.2 for a 90 degree bend. The results of a conventional analysis for the flow of incompressible liquid hydrogen in pipes are summarized in Figure 45 for the maximum engine fuel flow rate condition of 0.774 lb/sec, Table 18. It has been assumed that: (1) vapor/liquid ratio of the fluid delivered to the engine must be zero at maximum flow, and (2) low loss valves have been utilized in the system, so that line loss due to valves is approximately equal to their equivalent line length. Ball valves when used in liquid hydrogen systems satisfy this assumption. A nominal one-inch diameter line results in a pressure loss of 14 psi at max. flow.

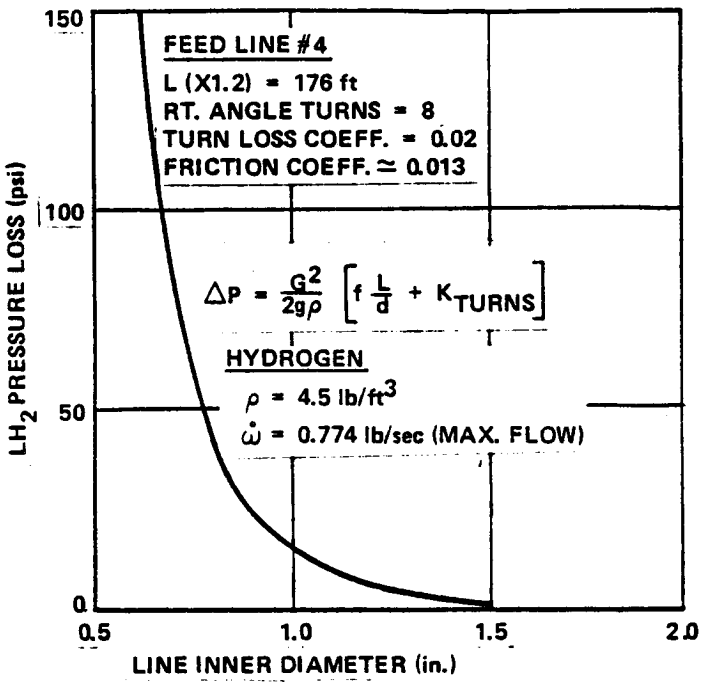

Figure 45. - LH_2 fuel feed line pressure loss.

Figure 46 shows the incremental ΔDOC determined from the sensitivity equation as a function of line diameter for the selected pump concept, determined in Section 5.1.2. A line diameter of 1.0 inches was determined to be optimal based upon this trade approach.

5.2.2 Insulation system comparison. - From the system optimization process described in Sections 5.1.2 and 5.2.1, a fuel-line inner diamter of 1.0 inch was chosen. Because the fuel to be pumped, LH_2, is cryogenic, the fuel lines must be insulated to prevent excessive heat input to, and consequent vaporization of, the fuel as it flows from the tanks to the engines, a distance of up to 160 feet. Two principal types of insulation systems were considered: vacuum and foam.

Where practical, vacuum insulation systems are usually utilized for ground-based cryogenic transfer systems, as the overall heat transfer can be minimized by means of an evacuated space filled with radiation shielding to control this mode of heat loss. The experience with vacuum-insulated systems for flight-weight systems is limited, but a significant drawback is found in manufacturing, installation, maintenance, and safety of the thin-walled tubing

necessary for a flight-weight system. On the other hand, to achieve the insulation properties of a vacuum system, foam-insulated lines must be relatively large and bulky. Foam systems can also degrade in performance over long periods of time. Thus, there is no clear-cut choice for the insulation approach. This section presents the results of the determination of the best present choice for insulation system. The approach incorporates consideration of both insulation properties and practical considerations such as weight, manufacture, maintenance, safety, etc.

5.2.2.1 Insulation requirements: Thermal insulation considerations are one factor in estimating the total feed-system weight. A primary requirement for the proposed aircraft engine design is that the hydrogen vapor volumetric fraction does not exceed .5 at the engine inlet under any flow condition. A second consideration relates to ground-hold conditions (i.e., zero H_2 flow) after initial line chilldown. The ground-hold condition will result in line venting and some fuel loss (boil-off) at various time intervals dependent on the insulation effectiveness. Excessive pressure in the line is prevented by thermal relief devices incorporated in the shutoff valves and a small hole in the pump check valve to allow venting into the fuel tank.

Various techniques have been developed for insulating cryogenic components. Some, such as those utilizing helium or nitrogen purges, do not appear suitable for aircraft feed line application. A vacuum jacket and/or closed cell type foam insulation appears suitable in terms of basic simplicity. A comparison of a typical foam insulation and a simple vacuum jacket in terms of heat leak rate is shown in Figure 47. It is apparent that the vacuum-jacket approach is superior in terms of minimizing heat leak rate. (Joints are not included).

Foam: The effect of line diameter (i.e., pressure drop) on required foam insulation thickness and total insulation weight is presented in Figure 48 for the condition $\dot{w}$ = 0.051 lb/sec. For the nominal 1.0 inch line diameter, the total insulation weight (all four feed lines) is about 50 pounds. Both the line and insulation weights are related to feed line diameter as shown previously. Since the line diameter determines hydrogen pressure drop, it is possible to relate the line and insulation weight to either the pump discharge pressure or pressure rise as shown in Figure 49. This approach in combination with a pump weight versus pressure rise curve permits direct determination of the minimum weight system, see Section 5.1.2.

The vacuum-jacketed line approach is superior to the foam insulation in terms of minimum heat leakage as noted previously in Figure 47. If the insulation system is a vacuum annulus only, the insulation weight is zero. If an aluminized mylar radiation shield is wrapped on the inner line, as is almost certainly necessary, the insulation weight is 0.07 lb/ft, or 40.3 pound for 576 feet total line length.

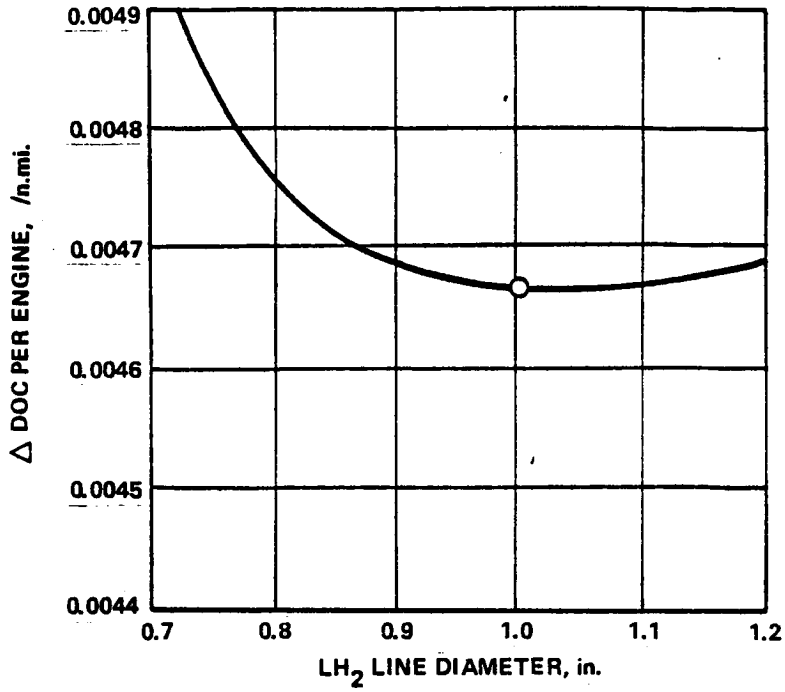

Figure 46. - Size optimization for engine fuel supply line.

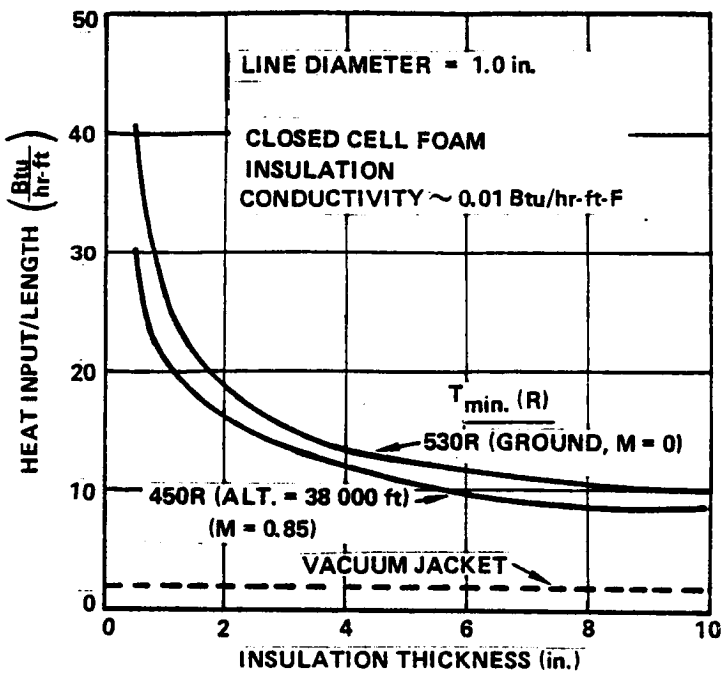

Figure 47. - Effect of insulation on heat leak rate.

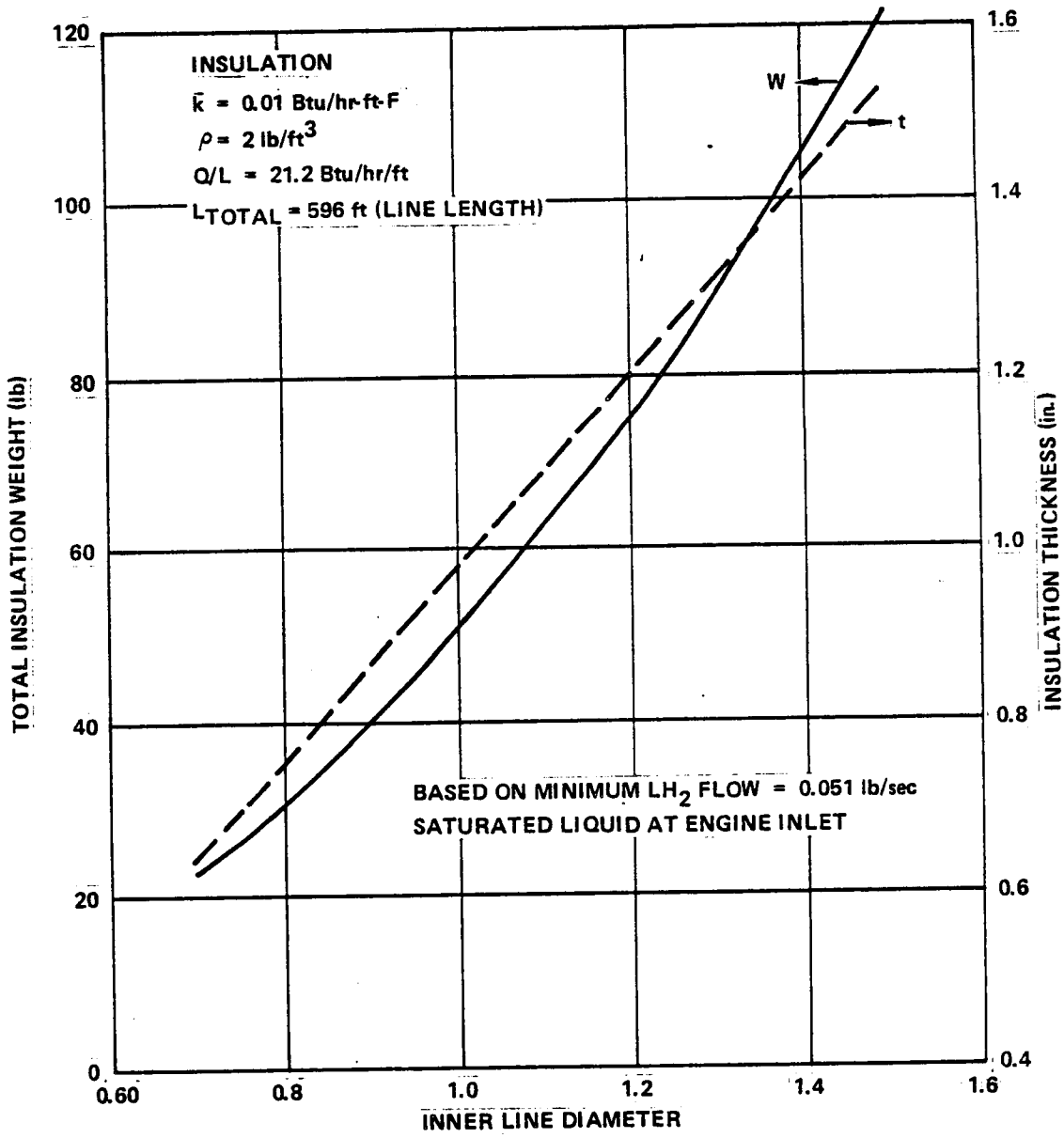

Figure 48. - Foam insulation requirements.

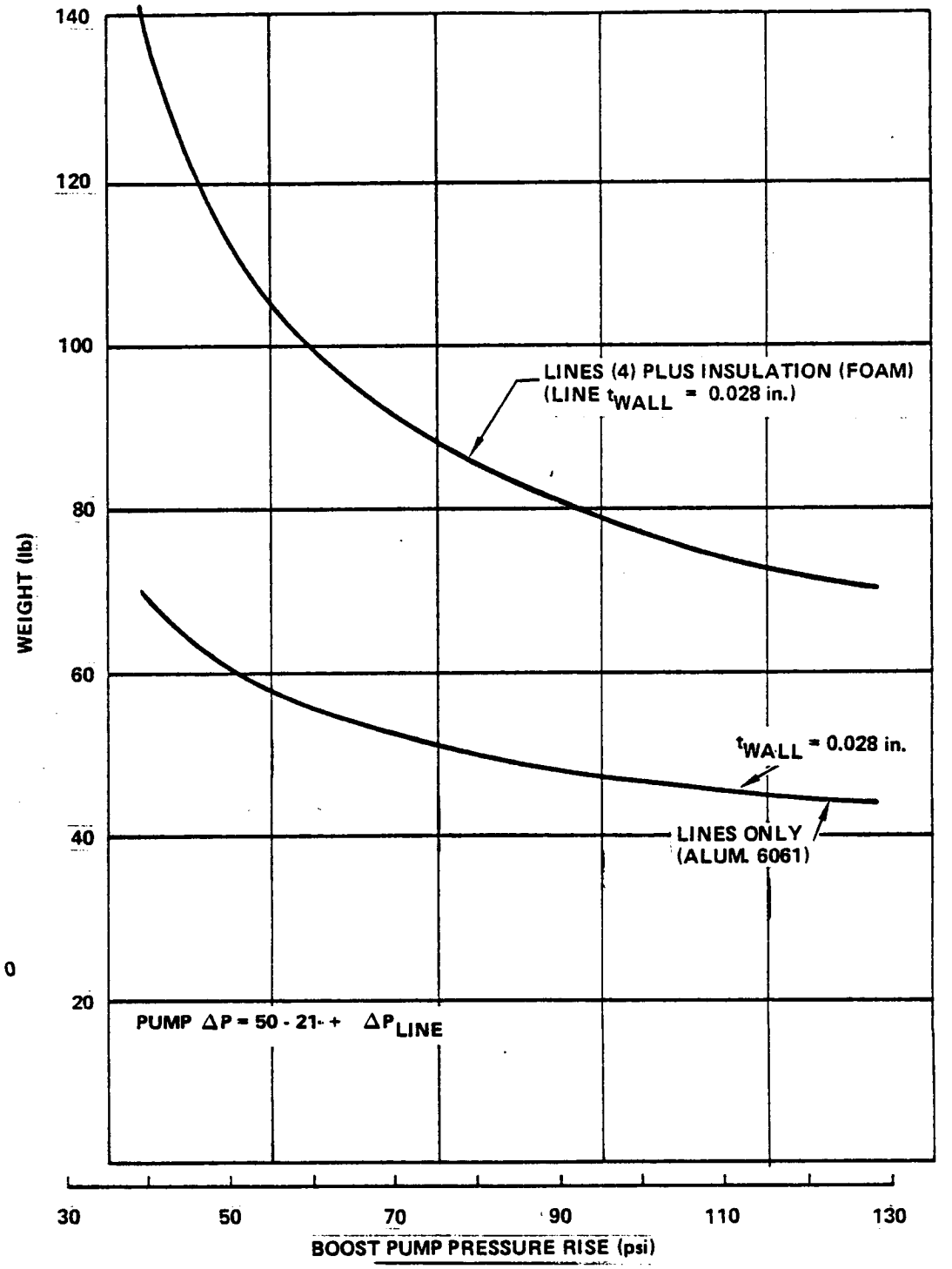

Figure 49. - Fuel feed line weight requirements.

5.2.2.2 Line configurations:

Vacuum jacket insulation: The inner line is wrapped with approximately 20 alternate layers of fiberglass cloth and aluminized mylar. The mylar acts as a radiation shield and the fiberglass prevents contact between the mylar sheets. Commercial manufacturers of cryogenic piping have found that vacuum insulated lines without radiation shields lose significant amounts of heat through radiative mechanisms. The space between the inner and outer lines is vacuum pumped to approximately 1 micron.

Line wall thickness calculated from flow pressure or minimum handling gage (Sec. 5.2.3) determines the tubing weights. However, the values chosen have been called into question during discussions with one manufacturer of cryogenic piping with whom the problem was discussed, CVI Corporation. CVI recommends somewhat thicker walls for three reasons: easier fabricability, easier repair, and greater structural strength. CVI suggested inner and outer wall thicknesses of 0.035 and 0.048 inch respectively, compared to Rocketdyne's estimates of 0.012 and 0.025 inch. However, CVI's experience lies primarily in the area of nonflight weight systems produced without advanced welding techniques. CVI's general concern must be considered, however. Therefore, a recommended technology effort for subsequent work includes fabrication, testing, and repair of flightweight cryogenic lines to establish minimum wall thicknesses that may be utilized for an operating system.

It is expected that the greatest stress loadings will be experienced by the outer line. A technique for wrapping the outer line with a nonmetallic composite material reinforcement may allow simultaneous reductions in weight at a fixed strength level and also a backup insulation system. In a NASA-funded study, engineers at Martin-Marietta Corporation showed that serviceable cryogenic lines could be constructed by wrapping thin metallic tubing with glass-fiber reinforcement. The metallic tube carried the cryogenic fluid, while the wrapped reinforcement provided both strength and thermal insulation. If the outer vacuum jacket were wrapped with glass reinforcement, the single wrap could act both as a reinforcement and as a backup insulation.

Another option for the outer jacket is the use (for all or part of the outer jacket) of semi-flex line. This approach would eliminate differential thermal expansion problems.

Provision of a 1 micron vacuum in the vacuum annulus may be accomplished in either of two ways; first, each fuel line could consist of a single annulus extending the entire length of the line. This annulus would be pumped by an onboard vacuum pump or by periodic pumping by ground-based equipment. Alternatively, the annulus could be pumped down and sealed during assembly and again only if measurements indicated a vacuum leak. Second, the vacuum line could be built from independent stand-alone units. Again, the individual segments, or spools, could be pumped by onboard or ground-based pumps, or they could be pumped out and sealed when constructed.

The spool approach is recommended due to its greater reliability. In the case of a single vacuum annulus, a single large leak imposed by some accident during flight could conceivably disable that fuel line. Further, vacuum pumping of a thin annulus is very slow, requires a large pump, or may require an extensive network of pumping lines throughout the aircraft. For the spool approach, as discussed in Section 5.6, loss of vacuum on a single spool will not cause vaporization of the fuel that passes through the spool. Thus, a single spool failure does not endanger the aircraft at any point of the flight profile.

Foam insulation: The foam insulation approach offers several distinct advantages compared to the vacuum approach principally in the areas of safety and reduction of technical complexity. From the standpoint of safety, foam insulation is not lost by catastrophic failure of spool sections, and the presence of the foam protects the inner fuel line from damage during handling and normal operations. Foam-insulated lines also present significant advantages in manufacturing and maintainability. Vacuum spool sections must be fabricated as complex double-concentric units and pumped at the fabrication or installation points. Construction for foam lines is much simpler: individual single tubes can be welded together and then covered by a foamed-in-place insulation cover. Repair is accomplished simply by cutting and removing the foam, repairing the inner line, and refoaming an insulation layer. Foam layers must be protected against the phenomenon of cryopumping, in which condensation of gases within the foam cells eventually degrades the insulation properties. Lightweight, metallic coverings can successfully protect against cryopumping problems. An additional advantage of foam is the elimination of one type of thermal expansion problem. For a concentric-tube vacuum insulation system, the differential contraction between the cold inner line and the warm outer line can be sufficient to damage the lines in the absence of a bellows in one of the lines to absorb the change in length. In current practice, no provision for differential thermal contraction is provided for foam-insultated lines, since the foam cells are sufficiently resilient to expand and compress to absorb the length change. Thus, the only thermal contraction which need be considered is the net length change of the metallic inner line. This effect is discussed in Section 5.2.3 below.

The only possible disadvantages of foam are weight, fire resistance, and long-life embrittling. Foam is expected to be 25 percent heavier than a vacuum line on per foot basis, but the elimination of complex spool connections should essentially offset weight penalties. Care must be taken that the foams selected for use are resistant to burning in short, relatively intense hydrogen fires. Finally, many existing foams tend to become embrittled during long exposure to cryogenic temperatures. At the present time, no known foams are completely unaffected by such conditions. Long-life foam development programs are presently underway, and it is expected that by 1955 fully stable foams will be available.

It is concluded that a foamed-insulated cryogenic piping system of the type is the most likely choice for use in the hydrogen powered aircraft. A further comparison of foam versus vacuum lines is presented in Sect. 5.6.2.

5.2.3 Design description. - This section includes discussion of materials for use in the fuel lines, thermal contraction, and weight.

5.2.3.1 Materials selection: Liquid hydrogen feed system materials which have been utilized successfully at Rocketdyne are summarized in Table 19. The cast aluminum alloy (Tens-50) and the highly alloyed stainless steel (A-286) materials are utilized mainly for fittings, valve bodies, or other complex shapes. The candidate materials for feed lines are the wrought aluminum (6061) alloy and 321 stainless steel. Use of a working-stress level equal to the lower value of either one-half of yield or one-fourth of ultimate strength results in the aluminum alloy having the highest strength-to-weight ratio. Because of its much lower thermal conductivity and thermal expansion characteristics, 321 stainless steel was chosen for the inner line. 6061 aluminum was used for the outer line.

5.2.3.2 Thermal contraction provisions: Two types of thermal contraction must be considered for lines which experience temperature changes from ambient to cryogenic temperatures. First, the overall length of the line may change, thereby affecting the system geometry and line-attachment provisions. This length change is on the order of 10×10^{-6} in/in/C, or 1.8 in for a 50 foot run of line cooled from ambient to cryogenic temperatures. Practically, this length change may be rendered harmless through the provision of sufficient bends in the line, a line-space envelope which allows the normal portion of the bend to absorb the length change elastically, and compliant mounting provisions (such as a cable-tray type of approach to supporting the fuel lines). Bellows might be provided where necessary, but normal practice has shown that the provisions suggested above are sufficient under ordinary operating conditions.

The second type of thermal contraction problem is the differential thermal expansion between the inner and outer lines. When the inner is cooled from ambient to cryogenic temperature and the outer line remains at essentially ambient temperature, differential thermal strains may be developed. For the case of foam-insulated lines, current practice with long, large diameter lines in the Space Shuttle has shown that thermal strains are accommodated without any need for special provisions such as bellows. Vacuum-insulated lines, on the other hand, generally require some type of mechanical strain-absorbing element such as a bellows. In addition, special configurations of foam-insulated lines may require large-deflection capability, so bellows arrangements were investigated for this application. Rocketdyne has extensive experience in cryogenic-line applications for rocket engines, such as the

TABLE 19. - CANDIDATE MATERIALS FOR LIQUID HYDROGEN APPLICATION (-423°F)

Material	Density (lb/in^3)	Yield Stress (psi)	Ultimate Stress (psi)	*Working Stress (psi)
Tens-50 Aluminum - Cast	0.096	54 000	66 000	16 500
6061 Aluminum - Wrought	0.096	46 000	60 000	15 000
321 Stainless Steel	0.286	43 000	190 000	21 500
A-286 Stainless Steel Machined	0.287	130 000	198 000	49 500

*Working Stress = Lower value of either 1/2 yield or 1/4 ultimate stress

Space Shuttle Main Engine. The general approach for insulation in the engine system is to apply foam over exposed lines, joints, valves, etc., wherever possible. Because the engine operates intermittently and then at very high fluid-flow rates, more efficient insulation approaches were rejected due to weight or complexity. A prime purpose for covering the exposed surface is preclusion of formation of LOX that could lead to an engine fire, and foams are effective in this role.

At some locations, however, foams cannot be used. The rocket engine is gimballed, and the cryogenic transfer lines must incorporate sufficient flexibility to permit several degrees of rotation. The bellows units are double walled with insulation provided by a vacuum in the annulus. This vacuum is produced by pumping the annulus to 1 micron, backfilling with pure argon gas, and sealing. When cryogenic fluid flows in the lines, the argon liquifies and a vacuum is produced. To achieve 1 micron vacuum in a bellows unit that has many slowly pumping regions requires several days of laboratory pumping, and the approach chosen allows attainment of a good vacuum without requiring heavy on-board pumping equipment. All lines and bellows are welded wherever possible.

5.2.3.3 Fuel feed line weight: Minimum fuel line wall thickness can be estimated from the hoop stress produced by the contained fluid, using the relation:

$$t = \frac{Pd}{2\sigma_w}$$

where

t = wall thickness

P = internal pressure

σ_w = working stress

and prior experience for line fabricability. In the case of the selected concept which uses a tank-mounted boost pump, the hydrogen pressure levels are so low (approximately 46 psia) as to result in unrealistically thin walls (approximately 0.001 - 0.003 inches) if only hoop stresses are considered. Rocketdyne manufacturing experience and Lockheed CL-400 experience indicate minimum wall thickness of 0.016 inch are required for practical considerations.

For the inner fuel-containment line, 321 stainless steel was chosen because of its thermal properties and because of ease of fabrication and welding, as well as proven structural integrity. 6061 aluminum was chosen for the outer line because of weight saving and compatibility with liquid hydrogen. Table 20 summarizes line-only and line-plus insulation weights. It is noted that the total weight of vacuum insulated line is only 10 pounds, or 3.4 percent less than foam-insulated line.

TABLE 20. - LINE WEIGHT SUMMARY

	Weight per Foot (lb)	Total Feed System Weight (596 ft) (lb)
Inner Line (0.016 Stainless Steel, 1.0 inch o.d.)	0.18	107
Outer Line (0.016 Aluminum, 4 inch o.d.)	0.23	137
Total	0.41	244
Insulation Weight		
Foam		50
Vacuum		40
Total Weights		
Foam		294
Vacuum		284

5.2.3.4 Fuel line summary: The selected fuel line configuration is summarized in Figure 50. Although vacuum insulation saves a small amount of weight in the fuel-line, the foam insulated line is selected due to safety, manufacturing, and repair considerations.

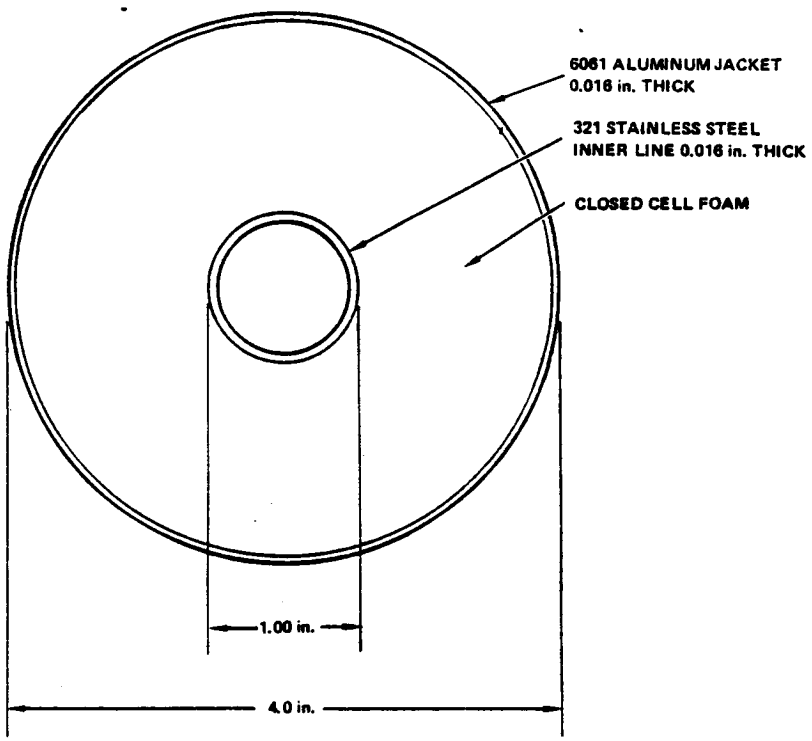

Figure 50. - Selected fuel-line configuration.

5.3 Boost Pump

In the fuel-system optimization effort (Sec. 5.1.2), it was determined that the boost pump should provide a minimum 46 psi boost over the entire range of fuel-flow, as specified in the schedule of Table 18. The objective of the boost pump design effort was to select the most attractive pump within

this constraint and other design requirements detailed in Sec. 5.3.1. This pump should not only attain minimum incremental ΔDOC, but it should also be amenable to long-life and easy maintenance in airline operations. It has been determined that two- or three-stage centrifugal pumps operating at speeds up to 36 000 rpm are the leading candidates for this application. However, there is no data for the operation of this or any other type of flight-weight pump in liquid hydrogen for times approaching the 8 000 hours desired for airline operations. Development of long-life, reliable cryogenic pumps of this type appears to rest on development of satisfactory bearings.

5.3.1 Design requirements. - The design philosophy for the boost pump system is based upon the premise that a single pump failure shall not compromise aircraft safety. In addition, aircraft operators are reluctant to ground an aircraft if one boost pump in any of its fuel tanks is incapable of being operated. In accordance with this philosophy, each tank in the hydrogen-fueled subsonic transport will incorporate a minimum of three boost pumps. The justification for this conclusion is discussed in the following paragraphs.

Although hydrocarbon-fueled aircraft can takeoff and climb to cruise altitudes with boost pumps inoperative most of the time, hydrogen-fueled aircraft engines would flameout if the boost pumps failued, due to vaporization in the line with loss of pressure. Hence, the boost pump system must entail a redundancy which precludes loss of thrust from any engine in the event of pump failure immediately after the aircraft becomes airborne. During takeoff and initial climb, this philosophy dictates that one tank supplies one engine and that two pumps in each tank must be operated simultaneously. Thus, with two pumps operating, a single boost pump failure just after takeoff could not cause a loss of engine thrust. The redundancy requirement further dictates that no two pumps within a given fuel tank can be supplied electrical power from the same source.

The above requirements indicate that each pump must be capable of supplying fuel at the pressure and flowrate required by one engine at the maximum flow condition which occurs during sea level climb operation. To permit engine performance growth without the necessity of redesigning the engine pumps, a margin of 10 percent excess capacity has been specified in the pump functional requirements. A draft of a general functional requirement specification for a pump system is shown in Table 21.

TABLE 21. - FUNCTIONAL REQUIREMENTS

Title:	Pump, Fuel Boost, tank-mounted, Plug-in Motor Driven
1.	Scope
	This document defines the functional requirements for a submerged, motor driven, liquid hydrogen fuel boost pump. The pump shall have provisions for quick removal and replacement from the tank without having to remove fuel, plumbing, or electrical wiring from the aircraft.
2.	Applicable Documents
	(to be added)
3.	Requirements
3.1	Ports
3.1.1	Discharge - The discharge port shall be a four bolt flange type sized for one inch tubing.
3.1.2	Pressure Sensing - Pressure sensing bosses shall be provided at each pump for sensing discharge pressure.
3.2	Lubrication - The pump and its driving motor shall be lubricated with a system compatible with hydrogen.
3.3	Pump Housing - A pump housing shall be provided which permits removal of the pumping element and driving motor without requiring that fuel be removed from the tank during the operation.
3.4	Check Valves - Check valves shall be provided in the inlet and discharge passages of the pump housing such that no fuel leakage can occur when the pump elements are removed.
3.5	Thermal Relief - The pump discharge check valve shall have a small hole vented to the tank to provide thermal relief.
3.6	Electrical -
3.6.1	Power - The pump motors shall be "Y" connected and shall be rated for continuous duty at 115/200 volts, 3 phase, 400 Hertz, or as an alternate, 270 V dc power.
3.6.2	Power Consumption - The power consumption shall be optimized for the cruise operation.

TABLE 21 Continued

3.6.3 Electrical Connection - The electrical connection between the removable element and the pump housing shall be automatically disconnected concurrently with removal of the pumping element and the motor subassembly.

3.7 Performance -

3.7.1 Fluid - The pump shall be compatible with liquid hydrogen fuel.

3.7.2 Operating Pressures - The pump inlet and discharge pressures shall be in accordance with the requirement of Figure ___

3.7.3 Flowrate - The pump flow requirements shall be as dictated by Figure ___.

3.7.4 Environment - The pumping element, housing and driving motor shall be capable of operating in an environment established by the presence of liquid hydrogen stored at a pressure of 145 kPa (21 psia) absolute.

3.7.5 Priming - The pumping element shall be capable of priming itself if initially filled with gaseous hydrogen at start up.

3.7.6 Maximum Pressure - The maximum pressure output of the pump under any condition shall be compatible with the limitations of the engine systems.

3.8 Reliability -

3.8.1 MTBF - The mean time between failures per element shall not be less than 2500 hours using the definition:

$$\text{MTBF} = \frac{\text{(Cumulative Flight Hours) (No. of Units/Aircraft)}}{\text{Cumulative Number of Chargeable Failures}}$$

3.8.2 TBO - The scheduled time between overhauls shall not be less than 8 000 flight hours.

3.8.3 Shelf Life - The unit shall have a shelf life of not less than 5 years with a capability of immediate service.

3.8.4 Safety - Safety concepts and design features shall be incorporated in the pump and drive design. The pump shall be capable of operating dry in a hydrogen gas environment without hazard.

3.9 Pump Mounting Attitude - The pump assembly shall be mounted vertically with the pump inducer located at the low point in the storage tank.

During cruise, when fuel flowrates and the hazard resulting from engine flameout are considerably reduced, each pump must be capable of supplying two engines by means of crossfeed for added redundancy and to reduce electrical power requirements if the operator chooses.

Boost pump performance requirements were determined from the flow-pressure requirements of Table 18 and as a result of the concept selection trade described in Section 5.1.2. The flow-pressure schedule is an unusually wide range from the standpoint of throttling of the pump output, and this factor has influenced pump selection considerably. The performance of the boost pump must be matched to that of the engine-mounted main pump since no engine-to-tank return line is provided in the hydrogen aircraft. The boost pump must provide a minimum NPSP of 0.5 psi to the engine-mounted pump with minimum weight and power consumption.

Other design requirements are determined from the intended mission of the pump system within the aircraft. The pump must be designed for long life, 8 000 hours being the baseline goal. The bearings must operate in LH_2 or, alternatively, an acceptable thermal isolation system must be found. The pump drive must operate on available aircraft power systems. Several candidates were considered, but the choices soon narrowed to electrically driven pumps. For the evaluation performed here, two aircraft electrical systems were considered. Present conventional systems utilize 400 cycle power. It is projected that by 1995 commercial aircraft may utilize 270 volt DC power systems, which have considerable advantages for aircraft applications. Both of these electrical systems were considered, and the details are given in Section 5.3.3. The tank-mounted boost pump must be safe in operation and easily maintainable. The manufacturing costs should be as low as possible consistent with meeting other operating needs. Finally, the boost pump must meet all general requirements of FAR 25.

5.3.2 Candidate pump types. - Four basic candidate pump types were considered: inducer, vane, piston, and centrifugal. In preliminary calculations, tandem row inducer pump designs were shown to have the lowest values of ΔDOC. However, at the minimum flow condition (flight idle at 38 000 feet and M = 0.85), they did not deliver enough pressure rise to meet the specified main pump NPSP (pressure above vapor pressure) requirement of 0.5 psi. This pressure rise might have been met by using the wide range, tandem row inducer design along with 50 percent flow recirculation around the motor-boost pump unit. However, this would result in a pump inlet vapor volume fraction that might be too high for the pump to operate because an inducer pump cannot pump two-phase flow if the inlet flow coefficient is too far off design. This, in combination with the fact that such a design would have to approach an unstable operating condition (which occurs in an axial pump that is operated at too low a flow) in order to meet the NPSP requirement, resulted in a decision to use a pump design with a wider operating range capability.

Positive displacement pumps would have design rotational speeds less than 10 percent of those of centrifugal or inducer pumps and, therefore, would be

too heavy for this particular combination of head rise and volume flowrate. Included in this positive displacement category are piston pumps and vane pumps. Additionally, positive displacement pumps typically have large surface areas that require some lubrication. This requirement would likely reduce operating life significantly, since liquid hydrogen is not a good lubricant. For these reasons, vane and positive displacement pumps were not considered further. The only remaining candidate is the centrifugal pump, with its wide operating range, forgiving stall characteristic, and relatively small lubrication requirement. Constant-speed and variable-speed centrifugals were evaluated as to ability to meet flow requirements and ΔDOC minimization. This evaluation is described in detail in Section 5.3.4.

For centrifugal pumps that are designed for maximum efficiency, the performance characteristics are shown parametrically in Figure 52 for design point operation (sea level climb at M = 0.38) and Figure 53 for minimum flow operation (flight idle at 38 000 feet and M = 0.85). It is apparent that stage numbers and design speeds can be varied over wide ranges to give whatever combination of characteristics is desired.

From Figure 52, it is apparent that, in this rotational speed range (less than 40 000 rpm to obtain an inlet diameter greater than 1 inch so as to pass the flow), multistaging is necessary in order to operate down to shutoff (P_m > 50 psi). With these high efficiency types of designs, operation down to shutoff is possible if the stage specific speed is greater than about 3 000. However, this may be done at a stage specific speed of only 1 150 by designing specifically to obtain a wide operating range. This is achieved at the expense of approximately a 14 point penalty in efficiency. It may be concluded that simplicity can be achieved at the expense of performance. Since both objectives are of interest here, wide range designs as well as high-efficiency designs were investigated.

5.3.3 Candidate pump drive systems. - Hydraulic, engine bleed air, and electrical pump drives were initially considered. Preliminary calculations showed that the fluid line and system weights necessary for the first two choices for use with remotely-located tank-mounted boost pumps were prohibitively high so that the choice was narrowed to an electrical drive. The aircraft electrical system may be either the standard 400 cycle ac system or a 270 volt dc system that has shown promise for future aircraft applications. Special controls are required if variable speed is to be used, whereas they are not if constant speed (which requires pump operation nearly down to shutoff) is to be used.

Brushless motors were assumed for the 270 volt dc case. The weights of these motors are shown in Figure 54 along with the weights of the corresponding electronic equipment required to operate a brushless motor over infinite ranges of torque and speed. In Figure 55 these motor and electronic equipment weights are summed to give the overall brushless motor assembly weights. For this brushless motor data, four additional assumptions were made: (1) the stator is hydrogen cooled to reduce resistance and, consequently, size

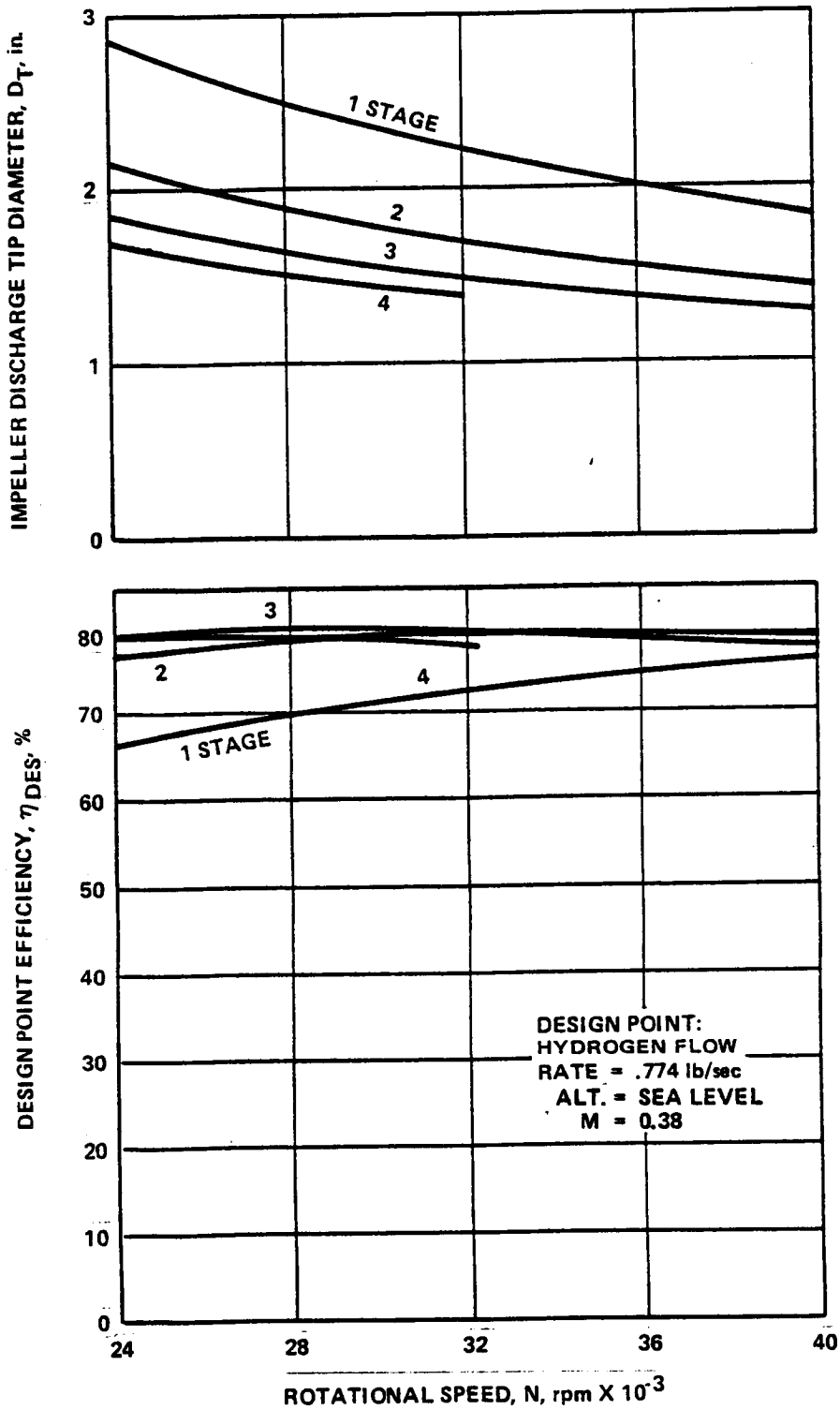

Figure 52. - Design point performance for centrifugal pumps designed for maximum efficiency.

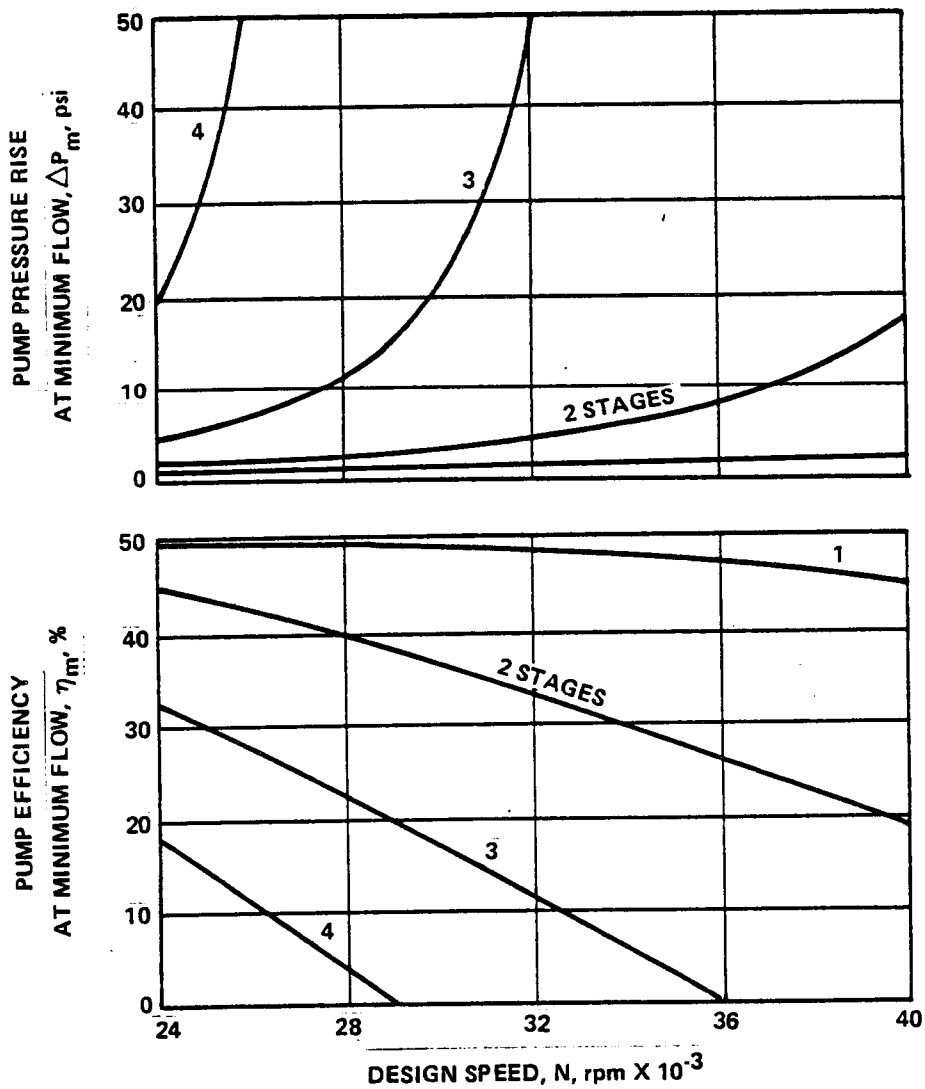

Figure 53. - Off design performance for centrifugal pumps designed for maximum efficiency.

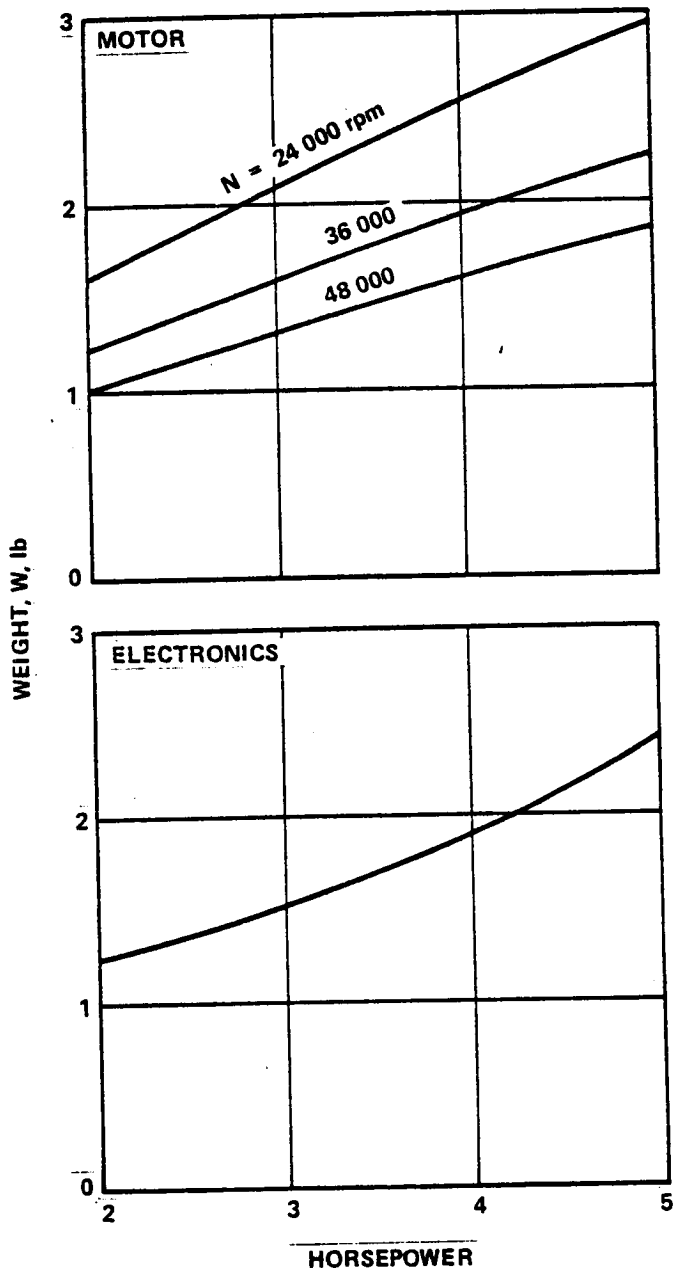

Figure 54. - 270 V brushless dc motor weight breakdown.

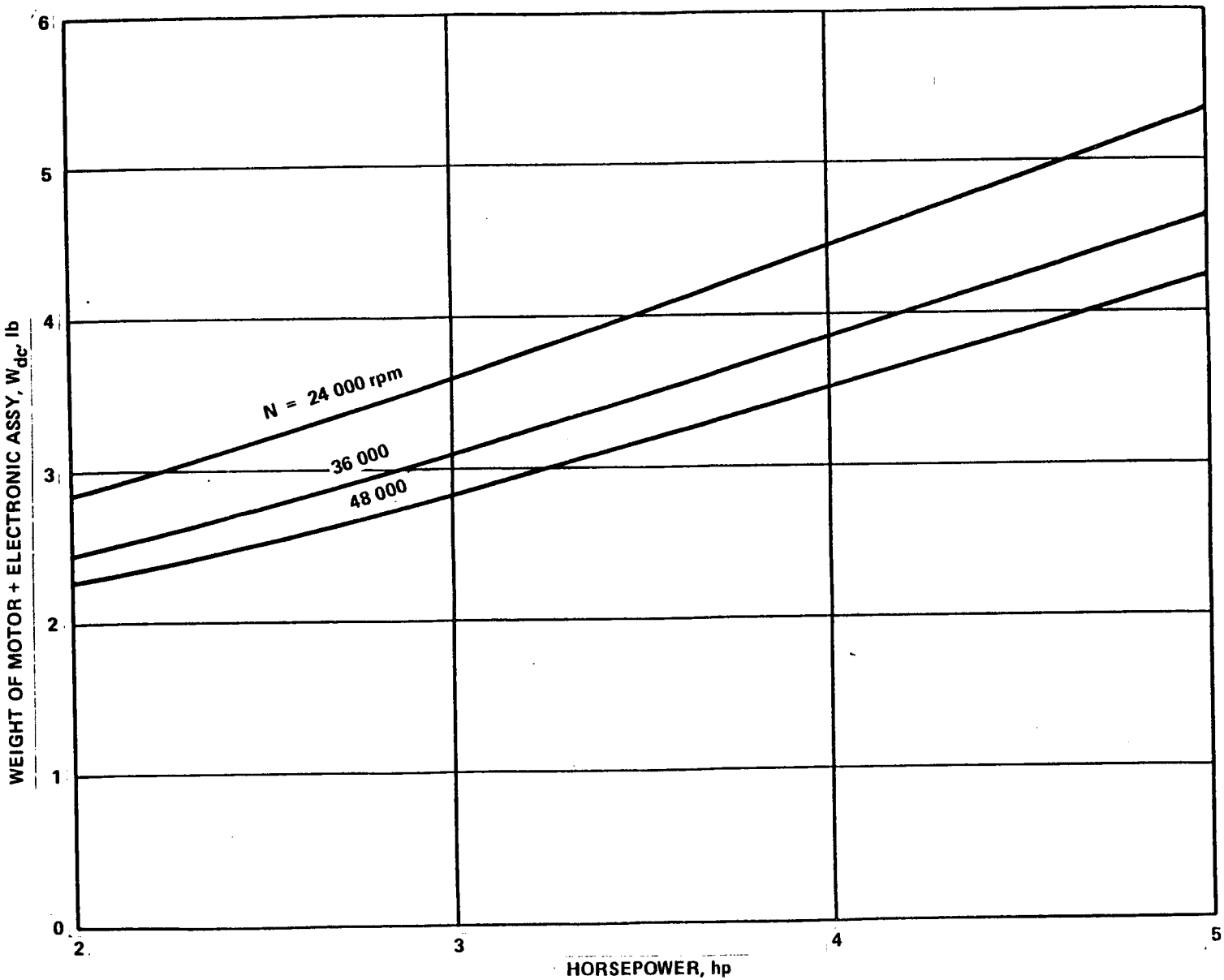

Figure 55. - 270 V brushless dc motor weights - includes weight of electronic assembly.

and weight, (2) there is no fluid in the air gap between the rotor and the stator, (3) hydrogen cooling does not result in any hydrogen vaporization, and (4) electro-magnetic interference is suppressed to existing military standards. Regarding these assumptions, it must be noted that keeping the hydrogen out of the air gap may be difficult to achieve and, in fact, may not even be desirable. Further investigation and, possibly, some technology efforts are required to establish the proper approach.

For 400 cycle ac motors, the weights for 24 000 rpm, 2 pole, constant speed motors are shown in Figure 56. If variable speed is desired, a rather large inverter weight must be added. This is also shown in Figure 56. Finally, the efficiencies of these motors are shown in Figure 57. Due to the electronic equipment losses, a brushless dc motor is slightly less efficient than a constant speed ac motor. However, if an inverter is used to make the AC motor variable speed, the large losses in the inverter drop the overall efficiency more than 10 percentage points. This is also shown in Figure 57.

5.3.4 Boost pump and drive candidate evaluation. - In order to evaluate candidate pumps, alternates must first be sized to meet the required flow conditions.

5.3.4.1 Pump sizing: The pump inlet diameter requirement in the tank was determined from isentropic equilibrium expansion (from a saturated liquid) curves for hydrogen (Figure 58) and the maximum hydrogen flowrate per engine of 0.774 lb/sec. The resulting line size requirements are shown in Figure 59 as a function of tank vapor pressure and pump inlet vapor volume fraction (assuming the flow has reached equilibrium). As shown, a one-inch diameter hole will pass the flow at a low vapor fraction for a tank vapor pressure of 21 psia. Since this is about as small a pump inlet as is practical from a manufacturing standpoint, this value was used throughout the pump selection procedure.

5.3.4.2 Pump selection: Six pump-drive combinations were investigated. As shown in Table 22 three were analyzed with ac motors and three were analyzed with dc motors. Within each motor category, two of the combinations used constant speed motors because there are two methods for obtaining throttling down to shutoff; (1) using a single stage, wide range pump (which has a lower efficiency), and (2) using a multistage, high efficiency pump. The other combination within each motor category used a variable speed motor and, since variable speed reduces the required number of stages, a high efficiency type pump.

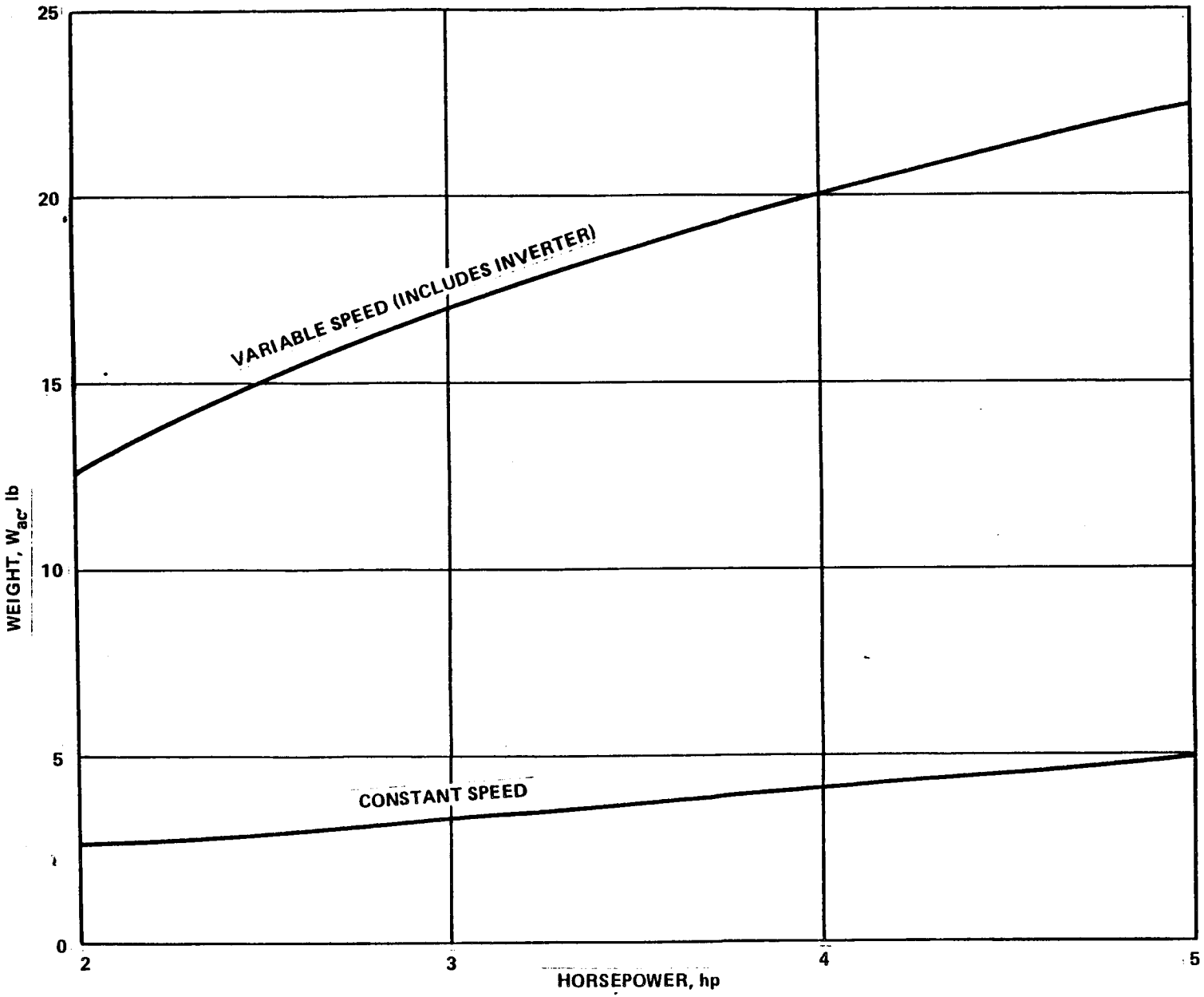

Figure 56. - 400 Cycle ac motor weights - 24 000 rpm, 2 pole.

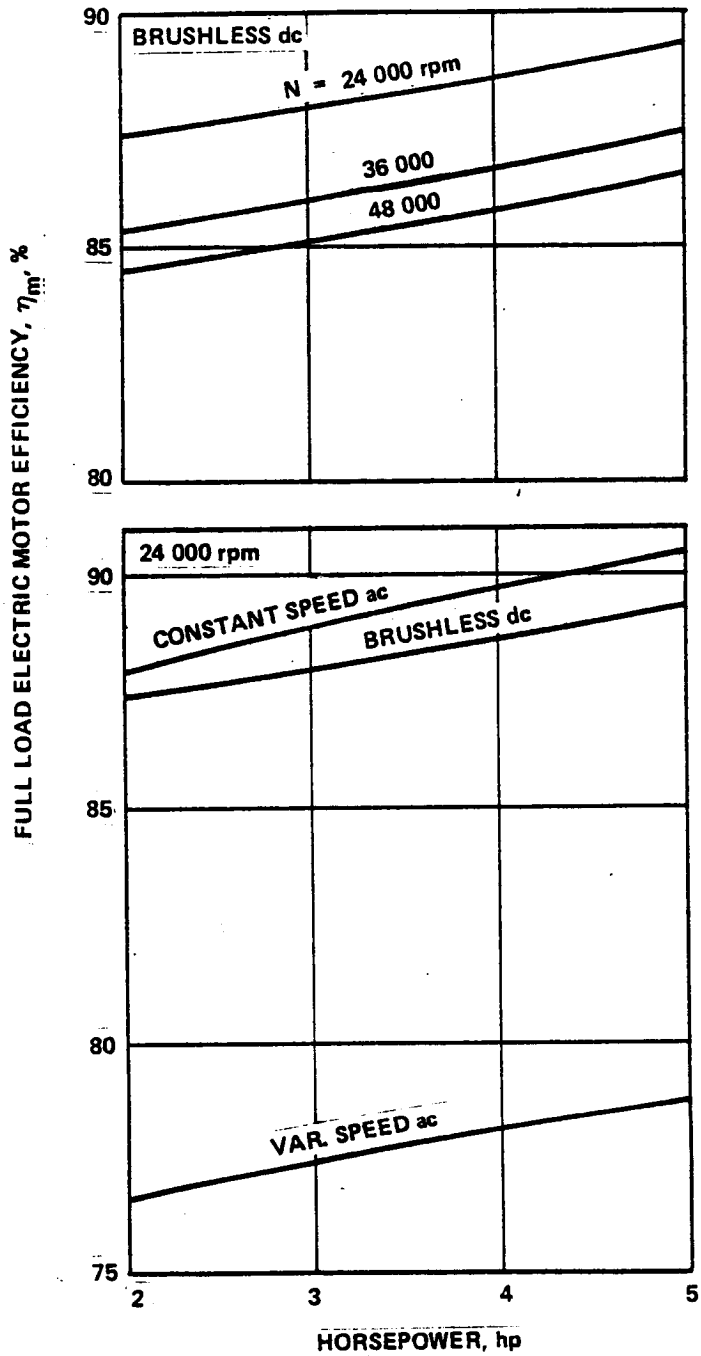

Figure 57. - Electrical motor efficiencies at full load.

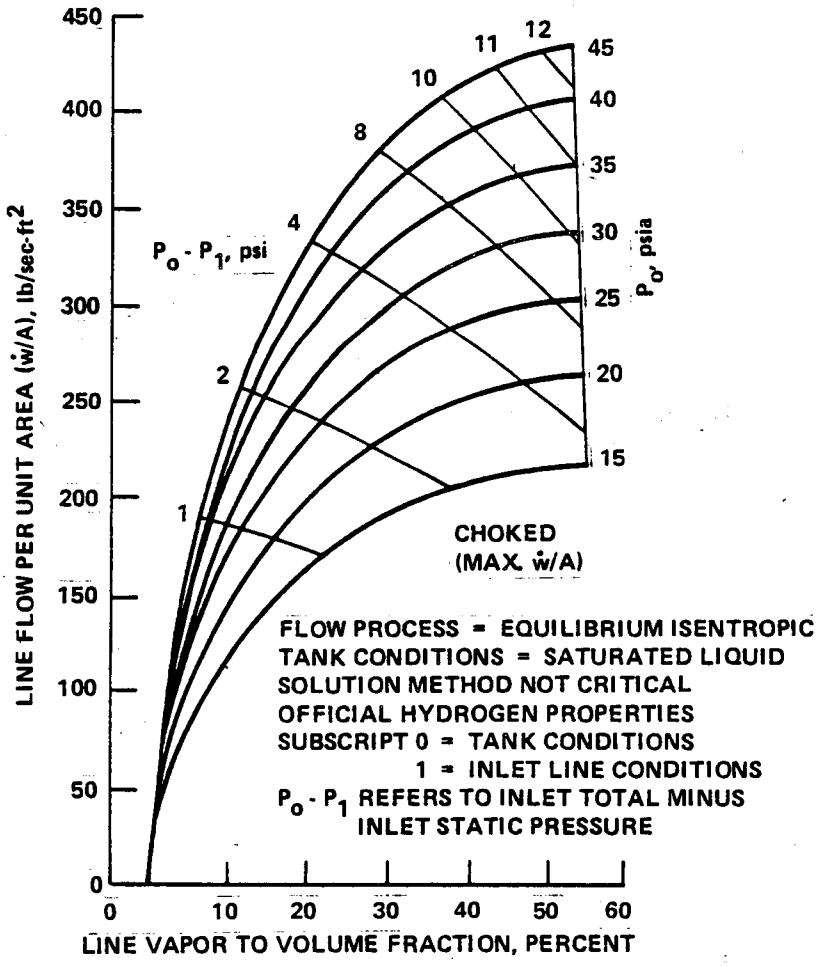

Figure 58. - Zero NPSH pumping capability requirements for hydrogen.

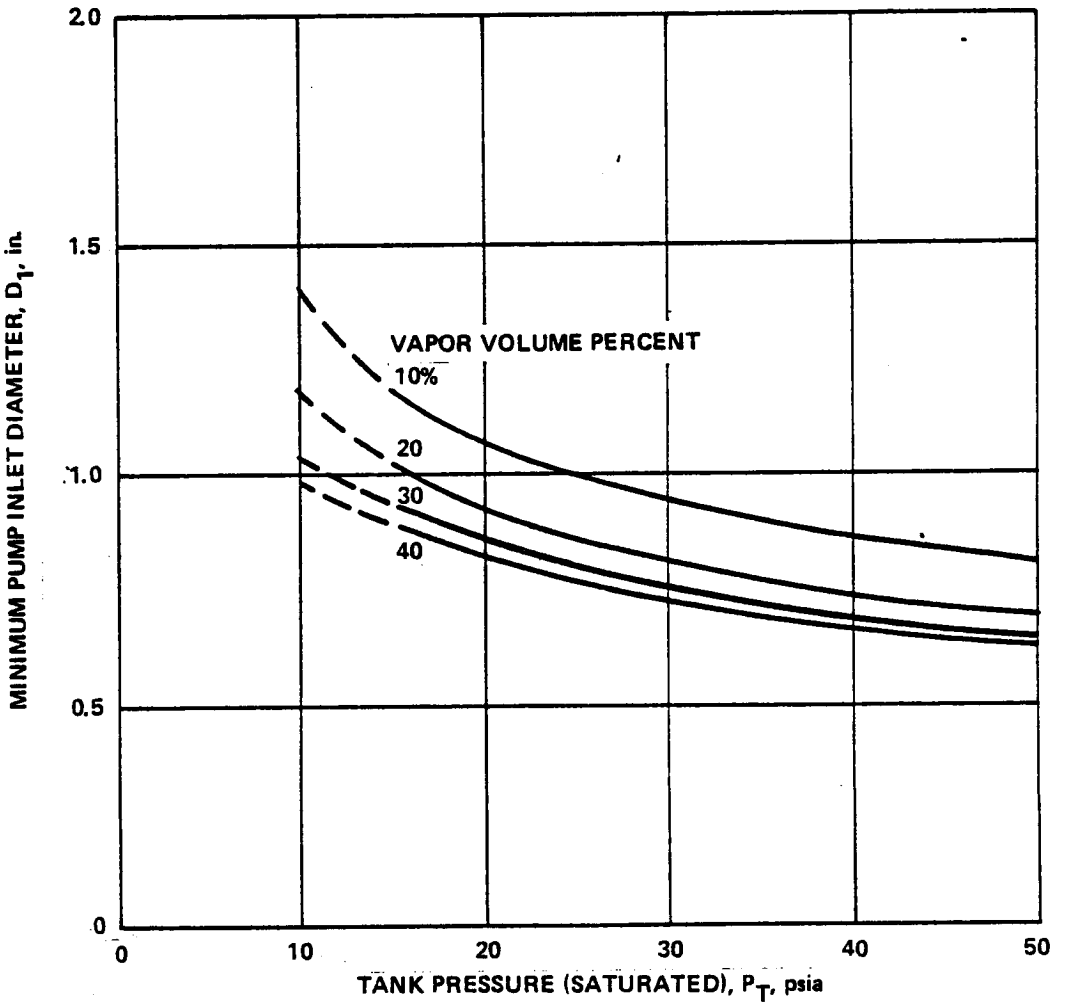

Figure 59. Boost pump inlet diameter requirements.

As shown in the last data block (Minimum Flow) in Table 22, all the constant speed designs delivered a high pressure rise of 62 psi during minimum flow operation. This high pressure rise provides more than enough net positive suction pressure (NPSP, pressure above the vapor pressure) to meet the main pump requirements. However, with a variable speed boost pump, the boost pump speed can be adjusted so that the pump puts in only enough pressure (approximately) to meet the main pump NPSP requirements. As shown, this was assumed for the two variable speed cases (configurations 3 and 6 in Table 22). This is also true during cruise. As a result, the boost pump power requirements are lower for the variable speed cases during off design operation. However, in the analysis that was made, the main pump was assumed to be independent of the boost pump discharge pressure during cruise operation, as is also shown in Table 22. As a result, the main pump discharge pressure probably exceeds the cruise requirements for the cases in which a constant speed boost pump is used. In these constant speed boost pump cases, variable speed main pumps would have to be used in order to match with the boost pump during both design and cruise operation. In summary, exact matching between the boost and the main pumps can be achieved only if one of the two pumps has a speed that can be set independently.

As shown in Table 22, configuration 2 (a 5-stage pump driven by a constant speed motor) has the lowest direct operating cost (ΔDOC) of the ac driven candidates and configuration 6 (a 2-stage pump driven by a variable speed motor) is best for the DC candidates. Configuration 3, which has a variable speed ac drive, cannot compete with configuration 2 because the frequency converter required to obtain variable speed with ac is very heavy. This is not true with DC because the converter is much lighter for dc and because it is required for both constant and variable speeds. As a result, the variable speed drive (configuration 6) was the best with dc. Also shown is that the use of wide range, single stage pumps to obtain simpler configurations results in a decrease in pump efficiency and, consequently, an increase in operating cost. This is particularly true with ac where the lower design speed results in a lower single stage pump specific speed which, in turn, results in a greater pump efficiency penalty.

Because the minimum allowable boost pump pressure rise during minimum flow operation was originally unknown, several variable speed designs, each with a different pressure rise at the minimum flow condition, were analyzed to determine their pump and motor efficiencies during minimum flow operation. The results are summarized in Table 23. These data, in turn, were used in a heat transfer analysis to determine the resulting NPSP's delivered to the main pump. Of the candidates listed in Table 23, the one with the lowest ΔP minimum (5 psi) delivered 0.9 psi NPSP to the main pump, which exceeds the requirement. All of the other designs had even high NPSP's. As a result, the variable speed configurations in Table 22 (configurations 3 and 6) will meet the main pump NPSP requirements. It is of interest to note that the second configuration in Table 23 (ΔP_{min} = 10 psi, N = 37 200 rpm) would supply more NPSP to the main pump than configuration 6 in Table 22, and would have ΔDOC that would be slightly less. The only drawbacks would be a somewhat higher speed and a somewhat smaller size, which could affect life and ease of fabrication somewhat.

TABLE 22. - ELECTRIC DRIVEN BOOST PUMP CANDIDATE SUMMARY

General	Configuration	1	2	3	4	5	6
	Speed	Const.	Const.	Var.	Const.	Const.	Var.
	Current	400 Hz AC	400 Hz AC	400 Hz AC	270 V DC	270 V DC	270 V DC
	Sync with source current	Yes	Yes	@ Design	No	No	No
	No. of pump stages	1	5	3	1	3	2
	Freq. conv./speed control	No/No	No/No	Yes/Yes	Yes/No	Yes/No	Yes/Yes
	ΔDOC, ¢/seat n. mi.*	0.00158	0.00134	0.00151	0.00139	0.00132	0.00127
Weights	Boost pump	9.64	2.58	2.83	2.10	1.12	1.50
	Boost motor	4.20	3.00	2.95	1.60	1.49	1.60
	Frequency conv.	0	0	12.75	1.62	1.44	1.44
	Total boost	13.84	5.58	18.53	5.32	4.05	4.54
	Line	29.3	29.3	29.3	29.3	29.3	29.3
	Main pump	25.0	25.0	25.0	25.0	25.0	25.0
	Total (2 boost)	82.0	65.5	91.4	64.9	62.4	63.4
Design (Max, hp - S.L. Climb @ M = 0.38)	Flow, $\dot{w}$, lb/sec	0.774	0.774	0.774	0.774	0.774	0.774
	Pressure rise, ΔP, psi	46	46	46	46	46	46
	Speed, N, rpm	24 000	24 000	24 000	40 000	36 000	33 000
	Pump η, percent	50	78	79	64	78	78
	Motor η, percent	90	89	77	86	86	86
	Electrical hp	4.69	3.06	3.46	3.84	3.16	3.14
Cruise (M = 0.85 @ 38 000 ft)	Flow, $\dot{w}$, lb/sec	0.292	0.292	0.292	0.292	0.292	0.292
	Electrical hp	3.54	2.31	0.74	2.90	2.38	0.67
	Main pump hp	19.0	19.0	19.0	19.0	19.0	19.0
Min. flow (Flt idle @ 38 000 ft and M = 0.85	Flow, $\dot{w}$, lb/sec	0.051	0.051	0.051	0.051	0.051	0.051
	Pressure rise, ΔP, psi	62	62	5	62	62	5
	Speed, N, rpm	24 000	24 000	6 850	40 000	36 000	9 410
	Pump η, percent	6.4	9.9	32	8.2	9.9	32
	Motor η, percent	88	87	28	83	83	42
	Electrical hp	3.33	2.18	0.17	2.74	2.27	0.11

* On a per engine basis

TABLE 23. - EFFECT OF PRESSURE RISE REQUIREMENT AT MINIMUM FLOW ON PUMP DESIGN AND MINIMUM FLOW PERFORMANCE

$\dot{w}_{min}$, lb/sec	ΔP_{min}, psi	Number of Stages	N_{des}, rpm	N_{min}, rpm	Pump η_{min}, %	Motor η_{min}, %	$hp_{elec.\ min.}$
0.051	5	2	33 000	9 730	31	42	0.116
↓	10	2	37 200	15 060	24	55	0.23
	20	3	29 900	17 170	17	71	0.50
	30	3	31 000	21 900	14	77	0.84
	40	3	31 700	26 300	12	80	1.26
	62	3	36 000	10 600	9.9	83	2.27

Pump = Centrifugal Designed for Maximum Efficiency
Motor = Variable Speed, Brushless DC

5.3.5 Selected boost pump and drive system. - The selection of the final boost pump configuration is dependent on the engine pump and fuel control characteristics and is described in Section 5.6.

5.3.6 Boost pump mounting and changing tool. - An important part of this program has been to find a method by which the fuel pumps may be replaced quickly and safely, without requiring that the liquid-hydrogen fuel tank be drained. In this section, a configuration devised with this requirement in mind is described. Included are drawings and description of the physical configuration of the pump mounting, the method of changing the pump without draining the fuel tank, and a tool designed to accomplish the changing of the pump. Particular consideration has been given to ensuring the safety and reliability of the configuration and the method for changing the pumps.

Figure 60 shows the physical configuration of the pump mounting. Three pumps are placed on a single mounting unit. Since FAA regulations require that two pumps be operable for all takeoffs and landings, this choice allows continuation of missions where one pump has failed at some intermediate time. This capability is desirable, since all intermediate stops of a flight may not be equipped or convenient for changing a cryogenically cooled pump.

The pump and housing are shown in cross section in Figure 60. Each pump has its own inlet while the discharge is common for the three pumps. The pump cavity housing is roughly cylindrical with the inlet located at the bottom of the fuel tank, so that the fuel may be used entirely. Fuel enters at the pump inlet and passes through the inducer and three impellers and exits through a check valve into the fuel line leading to the engine. The check valve is provided to ensure that fuel will not be pumped in reverse direction through a pump(s) that is not operating.

The pump is contained within the housing by means of locking lugs. To change a pump the insulated panel covering all three pumps is removed and the pump changing tool shown in Figure 61 is secured to the pump housing external locking lugs. An "O" ring is provided to seal the tool to the pump lower housing surface. The helium lines are then attached to the pump changing tool, the GHe inlet valve and air escape valves opened and the changing tool (and new pump) purged of air. When this is completed, the GHe line is connected to the pump purge port located in the pump lower housing plate. The tool is then rotated 45° to disengage the lugs and the pump pulled down so that the pump inlet closure sleeve blocks the pump inlet thereby preventing the escape of the LH_2 in the tank. At this point the pump GHe purge valve is opened admitting GHe to the top of the pump, forcing the LH_2 trapped in the pump back into the tank via the small check valve and discharge passage in the pump housing. When this is complete, the operating handle is turned another 45° to disengage the closure sleeve locking lugs and the pump is completely withdrawn and placed on the carrier plate in the changing tool. The new pump is then moved into position by means of the carrier plate operating rod and the procedure reversed to replace the pump (no further purging is required however). The purging lines are then removed, the changing tool removed and the cover plate replaced. The fluid discharge and

electrical connections are made simultaneously during the final travel of the pump into its locked position. Since the new pump is warm and quickly cools to liquid-hydrogen temperature, the bellows-mounted seal is provided to absorb the thermal expansion of the pump during its temperature change. Such seals have proven effective on previous Rocketdyne pumps producing considerably higher pressure than the approximately 60 psi maximum required here.

This approach to an easily replaceable pump unit has several advantages. Because both the pump cavity and the pump-changing tool are purged, there is no chance foreign matter such as particulates or vapor that might condense or freeze at liquid-hydrogen temperatures can find its way into the pump cavity, even if the pump changing operation is delayed with the pump cavity exposed. Second, the proposed approach ensures the safety of the mechanic who performs the operation. Should there be any failure during the pump-changing operation, the tool prevents the escape of hydrogen that might injure the mechanic or result in a hazardous condition. Third, the mechanism of the pump-changing tool, together with appropriate guides built into the pump cavity ensures that the replacement pump will be inserted into precisely the correct position to seal with the bellows-mounted seal. Finally because the replacement pump is protected inside the pump-changing tool, there is little chance of its being damaged prior to insertion. All handling of the pump itself may be accomplished within a controlled workshop environment rather than on the field.

It is estimated that a pump may be changed in 10-15 minutes by means of the approach described here, by one or two mechanics. Because the tool may be constructed of aluminum alloy, it should weigh on the order of 20-pounds. Thus, the replacement pump and tool unit should weight approximately 30-pounds and may be carried by a single person. However, a second person may be required to attach the tool to the lower side of the fuel tank, particularly if the access is in an awkward position. The tool will become cold as the pump-replacement operation is conducted through its contact with the cold pump and the tank. Thus, the mechanic must take the precaution of wearing gloves during the operation, but no other special protection is required.

5.4 Engine Fuel Pump

The engine fuel pump requirements are to provide a high pressure rise and to comply with the severe demands of air transport service while operating in the liquid hydrogen environment represented by a low net positive suction head (NPSH), cryogenic temperature, and low viscosity. This section discusses the implications of these requirements for the engine pump, presents the more significant design trade-offs, provides the results of a selected design approach, and recommends certain items for advanced technology development.

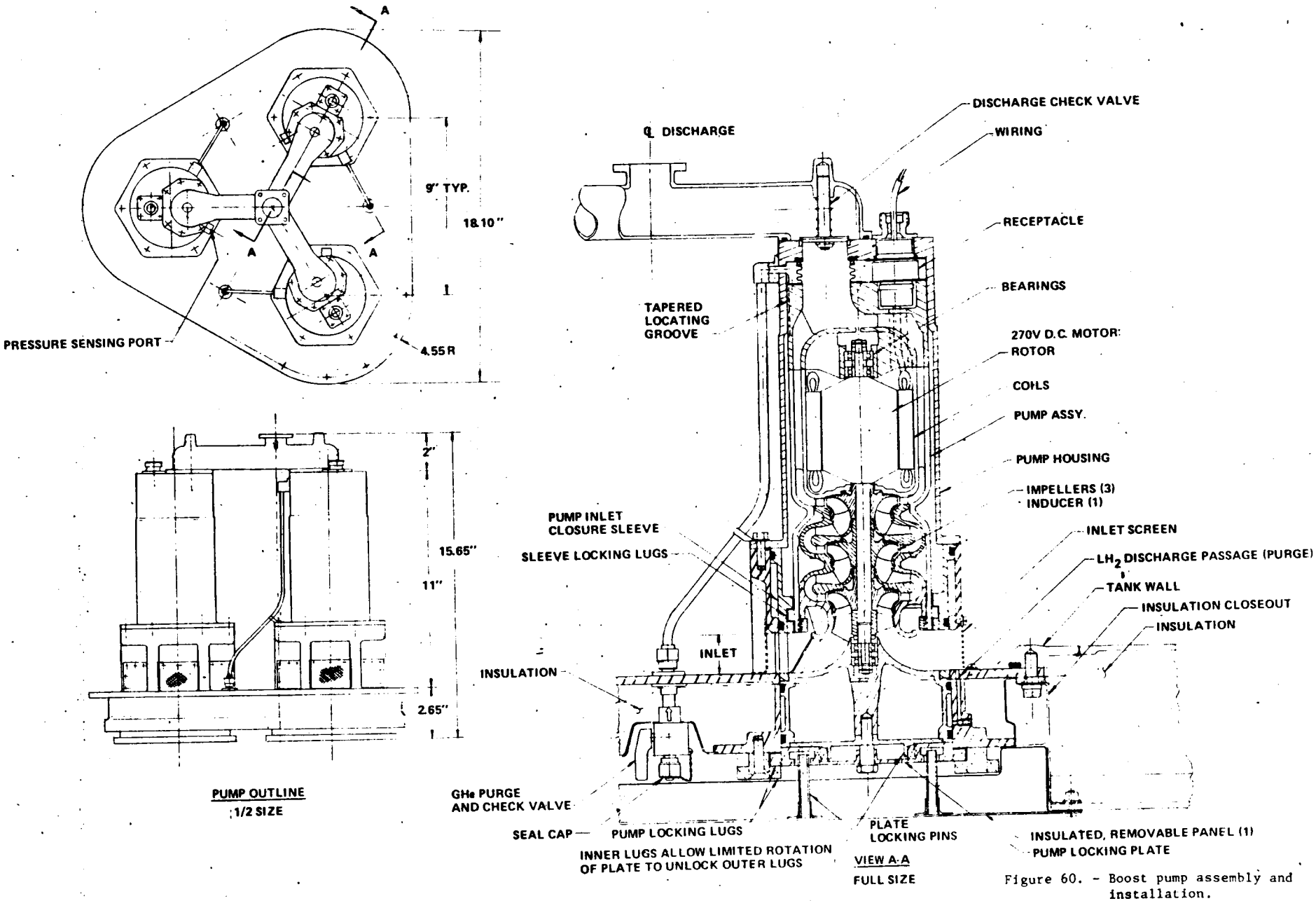

Figure 60. - Boost pump assembly and installation.

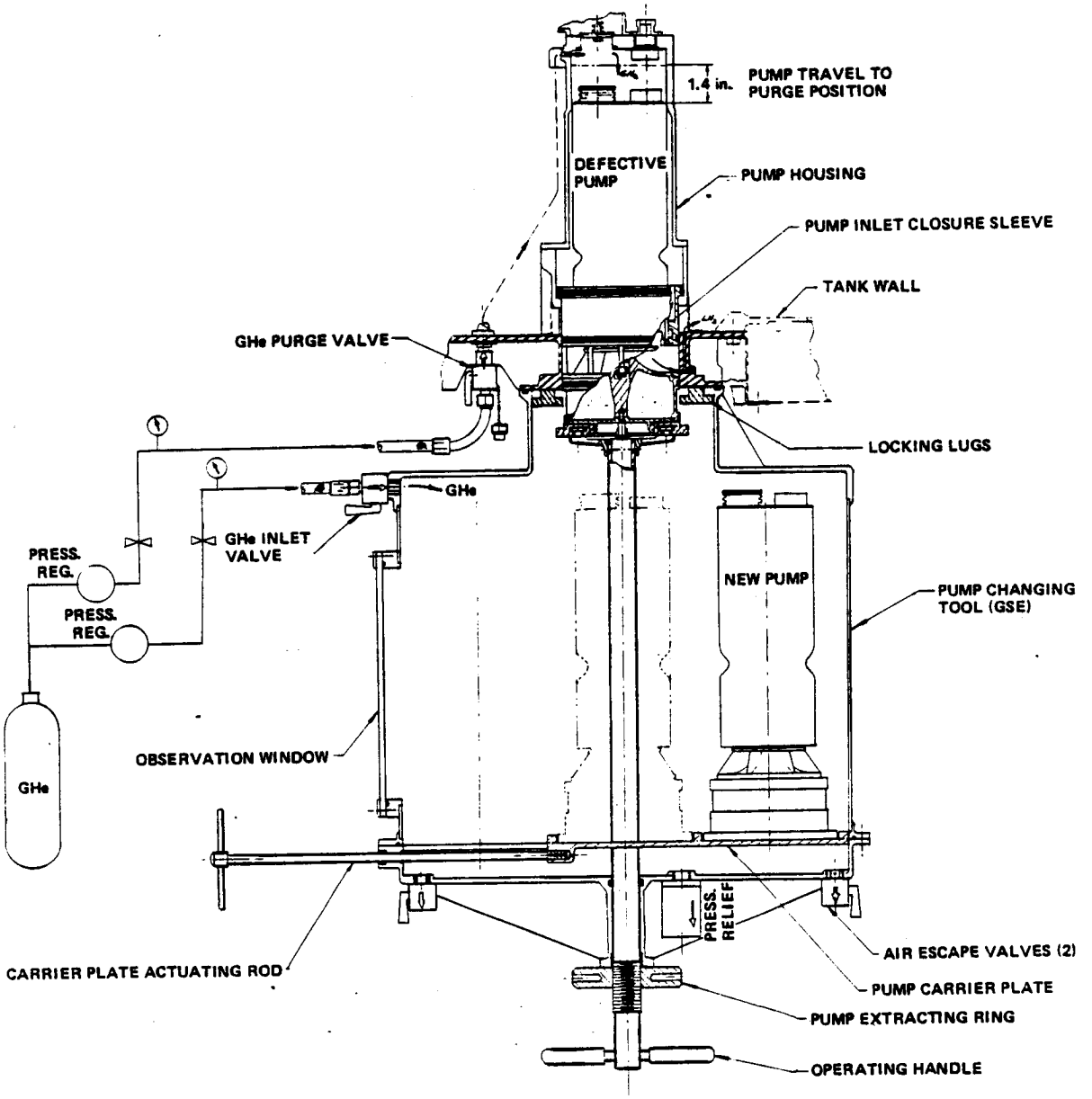

Figure 61. -Boost pump replacement concept

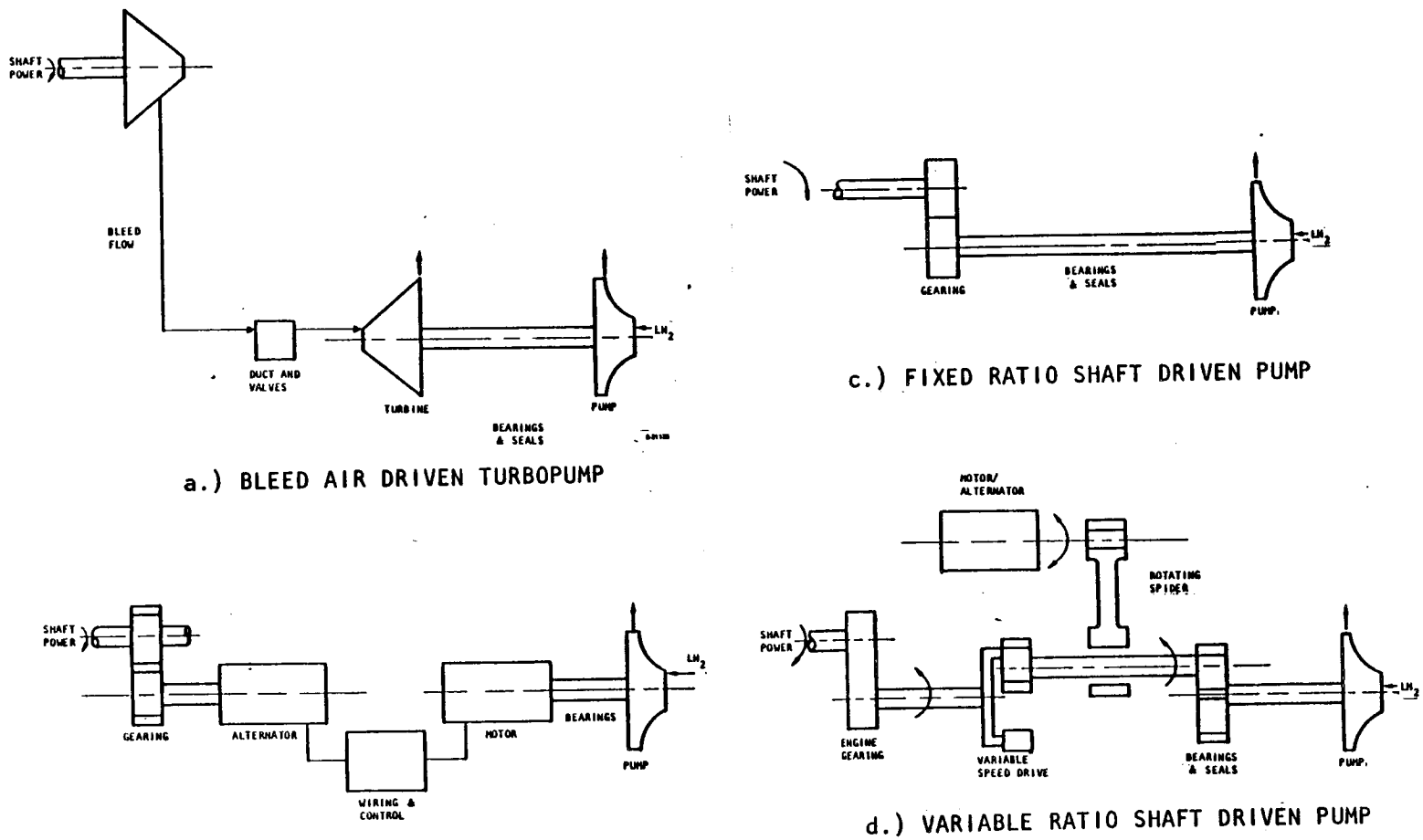

Figure 62. - Alternative pump drive concepts.

5.4.1 Design requirements. - The pump requirements start with the engine fuel flow and delivery pressure requirements which were developed in the engine study reported in Section 4.0. Table 24 presents a summary of the more significant operating conditions for the baseline engine, and tabulates the required fuel flow and fuel delivery pressure for each of these conditions. The engine LH_2 fuel pump is required to meet this set of requirements for engine fuel flow and delivery, with stable nonpulsating flow.

In order to avoid severely penalizing the engine fuel supply system which delivers LH_2 to the engine fuel pump, it is necessary that the engine pump not require an excessively high fuel inlet pressure. Based upon preliminary studies of the engine fuel supply system, it was agreed to consider the condition of a saturated liquid at 50 psia as a definition of the state of the LH_2 at the engine high pressure pump inlet for design purposes. All subsequent pump investigation was based upon this assumed pump inlet condition for steady state operation. Other pump design requirements were the following:

- During starts, it was assumed that the engine pump may encounter significant vapor associated with heat soak into the aircraft fuel line, and that either this vapor would have to be vented, or some scheme would have to be established for passing it through the pump.
- Pump rotational speed was not constrained, except as it may be by the selected drive system.
- The pump should be designed to minimize aircraft DOC, associated with pump weight and required input power.
- The minimum time between overhaul (TBO) upon entry into air transport service was established at 1 000 hours.
- Design for flight reliability and flight safety was an overriding requirement.
- Requirements for vapor venting, and pump thermal preconditioning, or other unusual operational constraints associated with the use of LH_2 fuel were to be eliminated or minimized.

5.4.2 Candidate pump types and selection of preferred concept. - Pump types which were considered to be potentially feasible for the proposed application were

- Centrifugal pumps, single or multistage
- Positive displacement piston pumps
- Positive displacement vane pumps.

TABLE 24. - SUMMARY OF BASELINE ENGINE OPERATING CONDITIONS

Operating Condition	Altitude, km (ft)	Mach No.	Thrust, daN (lb)	hp Spool Rotational Speed, rpm	hp Spool Rotational Speed, %	Fuel Flow, kg/sec (lb/sec)	Compressor Discharge Pressure, kpa (psia)	Sum of Heat Exchanger Pressure Drops, kpa (psid)	Injector and Metering Pressure Drop, kpa (psid)	Required Fuel Pressure, kpa (psia)
1. Ground Start	(0)	(0)	(0)	3 373	20.0	0.011 (0.024)	151.0 (21.9)	0.69 (0.1)	68.9 (10.0)	220.6 (32.0)
2. Ground Idle	(0)	(0)	(0)	10 456	62.0	0.044 (0.096)	579.2 (84.0)	5.5 (0.8)	68.9 (10.0)	653.6 (94.8)
3. Take-off	(0)	(0)	13 658 (30 706)	17 297	102.6	0.396 (0.874)	3 468.1 (503.0)	479.2 (69.5)	962.5 (139.6)	4 909.8 (712.1)
4. Take-off	(0)	0.40	9 116 (20 493)	17 316	102.7	0.411 (0.906)	3 606.0 (523.2)	513.7 (74.5)	1 034.2 (150.0)	5 155.2 (747.7)
5. Max. Climb	(0)	0.40	8 566 (19 258)	17 119	101.5	0.386 (0.851)	3 445.3 (499.7)	450.9 (65.4)	912.2 (132.3)	4 808.4 (697.4)
6. Start Cruise	10.67 (35 000)	0.85	2 910 (6 542)	16 886	100.1	0.166 (0.366)	1 516.2 (219.9)	75.4 (10.8)	168.9 (24.5)	1 759.5 (255.2)
7. Flight Idle	12.19 (40 000)	0.85	375 (842)	13 087	77.6	0.039 (0.086)	402.0 (58.3)	4.1 (0.6)	68.9 (10.0)	475.0 (68.9)

References 5 and 6 describe the preliminary development of a five cylinder piston pump for LH_2 service. This work demonstrated the feasibility of piston type pumps, but also highlighted the problems of leakage and life, and the necessity to operate at very low speed which resulted in a physically large pump for a given flow rate. Reference 3 reports similar work with a LH_2 piston type pump which was tested by the General Electric Co. In addition, Reference 7 reports that tests of a cryogenic vane pump were unsuccessful.

Because of these reported limitations of positive displacement pumps in the existing state of the art, and because centrifugal type pumps for LH_2 service have been relatively successful, the decision was made to concentrate the remainder of this limited investigation exclusively on the use of centrifugal type pumps. Further serious consideration of positive displacement LH_2 pumps for air transport service must be preceded by successful detailed investigation aimed at resolving the presently known design deficiencies of this type of equipment.

Both single and multistage centrifugal pumps were considered. The single stage pump represented the simplest design, whereas the use of multistage had the advantage of greater efficiency since it permitted the pump to operate at a more favorable specific speed.* In addition, the multistage pumps were smaller in diameter thus reducing the impeller thrust loads, and facilitating packaging. The following table shows the comparison of size and efficiency for various numbers of pump stages.

Number of Stages	Stage Ns	Impeller Dia (in.)	Estimated Efficiency %
1	257	5.28	50.5
2	432	3.73	60.2
3	585	3.05	66.0

Based upon this comparison, the 2 stage centrifugal design was selected as a reasonable compromise between design simplicity, pump efficiency, thrust load, and packaging feasibility. Subsequent work was based upon use of a two-stage design.

---

* Specific speed $Ns = \frac{N\,Q^{1/2}}{H^{3/4}}$

5.4.3 Candidate pump drive systems. - Four candidate pump drive systems were considered:

- Bleed air driven turbopump
- 270 Vdc electric motor driven pump
- Fixed ratio shaft driven pump
- Variable ratio shaft driven pump.

Figure 62a shows the bleed air driven turbopump system which was considered. The power source was high pressure bleed air extracted from the engine compressor. This was then ducted to a high speed air turbine and the flow to the turbine was modulated to an inlet valve. The air turbine was used to direct drive a centrifugal type LH_2 pump to provide LH_2 to the engine. One main advantage of this type of drive was the ease with which variations in pump speed could be obtained.

Another type of drive which was considered was based upon the recent development of high efficiency, 270 Vdc electric generators and motors having at once a capability for both high speed and variable speed. Control flexibility was a main advantage of this type of drive, if it should prove possible to design a system having a competitive weight. Figure 62b shows a schematic of a 270 Vdc pump drive system.

The simplest type drive which was considered was a fixed speed ratio shaft drive, using power extraction from the engine gearbox. This type drive is shown schematically in Figure 62c. The inability to vary the speed of the pump was seen as a possible major problem with this concept.

A variable speed mechanical drive can be used to obtain pump speed variation with a shaft driven system, and this scheme is shown in Figure 62d. Added mechanical complexity was seen as a possible major drawback for this approach.

The comparative evaluation of these drives is discussed in the next section.

5.4.4 Engine pump and drive candidate evaluation. - A trade-off analysis was conducted to select a preferred pump and drive system. In performing the analysis, engine operating conditions were first reviewed with particular reference to fuel delivery requirements as summarized on Table 24. Two conditions were selected as having particular significance in the pump drive trade-off analysis:

- Take-off (Condition 4) was selected as one point for comparison, since it represented the maximum pump power requirement and hence would determine the drive weight.

- Start of cruise (Condition 6) was selected as another point for comparison, since it was typical of long term cruise operation, and would reflect the influence of pump drive overall efficiency on engine SFC.

The pump drives to be compared represent two basic types, variable speed ratio and fixed speed ratio. The first three candidate drive types, discussed in Section 5.4.3, had a variable speed ratio. The variable speed type has the advantage of permitting adjustment of the pump speed and resulting fuel delivery to more nearly match the engine requirements. This results in a reduction of required pump input power at off-design conditions, such as cruise. A fixed speed ratio pump drive does not permit such a speed adjustment and hence requires relatively greater power input during the off-design operation, when compared to the variable speed systems. Tables 25 and 26 show summaries of pump operating conditions for both the variable speed ratio drives and a fixed speed ratio drive.

These data were then used in developing weight estimates and power requirements for the various drive systems. The attached summary chart, Table 27, shows a comparison of the significant characteristics of the alternative pump drives. Drive system overall efficiency is presented for both take-off and start of cruise conditions, and also the resulting required engine power extraction. System weights are shown. The change in DOC was calculated for the different systems, and is shown tabulated as a relative ranking. In addition, the various drives were ranked according to design simplicity, inherent reliability potential, and system cost.

In evaluating the results of trade-off analyses presented in this summary, it was decided that the delta DOC numbers developed for the start of cruise condition should be given relatively little weight since the absolute values were quite small. Primary significance was assigned to system design simplicity and inherent reliability potential, with system weight and cost considered next. On this basis, the fixed ratio shaft drive was selected as the preferred pump drive. The bleed air driven turbopump is considered to be the second most attractive alternative. The 270 Vdc system has the decided advantage of not requiring a shaft dynamic seal in the pump, but has the disadvantage of relatively high system weight. The variable speed ratio shaft drive has the disadvantage of mechanical complexity.

5.4.5 Pump bearing considerations. - The engine LH_2 fuel pump bearing system represents one of the key technical problems in the design of the overall system. The bearing system must be capable of operating at high rotational speeds (50 000 rpm); must be capable of carrying high loads, particularly high thrust loads under certain conditions; and must be compatible with the pumping of LH_2.

TABLE 25. - VARIABLE SPEED PUMP, SUMMARY OF OPERATING CONDITIONS

Operating Conditions (1)	Pump Speed Ratio, N/N_D	Fuel Flow kg/sec (lb/sec)	Fuel Flow ℓ/min (gpm)	Required Fuel Pressure, kPa (psia)	Fuel Supply Pressure kPa (psia)	Required Pressure Rise kPa (psid)	Pump Pressure Rise, kPa (psid)	Pump Flow Ratio,(3) W/W_D	Pump Efficiency %	Pump and Throttle Efficiency %	Pump Input Power kW (S hp)
1. Ground Start	0.100	0.011 (0.024)	10.7 (2.82)	220.6 (32.0)	(290) (42)	-262.0 (-38.0)	48.3 (7.0)	0.265	55.2	---	0.015 (0.02)
2. Ground Idle	0.189	0.044 (0.096)	42.8 (11.3)	653.6 (94.8)	482.6 (70.0)	171.0 (24.8)	171.0 (24.8)	0.561	66.2	---	0.186 (0.25)
4. Take-off (2)	1.000	0.411 (0.906)	385.0 (101.7)	5 155.2 (747.7)	344.7 (50.0)	4 810.5 (697.7)	4 810.5 (697.7)	1.000	69.0	69.0	44.7 (60.0)
6. Start Cruise	0.542	0.166 (0.366)	155.6 (41.1)	1 759.5 (255.2)	344.7 (50.0)	1 414.8 (205.2)	1 414.8 (205.2)	0.745	67.2	67.2	5.46 (7.32)
7. Flight Idle	0.100	0.039 (0.086)	38.2 (10.1)	475.0 (68.9)	482.6 (70.0)	-7.6 (-1.1)	48.3 (7.0)	0.949	62.9	---	0.052 (0.07)

(1) See Table 24, "Summary of engine operating conditions" for further definition.

(2) Condition 4 was pump design point.

(3) Pump flow ratio includes speed correction for W_D.

TABLE 26. - FIXED RATIO SHAFT DRIVEN PUMP, SUMMARY OF OPERATING CONDITIONS

Operating Conditions (1)	Pump Speed Ratio, N/N_D	Fuel Flow kg/sec (lb/sec)	Fuel Flow ℓ/min (gpm)	Required Fuel Pressure, kPa (psia)	Fuel Supply Pressure kPa (psia)	Required Pressure Rise kPa (psid)	Pump Pressure Rise kPa (psid)	Pump Flow Ratio,(3) W/W_D	Pump Efficiency %	Pump and Throttle Efficiency %	Pump Input Power kW (S hp)
1. Ground Start	0.195	0.011 (0.024)	10.7 (2.82)	220.6 (32.0)	482.6 (70.0)	-262.0 (-38.0)	182.7 (26.5)	0.136	37.0	---	0.09 (0.12)
2. Ground Idle	0.604	0.044 (0.096)	42.8 (11.3)	653.6 (94.8)	482.6 (70.0)	171.0 (24.8)	1 753.3 (254.3)	0.175	48.0	---	2.60 (3.49)
4. Take-off (2)	1.000	0.044 (0.906)	385.0 (101.7)	5 155.2 (747.7)	344.7 (50.0)	4 810.5 (697.7)	4 810.5 (697.7)	1.000	69.0	69.0	44.74 (60.0)
6. Start Cruise	0.975	0.166 (0.366)	155.6 (41.1)	1 759.5 (255.2)	344.7 (50.0)	1 414.8 (205.2)	4 569.8 (662.8)	0.415	58.0	18.0	20.43 (27.4)
7. Flight Idle	0.756	0.039 (0.086)	38.2 (10.1)	475.0 (68.9)	482.6 (70.0)	-7.6 (-1.1)	2 746.2 (398.3)	0.126	37.0	---	4.73 (6.34)

(1) See Table 24 "Summary of engine operating conditions" for further definition.

(2) Condition 4 was pump design point.

(3) Pump flow ratio includes speed correction for W_D

TABLE 27. - COMPARISON OF ALTERNATIVE PUMP DRIVES

	System Overall Efficiency (b)		Delta Engine Power kW (hp)		System Weight kg (lb)	Relative DOC Cruise	Relative Ranking (a)		
	Take-off	Start Cruise	Take-Off	Start Cruise			Simplicity	Reliability Potential	System Cost
Bleed Air Driven Turbopump	0.336	0.293	91.9 (123.2)	12.5 (16.8)	16.0 (35.3)	1.28	2	2	2
270 Vdc Electric Motor Driven Pump	0.429	0.418	72.0 (96.6)	8.8 (11.8)	18.7 (41.2)	1.10	3	2	3
Variable Ratio Shaft Driven Pump	0.502	0.488	61.5 (82.5)	7.5 (10.1)	18.3 (40.4)	1.00	4	3	3
Fixed Ratio Shaft Driven Pump	0.590	0.154	52.3 (70.2)	23.9 (32.0)	11.4 (25.2)	1.92	1	1	1

(a) Variation from 1 to 4, 1 being best.

(b) Includes engine to pump drive losses.

Rocket engine turbopumps have typically used rolling element bearings operating in LH_2. The LH_2 provides cooling but essentially no lubrication because of the very low viscosity; lubrication is provided by the use of teflon type separators, wherein the teflon transfers as a solid film lubricant to the rolling elements and races. These systems have demonstrated the required speed and load capability but have a demonstrated maximum life of about 10 hours, although extremely lightly loaded bearings have been run over 1 000 hours. Therefore, if rolling element bearings operating in LH_2 are to be used in the engine LH_2 pump, it will be necessary to assure extremely light loading under all operating conditions.

Hydrostatic LH_2 bearings, and hybrid bearings consisting of a hydrostatic bearing used in combination with a rolling element bearing have been proposed and tested experimentally, but have not yet demonstrated the inherent potential for meeting the engine fuel pump requirements.

Foil bearing systems have been tested by AiResearch with air and cryogenic helium, and appear to offer an attractive design alternative for LH_2 systems, although the loading would have to be controlled to a low value.

Industrial cryogenic turbomachines utilize oil lubricated bearings, both rolling element and plain journal bearing types, but require strict thermal control within the machine to prevent freezing the oil. However, the oil lubricated bearings have both high rotational speed capability, and substantial load carrying capacity.

Based upon these considerations, a preliminary selection of a bearing system was made for the proposed shaft driven pump described later. This system used an oil lubricated rolling element bearing at the shaft drive end of the pump. The bearing would receive oil from the engine gearbox and would operate at gearbox temperatures. Careful thermal design of the pump would be required to successfully use this design approach. The high load capacity of the oil lubricated bearing would be used to carry the pump thrust loads, which can be substantial under certain conditions of impeller seal wear and leakage. In addition, the oil lubricated bearing would carry the local radial loads at the shaft drive end of the unit. A foil type bearing (or rolling element alternative) was located between the two pump impellers and operated in the cryogenic hydrogen. With careful attention to dynamic and hydrodynamic balance, the loads on this bearing can be maintained at a suitable low value. It was considered that this hybrid approach offered the potential for meeting the engine LH_2 fuel pump bearing system design requirements, and it was recommended for advanced technology development.

5.4.6 Selected pump and drive system. -

5.4.6.1 General description: The selected engine high pressure pump was a two stage centrifugal design, and was shaft driven from the engine at a fixed speed ratio. The pump was designed to provide a flow of 387 ℓ/min (102 gpm) at a pressure rise of 4785 kPa (685 psid) and had a design rotational speed of 50 000 rpm. At the design point, the required shaft power input was 50.5 kW (67.7 hp) and the required condition for the hydrogen at the pump inlet was 345 kPa (50 PSIA) minimum at 25°K (45°R) maximum. These limits correspond to saturated liquid (0 NPSH) at 345 kPa (50 psia). Table 28 provides a more detailed summary of the pump operating conditions and design characteristics.

Referring to the pump cross-sectional drawing shown in Figure 63, it may be seen that the pump rotating group consisted of the two impellers and the shaft, fastened together with curvic couplings and an axial tie bolt. This construction is typical for modern, small, high speed turbomachines. The curvic couplings provide the required accuracy in alignment of the pump rotating parts and, in addition, can be made with convex-convex generated surfaces, thus reducing the surface contact area and increasing the resistance to conductive heat flow along the shaft. Minimizing the heat flow from the warm engine gearbox to the cryogenic end of the liquid hydrogen pump was an important design requirement.

A splined torsion drive shaft is used to connect the pump rotating group to the engine gearbox. The torsion shaft provides the torsional compliance necessary to isolate the gear tooth generated excitation from the inertia of the pump rotating group and, in addition, it provides additional resistance to conductive heat flow.

The pump rotating group is carried in an oil lubricated ball bearing at the gearbox end, and in a foil type journal bearing running in hydrogen at the pump end. This bearing arrangement has a particular advantage in that the high load capacity oil lubricated bearing not only carries the radial load at the gearbox end of the pump, but also carries all of the axial thrust load, so that the foil bearing running in the cryogenic hydrogen at the impeller end of the pump is only required to carry the local radial load. With accurate dynamic balancing of the impellers, the magnitude of this local radial load can be kept relatively small. This provision for carrying the thrust load was an important consideration, since the possibility of encountering high thrust loads always exists for high pressure centrifugal pumps, for instance if a labyrinth type thrust balance seal were to develop an abnormally high leakage rate.

The ball bearing is a preloaded duplex pair carried in a ring type flexible mount. The flexible mount provides the necessary radial compliance to accommodate the greater than normal temperature range expected for this application and, in addition, provides some angular compliance for the shaft,

TABLE 28. - LIQUID HYDROGEN PUMP

Conditions:	
Inlet Pressure	50 psia (Total Net)
Inlet Temperature	45 406°R (Saturated)
Discharge Pressure	735 psia
Flow	102 gpm (Liquid)
Design Data:	
No. of Stages	2.
Total Head	24 638.13 ft
Speed	50 000. rpm
First Stage TSH (a)	231.75 ft
First Stage S_V (b)	10,000.
Stage Specific Speed	431.5
Overall Efficiency	60.2%
Overall Power	67.7 hp
Impeller Diameter	3.730 in.
Impeller Reynolds No.	2.29×10^7
Impeller Eye Dia. First St.	0.985 in.
Impeller Eye Dia. Second St.	0.875 in.
Impeller Tip Width	0.055 in.

(a) TSH = Thermal Suction Head

(b) S_V = Suction Specific Speed = $\dfrac{N\,Q^{1/2}}{(NPSH + TSH)^{3/4}}$

necessary to accommodate the radial compliance of the foil bearing at the pump end. The ball bearing pair is lubricated by a slight oil mist from the engine gearbox, and a drain-back port is provided to return any collected mist to the gearbox. Direct spray lubrication was not planned for this bearing and may be objectionable because of the possibility for very low operating temperatures. A dynamic shaft seal was provided to retain the oil mist in the gearbox, and an overboard drain was provided to accommodate any oil leakage from the seal.

Because the thrust bearing is some distance from the impellers in the selected bearing arrangement, there is some possibility for axial misalignment of the impeller and diffuser center lines. To accommodate this without a harmful degradation in pump performance, the impeller tip width was made somewhat larger than the diffuser entrance width.

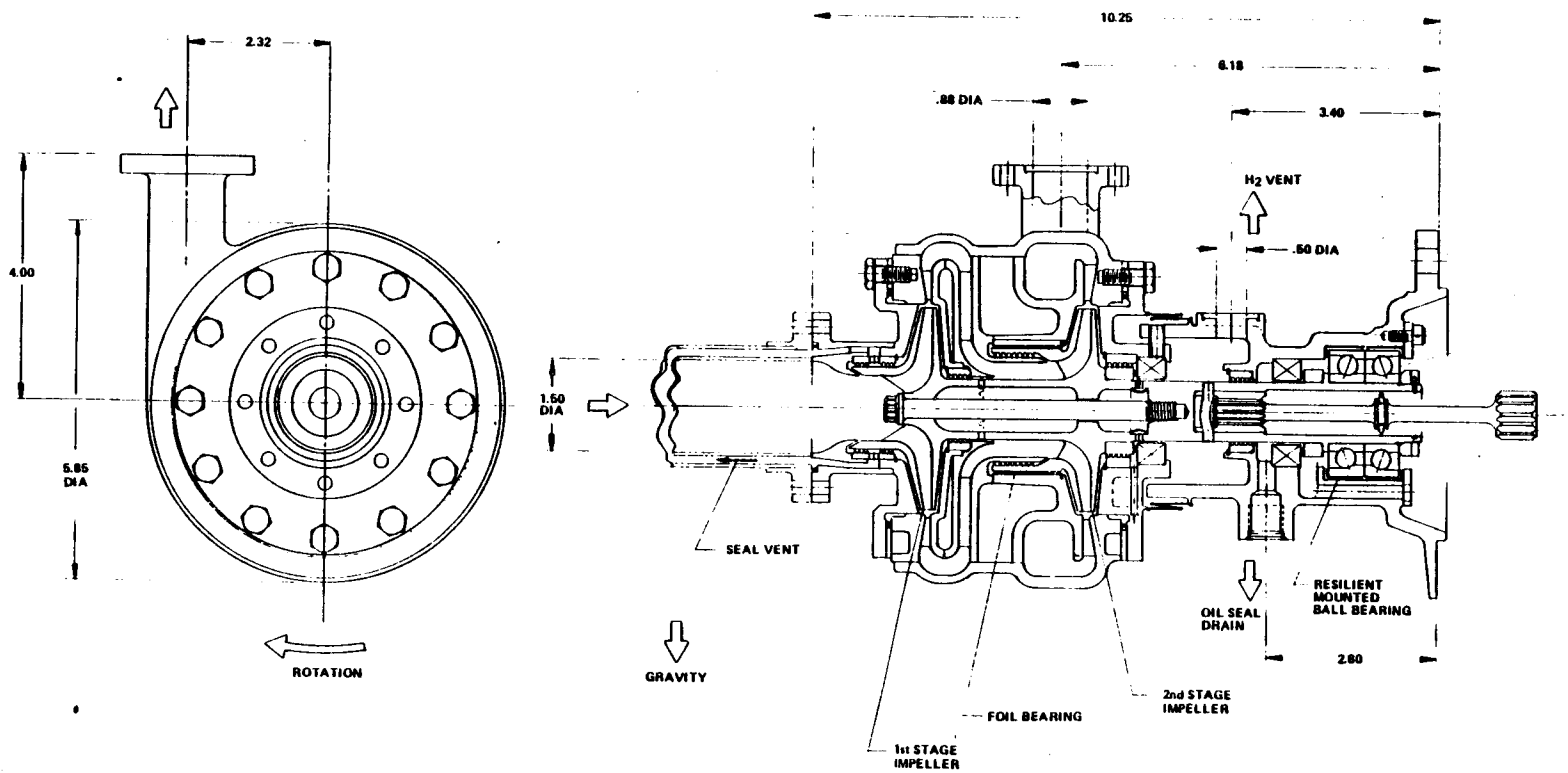

Figure 63. - Engine high pressure LH_2 pump.

The foil bearing located between the two pump impellers is an AiResearch proprietary design similar to the bearings used in a variety of other high speed turbomachines. The advantage of the foil bearing is that it offers the potential for a long service life in the cryogenic end of the pump where oil lubrication was not feasible. An alternative design approach was to use a rolling element bearing operating in the cryogenic hydrogen, in lieu of the foil bearing.

Labyrinth seals are used for controlling leakage and for obtaining thrust balance across the pump impellers. Referring to the cross-sectional drawing of Figure 63, it can be seen that the first stage impeller inlet labyrinth seal is vented to a location about six inches upstream of the pump inlet. This was done to minimize vapor flashing in the pump inlet, which would be detrimental to pump performance. The rear labyrinth seal for the second stage impeller is also vented, for the purpose of reducing the required design pressure of the hydrogen dynamic shaft seal. A hydrogen vent is provided in the housing to accommodate any leakage from the hydrogen dynamic shaft seal.

The pump inlet housing assembly is mounted to the bearing housing assembly by three radial pins. This arrangement facilitates radial contraction of the pump housing at cryogenic temperatures, and also reduces the conductive heat transfer. A thin gage convoluted seal is provided to preclude leakage. The pump assembly is mounted to the engine gearbox by a standard AND 20002 15.24 cm (6.00 in.) flange.

5.4.6.2 Materials: Materials selected for use in significant parts of the engine LH_2 pump were:

- Impellers - Inconel 718
- Diffuser housing - aluminum alloy
- Main housing - 300 series corrosion resistant steel
- Rolling element bearings - 400 C corrosion resistant steel
- Impeller shaft - Inconel 718
- Splined drive shaft - nitralloy
- Oil seal assembly - carbon, 400 C corrosion resistant steel, and 300 series corrosion resistant steel.

5.4.6.3 Weight: The estimated total weight for the two stage shaft driven centrifugal pump was 13.1 lb. This was obtained by detailed estimate of the weight of the individual components shown on the layout of Figure 63.

5.4.6.4 Performance: Performance maps showing pump head and efficiency as a function of pump flow and rotational speed are shown in Figure 64.

5.5 Fuel Control System

5.5.1 Design requirements. - The initial undertaking in the design of a fuel delivery and control system was to review the required functions, establish a list of inputs needed to perform those functions, and itemize the required output.

Functions of the engine fuel delivery and control system include:

- Provide the interface between the engine fuel supply system and the engine. The control system receives fuel from the engine fuel supply system within a limited range of thermodynamic states, and delivers this fuel to the engine in a condition which provides for efficient combustion, and at the proper flow rate for all engine operating conditions.

- Provide scheduling of compressor bleed valves used during starting, and compressor variable vane positions.

- Provide scheduling of other values and/or ignition required during engine prestart conditioning, and starting, and shut-down.

Inputs to the engine fuel delivery and control system include:

Physical Inputs

- Fuel from the engine fuel supply system, provided in accordance with a flow schedule established by the engine fuel flow requirements, and in accordance with a minimum pressure schedule established by the engine high pressure pump suction performance limits.

- Electrical power from the aircraft system for use in the engine fuel delivery and control system electronic control, for use in operation of valves and actuators, and for possible use as a pump drive.

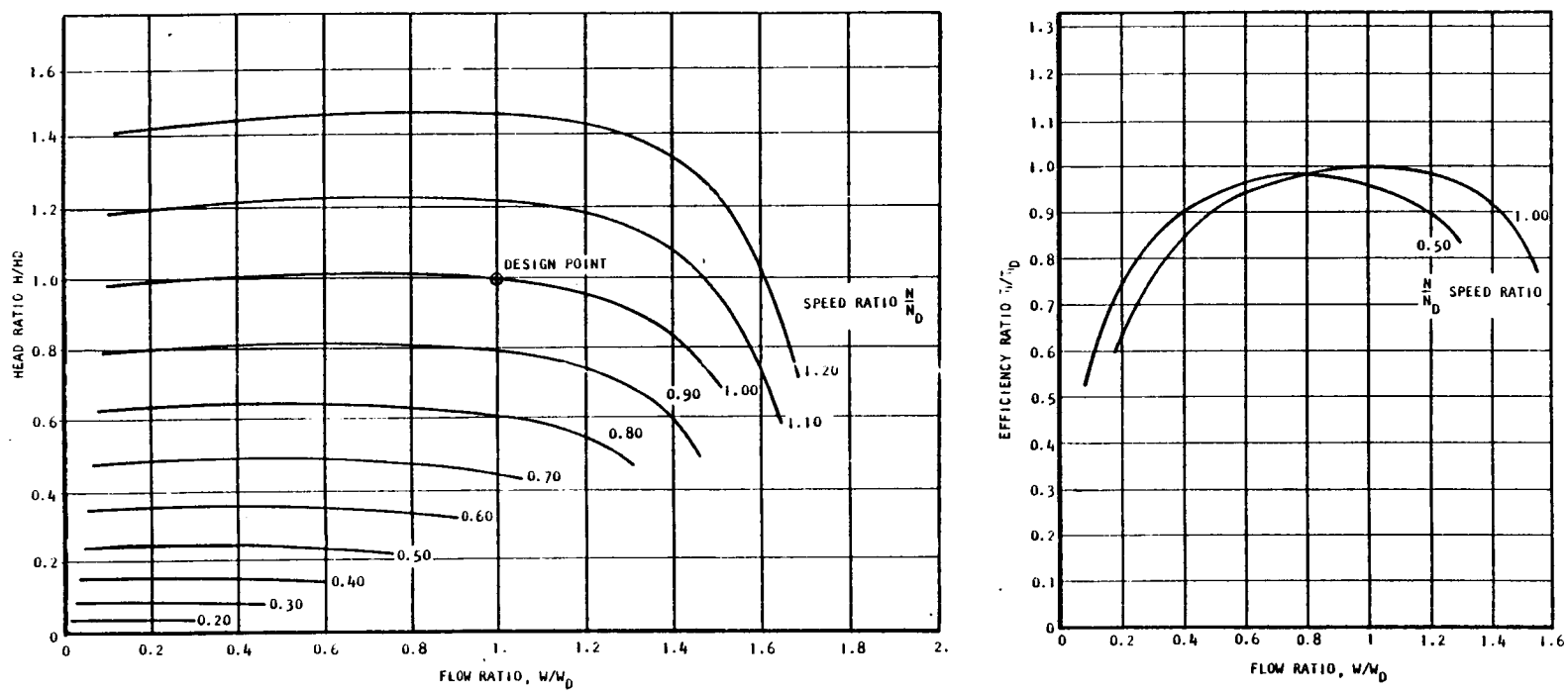

Figure 64. - Performance maps for two stage centrifugal pump.

- Engine compressor bleed air for use in the engine compressor variable vane actuators, and for possible use as a fuel turbopump drive.

- Engine shaft power for possible use as a fuel pump drive.

- Heat for use in vaporizing and heating the hydrogen fuel, to be obtained from the aircraft environmental control heat load, from the engine turbine cooling air, and from the engine exhaust.

Informational Inputs

- Command signals, including

  Electrical system master switch
  Engine fuel system purge operation
  Engine start signal
  Engine power level setting
  Engine stop signal.

- Informational inputs from the engine, including

  Fan rotational speed
  Compressor rotational speed
  Compressor inlet total temperature
  Compressor inlet total pressure
  Compressor discharge total pressure
  Compressor variable guide vane and stator vane positions
  Low pressure turbine inlet total temperature, or exhaust gas total temperature.

- Informational inputs generated within the fuel delivery and control system, including

  Pump inlet housing temperature
  Pump discharge pressure
  Pump discharge temperature
  Pump rotational speed
  Fuel flowmeter rotational speed

Outputs from the engine fuel delivery and control system include:

Physical Outputs

- Fuel delivered to the engine combustor, in a condition which provides for efficient combustion, and at a proper flow rate for all engine starting, transient, and steady state operating conditions.

- Vent gas during cool down or purging operations.
- Pump shaft dynamic seal vent gas.

Informational Outputs

- Engine speed or thrust indication*
- Scheduling of compressor bleed valve
- Scheduling of compressor variable vane positions
- Signals for monitoring of fuel delivery and control system significant parameters, such as fuel pump rotational speed, control valve positions, etc.

5.5.2 Candidate concepts. - Candidate concepts for the fuel control system which were studied and evaluated were based on use of the following pump drive systems:

- Bleed air driven turbopump system
- 270 Vdc motor driven pump system
- Engine shaft driven pump system, fixed speed ratio
- Engine shaft driven pump system, variable speed ratio.

System schematics for these concepts are shown in Figures 65 through 68. In each of these systems, electronic control circuitry was used in conjunction with the fluid pumping and metering elements. This use of electronic circuitry is consistent with modern engine design technique and will probably be used exclusively on this class engine in the 1985 time period.

All of the schemes use a flow modulating and shut-off valve downstream of the heat exchangers to reduce the effect of heat exchanger capacitance in fuel system transient performance. A turbine type flowmeter is included for fuel flow measurement upstream of the flow modulating valve.

5.5.3 Selected system.

5.5.3.1 Description: Selection of the design of the fuel control system was dependent on the choice of drive for the engine fuel pump. With the selection of the fixed speed ratio engine shaft driven pump system as

* Other engine monitoring parameters are not considered part of the engine fuel delivery and control system.

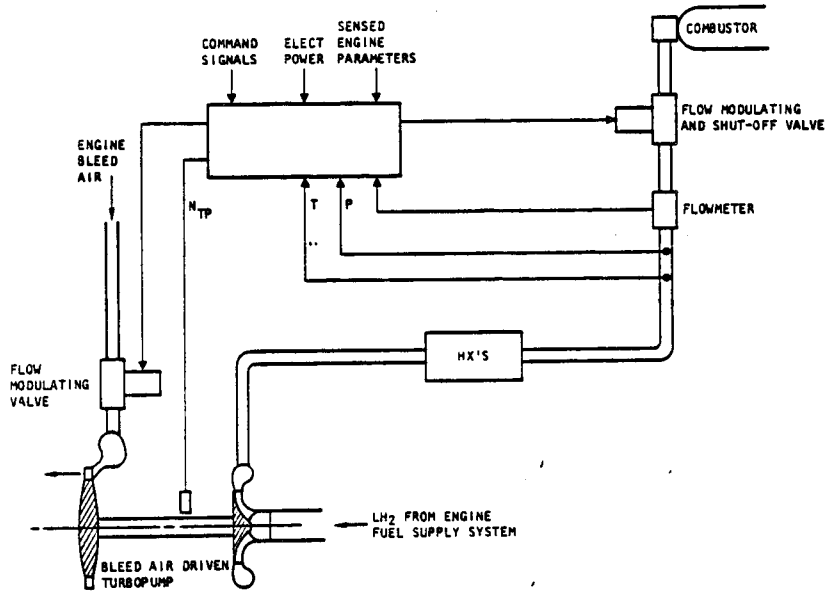

Figure 65.-Bleed air driven turbopump system.

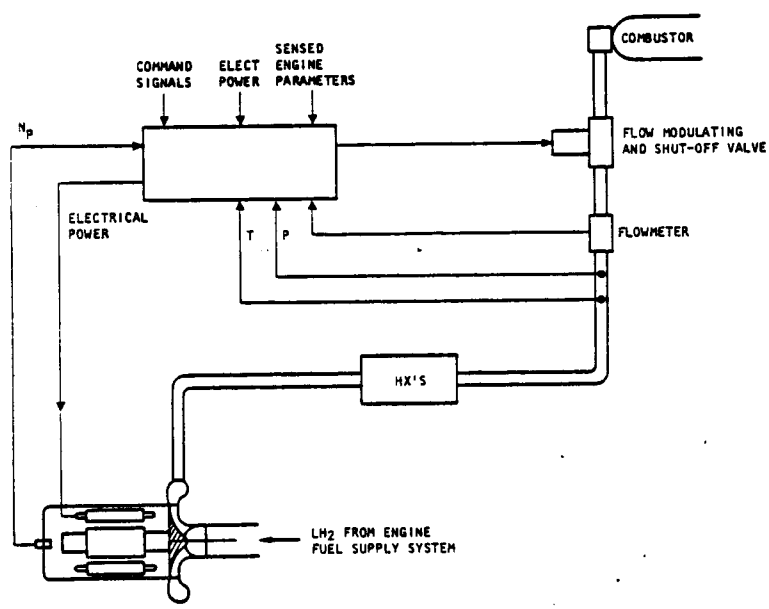

Figure 66.-270 Vdc motor driven pump system.

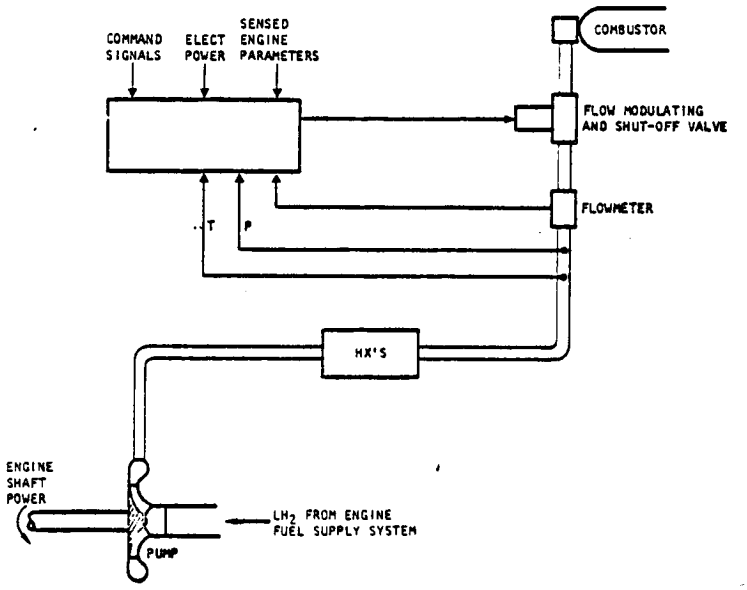

Figure 67.-Engine shaft driven pump system, fixed speed ratio.

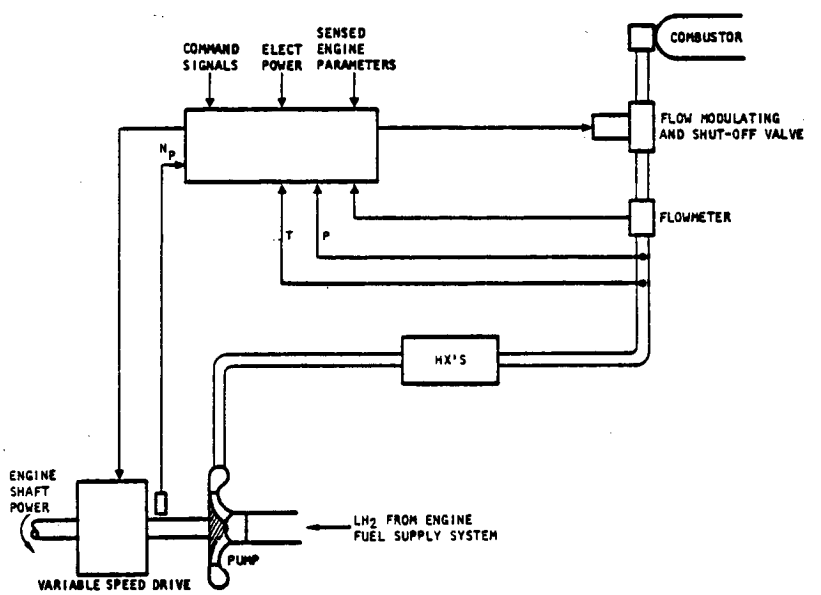

Figure 68.-Engine shaft driven pump system, variable speed ratio.

discussed in Section 5.4.4, the control system represented in Figure 67 became the preferred concept. Figure 69 shows the actual design arrangement of the components in the overall aircraft system. A description of the operation of this system is discussed in the following section.

5.5.3.2 Control response considerations: With the design arrangement shown in Figure 67, the potential problems associated with the effects of the large heat exchanger volume capacitance and the H_2 fluid compressibility are minimized. It is expected that control response characteristics comparable to that of a conventionally fueled engine can be readily achieved. Note that particular attention will have to be paid to the design and development of the fuel flow modulating valve and the turbine type flowmeter.

5.6 Engine Fuel Supply System Final Design and Performance

The critical problem in the delivery of fuel from the tank to the engine is to insure that the engine mounted pump is delivered a supply of liquid hydrogen at a pressure such that no significant amount of vapor is present (2 phase flow), although it is estimated that at low speeds the main pump could handle a voltumetric vapor fraction of approximately one half. This means that the heat added by the tank boost pump, motor, supply line, valves, etc., cannot exceed the fuel saturation enthalpy associated with the pressure at the engine pump inlet (zero net positive suction head). Since the heat added by the lines and system is proportional to the area of the line and inversely proportional to the flow rate, the lowest flow rate is the most critical. The heat added by the boost pump is proportional to the pressure rise but inversely proportional to the pump efficiency. A high pressure rise across the boost pump is desirable to suppress vaporization in the delivery system but the pump efficiency corresponding to the pressure rise must also be considered.

Another important consideration which influenced the system configuration and concept was the desirability of being able to use the hydrogen vapor in the delivery system during engine start. This would preclude the necessity for either having a long vapor return line back to the tank from the engine or providing a method to safely vent or dump the vapor. In addition, the residual vapor would then be useable in the engine. This could be accomplished by designing the engine fuel control system to handle vapor during the starting transient condition. The pressure required to insure fuel delivery to the engine and into the combustor could be supplied by the boost pump which is immersed in liquid. The increasing flow rate during acceleration from starting to ground idle would chill down the system so that liquid hydrogen would be available at the engine pump prior to reaching idle.

The above concept was pursued during the course of the study and was selected as the final approach described in the following sections.

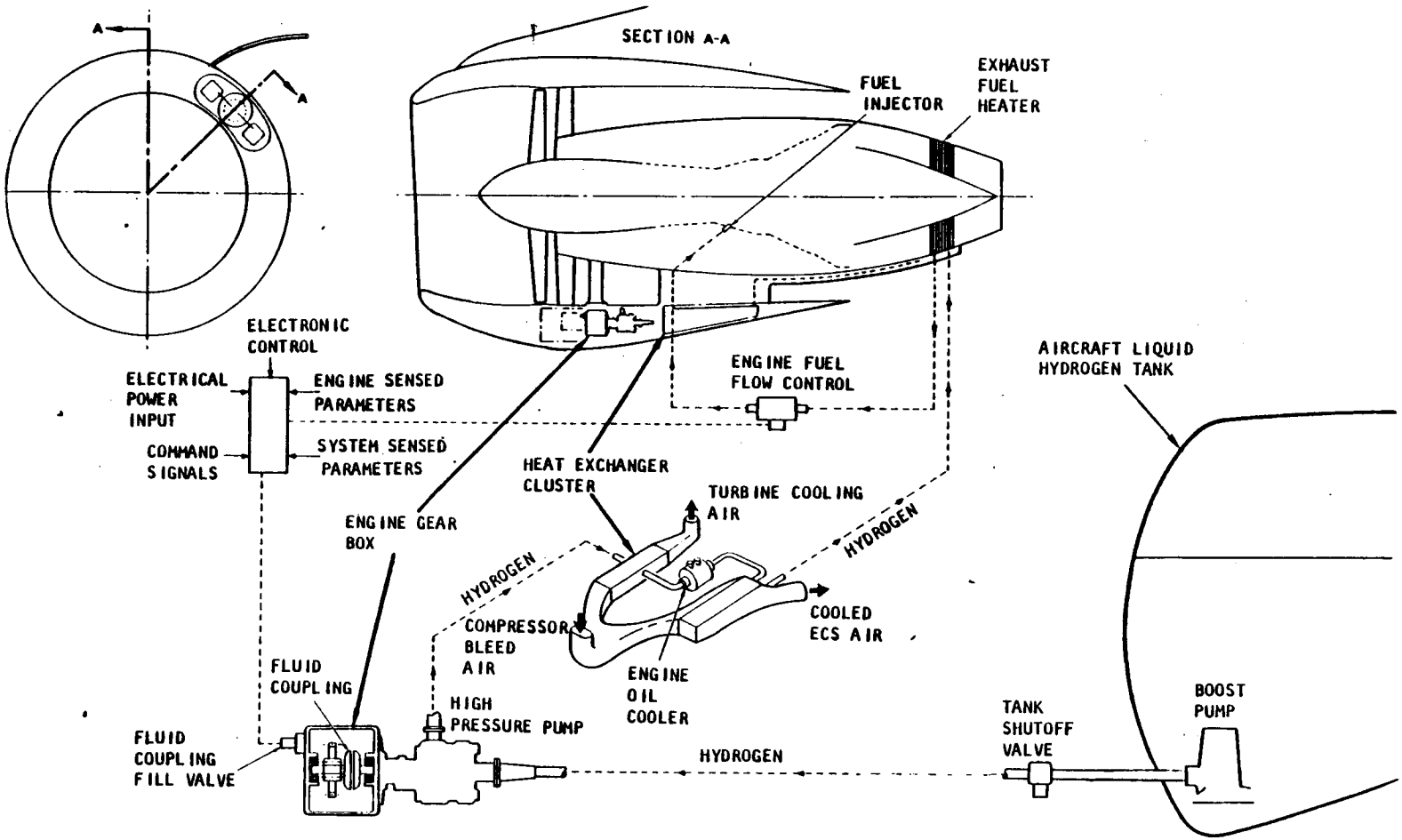

Figure 69. - LH_2 engine fuel delivery and control system.

5.6.1 Heat added to hydrogen. - During system operation, the liquid hydrogen temperature at the engine pump inlet will be higher than the tanked value due to heat inputs from the pump and (submerged) electric motor as well as heat input along the length of the fuel feed line. The primary concern is to ensure that zero vapor fraction hydrogen is delivered to the engines under all operating conditions. In actuality, it is desirable to ensure that some excess in engine delivered pressure compared to inlet saturation pressure is maintained. This excess pressure is usually referred to as Net Positive Suction Pressure (NPSP) and a minimum value of zero has been specified by AiResearch for normal operations.

The hydrogen saturation pressure at the engine pump inlet can be obtained from the calculated fluid enthalpy at the inlet in conjunction with hydrogen property tables. The engine inlet pressure is simply the tank pressure plus the boost pump pressure rise minus the feed line pressure loss. Therefore, we have

$$NPSP = P_{ENG} - P_{SAT} = P_{TANK} + \Delta P_{PUMP} - \Delta P_{LINE} - P_{SAT} \tag{1}$$

The engine pump inlet enthalpy is equal to the hydrogen enthalpy at tanked conditions plus the enthalpy rise attributed to line, pump and motor heating, respectively:

$$h_{eng} = h_{TANK} + \Delta h_L + \Delta h_p + \Delta h_M \tag{2}$$

The enthalpy rise due to line heating Δh_L is determined simply from:

$$\Delta h_L = \frac{Q/L \cdot L}{\dot{w}_{H_2}} \tag{3}$$

The enthalpy rise due to pump heating is given by:

$$\Delta h_p = \Delta P \cdot \left[\frac{1}{\rho}\left(\frac{1}{\eta_p} - 1\right) + 0.0175\right] \tag{4}$$

which for liquid hydrogen with a density of 4.3 lb/ft^3 and using the proper conversion factors to obtain consistent units reduces to:

$$\Delta h_p = \Delta P \cdot \left[0.0412\left(\frac{1}{\eta_p} - 1\right) + 0.0175\right] \tag{5}$$

where ΔP is pump pressure rise (psi) and η_p is pump efficiency. The numerical factor 0.0175 accounts for compressibility effects on the hydrogen internal energy.

The fluid enthalpy rise due to the submerged electric motor inefficiency is given by:

$$\Delta h_M = \frac{550}{778} \frac{hp}{\dot{w}_{H_2}} \left(1 - \eta_M\right) \tag{6}$$

where hp is motor horsepower and η_M is motor efficiency.

5.6.2 Final system selection. - The above relations, together with the line, joint, and valve heat leaks were used to determine conditions during the critical ground start of the engine. The boost pump selected to give maximum efficiency at low flows is a three stage, 270 volt dc driven centrifugal variable-speed pump as shown in outline in Figure 70.

The assumptions used in the analysis were:

- Starting flow rate is 0.024 lb/sec
- The longest line run was used (tank #4 to engine #4)
- Compartment temperature = 130°F at sea level
- 1 inch diameter stainless steel line
- Line is chilled down at engine start.

The objective was to compare foam versus vacuum insulation systems for the engine fuel supply line.

Since the in-service reliability of light weight vacuum jacketed line is unknown, but based on experience with static ground equipment is not expected to be very high, the foam jacketed concept was included in this analysis. The foam line consists of concentric tubes filled with 1.5 inches of closed cell foam with suitable bellows and connectors. Being a passive system, the consequences of a leak into the closed cell foam space will not, in the short term, increase the heat leak rate and it is expected to be more reliable and rugged overall.

The analysis was based on the boost pump and motor characteristics shown in Figure 71. Transient conditions during start are shown in Figure 72. Heat rejection to the fluid from the pump and motor as well as line, joint, and valve heat leaks, are included in the fuel temperature rise.

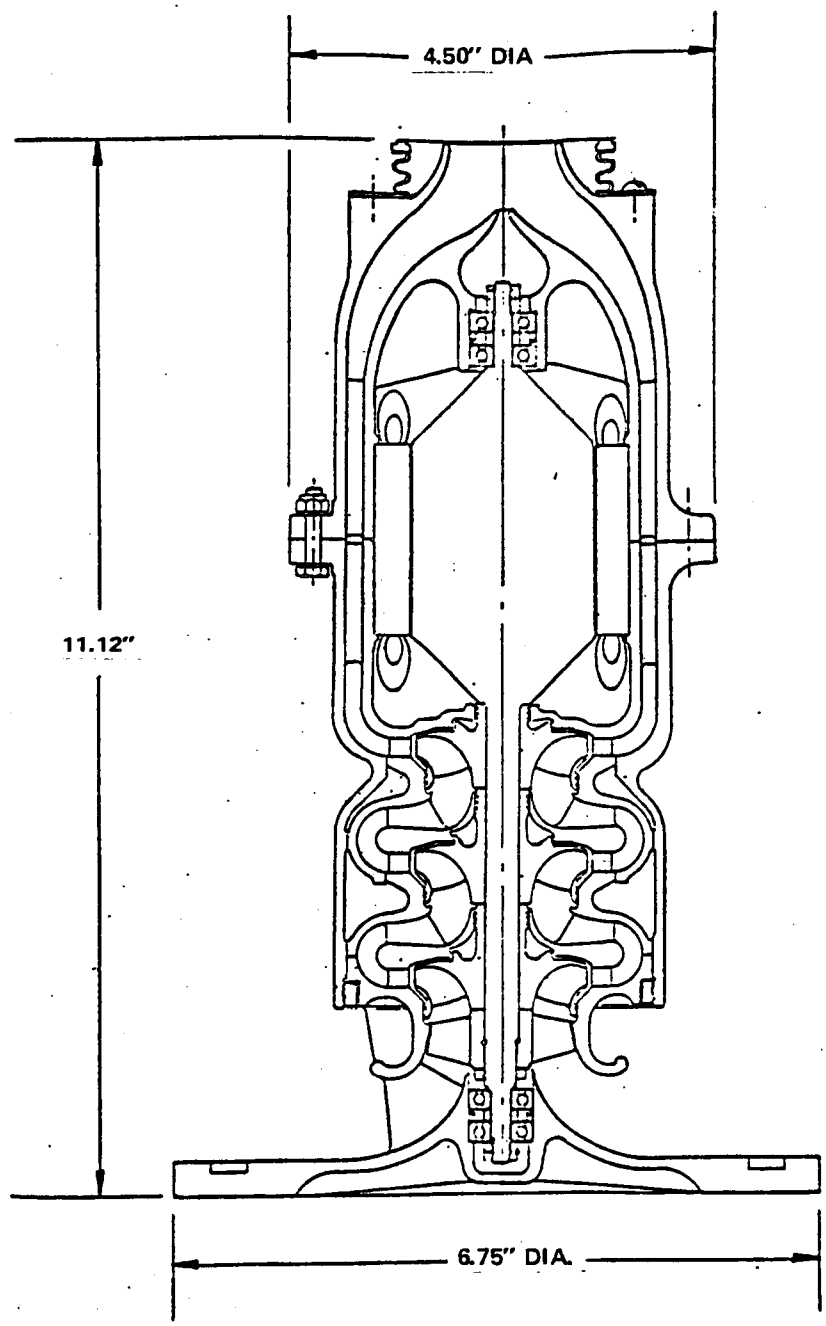

POWER	270 Vdc
PUMP WEIGHT	1.12 lb
RPM	36,000 max.
MAX. hp	3.16
SYSTEM WEIGHT	63.5 lb

3-STAGE, VARIABLE SPEED CENTRIFUGAL

Figure 70. - Selected LH_2 boost pump.

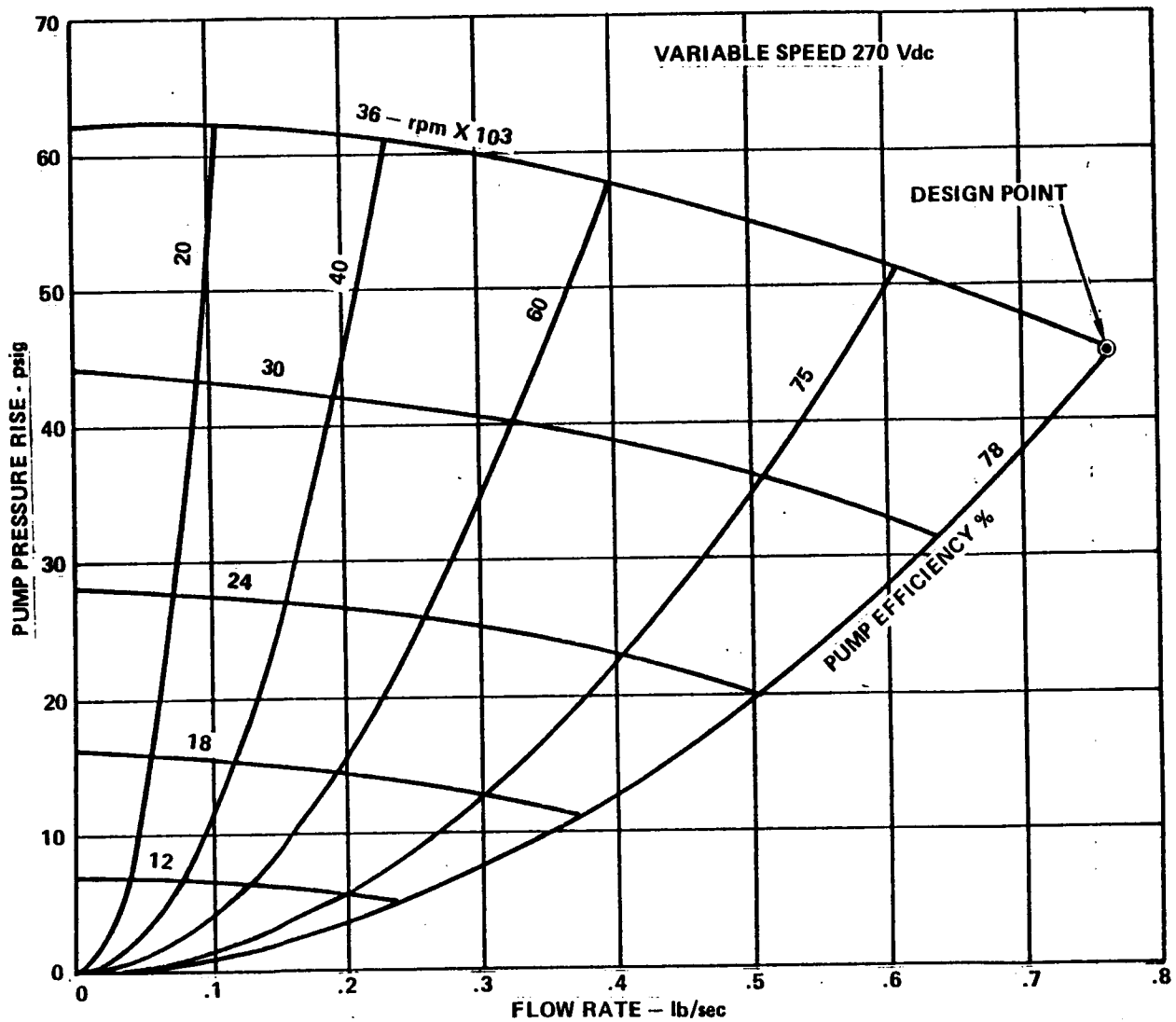

Figure 71. - Three stage pump characteristics.

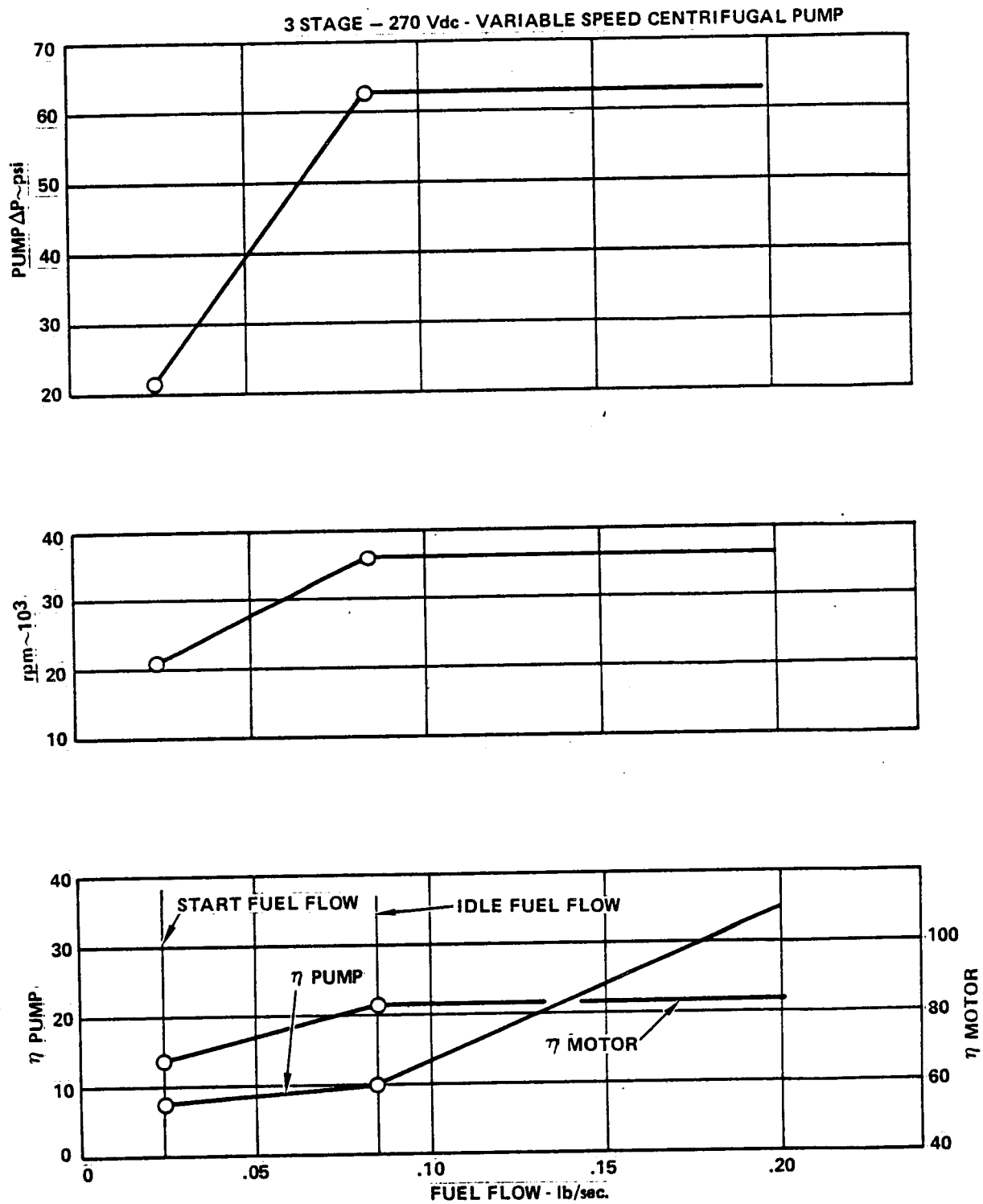

Figure 72. - Pump characteristics (transient).

Figure 73 shows the pump NPSP, V/L volume ratio, and percent of vapor at the pump inlet versus fuel flow. Also shown is the effect of GH_2 leakage into either 1 or 2 of the average 10 foot long vacuum jacketed line sections. Since it would not be reasonable to ground the airplane with a single vacuum leak, the assumption must be that a second leak could develop either inflight or at a location where repairs were not possible. With this assumption, the performance of the foamed line is seen to be nearly identical to the vacuum line with a GH_2 leak in two 10 foot sections. Since the weight of the foamed line is only about 10-15 percent greater, it would appear that the foam concept is more attractive in both reliability, original cost and maintenance.

In the case of an unchilled vapor filled line, the engine acceleration to idle will take a longer time that with a chilled line since the engine will not accelerate until the engine pump receives liquid H_2 (V/L = 0). This time could be reduced by using the intertank transfer system to increase the boost pump flow rate.

5.6.3 Final system configuration. - The final system layout and details are shown in figure 74. The lines are foam insulated and protected by an outer aluminum cover which would contain any H_2 leakage in the inner line. All components are purged and ventilated. An outer shroud (unpressurized) is provided where the fuel line runs through pressurized compartments. The motors and actuators of all shutoff and crossfeed valves can be removed without disturbing the line itself. Pump replacement can be done with LH_2 fuel in the tank. (See Section 5.3.6).

5.6.4 Engine operational procedures. - The procedures and requirements for operation of the engine, and its fuel delivery and control system, are as follows:

- Initial Condition

  Engine is stopped

  Electrical system is de-energized

  Engine fuel flow control valve is closed

  Tank shut-off valve is closed

  Boost pump is not running

  Entire fuel system down stream of the liquid hydrogen tank has reached a soak temperature of 560°R. The system is full of hydrogen gas at a temperature of 560°R, and the pressure has relieved to the 21 psia tank pressure through a reverse flow check valve in the tank shut-off valve.

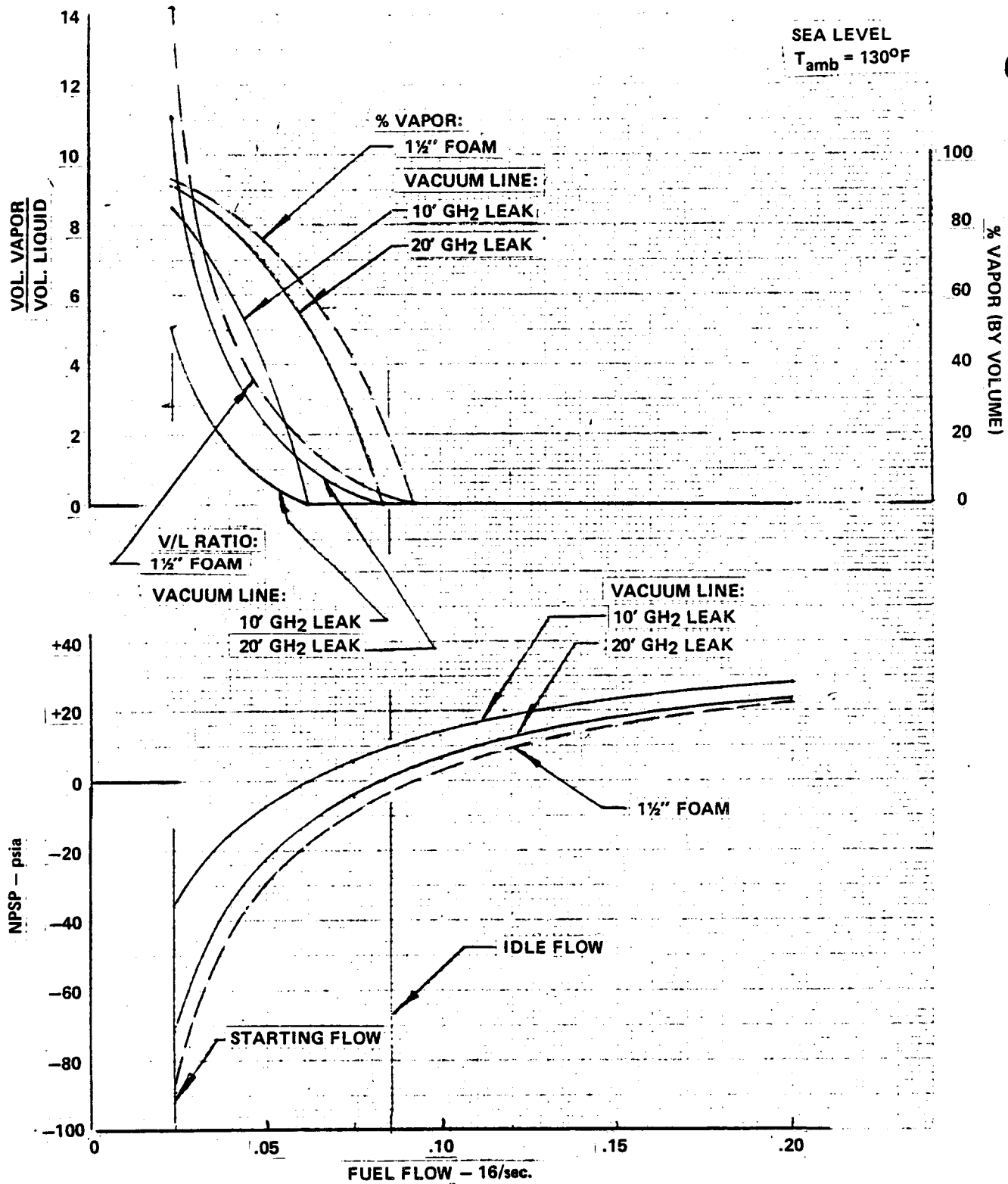

Figure 73. - Engine pump inlet conditions.

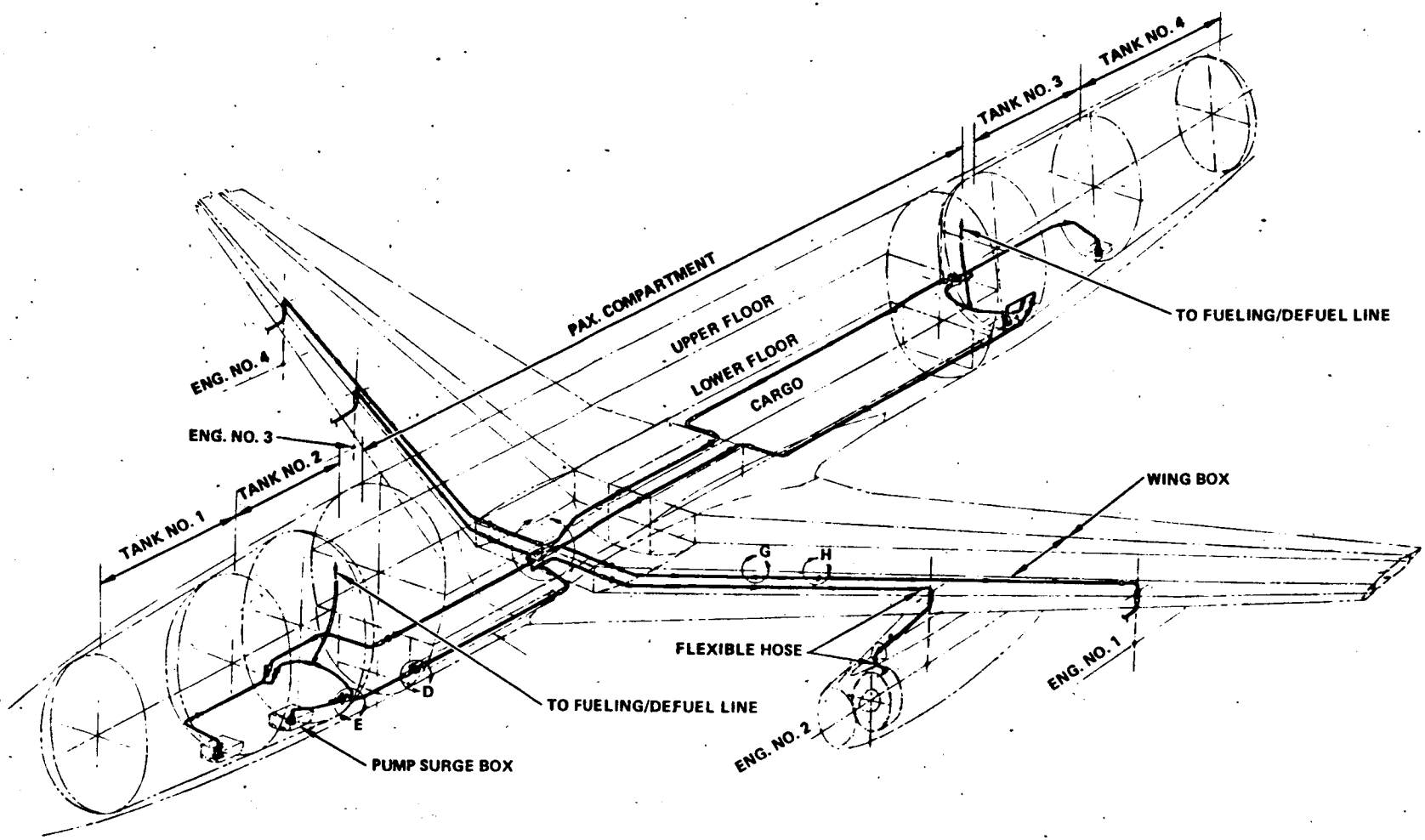

Figure 74. - Engine fuel supply system. (Sheet 1 of 2)

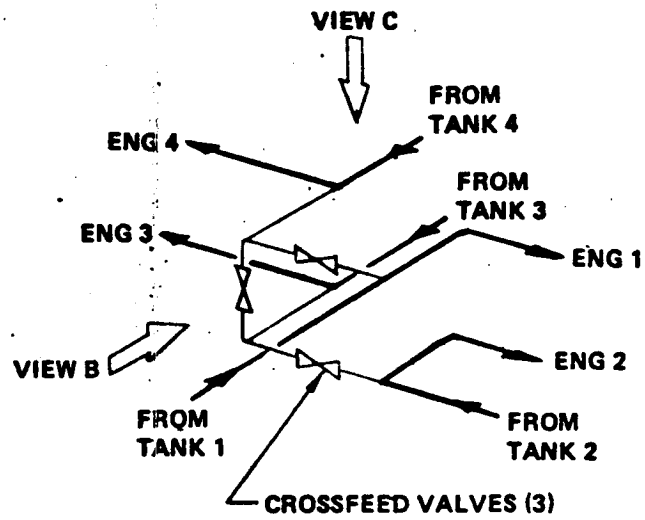

DET. A – CROSSFEED VALVE SCHEMATIC

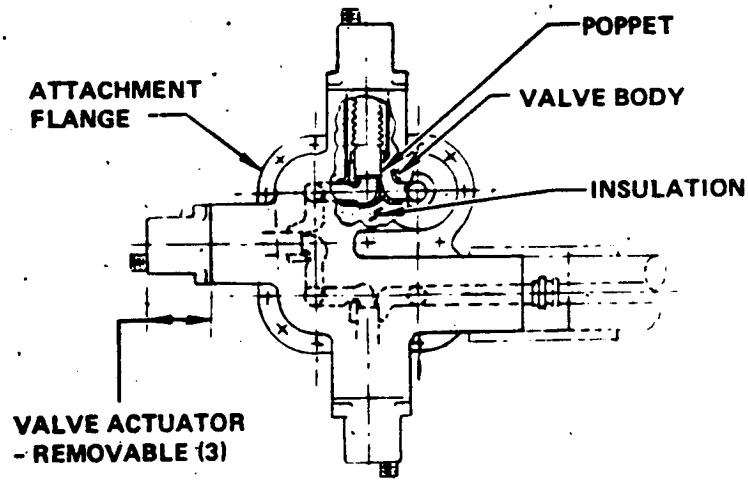

VIEW B

CROSSFEED VALVE ASSY - INSTALLATION

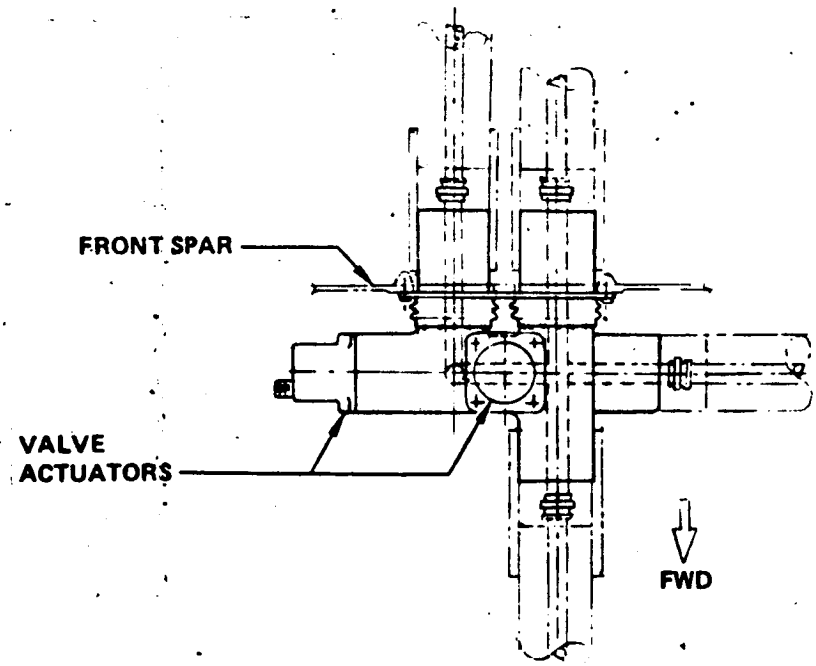

VIEW C

CROSSFEED VALVE ASSY.

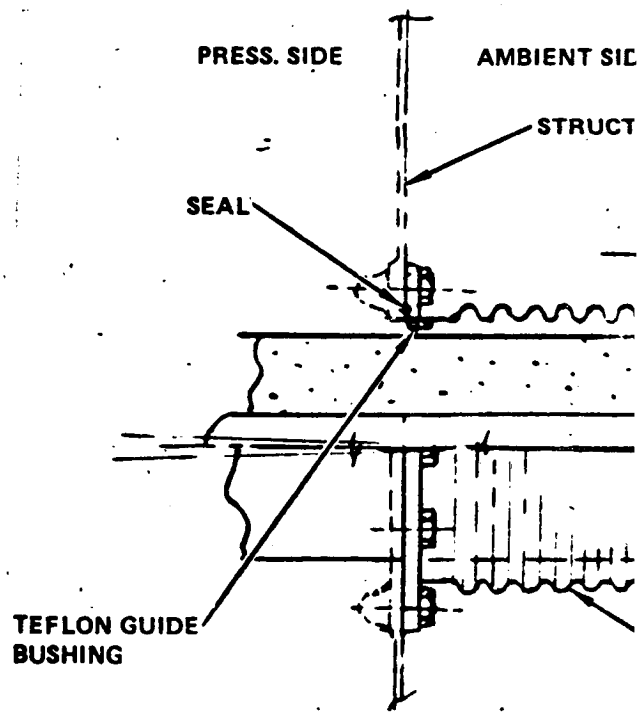

DET. D – BULKHEAD FTG. – I

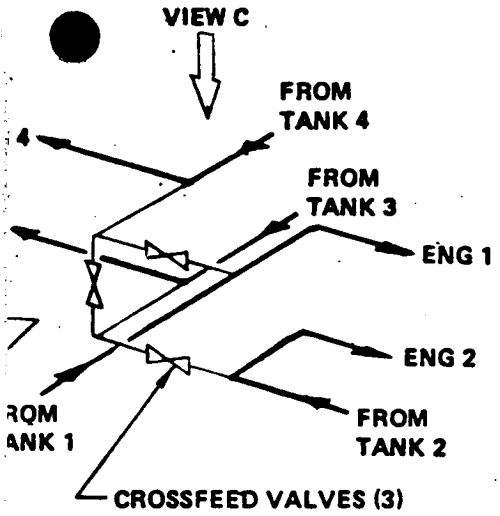

. A – CROSSFEED VALVE SCHEMATIC

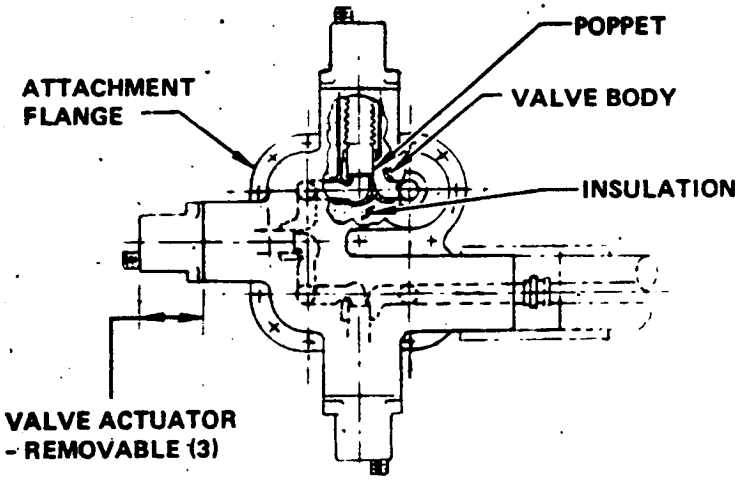

VIEW B

CROSSFEED VALVE ASSY - INSTALLATION

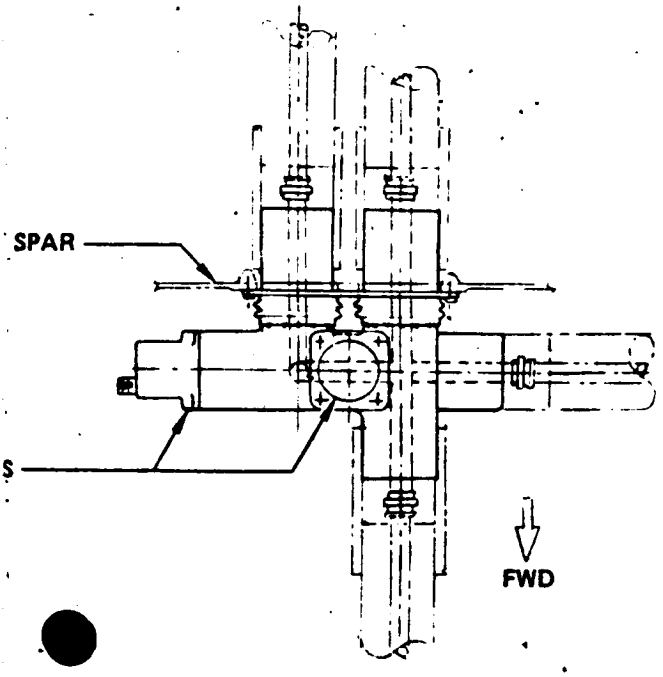

VIEW C

CROSSFEED VALVE ASSY.

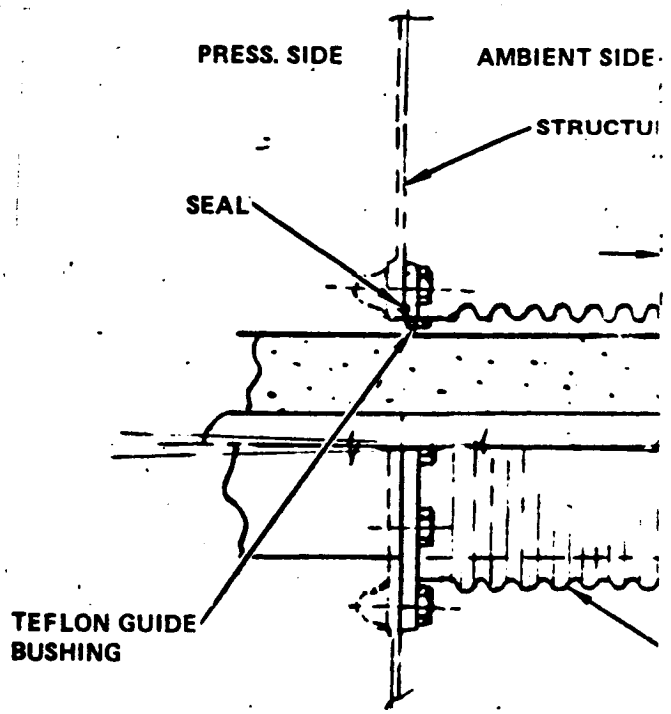

DET. D – BULKHEAD FTG. – FL

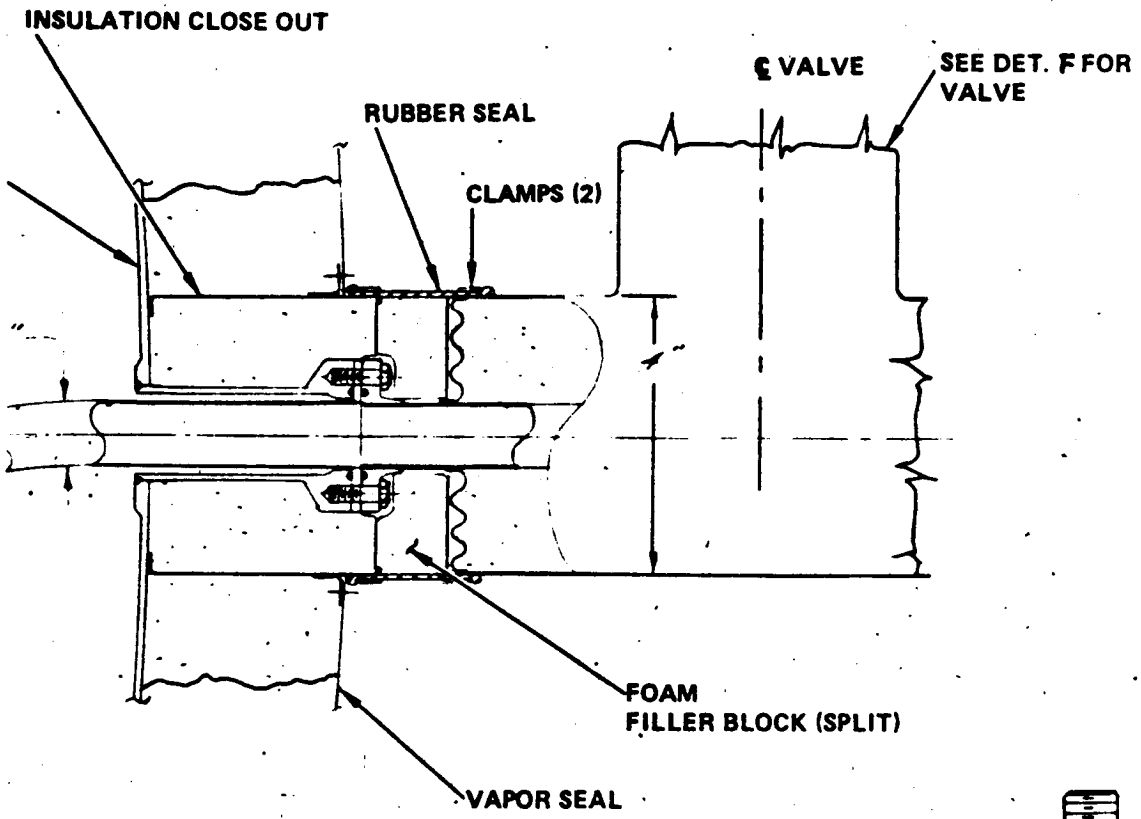

ET. E – TANK FTG AND VALVE INSTL.

RE

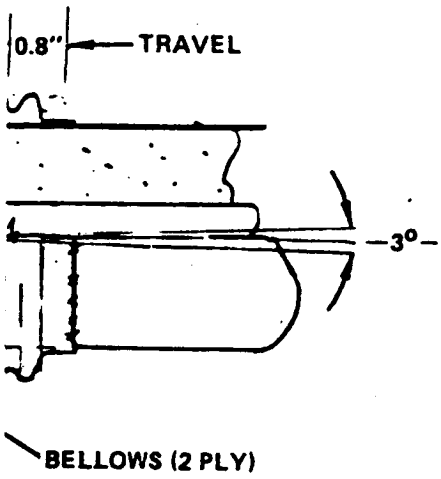

EXIBLE

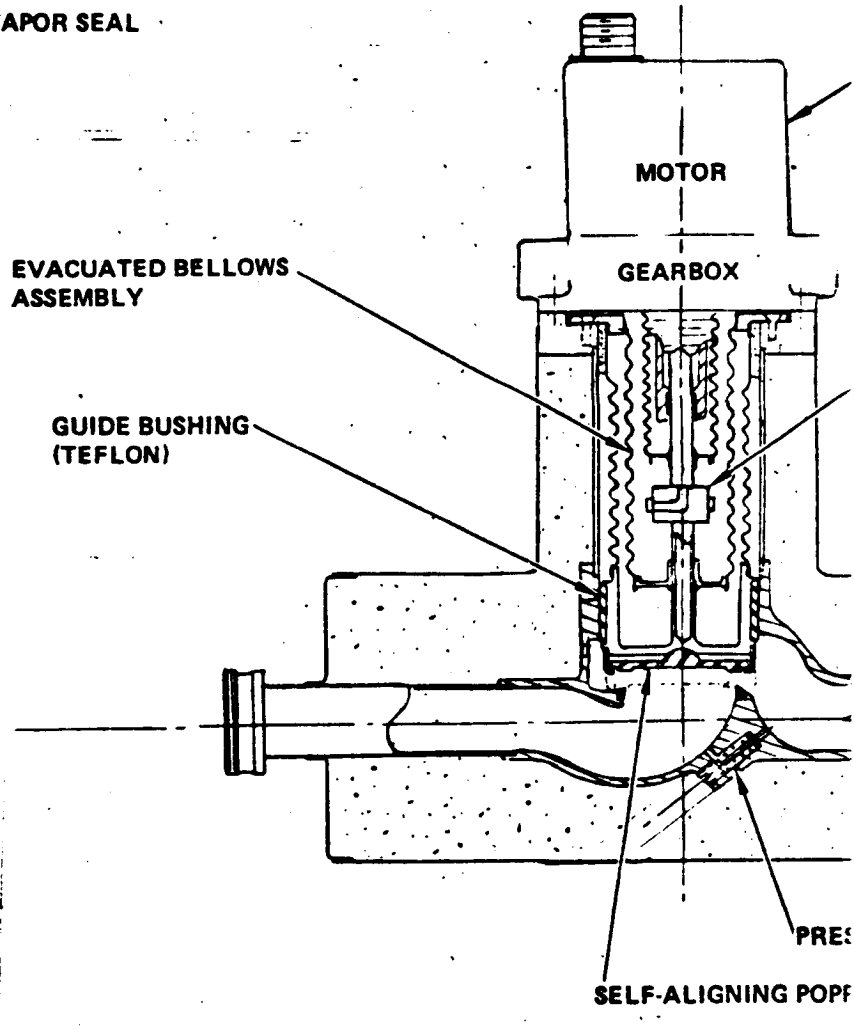

DET. F – TANK ISOLATION VALVE

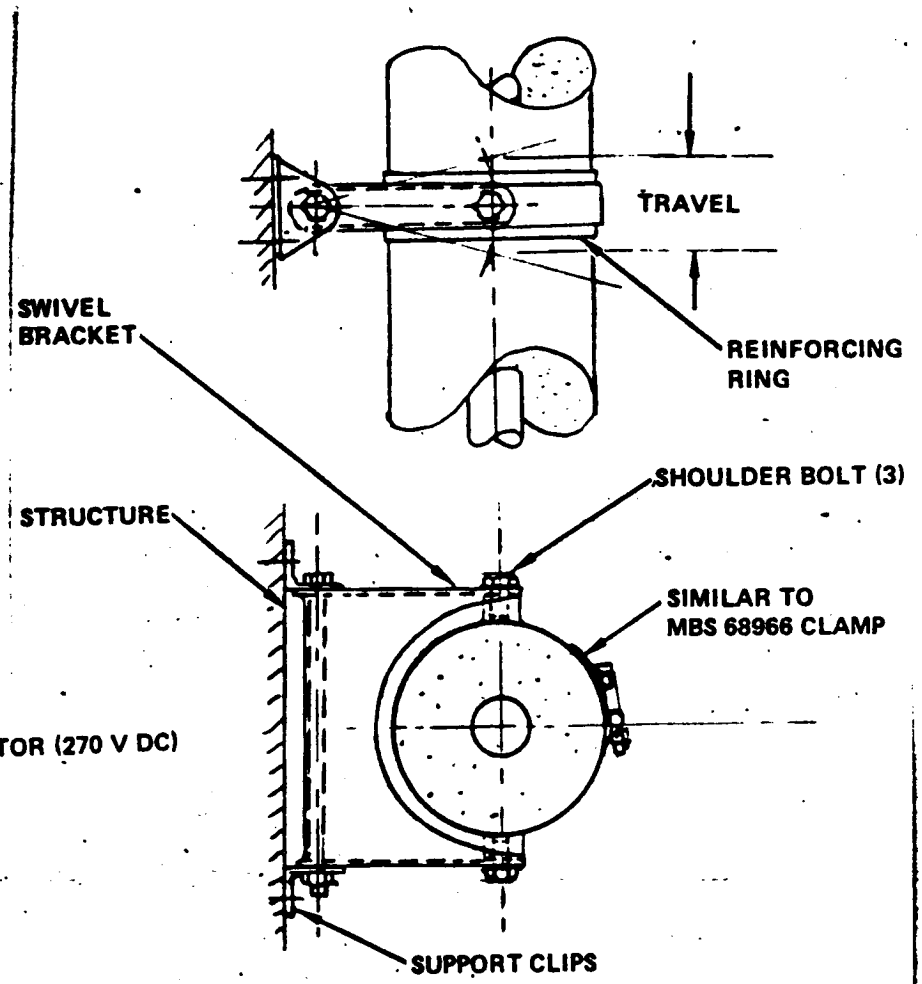

DET. G TUBE SUPPORT

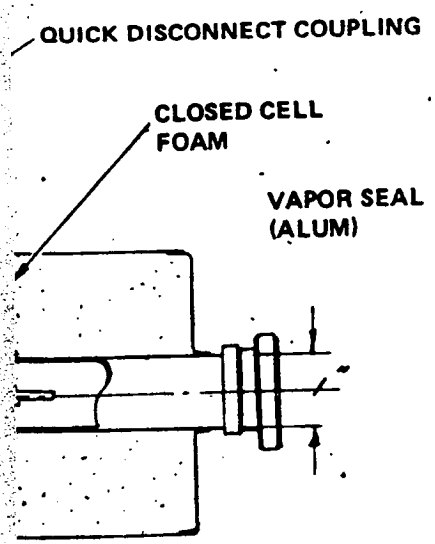

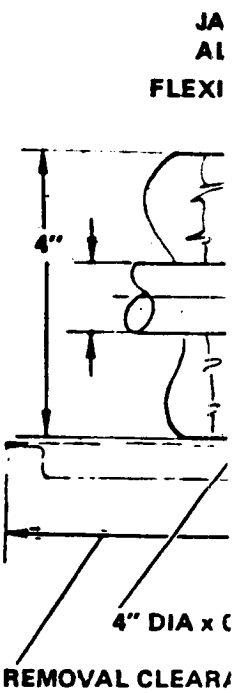

. RELIEF VALVE

T

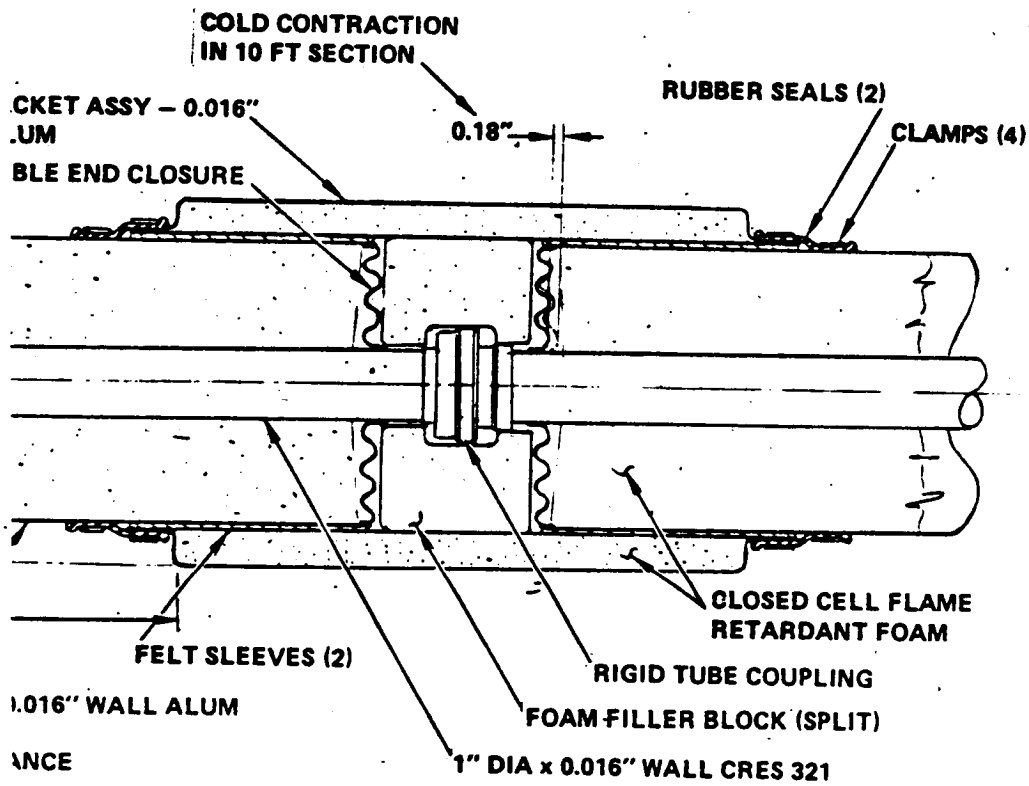

DET. H – JOINT-RIGID, ENGINE FUEL SUPPLY LINE

Figure 74. - Concluded.
(Sheet 2 of 2)

- Start Procedure

  Energize engine electrical system. This automatically opens the high pressure pump drive fluid coupling fill valve. The valve latches open and will remain open until electrically energized to close.

  Open tank shut-off valve.

  Start boost pump. Since the boost pump inlet is immersed in liquid hydrogen, the boost pump will pressurize the hydrogen gas in the line up to the engine fuel flow control valve to approximately 42 psia.

  Start cranking engine. Engine oil pressure develops during cranking, and fills the high pressure pump fluid drive coupling thus driving the pump.

  At 10% speed, turn on ignition, move throttle to idle position and the engine fuel flow control valve starts the admission of fuel to the engine fuel injector.

  Engine cranking continues until the engine is self-sustaining, and then the cranking is terminated.

  Engine continues acceleration to idle speed.

  Continue operation at idle speed until chill-down of the engine high pressure pump is completed. The time required for chill-down is approximately one minute. After chill-down of the engine high pressure pump is completed, normal engine operations may be commenced.

- Ground and Flight Operation

  System responds to command inputs in a manner similar to that of a conventional Jet A fueled turbofan engine.

- Shut Down

  Reduce engine speed to idle.

  Move throttle to idle cut-off.

  De-energize engine electrical system. This automatically energizes the high pressure pump drive fluid coupling fill valve to close. The valve latches close, and will remain closed after the electrical system is de-energized. With the valve closed, the fluid drive coupling drains, disconnecting the pump drive.

  Turn off boost pump.

  Close tank shut-off valve.

- Procedure After Aborted Ground Start

  Turn off ignition.

  Crank engine for a pre-determined time to ventilate engine and remove any hydrogen vapor.

  Determine reason for aborted start and take corrective action if required.

  Start engine using normal start procedure.

- Procedure for In-Flight Shut Down

  Reduce engine speed to idle.

  Move throttle to idle cut-off.

  De-energize engine electrical system. This automatically energizes the high pressure pump drive fluid coupling fill valve to close. With the valve closed, the fluid coupling drains permitting the fuel pump to stop, although the engine may be windmilling at moderately high speed.

  Turn off boost pump.

  Close tank shut-off valve.

- Procedure for In-Flight Start

  Open tank shut-off valve.

  Start boost pump.

  Energize engine electrical system. This automatically energizes the high pressure pump drive fluid coupling fill valve to open. Since the engine is windmilling, oil pressure is available and the coupling fills thus driving the pump at windmilling speed.

  Initiate ignition.

  Move throttle to idle position.

  When engine is started and operating normally at flight idle, move throttle to the desired power setting.

5.7 Technology Development Required

The study of the engine fuel supply system identified and brought into focus various areas of risk in the technology where advances in the state of the art are either necessary or highly desirable to facilitate the timely and economic development of a full scale system. This section lists the more significant of these technical risk items, and presents recommendations regarding appropriate advanced development.

5.7.1 Engine fuel pump. - The engine high pressure pump bearing system is a major technical risk item requiring advanced development. Rolling element bearings operating in cryogenic hydrogen, at the speeds and loads anticipated for the engine high pressure pump, have exhibited a life capability several orders of magnitude less than that required for air transport service. Hydrostatic/rolling element hybrid bearing systems have been designed and tested experimentally, but have not yet reached an acceptable state of development for the intended application. Foil bearings have not been demonstrated in cryogenic hydrogen, and hybrid bearing systems, using an oil lubricated bearing to carry the critical thrust loads, have not been demonstrated to verify the successful resolution of the critical thermal management problem. Clearly a program of advanced technology development is indicated here.

It is recommended that engine high pressure pump bearing system advanced development be undertaken, and that such advanced development start with the preliminary design of an engine high pressure pump in sufficient depth to establish the bearing requirements. This would then be followed by design, fabrication, and feasibility testing of a bearing system having the objective of meeting these requirements. Initial bearing tests would be in a bearing test rig, followed by tests in an actual pump.

5.7.2 Engine fuel control system. - Operation of the cryogenic hydrogen fuel control system presents several new problems such as starting with the supply line full of vapor, the necessity for extremely rapid chill down of the engine high pressure pump, the probable necessity to control the flow of fuel in both the vapor and liquid states, and the presence of significant volume capacitance in the fuel system combined with the use of the relatively compressible H_2 fuel. These new problems suggest the desirability of analysis and computer simulation of the selected engine fuel delivery and control system, to verify performance capability including flow, pressure, and thermal transients. Following analysis and computer simulation, fabrication and test of a breadboard system would be highly desirable.

5.7.3 Overall system. - It is desirable to make a preliminary investigation of systems interactions involved in utilizing H_2 as a heat sink for cabin air conditioning, engine oil cooling, engine stator vane and rotor blade cooling, in combination with the engine exhaust fuel heating concept. This may be done by computer simulation, and particular attention shall be paid to identifying critical off-design conditions.

It is also desirable to make a preliminary investigation of APU concepts for the H_2 fueled aircraft, including investigation of the utilization of H_2 boil-off as the fuel. Investigation of the feasibility of the external combustion concept to facilitate the utilization of H_2 boil-off should be included.

6. FUEL SUBSYSTEMS

The aircraft fuel subsystems, illustrated schematically in Figure 75, consist of all fuel-oriented systems up to the interface at the engine fuel control system. These systems cover the functions of storing fuel, fueling/defueling, supplying fuel to the engine and auxiliary power unit (APU), transferring fuel, pressurizing/venting, jettisoning, and purging and/or inerting systems. These systems are discussed in the following paragraphs.

6.1 Fuel Tank Arrangement

Fuel is stored in four thermally insulated tanks located within the fuselage. They are numbered sequentially beginning at the forward end of the airplane. Tanks 1 and 2 are located between the flight station and the forward end of the passenger compartment. Tanks 3 and 4 are located aft of the passenger compartment. Each tank has a nominal usable fuel capacity of 15 400 pounds of LH_2. Tanks 1 and 2 in the forward storage area are separated by a bulkhead which isolates the liquid fuel in each of the tanks. However, a vent system which is common to both tanks maintains an equal ullage pressure on both sides of the bulkhead. Tanks 3 and 4 are separated by a similar bulkhead in the aft fuselage area.

6.2 Fueling and Defueling

A fueling system shown in Figure 76 is provided which interfaces with the airport ground supply through two adapters located at the aft end of the fuselage below the vertical tail. Liquid hydrogen is supplied to the fueling adapter (Appendix B, Figure B-2) and displaced hydrogen gas from the aircraft fuel tanks is returned to the airport liquefaction facility for recycling by means of the vapor recovery adapter (Figure 77). A five-inch vacuum-insulated fueling manifold conveys fuel to Tanks 2, 3, and 4, reducing to a three-inch manifold between Tanks 1 and 2. Fuel is discharged into each tank by means of a perforated fueling manifold located near the bottom of the tank below the normal reserve fuel level. The perforations are sized to maintain a low discharge velocity to minimize turbulence in the bulk liquid.

The fuel level control system consists of a shutoff valve (Figure 76) actuated by a signal from a level sensor which terminates flow to each tank when it is full. When a given flight requires less than full tanks, the shutoff valves are actuated by a signal initiated by "bugs" on the tank fuel quantity indicators, located in the aircraft flight station, which have previously been set at the desired fuel quantity. The fuel quantity can also be selected at the refueling panel in the tail (Figure 76).

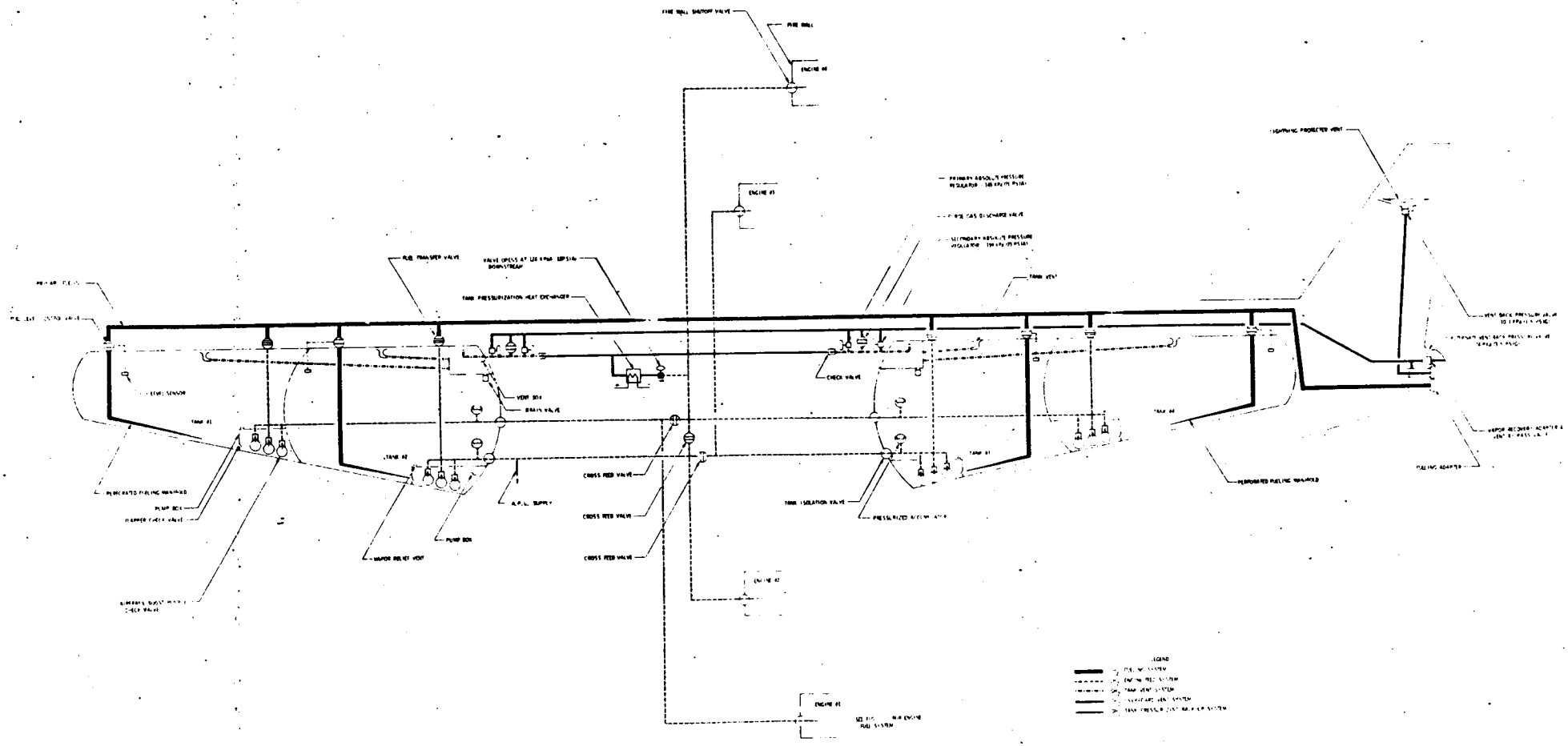

Figure 75. - Aircraft fuel system schematic.

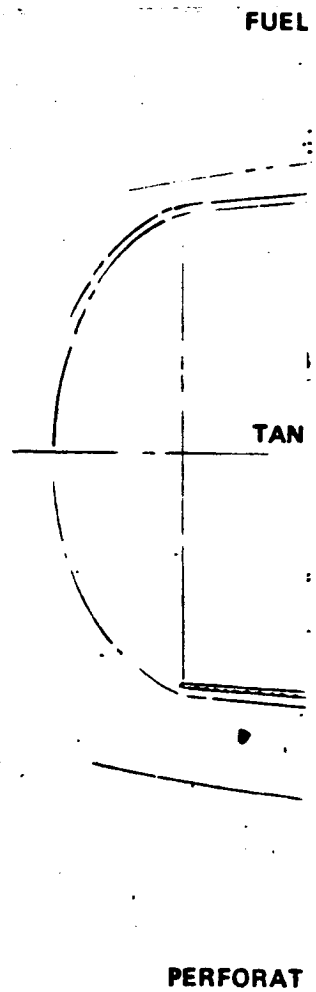
FUEL
TAN
PERFORAT

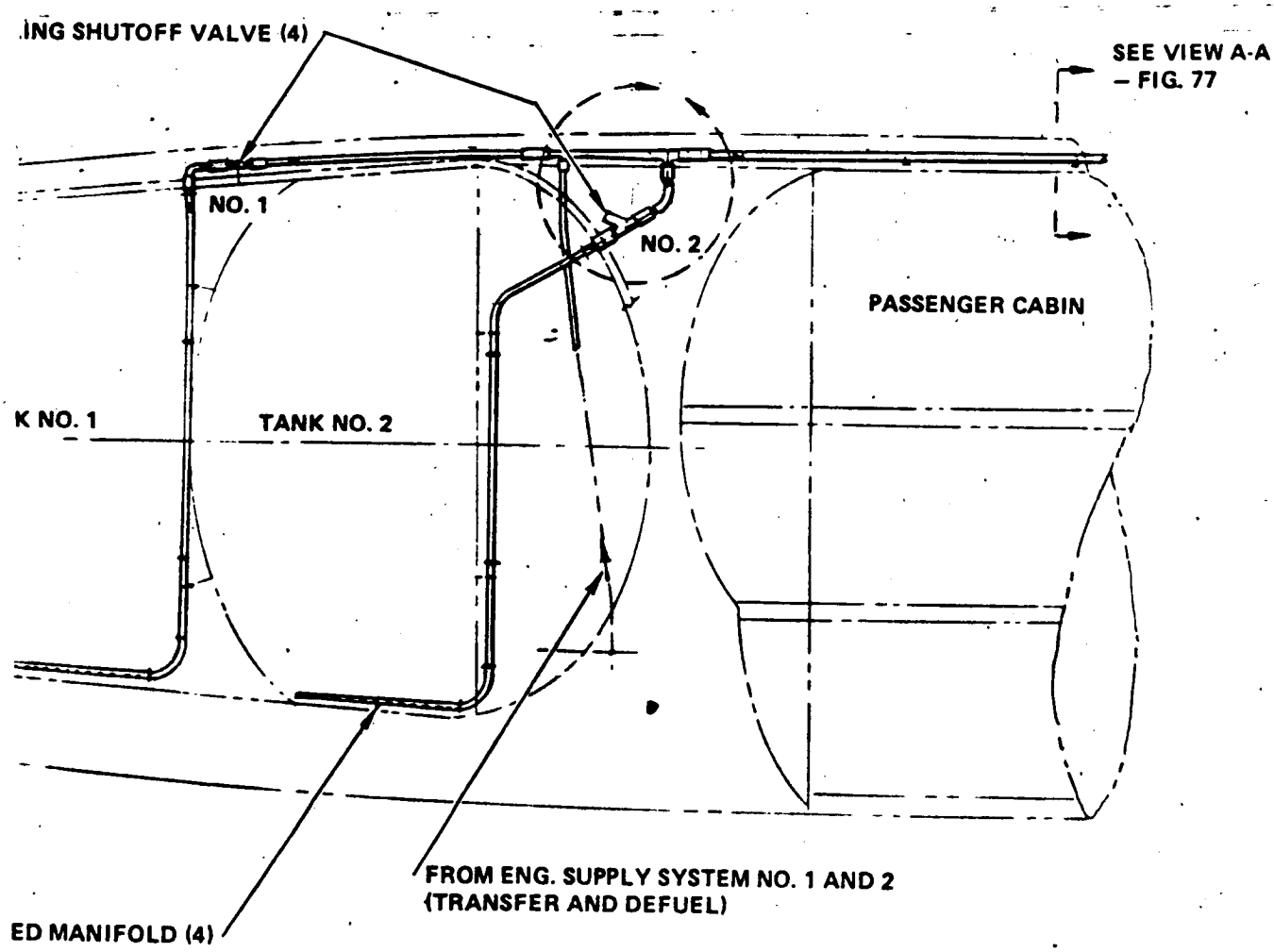
ING SHUTOFF VALVE (4)
SEE VIEW A-A
– FIG. 77
NO. 1
NO. 2
PASSENGER CABIN
K NO. 1
TANK NO. 2
FROM ENG. SUPPLY SYSTEM NO. 1 AND 2
(TRANSFER AND DEFUEL)
ED MANIFOLD (4)

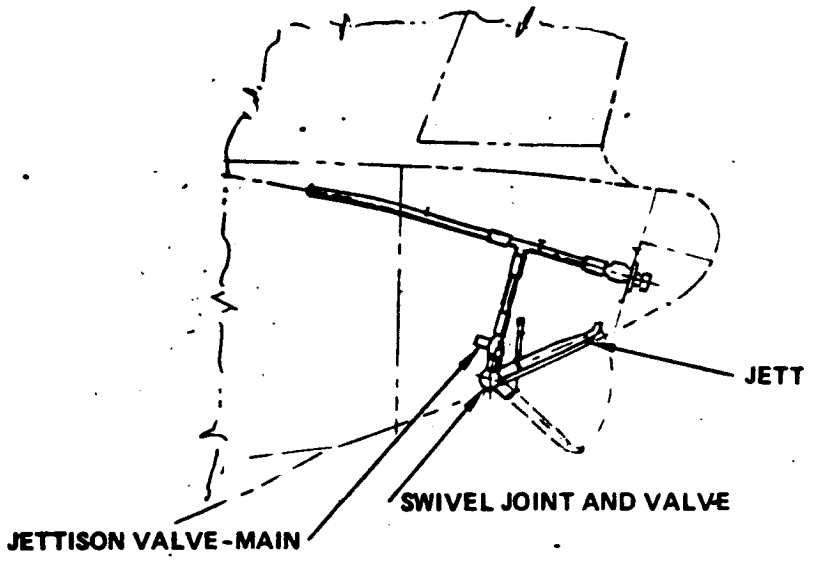

JETTISON ARRANGEMENT
(OPTIONAL)

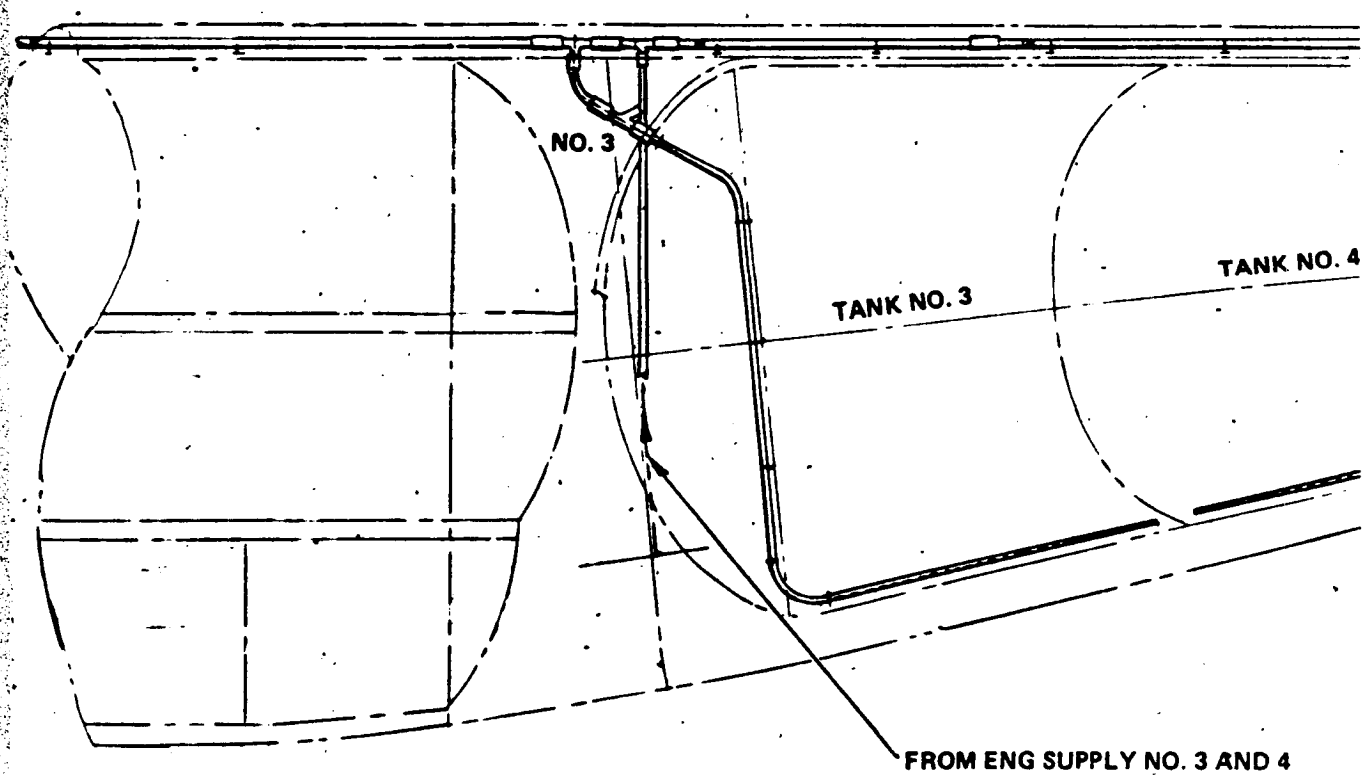

ISON CHUTE

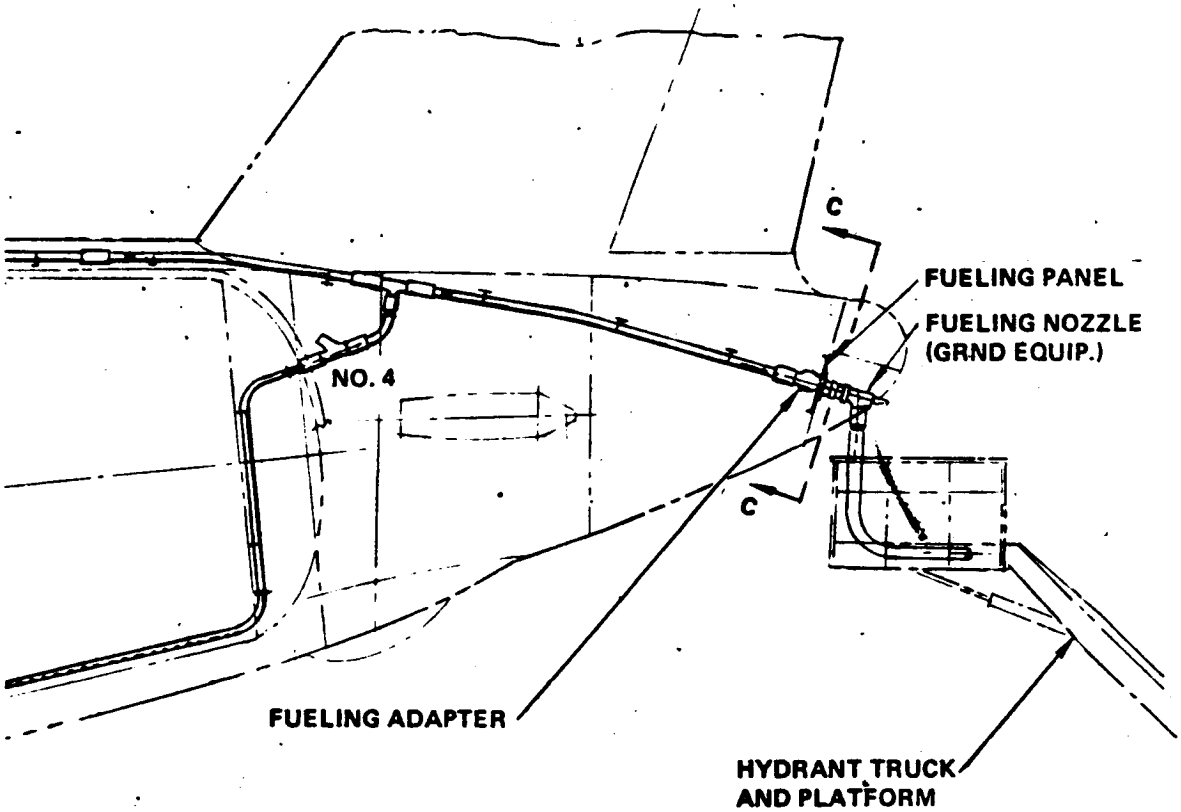

Figure 76. - Layout-fueling/defuel system. (Sheet 1 of 2)

TO TANK
NO. 1

TANK WALL

ADAPTOR

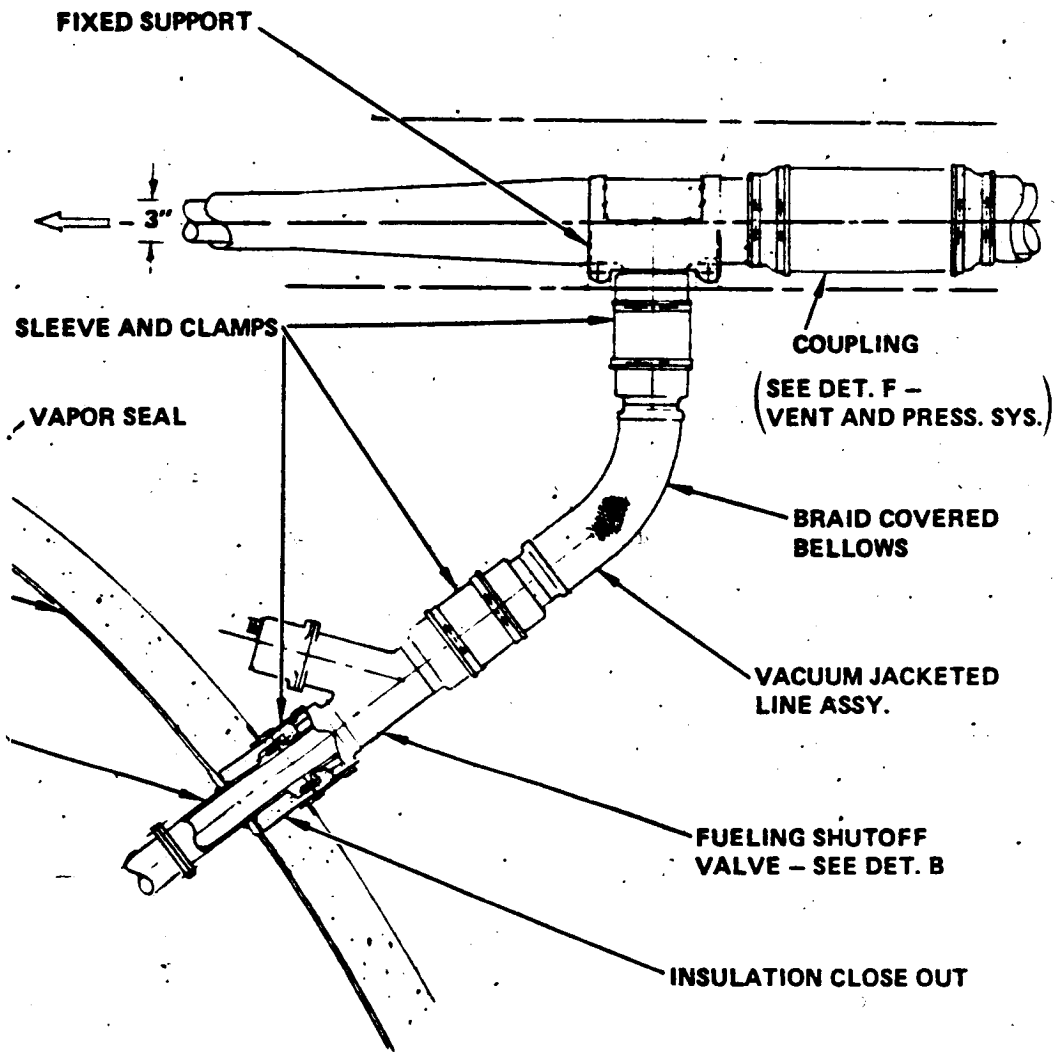

DET. A – FUELING VALVE INSTL.

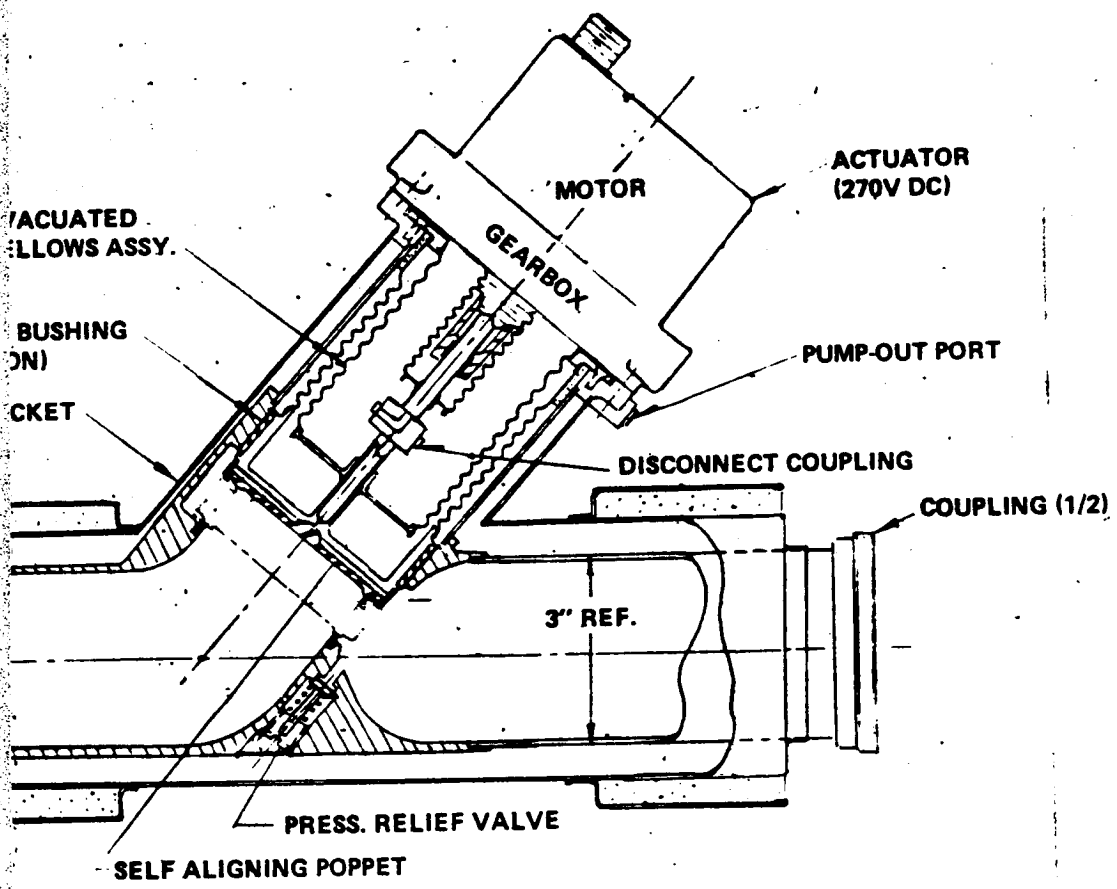

DET. B – FUELING SHUTOFF VALVE

DEFUEL VAL
– LIGHT ON
NOT IN SELEC

DEFUELING VAL

ADAP
AND S
REFU
CLOSE
ARE I

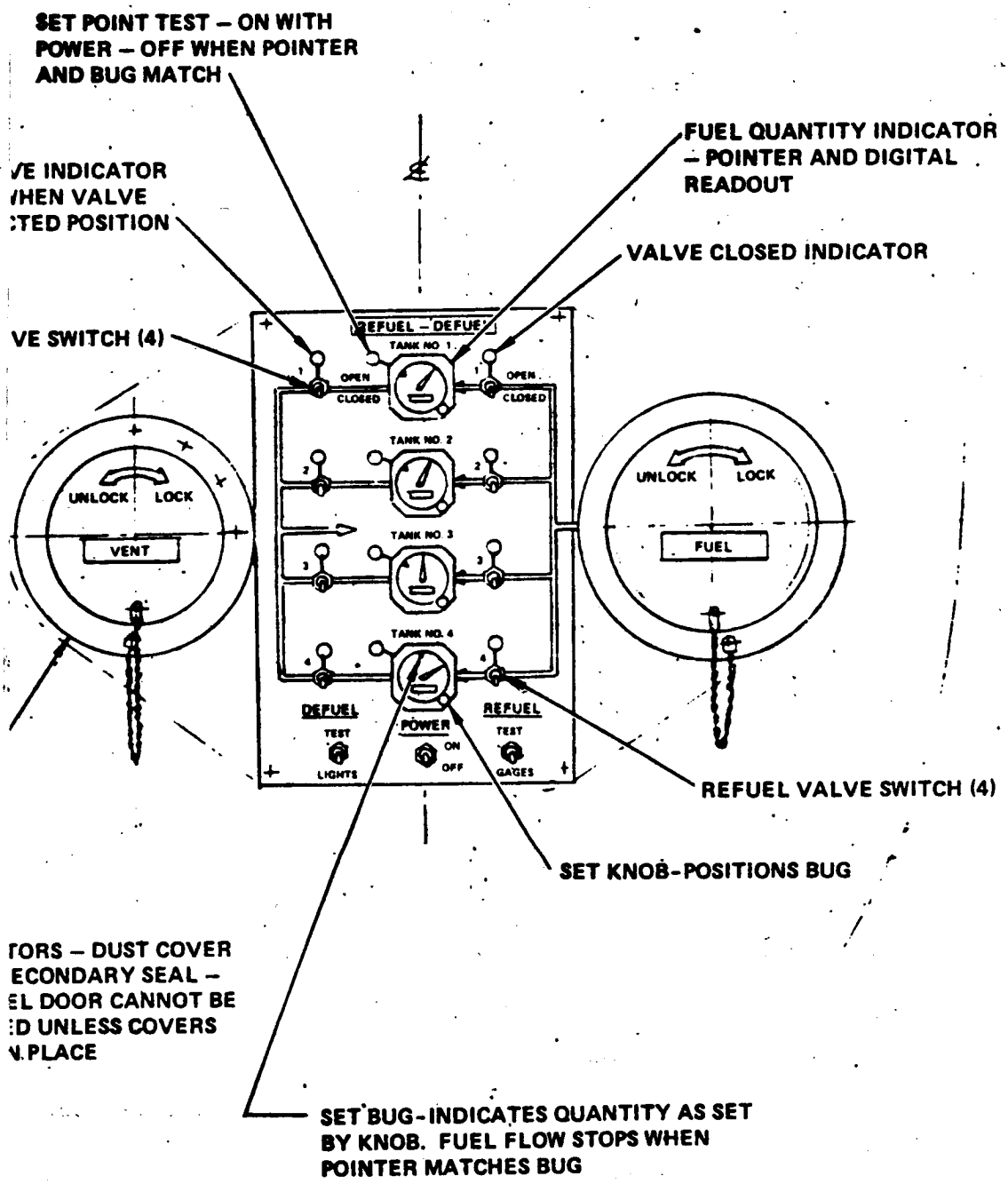

FIGURE 3. VIEW C-C – REFUEL PANEL

Figure 76. - Concluded.
(Sheet 2 of 2)

REM

VENT INTERCONNECT

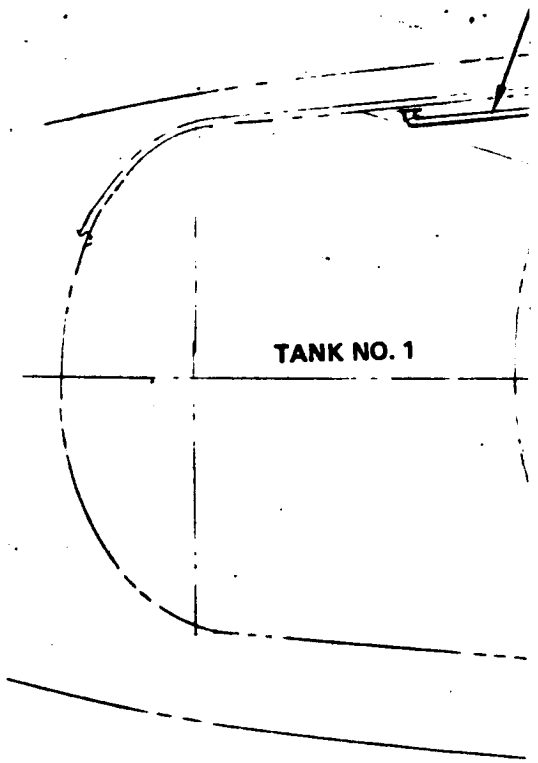

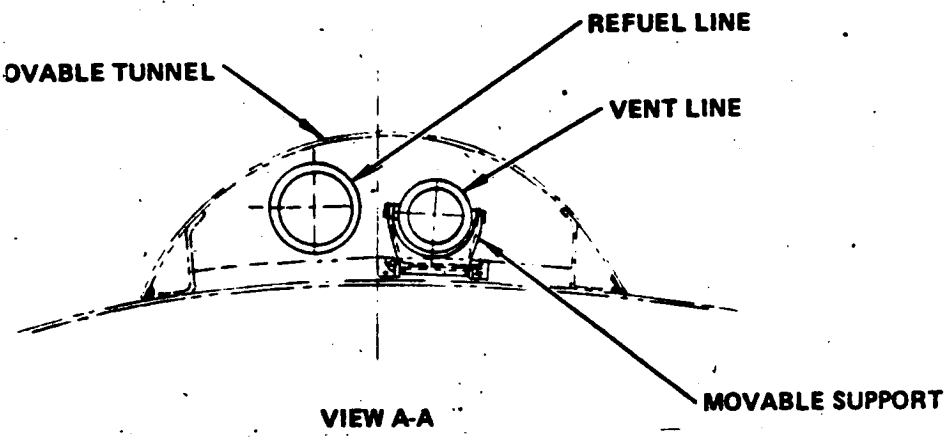
REFUEL LINE
OVABLE TUNNEL
VENT LINE
MOVABLE SUPPORT
VIEW A-A

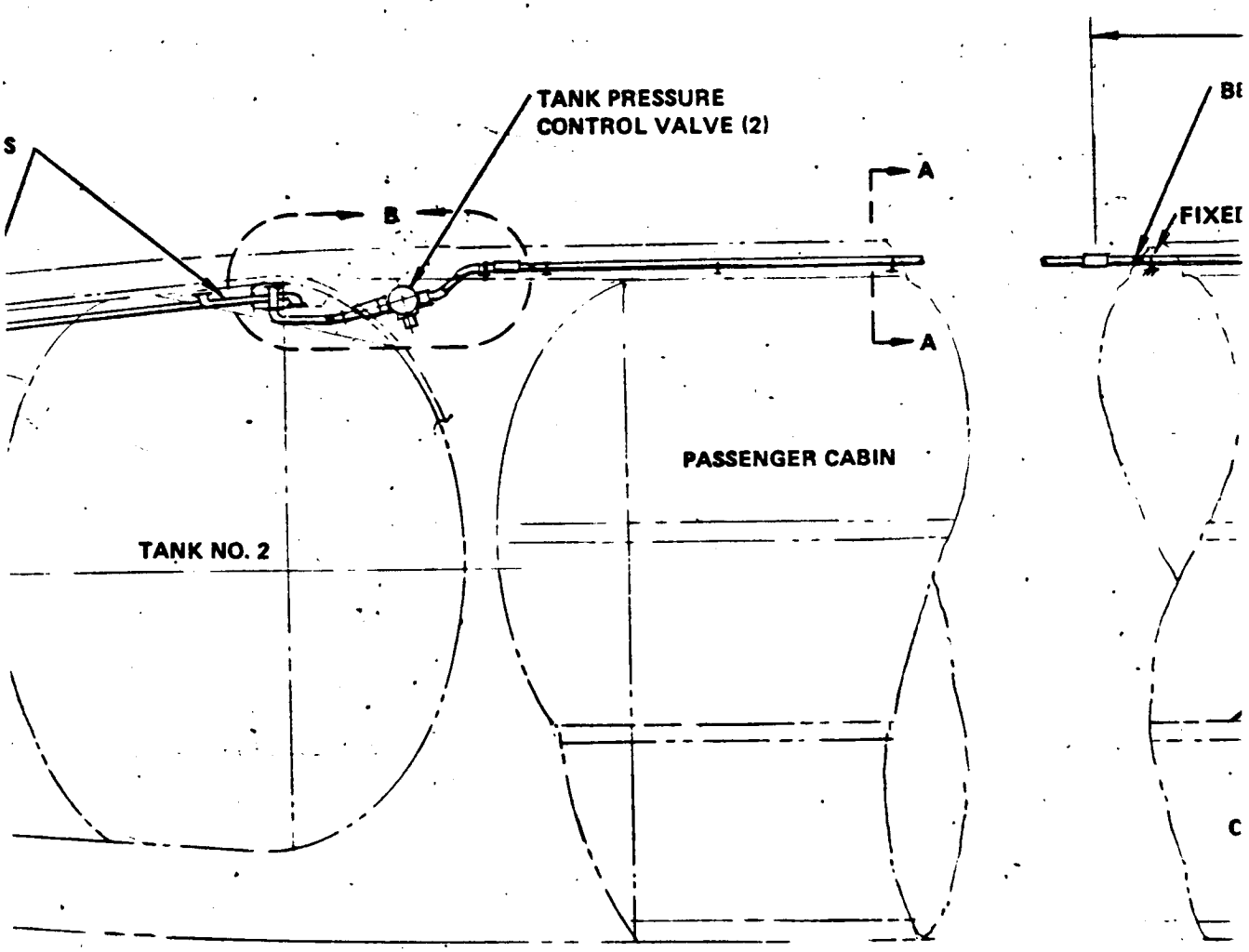
TANK PRESSURE
CONTROL VALVE (2)
S
B
A
A
PASSENGER CABIN
TANK NO. 2
BE
FIXED
C

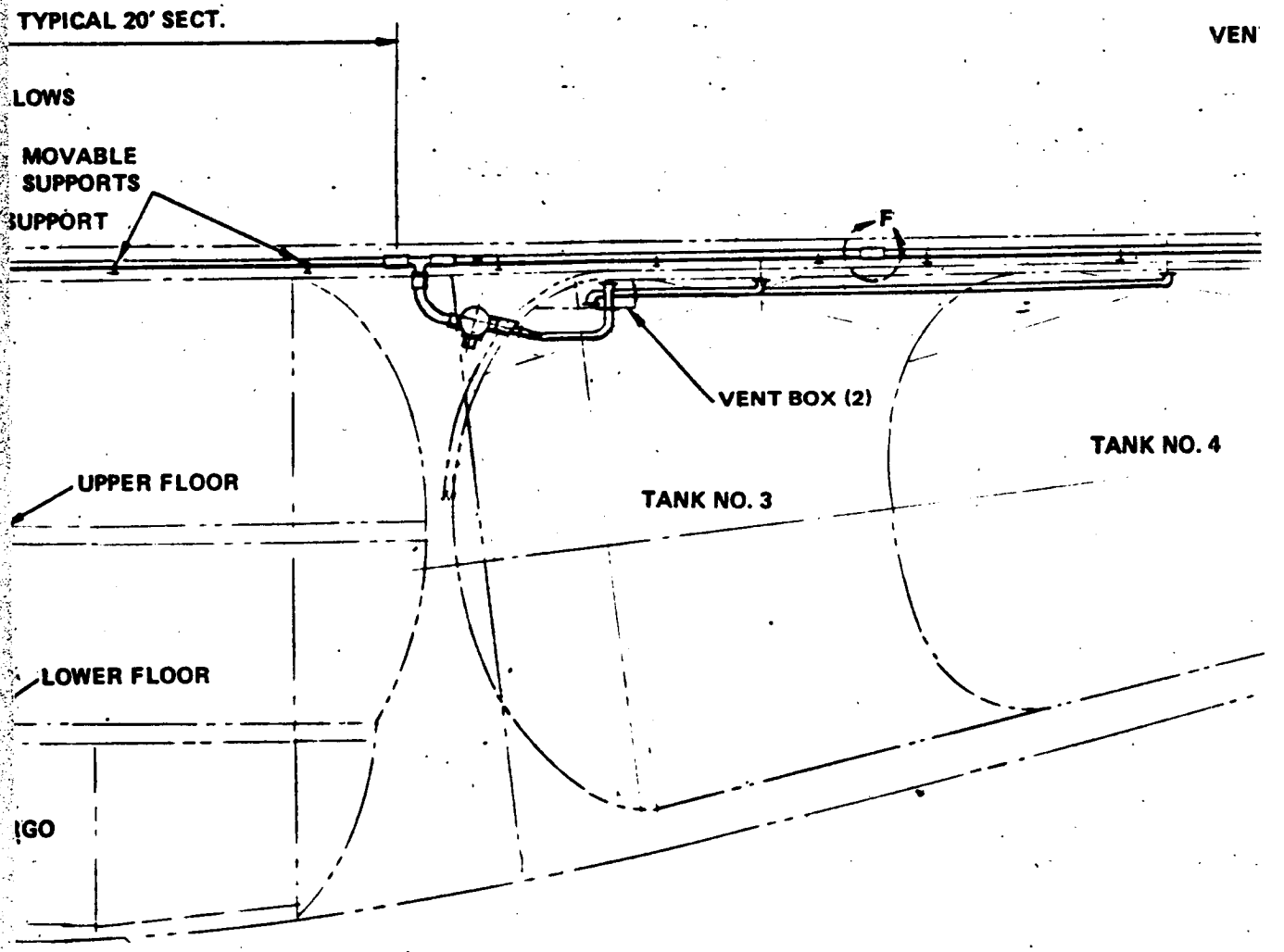
TYPICAL 20' SECT.
VEN
LOWS
MOVABLE
SUPPORTS
SUPPORT
F
VENT BOX (2)
TANK NO. 4
UPPER FLOOR
TANK NO. 3
LOWER FLOOR
GO

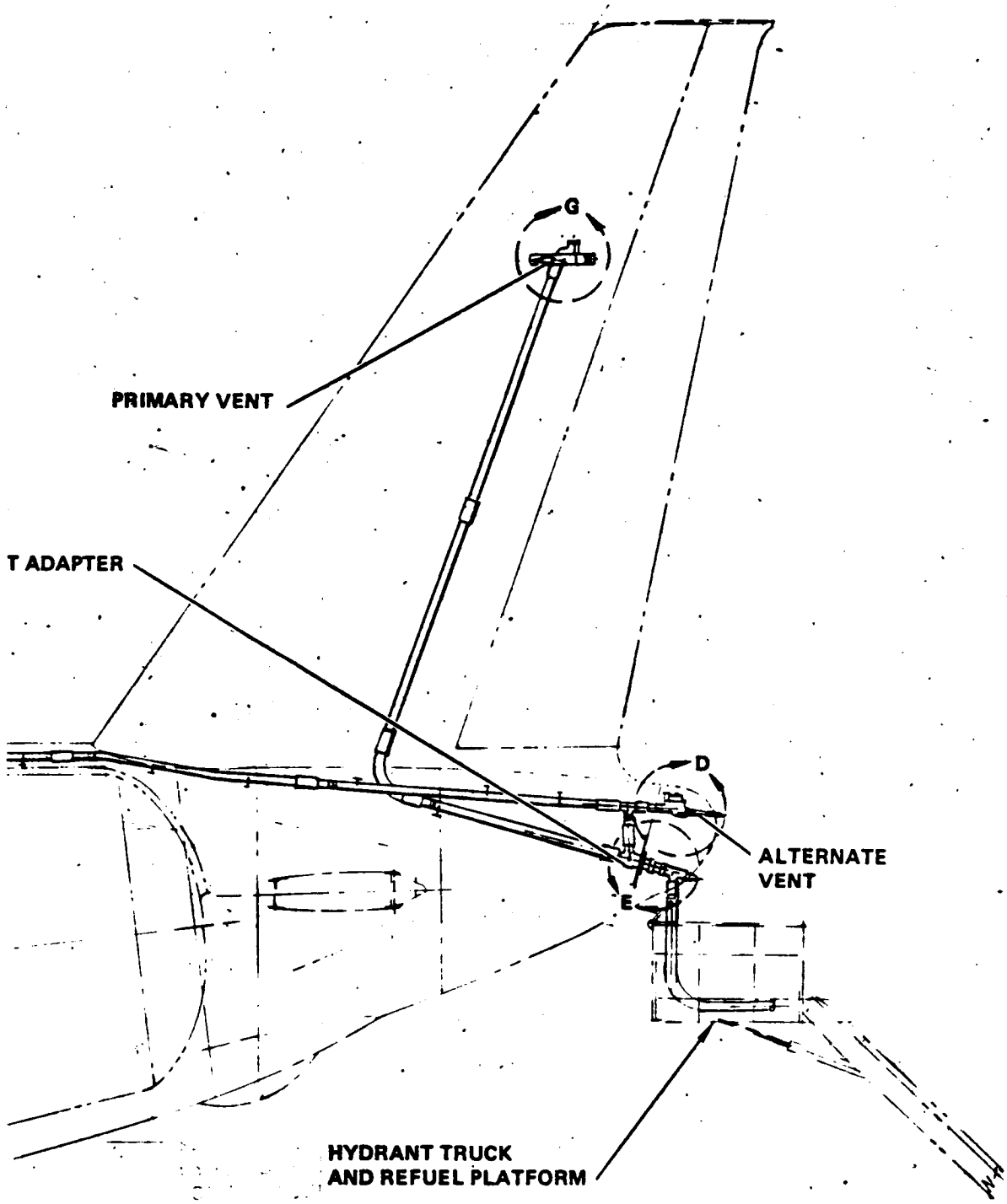

Figure 77. - Layout-vent and pressurization system. (Sheet 1 of 2)

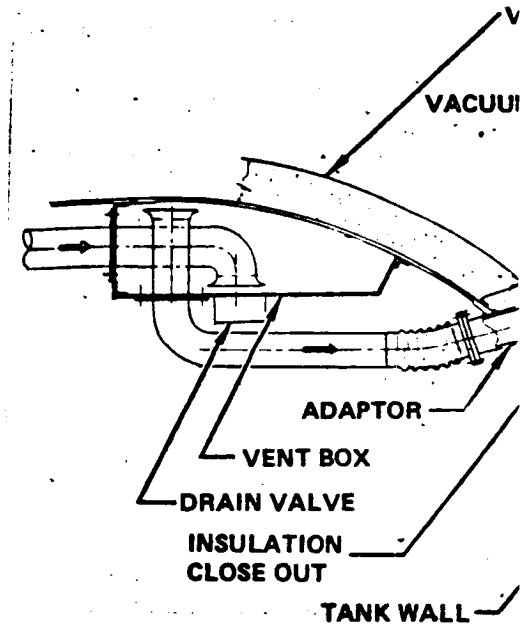
V
VACUUI
ADAPTOR
VENT BOX
DRAIN VALVE
INSULATION
CLOSE OUT
TANK WALL

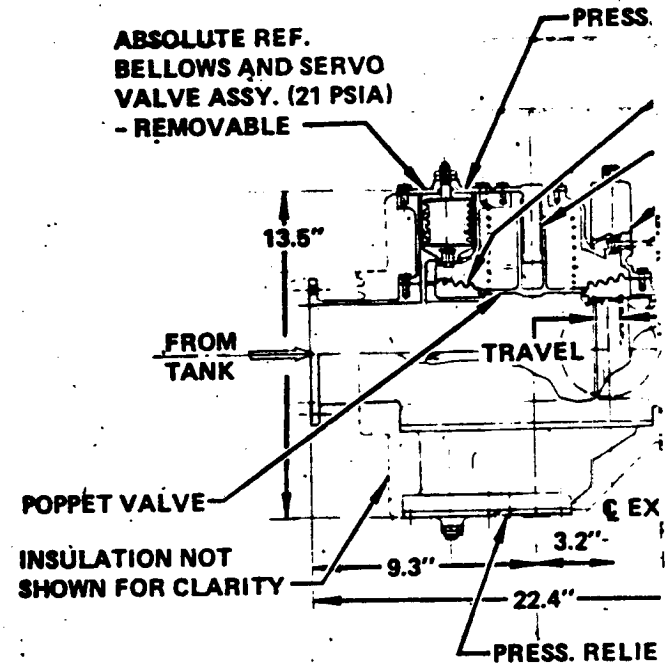

VIEW C-C – PRESS. CONTROL

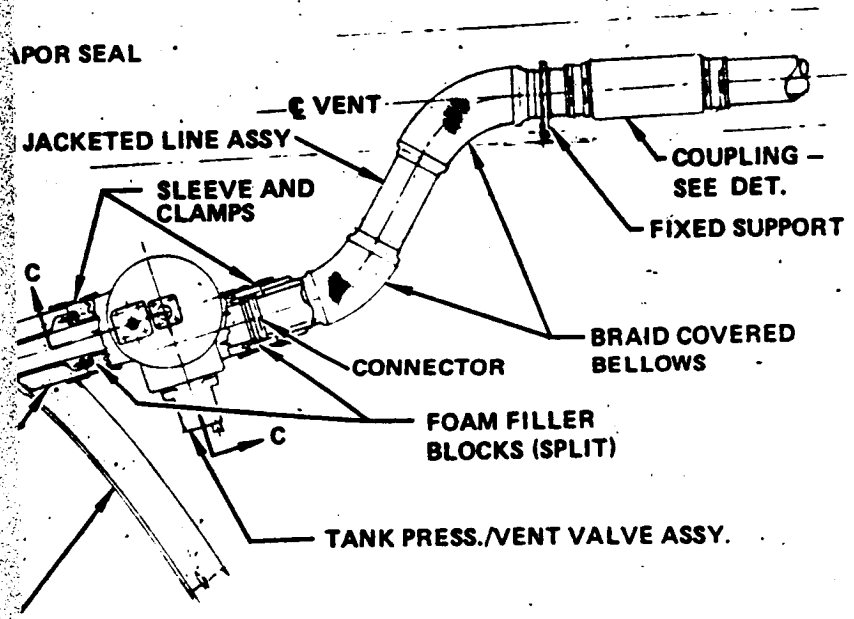

ET. B – TANK PRESSURE CONTROL
VALVE INSTL.

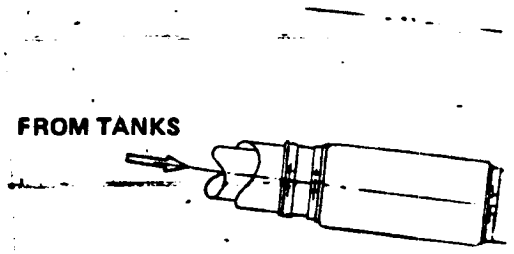

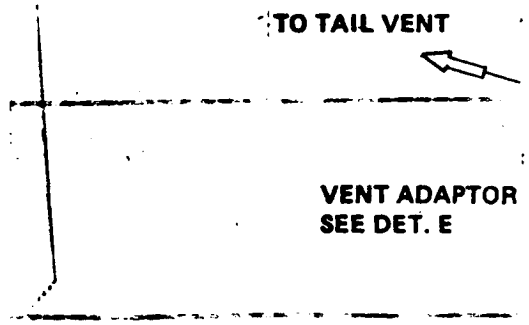

DET. D – A

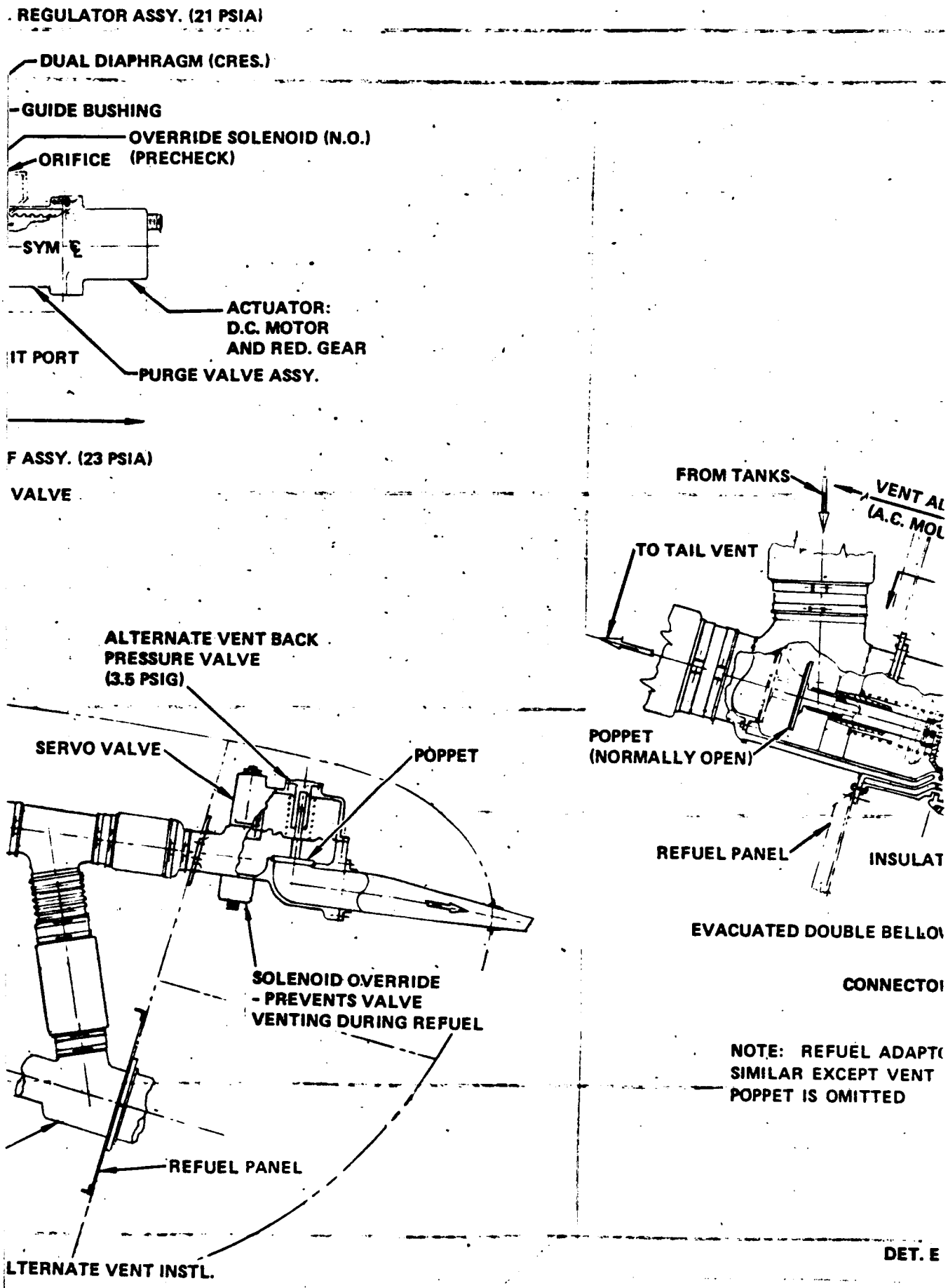
REGULATOR ASSY. (21 PSIA)
DUAL DIAPHRAGM (CRES.)
GUIDE BUSHING
OVERRIDE SOLENOID (N.O.)
(PRECHECK)
ORIFICE
SYM ℄
ACTUATOR:
D.C. MOTOR
AND RED. GEAR
IT PORT
PURGE VALVE ASSY.
F ASSY. (23 PSIA)
VALVE
FROM TANKS
VENT AL
(A.C. MOU
TO TAIL VENT
ALTERNATE VENT BACK
PRESSURE VALVE
(3.5 PSIG)
SERVO VALVE
POPPET
POPPET
(NORMALLY OPEN)
REFUEL PANEL
INSULAT
EVACUATED DOUBLE BELLOV
CONNECTOI
SOLENOID OVERRIDE
- PREVENTS VALVE
VENTING DURING REFUEL
NOTE: REFUEL ADAPTO
SIMILAR EXCEPT VENT
POPPET IS OMITTED
REFUEL PANEL
LTERNATE VENT INSTL.
DET. E

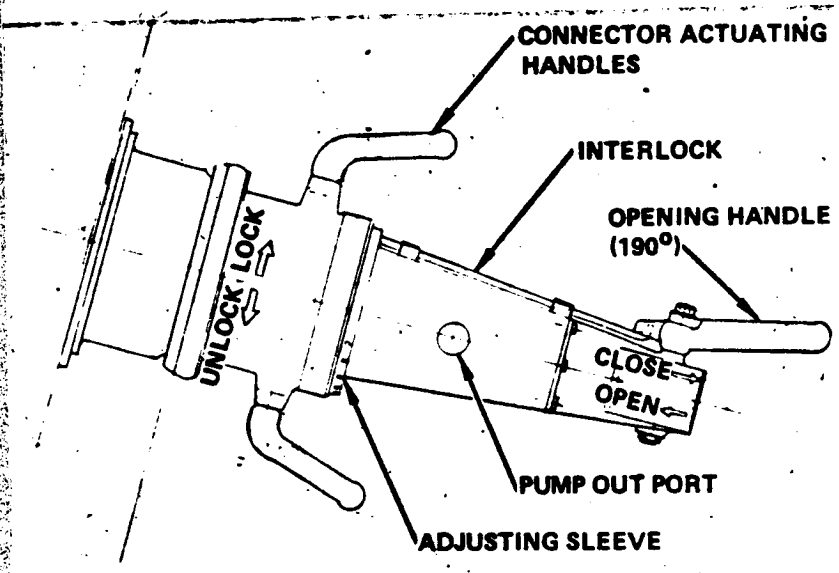

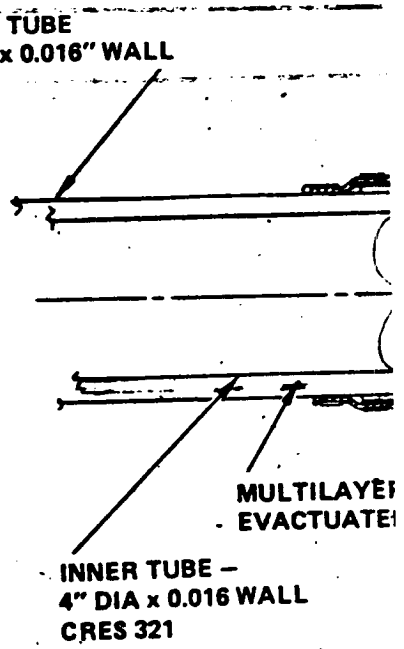

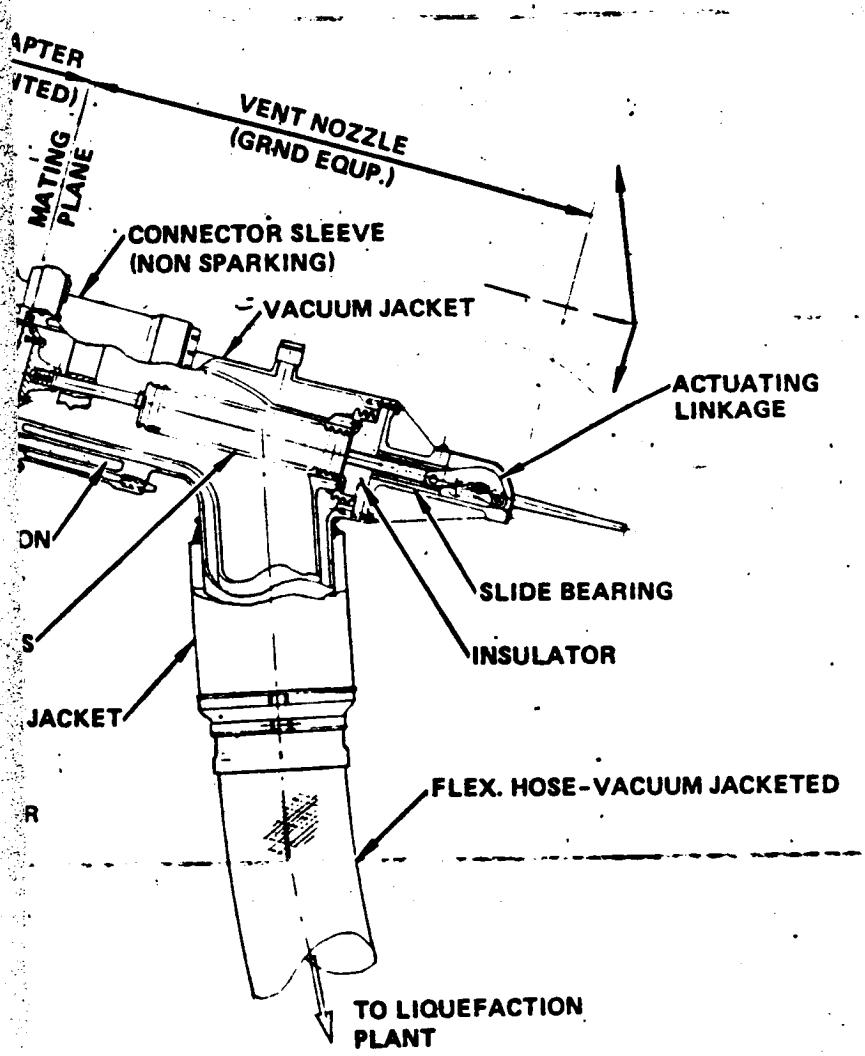

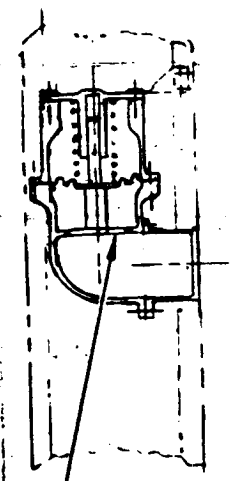

DET. G – P

VENT NOZZLE AND ADAPTOR

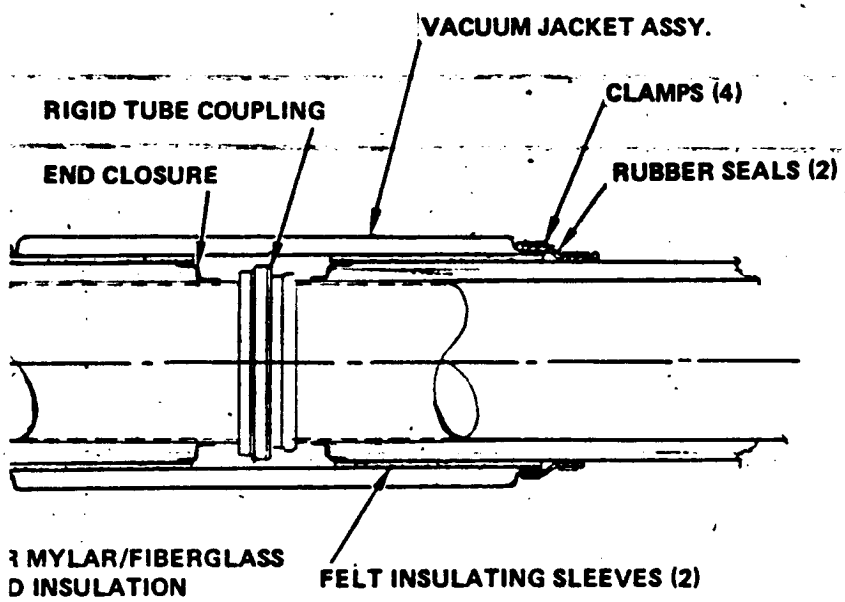

DET. F – TYPICAL VACUUM SYSTEM
RIGID JOINT

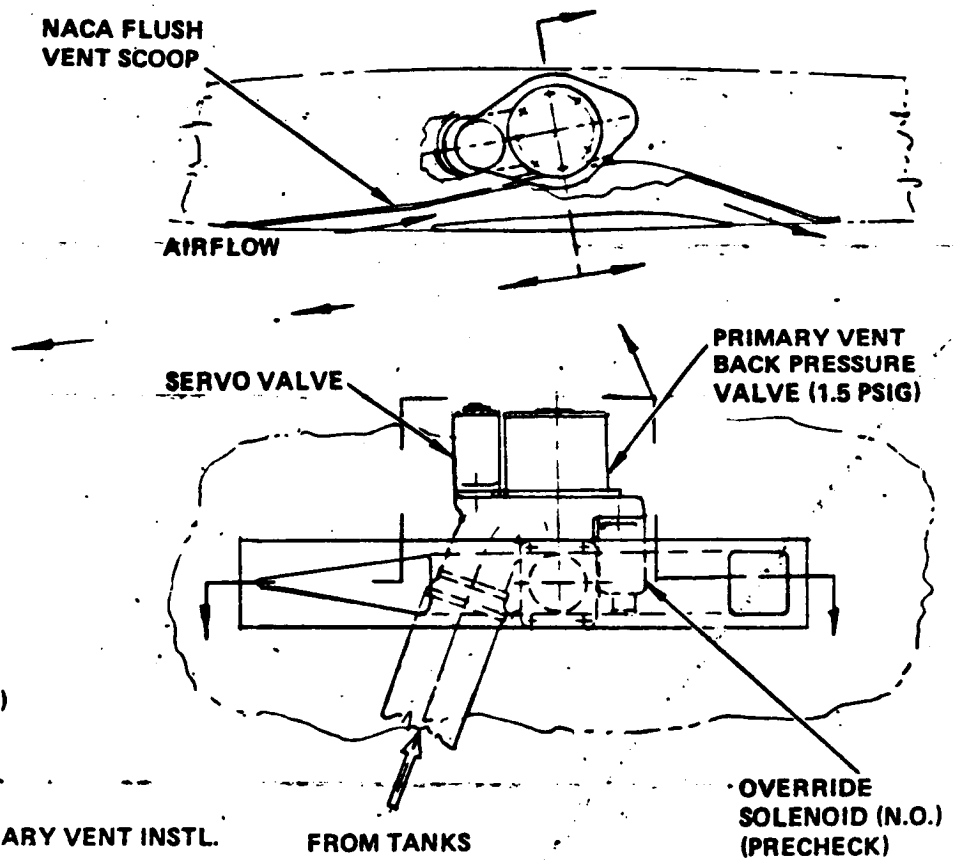

Figure 77. - Layout-vent and pressurization system. (Sheet 2 of 2)

Vapor released during the fueling operation flows through the absolute tank pressure regulators (Figure 76) into the common vent line where it is diverted to the vapor recovery adapter by means of a vent bypass valve built into the adapter and operated by the actuating linkage of the adapter (See Figure 76). The absolute pressure regulators prevent flashing of the fuel by maintaining the tank pressure above the saturation pressure of the delivered fuel.

The fuel tanks are protected from overpressurization in the event that a shutoff valve fails to close when the tank is full by limiting the ground system delivery pressure (Ref. 2) and by sizing the vent lines to allow liquid hydrogen overflow through the vent system to the vapor recovery adapter.

Defueling is accomplished with both fueling and vapor recovery adapters connected to the airport defueling facility (Ref. 2). The fuel transfer and refueling line tank isolation valves are then opened and the fuel level control valves are closed. Operation of the tank boost pumps will start the defueling operation. To maintain tank pressure above outside ambient, some heat may have to be added to the stored hydrogen by means of the fuselage-mounted tank pressurization heat exchanger which utilizes a calrod heating element to convert liquid hydrogen to gas. The tanks may be defueled individually or simultaneously.

6.3 Engine Fuel Supply

The engine fuel supply system is shown in Figure 74. Each engine is normally supplied fuel from its identically numbered fuel tank. In the event of engine failure, fuel from the tank which normally supplies the failed engine can be made available to the operating engines by a crossfeed system. However, the crossfeed system is not required for aircraft center of gravity control as will be discussed in Section 7.2, Operational Requirements of the Liquid Hydrogen Fuel System. A significant feature is the location and arrangement of the crossfeed valves. They are contained in one assembly for convenience in servicing and also to preclude long sections of transfer lines which would contain vapor and could result in engine flameout when switching from direct to crossfeed.

Lines leading to the engines are located in the wing box for protection and isolation. The lines are foam insulated within a protective metal outer tube. Evacuated double bellows lines with an outer braided cover are used where required for flexibility.

A surge box located at the low point in each fuel tank houses three boost pumps which supply fuel to each engine. The surge box traps fuel in the vicinity of the pumps to minimize unusable fuel, and to ensure its availability during unusual transient maneuvers. The present design utilizes a presurized accumulator downstream of the pump check valves to preclude engine starvation if the fuel migrates to the top of the surge box during negative or zero g flight.

The reasons for selection of a three pump system rather than the two pump arrangement used in conventional hydrocarbon fueled aircraft was discussed in Section 5.3.1.

6.4 Auxiliary Power Fuel Supply

The APU is supplied liquid fuel, normally from Tank No. 2, but available from any tank by crossfeed. During the initial APU startup, before electrical power is available to the tank-mounted boost pumps, it is expected that the normal tank pressure (21 psia) will preclude the need for a separate APU tank-mounted boost pump. It is also possible that an external combustion engine may be a feasible method of driving an APU. This represents a change from a previous study which had indicated that the APU might operate on boiloff hydrogen. More detailed studies showed that this was impractical because of the wide variation in boiloff rates, and also because of the high compressor power required to raise the gas to conventional APU combustor pressure.

6.5 Fuel Transfer

Fuel transfer between tanks can be accomplished by opening the appropriate fuel transfer valves and fuel level control valves while operating the tank boost pumps. A fuel transfer system is incorporated to preclude trapping of fuel in any tank should the feed line tank isolation valve fail in the closed position. The effect of this type of failure on center of gravity travel is discussed in Section 7.2 under Fuel Management.

6.6 Fuel Jettison

Inasmuch as this airplane meets the climb requirements of FAR 25.1001 (b) and (c) with full fuel load a fuel jettison system is not legally required. However, some situations can be postulated in which a jettison system might be desirable. For example, if a wheels up landing is anticipated fuel could be jettisoned to reduce the landing speed. Assuming a full fuel load and climb to 10 000 ft. the time to jettison fuel down to the reserve level would be approximately 1.4 hours.

6.7 Tank Vent and Pressurization System

The forward pair of tanks and the aft pair of tanks have separate pressurization and vent systems but share a common overboard vent system downstream of the pressure regulators (see Figure 77). The tanks are maintained at an absolute pressure of 145 kPa (21 psia) by a primary absolute pressure regulator located just downstream of the point where the vent line emerges from each pair of tanks. A secondard pressure regulator set at an absolute pressure of 159 kPa (23 psia) is mounted in parallel with the primary regulator to protect the tank from excessive pressure in the event of failure of

the primary regulator. A purge gas discharge valve for use during the initial tank fill and during tank purging for repair or inspection completes the valve assembly at this location. If the tank absolute pressure drops below 124 kPa (18 psia) when the boost pumps are operating, a back-up absolute pressure regulator allows liquid flow normally supplied from Tank No. 4 to be evaporated at the fuselage-mounted tank pressurization heat exchanger. Tank pressures are thus always maintained above the minimum level.

Vent boxes located within Tanks 2 and 3 act as liquid traps to preclude liquid from passing overboard through the common vent line. A drain valve at the bottom of each trap allows the liquid fuel to drop down into the tank below when the fuel level is below the float in the drain valve. Each vent box communicates with the tank it serves through a single vent line with its inlet in the ullage bubble above the point of intersection of the fuel surfaces for maximum pitch attitude extremes with full fuel tanks. This represents the simplest and most reliable vent design. If detail of the fuel tanks coupled with aircraft attitude studies reveals that no single inlet location will always be void of liquid fuel, an alternative design is available which incorporates two inlets in each vent line. The inlet which is remote to the vent box would be open at all times and the inlet near the vent box would be closed by means of a float-operated vent valve when under fuel but open when not covered by fuel. The added complexity of this system is to be avoided if possible since it places added moving components within the fuel tanks at a location which is relatively inaccessible for maintenance.

The common vent line downstream of the absolute pressure regulators serves a dual purpose. In flight, gas relieved through the pressure regulators is conveyed through the vent line to a lightning-protected overboard vent mounted in the vertical stabilizer. The overboard vent assembly includes a servo operated back-pressure valve set at 10.3 kPa differential (1.5 psig) to prevent air from being drawn into the vent where it could constitute a hazard. During fueling operations, the common vent serves as a means to recover large quantities of boil-off gases by routing them back to the vapor recovery adapter so that they can be recycled by the airport hydrogen liquefaction and distribution system. In the event of the failure of the primary vent an alternate servo operated vent set at 24.5 kPa (3.5 psig) is located in the tail cone area (Figure 77). This valve is closed by an override solenoid to prevent opening during fueling.

6.8 Nitrogen Inerting System

An investigation was made to determine the characteristics of a GN_2 inerting system which might be required to inert the space surrounding the nonintegral fuel tank (Candidate #1), and the engine supply system down to and including the engine pump and fuel control. The ground rules established for this study were:

1. The purge system is a flight dispatch item and must have dual redundancy in all functional aspects.

2. The quantity of N_2 carried must be sufficient to meet the most severe of the following: (a) 1 flight of 5500 n.mi. + alternate destination + ground hold, or (b) 2 flights of 2187 n.mi. with ground hold and diversion to an alternate destination.

3. The minimum purge space pressure must be at least 1 psig above ambient to preclude ingestion of air due to local flight pressures above ambient free stream.

4. Leakage rates through fuselage structure based on improved L-1011 production aircraft experience.

5. N_2 purge system must prevent air ingestion during maximum emergency rate of descent.

6. N_2 to be stored as a liquid.

The most difficult aspect of the analysis was to predict what leakage might occur in a service aircraft. As a starting point the functional test procedure (FTP) required of all production L-1011's was reviewed. This requires that after blocking of all valves, vents, and drains, the air leakage not exceed 87 lb/min with a cabin differential pressure of 7 to 8 psi. Correcting this rate for leakage area, 1 psi differential and N_2 properties and temperatures it was calculated that approximately 11,000 lb of N_2 would be required for the 5500 n.mi. flight profile. Since this is not reasonable, discussions were held with the L-1011 test personnel as to how this leakage might be reduced. The conclusion was that since much of the L-1011 leakage was due to the many door and window seals, feed-thrus, and hidden holes in structure, that in the LH_2 aircraft, with minimal access doors and careful attention to sealing of holes, this rate might be reduced to 10 or 15 percent. For purposes of this analysis the 10 percent value was assumed.

A schematic of the system is shown in Figure 6.8a. Cabin discharge air is used to heat the cryogenic LN_2.

The significant surface areas and volumes are:

	Surface Area (ft^2)	Vol. (ft^3)
Forward LH_2 tank compartment	2333	2854
Aft LH_2 tank compartment	2375	2536
Engine supply purge jacket (including engine pump and fuel control)	442	99
Total	5150	5489

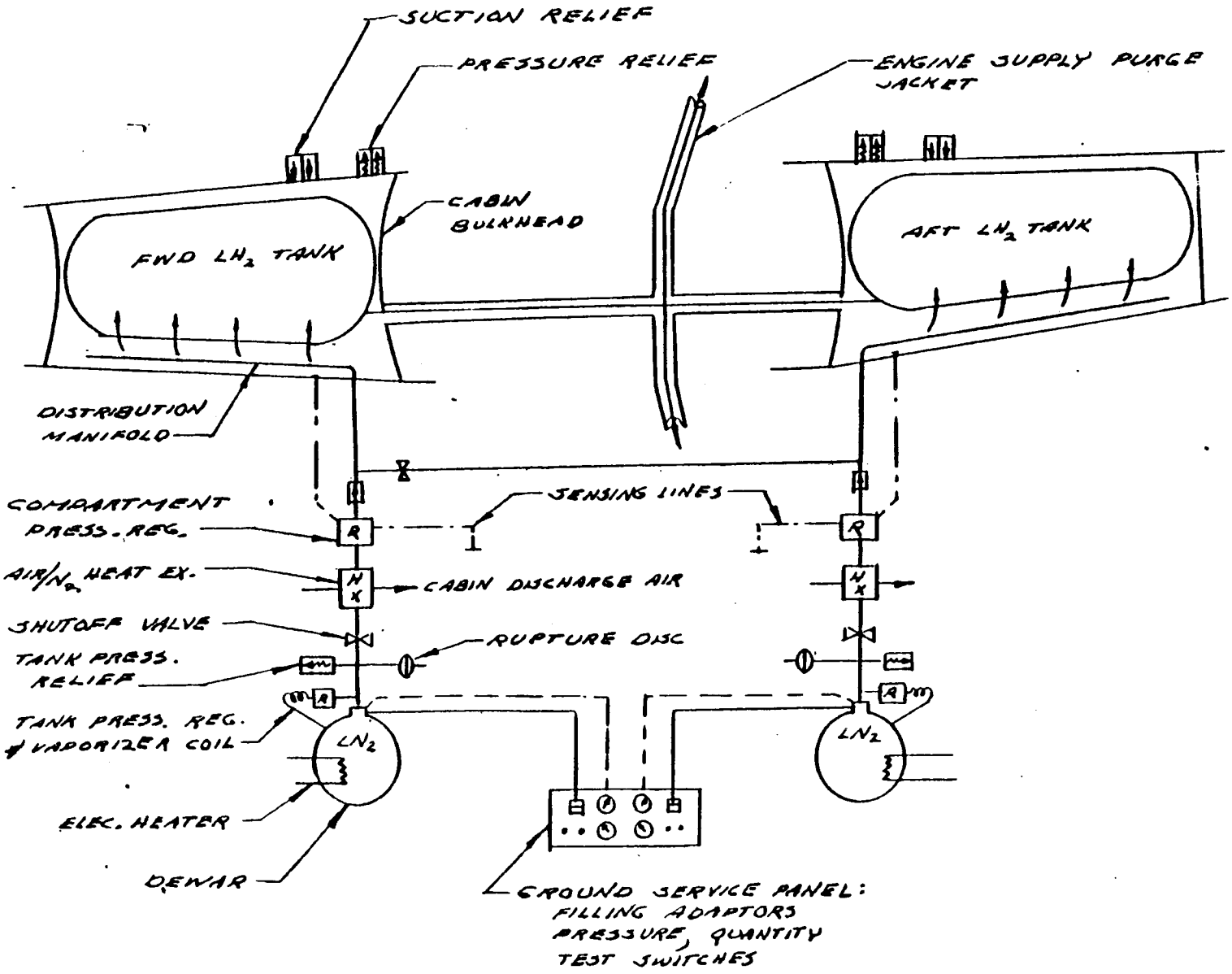

Figure 6.8a. N_2 purge system schematic.

Comparison of the mission profiles showed that the two 2187 n.mi. trips constituted the more severe requirement with regard to quantity of N_2 because of the more frequent climbs and descents. N_2 venting is required on climb with subsequent replenishment being necessary on descent. On this basis the following weights were estimated for the system:

LN_2 Required:	
Compartment charging	1849 lb
Leakage	1030
Residual N_2	71
Total	2950 lb
System Weights:	
LN_2 Dewars (60 psig)	258 lb
Equipment	100
Plumbing and shrouds	396
	754 lb
+ 10 percent contingency	76
Total System	830 lb
+ LN_2	2950
Total installed system + gas	3780 lb

The effect on DOC (assuming the LN_2 costs nothing since it is required for H_2 liquefaction) is equivalent to an increase of 1.53 percent in the baseline value of 1.8334¢/seat n.mi. This is clearly undesirable, not only for the direct economic penalty, but also from the point of view of logistics and servicing.

An alternate concept was also examined in which the compartments are held at a constant absolute pressure. This saves the quantity of N_2 required for charging and recharging but increases the leakage so that the first quantity of LN_2 required is 2760 lb, almost as much as before. Further structural penalties would result from designing the tank compartments to withstand this pressure.

If the internal pressure differential could be reduced to 1/2 psig the total system weight would be 3430 lb, a 9 percent reduction. The 1/2 psi might be marginal, however, in preventing air ingestion under certain flight conditions.

The approach selected for the final candidate fuel containment systems #1, 2, 3 and 4 consists of air purging and compartment ventilation where applicable, together with the leak detection at purge exits. This approach is further described in Section 8.6.1. N_2 inerting is used, however, in the flexible foam outer insulation layers of candidates #3 and #4 as described in Section 8.6.2.

The need for active inerting and choice of a final concept is dependent on service experience with an actual LH_2 fuel system in a developmental aircraft program.

6.9 Technology Developments Required

To establish the most promising fuel system design will require component and system design evaluations followed by detailed laboratory developmental testing. Areas in which this effort should be concentrated include the following:

6.9.1 Negative "g" operation. - The availability of fuel to the tank boost pumps must be assured at all times to prevent engine starvation. The present design proposes a pressurized accumulator downstream of the boost pumps. Other methods, such as double-ended boost pumps, should be investigated inasmuch as they may be lighter in weight and more reliable than the proposed accumulators.

6.9.2 Engine starting without boost pumps operating. - If the airplane is to be self-supporting, the engines and/or the APU must be capable of being started without the aircraft fuel tank boost pumps operating. Hence, the minimum inlet fuel pressure for starting the engines and/or the APU should be determined and compared to available pressure at the engine/APU inlet as a result of fuel tank pressurization.

6.9.3 Float-operated valve development. - Because of the low density of liquid hydrogen and permeability of most materials when subjected to hydrogen, the design of a float presents problems in sizing and material selection. The feasibility of floats to operate shutoff valves or switches should be investigated at an early date since they offer the simplest and most reliable method of sensing liquid levels.

6.9.4 Fuel quantity gauging. - A neutron radiation fuel gauge should be investigated for fuel quantity gauging. Neutrons will pass through the walls of the fuel tank quite easily and yet are attenuated proportionately to the density of the hydrogen they pass through. This would allow the gauging components to be placed external to the tank.

As an alternate, capacitance gauging is feasible and has been used in LH_2 but would require the insertion and support of long probes at multiple locations in each tank.

7. FUEL CONTAINMENT SYSTEM

As used herein, the term fuel containment system refers to two basic subsystems; the fuel tank structure and its associated supporting structural components, and the tank cryogenic insulation system. Both integral and nonintegral fuel tanks were evaluated. An integral tank is defined as one which provides the aircraft structure in the tank area to carry fuselage structural loads as well as providing for fuel containment. A nonintegral tank is mounted within a conventional airframe and serves only as a fuel containment vessel.

The methodology used in the selection of a preferred design of fuel containment system was to apply a consistent set of criteria to a three-step process, varying only in extent of analysis, proceeding from concept screening, to evaluation of preferred candidates, to selection of a final configuration. This process is shown diagramatically in Figure 78 using the insulation system as an example.

In order to focus design and analysis attention as much as possible on constructive aspects, the aft tank of the aircraft was selected and used as the model for evaluation of candidate structure and insulation concepts. After a preferred aft tank design was established, the forward tank was sized and weighed using the same design concepts for both structure and insulation based on spot analysis as deemed necessary to account for local differences.

The procedures and results of the investigation of tank insulation systems are presented in Section 7.1. Section 7.2 contains this information relative to the tank structure.

7.1 Tank Insulation

A total of 15 candidate tank insulation concepts were evaluated in the initial screening operation to find the two most promising for use with integral-type tanks and the two most promising for nonintegral tanks. The 15 candidates included both active (inert gas purged and dynamically pumped vacuum systems) and passive concepts. A closed cell polymeric foam insulation, applied to the external surfaces of an integral tank was used as the baseline system for comparative evaluation purposes.

The four preferred insulation systems (two for integral and two for nonintegral tanks) were subjected to a more rigorous analysis, leading finally to selection of one concept to be incorporated in the design of the subject LH_2-fueled transport aircraft.

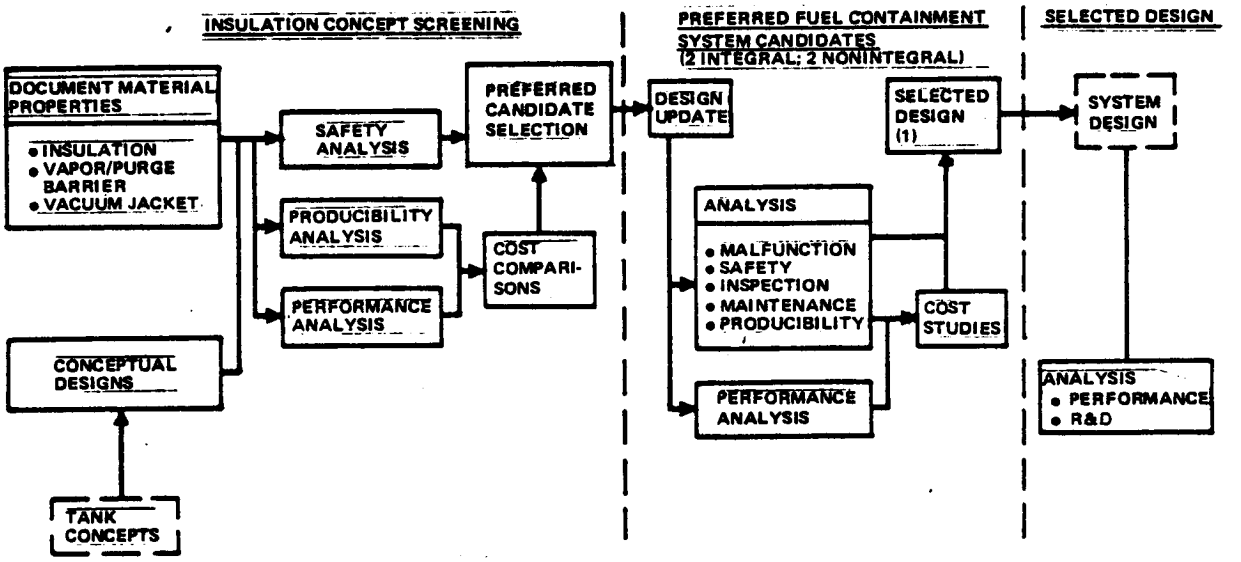

Figure 78. Tank insulation analysis procedure.

The procedures employed in each step of this selection process, and the results which were obtained, are discussed in this section.

7.1.1 Design requirements and evaluation criteria. - Selection of the insulation system for a commercial transport aircraft LH_2 fuel tank is constrained by the requirements of minimum operating costs and the achievement of a very high level of safety throughout the aircraft lifetime. In order to realize cost goals, the system must combine lightweight construction with low heat transfer characteristics which are consistent with in-flight tank pressurization requirements; have a high reliability, low maintenance, long life-cycle; and have development and fabrication cost commensurate with commercial aircraft practices. Safety considerations must include freedom, not only from loss of life or aircraft during a flight or ground operation incident, but also failures potentially dangerous to maintenance operations. Design requirements, and safety, performance, and operational criteria were established for the fuel containment system of the aircraft.

The aft tank configuration was used for the screening and preferred systems studies to focus the analysis effort to the maximum degree. Prior aerospace research and development results and commercial experience with cryogenic storage vessels were used to evaluate potential problem areas and to assess the applicability of each insulation concept.

The general criteria used in evaluation and ranking of the insulation concepts were:

- Safety - No single or probable combination of failures shall lead to loss of life or aircraft. Assessment of failure modes and their overall impact was consistent with current or anticipated safety practices applicable to commercial aircraft in 1990-1995 and to storage and handling of liquid hydrogen. Modes of failure considered were: accidental penetration of exterior surfaces, air or GH_2 leakage into insulation or aircraft, cryopumping of O_2 in organic materials, malfunction of purge or vacuum system and associated control components, toxicity of products in event of external fire.

- Performance - Minimization of aircraft DOC. DOC was evaluated as a function of system inert weights (including accessories associated with purge/vacuum concepts); fuel vaporized to maintain tank pressure as well as nonrecoverable fuel loss (vent) weights; system volume; and maintenance requirements (inspection/repair/replacement).

- Producibility - Each system must be designed so it can be fabricated, assembled, inspected and maintained consistent with aircraft practices.

Cost estimates were based on production of 350 ship sets plus 20 percent spares. If costs were competitive, the concept which provided the aircraft with the lowest energy consumption was selected.

7.1.2 Candidate insulation concepts. - Insulation systems for aircraft LH_2 fuel tanks serve the following basic purposes:

- To reduce the heat rates to the tanks and thus prevent boiloff to a level consistent with minimizing direct operating costs.

- To prevent the buildup of parasitic weight on the aircraft in flight due to gas condensation or freezing, in particular, water vapor.

Since all atmospheric gases will freeze at LH_2 temperature, air in the insulation system must either be evacuated by active pumping and/or passive cryopumping, or a non-condensible gas such as helium or hydrogen must be substituted in the insulation. Consequently, integrity of the vapor barrier is a critical item in the design of external insulation systems. The

insulation thickness on all candidate systems must be sized, as a minimum to keep the external sealed surface above the dew point (the insulation surface for an external application or the tank surface for an internal insulation).

Fifteen insulation system concepts, shown in Table 29, were selected for analysis. Table 30 shows the status of development work on current insulation systems which is applicable to the list of candidate system designs. Thermal performance test data from these programs were used in the analysis of the systems for the subject aircraft use.

Plumbing schematics for the "active" systems, i.e., those requiring either vacuum pumps or purging, are shown in Figures 79 through 81. The plumbing schematic for concept 1, Figure 79, shows the automatic controls used to maintain the correct helium pressure during aircraft ascent and descent so as to prevent structural failure of the purge jacket. Dual N_2/He purge system controls for concept 2 are shown in Figure 80. The differential pressure measurement across the inner purge barrier controls the helium pressure; the nitrogen pressure control is referenced to ambient pressure. The 10^{-4} torr pressure requirement for concept 9 requires a turbomolecular pump and fore pump in addition to the blowers as shown in Figure 81. Systems 10, 11, and 12 do not require complex turbomolecular and fore pumps because of the more modest vacuum pressures used in those concepts. Their plumbing schematics are shown in Figure 82. In all concepts the pumping systems operate only when the specified vacuum pressures are exceeded.

7.1.3 Concept screening procedure. - In the concept screening, each insulation concept was analyzed with regard to safety, performance, producibility and operational requirements. These analyses considered the following aspects:

Safety

- Malfunction
- Leak Detection
- Flammability and Toxicity
- Inspectability

Performance

- Heat Input to Fuel (Evaporated and Vented)
- Weight and Volume
- DOC

CONCEPT / CHARACTERISTIC	PURGED		CRY
	1 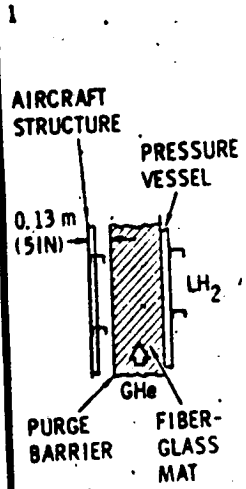	2 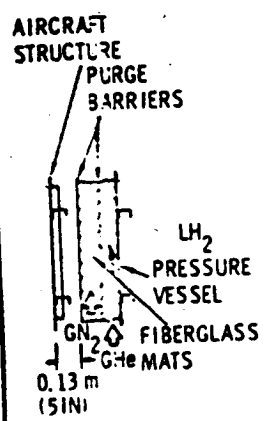	3 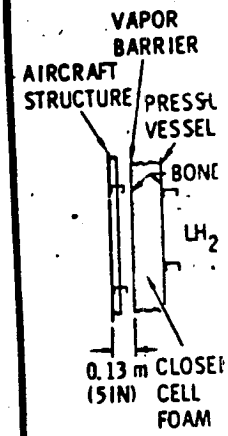
INSULATION TYPE	He PURGE 1.4×10^4 N/m^2 (2 PSI) GAGE PRESSURE	PURGE GAS / GAGE PRESSURE He: 2.8×10^4 N/m^2 (4 PSI) N_2: 1.4×10^4 N/m^2 (2 PSI) INTERMEDIATE PURGE BARRIER TEMPERATURE > 83°K (150°R)	CRYOPUMPED AIR FILLED FOAM; AMBIENT PRESSUI LOAD ON THE FOAM
PRESSURE VESSEL CONSTRUCTION INTEGRAL (I) NONINTERGRAL (N)	N	N	N
MATERIALS	• FIBERGLASS MAT 16 kg/m^3 (1 lb/ft^3) • PURGE BARRIER EPOXY/GLASS/TEFLON COMPOSITE 0.69 kg/m^2 (0.14 lb/ft^2)	• FIBERGLASS MATS 16 kg/m^3 (1 lb/ft^3) • PURGE BARRIERS EPOXY/GLASS TEFLON COMPOSITE 0.69 kg/m^2 (0.14 lb/ft^2)	• CLOSED-CELL PI METHACRYLIMI FOAM 35 kg/m^3 (2.2 lb/ft^3) • MAAMF VAPOR BARRIER 0.673 kg/m^2 (0.138 lb/ft^2) • POLYURETHANE ADHESIVE (0.15 kg/m^2 (0.03 lb/ft^2) PER BOND LINE
OPERATION	PURGE AIR TO 1%; MAINTAIN POSITIVE PRESSURE IN SERVICE; VENT DURING ASCENT; REPLENISH DURING DESCENT; LOAD He AFTER EACH FLIGHT	SAME AS SYSTEM 1 FOR BOTH PURGE GASES	PASSIVE

YOPUMPED	GH_2-FILLED	AIR-FILLED / GH_2-FILLED	GH_2-FILLED	
4 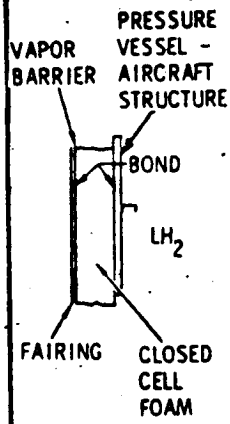	5 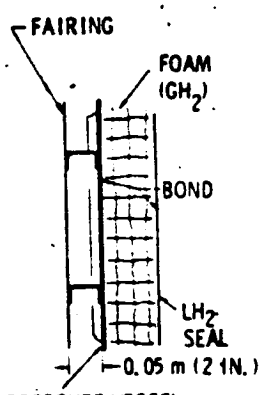	6 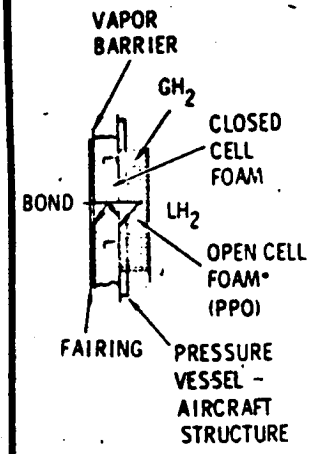	7 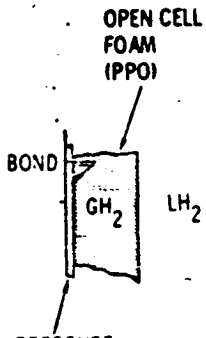	8 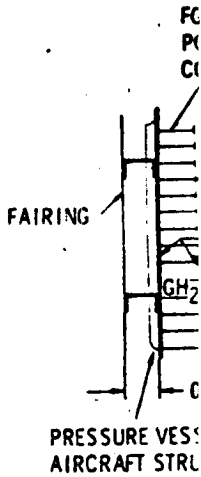
CRYOPUMPED AIR-FILLED FOAM; AMBIENT PRESSURE LOAD ON FOAM	GH_2-FILLED AT TANK PRESSURE	CLOSED FOAM - AIR-FILLED OPEN FOAM - GH_2-FILLED AT TANK PRESSURE TANK TEMPERATURE > 97°K (175°R)	GH_2-FILLED AT TANK PRESSURE	GH_2-FILLED AT PRESSURE
1	1	1	1	1
• CLOSED-CELL POLY-METHACRYLIMIDE FOAM 35 kg/m³ (2.2 lb/ft³) • MAAMF VAPOR BARRIER 0.673 kg/m² (0.138 lb/ft²) • POLYURETHANE ADHESIVE 0.15 kg/m² (0.03 lb/ft²) PER BOND LINE	• CLOSED CELL POLYURETHANE FOAM WITH 3-D GLASS FIBER REINFORCEMENT, POLYURETHANE/GLASS LH_2 SEAL, AND POLYURETHANE ADHESIVE 96 kg/m² (6 lb/ft²) 0.15 kg/m² (0.03 lb/ft²) PER BOND LINE	• CLOSED CELL POLYURETHANE FOAM 35 kg/m³ (2.2 lb/ft³) • PPO OPEN-CELL FOAM* 40 kg/m³ (2.5 lb/ft³) • MAAMF VAPOR BARRIER 0.673 kg/m² (0.138 lb/ft²) • POLYURETHANE ADHESIVE 0.15 kg/m² (0.03 lb/ft²) PER BOND LINE	• PPO OPEN-CELL FOAM* 40 kg/m³ (2.5 lb/ft³) • POLYURETHANE ADHESIVE 0.15 kg/m² (0.03 lb/ft²) PER BOND LINE	• POLYIMIDE COMB CORE CELL, FILLE F.G. BATTI 40 kg/m³ (2. • PERFORATED POLYIMIDE SHEET 3.5 x (7.3 x 10⁻³ • POLYURETH ADHESIVE 0 0.03 lb/ft²) LINE
PASSIVE	PASSIVE	PASSIVE	PASSIVE	PASSIVE

*THE MAXIMUM THICKNESS PPO FOAM CAN BE MADE IS ~0.1 m (4 IN.) DUE TO THE DRAWING PROCESS. BEYOND THIS THICKNESS, MULTIPLE LAYERS HAVE TO BE BONDED TOGETHER.

	EVACUATED			
FILLED YIMIDE RE PERFORATED POLYIMIDE FACE -BOND LH_2 5 m (2 IN.) L - TURE	9 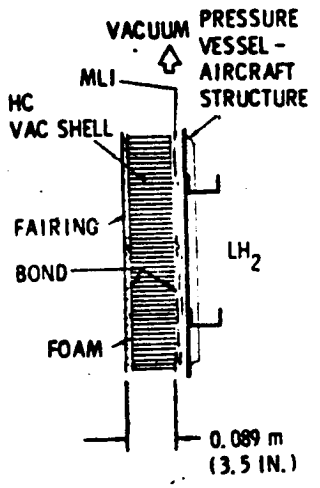 	10 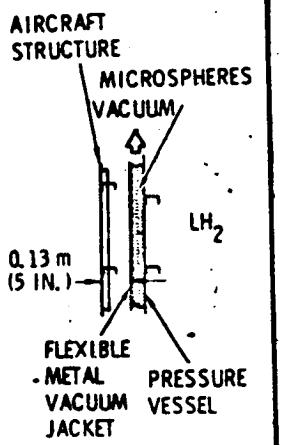 	11 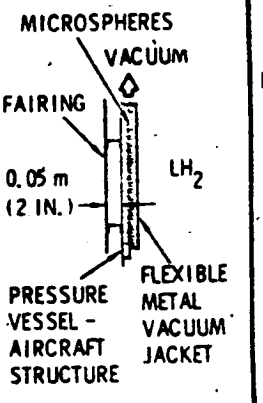 	12 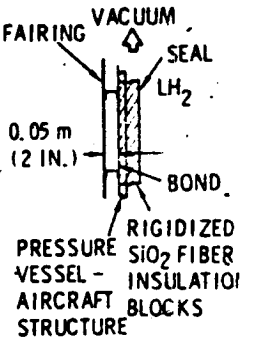
NK	HONEYCOMB AND MLI EVACUATED TO $<10^{-5}$ TORR; NO LOAD ON MLI; AMBIENT PRESSURE LOAD ON JACKET	MICROSPHERES EVACUATED TO $<10^{-2}$ TORR: AMBIENT PRESSURE LOAD ON MICROSPHERES	MICROSPHERES EVACUATED TO $<10^{-2}$ TORR; TANK PRESSURE LOAD ON MICROSPHERES	RIGIDIZED SiO_2 FIBER EVACUATED TO $<10^{-1}$ TORR; TANK PRESSURE LOAD ON FIBER BLOCKS
	I	N	I	I
ONEY- 3/8-IN. WITH lb/ft^3) ACE 0^{-2} kg/m^2 /ft^2) E 5 kg/m2 ER BOND	• ALUMINUM HONEYCOMB CORE 50 kg/m^3 (3.1 lb/ft^3) • ALUMINUM FACE SHEETS, EACH 1.36 kg/m^2 (0.28 lb/ft^2) • EPOXY ADHESIVE 3.7×10^{-2} kg/m^2 (7.5×10^{-3} lb/ft^2) PER BOND LINE • DAM/DARON NET MLI UNIT WEIGHT PER LAYER DAM: 8.8×10^{-3} kg/m^2 (1.8×10^{-3} lb/ft^2) DACRON: 11.7×10^{-3} kg/m^2) (2.4×10^{-3} lb/ft^2)	• MICROSPHERES 69 kg/m^3 (4.3 lb/ft^3) • 321 S. S. FLEX VACUUM JACKET 1.0 kg/m^2 (0.21 lb/ft^2)	• MICROSPHERES 69 kg/m^3 (4.3 lb/ft^3) • 321 S. S. FLEX LINER 1.0 kg/m^2 (0.21 lb/ft^2)	• SiO_2 RIGIDIZED FIBER BLOCKS 112 kg/m^3 (7 lb/ft^3) • INVAR LINER 0.97 kg/m^2 (0.21 lb/ft^2) • POLYURETHANE ADHESIVE 0.15 kg/m^2 (0.03 lb/ft^2) PER BOND LINE
	EVACUATE HONEYCOMB AND MLI; MAINTAIN VACUUM IN SERVICE (PUMPS OPERATE ONLY WHEN 10^{-5} TORR IS EXCEEDED)	EVACUATE MICRO-SPHERES; MAINTAIN VACUUM IN SERVICE (PUMPS OPERATE ONLY WHEN 10^{-2} TORR IS EXCEEDED)	EVACUATE MICRO-SPHERES; MAINTAIN VACUUM IN SERVICE (PUMPS OPERATE ONLY WHEN 10^{-2} TORR IS EXCEEDED)	EVACUATE SiO_2 BLOCKS; MAINTAIN VACUUM IN SERVICE (PUMPS OPERATE ONLY WHEN 10^{-1} TORR IS EXCEEDED)

TABLE 29. - TANK INSULATION SYSTEM CONCEPTS

CRYOPUMPED (MULTIPLE SEAL)	AIR-FILLED/CRYOPUMPED (DOUBLE-SEAL)	GN_2 PURGE/CRYOPUMPED
13 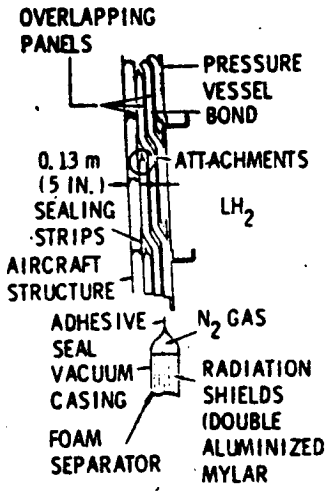 	14 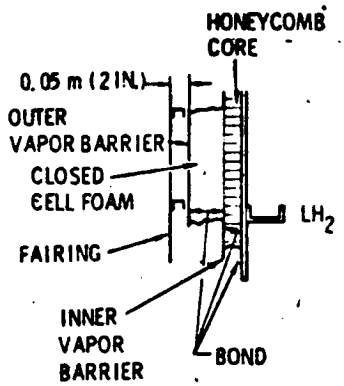 	15 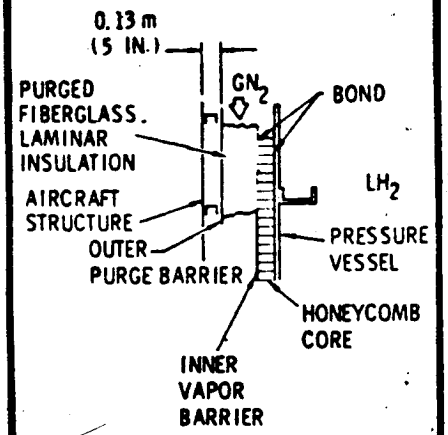
CRYOPUMPED N_2 IN PANELS; AMBIENT PRESSURE LOAD ON THE INSULATION	AIR IN HONEYCOMB CRYOPUMPED; CLOSED-CELL FOAM AIR-FILLED; INNER VAPOR BARRIER TEMPERATURE >97°K(>175°R)	AIR IN HONEYCOMB CRYOPUMPED; N_2 PURGE IN BATTING AT 1.4×10^4 N/m^2; (2 PSI) GAGE PRESSURE; INNER VAPOR BARRIER TEMPERATURE >83°K(>150°R)
N	I	N
SEALED PANEL CONSISTS OF: • 6 DAM SHIELDS • 12 FOAM SPACERS • 2 MAAM CASINGS $0.55\ kg/m^2$ ($0.113\ lb/ft^2$) PER PANEL • MAAM SEALING STRIP, EACH $5.2 \times 10^{-2}\ kg/m^2$ ($1.1 \times 10^{-2}\ lb/ft^2$) • POLYURETHANE ADHESIVE $0.15\ kg/m^2$ ($0.03\ lb/ft^2$)	• 3/8-IN. CELL MYLAR HONEYCOMB $34\ kg/m^3$ ($2.1\ lb/ft^3$) • MAAM INNER VAPOR BARRIER $5.2 \times 10^{-2}\ kg/m^2$ ($1.1 \times 10^{-2}\ lb/ft^2$) • POLYURETHANE CLOSED-CELL FOAM $35\ kg/m^3$ ($2.2\ lb/ft^3$) • MAAMF OUTER VAPOR BARRIER $0.673\ kg/m^2$ ($0.138\ lb/ft^2$) • POLYURETHANE ADHESIVE $0.15\ kg/m^2$ ($0.03\ lb/ft^2$) PER BOND LINE	• 3/8-IN. CELL MYLAR HONEYCOMB $34\ kg/m^3$ ($2.1\ lb/ft^3$) • MAAM INNER VAPOR BARRIER $5.2 \times 10^{-2}\ kg/m^2$ ($1.1 \times 10^{-2}\ lb/ft^2$) • FIBERGLASS LAMINAR BATTING $16\ kg/m^3$ ($1\ lb/ft^3$) • PURGE BARRIER EPOXY/GLASS/TEFLON COMPOSITE $0.69\ kg/m^2$ ($0.14\ lb/ft^2$) • POLYURETHANE ADHESIVE $0.15\ kg/m^2$ ($0.03\ lb/ft^2$)
PASSIVE	PASSIVE	PURGE AIR TO <1%; MAINTAIN POSITIVE N_2 PRESSURE IN SERVICE; VENT DURING ASCENT; REPLENISH DURING DESCENT; LOAD N_2 AFTER EACH FLIGHT

TABLE 30. - STATUS OF DEVELOPMENT APPLICABLE TO THE INSULATION SYSTEM CONCEPTS

Insulation System Concept	Applicable Development		
	Reusable System Design?	Demonstrated on:	Comments
1. He Purged	Yes (Space Shuttle Application Technology)	NAS 8-27419, 2.2 m (7.2 ft) tank	Purge jacket is epoxy glass, Teflon coated. Insulation is multilayers. 100 Space Shuttle flight cycles demonstrated with LH_2.
2. He/N_2 Double Purge	No. (Orbital Application Technology)	NAS 3-4199, 2.1 m (6.9 ft) tank	Used helium purged fiberglass substrate, nitrogen filled multilayers. Simulated one ground hold, launch, orbit flight cycle with LH_2. Thickness of He to N_2 layers must be controlled accurately to prevent N_2 liquefaction.
3. External Polymethacrylimide (Rohacell) Foam (Non-integral Tank) 4. External Polymethacrylimide (Rohacell) Integral Tank	No. (Apollo Flight Program)	Saturn S-II Stage, 10m (33 ft) diam.	Polyurethane foam sprayed on, machined, covered with polyurethane sealer. Conductivity rises with time due to displacement of blowing gas with air. Flight demonstrated.
5. Internal Polyurethane Foam	No. (Apollo Flight Program)	Saturn S-IVB Stage 6.7 m (22 ft) diam.	Glass fiber reinforced foam tiles, individually bonded, fiberglass polyurethane resin liquid barrier (GH_2 filled). 135 thermal cycles.

TABLE 30. - STATUS OF DEVELOPMENT APPLICABLE TO THE CANDIDATE INSULATION SYSTEMS (Continued)

Candidate Insulation System	Applicable Development		
	Reusable System Design?	Demonstrated on:	Comments
6. PPO Internal Foam/ Polyurethane External Foam	-	This combination has not been demonstrated. See comments on Systems 3 and 7.	
7. PPO Internal Open Cell Foam	Yes (Space Shuttle Technology)	NAS 9-10960, 1.75m (5.8 ft) tank	Individual tiles bonded to wall. Conductivity higher than GH_2, varies with orientation. 100 Space Shuttle flight cycles demonstrated with LH_2.
8. Honeycomb Gas Layer Barrier	Yes (SST Methane Tank Technology; Space Shuttle Technology)	NAS 3-12425 NAS 8-25974	GH_2 filled insulation.
9. Rigid Vacuum Shell	Yes (Space Shuttle System Technology)	NAS 3-14369, 2.6 m (8.7 ft) diam. Tank	Aluminum honeycomb rigid vacuum shell with aluminum face sheets. Shell collapsed after cycling 29 times due to peeling of inner face sheet. External face sheet should be made vacuum seal to prevent this. Problems making system vacuum tight to 10^{-5} torr.

TABLE 30. - STATUS OF DEVELOPMENT APPLICABLE TO THE CANDIDATE INSULATION SYSTEMS (Continued)

Candidate Insulation System	Applicable Development		
	Reusable System Design?	Demonstrated on:	Comments
10. Microspheres with External Flexible Metal Jacket	Yes (Space Tug System Technology)	NAS 3-17817 1.2 m (3.9 ft) diam. Tank	Stainless steel jacket, .003 in. thick, has demonstrated vacuum integrity to 10^{-6} torr. None of 4 m (76 ft) of resistance seam welds leaked. Test program demonstrated 13 flight cycles using LN_2 with no change in thermal performance. Microspheres have been loaded compressively in a flat plate 100 times with no change in thermal performance.
11. Microspheres with Internal Liner	Yes (LH_2 aircraft application technology)	This design modification to System 10 has not been demonstrated.	
12. Silica insulation with Internal Liner	Yes (Space Shuttle high temperature insulation)	Properties of insulation have been determined. Liner has not been demonstrated.	
13. Self-evacuating Shingles	No (Orbital Application Technology)	NAS 3-6289, .8 m (2.5 ft) calorimeter tank.	Leak tight shingles were not obtained; sealing strips opened upon thermal cycling. This system did not perform as designed; requires further development.

TABLE 30. - STATUS OF DEVELOPMENT APPLICABLE TO THE CANDIDATE INSULATION SYSTEMS (Continued)

Candidate Insulation System	Applicable Development		
	Reusable System Design?	Demonstrated on:	Comments
14. Self-evacuating Honeycomb/Foam		This combination has not been demonstrated. See comments on Systems 3 and 15.	
15. Self-evacuating Honeycomb/N_2 Purge.	No. (Orbital Application Technology)	NAS 8-11747 .8 m (2.5 ft) calorimeter tank.	Conductivity of honeycomb degraded with number of LH_2 cycles (up to 14) as gas permeated the honeycomb. Had problems with nitrogen purge gas liquefying in the multilayers (Honeycomb sub-layer should have been thicker).

Producibility

- Approach
- Development and Manufacturing Requirements

Operations

- Inspection, Maintenance and Operational Requirements
- Life Expectancy

Results of these studies were then compared to rank each concept so that the four most promising could be selected for more detailed study.

7.1.3.1 Safety analysis: The safety analysis considered four major aspects. These were evaluated against the criteria shown in Table 31 and a numerical weighting factor assigned to each. The parameters considered under the malfunction testing included the type of failure (e.g., vacuum jacket leakage),

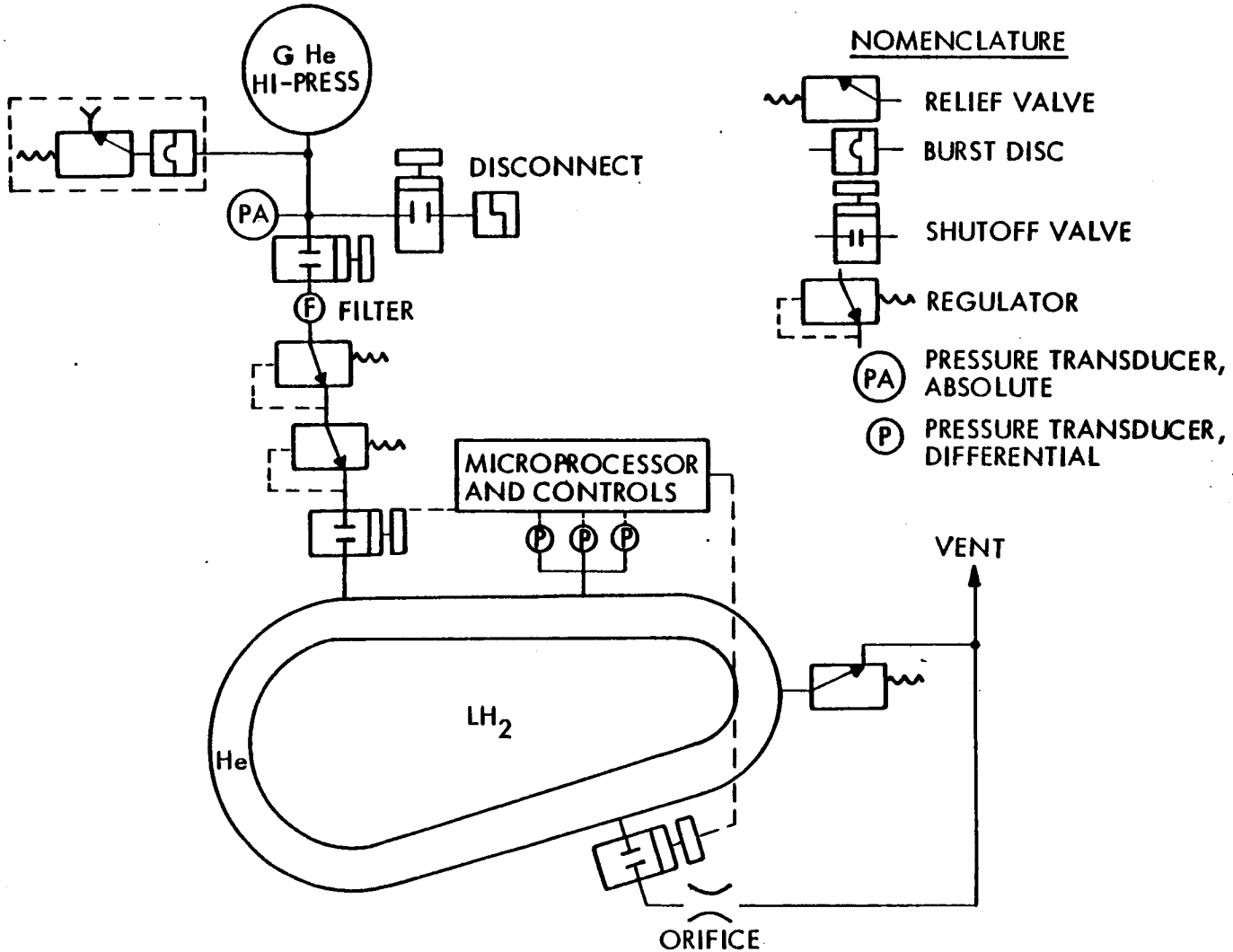

Figure 79. - Plumbing schematic for system 1.

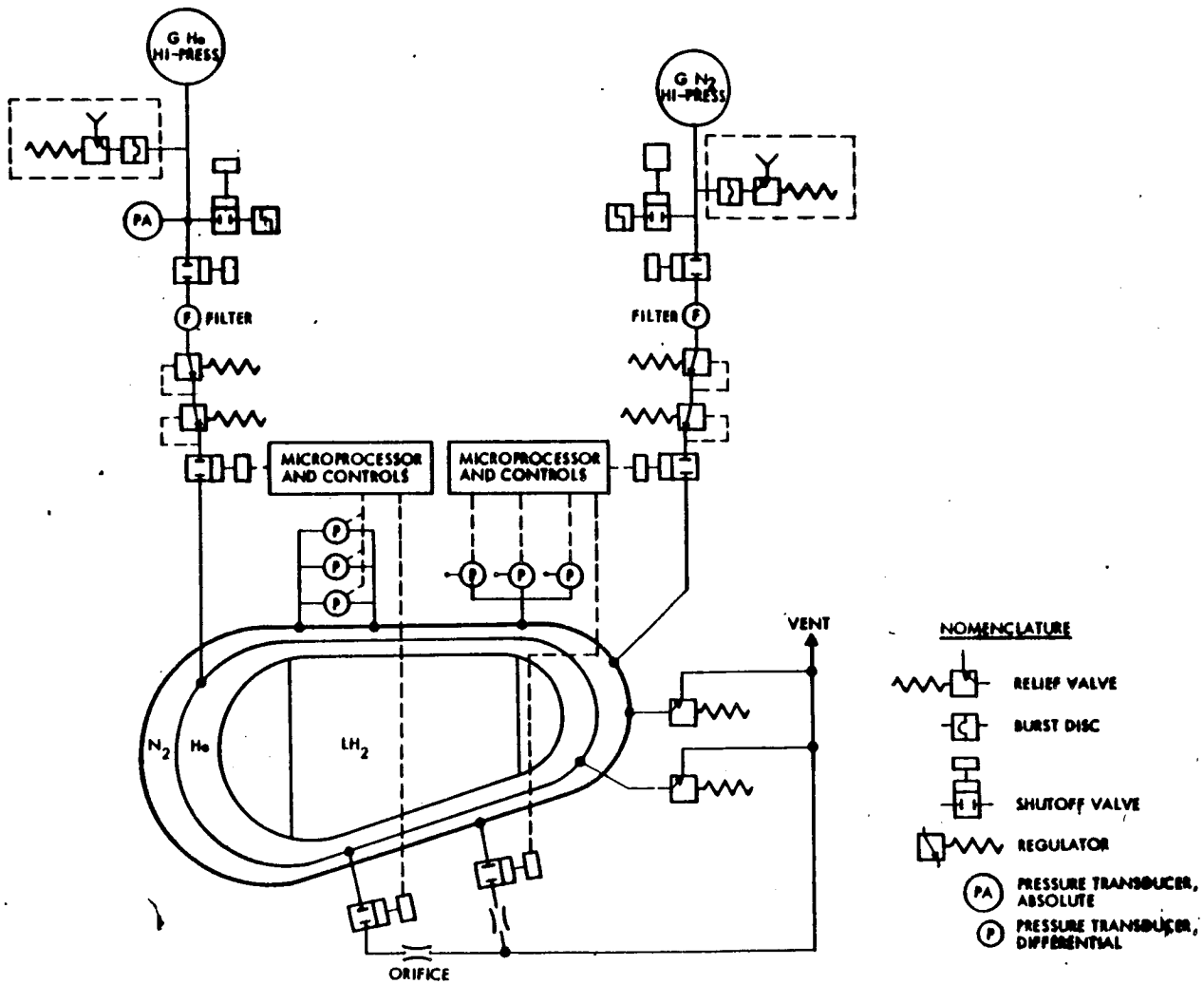

Figure 80. - Plumbing schematic for system 2.

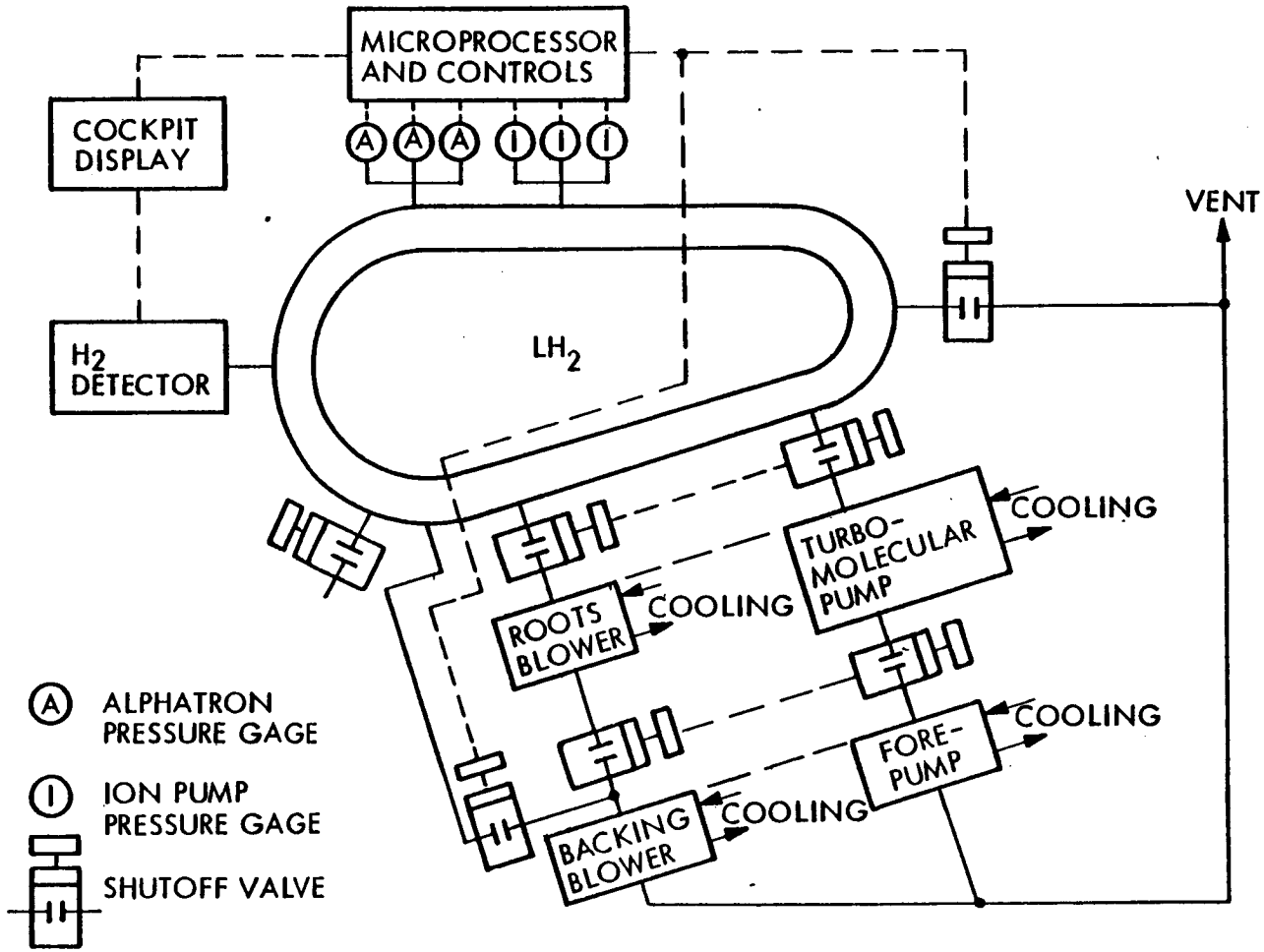

Figure 81. - Plumbing schematic for system 9.

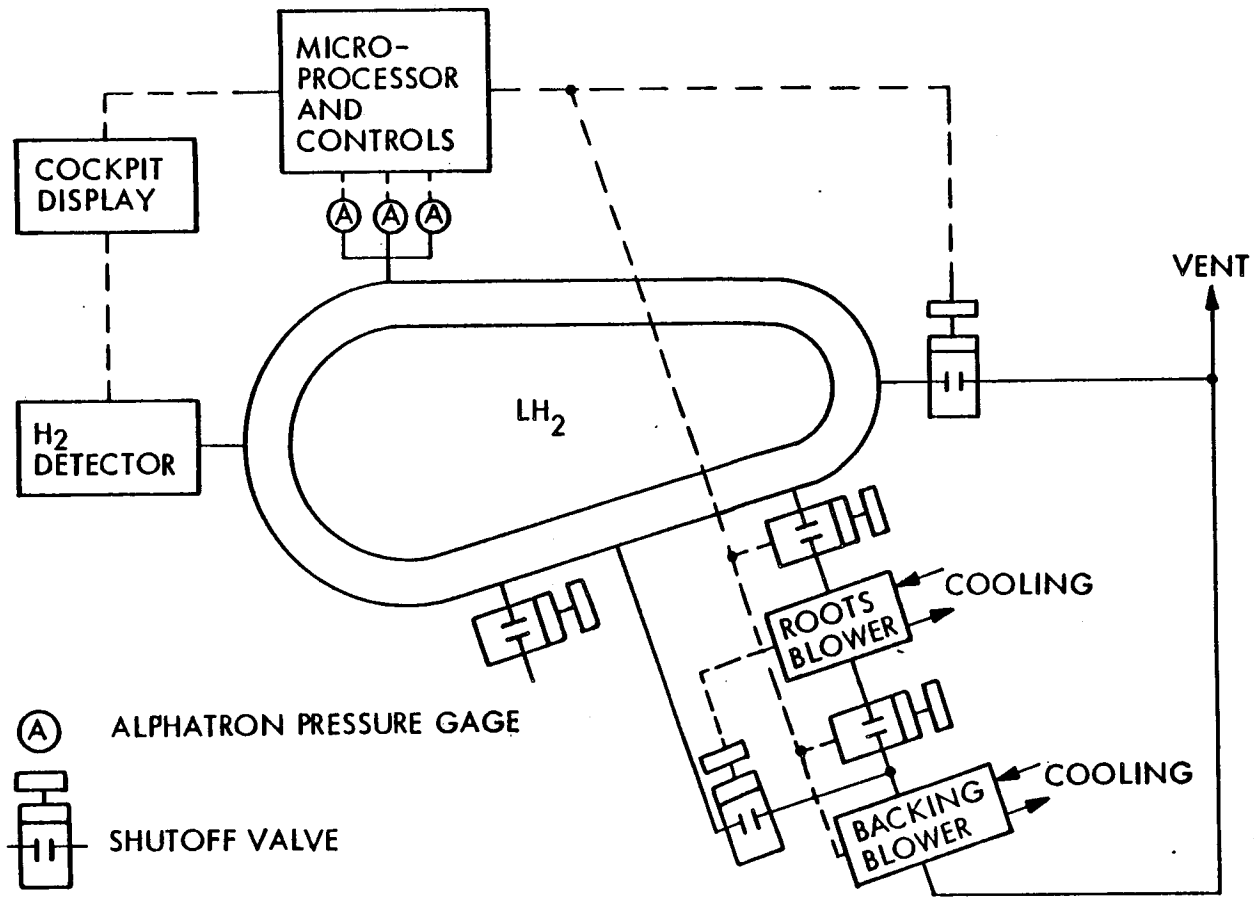

Figure 82. - Plumbing schematic for systems 10, 11, and 12.

TABLE 31. - SAFETY RANKING CRITERIA

Criteria	Ranking Weight*	
Malfunction		
Barriers		
• Permeability and leakage	4 (mixing of H_2 and air)	For Each Consideration
	4 (LO_2)	
• ΔP and flow direction	2 (H_2)	
	2 (Air)	
• Effect of thermal cycles	3	
• Resistance to accidental penetration	4	
Active systems	3	
Leak detection and control		
Time	1	
Sensitivity	1	
Safe removal in service	3	
Safe removal for tank inspection	1	
Flammability and toxicity	2	
Inspectability		
Tank	1	
Barrier	1	

*4 = Maximum importance:

Total of 44 = Maximum safety

the condition resulting from this failure, its effect on flight operation and aircraft safety, and protective measures that could be provided to overcome or minimize the failure effect. The problem of GH_2 leakage from the tank was examined in terms of the ability to detect leakage into the insulation, and into the airframe interior in the case of a nonintegral tank. A second aspect of the safety analysis considered the potential for removal of hydrogen or inerting of the system during aircraft operation, as well as when it is necessary to enter the fuel tank for inspection or repair. Flammability of the materials used in the system, and the possible toxic products resulting from combustion of a material were included in the third category of the safety analysis. The final aspect was how the system design affects the capability to inspect for tank wall or vapor barrier leakage.

For purposes of comparison, numerical ranking factors were assigned to each individual parameter. A value of four signifies maximum importance with smaller values indicating considerations of lesser impact on aircraft and passenger safety. The ranking scale was selected to give an acceptable value of resolution for comparison between concepts and was consistent with the level of analysis in this screening operation.

7.1.3.2 Performance analysis: The procedure followed in developing performance data for each system in the concept screening phase was to compute the amount of fuel evaporated during flight and ground segments as a function of insulation thickness. From the weight of fuel required to fly the design mission, plus allowance for necessary reserves, the required fuel load (the weight of liquid + evaporated fuel) and subsequent tank volumes were computed. Fuel containment system dry weight and fuselage length requirements were then calculated. These parameters, together with total fuel and ground vent loss weights, were then used to calculate DOC as a function of insulation thickness. Optimum thickness was selected as that corresponding to the minimum DOC, as obtained graphically from the DOC versus insulation thickness results.

7.1.3.2.1 Fuel tank geometry: As stated earlier, the aft tank of the aircraft was used as a basis for both the screening and preferred candidate analysis phases. The general configuration of the tank and its geometric relationships which were assumed for preliminary analysis purposes are illustrated in Figure 83. Solutions to the relationships between required volume and insulation thickness and the tank length and forward diameter parameters are represented in Figures 84 and 85. These graphical relationships were used in the iterative process of tank sizing as a function of insulation system heat transfer characteristics and the corresponding thickness of the candidate insulation system.

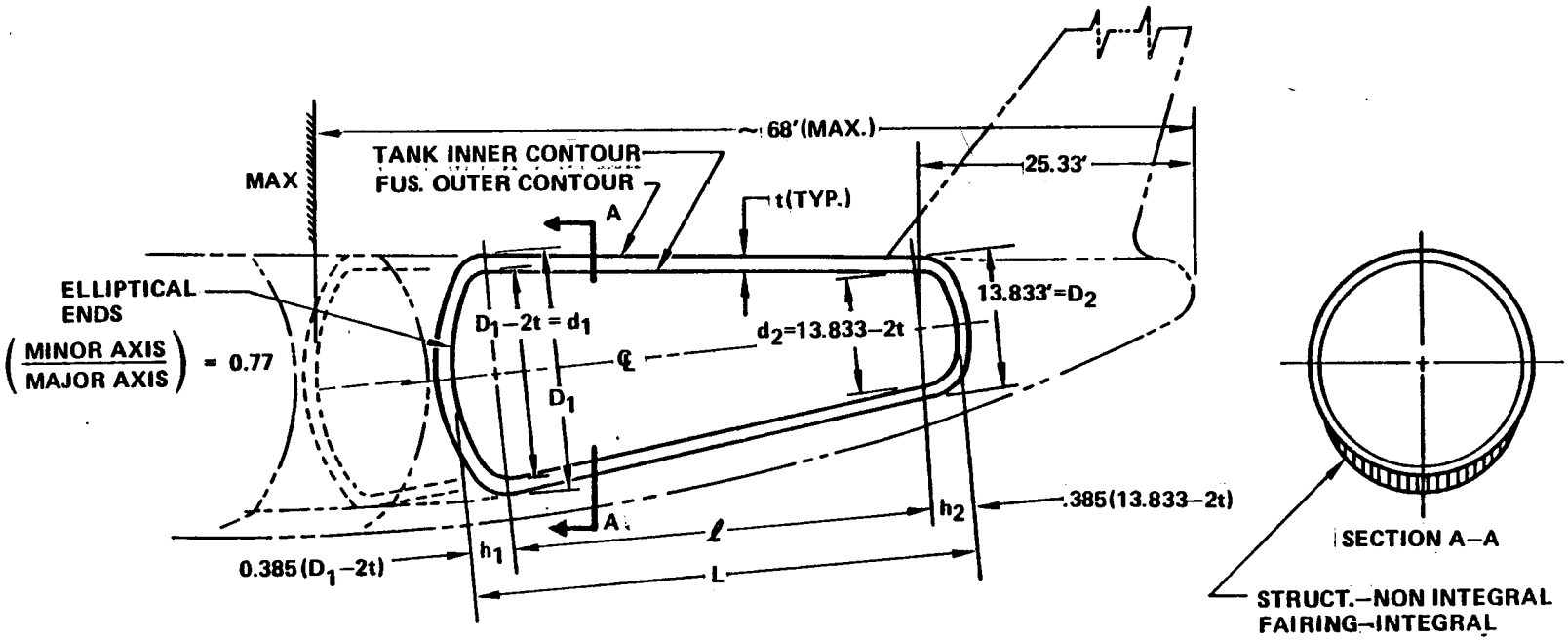

Figure 83. - General configuration of aft tank.

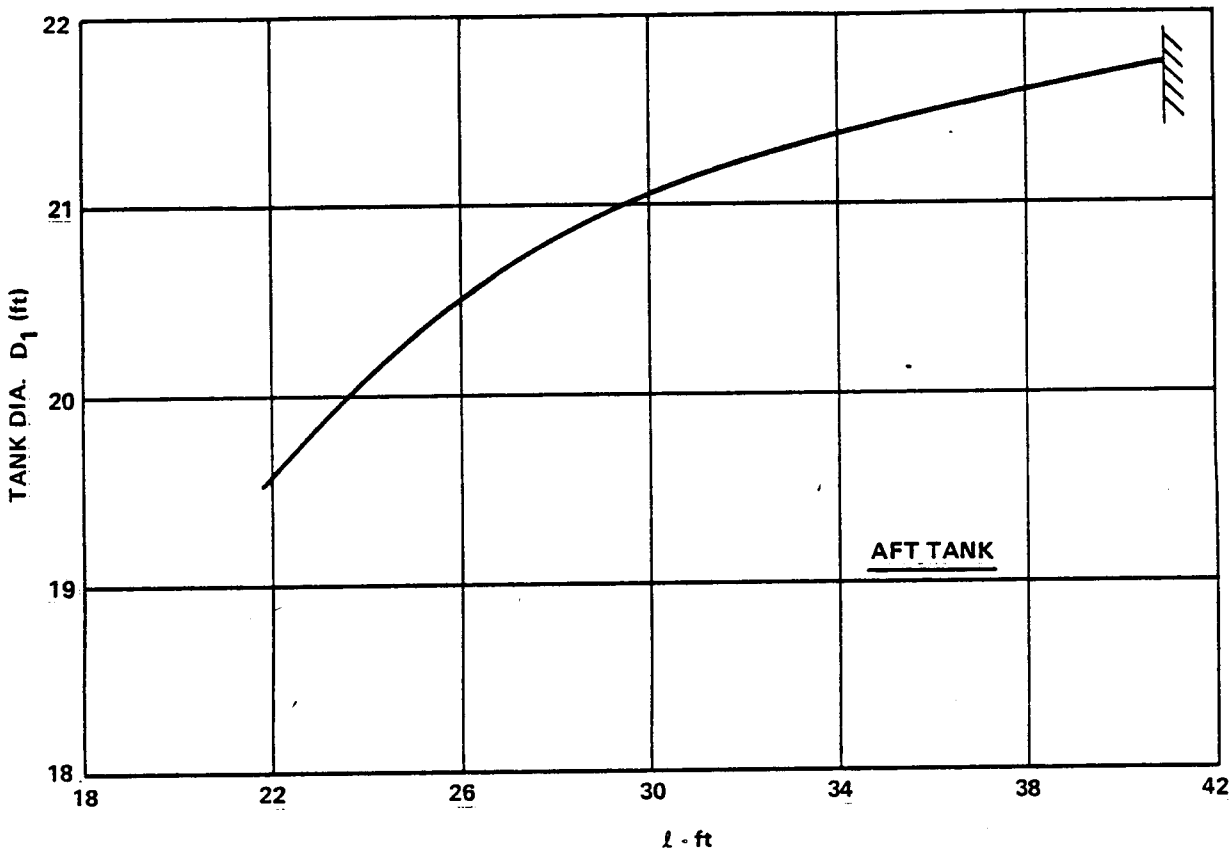

Figure 84. - Tank diameter D_1 vs tank length ℓ.

7.1.3.2.2 Thermal analysis: The thermal model used in the concept screening phase was developed as a closed form type of solution which considers the heat transfer in both liquid and vapor phases present in the tank as a function of liquid fraction, vapor and liquid wetted wall heat fluxes, exterior temperature, and tank wall and insulation thermal properties. Net heat input to the liquid (and vapor generation) is a function of heat transfer across the liquid wetted portion of the tank wall, the liquid/vapor interface, along the tank wall from the ullage to liquid region, and radiation from the ullage portion of the tank wall to the liquid. The model is illustrated in Figure 86. Derivation of the model for wall and vapor heat transfer to the liquid is presented in Appendix C.

Vent rates were calculated for a constant vent pressure of 145kPa (21 psia). The differential equation includes variable thermodynamic properties for the liquid and vapor as well as for the insulation and tank wall. Radiation heat input to the liquid surface was computed as a function of average ullage region wall temperature for each of three areas corresponding to equal area times view factor products. Interior tank wall and liquid surfaces were assumed to be grey and to have absorptances of 0.3 and 1.0, respectively.

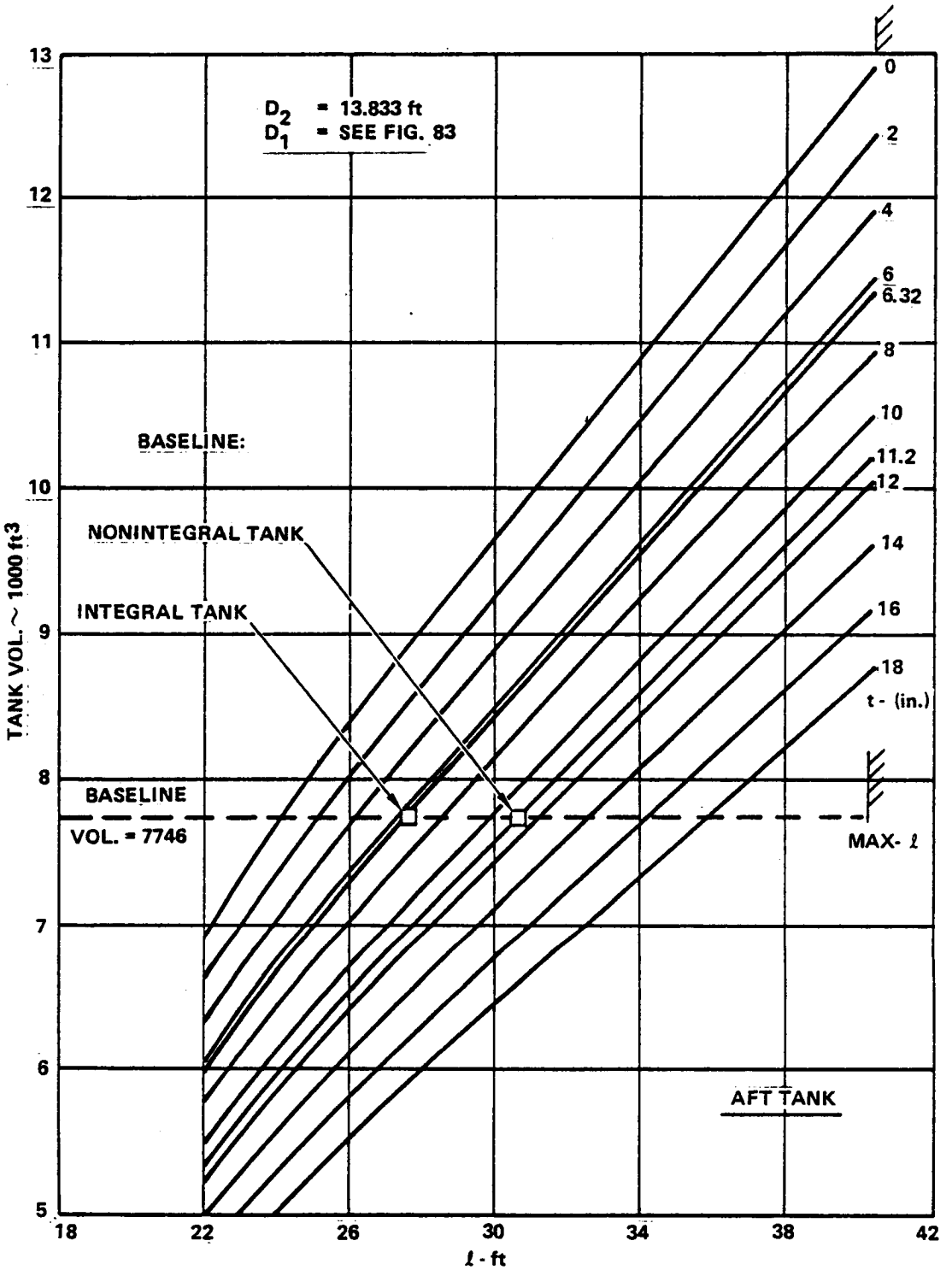

Figure 85. - Tank length ℓ vs volume and thickness

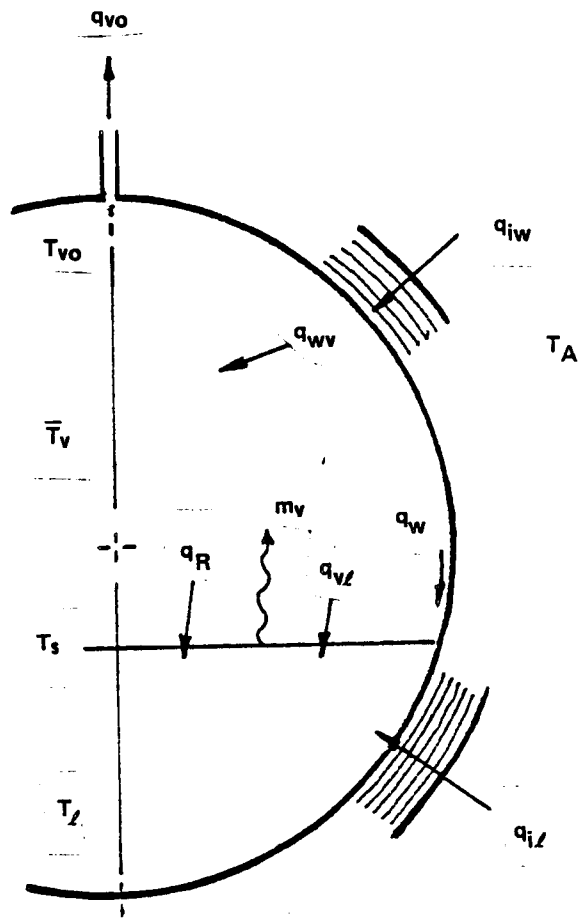

Figure 86. - Thermal model used for concept screening.

The major uncertainty in the thermal analysis, which also applied to the preferred candidate analysis, was the definition of the vapor-wall Nusselt number. This parameter governs the wall temperature distribution opposite the vapor and the subsequent mean vapor temperature. A thorough search of the literature did not reveal a satisfactory correlation for a non-isothermal wall exposed to a non-isothermal fluid for low Prandtl numbers (i.e., H_2 vapor). Consequently, initial studies were conducted varying the Nusselt number from a conduction dominate situation (Rayleigh Number $< 6 \times 10^3$) to a turbulent boundary layer condition (RA $\geq 10^8$). Change of this parameter resulted in a very significant variation in vapor-wetted wall temperature distributions. As an example, the temperature of the top of the tank for

a 50 percent ullage condition showed a variation from 185°K to 28°K as the Nusselt number was varied by a factor of 400 (going from a condition of highly stratified vapor to a turbulent boundary layer). The heat rate to the liquid decreased as the Nusselt number was increased to approximately 10 times the conduction limit. Further increase in Nu resulted in an increase in liquid heat rate. The initial decrease is due to lower conduction heat transfer along the tank wall, a smaller vapor-liquid temperature difference and a decrease of radiation from the vapor space wall to the liquid. Table 32 illustrates the influence of vapor-wall Nusselt number on mass of liquid evaporated and vented for a 50 percent liquid level with a liquid-wetted wall heat flux of 97.7 W/m (31 Btu/hr ft^2).

The experimental data found in the literature which could be used for correlation of the vapor-wall Nusselt number were very limited. Schalla (Ref. 8) reported the results of heat transfer testing on a small diameter (50-inch) liquid hydrogen tank. His vapor-wetted tank wall temperature data were used to correlate Nusselt number using the screening model. For the test tank, the best correlation of predicted and measured temperatures as a function of liquid level was obtained for a Nusselt number of approximately 17 which corresponds to a laminar condition. This comparison is

TABLE 32. - EFFECT OF VAPOR NUSSELT NUMBER ON HEAT INPUT TO LIQUID
[50% LIQUID LEVEL, q_w = 97.7 W/m^2 (31 Btu/hr/ft^2)]

N_u	Conduction	2X Conduction	4X Conduction	40X Conduction	110X Conduction
Average Wall °K Temperature (°R)	153 (276)	123 (221)	96 (173)	46 (83)	33 (59)
Vapor Exit °K Temperature (°R)	33.3 (60)	38.3 (69)	42.2 (76)	38.9 (70)	32.2 (58)
Ratio of Mass Vented*	1.0	0.926	0.878	0.939	1.080
Ratio of Vent Gas Sensible Heat*	1.0	1.287	1.505	1.366	1.059

*Compared to Nusselt No. corresponding to highly stratified gas.

shown in Figure 87 where tank top surface temperature is plotted as a function of Nusselt number for various liquid levels. The dashed line represents the best fit of the experimental data corrected for a 290°K outer surface temperature. Computed and measured liquid heat rates are compared in Figure 88 as a function of liquid fraction. Because of this reasonable correlation with the experimental data a Nusselt number of 17 was employed to generate tank wall temperature distributions and liquid heat rates for the Concept Screening phase.

Computation of design mission fuel loss for four insulation thicknesses for each concept was performed using the following procedure. Initial tank sizing to determine heat transfer area was based upon the liquid heat input for a 90 percent full tank under cruise conditions. This tank size was used to compute fuel losses for seven segments of a 24-hour period having fuel withdrawal increments, ambient temperatues, and times as shown in Table 33. An initial tank pressure of 145kPa (21 psia) and a minimum allowable pressure of 124kPa (18 psia) was assumed for the mission. At low heat rates it may be necessary to vaporize some fuel to maintain the minimum pressure level in the tank. By successive iterations the tank size and fuel loss converged to give the correct tank dimensions for the design mission fuel requirement. Transient conditions were accounted for by computation of the time constant for each insulation using a stepwise ambient temperature change from ground to cruise and proportioning the cruise and ground segment (5 and 7) into two ambient temperature conditions. This resulted in a gross approximation of heat storage within the system.

7.1.3.2.3 Thermal properties: The temperature dependent properties required for the thermal analysis of the concepts, and the sources from which the data was obtained, are as follows:

- Hydrogen - Liquid and vapor phases
  - Density
  - Compressibility
  - Vapor Pressure
  - Thermal Conductivity
  - Specific Heat
  - Latent Heat of Vaporization
  - Viscosity
  - Sonic Velocity

  Properties data were taken from Reference 9.

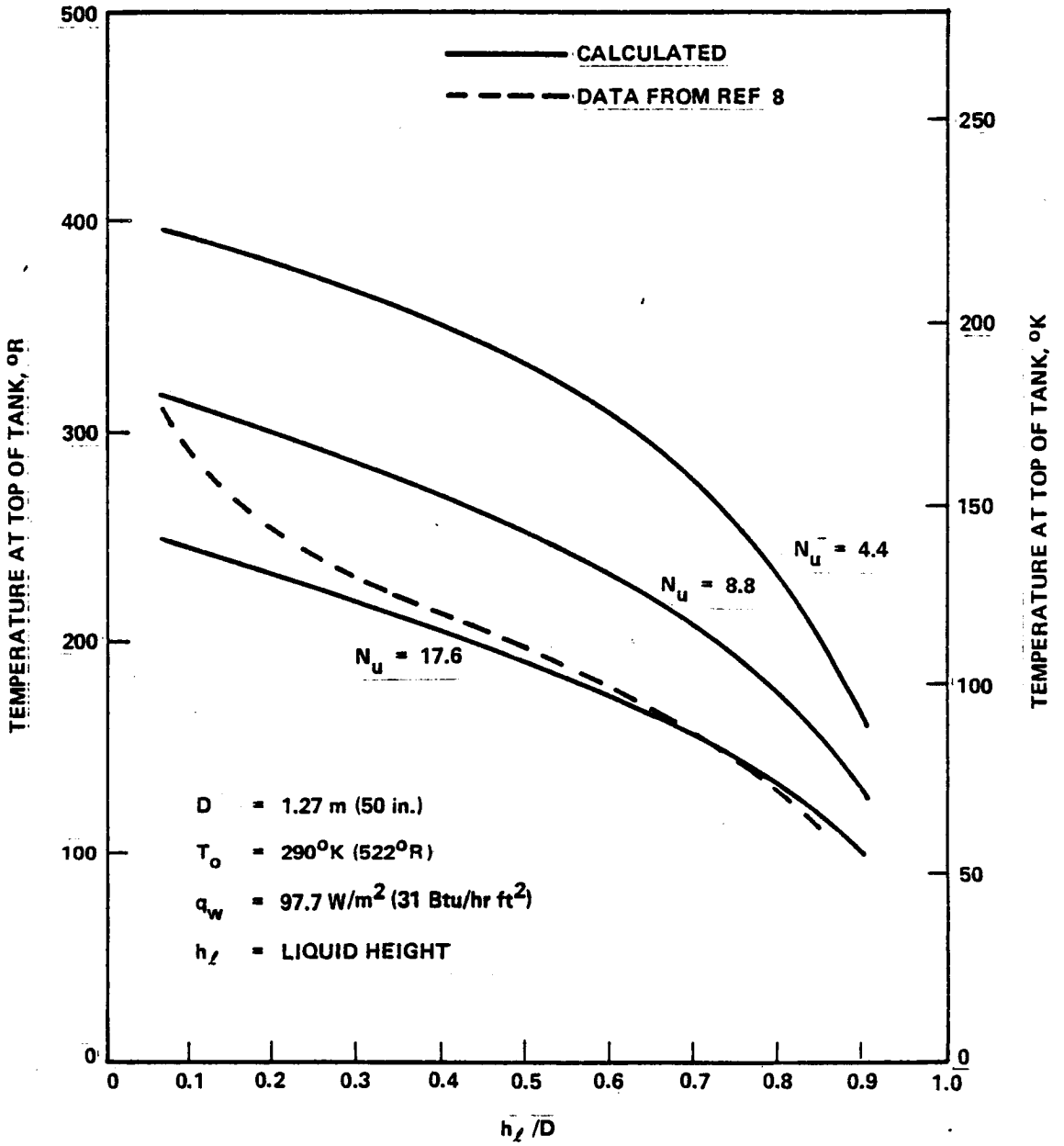

Figure 87. - Correlation of tank top surface temperature with Nusselt number for various liquid levels.

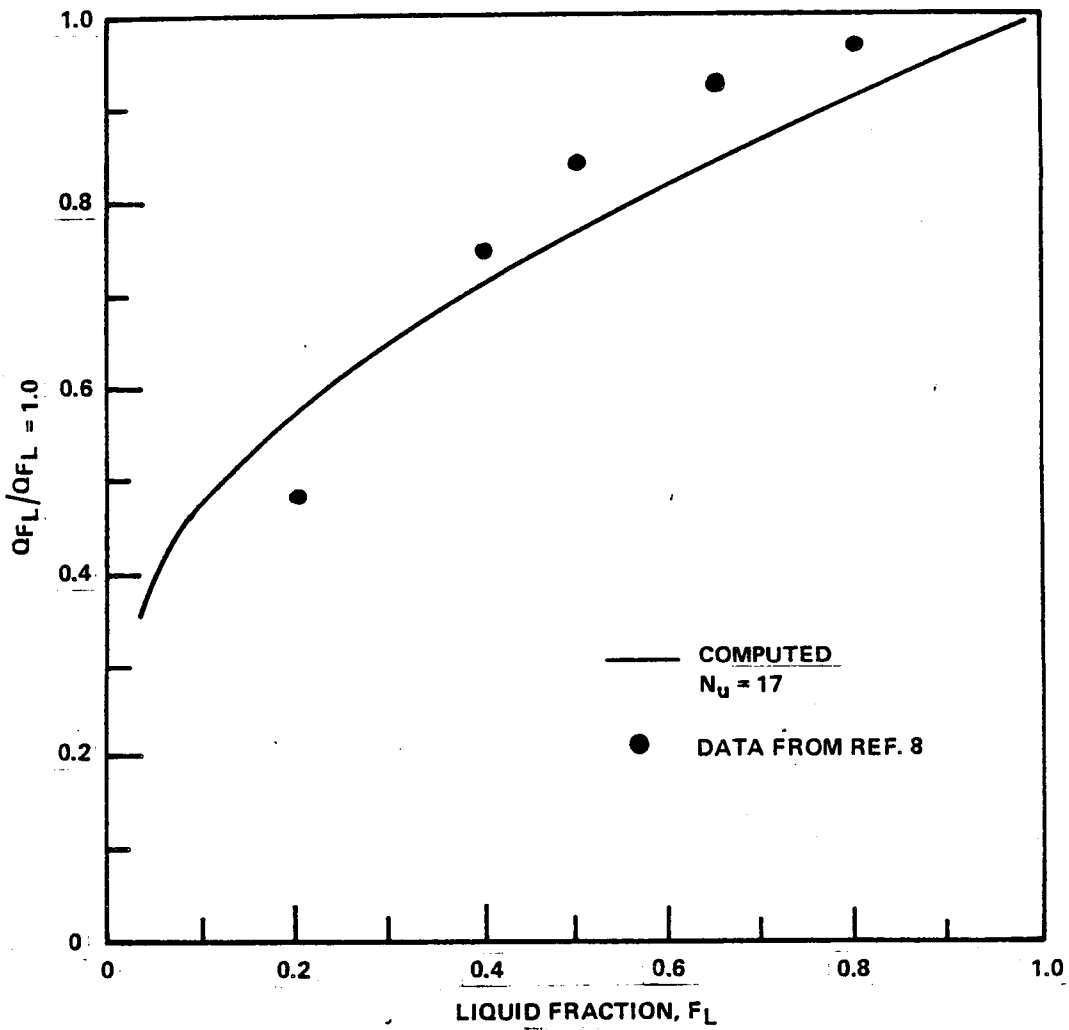

Figure 88. - Comparison of measured and computed liquid heat rate ratio as a function of tank liquid fraction.

- Tank and Fuselage - Aluminum - 2219 alloy for tank and 2024 alloy for fuselage
  - Density (REf. 10)
  - Thermal conductivity (Ref. 11)
  - Specific Heat (Ref. 10)
- Insulations - Where available, data were taken from the literature for the specific material. In cases where data were not available, the properties were estimated using those of similar materials.

TABLE 33. - MISSION FUEL SCHEDULE - AFT TANK

Segment	Time (hrs)		Fuel Withdrawal		Ambient Temperature	
	Segment	Total	kg	lb	°K	°R
1. Ground, After Fueling, Engines Off (a)	0.283	0.283	0	0	290	522
2. Taxi	0.233	0.516	35.4	78	290	522
3. Take-Off	0.0817	0.598	221	487	290	522
4. Climb	0.743	1.341	1,086	2,394	290	522
5. Cruise	10.273	11.614	10,466	23,073	222	400
6. Descent-Land	0.383	11.997	178	393	222	400
7. Ground	12.003	24.000	(b)		290	522

(a) APU Fuel not Included

(b) Approximately 1134 kg (2500 lb) of fuel remain in aft tank at start of assumed out-of-service period.

- Density
- Thermal Conductivity
- Specific Heat

Sources of property values used for each concept are given in Table 34. For the external foam, LI900, and microspheres, the data shown in Figure 89 were used for thermal conductivity values. In the case of polyurethane a composite of the data for densities from 27 to 35 kg/m^3 was used to derive an effective thermal conductivity. Only a single data point at ambient temperature was available for the Rohacell foam. As it falls on the curve for PVC foam, Figure 89, these data were used to represent the temperature dependent conductivity of Rohacell. Because of the long aircraft lifetime and the capability of hydrogen to permeate such materials, the thermal conductivity of the internal polyurethane foam in system 5 was considered as a GH_2 filled foam for this analysis. For the two purged systems, numbers 1 and 2, thermal conductivities were taken to be those of the specific purge gas, assuming the contribution of the low density glass batt material to heat transport was insignificant. (Reference 10)

TABLE 34. - DATA SOURCES FOR PROPERTIES OF INSULATION CONCEPTS

Concept Number	Material	Property and Data Source
1.	He filled fiberglass	Thermal conductivity and specific heat; ref. 10
2.	He and N_2 filled fiberglass	Same as No. 1
3.,4.	Rohacell foam	Thermal conductivity; see Fig. 89, extrapolated using PVC data. Specific heat; ref. 12 for polyurethane
5.	Internal Polyurethane foam, 3D reinforced	Density and thermal conductivity for GH_2 filled condition; ref. 5-9. Specific heat from ratio of foam and glass reinforcement refs. 10 and 12
6.	Internal PPO plus external Polyurethane foam	Density and thermal conductivity; PPO, ref. 5-10; Polyurethane - see Fig. 89. Specific heat; PPO assured same as Polyurethane - ref. 12
7.	Internal PPO foam	See No. 6
8.	Internal gas filled honeycomb	Density and thermal conductivity; ref. 14 and 15. Specific heat; extrapolated using ratios of constituents and ref. 12
9.	Polyurethane foam	See Fig. 89, 32 kg/m^3. Specific heat; ref. 12
10., 11.	Microspheres	Density and thermal conductivity; ref. 16. Specific heat; ref. 10
12.	LI-900	Density, thermal conductivity and specific heat; ref. 17
13.	Self-evacuation shingles	Density and thermal conductivity, ref. 18. Specific heat, estimate using ratio of constituents, refs. 10 and 12.

TABLE 34. - DATA SOURCES FOR PROPERTIES OF IN SULATION CONCEPTS (Continued)

Concept Number	Material	Property and Data Source
14.	Self-evacuated honeycomb plus Polyurethane foam	Density and thermal conductivity: Polyurethane foam - see Fig. 89, 32 kg/m^3; honeycomb, ref. 19. Specific heat estimated using ratios of components; refs. 10 and 12
15.	Self-evacuated honeycomb plus GN_2 purged fiberglass	See No's. 2 and 14

- Purge Barrier/Vapor Barrier/Vacuum Jacket - Two types of vapor barriers were considered for use with closed cell form insulations to prevent infusion of air or hydrogen. One was a simple plastic sheet such as mylar or Kevlar. The other was a multilayer sandwich called MAAMF, which consists of the following:

Layer	Material Description
1	0.5 mil Mylar, Type A
2	Adhesive
3	0.5 mil Aluminum Series 1100.0 Foil
4	Adhesive
5	0.5 to 1.5 mil Aluminum Series 1100.0 Foil
6	Adhesive
7	0.5 mil Mylar, Type A
8	Dacron or Glass Net Fabric

The total thickness is 5 to 6 mils and it weighs 0.225 kg/m^2 (0.046 lb/ft^2).

Thermal conductivity of the vapor barriers and the thin (5 mil) stainless steel vacuum jacket was not considered because the thermal resistances introduced by these components is negligible. Thermal conductance of the honeycomb composite rigid vacuum shell was computed using both composite and aluminum core conductance data from Reference 22, together with overall thermal resistance data of References 23 and 24 to account for the resistance of the adhesive bonded core-to-face sheet interfaces.

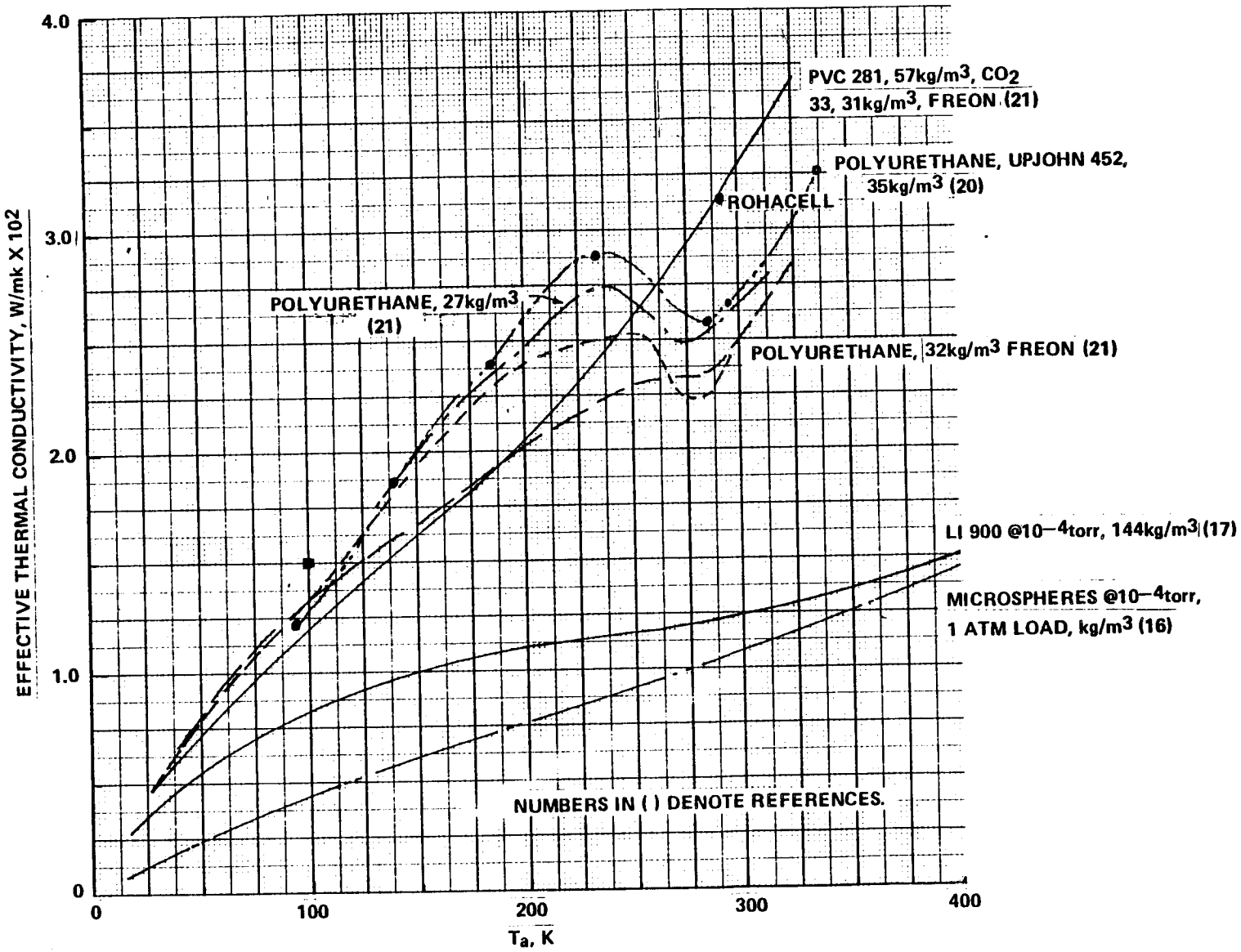

Figure 89. - Thermal conductivity of foams, rigidized silica and microsphere insulations.

Specific heat data were used in the transient program for evaluation of the preferred candidates. For the stainless steel vacuum jacket data were taken from Reference 10. Vapor and purge barrier specific heats were calculated from the specific heats of the constituents of each material weighted by the mass fraction of each in the total composite.

7.1.3.3 Producibility analysis: A preliminary producibility analysis was made for each concept to identify development items, potential fabrication and assembly procedures, and specialized manufacturing inspection requirements. These analyses were made to obtain an order of magnitude estimate of development and production costs which could be translated into DOC increments.

7.1.3.4 Operations analysis: The operations analysis was conducted to define projected maintenance and inspection requirements. Items requiring service were identified and frequencies of inspection and servicing were postulated. These analyses were conducted at the lowest level which would provide a relative comparison between systems.

7.1.4 Screening results. - The 15 candidate fuel tank insulation concepts were subjected to the screening analysis. They represented twelve basic types, three of which had two variations each. The objective was to provide a basis on which recommendations could be made for two concepts to be evaluated as preferred candidates for use with integral tanks and two for use with nonintegral tank designs.

7.1.4.1 Safety: As outlined in Section 7.1.3.1 the safety analysis was a four step process. First, a malfunction analysis was performed to determine if any of the systems had failure modes that were dangerous to life on aircraft. The details of the malfunction analysis are given in Appendix E. Second, requirements for hydrogen detectors were established. Third, an assessment of flammability and toxicity was made. Fourth, the ability to perform inspections of barriers and tank structure was evaluated.

The results of the evaluation of each concept with regard to the safety criteria (Table 31) are presented in Table 35. Under each specific criterion the concepts are ranked in order of decreasing merit. Numerical ranking weights were assigned at each level within a category, based upon the maximum value which corresponds to the importance of the specific consideration. For example: in the category of permeability to gases to allow mixing of air and H_2, concept 4 was assigned a value 4, concept 2 a value of 3 and concept 5 a value of 1. The summation of the category ranking values was then converted to a scale of 0 to 100 to yield a relative ranking of all systems. The resulting composite ranking is presented in Table 36.

TABLE 35. - RANKING OF CANDIDATE INSULATION SYSTEMS BASED ON SAFETY CRITERIA

Criteria: Permeability of Barriers to Gases to Allow Mixing of Air and H_2 [4]	Criteria: Permeability of Barriers to Gases to Allow O_2 Cryo-pumping in Organic Material [4]	Criteria: Potential Rate of H_2 leakage Based on Pressure Drop Across Barrier [2]	Criteria: Potential Rate of Air Leakage into the Insulation Based on Pressure Drop and Flow Direction Across Barrier [2]
Concept Ranking: 3M,9,10,11,12 (2 Barriers, both Metal)	1,2,5,7,8 (Gas Flow outward) 10,11,12 (Min Organics 3M (Metal Barrier	1,2 ($\Delta P \ll$ Amb)	5,7,8 (Gas Flow Outward)
2,14,15 (3 Barriers, one Metal)	6,9,14,15 (No LO_2 Liquefaction)	6 ($\Delta P \ll$ Amb)	1,2,15 ($\Delta P \ll$ Amb)
1,3,6,13 (2 Barriers, one Metal)	3,4,13 (Potential LO_2 in Organics)	3,4,5,7,8,9,10,11, 12,13,14,15 (ΔP = Amb)	6,14 ($\Delta P \ll$ Amb)
5,7 (one Metal Barrier)			3,4,9,10,11,12,13 (ΔP = Amb)

Criteria: Potential Barrier Leakage due to 4900 Thermal Cycles [4]	Criteria: Resistance to Accidental Penetration of External Surface [4]	Criteria: Reaction Time to Detect H_2 Leakage [1]	Criteria: Sensitivity of Leak Detection Method [1]
Concept Ranking: 1,2,9 (Barrier Moves Independently of Tank) 7,8 (Barrier Seal not Required) 10 (Barrier Seal designed to Flex Elastically) 11,12 (Barrier Seal not flexed, 10,000 psi Stress in Liner Well Within Elastic Limits)	Concept Ranking: 5,7,8,11,12 (Tank or Ext Fairing)	Concept Ranking: 9,10,11,12 (Positive ΔP, Leak into Vacuum)	Concept Ranking: 9,10,11,12 Low Pressure Detection
3M (Metal Barrier may Buckle during Thermal Cycling) 5 (Liquid Seal may Chip during Cycling) 14,15 (Honeycomb Seal is Cold Worked during Cycling)	1,2,3,4,6,9,14,15 (Vapor Barrier)	5,7,8 (Positive ΔP, Detectors Outside Tank)	1,2,3,4,5,6,7,8 Amb Pres 13,14,15 Detection
3,4,6,13 (Organic Seal is not as Resistant to Thermal cycle Induced Leaks at Lower Temperatures as Metals)	10 (Thin Metal Barrier) 13 (Plastic Film Barrier)	2,15 (Positive ΔP, 1 Barrier, Detectors in N_2 Layer)	
		1 (Positive ΔP, 1 Barrier, Detectors Outside Tank)	
		3,6,13 (Negative ΔP, 1 Barrier, Detectors Outside Tank)	
		14 (Negative ΔP, 2 Barriers, Detectors Outside Tank)	

Criteria: Capability to Remove Leaking H_2 Safely in Service [3]	Criteria: Tank Inspectability [1]	Criteria: Secondary Barrier Inspectability [1]	Criteria: Malfunction of Active Systems [3]	Criteria: Ease of GH_2 Removal from Tank for Internal Inspection [1]	Criteria: Flammability and Toxicity of Materials in Case of Fire [2]
Concept Ranking: 9,10,11,12 (Pump) 1,2,15 (Purge)	Concept Ranking: 5,7,8,11,12 (Ext. Insp.)	Concept Ranking: 1,3,4,6,9,10 (Ext. Insp.)	Concept Ranking: 3,4,5,6,7,8,13, 14,15 (Passive)	Concept Ranking: 1,2,3,4,9,10,11, 12,13 14,15 (Metal)	Concept Ranking: 10,11,12 (Min Organics)
4,5,6,7,8,13,14 (Nonactive)	1,2,3,4,9 (Int. Insp) 10,13,14,15	5,7,8,11,12 (Int. Insp.)	1,10,11,12 (Active)	6,7,8 (Open Cell)	1,2,9,15 (Mod Organics)
	6 (Tank Surface not Visible)	2,13,14,15 (One Barrier can't be inspected)	2,9 (Active Most Complex)	5 (Closed Cell)	5,7,8 (Inside Tank)
					3,4,5,13,14, (Most Organic Ext. to Tank)

LEGEND

Criteria:

X

Concept Ranking:

Safest

Least safe

Ranking Weight

TABLE 36. - SUMMARY OF SAFETY RANKING

Concept	Ranking Score[a]
11, 12	89
10	84
9	80
7, 8	78
3, 4[b]	77
2	75
1	74
5	73
15	70
14	56
6	54
3, 4[c]	49
13	42

[a] 100 = maximum possible
[b] MAAMF is used as vapor barrier
[c] Plastic film is used as vapor barrier

INSULATION CONCEPT NUMBER/TYPE

1. GHe Purged FG
2. GHe-GN_2 Purged FG
3. Ext. Foam, Non-Integral
4. Ext. Foam, Integral
5. Internal PU Foam
6. Int. PPO, Ext. PU Foams
7. Int PPO Foam
8. Int. Perf HC
9. Rigid Vac Shell
10. Ext. Microspheres
11. Int. Microspheres
12. Int. LI 900
13. Self-Evac. Shingles
14. HC/Foam
15. HC/GN_2 Purged FG

Considering safety alone, concepts 2, 3, 9, and 10 would be the choices for the nonintegral tank design, and concepts 4, 7, 11, and 12 the choices for the integral design.

7.1.4.2 Performance: Results of the thermal performance studies are tabulated in Table 37 for each system. The values presented are those for the insulation thickness giving the minimum DOC as determined graphically from a plot of DOC versus insulation thickness. Weight and volume statements were then recalculated for the thickness corresponding to minimum DOC. Ranking of the concepts based upon DOC is shown in Table 38. The table also shows fuel weight and fuel volume fractions as dimensionless parameters normalized to the values calculated for the baseline system, Concept No. 4.

The values of DOC are based upon consideration of both flight and ground fuel losses. A comparison between DOC calculated in this manner and that calculated for flight loss only is given in Table 39. The only impact consideration of flight boiloff alone has on the ranking is that Nos. 6 and 9 change positions, No. 6 ranking higher than No. 9.

On the basis of DOC, concepts 4, 14, 11, and 12 remain as logical choices for the integral tank design and concepts 13, 10, 3, and 15 for the nonintegral tank.

7.1.4.3 Producibility and operational: A preliminary producibility analysis was made for each candidate system to identify development items, potential fabrication and assembly procedures, and inspection requirements following or during fabrication as shown in Table F-1 of Appendix F. All systems appear feasible to fabricate although a much more detailed analysis is required, particularly around tank penetrations. From the data in the Appendix, cost differences were developed between the 15 insulation candidates for the development and manufacture of the insulation systems. When the difference in costs is expressed as a percent of direct operating cost per seat nautical mile, it varies up to only 0.2 percent between 14 of the systems. For the other system, No. 9, the percentage increased up to 0.4 percent over the lowest cost system. These cost differences have a minor impact on selection of a candidate insulation system. For example: a development cost of 10×10^6 dollars spread over 350 aircraft having a 14 year lifetime and operated 350 days per year represents a DOC increment of 3×10^{-4}¢/s n.mi. Thus, a 0.4 percent range in these costs is insignificant to DOC. No DOC figures were calculated for production costs in the concept screening phase because of the scope of the analysis that would be required to obtain valid data for the many systems involved.

Estimates for inspection, maintenance and operational requirements of the systems are shown in Table F-2, Appendix F. From these requirements, the magnitude of direct operating costs was estimated assuming a labor cost of $25 per man hour. The estimates vary from 0.0005 to 0.0001 ¢/s n.mi.

TABLE 37. - CONCEPT SCREENING PERFORMANCE ANALYSIS SUMMARY

Concept Number	1	2	3	4	5	6	7	8	9	10	11	12	13	14	15
Insulation	fg/Gle purge	fg/Gle-GN_2 purge	Rohacell Foam Ext.	31	PU Foam Int	Int PPO/ Ext PU Foam	Int PPO Foam	Perf HC	Rigid Vac Shell(g)	Micro-sphere Ext Vac	Micro-sphere Int Vac	LI-900 Int. Vac	Self-Evac Shingles	HC/Foam	HC-GN_2 Purge
Tank Type	N I(a)	N I	N I	I	I	I	I	I	I	N I	I	I	N I	I	N I
FCS Weight kg (lb)	13 279 (29 275)	12 891 (28 420)	10 134 (22 341)	7 839 (17 282)	11 576 (25 521)	9 505 (20 955)	10 689 (23 536)	10 676 (24 899)	11 294 (22 542)	10 225 (22 542)	8849 (19 509)	9537 (21 025)	8994 (19 827)	8046 (17 739)	11 760 (25 925)
FCS Thickness cm (in.)	33.83 (13.32)	25.25 (9.92)	23.38 (8.81)	10.54 (4.15)	13.11 (5.16)	14.15 (5.57)	20.96 (8.26)	17.17 (6.76)	15.60 (6.15)	20.02 (7.88)	10.69 (4.21)	9.88 (3.89)	15.75 (6.20)	10.87 (4.28)	24.49 (9.64)
Fuel Vaporized Flight (b) kg (lb)	1615 (3560)	1090 (2404)	889 (1960)	916 (2020)	4559 (10 050)	1625 (3582)	4291 (7460)	3664 (8078)	372 (820)	260 (574)	523 (1152)	1021 (2250)	374 (824)	865 (1906)	464 (1024)
Fuel Vaporized Ground (c) kg (lb)	1737 (3830)	1842 (4060)	1617 (3564)	1733 (3820)	5094 (11 230)	3373 (7435)	4491 (9900)	4022 (8855)	191 (420)	1016 (2240)	761 (1678)	1243 (2740)	805 (1775)	1229 (2710)	1017 (2242)
DOC(d)	2.0043	1.9340	1.8818	1.8269	1.9961	1.8866	1.9857	1.9524	1.8675	1.8635	1.82884	1.8531	1.8322	1.8528	1.8961
Fuel Weight Fraction (W_{FCS}/W_{FUEL})(e)	0.475	0.461	0.353	0.280	0.414	0.340	0.382	0.382	0.406	0.366	0.317	0.341	0.322	0.288	0.421
Fuel Volume Fraction (V_{FUEL}/V_{FCS}) (f)	0.569	0.645	0.607	0.739.	0.649	0.701	0.614	0.639	0.696	0.714	0.741	0.731	0.726	0.733	0.667

(a) N I = nonintegral, I = integral

(b) Includes pressurant gas

(c) Includes tank cooldown for fueling

(d) Fuel vented on ground not included

(e) W_{fuel} = mission fuel weight, 61 630 lb

(f) V_{fuel} = mission fuel volume

(g) HC vac jacket carries aircraft loads

TABLE 38. - DOC, WEIGHT, AND VOLUME SUMMARY FOR CONCEPT SCREENING

	Concept Number													
	14	11	13	12	10	9	3	6	15	2	8	7	5	1
	(Ranked According to DOC)													
$\frac{DOC}{DOC_4}$	1.000	1.001	1.003	1.014	1.020	1.022	1.030	1.033	1.038	1.059	1.069	1.087	1.093	1.097
$\frac{W'_f}{W'_{f4}}$	1.029	1.132	1.150	1.218	1.307	1.450	1.296	1.214	1.504	1.646	1.364	1.364	1.479	1.696
$\frac{V'_f}{V'_{f4}}$	0.992	1.003	0.982	0.989	0.966	0.942	0.907	0.949	0.903	0.873	0.865	0.831	0.878	0.770

DOC_4 = 1.8269 ¢/S.n. mi.

W'_{f4} = 0.280 where $W'_f = W_{FCS}/W_{FUEL}$

V'_{f4} = 0.739 where $V'_f = V_{FUEL}/V_{FCS}$

TABLE 39. - IMPACT OF GROUND BOILOFF (RECOVERED) ON DOC

Insulation Concept Number/Type	DOC (¢/S n. mi.)	
	Ground Boiloff Not Included	Ground Boiloff Included
1. GHe Purged FG	1.9899	2.0043
2. GHe-GN_2 Purged FG	1.9197	1.9349
3. Ext. Foam, Nonintegral	1.8674	1.8818
4. Ext. Foam, Integral	1.8126	1.8269
5. Internal PU Foam	1.9540	1.9961
6. Int. PPO, Ext. PU Foams	1.8587	1.8866
7. Int PPO Foam	1.9486	1.9857
8. Int. Perf HC	1.9267	1.9524
9. Rigid Vac Shell	1.8659	1.8675
10. Ext. Microspheres	1.8551	1.8635
11. Int. Microspheres	1.8221	1.8284
12. Int. LI 900	1.8428	1.8531
13. Self-Evac. Shingles	1.8255	1.8322
14. HC/Foam	1.8156	1.8528
15. HC/GN_2 Purged FG	1.8877	1.8961

As in the case of evaluating differences in production cost, these differences are too small to be meaningful in influencing selection of a preferred concept.

There is not sufficient data for any of the insulation systems to quantitatively predict their useful life for an aircraft flying 350 times a year for 14 years (4900 thermal cycles). However, based on the limited test data available and characteristics inherent in their design, a qualitative ranking was made as shown in Table F-3 of Appendix F. The concepts were ranked as 1, 2 or 3 with 1 having the longest projected life system. Concepts 1, 2, 6, 7, 8, 10, 11, and 12 are ranked the highest with 3, 4, 5, 9, 14, and 15 falling into the middle category. It must be emphasized that insufficient information is available at this time to make more than a very tentative judgement of this criterion.

7.1.5 Selection of preferred candidates. - The selection of the concepts to be evaluated as preferred candidates was made primarily on the basis of rankings from the safety and performance results. Analysis of producibility and operations did not yield any quantitative information which would influence the selection. At this stage of development all concepts appear to be feasible in these regards, and qualitative estimates of DOC increments due to differences in producibility and operations aspects did not result in any large percentage variations between concepts.

Initially, four candidates for each tank concept (integral and nonintegral) were selected on the basis of DOC. Candidates numbers 4, 14, 11, and 12 were selected for the integral tank. For the nonintegral design, numbers 13, 10, 3 and 15 were selected. These were then compared with a ranking of safety criteria to arrive at the final candidates for each tank concept. Candidates 13, 14, and 15 were eliminated on the basis of poor safety rankings and the fact that satisfactory performance has never been demonstrated in prior development programs. For example, an airtight seal has never been maintained on Concept 13 and a leak-tight honeycomb construction could not be achieved for multiple cyclic exposure with Concept 14. Candidate 15 was also eliminated on the basis of the consideration of failure of previous development efforts to demonstrate satisfactory leak tight construction techniques with honeycomb substrates for cryogenic tanks.

Recommendation of the five remaining concepts was made to NASA. As a result of discussions between Lockheed and NASA it was mutually agreed to include concepts 3 and 4 with the substitution of modified versions of 9 and 11 for nonintegral and integral tanks respectively. Concept 9 was substituted for 10 in order to include the hard vacuum system in the final evaluation. Further, concept 11 was modified to place the insulation exterior to the tank. The external vacuum jacket was protected with a composite formed by an exterior aerodynamic fairing and a flexible foam layer between the fairing and the jacket. The disadvantages of the original design for concept 11 were: (1) the use of honeycomb for the fuel tank structure; (2) making the 5-mil stainless steel liner LH_2 leak proof; (3) fabrication difficulties; and (4), the reduction of allowable stresses in the tank structure due to the warm tank. It was felt that the new concept presented a more reasonable approach and would minimize operational and production problems.

In summary the concepts approved for the preferred candidates analysis phase were:

Candidate No. 1 (Concept 3): Nonintegral tank - external foam.

Candidate No. 2 (modified Concept 9): Nonintegral tank - hard shell vacuum jacket.

Candidate No. 3 (Concept 4) Integral tank - external foam.

Candidate No. 4 (modified Concept 11): Integral tank - external microspheres.

Descriptions of these systems are given in Section 7.1.6.

7.1.6 Analysis of preferred candidates. - Parametric thermal analysis studies were conducted to develop fuel loss and required tank volume as a function of insulation thickness for each candidate. These data were then translated into DOC for design optimization.

Two different methods of thermodynamic analysis were used for the concept screening and preferred candidate phases of the program. As described in Section 5.1.3.2, for concept screening a closed form steady-state solution was used to compute heat inputs as a function of tank liquid fraction. These inputs were modified by a heat storage term applied in a stepwise manner to give a pseudo-transient result which followed a seven segment mission profile for exterior temperature and fuel fraction.

Analysis of the preferred candidates was done in a manner to represent a true transient condition using a finite difference program which followed the specified design mission using inputs of Mach number, altitude, and rate of fuel usage in steps of 5 min time intervals. In addition to the normal flight mode, a subroutine was included to simulate the effects of severe flight turbulence by assuming complete liquid disorientation and wetting of the inner tank wall, so that the liquid, vapor and inner tank wall reach an equilibrium temperature. The stratification process then resumes following this simulation of a severe, short-term flight disturbance.

7.1.6.1 Description of candidates: The four insulation candidates, selected with NASA concurrence, are:

- Candidate No. 1 - Nonintegral fuel tank with an exterior rigid closed-cell foam insulation system using the MAAMF vapor barrier concept.

- Candidate No. 2 - Nonintegral fuel tank with a hard shell vacuum jacket; 1.27 cm (0.5 inch) of rigid closed-cell foam located at tank wall to prevent air liquefication in event of external leakage into vacuum space; aluminized Mylar bonded to interior surface of jacket and exterior surface of foam to reduce radiation heat transfer.

- Candidate No. 3 - Integral fuel tank with rigid closed cell foam primary insulation; open-cell flexible foam exterior to primary insulation vapor barrier (MAAMF concept) to accommodate dimensional changes and support exterior fairing.

- Candidate No. 4 - Integral fuel tank with external evacuated microsphere insulation having flexible metal vacuum jacket; open-cell flexible foam located exterior to flexible vacuum jacket to support fairing.

Cross-sectional views of the four systems are shown in Figures 90 through 93 with the appropriate fixed dimensional properties and component specific weights and densities.

7.1.6.2 Thermal analysis of preferred candidates: The model used for thermal evaluation of the four preferred insulation system candidates was a transient computer program, "THERM". The THERM Thermal Analyzer Program, described in Appendix D, solves transient heat flow problems by use of a forward finite-difference algorithm for solving an analogous resistance-conductance (R-C) electrical network. It is structured to allow maximum flexibility in describing energy transport phenomena unique to a specific application. This program computes the tank pressure and vapor vent rates (including vapor required for pressurization) as well as the transient temperature distributions in the tank walls, in the insulation systems, and in the liquid and vapor components. The model uses the design mission fuel flow schedule, (Appendix A) and the environment temperatures during flight are from Standard Atmosphere Tables (Reference 25). The program models both integral and nonintegral tanks. Thermal conductivities and specific heats of the tank wall, insulation system materials, and the hydrogen liquid and vapor are specified as a function of temperature throughout the model.

In the thermal model the liquid and vapor volumes are divided into 9 and 10 horizontal layers, respectively, as shown in Figure 94. The liquid/vapor interface is at the saturation temperature, T_s, corresponding to the tank pressure. Located opposite each liquid and vapor node are a tank wall node, 3 insulation nodes, and two outer structure nodes for the aircraft fuselage or exterior fairing.

The liquid volume consists of 8 nodes of increasing thickness down from the surface in the temperature stratified layer of the upper LH_2 region. The ninth and bottom liquid node corresponds to the uniform bulk liquid temperature, T_B, layer at the bottom of a stratified tank that experiences some degree of bottom heating. The transient stratification analytical model of Reference 26 is used in this program. It was modified to account for the changes in the liquid level that occur during the simulated flight mission.

The vapor volume consists of 10 horizontal layers in which conduction, convection, mass flow and radiation effects between the nodes and their surroundings are modeled. The mass, volume, temperature and pressure of the vapor are computed from liquid/ullage coupling models that consider the thermodynamics of the two modes of tank pressurization and venting. One mode is represented by a closed tank, self-pressurization model; while the second mode is represented by a constant pressure, continuous tank venting model.

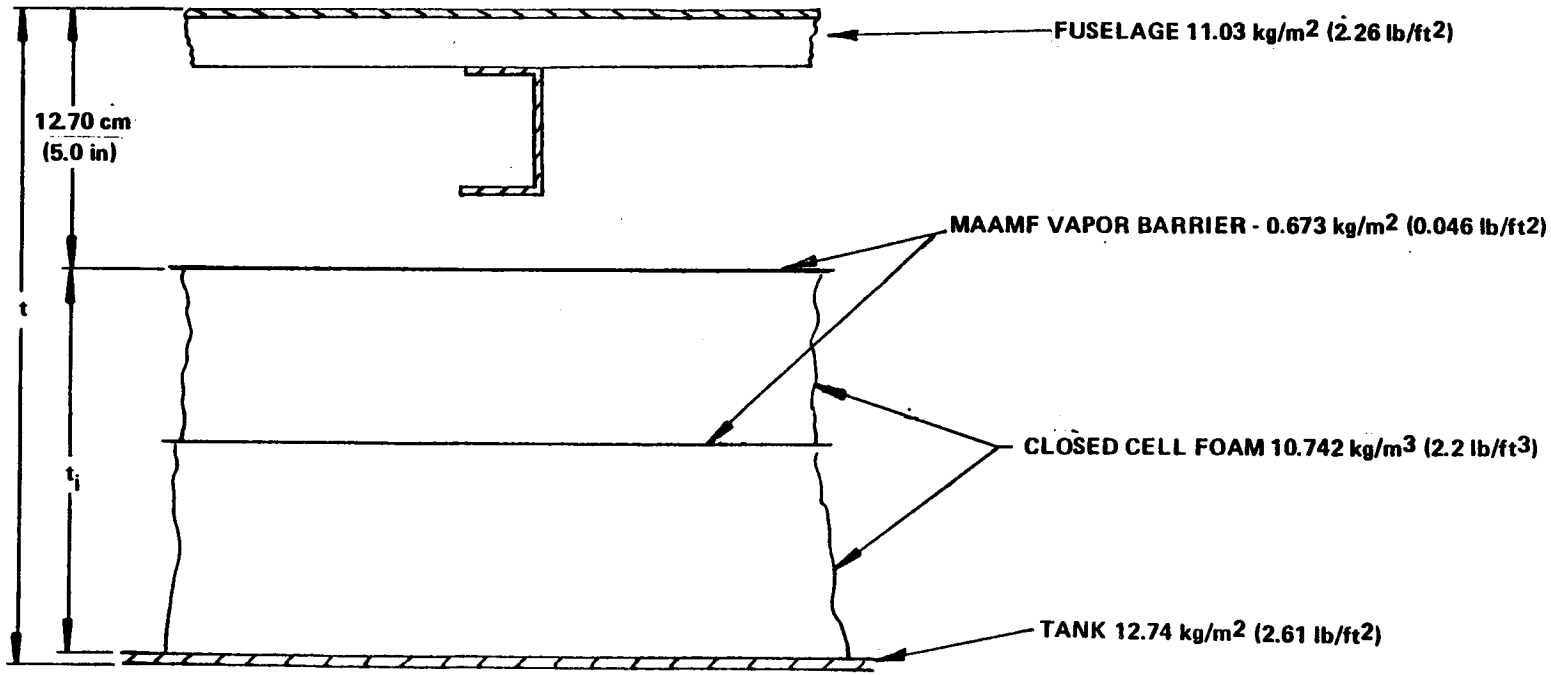

Figure 90. - Candidate no. 1, nonintegral tank - external foam.

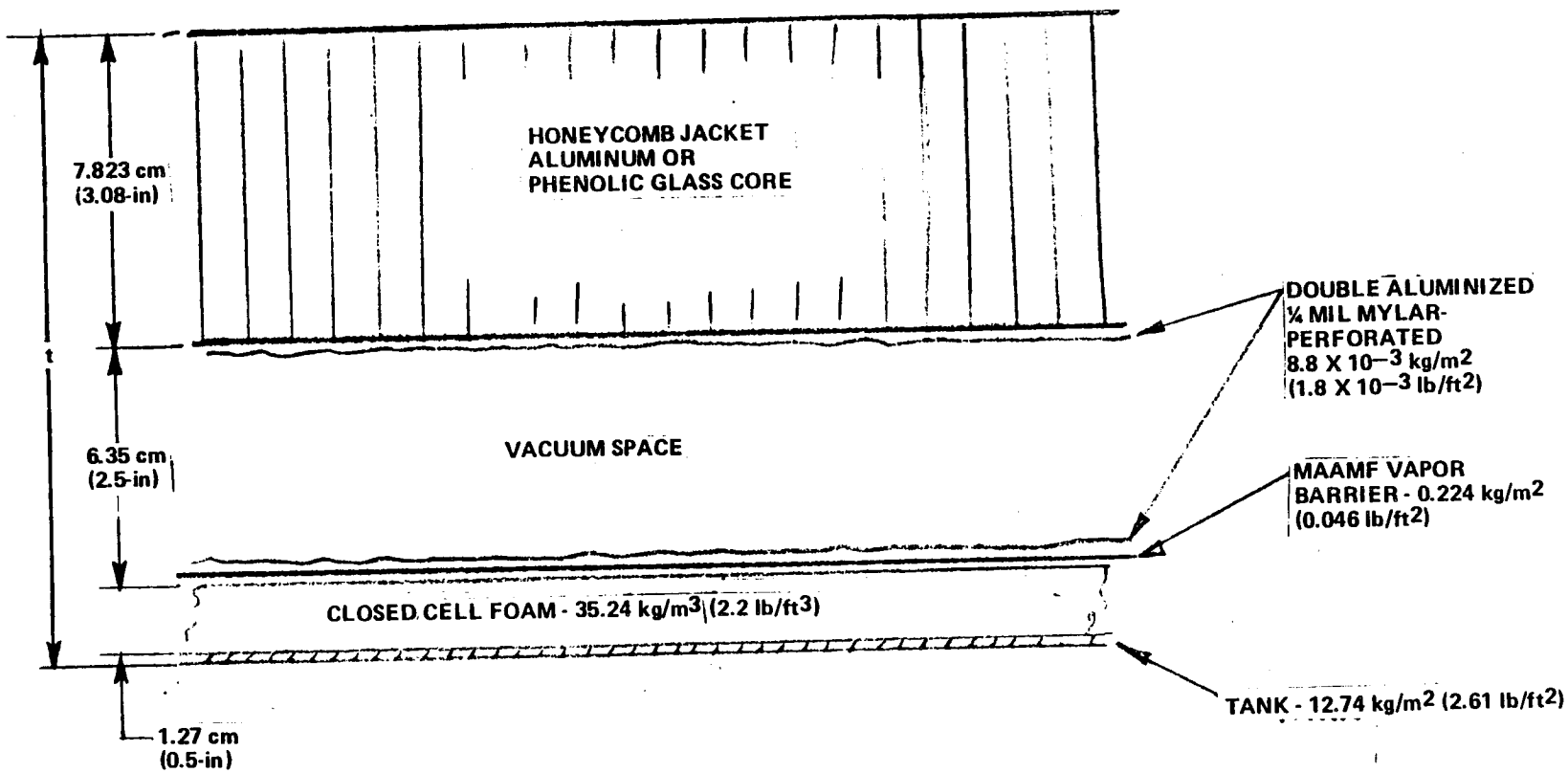

Figure 91. - Candidate no. 2, nonintegral tank - hard shell vacuum.

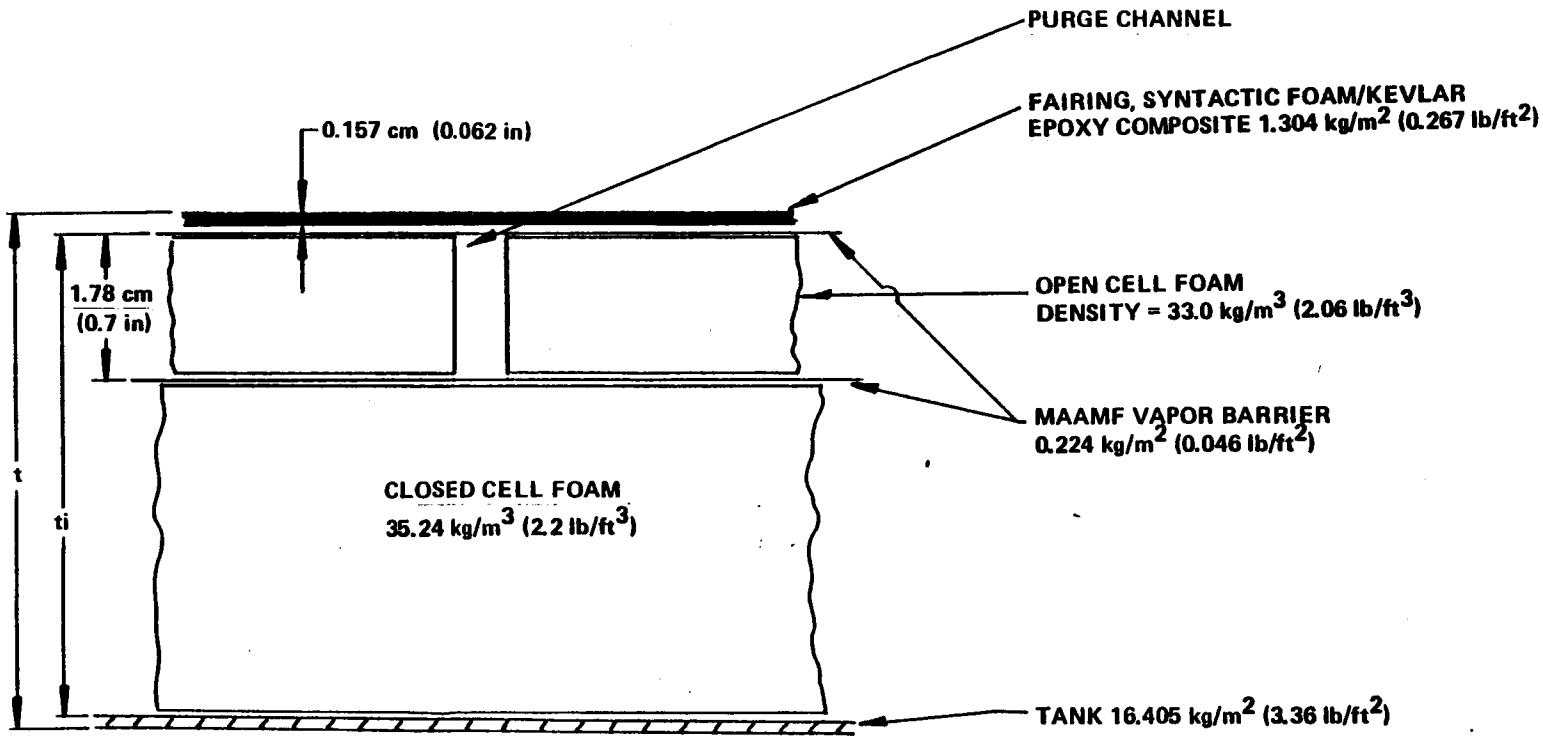

Figure 92. - Candidate no. 3, integral tank - external foam.

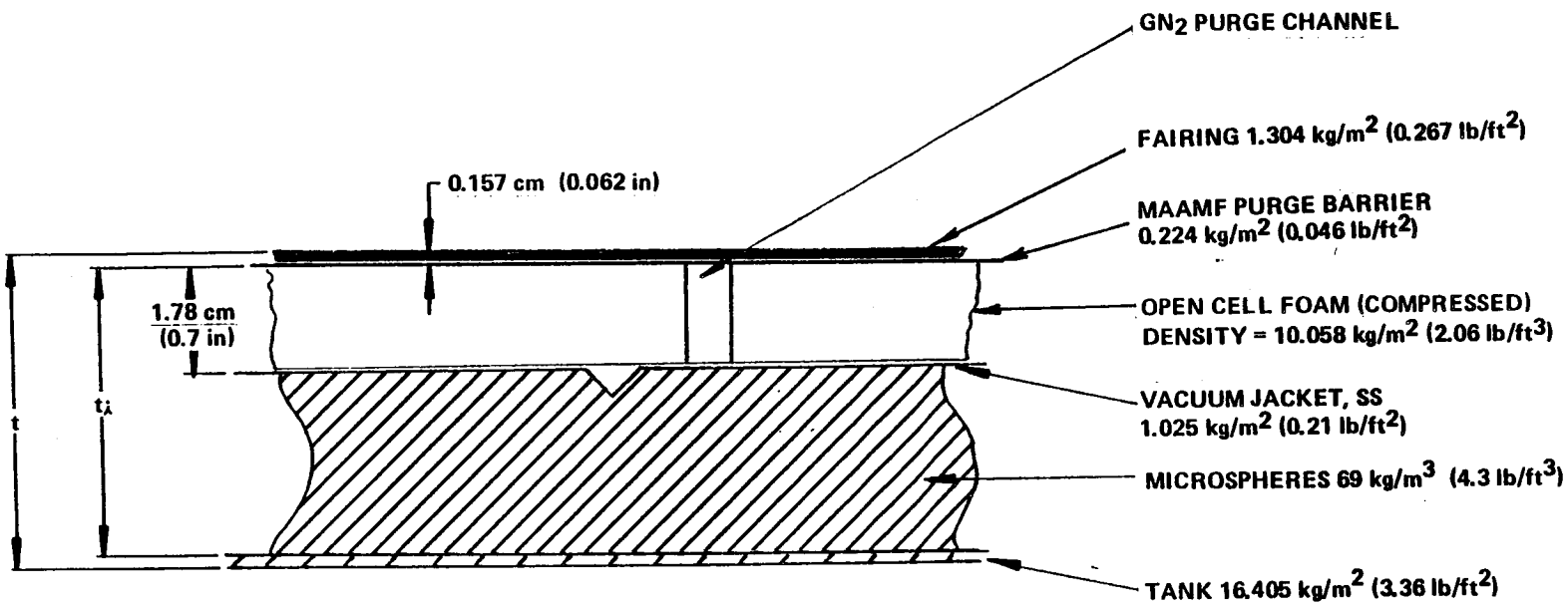

Figure 93. - Candidate no. 4, integral tank - external microspheres.

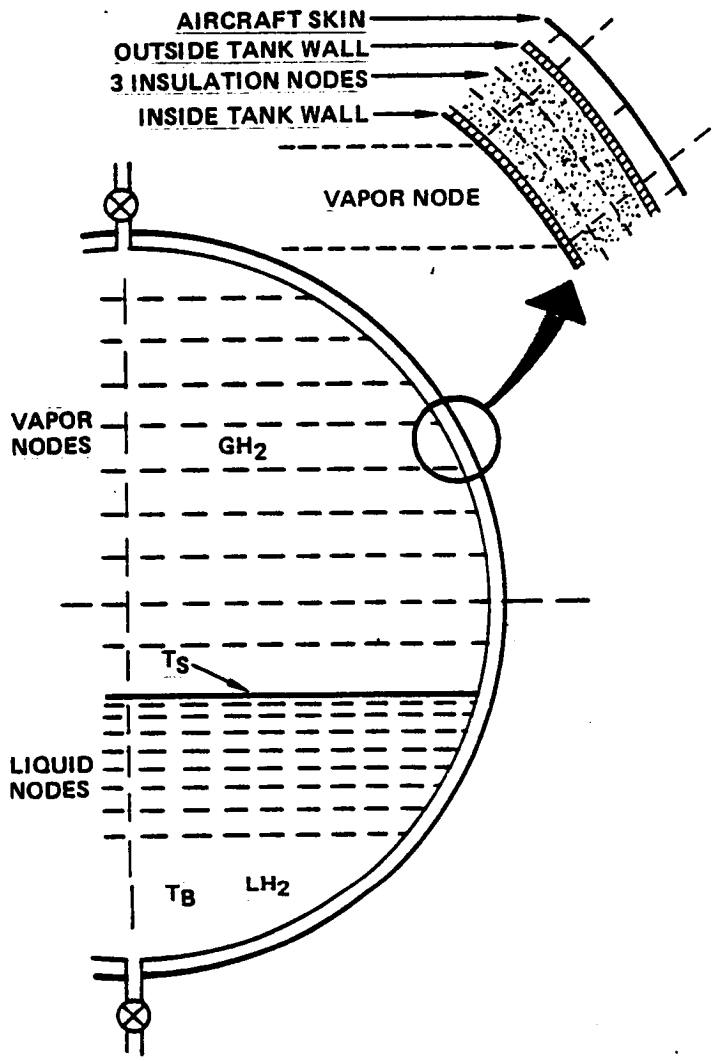

Figure 94. - Tank insulation and vent model for analysis of preferred candidates.

This program has the ability to switch between the two tank pressurization and venting modes depending upon the tank heat input, LH_2 fill level, liquid hydrogen withdrawal rates, etc. In this program a severe flight disturbance that would completely mix the stratified liquid, the vapor, and wet the tank walls, can also be simulated. Following this instantaneous event, the liquid restratifies and the tank self-pressurizes and/or vents.

In operation of the program an initial estimate is made of required tank volume for a given insulation thickness, based upon the results of the concept screening analysis. Using the output data from the first computer run an iterative procedure is then used to obtain convergence of volume in terms of mass of liquid evaporated. Basic output of the program is node temperatures, liquid and vapor mass and volume fractions, vented and evaporated masses and ullage pressure in 5 min. time steps.

The major output parameters of the thermal analysis which were used to evaluate the concepts are:

- Fuel evaporated and fuel vented during flight
- Fuel evaporated during ground hold and filling
- Fuel tank ullage pressure during flight
- Temperature distributions of tank wall, insulation and outer structure
- Vent rate during filling

Additional analyses were conducted to assess the benefit in terms of fuel loss of operating at higher tank pressures, 207 kg (30 psia) and 276 kPa (40 psia). These were done for candidate No. 3 only. Also, the effects of air and hydrogen leakage into the vacuum spaces of Candidates Nos. 2 and 4 were examined in limited depth.

7.1.6.2.1 Fuel losses: The fuel losses associated with the filling, flight, and ground hold portions of the aircraft mission were computed for each candidate. Insulation thickness was the variable for Nos. 1, 3, and 4. Five different values were examined. Since geometry is fixed for No. 2, losses were computed for the nominal vacuum space pressure of 1×10^{-4} torr, and for values an order of magnitude above and below (10^{-3} and 10^{-5} torr). In addition, an emergency condition of 760 torr, corresponding to loss of vacuum was also calculated. The loss terms are fuel evaporated during flight (vented plus amount required for tank pressurization), fuel vented during flight, and fuel vented during fill and ground hold.

Fuel losses as a function of insulation thickness are shown in Figures 95 through 97 for candidates Nos. 1, 3, and 4, respectively. Table 40 presents fuel loss data calculated at each insulation thickness. Overall system thickness, (t), is defined as the distance from the interior of the tank wall to the exterior of the fuselage. Primary and total insulation thicknesses are denoted by t_{ip} and t_i, respectively. Vacuum influence on fuel loss for candidate No. 2 is also given in the Table. Comparing the rigid, closed cell foam candidates, Nos. 1 and 3, it is seen that equal thicknesses of insulation give nearly equal fuel loss data. This is as anticipated because the primary insulations are identical and the secondary foam wrap for No. 3 has a thermal conductivity close to that of the primary material. On the basis of system thickness, t, however, No. 3 is much more effective from a volume standpoint.

A comparison between candidates No. 3 and No. 4 shows that the latter is a more thermally efficient concept. Although the microspheres have nearly twice the bulk density of the rigid foam (69 versus 35 kg/m^3), for an equal weight insulation the microsphere concept, No. 4, shows appreciably lower fuel losses. As an example: with 5.08 cm of rigid foam for No. 3 the flight and ground losses are 537 and 780 kg, respectively (per tank). For No. 4 at 2.54 cm thickness of microspheres (equal weight of insulation) the flight and ground losses are 397 and 621 kg, respectively. This corresponds to a 279 kg saving for non-recoverable losses and a 317 kg reduction in recoverable loss (for 2 tanks). Candidate No. 4 is also slightly more effective on a volume basis because of the superior thermal conductivity of the microspheres.

Candidate No. 2 shows the minimum in fuel loss, even for vacuum space pressures as high as 10^{-3} torr. For flight conditions little difference in fuel loss is observed with pressure changes from 10^{-5} to 10^{-3} torr. This provides a comfortable design margin for the vacuum system. Ground loss is, of course, affected significantly as all heat input goes to vented mass rather than pressurization.

For the case of the honeycomb and annulus at atmospheric pressure of air (simulating a catastrophic vacuum failure) the evaporation rate at altitude is 102 kg/hr (235 lb/hr) with a vent rate of 74 kg/hr (170 lb/hr). This vent rate is less than that required for fueling so no limitations are placed on the vent system design. Also, the 1.27 cm of rigid closed cell foam with the MAAMF barrier prevents liquefaction of air in the event of vacuum failure. Solidification of water vapor would of course occur at a rapid rate at the lower altitudes.

A nonmetallic honeycomb core (Hexcel - 3/8 in. cells HRP phenolic-glass, having the same specific weight and thickness as the aluminum core) was also investigated for candidate No. 2. Under normal operating conditions (vacuum of 10^{-4} torr) the fuel loss parameters are essentially independent of core conductance as the vacuum space provides the controlling thermal resistance. Results of the system thermal analysis comparing candidate No. 2 with aluminum versus composite honeycomb core are:

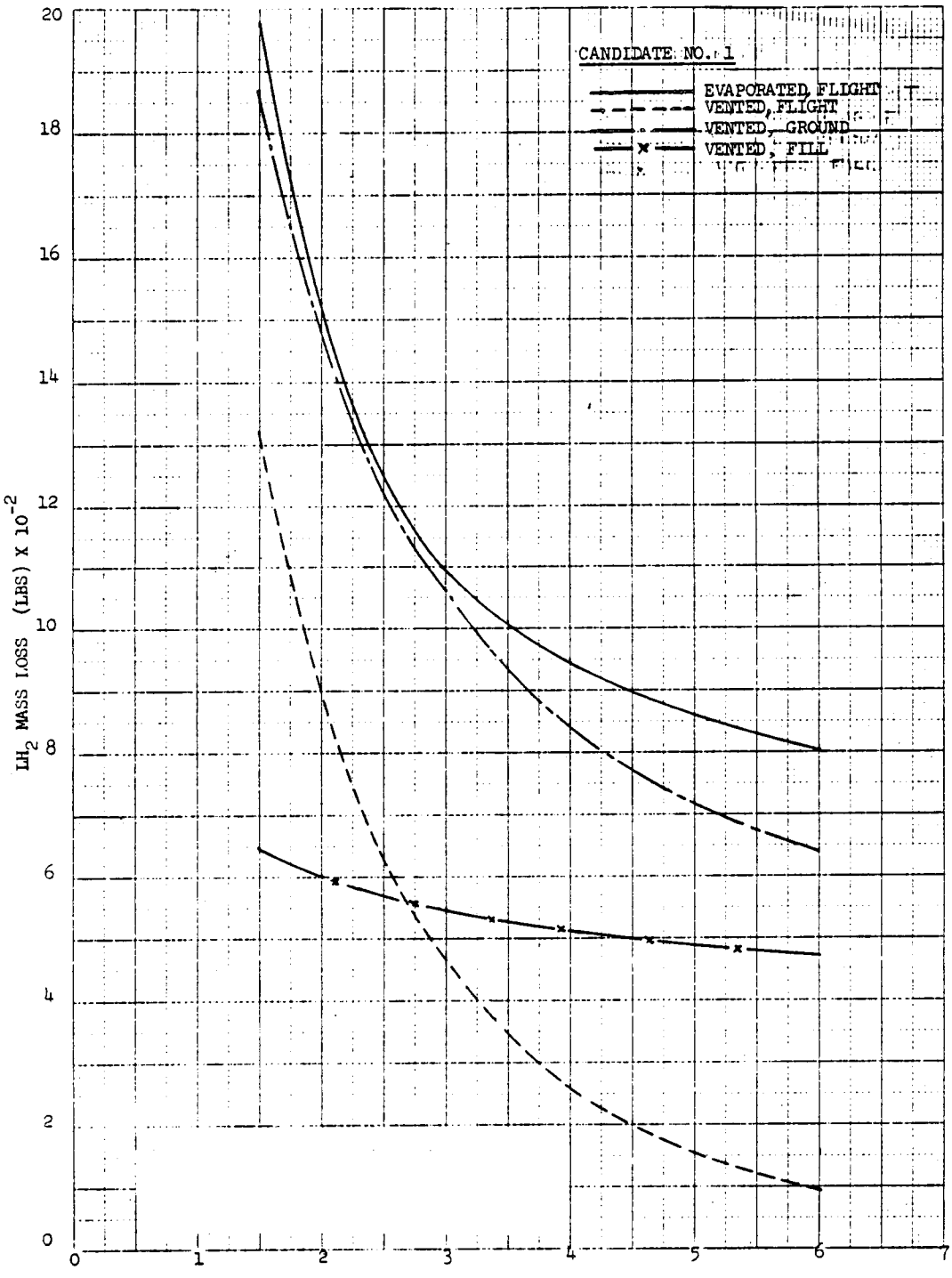

Figure 95. - Fuel losses as a function of insulation thickness for candidate no. 1, aft tank.

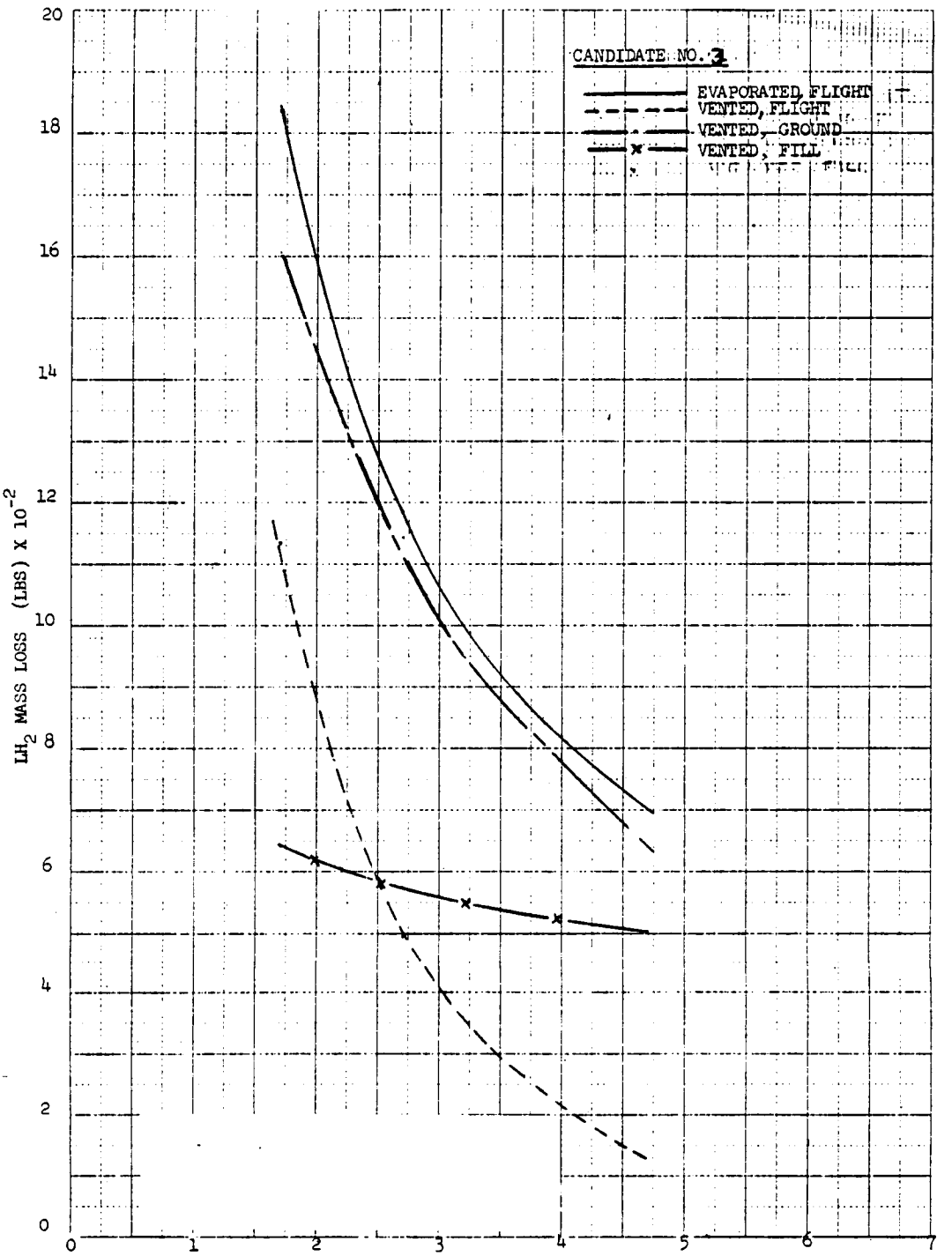

Figure 96. - Fuel losses as a function of insulation thickness (primary and open cell foam) for candidate no. 3, aft tank.

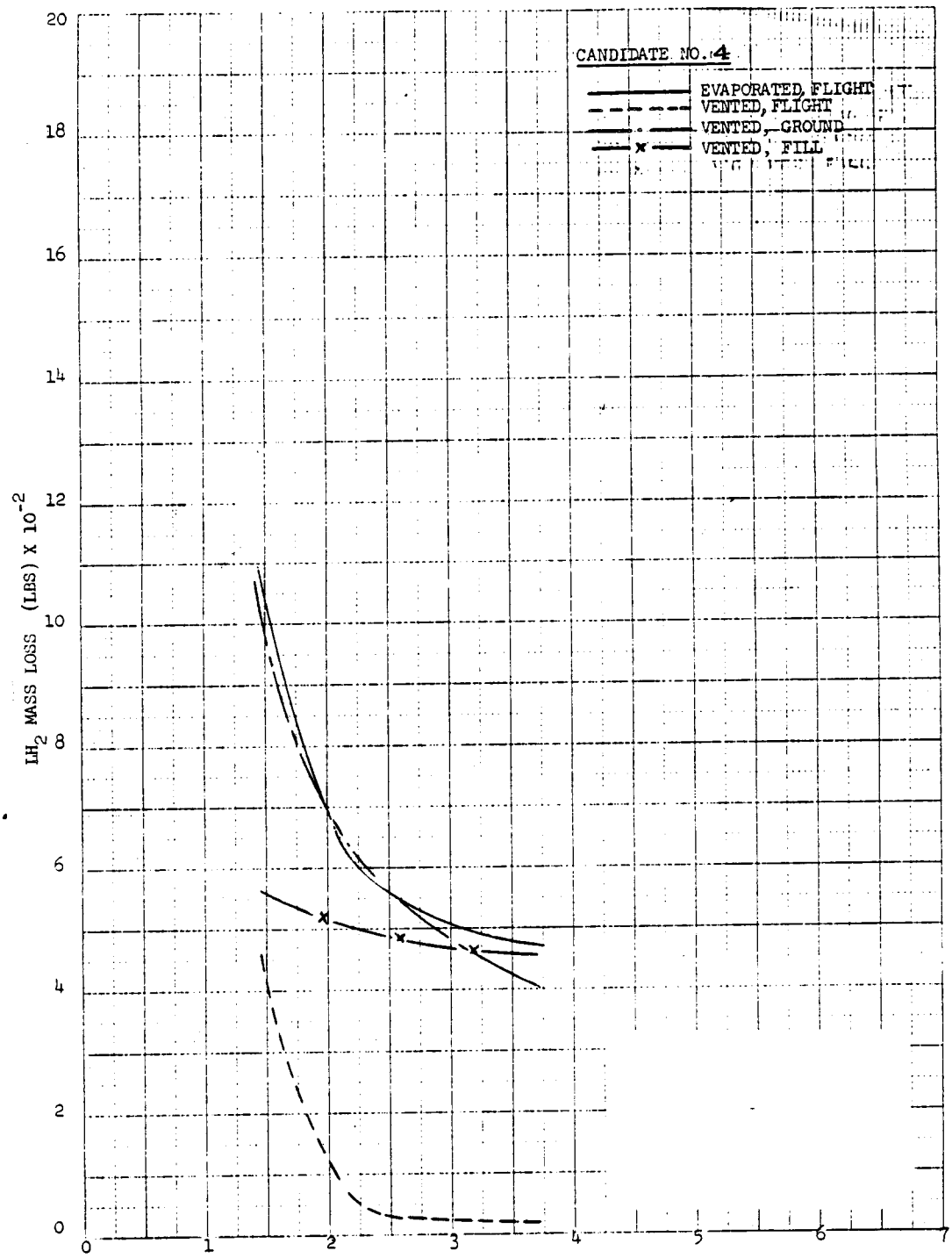

Figure 97. - Fuel losses as a function of insulation thickness (microspheres and open cell foam) for candidate no. 4, aft tank.

TABLE 40. - SUMMARY OF THICKNESS PARAMETERS AND FUEL LOSSES FOR THE FOUR PREFERRED CANDIDATE INSULATION SYSTEMS (AFT TANK ONLY)

		Candidate Insulation System																	
		1					2			3					4				
Insulation (Type Tank)		Rigid Closed Cell Foam (Nonintegral Tank)					Hard Shell Vacuum (Nonintegral Tank)			Rigid Closed Cell Foam + Flex Foam (Integral Tank)					Microspheres with Flex Foam (Integral Tank)				
t_{ip} (a)	cm	3.81	5.08	7.62	0.16	15.24	15.24 (a)	15.24 (a)	15.24 (a)	2.54	3.81	5.08	7.62	10.16	1.91	2.54	3.81	5.08	7.62
	(in)	(1.50)	(2.00)	(3.00)	(4.00)	(6.00)		(6.00)		(1.00)	(1.50)	(2.00)	(3.00)	(4.00)	(0.75)	(1.00)	(1.50)	(2.00)	(3.00)
t_i (b)	cm	3.81	5.08	7.62	10.16	15.24				4.32	5.59	6.86	9.40	11.94	3.68	4.32	5.59	6.86	9.90
	(in)	(1.50)	(2.00)	(3.00)	(4.00)	(6.00)				(1.70)	(2.20)	(2.70)	(3.70)	(4.70)	(1.45)	(1.70)	(2.20)	(2.70)	(3.70)
t (c)	cm	17.20	18.47	21.01	23.55	28.63	15.24	15.24	15.24	5.11	6.38	7.65	10.19	12.73	4.45	5.08	6.35	7.62	10.16
	(in)	(6.77)	(7.27)	(8.27)	(9.27)	(11.27)		(6.00)		(2.01)	(2.51)	(3.01)	(4.01)	(5.01)	(2.01)	(2.51)	(3.01)	(4.01)	(5.01)
MEF (d)	kg	897	691	495	429	365	219	222	242	831	653	537	396	318	495	397	278	242	214
	lb	(1978)	(1524)	(1092)	(945)	(805)	(483)	(489)	(534)	(1832)	(1439)	(1184)	(872)	(702)	(1092)	(876)	(613)	(534)	(472)
MVF (e)	kg	596	407	211	117	43	9	10	13	515	335	228	119	59	209	117	27	11	9
	lb	(1313)	(897)	(465)	(257)	(94)	(19)	(21)	(29)	(1135)	(739)	(502)	(262)	(129)	(460)	(259)	(60)	(25)	(20)
MVG (f)	kg	1139	948	728	616	503	328	362	480	1017	878	780	619	515	723	621	512	457	369
	lb	(2510)	(2090)	(1605)	(1357)	(1110)	(724)	(798)	(1059)	(2241)	(1936)	(1719)	(1365)	(1135)	(1594)	(1370)	(1129)	(1007)	(816)
Vacuum, torr		N/A					10^{-5}	10^{-4}	10^{-3}	N/A					10^{-1}				

NOTES:

(a) Thickness, primary insulation: i.e.; rigid closed cell foam or microspheres.

(b) Thickness, total insulation: i.e.; rigid closed cell foam plus flexible open cell foam.

(c) Total thickness, insulation plus structure plus fairing, i.e., from inside surface of fuel contaminent system to external surface of aircraft.

(d) Total weight of fuel evaporated during flight.

(e) Fuel weight vented during flight.

(f) Total fuel weight vented on ground (recoverable); sum of fill plus ground hold.

(g) 1.27 cm (0.5 in) closed cell rigid foam with MAAMF vapor barrier, plus 2-layers double-aluminized 1/4 mil mylar, 6.35 cm (2.5 in.) clearance, 7.62 cm (3 in.) aluminum honeycomb.

		Core Type	
		Aluminum	Phenolic/FG
Fuel Evaporated - Flight	kg	444	443
	(lb)	(978)	(976)
Fuel Vented - Flight	kg	19	18
	(lb)	(42)	(40)
Fuel Vented - Ground	kg	724	715
	(lb)	(1596)	(1576)

Under the emergency condition of atmospheric pressure of air in the vacuum space, the evaporation rate with the composite honeycomb core under cruise conditions is 78 kg/hr (172 lb/hr) and under ground conditions is 109 kg/hr (240 lb/hr). Although the lower thermal conductance core reduces fuel losses in this condition, the loss rates in either case do not present an unsafe flight condition. The vent system is designed for the larger vent gas mass flows experienced during filling, and the quantities of fuel lost in flight do not significantly reduce flight duration capability.

7.1.6.2.2 Tank pressure control: A minimum design tank pressure during flight was input into the computer program. For purposes of this analysis a minimum pressure of 110 kPa (16 psia) was arbitrarily assumed. (Note that a minimum pressure of 124 kPa (18 psia) was later selected as a system design value.) If at any time tank pressure falls to this value a subroutine is called, and it computes the additional amount of fuel which must be vaporized to maintain this level of pressure. This additional quantity of vaporized fuel is added to that resulting from heat transfer to the liquid.

For Candidate No. 2 at vacuums of 1×10^{-5} and 1×10^{-4} torr, additional fuel vaporization was required at the end of cruise to maintain the minimum pressure level. Without this additional vaporization, tank pressure falls below the minimum value for vacuums of 1×10^{-4} and 1×10^{-5} torr, as shown in Figure 98.

No additional vapor generation was required for the insulation thicknesses investigated for Candidate Nos. 1 and 3. Vapor generation was required for Candidate No. 4 at the largest value of insulation thickness; however, this case was not viable because its DOC was not the minimum value for the candidate.

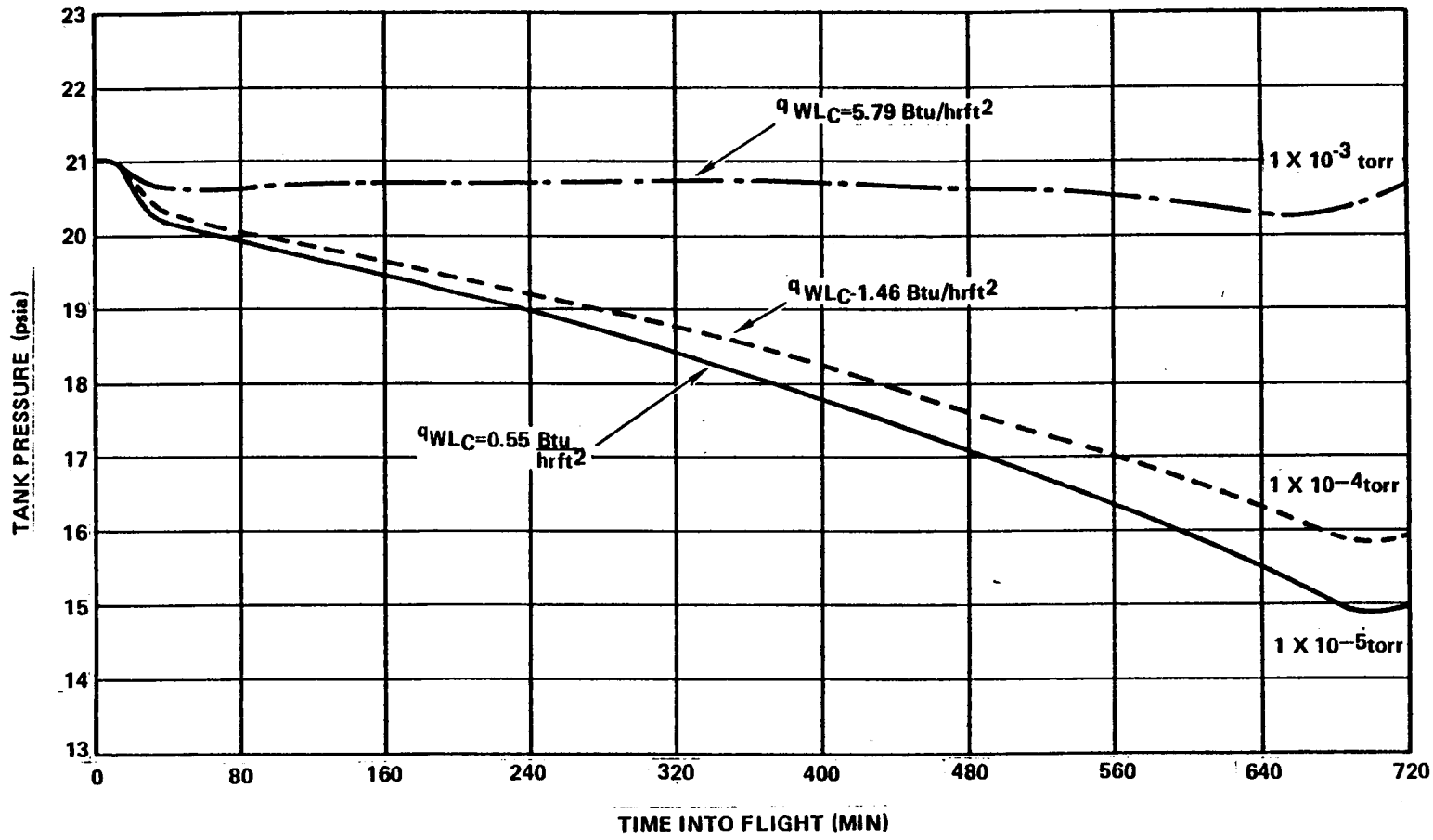

Figure 98. - Tank pressure during flight as a function of vacuum level, candidate no. 2 - aluminum core HC.

Using the thickness of insulation consistent with minimum DOC, analysis of the tank pressure variation as a function of time of flight during the mission showed that both candidates 1 and 3 vented excess boiloff continuously. The result of the calculation for candidate No. 4 is plotted in Figure 99. No venting is required during a period extending from 15 minutes after takeoff until landing.

7.1.6.2.3 Tank pressure level: A separate analysis was performed to determine the effect of higher tank pressures on venting losses. By increasing the tank venting pressure above the 145 kPa (21 psia) value the amount of fuel vented during filling and flight can be reduced by using the sensible heat capacity of the liquid. For example, as the tank is filled with liquid saturated at 138 kPa (20 psia), a relatively large temperature difference exists between the liquid surface and the bulk of the liquid. For a 276 kPa (40 psia) vent pressure setting this temperature difference is 2.09°K (3.76°R) as compared to a difference of 0.17°K (0.3°R) for a 145 kPa (21 psia) vent pressure. The results of an analysis, performed using candidate No. 3 as a basis, shows liquid temperatures as a function of time for three pressure levels in Figure 100. The variation of ullage pressure during flight as a function of vent pressure is shown in Figure 101. Venting occurs only during the initial 15 minute period for both 276 kPa (40 psia) and 207 kPa (30 psia) vent pressure.

During filling the fuel evaporated is 33 kg (73 lb) for the 276 kPa (40 psia) case and 34 kg (75 lb) for a 207 kPa (30 psia) vent pressure. Fuel evaporated and fuel vented during flight are 317 kg (698 lb) and 13.6 kg (30 lb), respectively, for a 276 kPa (40 psia) vent pressure. Similarly, for a 207 kPa (30 psia) vent pressure, these weights are 311 kg (686 lb) and 15.4 kg (34 lb). These compare with 538 kg (1186 lb) and 227 kg (500 lb) for the 145 kPa (21 psia) vent pressure condition. The higher vapor density in the 276 kPa (40 psia) case accounts for the slight increase in fuel loss over that of the 207 kPa (30 psia) condition.

7.1.6.2.4 Liquid stratification: The degree of liquid stratification in the tank during flight is small for all candidates. As shown by Figures 102 and 103, the temperature differences between the liquid at the surface and at the bottom of the tank is less than 0.22°K (0.40°R). During filling, stratification is shown to occur because in the analytical model subcooled liquid is introduced at the bottom of the tank. However, within 100 minutes after start of filling the stratification has essentially disappeared. Figure 102 is representative of the candidate having the highest heat flux, and Figure 103 illustrates a lower heat flux candidate. Because of the essentially uniform liquid temperature during flight there is little possibility of a sudden pressure reduction by mixing of the liquid as the result of a sudden maneuver or turbulence.

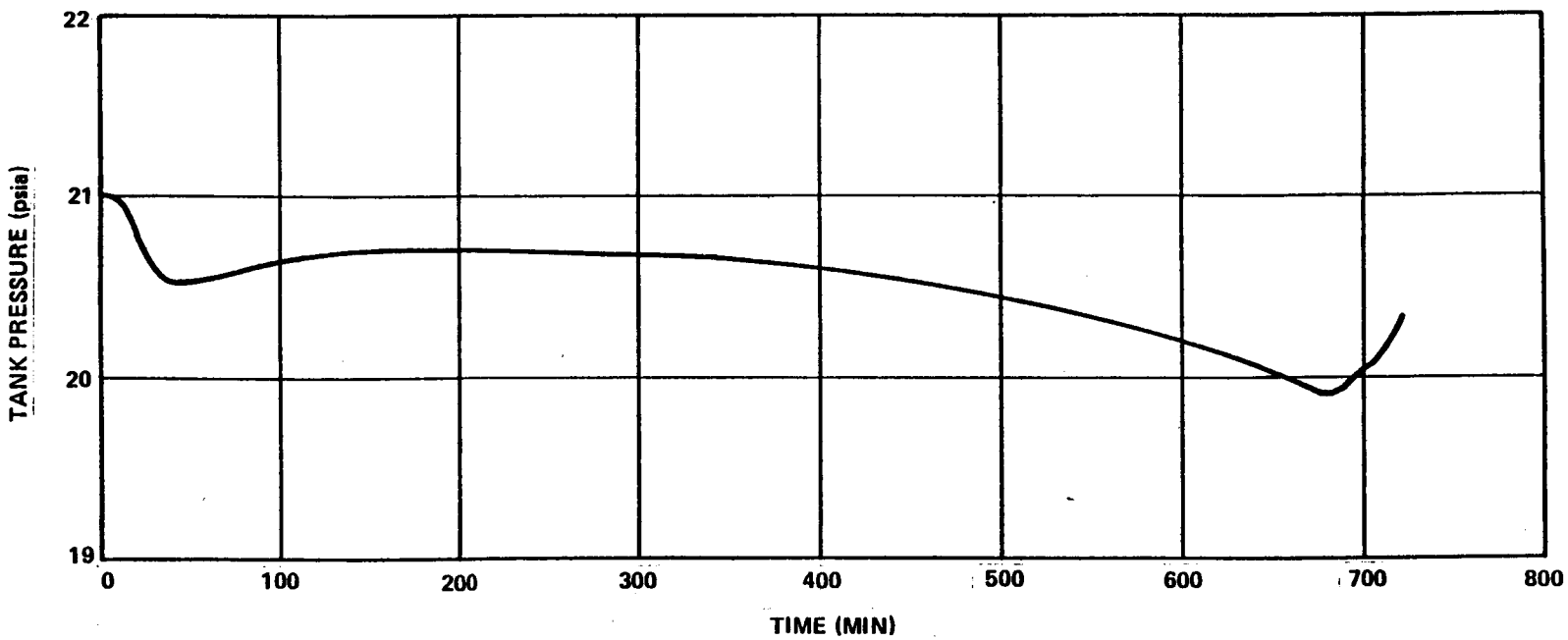

Figure 99. - Tank pressure variation during flight for candidate no. 4.

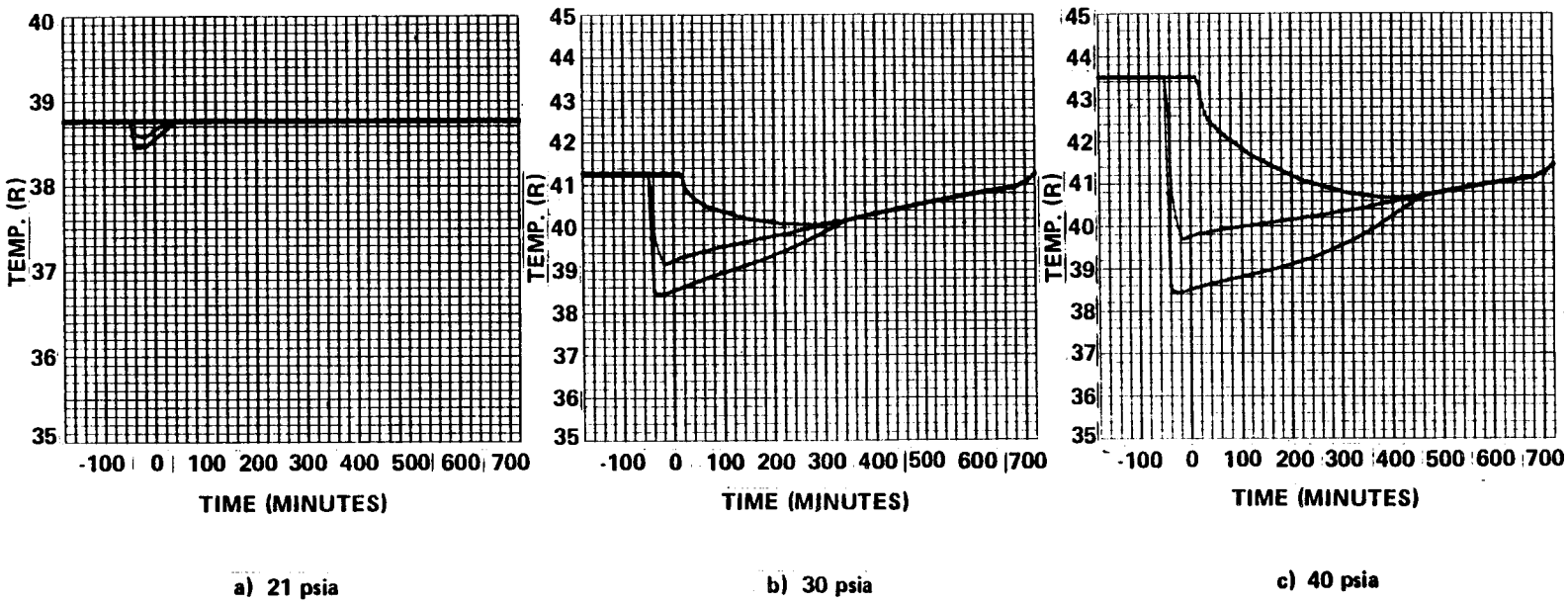

Figure 100. - Liquid temperature differences for three vent pressure settings for candidate no. 3.

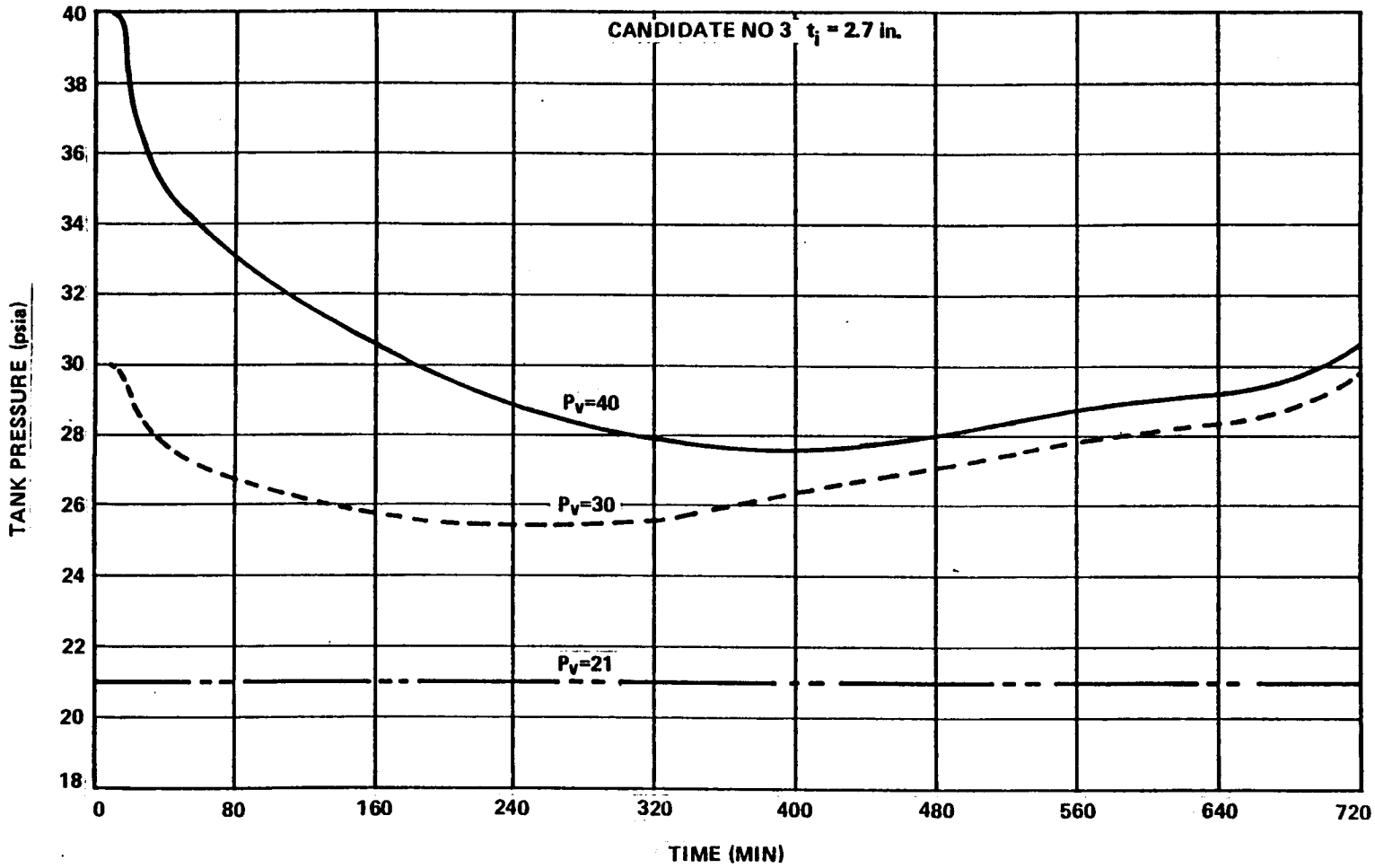

Figure 101. - Tank pressure variation during flight for vent pressure settings of 21, 30 and 40 psia.

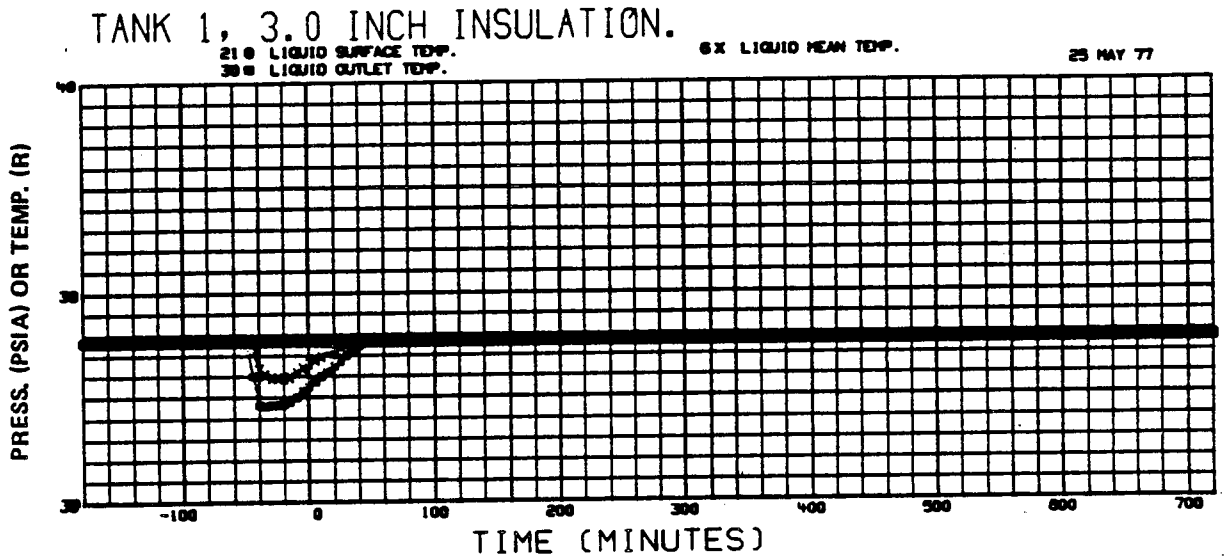

Figure 102. - Liquid temperature differences as a functional of flight time for candidate no. 1.

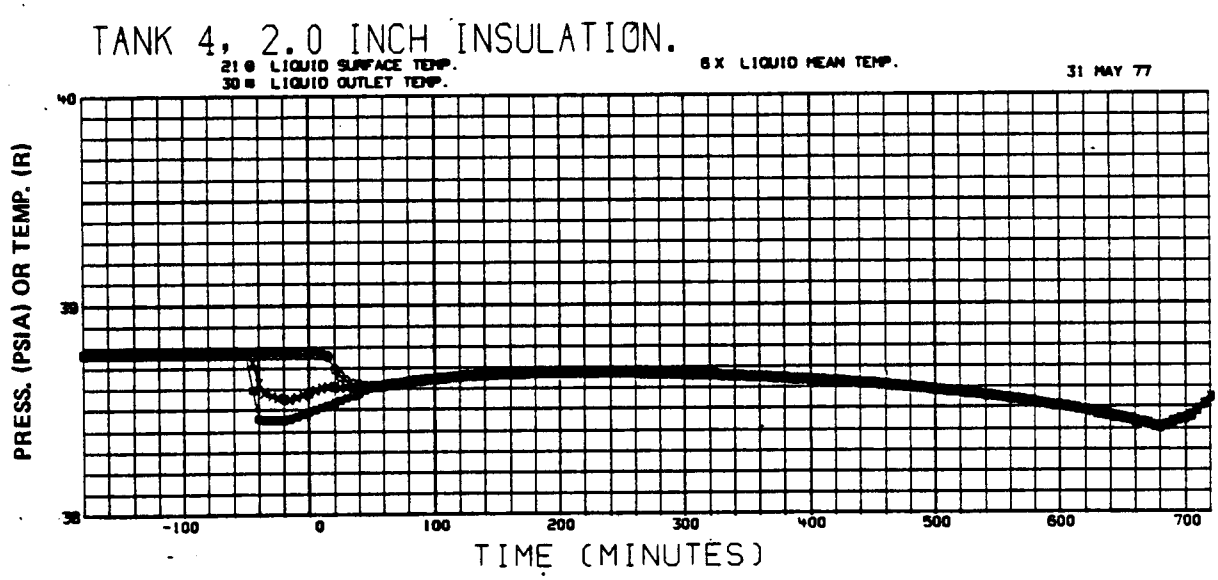

Figure 103. - Liquid temperature differences as a function of flight time for candidate no. 4.

7.1.6.2.5 FCS temperature distributions: Computed temperature distributions for the tank wall, insulation, vapor barrier and exterior structure are shown in Figures 104 through 109 for the four candidates. For candidate No. 2, temperatures are presented for the normal operating condition and for the case where the vacuum space is filled with air for both aluminum and nonmetallic honeycomb cores (Figures 105 through 107). The nodal temperature data are plotted as a function of a dimensionless distance parameter relative to the circumference of the tank wall, ℓ/c. The top of the tank is represented by $\ell/c = 0$ and the bottom by $\ell/c = 1.0$. Distributions are shown for liquid fractions of 0.90, 0.50 and 0.15, with 0.50 corresponding to cruise ambient conditions and 0.90 and 0.15 at ground ambient.

The most severe temperature gradients occur in the area of the liquid-vapor interface at the tank wall and inner insulation nodes. The maximum gradients at these locations are given in Table 41. The maximum gradient in the tank wall occurs at the liquid vapor interface and it decreases with decreasing wall heat flux. Also, the gradient increases with decreasing liquid level because of the higher tank wall temperatures as the ullage volume increases. Gradients shown in the insulation are for the midplane location of the primary insulation. The exterior vapor barrier location of Table 41 denotes the purge barrier for candidate No. 4 and the foam insulation vapor barrier for the other candidates.

7.1.6.2.6 Emergency conditions: The effects of both GH_2 and air leakage into the vacuum space of candidates Nos. 2 and 4 were evaluated from the standpoint of heat rate to the liquid and vapor barrier (or to the vacuum jacket for No. 4) and their resulting temperatures. A summary of these results is given in Table 42.

For candidate No. 2 the vapor barrier temperature remains significantly above the oxygen liquefaction temperature, 91°K (163°R), for the conditions of air leakage into the vacuum space. The maximum liquid heat rates for a full tank will not result in vent rates in excess of the vent system capacity. This calculated heat rate corresponds to an evaporation rate of 347 kg/hr 765 lb/hr). If a failure occurred at the midpoint of cruise, the evaporation rate of 243 kg/hr (535 lb/hr) would require approximately 1500 kg (3300 lb) of reserve fuel to continue the planned flight. It appears that neither failure mechanism would jeopardize the aircraft safety.

A similar conclusion is made for candidate No. 4. Vent rates are lower than for No. 2 (even assuming the open cell foam is permeated by GH_2 through the metal vacuum jacket provided for the microspheres). For the condition of GH_2 leakage into the microspheres the consequences of a double failure with subsequent air leakage into the open cell foam was not considered because of the GN_2 purge system. The air leakage condition was based upon the assumption that the 5 mil stainless steel vacuum jacket has a small leak. The data shown in this case are based upon a small localized leakage which was felt to be representative of that which might occur in a welded jacket seam during prolonged service. For these purposes the leakage rate was postulated to be

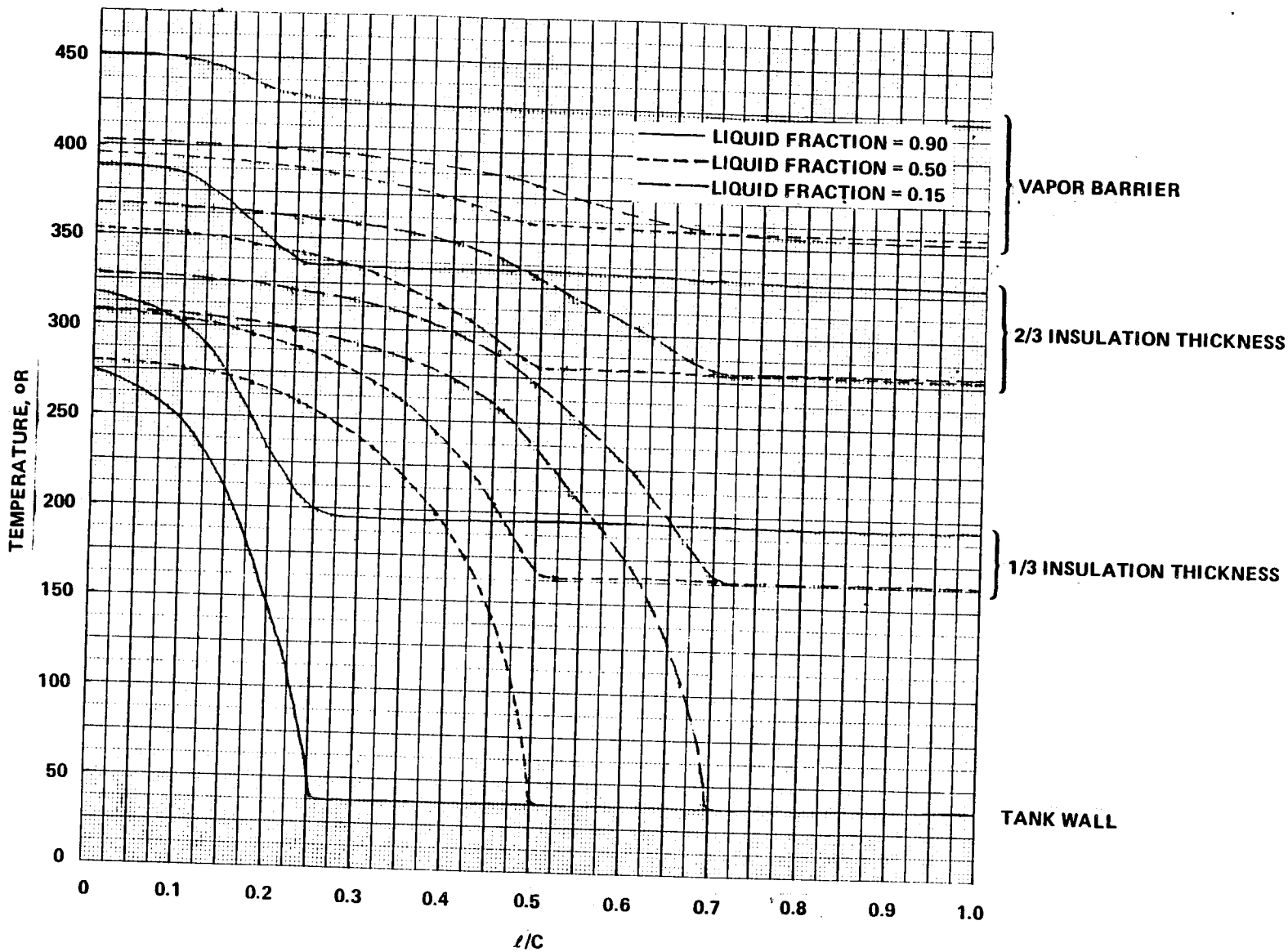

Figure 104. - Candidate no. 1 circumferential temperature distributions for liquid fractions of 0.90, 0.50 and 0.15.

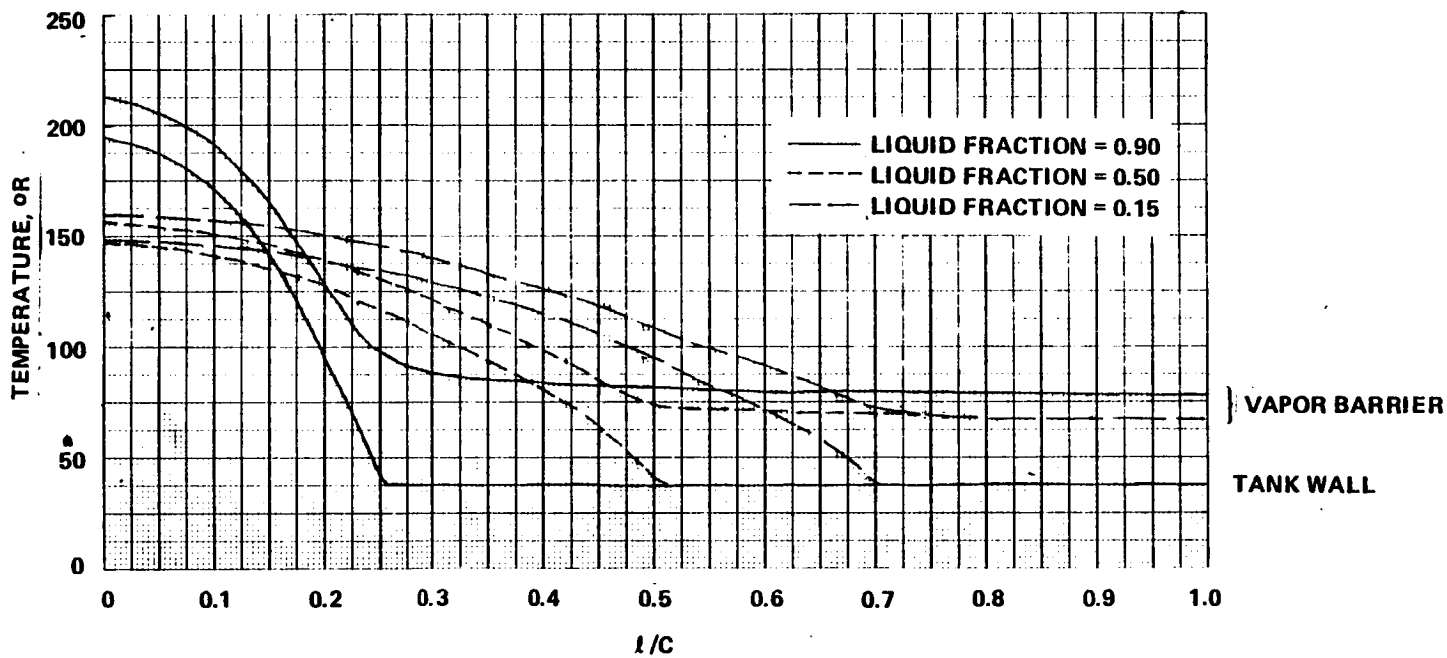

Figure 105. - Candidate no. 2, aluminum core, circumferential temperature distributions in tank wall and vapor barrier for liquid fractions of 0.80, 0.50 and 0.15, vacuum = 1 x 10^{-4} torr.

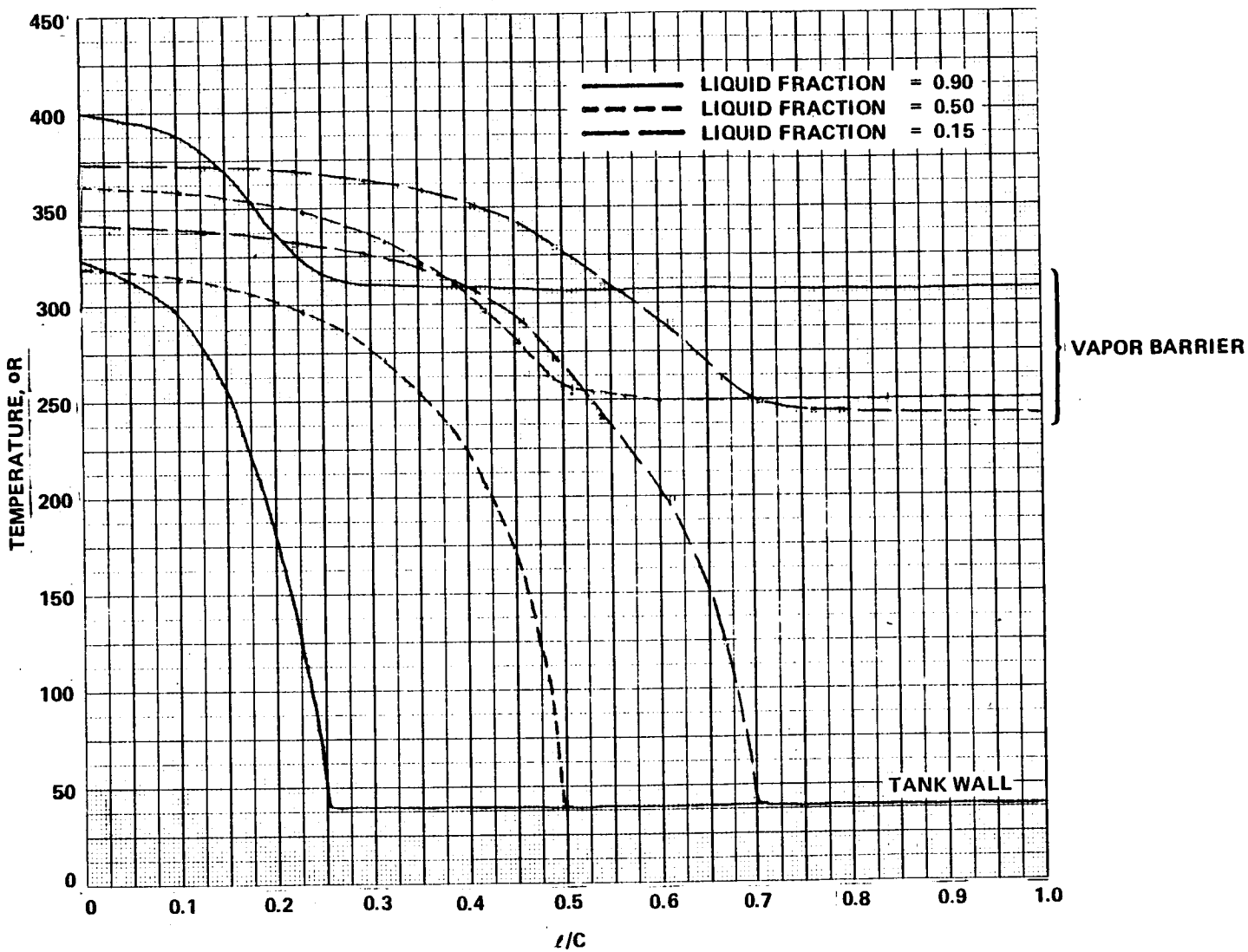

Figure 106. - Candidate no. 2, aluminum core, circumferential temperature distributions in tank wall and vapor barrier for liquid fractions of 0.90, 0.50 and 0.15 with vacuum space at atmospheric pressure.

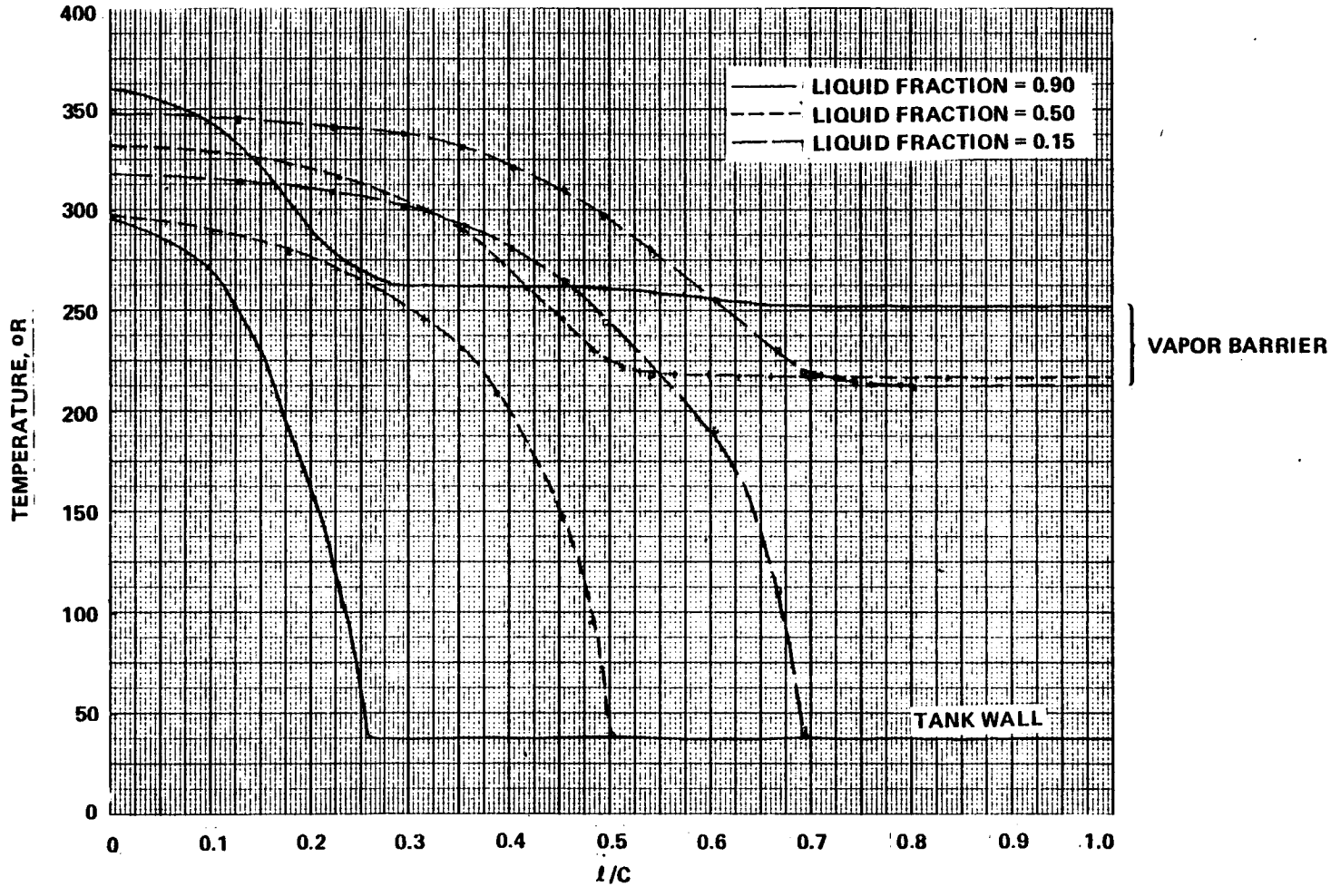

Figure 107. - Candidate no. 2, composite core, circumferential temperature distributions in tank wall and vapor barrier for liquid fractions of 0.90, 0.50 and 0.15 with vacuum space at atmospheric pressure.

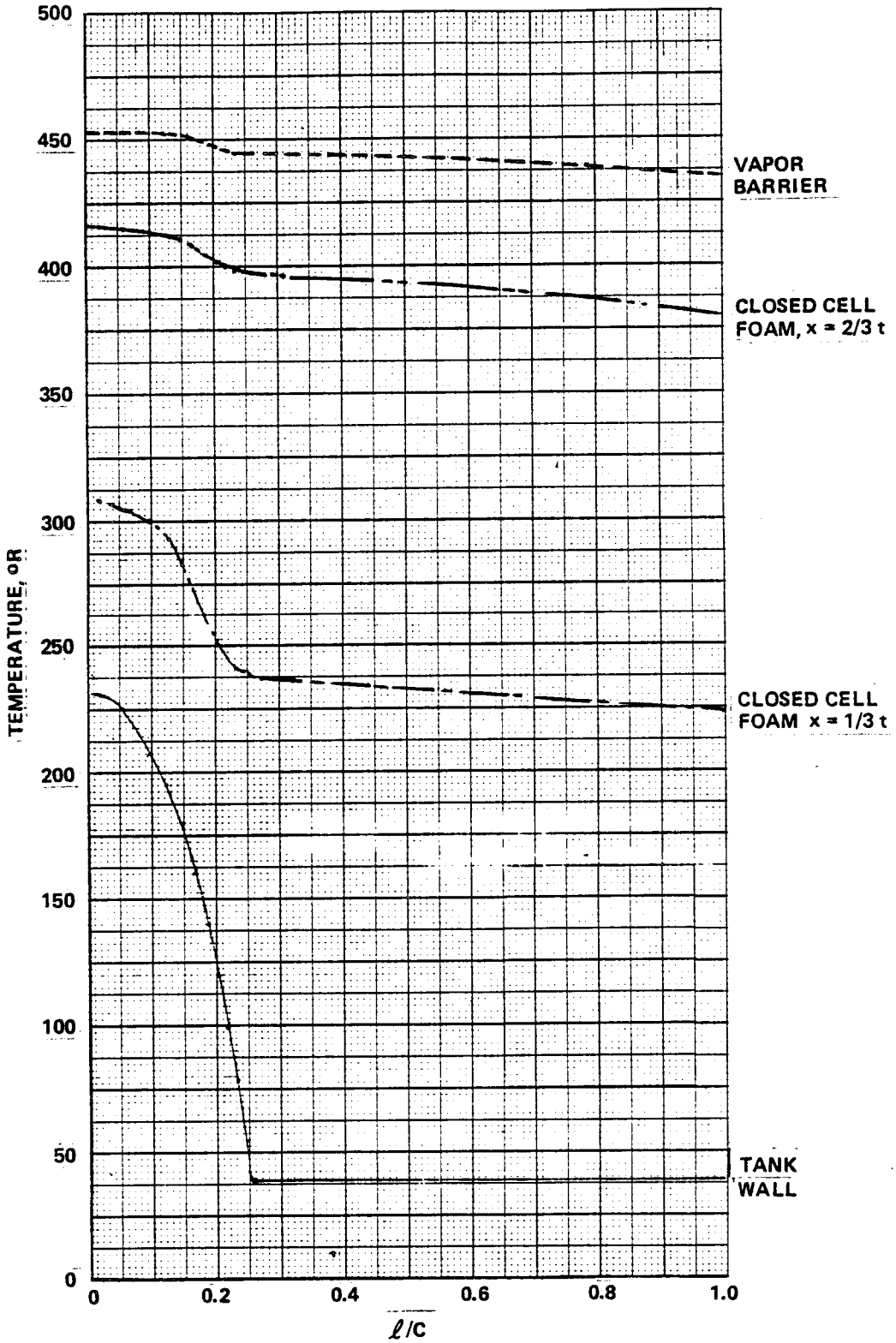

Figure 108. - Candidate no. 3 circumferential temperature distributions for liquid fraction = 0.90 (Sheet 1 of 3).

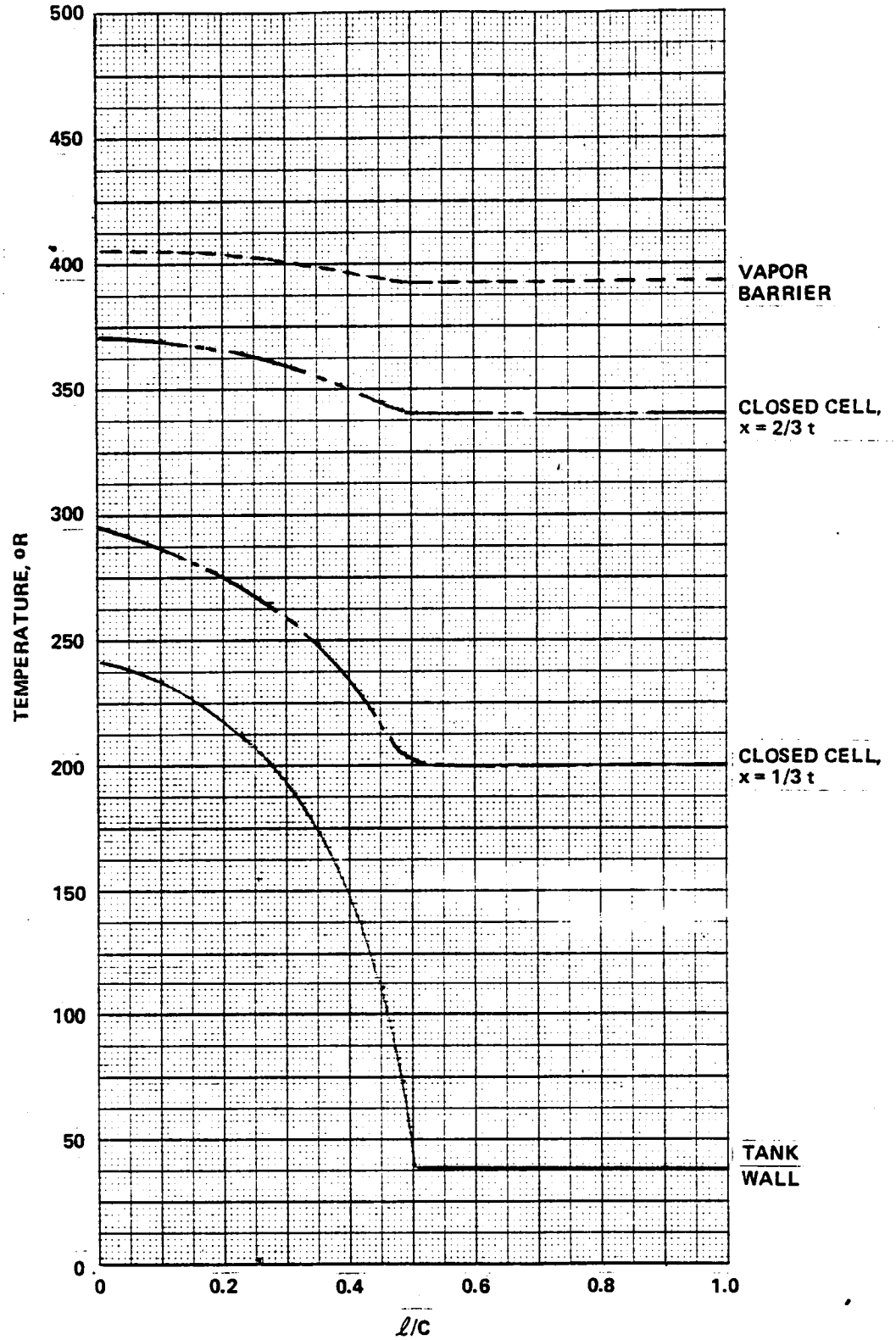

Figure 108. - Candidate no. 3 circumferential temperature distributions for a liquid fraction = 0.50 (Sheet 2 of 3).

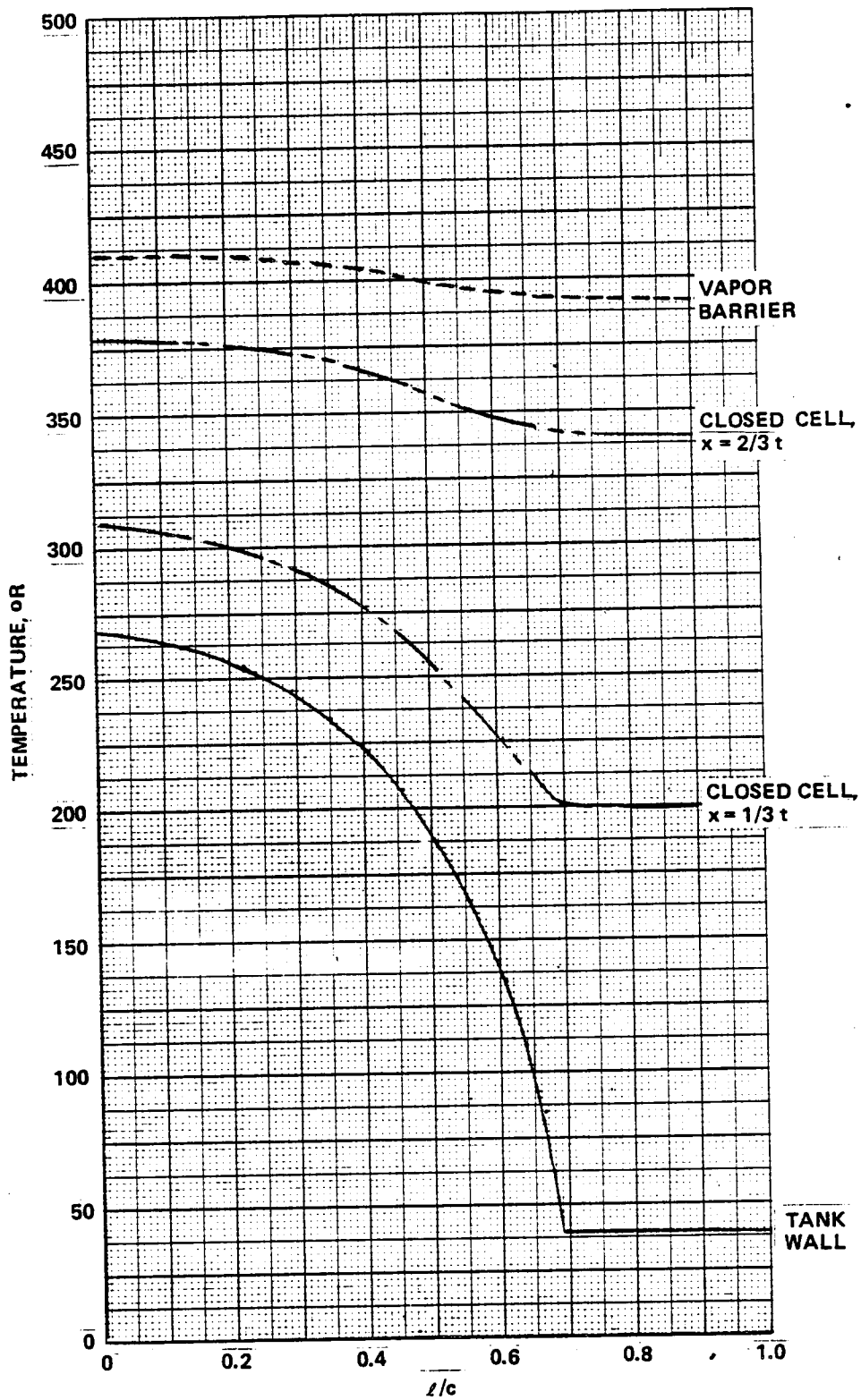

Figure 108. - Candidate no. 3 circumferential temperature distributions for a liquid fraction = 0.15 (Sheet 3 of 3).

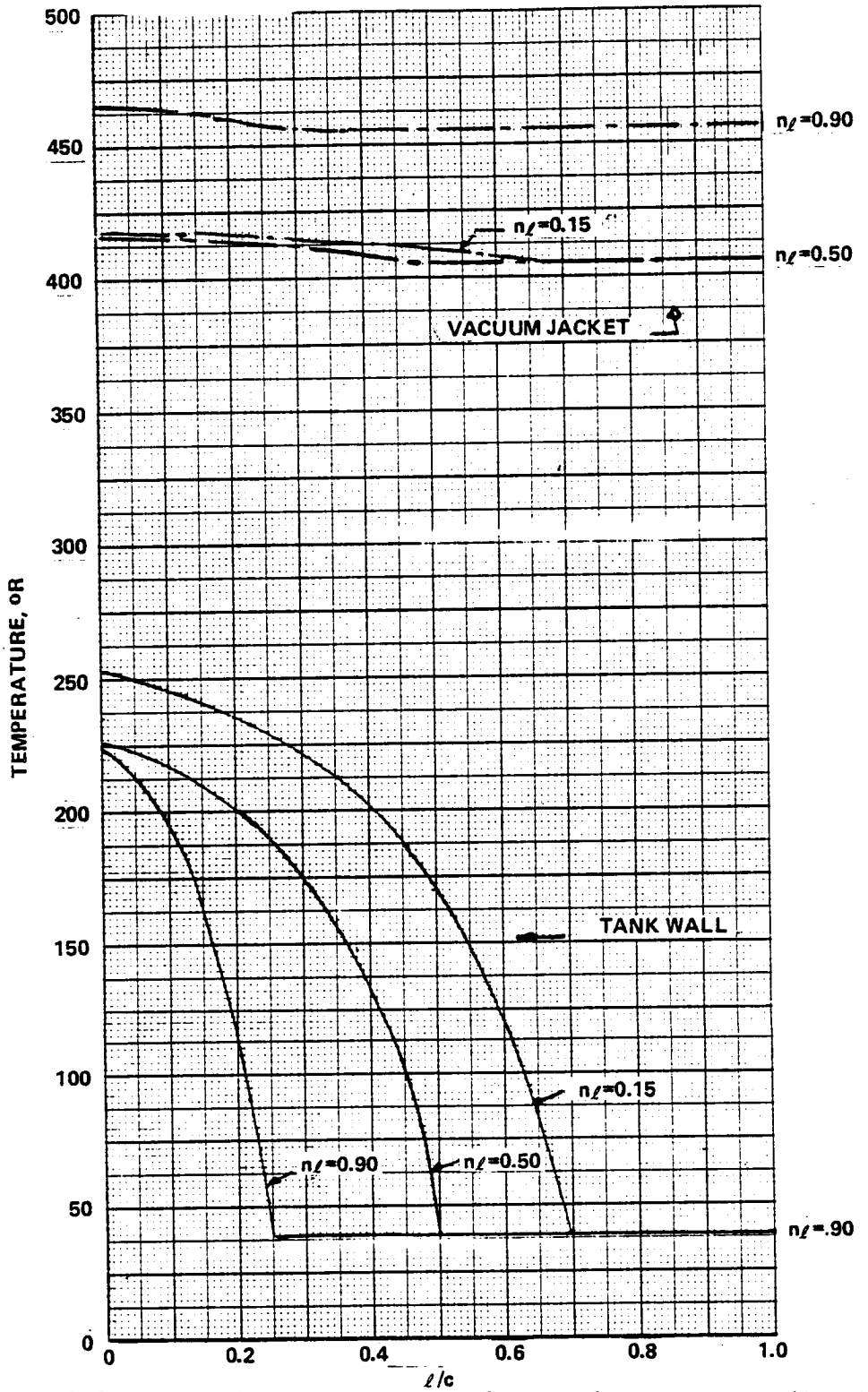

Figure 109. - Candidate no. 4, circumferential temperature distributions for tank wall and vacuum jacket.

TABLE 41. - MAXIMUM COMPUTED CIRCUMFERENTIAL TEMPERATURE GRADIENTS IN TANK WALL AND INSULATION SYSTEM FOR NORMAL OPERATING CONDITIONS

Candidate No.	Liquid Fraction	Maximum Gradient at Location °K/m(°F/in.)					
		Tank Wall		Insulation (Mid thickness)		Exterior Vapor Barrier	
1	0.90	157	(7.2)	37	(1.7)	4	(0.2)
	0.50	339	(15.5)	74	(3.4)	20	(0.9)
	0.15	464	(2.12)	112	(5.1)	33	(1.5)
2	0.90	68	(3.1)	39	(1.8)	33	(1.5)
	0.50	74	(3.4)	44	(2.0)	35	(1.6)
	0.15	116	(5.3)	63	(2.9)	46	(2.1)
3	0.90	125	(5.7)	31	(1.4)	7	(0.3)
	0.50	282	(12.9)	55	(2.5)	22	(1.0)
	0.15	381	(17.4)	90	(4.1)	33	(1.5)
4	0.90	98	(4.5)	17	(0.8) [a]	4	(0.2)
	0.50	232	(10.6)	22	(1.4) [a]	4	(0.2)
	0.15	313	(14.3)	28	(1.3) [a]	4	(0.2)

(a) Microspheres are a packed bed type of insulation and do not transmit tensile loads.

equivalent to that from a 1/8-inch diameter orifice. With the vacuum pumps operating the insulation annulus pressure can be maintained at 1 torr under these conditions (compared to the design pressure of 0.1 torr). Even assuming the entire microsphere volume is filled with air, the wall heat input due to cryopumping is negligible compared to that through the insulation at the higher pressure.

A second consideration for the vacuum system of candidate No. 4 is to assume a catastrophic failure of the vacuum enclosure, such as might be experienced by penetration of the aircraft wall by a foreign object. The flow of air into the vacuum space might not be limited by the jacket, and condensation of air products would occur at a high rate.

TABLE 42. - EFFECTS OF GH_2 AND AIR LEAKAGE INTO EVACUATED INSULATION CANDIDATES

	Candidate No. 2	Candidate No. 4
GH_2 Leakage		
q_w Cruise -w/m^2 (Btu/hr ft^2)	150.3 (47.4)	109.4 (34.7)
q_w Ground -w/m^2 (Btu/hr ft^2)[a]	210.2 (66.7)	137.1, 160.7 (43.5, (51.C)[b]
T_{VB} Cruise ^oK (^oR)	167 (300)	117 (201)
T_{VB} Ground ^oK (^oR)[a]	206 (371)	134 (242)
T_F Ground ^oK (^oF)[a]	-	260 (468)
Air Leakage		
q_w Cruise -w/m^2 (Btu/hr ft^2)	79.1, 60.2 (25.1), (19.1)[c]	42.2 (13.4)
q_w Ground -w/m^2 (Btu/hr ft^2)[a]	126.1, 84.2 (40.0), (26.7)[c]	57.4 (18.2)
T_{VB} Cruise ^oK (^oR)	118, 109 (213), (196)[c]	-
T_{VB} Ground ^oK (^oR)[a]	150, 127 (270), (228)[c]	-
T_F Ground ^oK (^oR)[a]	277 (498)	279 (502)

[a] $T_{ambient}$ = 289^oK (520^oR)

[b] GH_2 Leakage into microspheres and open cell foam

q_w = Wetted Wall Heat Flux, T_{VB} = temperature of Vapor Barrier or Vacuum Jacket (No. 4)

T_F = Exterior Temperature of Fairing or Vacuum Jacket

[c] Glass/phenolic core

The rate of condensation and solidification is a complex function of heat and mass transport within the porous insulation and its accurate representation is beyond the scope of this program. The microsphere insulation conductance for GN_2 at atmospheric pressure and 293°K is $5x10^{-4}$ (gm/sec cm^2) (cm/torr) so the insulation limits the lateral mass transfer from the opening in the jacket. Also, the void volume for microspheres is on the order of 35 percent so the thermal conductivity of the liquid or solidified layer would be reduced over that of nitrogen in either phase.

During use the jacket is under a mechanical compressive load of approximately 3.5 kPa (1/2 psi) resulting from the compression of the open cell foam by the aircraft exterior skin. This load will keep the microspheres in a densely packed configuration, and they will not flow out of an opening in the jacket other than in the immediate area of puncture. Another consideration is that condensed and solidified air may plug the area adjacent to the opening and further restrict flow of air into the microsphere annulus so it could not cryopump a significant distance from the opening. Because of the very small pores interconnecting each interparticle void, liquid air will be constrained from flowing freely throughout the annulus. With increasing time increments the liquid air will solidify.

Because of the uncertainties associated with the above assumptions and the complexity of a rigorous analysis, an upper limit for LH_2 boiloff was calculated for a worst case condition resulting from a catastrophic failure. This assumes that air flow is not restricted by the insulation and that air can flow freely to the entire tank surface. It is emphasized that this worst case condition is not considered realistic in that it is highly improbable that air could penetrate to all areas around the tank.

The void volume of the insulation space (solid fraction of microspheres is 0.65) is 2.36 m^3 (83.3 ft^3). Assuming a solid nitrogen density of 962 kg/m^3 (60 lb/ft^3), 2270 kg (5000 lb) of solid air could form in this annular volume. A wall heat rate during condensation was assumed to be 3150 W/m^2 (1000 Btu/hr ft^2) which results in a time of 12 minutes to fill the volume. Including the heat of fusion this corresponds to a mean heat rate, 3546 W/m^2 (1125 Btu/hr ft^2). After 12 minutes, in this worst case situation, the microsphere space is filled and further condensation would occur in the outer covering of open-cell foam. However, the thermal resistance of the solid nitrogen layer will limit tank wall heat rate. For a jacket temperature corresponding to the freezing point of nitrogen and a solid nitrogen thermal conductivity of 0.29 W/m °K (0.17 Btu/hr ft °F) the tank wall heat flux is reduced to 353 W/m^2 (112 Btu/hr ft^2).

The conductivity of the solid layer would actually be less than the above value due to the inclusion of the microspheres (evacuated inner volume) in the layer, but as this value is not known, the higher figure was used for the worst case estimate.

For a full fuel tank the boiloff during the initial 12 minute period would be 1145 kg (2525 lb). After this period the boiloff rate would be

558 kg/hr (1230 lb/hr). This maximum fuel loss rate would probably require the addition of an emergency vent.

A major rip or puncture in the vacuum jacket of candidate No. 4 is thus seen to not represent a critical safety hazard to the aircraft. It will, of course, be cause for the pilot to seek an emergency landing, exactly as he would in the event of a similar puncture of the fuselage of a conventionally fueled aircraft.

A critical sequence in the situation postulated will occur after the aircraft has landed, when the tank is being emptied for repair. As the LH_2 is removed from the tank the solid air will warm, liquefy, and then boil. Unless special procedures are followed, the cryopumped air can expand so rapidly large areas of the vacuum jacket may be blown off. Proper handling can obviate this situation.

7.1.6.3 Direct operating cost: On the basis of the required tank volumes derived from the thermal analysis procedures for each insulation type and thickness, estimates of weights of all components were made to determine dry weight of the fuel containment system. The following components were included in the dry weight statements for each system:

- Tank shell, integral or nonintegral design
- Tank supports and internal baffle
- Insulation material
- Vapor barriers, where applicable
- Purge barrier(s), where applicable
- Vacuum jacket, where applicable
- Fuselage structure, nonintegral tank
- Fairing, integral tank
- Vacuum pumps and controls, where applicable
- Purge gas storage and controls, where applicable

This total dry weight, combined with design mission fuel weight, weight of fuel evaporated in flight, weight of fuel vented on the ground, and the fuselage length associated with the tank volume, were then input into the DOC equation. This was repeated for each insulation thickness, and the values of DOC were plotted against the insulation thickness to graphically determine the thickness associated with the minimum in DOC for a particular system. The form of the DOC equation which was used in analysis of the fuel containment system is shown in Section 3.4.

For each DOC calculation in this analysis of the four preferred candidates, the dry fuel containment system weight and fuel loss weights were computed on the basis of the aft tank only, and the results were then multiplied by a factor of two to provide a reasonable approximation of total aircraft system weights for application to the DOC equation.

Using the data from Table 40 for system sizing, DOC was calculated as a function of total FCS thickness (t). By plotting DOC versus t, a minimum value of DOC was obtained with a corresponding FCS thickness for candidates 1, 3 and 4; Figure 110. These selected thicknesses were, respectively, 20.32 cm (8.00 in.), 9.14 cm (3.60 in.), and 6.12 cm (2.41 in.). Since candidate 2 has a fixed geometry, it therefore has a singular value of DOC for the selected vacuum pressure of 10^{-4} torr.

The characteristics of each of the four candidate insulation systems, using the thicknesses of Nos. 1, 3, and 4 so chosen, were individually entered into the ASSET computer program for aircraft optimization, along with representation of the preferred tank structural concepts, the LH_2-fueled engine, and the other components of the LH_2 fuel system previously described. The results of this investigation, which provided the basis for selecting a final insulation system concept, are presented in Section 7.3.

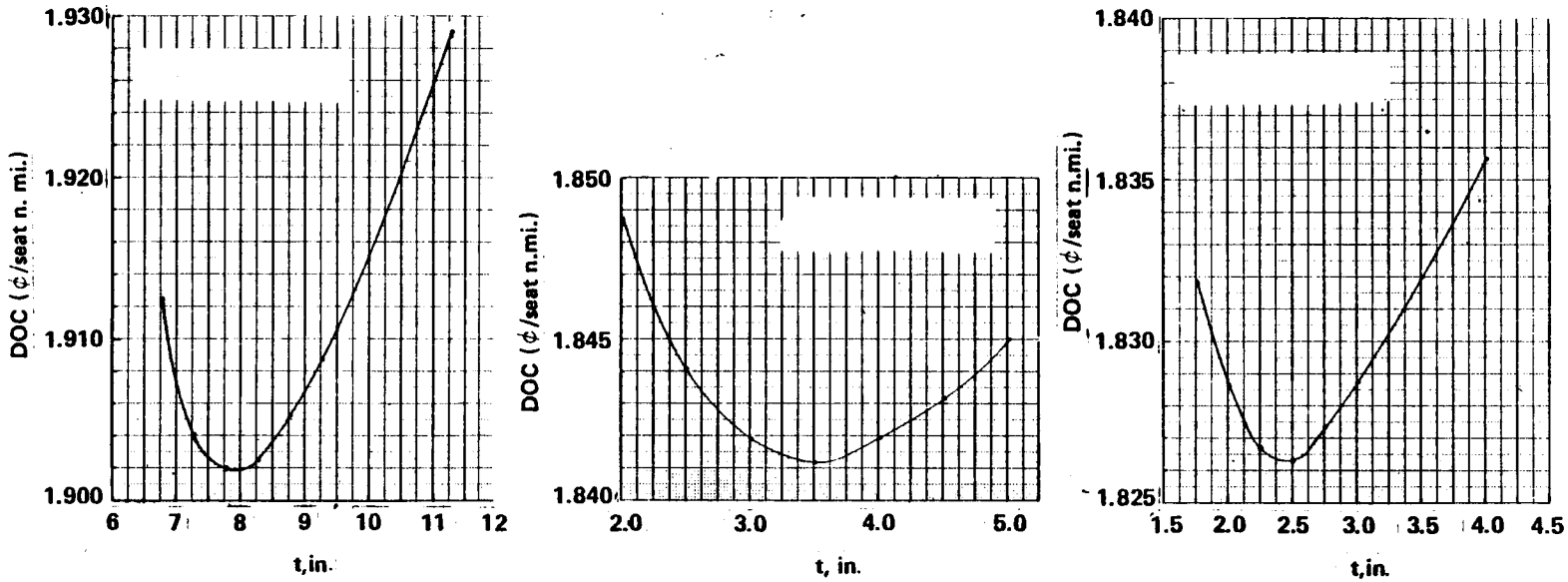

a. CANDIDATE NO. 1

b. CANDIDATE NO. 3

c. CANDIDATE NO. 4

NOTE:

DOC VALUES ARE BASED ON PRELIMINARY SYSTEM WEIGHT ESTIMATES.

Figure 110. - Change in DOC with overall fuel containment system thickness (t).

7.2 Tank Structure

An investigation to determine a preferred concept for the fuel tank structural design proceeded in parallel with that of the insulation study. This section presents results of that structural investigation. Design criteria and loads are established, structural concepts for both integral and nonintegral type tanks are described, and the results of the analyses are presented. In addition, the results of parametric studies are reported which determined 1) a preferred shape for the fuel tank dome ends, 2) the effect on economics of specifying a reduced design life for the tank structure, 3) the effect of designing for different pressure levels, 4) the viability of using pressure stabilized structure, and 5) the preferred tank suspension method.

7.2.1 Structural design criteria and loads. - The structural design criteria and loads defined in this section were developed to provide 1) the basis for the evaluation of the candidate tank configurations and 2) a level of structural safety equivalent to current transports for assessing structural mass trends resulting from application of these criteria.

In general, the criteria are based on the structural requirements of the Federal Aviation Agency, FAR 25 with specific criteria being the same as that used for the L-1011 aircraft. This section presents the following criteria: basic airplane performance data (airplane mass, design speeds, maneuver envelope, etc.), design pressure, emergency landing, thermal stress, combined loads, fatigue and fail-safe. In addition, the design loads are presented for four flight conditions.

7.2.1.1 Airplane weight and inertia data: The loads are based on the design weights shown in Table 43 which were taken from Reference 1 for use as preliminary values. The inertia distribution data has been estimated based on these weights and the basic geometry and layout of the configuration. Forward c.g. limit was assumed to be 20 percent MAC. Structural reserve fuel is 7 percent of total fuel, the same criterion as used on the L-1011.

7.2.1.2 Design speeds: The design speed altitude variation is presented in Figure 111. It is the same as the L-1011 airplane. This figure shows the variation with altitude of cruise speed, dive speed and maneuver speed.

TABLE 43. — INITIAL VALUES, DESIGN WEIGHT SUMMARY

Condition	Weight	
	kg	lb
Maximum Take-off Gross Weight	181 000	400 000
Landing Gross Weight	172 000	380 000
Operating Weight Empty	108 000	238 000
Structural Reserve Fuel	2 200	5 000
Maximum Weight with Structural Reserve Fuel	168 000	370 000
Minimum Flying Weight	110 000	243 000

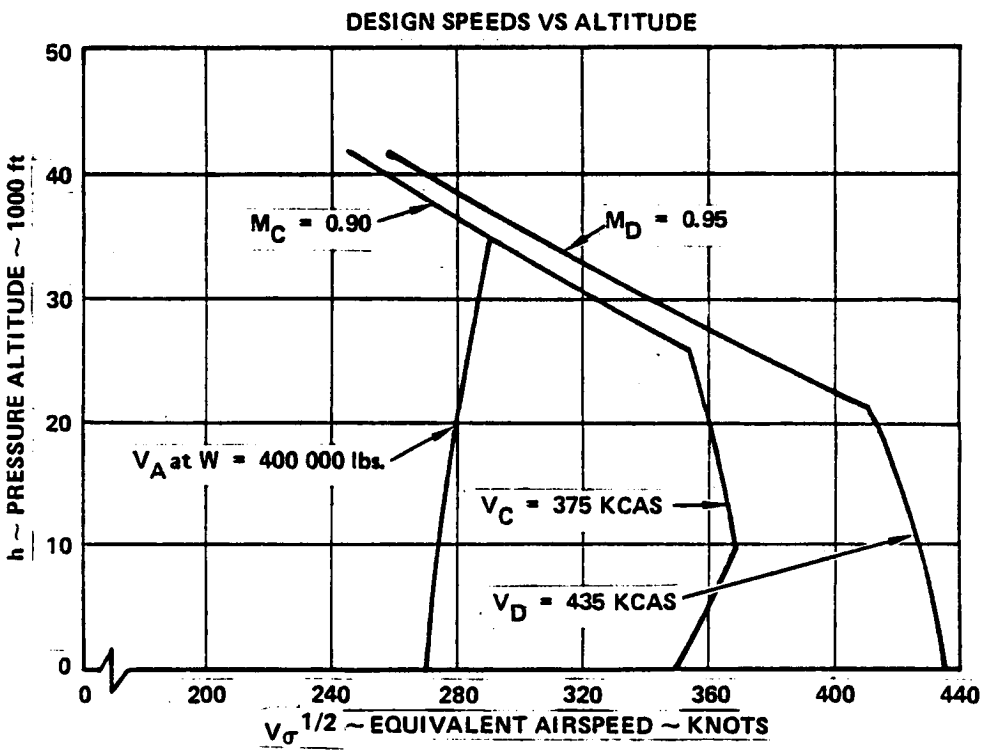

Figure 111. – Design speeds vs altitude.

Design cruising speed, V_C, is the maximum speed at which encounter of high-intensity nonstorm turbulence (U_{de} = 50 fps) must be considered.

Design dive speed, V_D, is established so that the probability of inadvertently exceeding dive speed is extremely remote even while operating at maximum operating speed.

Design maneuvering speed, V_A, is determined from the aircraft stall characteristics. It is very near to the minimum speed at which the design limit load factor can be attained.

7.2.1.3 Maneuver envelope: The maneuver envelope is a function of weight and altitude. At low speed the attainable load factor is limited by weight and maximum lift. At speeds above V_A the allowable maneuver load factor is defined by FAR Part 25.

The envelope shown in Figure 112 corresponds to the altitude at which the constant M_C line intersects the constant V_C line (M_C = 0.9, V_C = 375 KCAS). Other points of interest are defined by; the intersection of the constant M_D line and the constant V_D line (M_D = .95, V_D = 435 KCAS, h = 21 800 ft), the point where V_C is a maximum (V_C = 375 KCAS = 368 KEAS, h = 10 000 ft) and sea level where V_D is a maximum (V_D = 435 KCAS = 435 KEAS).

7.2.1.4 Design loads: Four flight conditions were investigated for static strength of the fuselage aftbody:

(1) A PLA (positive low angle of attack) condition at 21 800 feet of 2.5 g's and a download on the horizontal tail of 100 000 pounds (Figure 113).

(2) An abrupt pitching maneuver at sea level of 1.0 g with a download on the horizontal tail of 130 000 pounds, included on Figure 113.

(3) A vertical gust condition at 10 000 feet was found to be not critical.

(4) A negative maneuver condition of -1.0 g with an upload on the horizontal tail of 16 000 pounds (Figure 114).

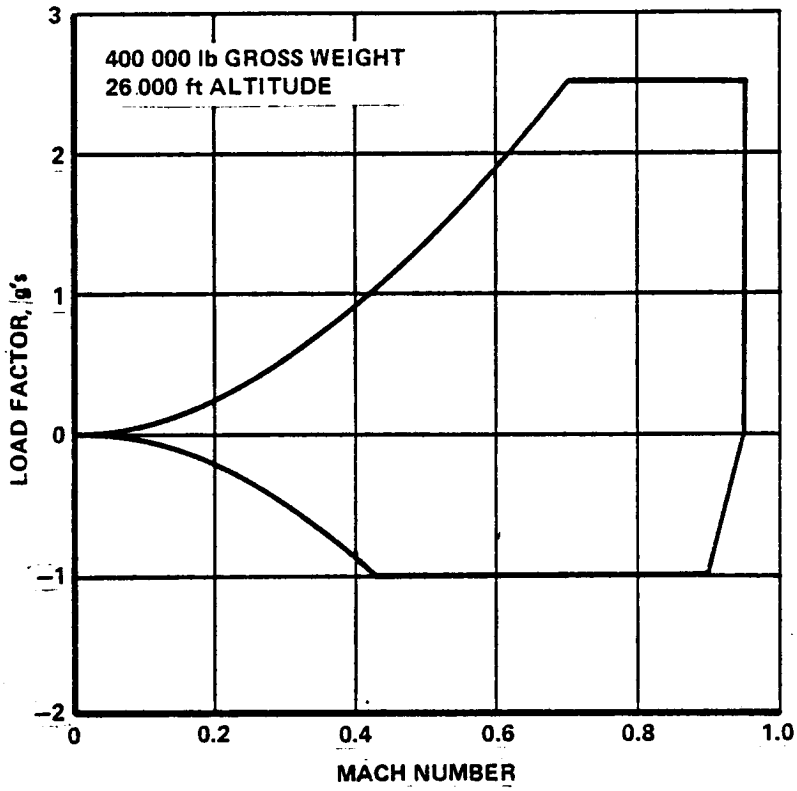

Figure 112. - Maneuver envelope - 400 000 lb gross weight, 26 000 ft altitude.

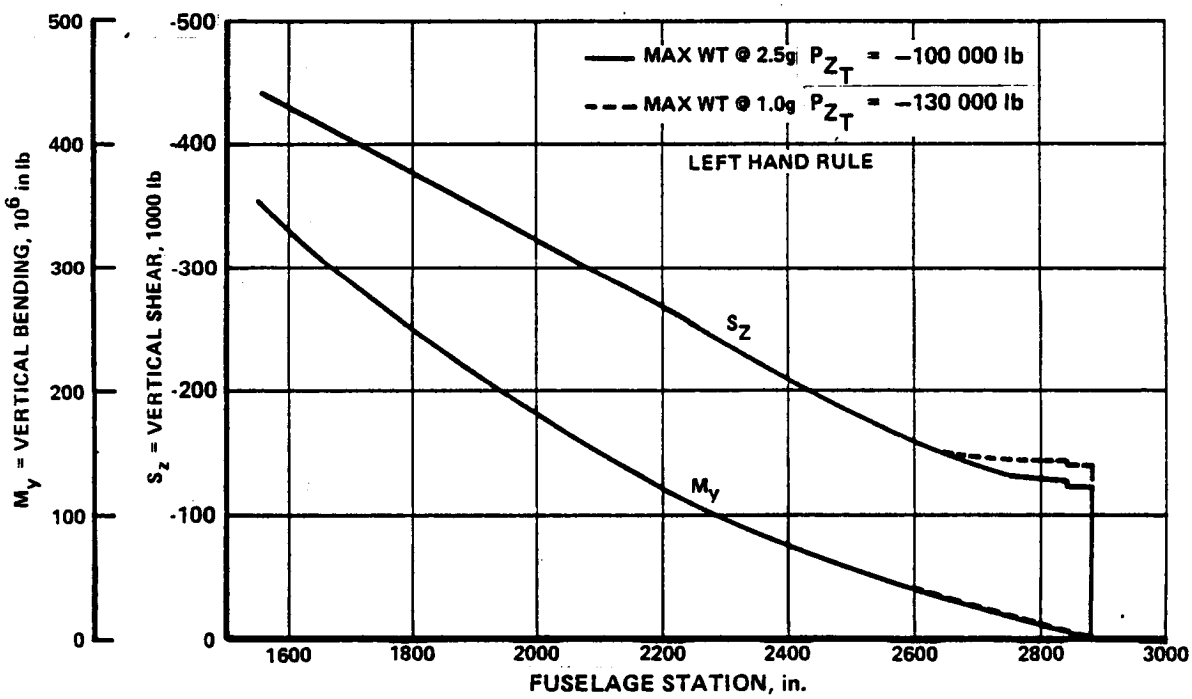

Figure 113. - LH_2 subsonic transport fuselage aftbody limit loads, fuselage tank configuration.

In addition to the above limit load conditions, a cruise condition was investigated in support of a fatigue evaluation. The condition selected was 1.0 g at start of cruise with a down load on the horizontal tail of 50 000 pounds (Figure 115).

7.2.1.5 Tank design pressures: LH_2 tanks for the baseline aircraft were designed to operate at a nominal pressure of 14.5 k Pa (21 psia). Factors required for cabin pressure (FAR 25) are assumed applicable to the LH_2 tank design and the maximum cruise altitude is assumed to be 11 600 m (38 000 ft).

$$p = 14.5 \text{ k Pa } (21.0 \text{ psia})$$

The differential pressure (Δp) acting on the LH_2 tanks is

$$\Delta p = p - p_{at}$$

$$p_{at} = \text{atmospheric pressure}$$

The differential pressure was multiplied by a factor of 1.1 to account for relief valve tolerance and inertia effects, to provide an operating pressure.

$$p_{op} = 1.1 \Delta p$$

- Differential Pressure for Combination with Limit Loads - A limit pressure, equivalent to the operating pressure, is combined with the limit loads due to maneuver or gusts.

$$p_{limit} = p_{op}$$

- Differential Pressure for Combination with Ultimate Loads - An ultimate pressure that corresponds to the operating pressure multiplied by 1.50, was defined for combining with the ultimate loads due to maneuver or gusts.

$$p_{ult} = 1.50 \times p_{op}$$

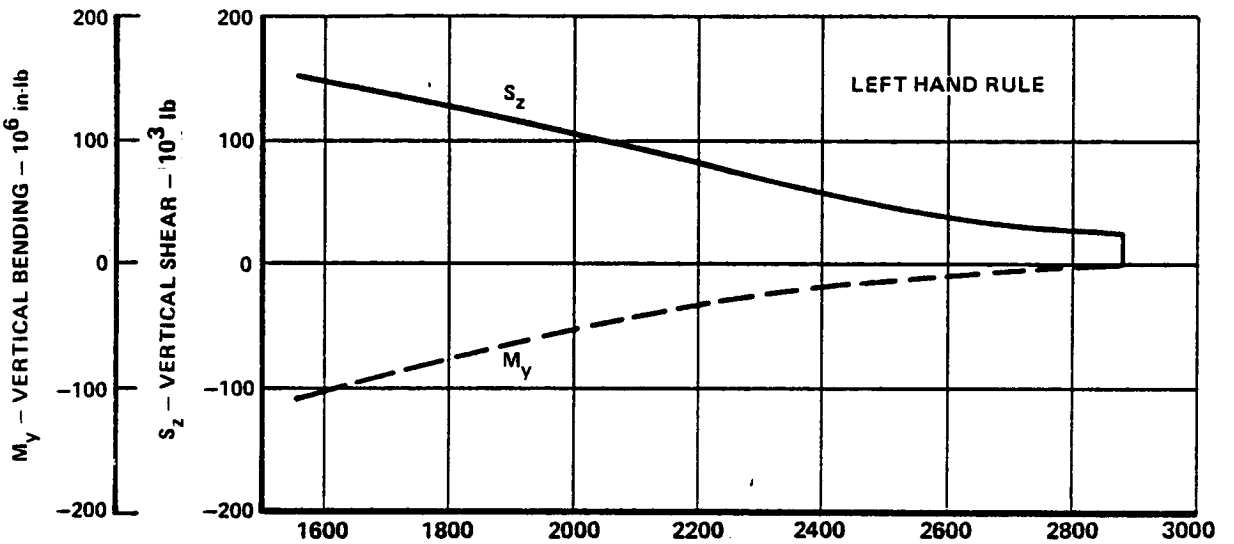

Figure 114. - LH_2 subsonic transport fuselage aftbody limit loads (-1.0 g max, P_{z_T} = 16 000 lb).

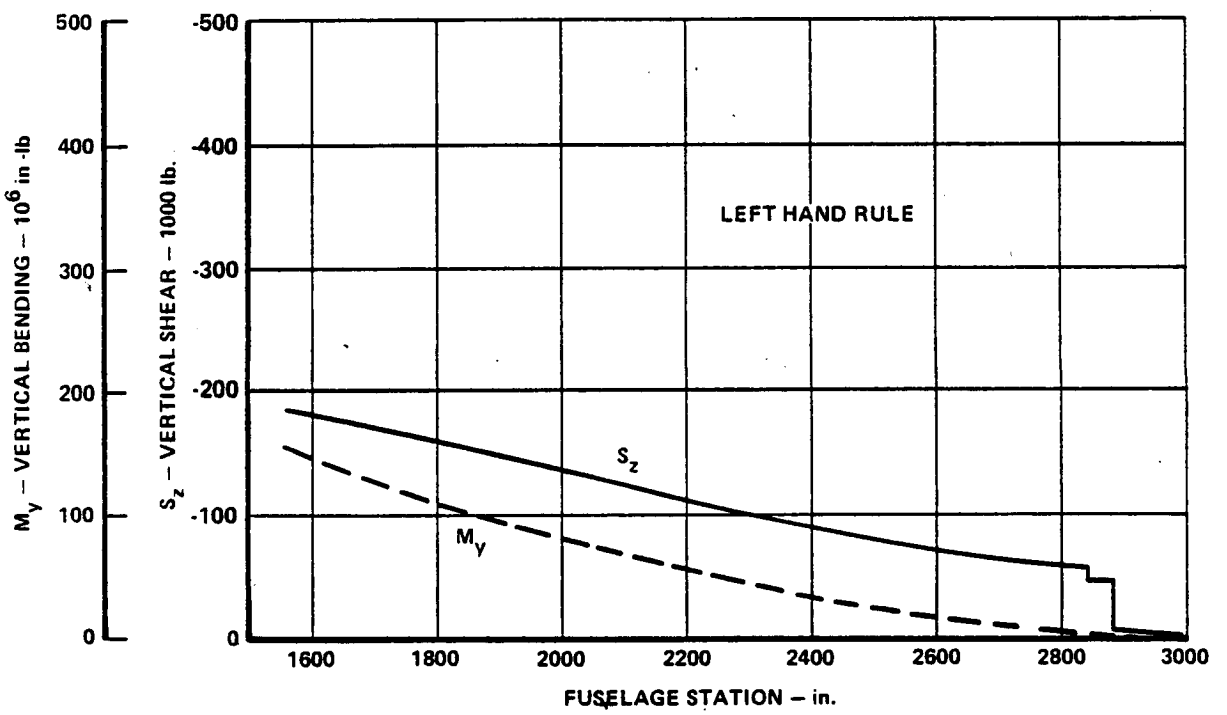

Figure 115. - LH_2 subsonic transport fuselage aftbody limit loads (1.0 g max. weight start of cruise, P_{z_T} = 50 000 lb).

- Ground Test Differential Pressure - A proof pressure corresponding to the operating pressure multiplied by 1.33, was specified. No detrimental deformation shall result from this condition.

$$p_{proof} = 1.33 \times p_{op}$$

A burst pressure equivalent to the operating pressure multiplied by 2, was defined. Catastrophic failure of the tank shall not occur.

$$p_{burst} = 2.00 \times p_{op}$$

7.2.1.6 Emergency landing condition: The following ultimate inertia load factors (FAR 25.561) were applied to the tank suspension system and fuel within the tank.

upward: $n = 2.0$

forward: $n = 9.0$

sideward: $n = 1.5$

downward: $n = 4.5$

Each load factor was applied on an arbitrary independent condition.

7.2.1.7 Thermal stress criteria: Thermal stresses reflecting the maximum individual or combination of through-the-wall, circumferential, and longitudinal temperature gradients were investigated. For the critical flight condition(s) the external loads were combined with the appropriate temperature gradients associated with the insulation system, tank suspension method and tank ullage condition.

- Limit Thermal Stresses/Strains - For limit design purposes, thermal stresses were calculated for the design flight condition that are compatible with the limit-load design condition. No additional factor of safety was applied to the thermal stresses/strains.

- Ultimate Thermal Stresses/Strains - The stress-strain relationship may not be linear when ultimate design stress levels are being considered. In these cases the thermal strain was held invariant and the stress ($E \times \epsilon$) was combined with the load stress which is thickness dependent. Where the thermal strain was of the same sign as the load stress a factor of safety of 1.25 was applied to the thermal strain. A factor of 1.00 was applied when they were subtractive.

7.2.1.8 Combined Loads Criteria: Flight loads, tank pressure and thermal stresses were combined as specified.

The factor of safety as defined for the loads, pressures and thermal strains in the foregoing section, was used to combine the loads and form the final stress resultants.

For compression design, the tensile force produced by the internal pressure was ignored and only the shear and/or compressive forces produced by the external loads were considered with the temperature induced strains/stresses.

For tension design, the sum of the membrane forces produced by the internal pressure and external loads was considered with the appropriate thermal strain/stresses.

The flight and ground conditions considered are specified in Table 44 with the design levels (factors of safety) of the load and thermal environment defined.

7.2.1.9 Fatigue design criteria: Fatigue design requirements can be met by limiting the permissible design tension stress levels for static ultimate design and normal operating conditions.

An average flight time of approximately 5 hours per flight was used for the LH_2 fueled transport. For 2219-T851 Aluminum Alloy at -423°F, Figure 116 presents the relationship between fuel tank circumferential design stress and fatigue quality for 50 000 hours of service with the average flight time, one internal pressure cycle per flight, and a life reduction factor of four. The upper curve reflects the ultimate design stress levels applicable to fuel tank substructure other than skin, such as frames, which are uniaxially loaded by pressure and thermal loads. The ultimate design stress levels to be applied to fuel tank skin hoop tension are represented by the second curve on this figure. These values are reduced, to approximately 71.5 percent of the substructure design allowable, because the skin is subjected to biaxial stresses from internal pressure, external loads and thermal loads. The allowable gross area tension stress for the operating condition for 2219 aluminum is presented as the lower curve of Figure 116. For other materials the tension allowables in other than fuel tank regions are related to prior experience and successful service experience with similar types of aircraft, such as the L-1011 commercial transport.

The fatigue life for the materials selected for the integral and non-integral tank designs are achieved by limiting the ultimate design stress values. Table 45 contains the allowable gross area tension stresses for 2024 and 2219 aluminum alloys with a fatigue quality index (K_t) of 5.0.

TABLE 44. - COMBINED LOADS AND THERMAL CRITERIA

Condition	External Loads	Internal Pressure	Thermal Stress/Strain
Operating (Cruise Cond.)	Limit	Limit	Limit
Limit Design	Limit	Limit	Limit
Ultimate Design	Ultimate	Ultimate	Ultimate
Fail-Safe Design	Limit	Limit	Limit
Emergency Landing	Ultimate	Ultimate	Ultimate
Proof Test	-	Proof	-
Burst	-	Burst	-

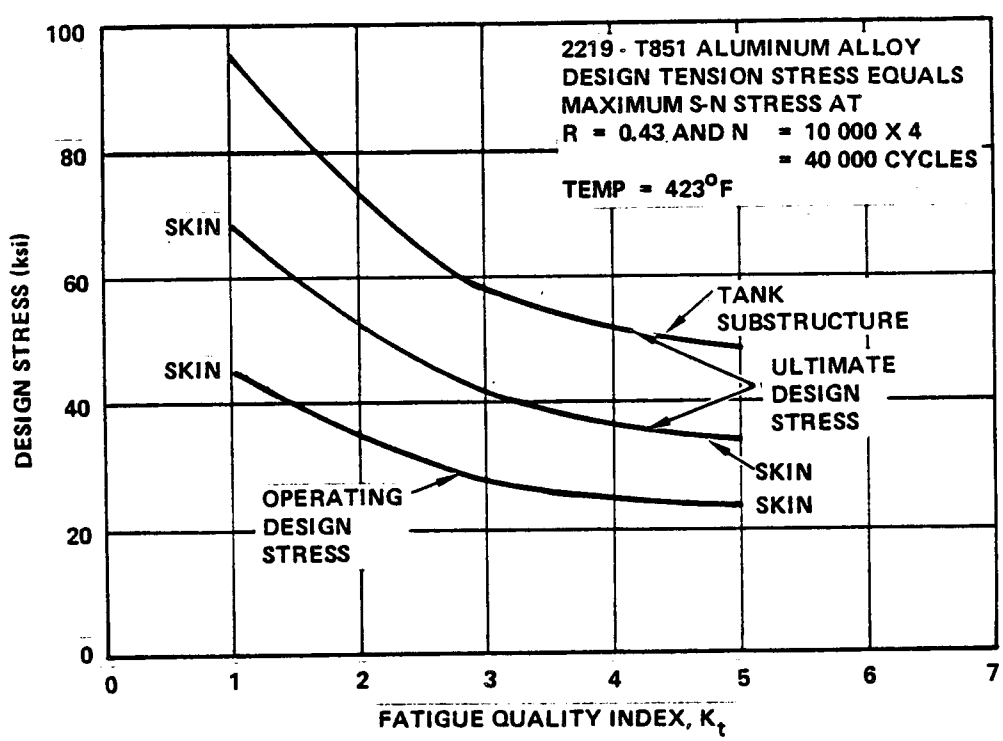

Figure 116. - Variation in circumferential design stress with fatigue quality for 10 000 flights including a life reduction factor of four on number of flights.

TABLE 45. - FUSELAGE ALLOWABLE GROSS AREA TENSION STRESSES FOR ULTIMATE DESIGN AND OPERATING CONDITIONS

Components	Nonintegral		Integral
	Shell	Tank (1)	Both (1)
	2024 Alum (RT)	2219 Alum (-423°F)	2219 Alum (-423°F)
Ultimate Design Condition			
• General Structure	45 000	NA	NA
• Concentrated Loads and Biaxial Stress Areas	35 000	34 000	34 000
Operating Condition			
• Skin Hoop Tension at Operating Pressure, External Loads and Thermal Stress	NA	23 000	23 000

Notes:

1. Design allowables based on a fatigue quality index of 5.0, 50 000 hr of service life and a life reduction factor of 4.

For the nonintegral tank design, 2024 aluminum alloy was used for the fuselage bending material. The ultimate gross area tension stress for symmetrical flight and ground conditions was limited to 45 000 psi. In addition, the basic design allowable stress was further reduced to 35 000 psi in local areas subjected to biaxial loading, regions adjacent to highly concentrated loads, blind areas and single load paths in primary structure. For the 2219 aluminum alloy which is used for the fuel tank design in both the integral and nonintegral designs, the allowable stress in areas subjected to concentrated loads and biaxial stresses was limited to 34 000 psi.

Table 45 presents the design allowables for the special fatigue considerations required for the operating design condition for pressurized fuel tank structure. For both integral and nonintegral tank designs the allowable gross-area tension stress of 23 000 psi (K_t = 5) for fuel tank skin circumferential stresses is related to fuel temperature, number of landings, and related values of life reduction and stress concentration factors. The allowable stress for fuel tank substructure, such as frames, would be higher than that required for fuel tank skins because the loading on the substructure is primarily uniaxial.

7.2.1.10 Fail-safe (damage tolerance) design criteria: The objective of the fail-safe (damage tolerance) design criterion is to ensure that flight safety is maintained in the event of structural damage of reasonable magnitude. Such damage may arise from fatigue as well as accidental impact or other sources. To meet the objective, a fracture control plan consisting of the following aspects was implemented.

Minimum requirements on material fracture properties shall be established for material selection. The required properties shall include fracture toughness, fatigue crack growth, and threshold for stress corrosion cracking. Materials in as received condition as well as after undergoing major fabrication processes such as cold work, welding, and heat treatment shall be tested.

Based on production inspection capabilities, the maximum size flaw that is likely to be missed shall not grow to critical proportions during the life of the structure; i.e., 10 000 flights or 50 000 hours. The inspection requirement shall be met by using a combination of quality control and NDI requirements.

The operating stress levels and material selection shall be chosen to ensure that, under normal service conditions, undetected flaws will remain as subcritical through-the-thickness cracks for a sufficiently long period. Thus the detection of such flaws by leakage can be ensured.

For the above criteria, the critical damage size is that which can sustain the operating pressure in combination with the limit loads due to maneuvers or gusts.

For fail-safe, the tank structure must be capable of supporting the operating pressure loads and appropriate fail-safe loads for accidental damages equivalent to a 12.0 inch through-the-thickness crack anywhere in the structure, including members attached to the structure across the damaged section. The fail-safe loads shall be equal to the maneuver and gust loads that can reasonably be expected during completion of the flight in which the damage occurred.

Fail-safe for the remainder of the structure shall be designed to meet the fatigue and damage tolerance requirements of FAR 25.571.

Besides the customary quality control and NDI procedures which applied to the material received and during fabrication process, a leak test shall be conducted concurrently with the ground proof test discussed previously.

7.2.2 Structural design concepts and materials. - Two basic types of tank designs were considered for this study:

- Integral, where the tank serves both as the container of the fuel and also supports the body loads

- Nonintegral, in which the tank is simply a fuel container and does not participate in the support of the body loads which are carried by a separate shell structure.

Promising structural design concepts were evaluated for each of the above basic types of LH_2 tank designs and are shown in Table 46.

For the Integral tank design, three wall concepts were considered with all designs being restricted to one-piece configurations to minimize potential sources of leaks. These concepts were the blade-stiffened, zee-stiffened and tee-stiffened designs. In addition, an unstiffened wall design was included in the candidate concepts for the tank design.

The wall concepts considered for the nonintegral tank design were the conventional construction zee- and hat-stiffened concepts for the fuselage shell and the same one-piece wall designs as described for the integral tank being used for the tank design.

For the fuselage shell structure of the nonintegral tanks the conventional 2024 and 7075 aluminum alloys currently being employed on wide bodied transport were used for the baseline material; whereas, the aluminum alloy 2219 was selected for the tank material for both basic types of tanks.

The 2219 aluminum alloy was selected because of its ductility at cryogenic temperatures, as well as its weldability, formability, stress corrosion resistance, and its high fracture toughness and resistance to flaw growth, References 27 and 28.

Table 47 presents a compilation of materials data applicable to the design of LH_2 fuel containment tankage and fuselage shell structure.

TABLE 46. - STRUCTURAL DESIGN CONCEPTS

Structural Component	Tank Design	
	Nonintegral	Integral
Fuselage	Zee-stiffened Hat-stiffened	Not applicable
Tank	Blade-stiffened Zee-stiffened Tee-stiffened Unstiffened	

TABLE 47. - MATERIALS DATA PERTINENT TO LH_2 FUELED SUBSONIC TRANSPORT FUEL CONTAINMENT TANKAGE/FUSELAGE STRUCTURES

Materials																		
Structural			Identity				Properties and Characteristics											
	Concept						F_{tu} (ksi)		F_{ty} (ksi)		F_{cy} (ksi)		e (%)		K_{IC} (ksi/in)			
Assy	Int.	Non-Int.	Type	Alloy	Prod. Form	Thickness	AMB.	LH_2	AMB.	LH_2	AMB.	LH_2	AMB.	LH_2	AMB.	LH_2	Comments	
Tank	√	√	Alum.	2219-78 or 2419-78	Sht.	To 249	62	98	47	63	48	*	7	16	64	78	Density .102 lb/in^3, 2219 and 2419 properties the same except 2419 K_{IC} is guaranteed; hydrogen environment embrittlement is negligible.	
					Plt.	To 1.0	62	98	47	63	48		8	15	-	47		
						1.0-2.0	62	98	47	63	47		7	15	34	-		
					Ext.	To .5	53	92	42	57	43		6	15	-	-		
						.5-30	58	92	42	57	42		6	15	-	-		
			Gres	21-6-9	Sht	To .249	100	234	60	181	60		40	56	-	-	Density 0.283 lb/in^3; high resistance to hydrogen environment embrittlement.	
					Bar	All	90	245	50	146	50		40	15	-	-		
				321	Sht	To .249	75	230	30	60	27		45	35	-	-	Density 0.286 lb/in^3; high resistance to hydrogen environment embrittlement	
					Bar	All	75	270	30	60	27		45	35	-	-		
Fus. Shell	N.A.	√	Alloy	2024-73 Clad	Sht	To .128	64	110	47	74	39		15	17	83	-	Density 0.100 lb/in^3; hydrogen environment embrittlement is negligible.	
						.129-.249	65	110	47	74	39		15	17	87	-		
					Plt	.25-.49	65	97	47	80	40		12	10	-	-		
						.50-1.0	63	97	47	80	39		8	10	21	-		
				7075-776 Clad	Sht	To .187	67	106	57	70	56		8	15	49	-	Density 0.101 lb/in^3; hydrogen environment embrittlement is negligible	
						.188-.249	69	106	59	70	58		8	15	53	-		
					Plt	To .449	68	95	58	80	57		8	9	25	-		
						.50-1.0	68	95	57	80	56		6	9	25	-		
				7075-776 Bare	Sht	.64-.125	78	115	70	100	64		8	11	61	-	Density 0.101 lb/in^3; hydrogen environment embrittlement is negligible.	
						.125-.249	78	115	71	100	70		8	11	59	-		
					Plt	.25-.49	77	110	69	95	65		9	10	-	-		
						.50-1.0	77	110	70	95	68		9	10	23	-		
						1.0-2.0	76	110	69	95	66		6	10	23	-		
					Ext	.25-.49	81	117	73	100	73		7	20	-	-		
						.50-.74	81	117	72	100	72		7	20	24	-		
						.75-1.5	81	117	72	100	72		7	20	24	-		

*F_{cy} @ LH_2 temperature not available as of 12-2-76 but $F_{cy} \approx F_{ty}$ @ -423°F assures a reasonable assumption.

**All facture toughness values are for L-T orientation.

For fuselage shell structure, independent of the fuel containment system, data for the 2024 and 7075 materials indicate that such materials can remain in contention for independent fuselage shell structure of the LH_2 transport.

Comparison of data for 2219, 21-6-9 (Nitronic 40) and 321 materials for the tank structure show the strength/density advantage for the 2219 material in fuel containment applications.

7.2.3 Concept screening. - The design of an economically viable LH_2 fueled aircraft requires the lowest attainable structural mass-fracture commensurate with the assumed technology period. To achieve this goal promising structural design concepts were evaluated for each basic tank configuration (i.e., integral and nonintegral) using a representative load/temperature environment and the design criteria specified in Section 7.2.1. The candidate structural design concepts are described in Section 7.2.2.

7.2.3.1 Evaluation procedure: To provide a rational basis for evaluating the candidate tank wall concepts for the integral and nonintegral tanks, a structural investigation was conducted which proceeded in parallel with that of the insulation system described in Section 7.1. The structural evaluation consisted of the following steps:

1. Baseline tank configurations were established for the integral and nonintegral tank designs. Structural configurations and a typical insulation system were postulated for a constant volume tank to define the basic tank dimensions.

2. A BOSOR 4 finite difference structural model was established for the integral and nonintegral tanks using the basic dimensions defined for the above baseline tanks. A representative wall concept was selected for each tank from the candidate concepts which provided the property data for the models.

3. Using the external loads, static solutions were obtained using the BOSOR 4 structural models. Displacements, inplane stress resultants, and bending moment resultants were defined for each tank design.

4. Point design regions were selected and typical structural components for each tank design were defined for conducting the detail analysis. The results of the BOSOR 4 static solutions were used to define the load/temperature environment.

5. Detail structural analyses were conducted on each candidate tank wall concept using the internal load/temperature environment corresponding to the basic tank design being investigated. This environment, in conjunction with computerized stress analysis programs, were used to define the minimum-weight proportions and corresponding weight of the candidate concepts. Included in this study were basic strength, stability, and fatigue and fail-safe analyses.

6. The total tank weight for each candidate concept was extrapolated from the results of the point design analysis. These results were then used to select the most promising tank wall concept for the integral and nonintegral tank designs.

7.2.3.2 Analytical methods: Established methods were employed to analytically evaluate the candidate tank concepts during the concept screening analysis; they were of two general types: 1) computerized shell programs to define the internal loads and conduct the general stability analysis, and 2) stress analysis programs and methods for sizing the major structural components. A description of these programs and analytical methods is presented in the following text.

7.2.3.2.1 Shell analysis: The computerized shell analysis programs, BOSOR 4 and STAGS (References 29 and 30), were used to define the internal loads and conduct the stability analyses. Both of these programs use a finite-difference solution method based on an energy formulation and can perform stress, stability, and vibration analyses of segmented, ring-stiffened shells. The BOSOR 4 program is limited to shells of revolution, whereas the STAGS program is a more general program capable of handling asymmetrical wall thicknesses and applied loads.

7.2.3.2.2 Structural analysis: The basic strength and stability analyses of the candidate tank wall concepts were conducted using existing structural analysis computer programs. In addition to these programs, established methods were used to analyze the damage tolerance aspects of the wall concepts, as well as, the basic strength of the other major structural components.

For the tank wall concepts a computer program which links general purpose random search algorithms with available stress analysis programs was used to define the minimum weight panel proportions. These stress analysis programs are similar to those reported in Section 12 of Reference 31. Included in these programs is a strength evaluation of the complex stress state, i.e., inplane and normal stress resultants. The search Algorithm, entitled MONTE CARLO I, employed in these programs contains a sequence of two previously reported and well known approaches: Random Selection and Random Rays, Reference 32.

The sizing of the frames for this study were based on the theory derived by Shanley in Reference 33, which is premised on providing sufficient frame stiffness to preclude a general instability failure of the shell in bending. Shanley's expression for the required frame stiffness is:

$$(EI) = C_f MD^2/L$$

This expression relates the frame stiffness (EI) to the applied bending moment (M), the shell diameter (D) and frame spacing (L).

7.2.3.2.3 Fatigue analysis: A detailed description of the fatigue criteria is presented in Section 7.2.1.9. The intent of this section is to describe the application of this criteria to the structural components.

The fatigue design requirements are met by restricting the permissible design tension stress levels used for design. Design allowables for both the operational and ultimate design conditions were established and are shown in Figure 116.

For the operating condition, the limit loads for the cruise condition were used and the fuel tank skin circumferential stress was restricted to a stress level of 23 000 psi, $k_t = 5$.

The design allowables for the skin and substructure of the tank for the ultimate design conditions are also shown on Figure 116. The application is similar to that of the operating conditions, with the exception that the applied loads reflect the maximum ultimate design loads from any of the flight conditions.

7.2.3.2.4 Fail-safe analysis: The objective of the fail-safe analysis was to ensure that the structure in the presence of an assumed damage condition was capable of supporting the design load of 100-percent limit load. Both circumferential and longitudinal skin crack damages were assumed as specified in the design criteria, Section 7.2.1.10.

In general, for all concepts which have attached stiffeners (welded or mechanically fastened), the stiffener reinforces the skin and provides crack arresting capability; conversely, for one-piece skin/stiffener designs no reinforcement capability is provided by the stiffener. In the latter case, the fail-safe criteria is met by lowering the axial stress level (i.e., increasing the cross-sectional area) and/or by providing external straps.

The analysis methods used for conducting the fail-safe analysis are presented in Reference 34. Figures 117 and 118 outline the general equations used in determining the residual strength of the damaged structure for the circumferential and longitudinal crack conditions, respectively.

7.2.3.3 Baseline tank configurations: Baseline integral and nonintegral tank configurations were defined for use in the analysis and evaluation of the candidate structural concepts in the concept screening analysis. The size and geometry of these nominal tanks were established based on the following:

- The tank is of conical configuration with ellipsoidal closures having an aspect ratio (a/b) = 1.30
- The tanks are covered with an insulation having a thickness of 6.00 inches
- The tanks are sized by using an overall effective fuel density of 3.978 lb/ft^3.

For the baseline aircraft,

$$W_g = 391\ 740\ lb$$

$$\text{Usable fuel per tank} = \frac{61\ 630}{2} = 30\ 815\ lb$$

$$\text{Tank volume (in as-built, warm condition)} = \frac{30\ 815}{3.978} = 7\ 746\ ft^3$$

As mentioned earlier, the basic analysis of both structure and insulation systems was performed using the aft tank of the aircraft as a model. The geometry of the aft tank and its relation to the aircraft was presented previously in Figure 83. Table 48 shows the assumed structural concepts and the major dimensions of the baseline integral and nonintegral aft tanks.

7.2.3.4 Structural models: BOSOR 4 math models were constructed for each basic tank design (integral and nonintegral) to define the internal loads for the concept screening analysis. The tank dimensions used for the models reflected the size and geometry of the nominal baseline tank configurations. Representative wall concepts were selected from the list of candidate structural concepts and their corresponding stiffnesses were used as input to the structural models.

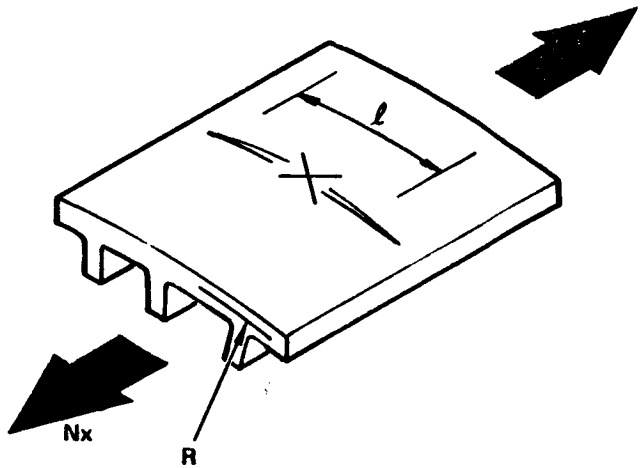

THE RESIDUAL STRENGTH OR ALLOWABLE STRESS IS DEFINED BY

$$F_g = \frac{\gamma n K_o}{\sqrt{\ell}}$$

WHERE:

γ = REINFORCEMENT EFFICIENCY PARAMETER

n = CURVATURE REDUCTION FACTOR, $n = 1/2$

K_O = STRESS INTENSITY FACTOR FOR CONDITIONS OF PLANE STRESS USED FOR THROUGH-THE-THICKNESS CRACKS, $K_O = K_C / \sqrt{\pi/2}$

K_C = PLANE STRESS FRACTURE TOUGHNESS (ASTM NOTATION)

ℓ = TOTAL CRACK LENGTH, $\ell = 2a$

Figure 117. - Fail-safe analysis of circumferential damage condition.

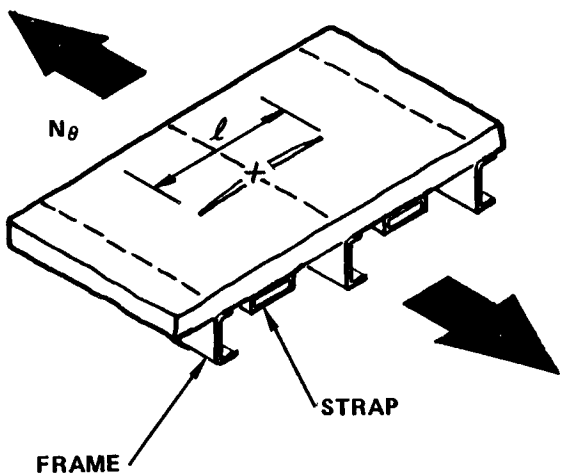

THE RESIDUAL STRENGTH OR ALLOWABLE STRESS IS DEFINED FOR A REINFORCED PANEL BY

$$F_{pg} = 1.2\, F_{tus} \left(\frac{2We + \sum \frac{Ae}{t_s}}{C_1 \ell + 2We} \right)$$

AND FOR AN UNREINFORCED PANEL BY

$$F_{po} = 1.2 \left(\frac{2We\, F_{tus}}{C_1 \ell + 2We} \right)$$

WHERE:

$2W_e$ = AN EFFECTIVE WIDTH PARAMETER

ℓ = TOTAL CRACK LENGTH, $\ell = 2a$

F_{tus} = ULTIMATE TENSILE STRENGTH OF THE SKIN MATERIAL

C_1 = LONGITUDINAL CRACK EXTENSION PARAMETER FOR PRESSURIZED FUSELAGE PANEL. A FUNCTION OF THE STRESS INTENSITY FACTOR K_O.

$\left(\frac{\sum Ae}{t_s} \right)$ = EFFECTIVE REINFORCEMENT AREA DIVIDED BY SKIN THICKNESS.

Figure 118. - Fail-safe analysis of longitudinal damage condition.

TABLE 48. - CONCEPTS AND DIMENSIONS OF BASELINE INTEGRAL AND NONINTEGRAL TANKS

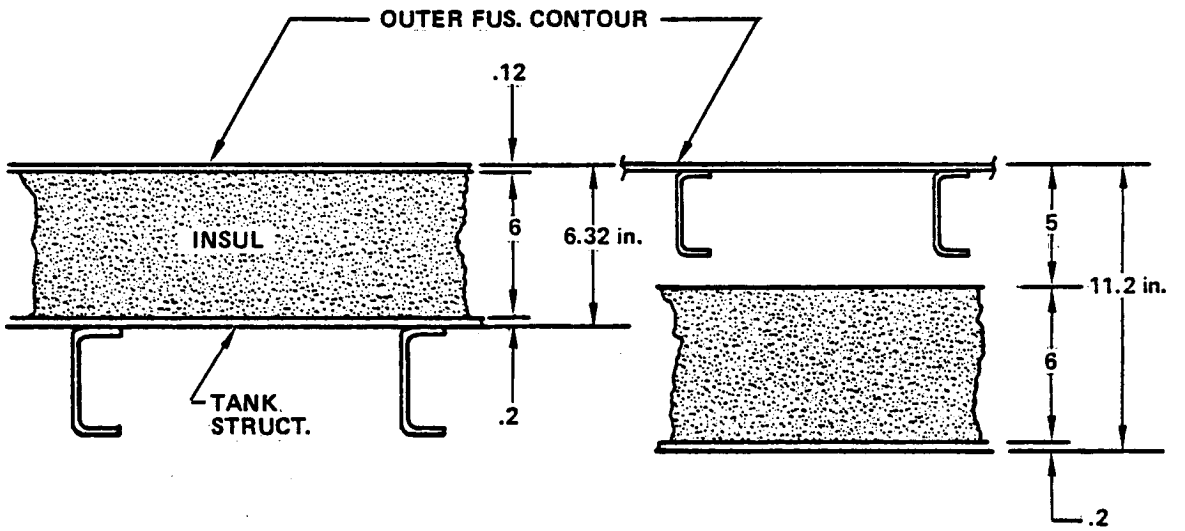

	INTEGRAL	NONINTEGRAL
Vol - ft^3	7746	7746
D_2 - ft	13.833	13.833
D_1 - ft	20.75	21.12
D_2 - ft	12.78	11.967
d_1 - ft	19.697	19.254
ℓ - ft	27.52	30.59
h_1 - ft	7.58	7.41
h_2 - ft	4.92	4.61
L - ft	40.02	42.61

7.2.3.4.1 Nonintegral tank model: The representative structural/material arrangement selected as a baseline for this design consisted of a zee-stiffened panel concept for the shell (the fuselage structure surrounding and supporting the tank) with sheet metal frames at approximately 20-inch spacing. The materials for the shell structure are the conventional 2024 and 7075 aluminum alloys. The structural configuration selected for the LH_2 tank was the blade-stiffened configuration fabricated from 2219 aluminum alloy.

A preliminary sizing of this representative concept was conducted to define the input properties for the model. For the fuselage, the shell wall had an area of 0.095 in^2 per stringer pitch which included an 0.033 in. thick skin. The internal frames were of conventional sheet metal construction with an area of approximately 0.65 in^2 (excluding any effective skin) at approximately 20 in. spacing.

The configurations used for modeling the tank reflected the baseline tank configuration, i.e., ellipsoidal closures and a conical tank. The tank closures were an unstiffened wall design with a constant thickness of 0.10 in. External rings were provided at the junction of the closures and the conical section for supporting the tank.

Pertinent dimensions of the baseline fuselage shell and tank are shown in the structural model represented in Figure 119. The tank was supported at the equators of the forward and aft tank closures. At the aft support, the tank and shell had compatible deflection (axial and radial) and rotational degrees of freedom; whereas, only radial deflection was permitted at the forward support.

The structural computer model is characterized by 150 axial node points in the tank, and 99 in the fuselage shell. Figure 120 shows the structural model with the components of the applied loads indicated. These loads reflect the limit loads components of the PLA symmetrical maneuver condition at 2.5 g. These components include the tail loads (moment and shear) applied at aft end of fuselage, the tank internal pressure and inertia loading, and the tank and fuselage temperatures. The tail loads applied at the aft fuselage were adjusted so that the combined effect of these loads and the tank inertia load would meet the specified shear and moment values at the forward end of the tank, FS 2335.

BOSOR 4 static solutions were conducted to assess the internal membrane and bending forces associated with the tank and fuselage structure. Separate solutions were obtained using each component of the applied loads to assess the impact of the individual load components as well as providing the basis for defining other load conditions.

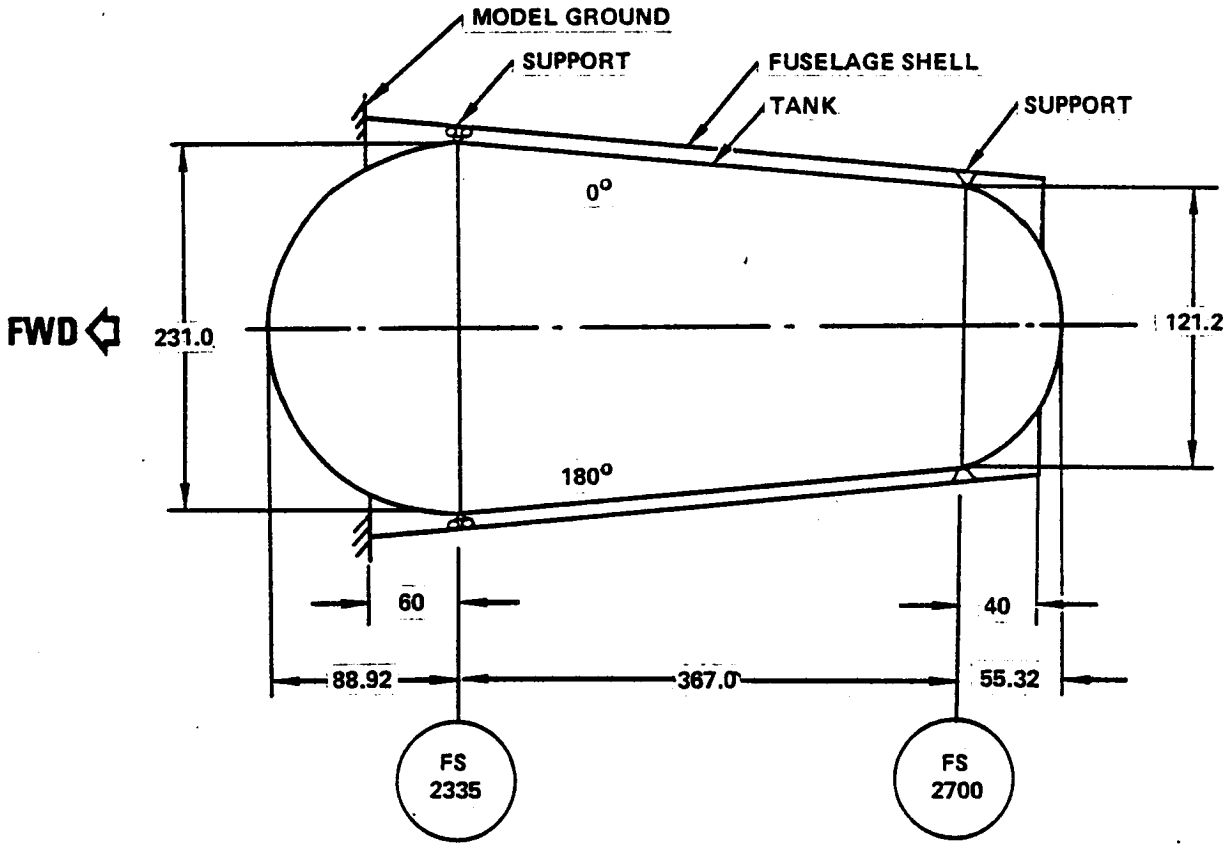

Figure 119. - Fuselage and tank dimensions used for the nonintegral tank structural model.

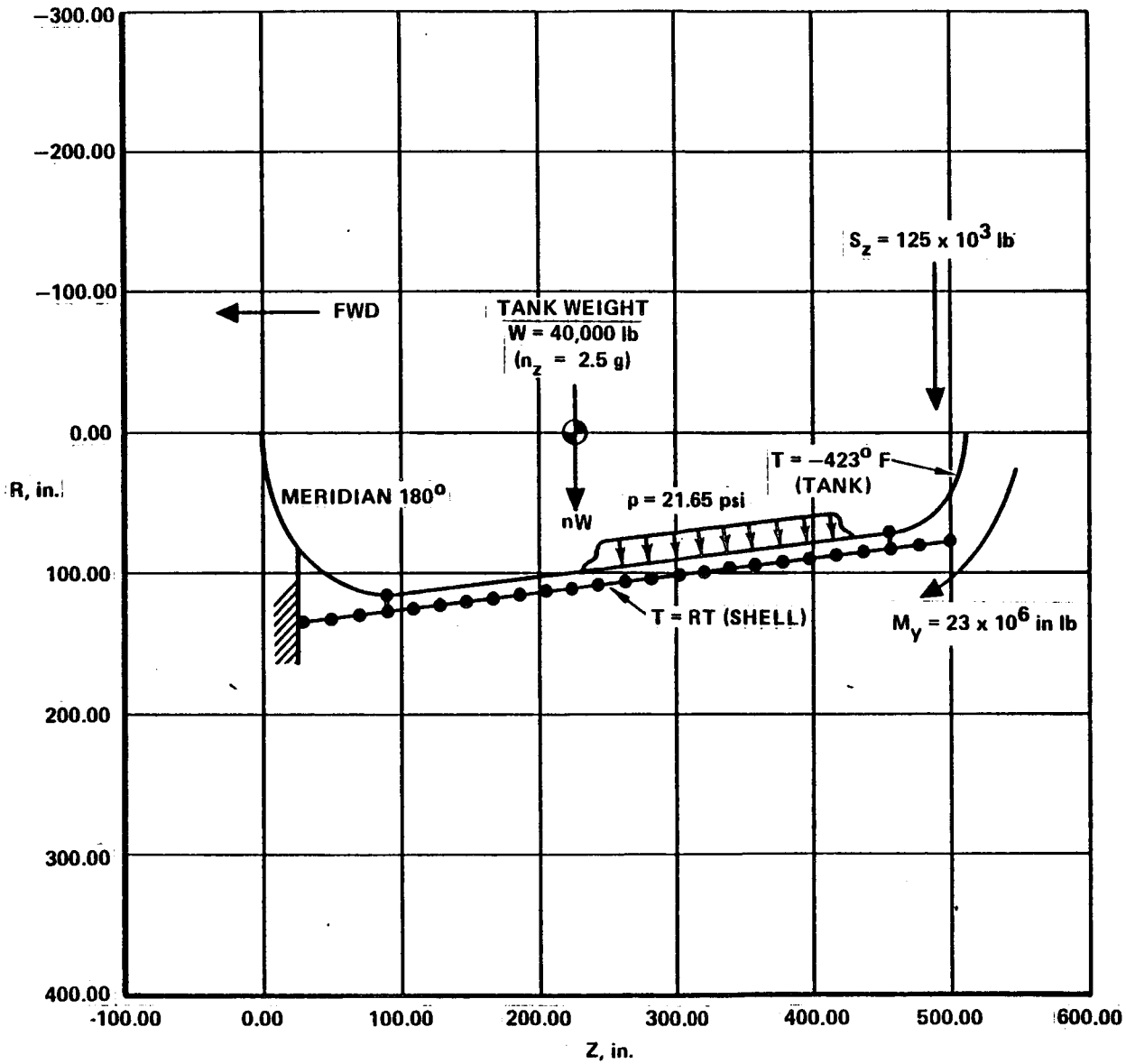

Figure 120. - Applied loads and structural model for the nonintegral tank design.

Results of the static solutions include both printout and plots of the displacements, membrane forces, and bending moments as a function of arc length. The arc length is measured from the apex of the forward tank closure aft along the tank meridian to the apex of the aft tank closure, approximately 640 inches. The plots then proceed to the forward end of the shell (fixed boundary) aft along the shell meridian.

The three displacement components: meridional (U), circumferential (V) and normal (W) were defined for each load component. Figure 121 displays a plot of the normal displacement (W) for each of the load components, i.e., the temperature, air load, and internal pressure conditions.

The inplane stress and bending moment resultants for each of the applied load conditions are shown in Figures 122 through 127. The meridional (N_1), hoop (N_2) and inplane shear (N_{12}) stress resultants are displayed in Figures 122, 124 and 126 for the internal pressure, airload and temperature conditions, respectively. The corresponding meridional (M_1), hoop (M_2) and twisting (M_T) moments are shown in Figures 123, 125, and 127.

7.2.3.4.2 Integral tank model: The representative structural candidate selected for the modeling effort on the integral tank design used the zee-stiffened panel concept with sheet metal frames at approximately 20 inch spacing. Tank material was 2219 aluminum alloy. Truss structures composed of Boron/Epoxy tubular members were provided as interface skirts between tank and fuselage. Conventional zee-stiffened structure using 2024 aluminum alloy was selected for the short segments of fuselage at both ends of the model.

The integral tank design represented in the structural model is shown in Figure 128. The tank was cantilevered from the forward end of the fuselage segment approximately 60.0 inches forward of the interface structure. The structural model for the integral tank design was characterized by approximately 150 axial node points for the tank, and 72 points in the fuselage segment and interface skirts.

The preliminary sizing of the structural concepts provided the necessary input data for the model. For the small segments of fuselage at the forward and aft end of the model, conventional zee-stiffened structure was utilized with the same material properties as described for the nonintegral tank design. The input data for the interface trusses reflected Boron/epoxy tubular elements having an area of 2.2 in^2 and a inertia value of 1.0 in^4. The input for the tank structure, which must support both the flight and internal pressurization loads, reflected the zee-stiffened design with an area of approximately 0.20 in^2 per stringer pitch. The tank closures were ellipsoidal in configuration and of unstiffened wall design with a constant thickness of 0.10 in.

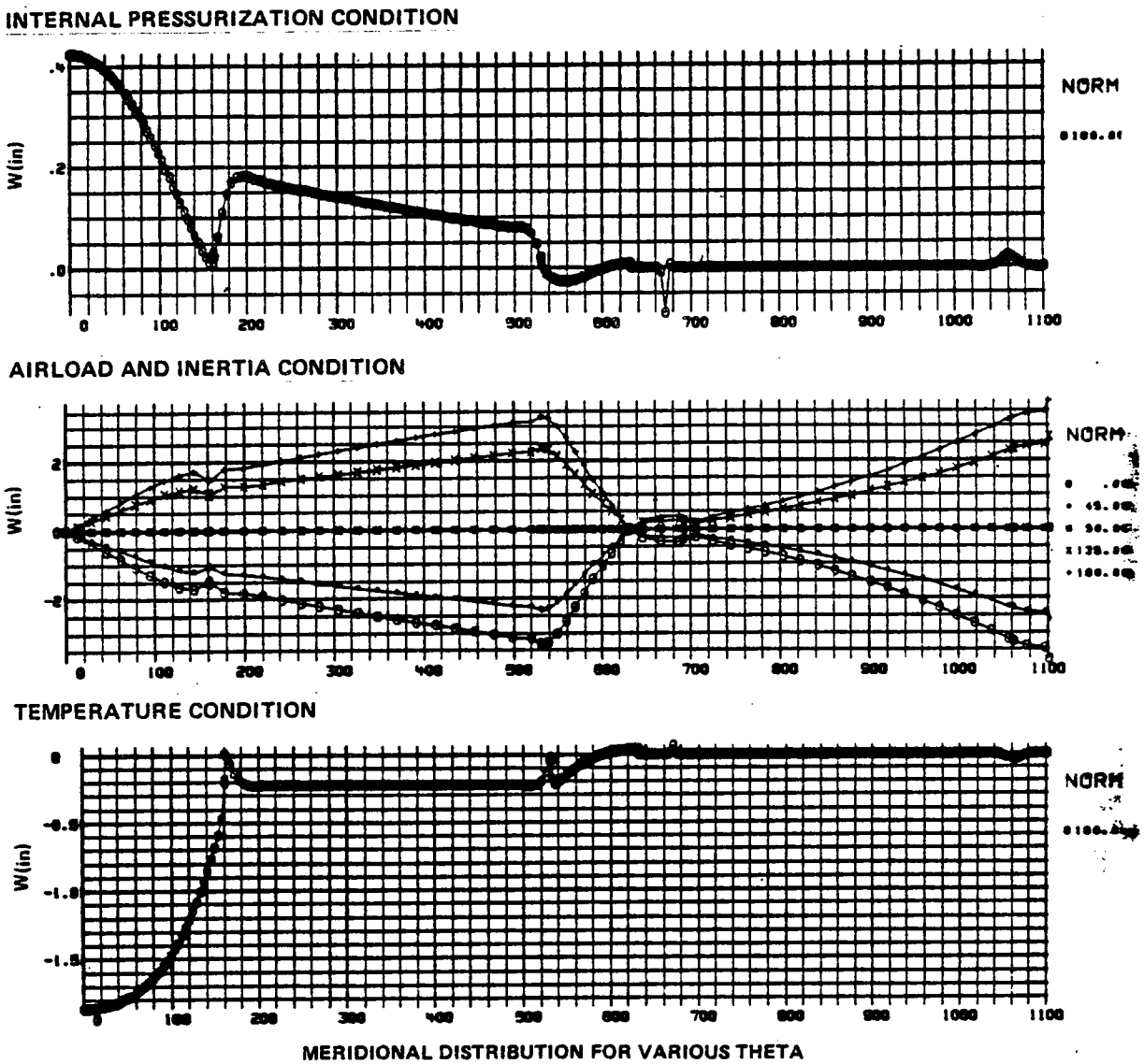

Figure 121. - Normal displacements of the nonintegral tank structural model.

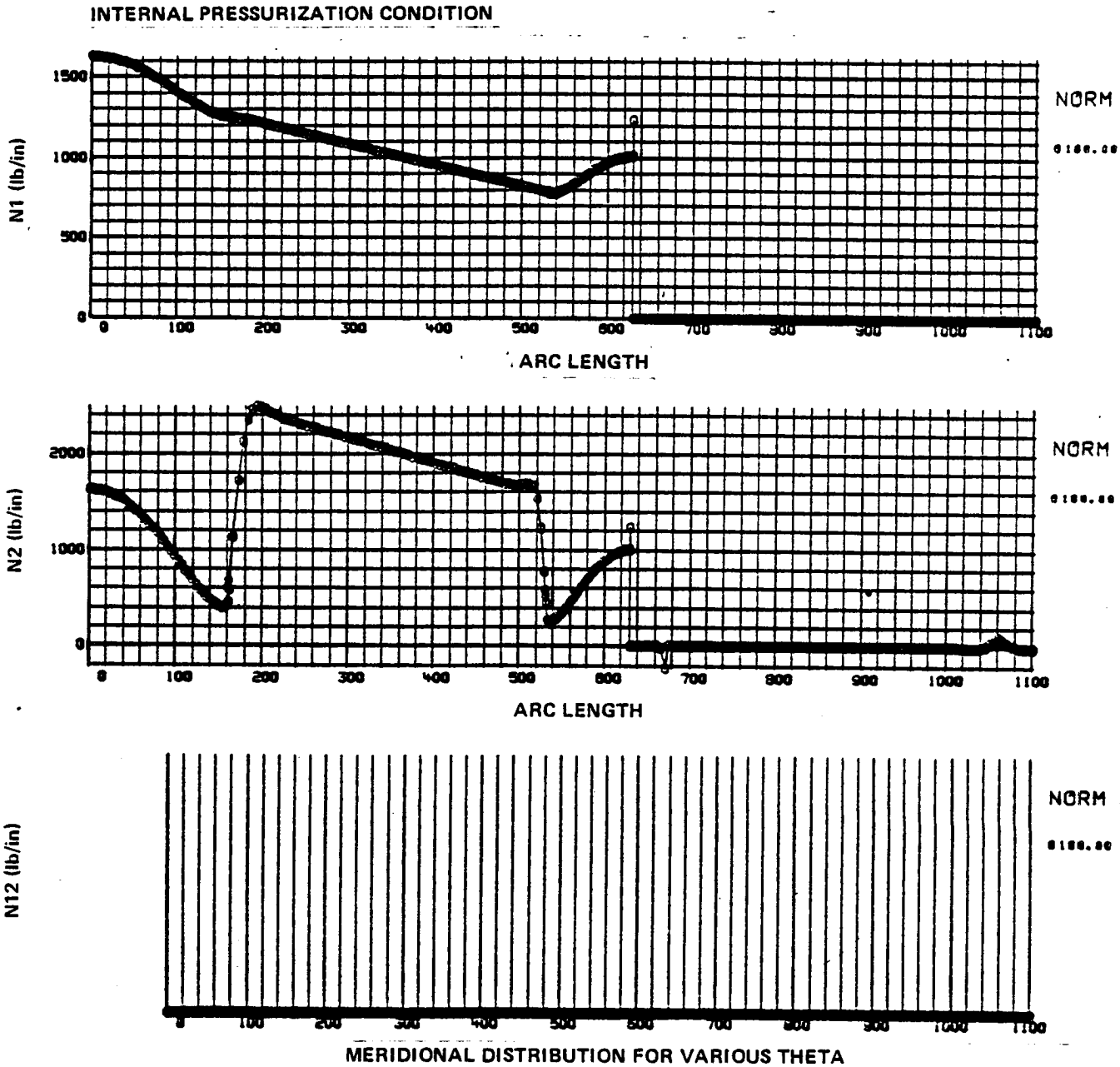

Figure 122. - Inplane stress resultants for the internal pressurization condition, nonintegral tank design.

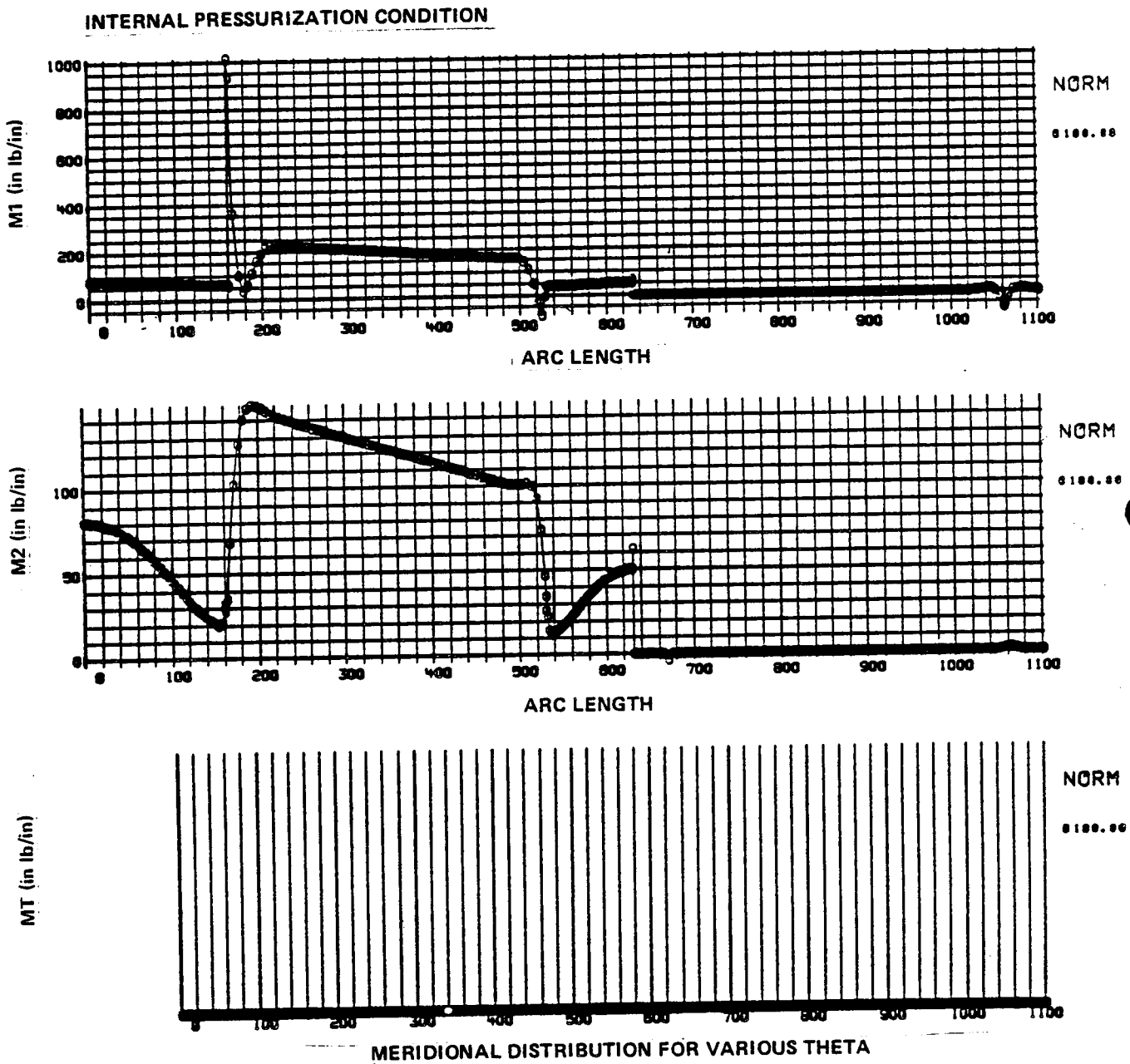

Figure 123. - Bending moments for the internal pressurization condition, nonintegral tank design.

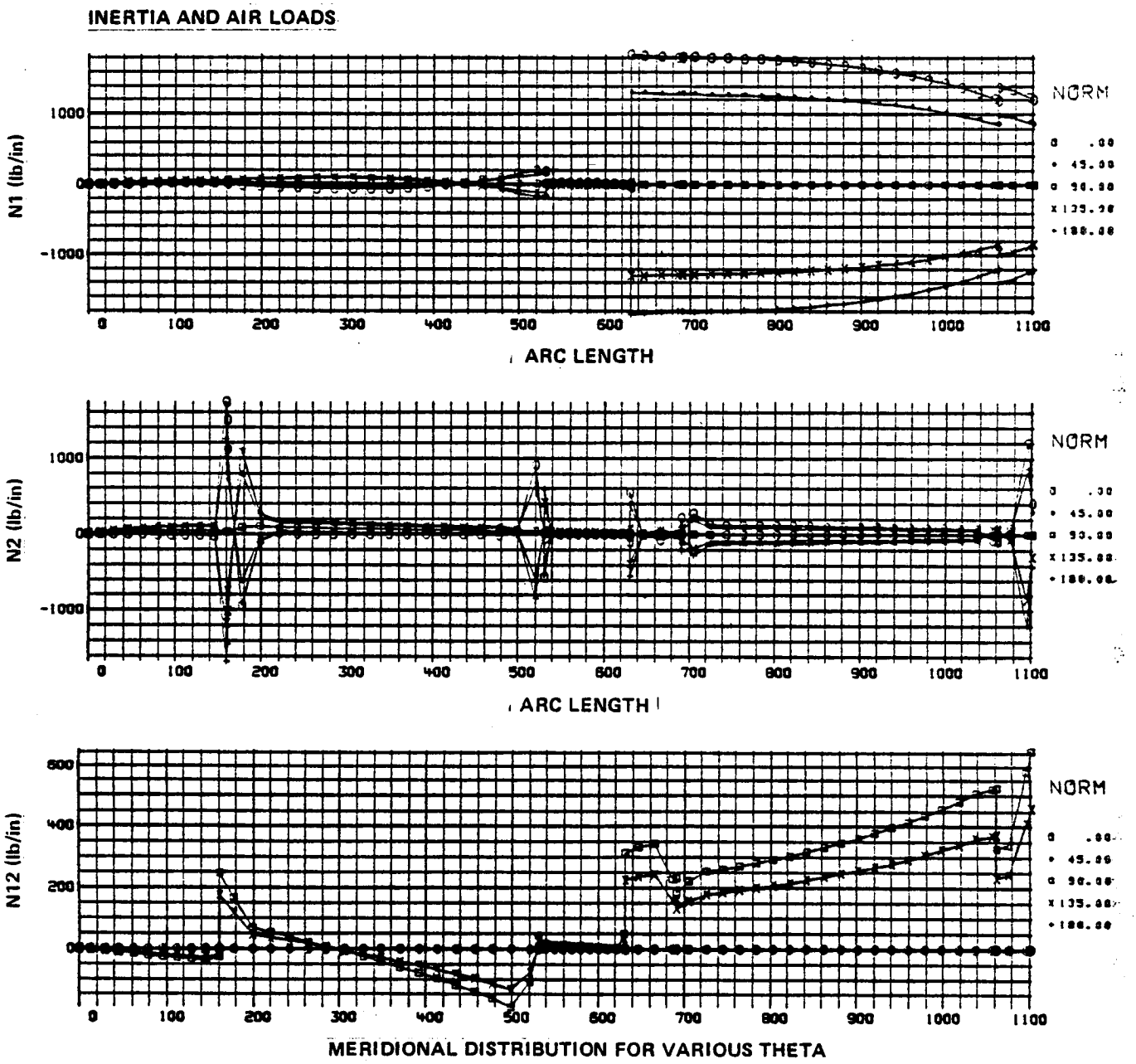

Figure 124. - Inplane stress resultants for the inertia and air load condition, nonintegral tank design.

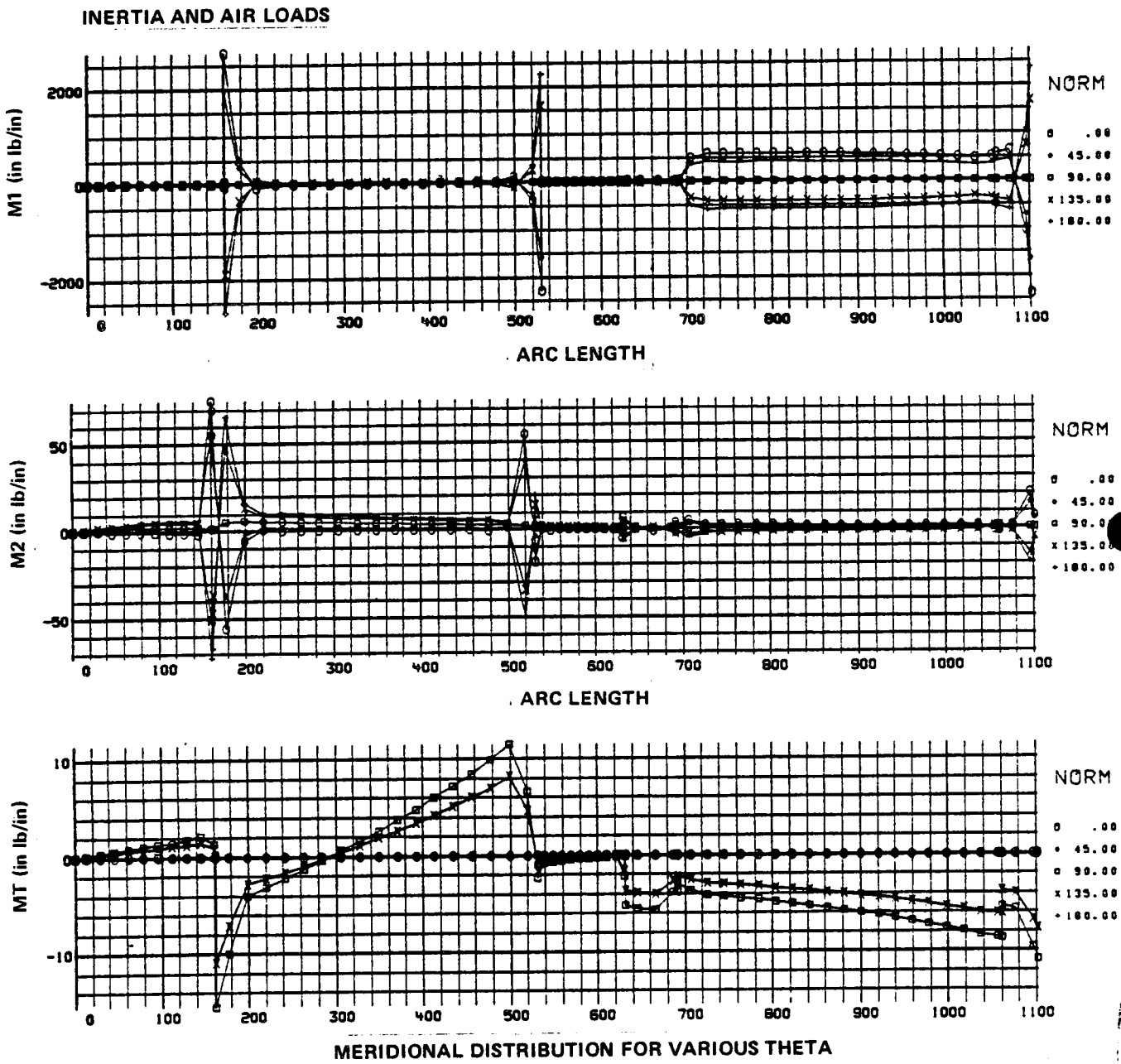

Figure 125. - Bending moments for the inertia and air load condition, nonintegral tank design.

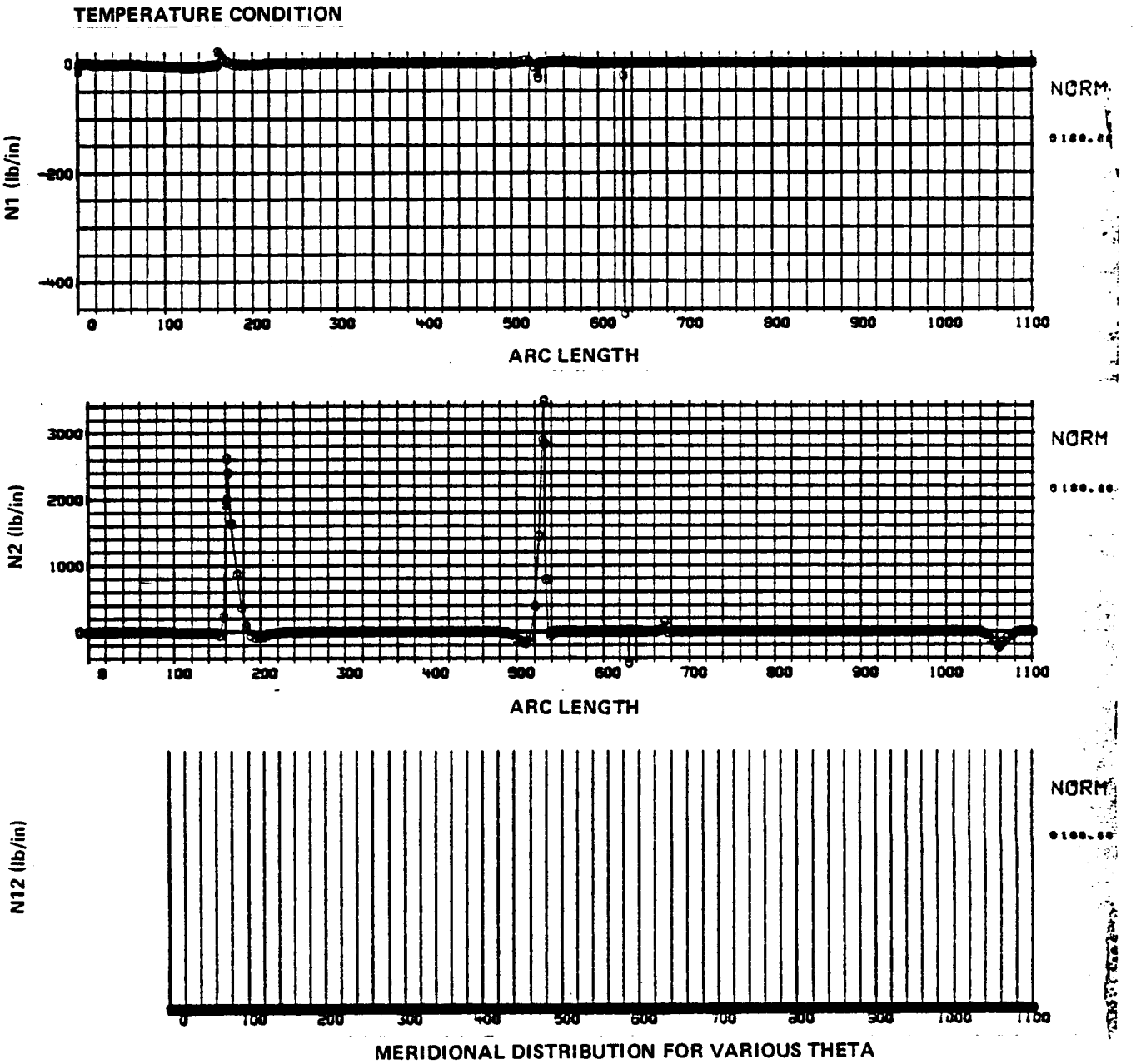

Figure 126. - Inplane stress resultants for the temperature condition, nonintegral tank design.

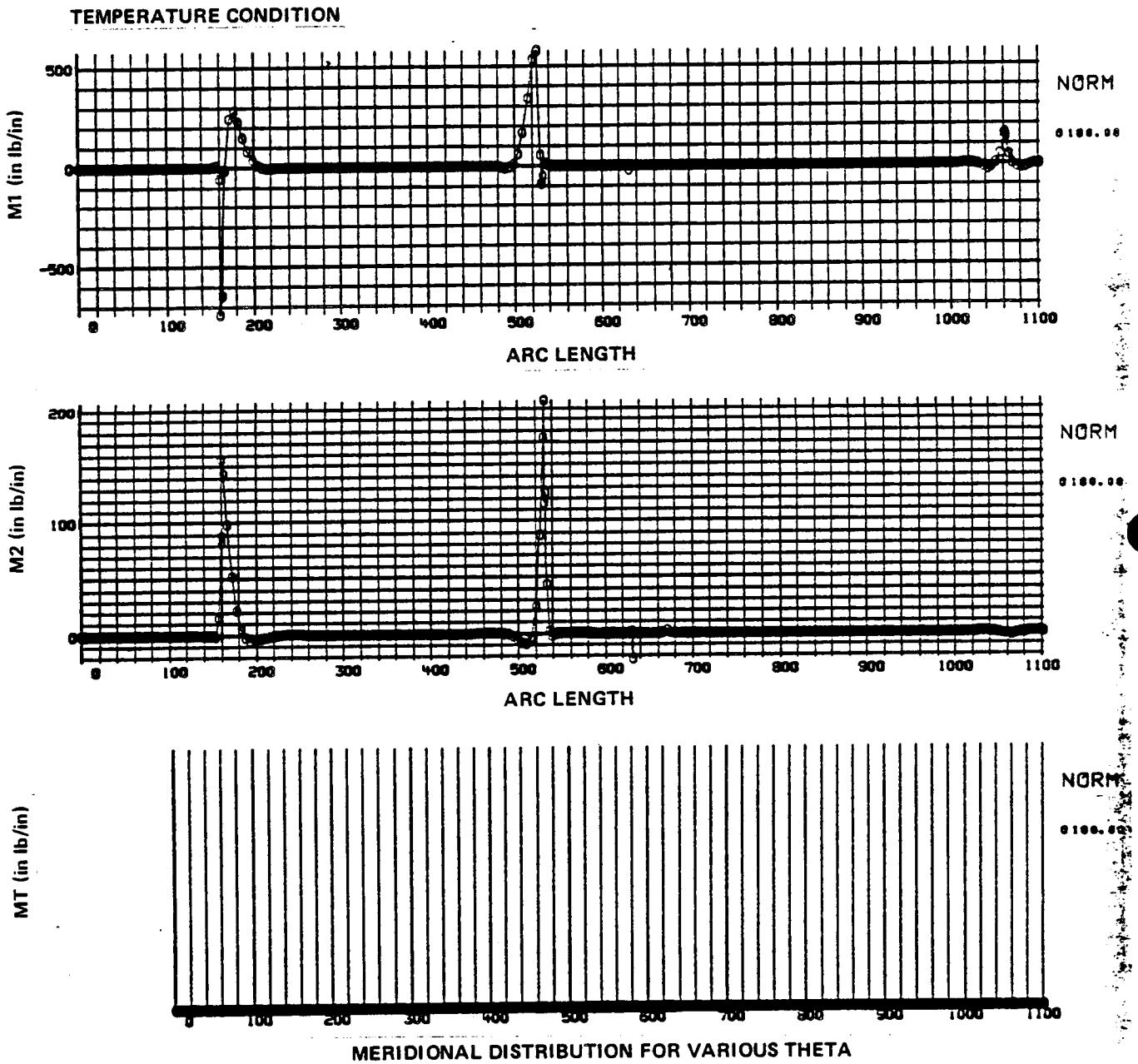

Figure 127. - Bending moments for the temperature condition, nonintegral tank design.

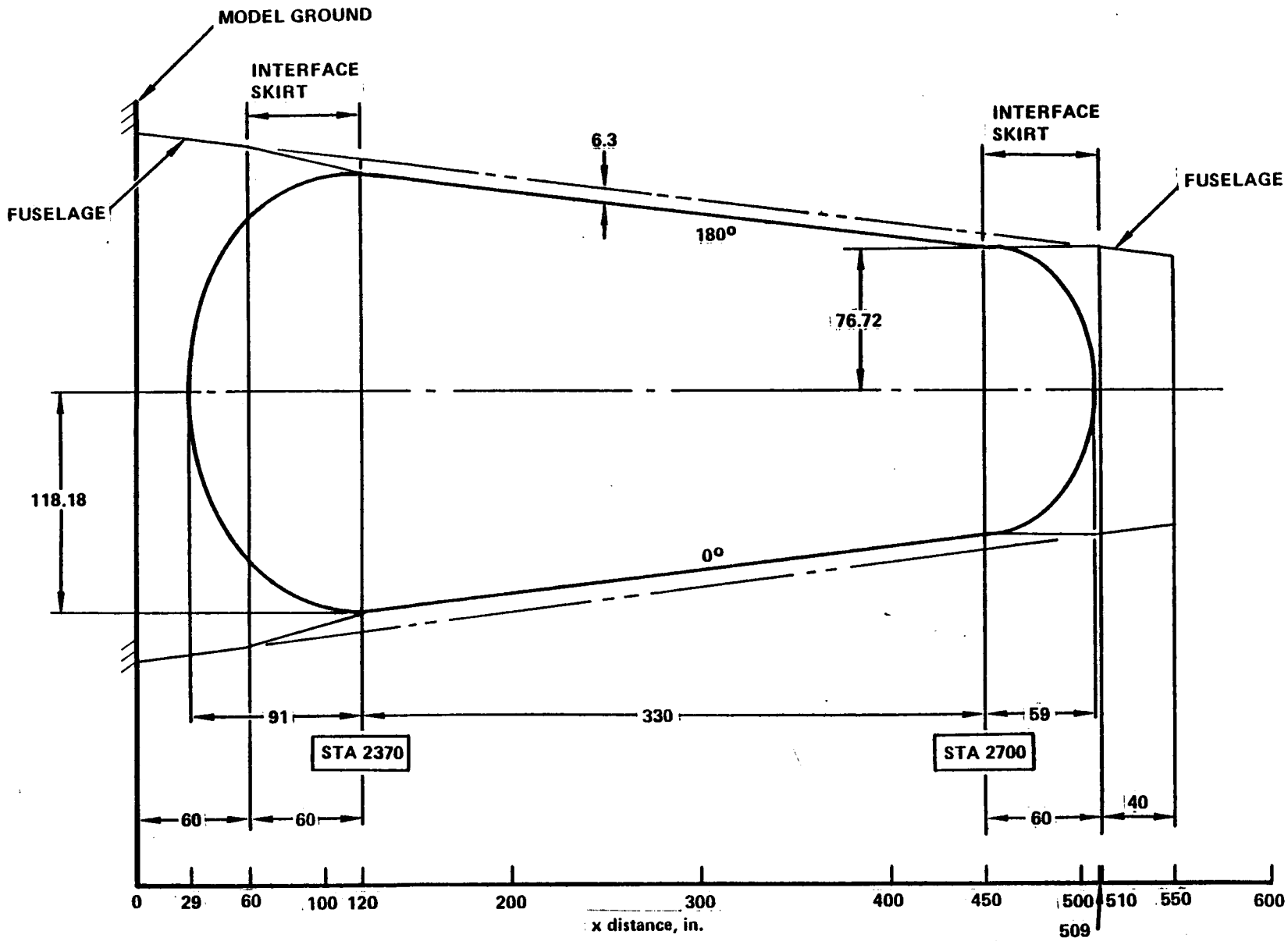

Figure 128. - Fuselage and tank dimensions used for the integral tank structural model.

Figure 129 represents a lot of the structural model with the applied loads simulating the PLA flight condition shown. Similar to the nonintegral tank design, static solutions were conducted on the integral tank model and displacements and stress resultants were obtained.

The normal displacements (W) for each component of the PLA flight condition are shown in Figure 130. The plots on this figure present the displacements due to the temperature condition, the airloads, and pressurization conditions respectively, starting from the bottom. This figure presents the displacements as a function of arc length measured along the shell meridian. This measurement initiates at the forward end of the fuselage shell (fixed boundary) and proceeds aft along the meridian to the equator of the forward tank closure. The arc length is then measured from the apex of the forward tank closure to the equator, and then proceeds along the tank cylinder to the equator of the aft tank closure and continues to the apex of the aft closures. The arc length then proceeds from the forward end of the aft interface skirt through the skirt and aft fuselage shell. The arc length in Figure 130 is segmented and titled to indicate the various structural components.

The inplane stress and bending moment resultants for each of the applied load components are displayed in Figures 131 through 136. The first two figures present the stress and bending moment resultants for the internal pressurization condition, and the remaining figures present the resultants in the same order for the airload and temperature conditions, respectively.

7.2.3.5 Point design environment: The internal load environment imposed on the aft tankage of the liquid hydrogen-fueled subsonic transport was defined at selected locations, hereafter known as point design regions, and used as the basis for the evaluation of the candidate concepts.

The design conditions and their associated flight parameters were prevented in Section 7.2.1.4. Also included were the resulting external loads (vertical shear and bending moment) imposed on the fuselage afterbody by these flight conditions. The load components for these conditions include the airloads (tail and inertial loads), the internal pressurization of the

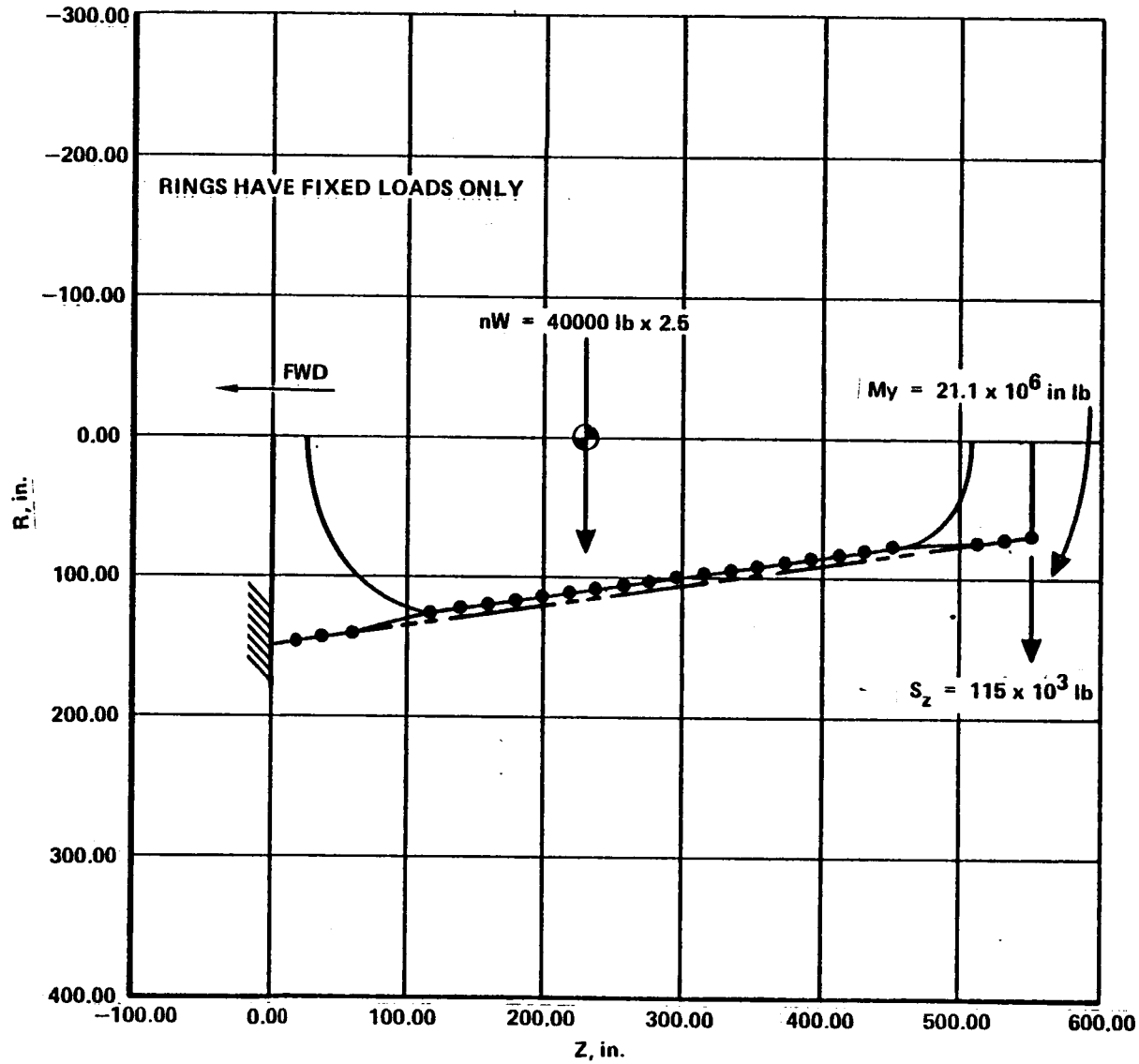

Figure 129. - Applied loads and structural model for the integral tank design.

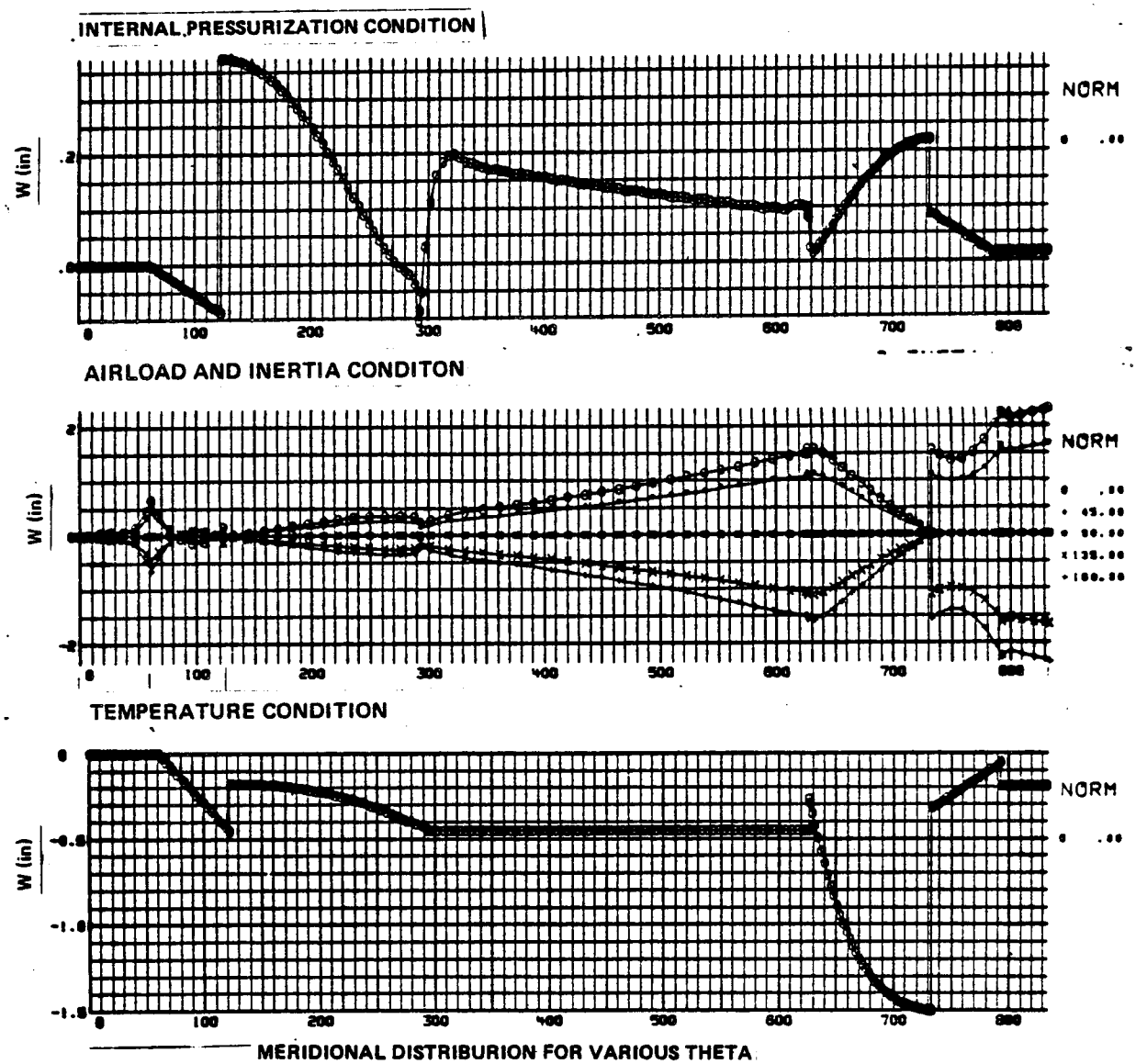

Figure 130. - Normal displacements of the integral tank structural model.

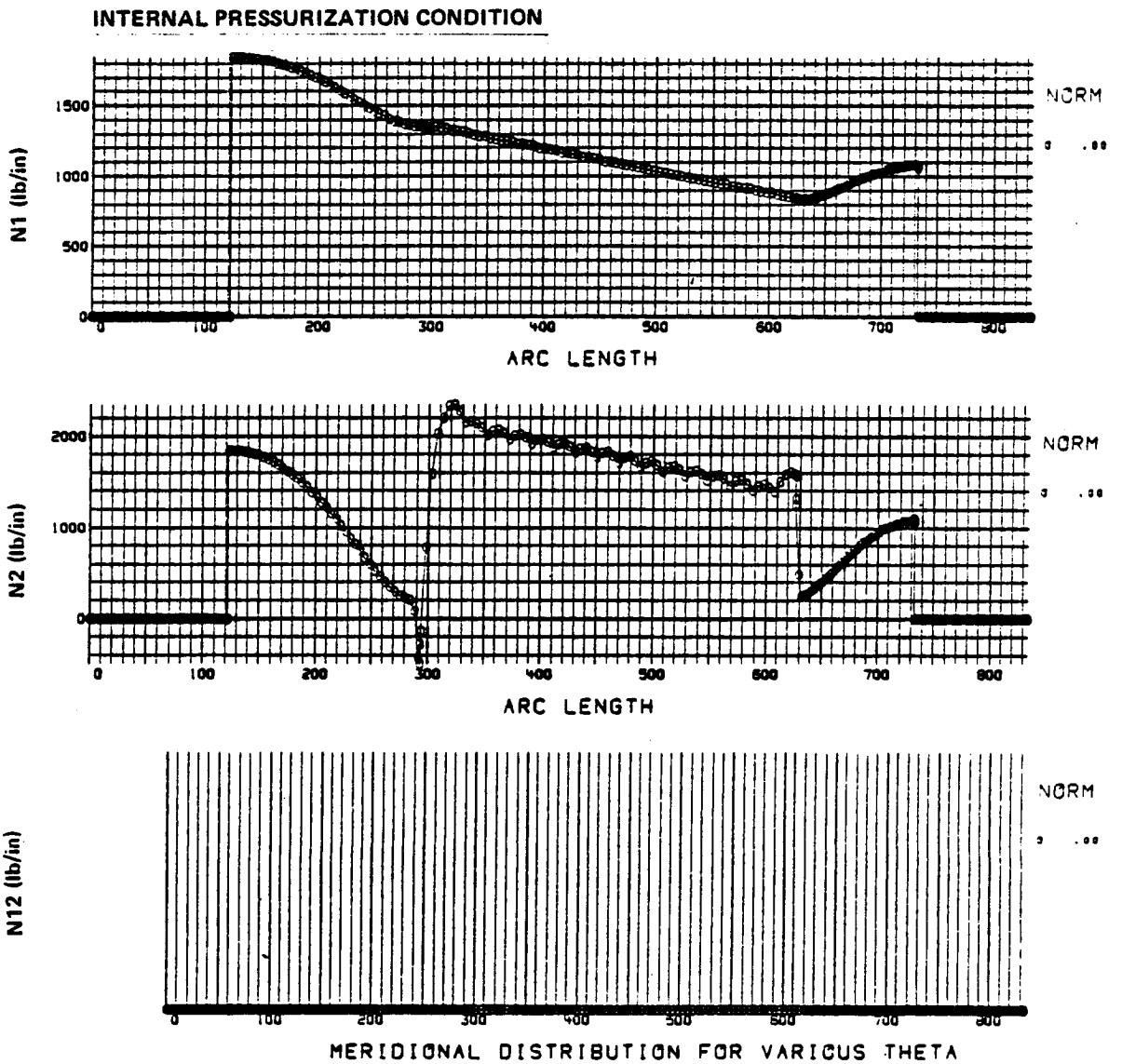

Figure 131. - Inplane stress resultants for the internal pressurization condition, integral tank design.

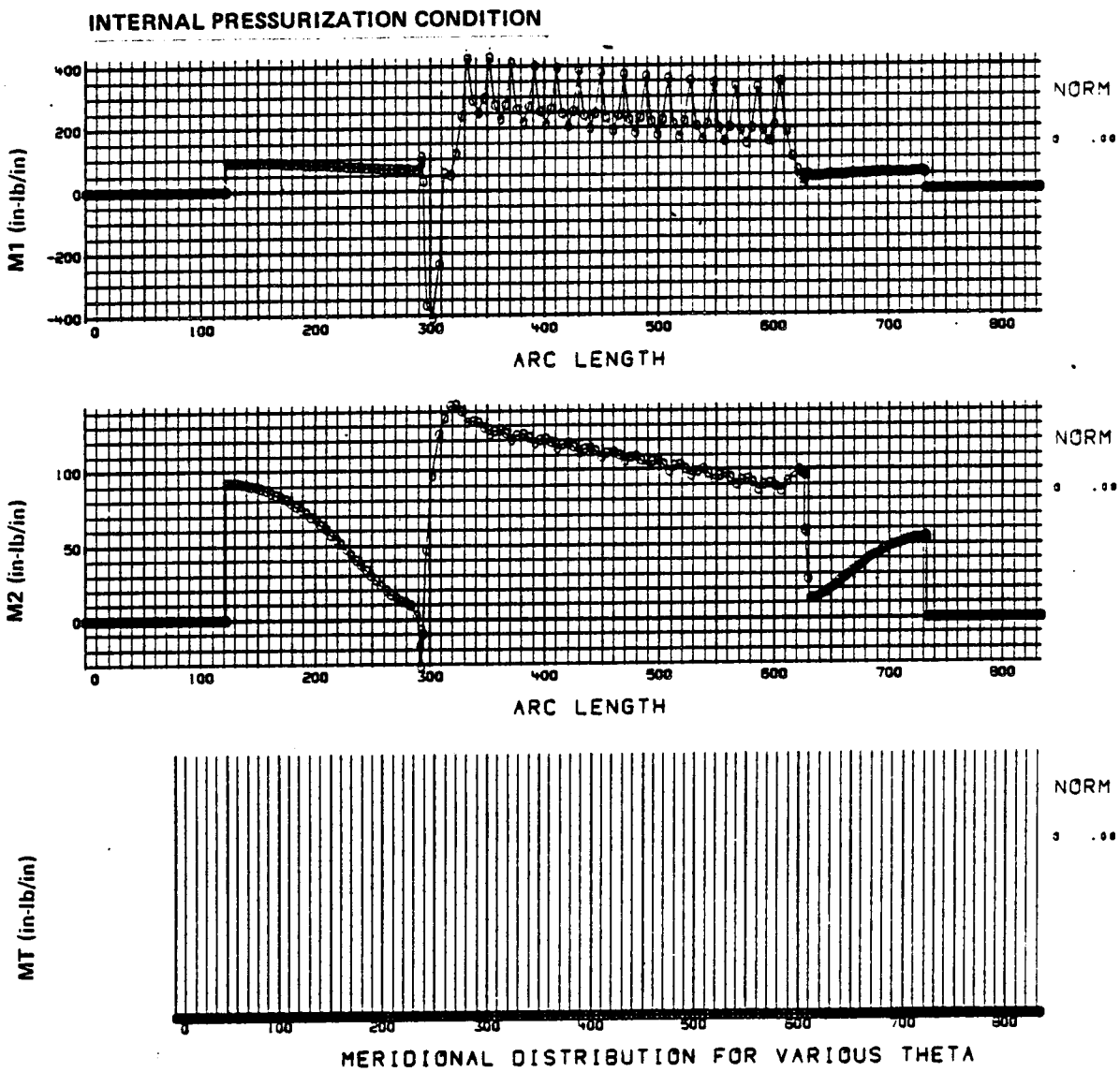

Figure 132. - Bending moments for the internal pressurization condition, integral tank design.

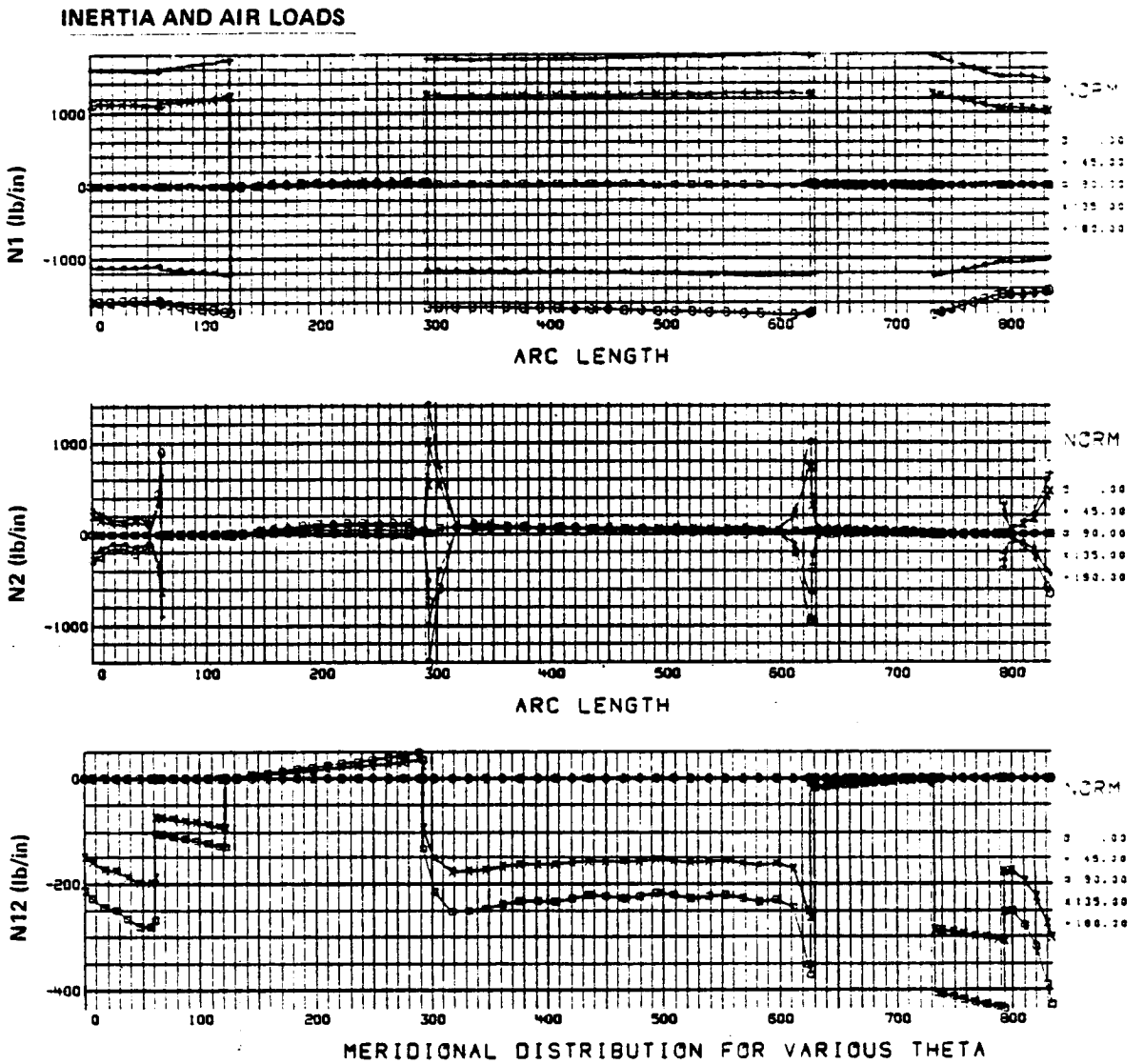

Figure 133. - Inplane stress resultants for the inertia and air load condition, integral tank design.

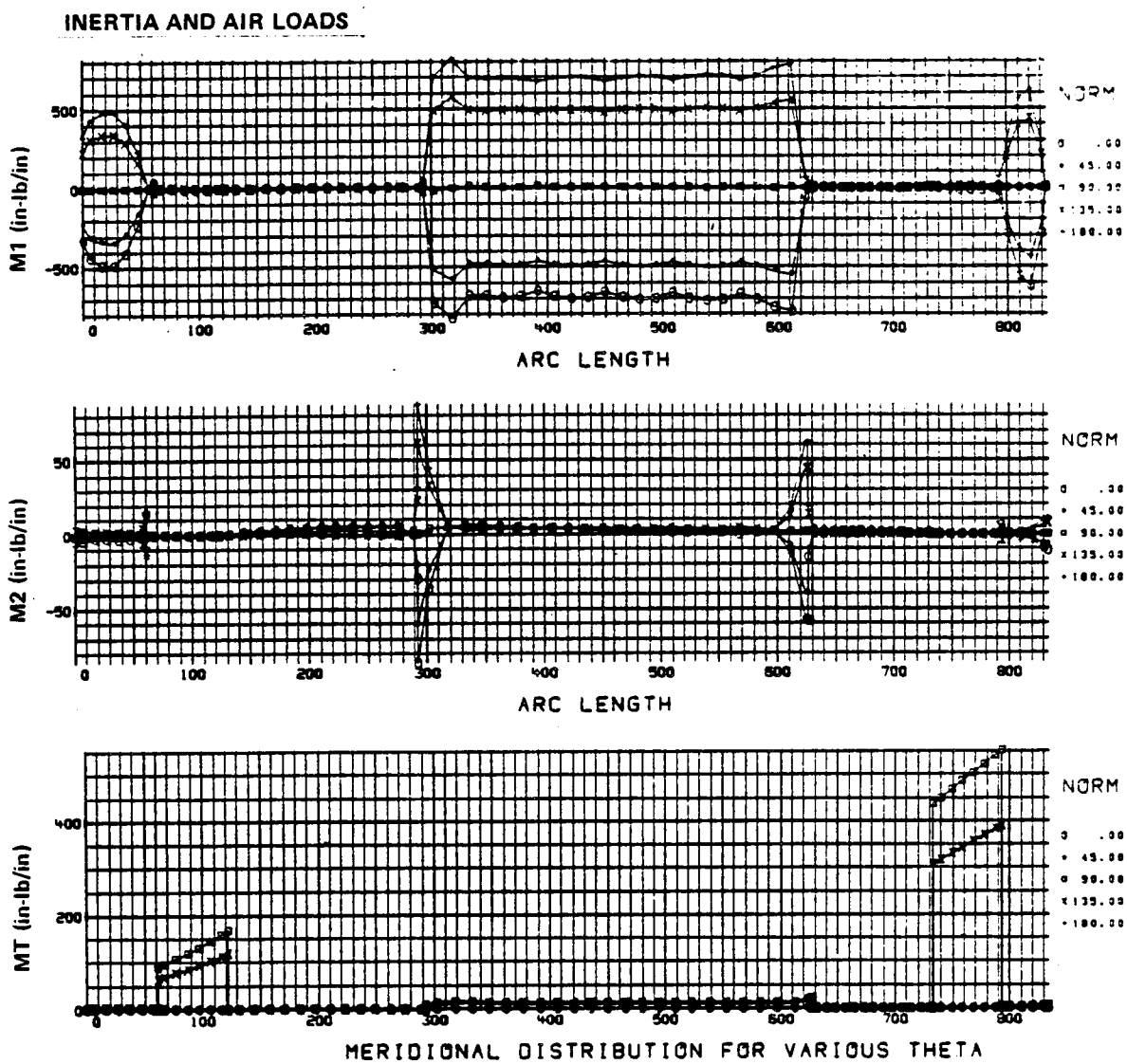

Figure 134. - Bending moments for the inertia and air load condition, integral tank design.

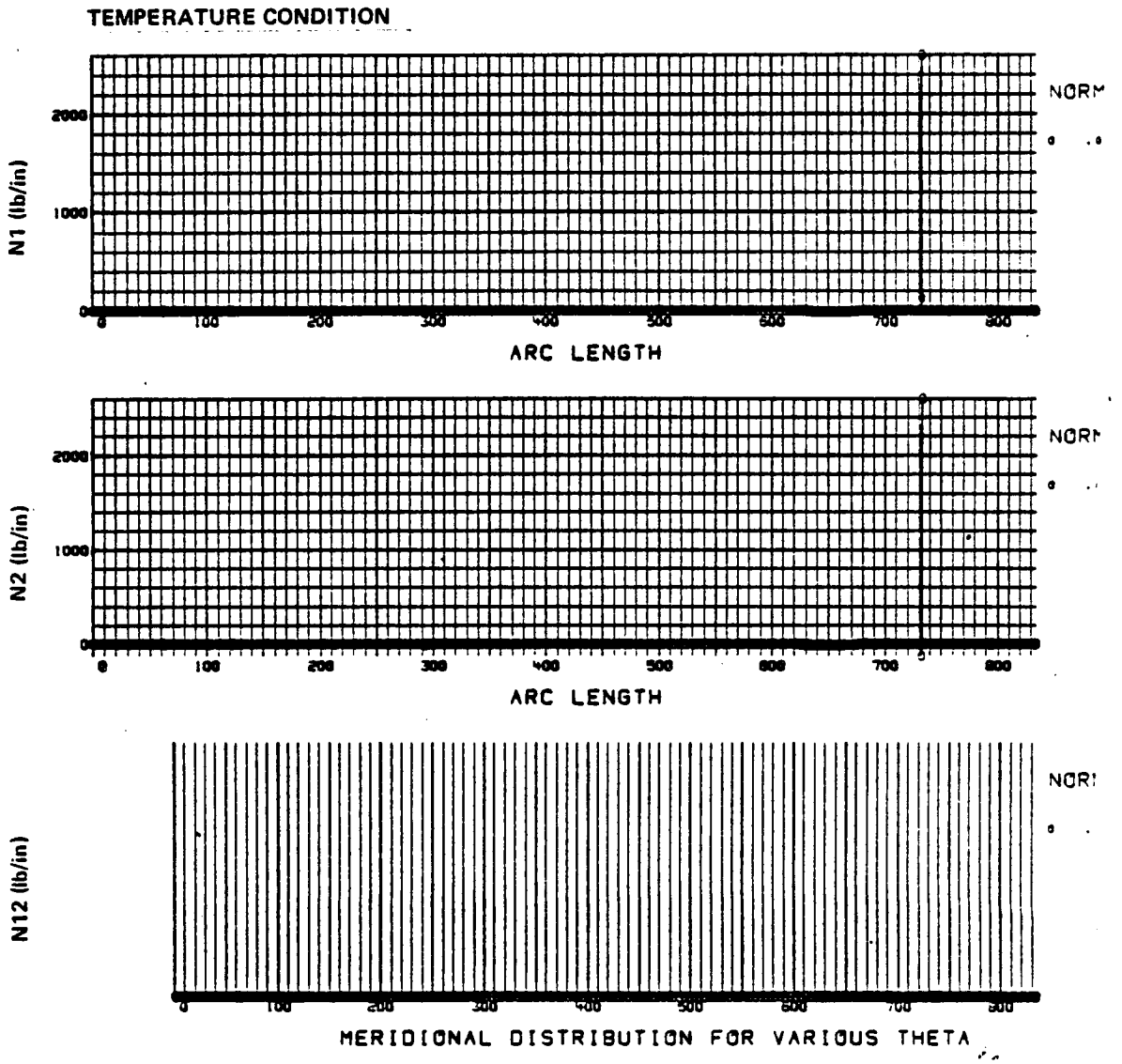

Figure 135. - Inplane stress resultants for the temperature condition, integral tank design.

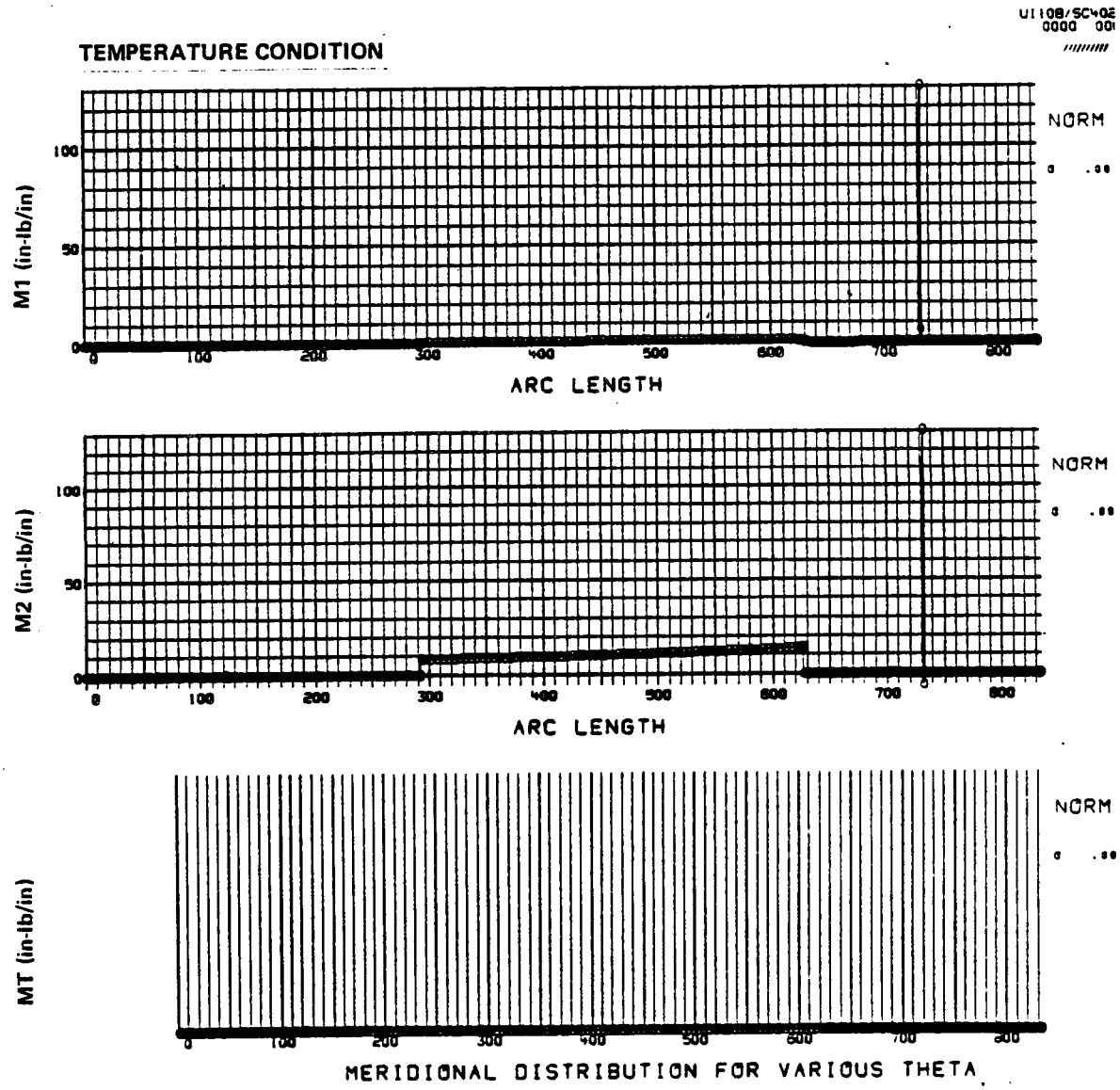

Figure 136. - Bending moments for the temperature condition, integral tank design.

tank, and the temperature environment. BOSOR static solutions were conducted for each of these load components to define the overall internal load distribution for each basic tank design, i.e., integral and nonintegral. These results were presented in the preceding Section (7.2.3.4) entitled Structural Models. These internal loads were then used to define the point design environment for each flight condition. For example, the inplane and bending stress resultants due to the internal pressure condition from the structural model were multiplied by the pressure ratio to form the corresponding stress resultants for each flight condition.

The tank pressure schedule for each of the design flight conditions is presented in Table 49. The nomenclature and safety factors used in developing this schedule are described in Section 7.2.1.

The point design regions selected for the structural analysis of the nonintegral and integral tank designs are presented in Figure 137. These regions, which are shaded on this figure, correspond to the one-quarter and three-quarter lengths between the equators of the forward and aft tank closures.

The load/temperature environments were defined at three circumferential locations at each of the above design regions. Examples of these results are presented in Tables 50 through 52. These tables show the inplane stress resultants for the PLA, Negative Maneuver and Cruise conditions at the tank quarter-length point design region.

TABLE 49. - TANK PRESSURE SCHEDULE

Flight Cond.	Alt (ft)	$P_{nom.}$ (psia)	$P_{atm.}$ (psi)	ΔP (psi)	P_{op} (psi)	P_{Limit} (psi)	P_{ult} (psi)
Positive Low Angle	22 000	21.0	6.2	14.8	16.3	16.3	24.4
Pitching Maneuver	S.L.	21.0	14.7	6.3	6.9	6.9	10.4
Negative Maneuver	22 000	21.0	6.2	14.8	16.3	16.3	24.4
Cruise	35 000	21.0	3.4	17.6	19.4	19.4	29.1

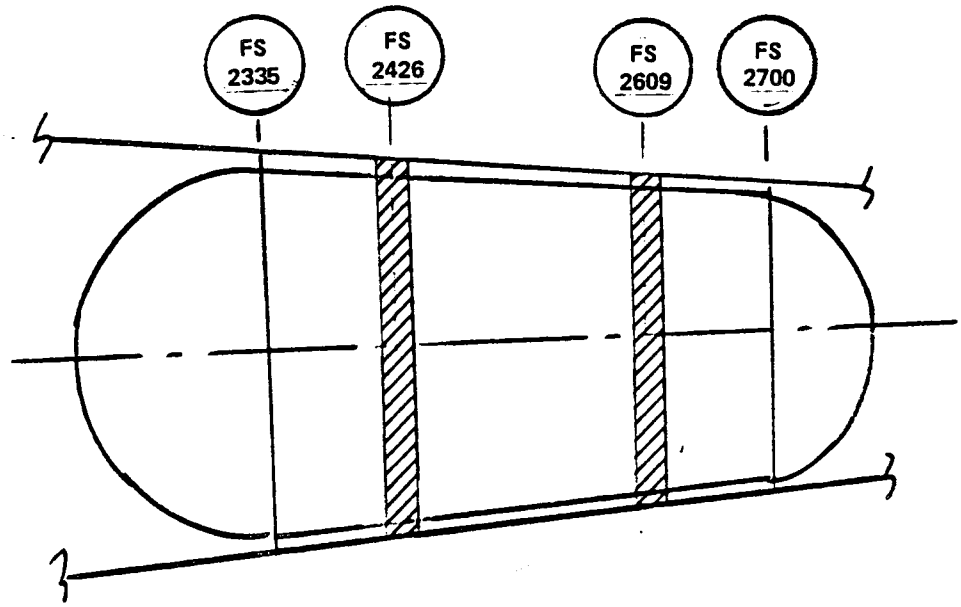

NONINTEGRAL TANK

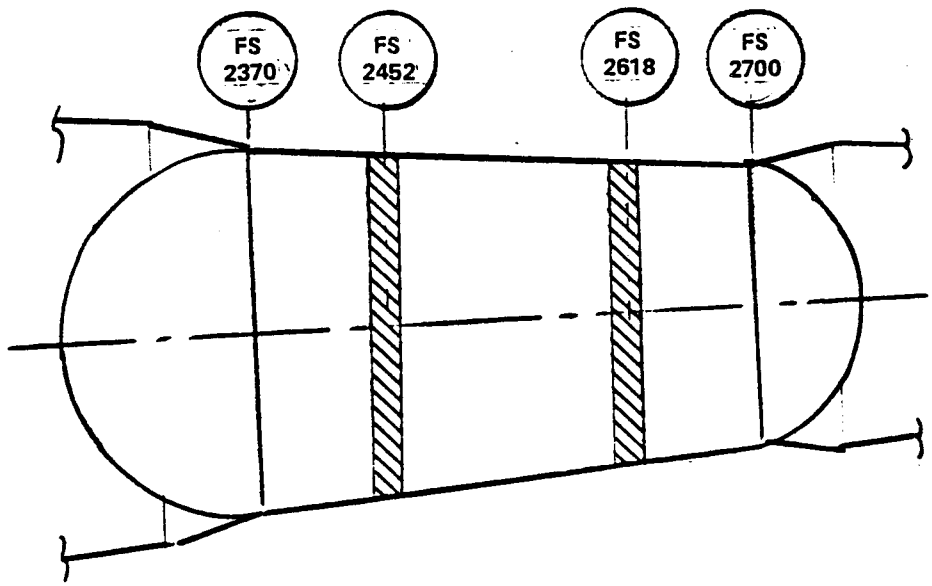

INTEGRAL TANK

Figure 137. - Point design regions.

TABLE 50. - POINT DESIGN LOAD ENVIRONMENT, PLA FLIGHT CONDITION

Structural Component	Circumf. Location (Degrees)	Nonintegral Tank Design			Integral Tank Design		
		Membrane Forces (lb/in)			Membrane Forces (lb/in)		
		N_1	N_2	N_{12}	N_1	N_2	N_{12}
Fuselage	0	2669	173	0			
	90	0	0	423			
	180	-2670	-174	0			
Tank	0	1184	2545	0	3983	2370	0
	90	1313	2667	33	1429	2378	347
	180	1442	2789	0	-1129	2386	0

1. Ultimate loads.
2. Tank quarter-length location from the forward head equator.

TABLE 51. - POINT DESIGN LOAD ENVIRONMENT, NEGATIVE MANEUVER CONDITION

Structural Component	Circumf. Location (Degrees)	Nonintegral Tank Design			Integral Tank Design		
		Membrane Forces (lb/in)			Membrane Forces (lb/in)		
		N_1	N_2	N_{12}	N_1	N_2	N_{12}
Fuselage	0	-534	-35	0			
	90	0	0	85			
	180	534	35	0			
Tank	0	1307	2545	0	514	2285	0
	90	1256	2497	13	1394	2287	69
	180	1204	2448	0	2256	2288	0

1. Ultimate loads.
2. Tank quarter-length location from the forward head equator.

TABLE 52. - POINT DESIGN LOAD ENVIRONMENT, CRUISE CONDITION

Structural Component	Circumf. Location (Degrees)	Nonintegral Tank Design			Integral Tank Design		
		Membrane Forces (lb/in)			Membrane Forces (lb/in)		
		N_1	N_2	N_{12}	N_1	N_2	N_{12}
Fuselage	0	1067	70	0			
	90	0	0	169			
	180	-1067	-70	0			
Tank	0	1582	3097	--	2692	2740	0
	90	1563	3145	13	1698	2743	139
	180	1615	3194	--	648	2746	0

1. Ultimate loads.
2. Tank quarter-Length location from the forward head equator.

7.2.3.6 Point design analysis results: The candidate structural concepts were subjected to point design analysis to define the most promising structrual concept for each of the basic types of tanks, i.e., integral and nonintegral. The candidate concepts were presented in Section 7.2.2, with the analytical methods and point design environments described in Sections 7.2.3.2 and 7.2.3.5, respectively. The structural components included in the point design analysis are represented in Figure 138. A typical insulation system is shown for reference purposes only.

7.2.3.6.1 Nonintegral design: The candidate wall concepts identified for the tank and fuselage were subjected to point design analyses to define the minimum-weight proportions. For the fuselage, zee-stiffened and hat-stiffened concepts fabricated from conventional aluminum material were investigated; whereas, for the tank, an unstiffened design (monocoque shell) was considered along with several stiffened designs (blade, zee, and tee), all based on the use of 2219 aluminum alloy

Two candidate shell configurations for the fuselage were sized for a range of frame spacings using the previously described analytical methods and point design environment.

The resultant panel cross-sectional data for the upper, mid, and lower fibers at the quarter-length location are shown in Figure 139. As can be

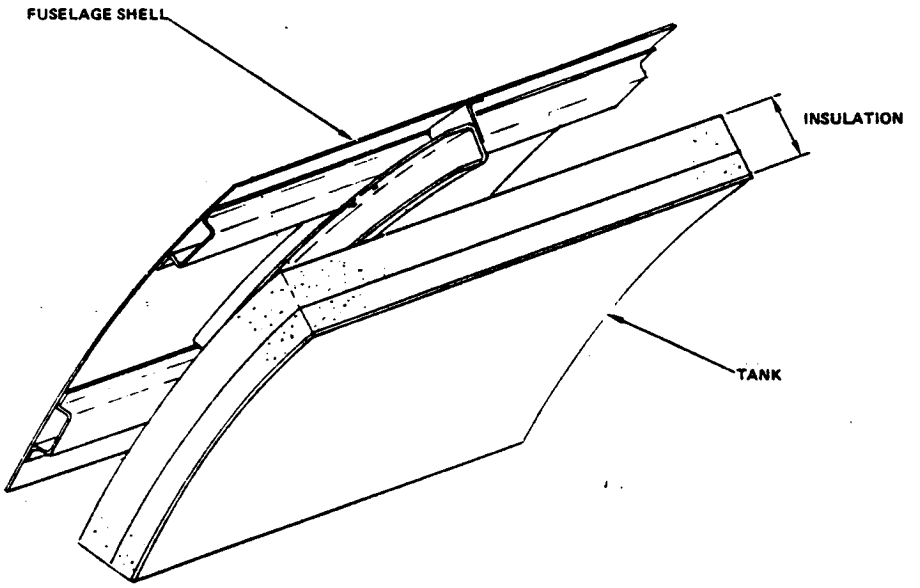

a) NONINTEGRAL TANK

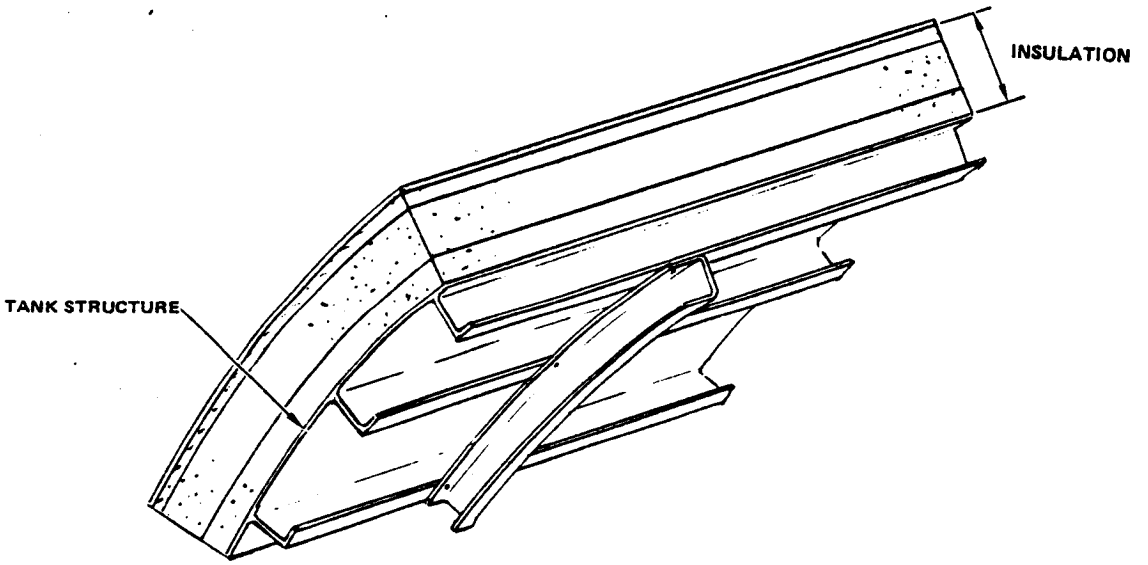

b) INTEGRAL TANK

Figure 138. - Point design structure.

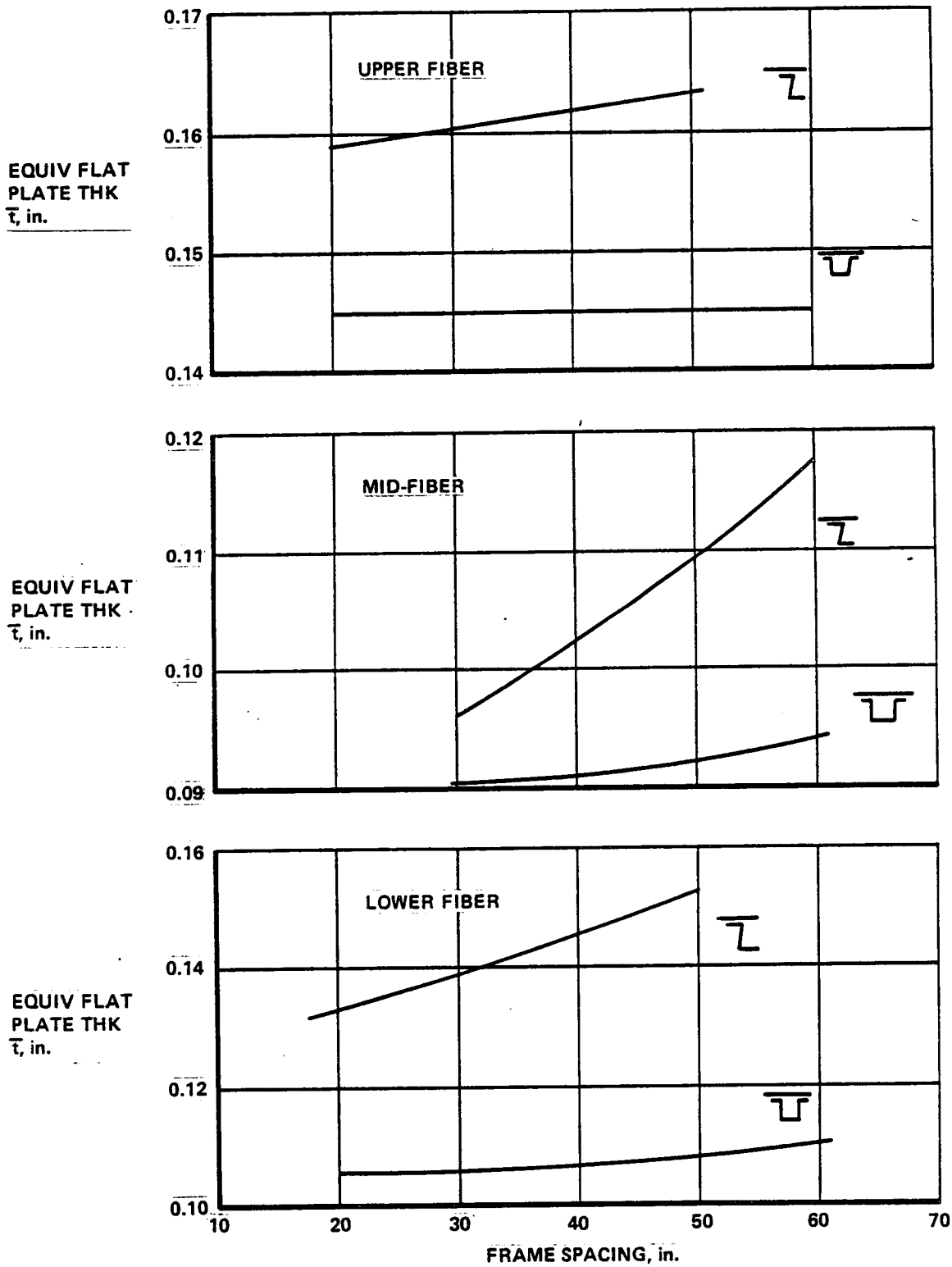

Figure 139. - Fuselage shell equivalent thickness, nonintegral design.

seen from this figure the hat-stiffened design has smaller thicknesses than the zee-stiffened design at all of the circumferential locations investigated. The equivalent thickness curves for the hat-stiffened concept are relatively insensitive to frame spacing with approximate values of 0.145 in., 0.090 in., and 0.105 in. indicated for a frame spacing of 40.0 in. for the upper, mid and lower fibers, respectively.

The minimum weight designs for the zee-stiffened concept occur at the minimum frame spacings studies and in general are very senstive to changes in frame spacing. For comparison purposes, the corresponding thicknesses of the zee-stiffened design at 40.0 in. spacing are 0.161 in., 0.103 in., and 0.146 in. for the upper, mid and lower fibers, respectively.

Representative sheet metal frames were sized for application to both fuselage shell concepts. The frame designs were evaluated for both strength and stiffness at the two point design regions on the fuselage.

The frame stiffness requirements were predicated using the criteria developed by Shanley in Reference 33, which ensures failure of the sheet-stringer panel between frames, i.e., prevents general instability. The frame bending stiffness (EI), and the corresponding area and equivalent panel thickness for various frame spacings at the two point design regions are shown in Table 53. The maximum bending moments and shell diameters are also indicated on this table.

The basic strength of the frames were assessed using the loads obtained from the BOSOR static analysis. Figure 140 displays the internal hoop forces acting in the frame as a function of the circumferential angle. The internal forces for both the maximum up-bending (PLA condition) and downbending (negative maneuver) conditions are presented. At the fuselage quarter length location a maximum hoop force of ± 2 400 lb (limit) is indicated; whereas, only ± 1 750 lb (limit) is shown at the three-quarter length location.

Table 54 presents the frame analysis conducted using the internal frame loads from the model. The frame hoop forces were adjusted for frame spacings greater than that used in the model. Representative tension and compression allowables and a minimum frame area were defined and are noted on the table.

A summary of the area requirements defined by the stiffness and strength analyses are presented in Table 55. The required design areas, i.e., the maximum value between stiffness and strength requirements, and their equivalent panel thicknesses are specified.

The combined results of the fuselage shell and frame analysis are presented in Tables 56 and 57 for the hat- and zee-stiffened fuselage concepts, respectively. These tables reflect the component and total equivalent thicknesses for the shell and frame as a function of frame spacing. The equivalent unit weights for these designs are also displayed graphically in Figure 141.

TABLE 53. - FUSELAGE FRAME STABILITY REQUIREMENTS, NONINTEGRAL TANK DESIGN

Point Design Region	Fuselage Bonding Moment M, in-lbs	Shell Dia D, in.	Frame Spacing L, in.	$(EI)_f$ (lb-in^2)	Frame Area A_{f_2} in^2
Quarter Length (FS 2426)	97.5×10^6	231.6	20	16.3×10^6	1.03
			30	10.9	0.69
			40	8.17	0.52
			50	6.54	0.42
			60	5.45	0.34
Three-Quarter Length (FS 2609)	60×10^6	187.86	20	6.62×10^6	0.42
			30	4.41	0.28
			40	3.31	0.21
			50	2.65	0.17
			60	2.21	0.14

$$(EI)_f = C_f \frac{MD^2}{L}$$

where: $C_f = 1/16\,000 = 6.25 \times 10^{-5}$

$E_f = 10.5 \times 10^6$

$A = 6.0t$

$I \approx 9t$

$I \approx 1.5A$

$$I_f = \frac{(EI)_f}{E}$$

or

$$A_f = \frac{(EI)_f}{1.5E}$$

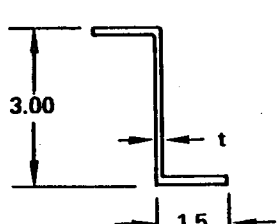

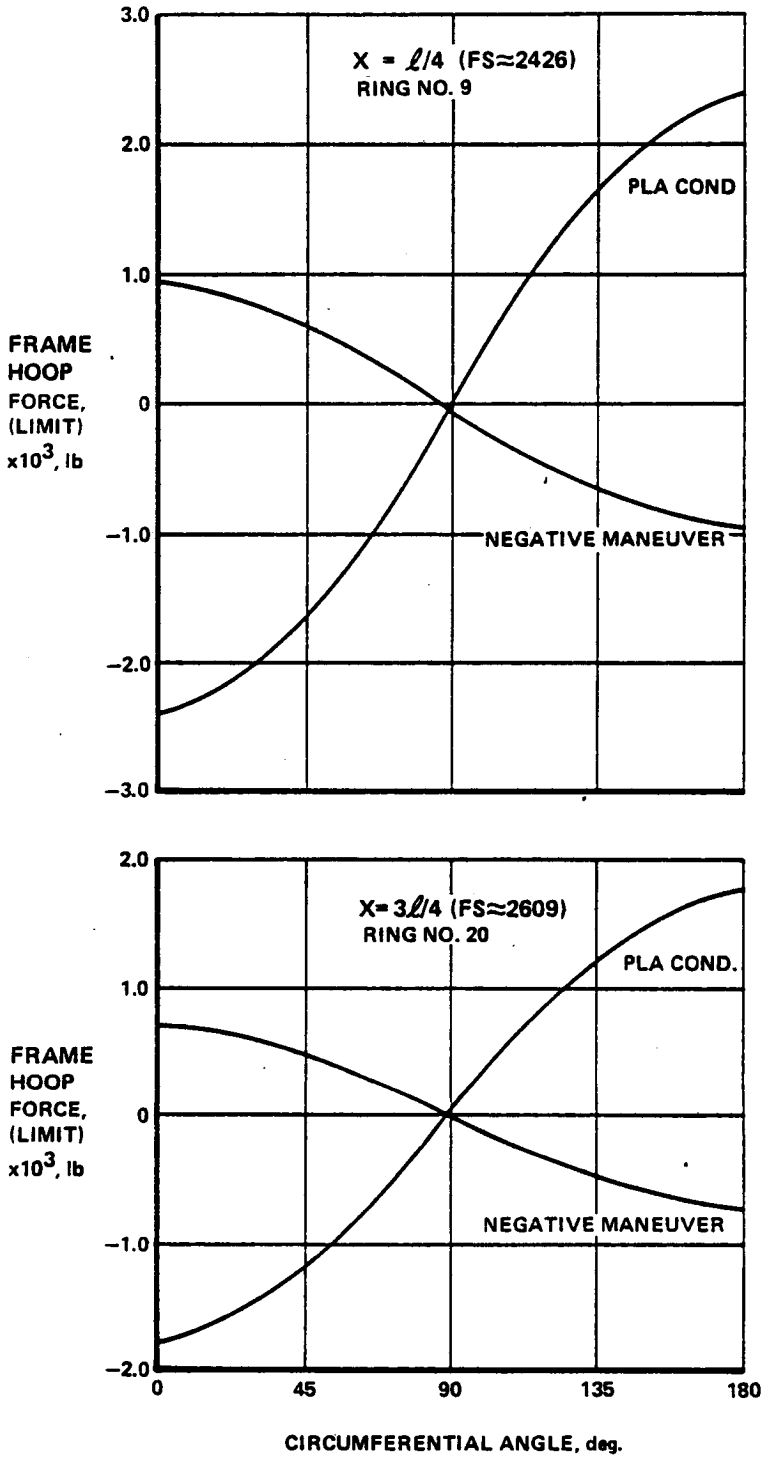

Figure 140. - Fuselage frame loads, nonintegral design.

TABLE 54. - FUSELAGE FRAME STRENGTH REQUIREMENTS, NONINTEGRAL DESIGN

Circum. Location		L = 20 in.(1)		L = 30 in.		L = 40 in.		L = 50 in.		L = 60 in.	
		P (lb)	A (in^2)	P (lb)	A (in^2)	P (lb)	A (in^2)	P (lb)	A (in^2)	P (lb)	A (in^2)
$\ell/4$	0	3525	(0.30)	5288	(0.30)	7050	(0.30)	8812	(0.30)	10575	(0.30)
	90	--	(0.30)	--	(0.30)	--	(0.30)	--	(0.30)	--	(0.30)
	180	-3525	(0.30)	-5288	.35	-7050	0.47	-8812	0.59	-10575	0.71
	A_{AVG}		(0.30)		0.31		0.34		0.37		0.40
$3\ell/4$	0	2625	(0.30)	3938	(0.30)	5250	(0.30)	6562	(0.30)	7875	(0.30)
	90	--	(0.30)	--	(0.30)	--	(0.30)	--	(0.30)	--	(0.30)
	180	-2625	(0.30)	-3938	(0.30)	-5250	0.35	-6562	0.44	- 7875	0.52
	A_{AVG}		(0.30)		(0.30)		0.31		0.34		0.36

1. Structural Model Data, Frame Spacing = 20 in.
2. $P_L = P_{20} \times \left(\frac{L}{20}\right)$
3. Allowables: Tension, F_t = 45 000 psi; Compression, F_c = 15 000 psi
4. $A = P/F_{t,c}$ or $A = A_{min} = 0.30\ in^2$
5. Average Area (A_{AVG}) = $(A_o/4\ t\ A_{90}/2 + A_{180}/4)$

TABLE 55. - SUMMARY OF FUSELAGE FRAME REQUIREMENTS, NONINTEGRAL DESIGN

Sta.	Frame Spacing (in)	Area (in^2)		A_R (in^2)	$\bar{t}$ (in.) (A/L)
		Stiffness Reqmt.	Strength Reqmt.		
$\ell/4$	20	1.03	0.30	1.03	.052
	30	0.69	0.31	0.69	.023
	40	0.52	0.34	0.52	.013
	50	0.42	0.37	0.42	.008
	60	0.34	0.40	0.40	.007
$3\ell/4$	20	0.42	0.30	0.042	.021
	30	0.28	0.30	0.30	.010
	40	0.21	0.31	0.31	.008
	50	0.17	0.34	0.34	.007
	60	0.14	0.36	0.36	.006

In similar fashion the candidate structural concepts for the tank of the nonintegral design were subjected to point design analysis to assess the relative merit of each concept. General instability analysis of the tank was conducted using BOSOR to ascertain if frames were required to prevent this failure mode. The concepts and associated stiffnesses used for this model were described in Section 7.2.3.4. The tank design for this model contained no frames except at the forward and aft suspension points. The results of the BOSOR bifurcated stability analysis showed that internal frames were not required to stabilize the tank design; therefore, they were not considered in the evaluation of the candidate concepts.

The tankage of the nonintegral design experiences only minor thermal loadings and flight inertia loads; therefore, the predominate loading was caused by the internal pressurization. Since the tank wall is tension designed, the structural concepts were designed by applying the fatigue and damage tolerance criteria. The basic tank wall cross-sectional data defined using this criteria was in all cases sufficiently strong to meet the basic strength requirements.

In general, the fatigue allowable defined for the operating condition established the minimum skin gage, whereas the fail-safe criteria was used to define the cross-sectional area and strap requirements. Both circumferential

TABLE 56. - SUMMARY OF FUSELAGE WEIGHT DATA FOR THE HAT-STIFFENED DESIGN, NONINTEGRAL TANK

Sta	Location	Frame Spacing (in.)	Equiv. Thk., $\bar{t}$, (in.)			Total[a] Unit Wt. (lb/ft^2)
			Shell	Frame	Total	
$\ell/4$	Upper Fiber	20	0.145	0.052	0.197	2.84
		30	0.145	0.023	0.168	2.42
		40	0.145	0.013	0.158	2.28
		50	0.145	0.008	0.153	2.20
		60	0.145	0.007	0.152	2.19
$\ell/4$	Mid Fiber	20		0.052		
		30	0.091	0.023	0.114	1.64
		40	0.091	0.013	0.104	1.50
		50	0.092	0.008	0.100	1.44
		60	0.094	0.007	0.101	1.45
$\ell/4$	Lower Fiber	20	0.106	0.052	0.158	2.28
		30	0.106	0.023	0.129	1.86
		40	0.107	0.013	0.120	1.73
		50	0.108	0.008	0.116	1.67
		60	0.110	0.007	0.117	1.68

(a) $w = 144 \rho \bar{t} = 14.4 x\bar{t}$

TABLE 57. - SUMMARY OF FUSELAGE WEIGHT DATA FOR THE ZEE-STIFFENED DESIGN, NONINTEGRAL TANK

Sta	Location	Frame Spacing (in.)	Equiv. Thk., $\bar{t}$, (in.)			Weight[a] (lb/sq. ft)
			Shell	Frame	Total	
$\ell/4$	Upper Fiber	20	0.159	0.052	0.211	3.04
		30	0.161	0.023	0.184	2.65
		40	0.161	0.013	0.174	2.51
$\ell/4$	Mid Fiber	30	0.096	0.023	0.119	1.71
		40	0.103	0.013	0.116	1.67
		50	0.111	0.008	0.119	1.71
		60	0.117	0.007	0.124	1.78
$\ell/4$	Lower Fiber	20	0.134	0.052	0.186	2.68
		30	0.140	0.023	0.163	2.35
		40	0.146	0.013	0.159	2.29

(a) $w = 144\ \rho\bar{t} = 14.4\ \bar{t}$

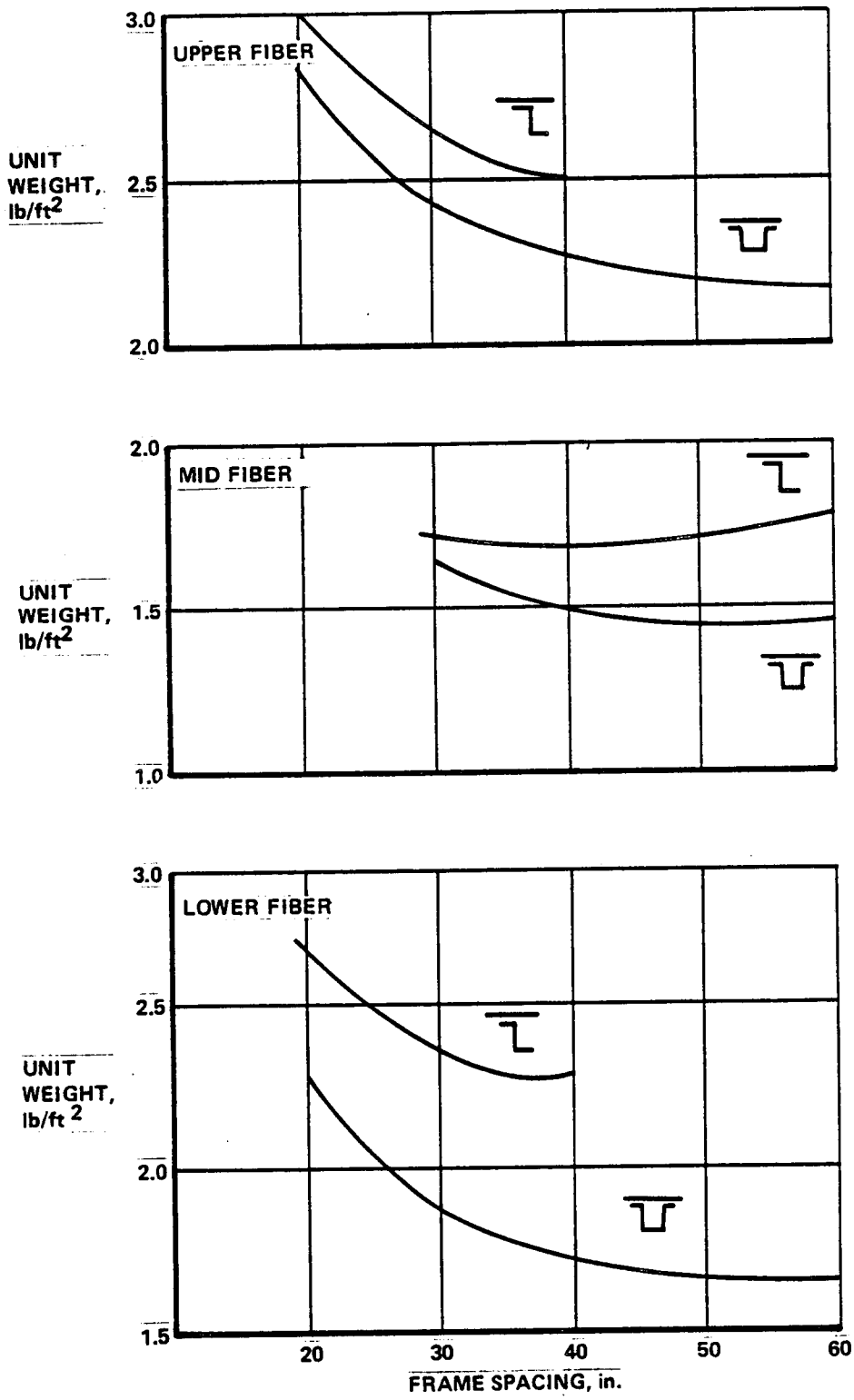

Figure 141. - Fuselage unit weight at the quarter-length location, nonintegral design.

and longitudinal crack damages were considered for the fail-safe analysis. Table 58 presents the fatigue and fail-safe analysis (circumferential damage condition) conducted at the two point design regions. This data reflects all the stiffened wall designs as well as the unstiffened design at these two locations. All designs require the same equivalent axial thickness ($\bar{t}$), whereas the skin thickness of the stiffened concepts can approach the minimum thickness dictated by the fatigue criteria.

The requirement for hoop straps was investigated using the longitudinal damage fail-safe criteria, see Section 7.2.3.2. Table 59 presents an example of the analysis conducted at the upper fiber location of the quarter-length point design region. This table presents the strap requirements for both the stiffened and unstiffened designs as a function of a variable strap spacing. The strap areas and their equivalent thicknesses for the stiffened skin designs are slightly higher than those of the unstiffened design for all strap spacing investigated. This situation is caused by accepting the minimum skin thickness and the correspondingly higher hoop stress dictated by the fatigue criteria.

Integral weld lands are provided on the tank wall for the attachment (spot welds) of the hoop fail-safe straps. The dimensions of these weld lands were postulated to be the width of the strap (2.0 in.) and one-quarter the thickness of the skin ($t_s/4$). Typical equivalent thickness calculations for these lands are included on Table 59.

Table 60 summarizes the results of the point design analysis conducted on the upper fibers at the quarter-length location on the tank. These unit weights reflect the component and total weights of the fuselage and tank as a function of hoop strap spacing. Insignificant weight differences are noted between the candidate concepts at any of the strap facings. The weight for any of the concepts is approximately 4.90 lb/sq ft and is relatively insensitive to the placement of the tank hoop fail-safe straps. The corresponding unit weight data for the lower fiber is shown in Table 61. The same insensitive weight trends are noted between concepts with all concepts weighing approximately 4.4 lb/sq ft.

The average circumferential unit weight and the component unit weights at the upper, mid and lower fibers are shown in Figure 142 as a function of fail-safe strap spacing for the tank quarter-length location. Because of the very little variation in weight between any of the concepts, it reflects both the stiffened and the unstiffened designs. An average unit weight of 4.62 lb/sq ft is noted at this tank location.

7.2.3.6.2 Integral design: The candidate wall concepts for integral tank design were subjected to point design analysis. These concepts included the blade-stiffened and the zee-and tee-stiffened concepts. All concepts are one-piece configurations to minimize the potential sources of leaks.

TABLE 58. - TANK FATIGUE AND FAIL-SAFE REQUIREMENTS, NONINTEGRAL TANK DESIGN

Point Design Region	Fiber Location	Limit Loads Nx (lb/in.)	Limit Loads Nθ (lb/in.)	Minimum[1] Skin Thk. t_s, (in.)	Equivalent[2] Axial Thk. $\bar{t}$, (in.)
X = ℓ/4	Upper	1 055	2 065	0.090	0.153
	Mid	1 042	2 097	0.091	0.151
	Lower	1 077	2 129	0.093	0.156
X = 3ℓ/4	Upper	839	1 658	0.072	0.121
	Mid	837	1 679	0.073	0.121
	Lower	836	1 700	0.074	0.121

1. Fatigue Criteria (Operating Conditions)

$$t_s = \frac{N_\theta}{F} + \frac{N_\theta}{23\ 000}$$

2. Fail-safe Criteria (Circumferential Damage)

$$\bar{t} = \frac{Nx}{Fg} \quad \text{where:}$$

$$Fg = \frac{1\ K}{2\sqrt{\ell}} = \frac{47\ 870}{2\ \sqrt{12}} = 6\ 910$$

STIFFENED

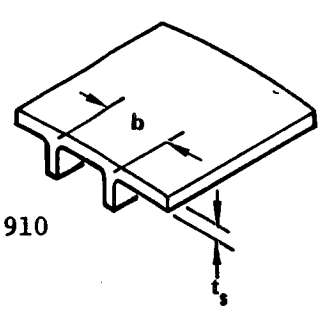

UNSTIFFENED

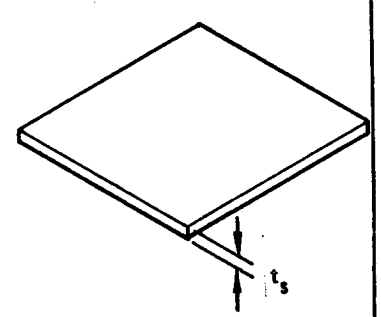

t_s = Skin Thk.

$\bar{t}$ = A/b

$\bar{t} = t_s$

TABLE 59. - TANK FAIL-SAFE STRAP AND WELD LAND REQUIREMENTS, NONINTEGRAL TANK DESIGN

Structural Concepts	Location Fiber	Skin Thk. t_s (in.)	N_θ (lb/in.)	f_θ (psi)	Strap Spacing b (in.)	Crack Length $\ell = 2b$ (in.)	Fail-Safe Straps: Area A_s (in^2)	Fail-Safe Straps: Equiv. Thk., $\bar{t}$ (in.)	Weld Land $\bar{t}$ (in.)
All Stiff.	Upper	0.090	2 065	22 900	6	12	0.143	0.024	0.0075
Skin	↓	↓	↓	↓	10	20	0.260	0.026	0.0045
Concepts					15	30	0.406	0.027	0.0030
1, Z, T					20	40	0.553	0.028	0.0023
Unstiff	Upper	0.153	2 065	13 500	6	12	0.110	0.018	0.0128
Skin	↓	↓	↓	↓	10	20	0.227	0.023	0.0076
Concept					15	30	0.374	0.025	0.0051
					20	40	0.520	0.026	0.0038

1. Fail-safe requirements (Section 5.2.3.2)

$$f_\theta = F_{pg} = 1.2\, F_{tu} \left(\frac{2We + \Sigma Ae/ts}{C_1 \ell + 2We} \right)$$

where:

$2We = 1.05 \qquad 1.20\, F_{tu} = 74\ 400$

$C_1 = 1.055 \qquad \Sigma A_e = 2A_s$

then:

$$A_s = \left[\frac{f_\theta}{74{,}400} (1.055\,\ell + 1.05) - 1.05 \right] \frac{t_s}{2}$$

2. Weld land requirement

$$\bar{t} = A_{LAND}/b$$

where:

$$A_{LAND} = 2.00x\ t_s/4$$

then:

$$\bar{t} = t_s/2b$$

TABLE 60. - SUMMARY OF UPPER FIBER UNIT WEIGHTS AT THE QUARTER-LENGTH LOCATION, NONINTEGRAL TANK DESIGN

Hoop Strap Spacing (in.) [a]		10	15	20
Unstiffened Design	Fuselage[b] (lb/sq ft)	(2.267)	(2.267)	(2.267)
	Shell	2.094	2.094	2.094
	Frame	0.173	0.173	0.173
	Tank (lb/sq ft)	(2.635)	(2.629)	(2.628)
	Shell	2.199	2.199	2.199
	Straps	0.327	0.359	0.374
	NOF	0.109	0.072	0.056
	Total (lb/sq ft)	4.902	4.896	4.895
Integral Stiffened[c] Design	Fuselage[b] (lb/sq ft)	(2.267)	(2.267)	(2.267)
	Shell	2.094	2.094	2.094
	Frame	0.173	0.173	0.173
	Tank (lb/sq ft)	(2.637)	(2.631)	(2.629)
	Shell	2.199	2.199	2.199
	Straps	0.351	0.374	0.387
	NOF	0.086	0.058	0.043
	Total (lb/sq ft)	4.904	4.898	4.896

(a) Tank fail-safe straps.

(b) Fuselage represents least-weight concept (hat stiffened) and corresponding frame spacing (40.0 in.).

(c) All integral designs (blade-, zee-, and tee-stiffened concepts).

At the point design regions, each component associated with the definition of a unit segment of structure was sized as a function of frame spacing. These components included the basic panel, frame, fail-safe strap and non-optimum factor; and were sized using the previously discussed design criteria, analytical methods and point design environment.

The resultant panel cross-sectional data for the upper and lower fibers at the quarter-length location are shown in Figure 143. This figure presents the equivalent thicknesses of the blade, zee and tee-stiffened designs as a function of frame spacing. Due to the fail-safe requirements (circumferential crack condition) all designs had the same thickness at the smaller frame spacings; whereas when the compression loads became dominate the less efficient compression design (blade) required a greater thickness at the higher frame spacings.

TABLE 61. - SUMMARY OF LOWER FIBER UNIT WEIGHTS AT THE QUARTER-LENGTH LOCATION, NONINTEGRAL TANK DESIGN

Hoop Strap Spacing (in.) [a]		10	15	20
Unstiffened Design	Fuselage[b] (lb/sq ft)	(1.711)	(1.711)	(1.711)
	Shell	1.538	1.538	1.538
	Frame	0.173	0.173	0.173
	Tank (lb/sq ft)	(2.694)	(2.689)	(2.687)
	Shell	2.244	2.244	2.244
	Straps	0.338	0.370	0.387
	NOF	0.112	0.075	0.056
	Total (lb/sq ft)	4.405	4.400	4.398
Integral Stiffened Designs[c]	Fuselage[b] (lb/sq ft)	(1.711)	(1.711)	(1.711)
	Shell	1.538	1.538	1.538
	Frame	0.173	0.173	0.173
	Tank (lb/sq ft)	(2.696)	(2.691)	(2.687)
	Shell	2.244	2.244	2.244
	Straps	0.366	0.389	0.400
	NOF	0.086	0.058	0.043
	Total (lb/sq ft)	4.407	4.402	4.398

(a) Tank fail-safe straps.

(b) Fuselage represents least-weight concept (hat stiffened) and corresponding frame spacing (40.0 in.).

(c) All integral designs (blade-, zee-, and tee-stiffened concepts).

For each of these concepts, unstiffened skin panels were found to be the lightest concept for the design of the mid-panels at the quarter-length location. A panel thickness of 0.164 in., invariant with frame spacing, was used for these designs.

The frames for these designs were analyzed in a similar manner as the fuselage frames for the nonintegral design. Both strength and stability were considered. Figure 144 presents these results along with added requirements imposed by the fail-safe criteria. An example of this fail-safe analysis as summarized in Table 62 for the 30.0 in. frame spacing design. Note that the assumed location and size of the damage dictates the respective area of the frame or strap. The methods employed in this analyses are described in the Analytical Methods Section.

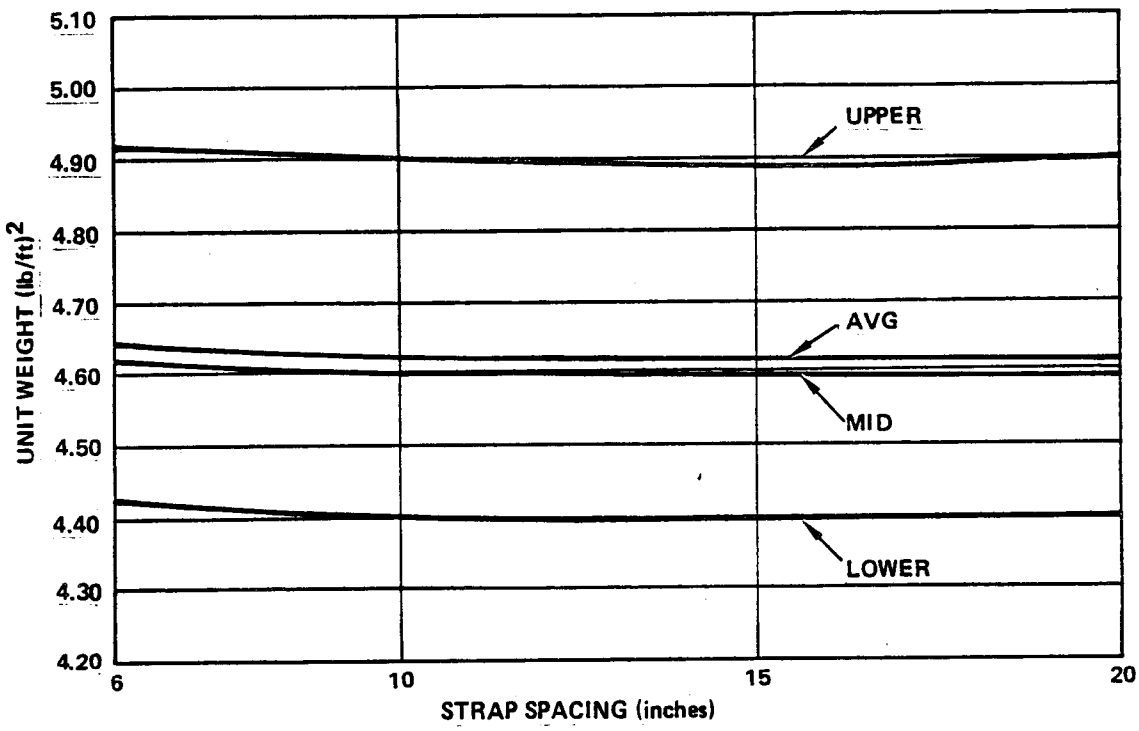

Figure 142. - Unit weights vs strap spacing for nonintegral tank (quarter-length point design region).

Table 62 describes the frame and strap requirements as a function of the number of straps, but does not indicate the selection process used in defining the spacing for the minimum weight design. Table 63 summarizes the frame area requirements due to stability, strength, minimum gage and fail safe. In addition, the strap area requirements for fail safe and the total area of the frame and straps are presented. It can be seen from this table that the fail safe requirements dictates the areas of the frames when no straps or one strap is used; whereas, the stability requirements designs the higher strap spacings. Using these frame areas and combining them with the required strap areas a total equivalent thickness was obtained. Minimum-weight designs are indicated for the two and three strap designs. The smaller number of straps was chosen for the 30.0 in. frame spacing design.

The results of the analyses conducted on the hoop straps and frames dictated the minimum-weight combination for each of the frame spacings investigated. Table 64 summarizes these results and indicates the unit strap areas, total strap areas and the equivalent thickness for each design.

Integral strap weld lands and panel closeouts were postulated for each tank design. The strap weld lands were similar to those described for the nonintegral tank. To provide for attachment of the frames the panel stiffeners were assumed to be tapered-out with a flat land of sufficient thickness provided to carry the axial and bending stresses. These results are presented in Tables 65 and 66 under the heading of nonoptimum factor (NOF).

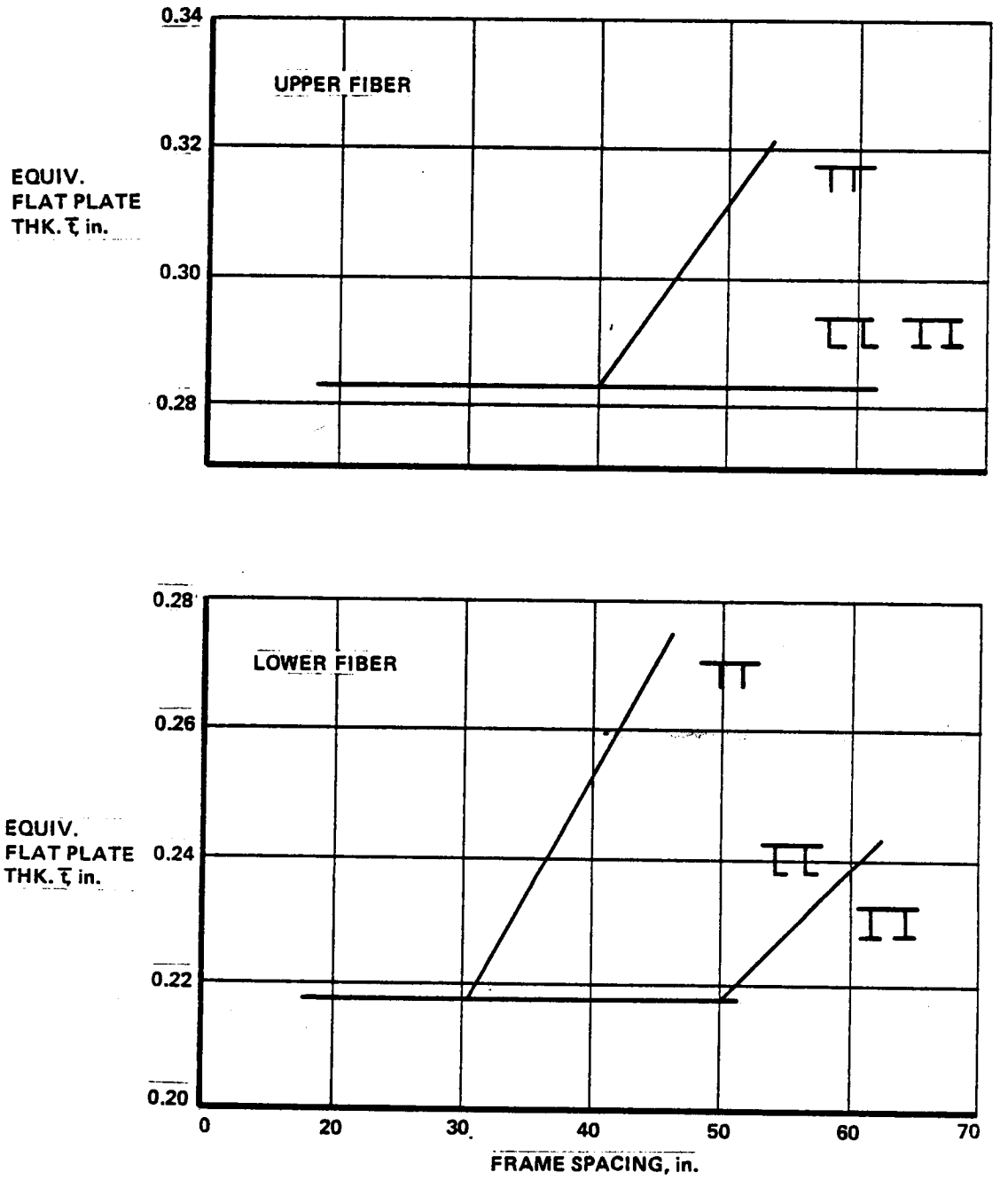

Figure 143. - Tank equivalent thickness, integral design.

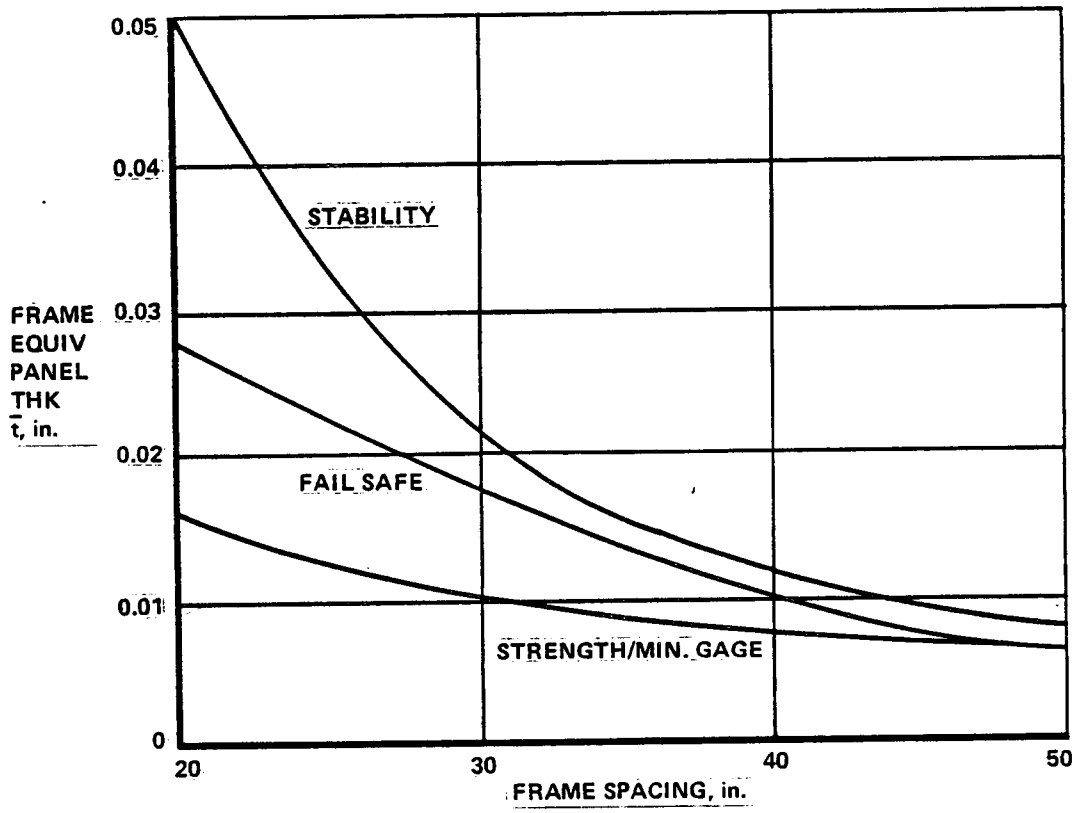

Figure 144. - Frame equivalent thickness as a function of spacing, integral design.

Tables 65 and 66 summarize the results of the point design analysis conducted on upper and lower fibers at the quarter-length location. These weights reflect the component and total weights of the tank as a function of the variable frame spacing. In general, at both locations the blade-stiffened designs are competitive from a weight standpoint with the tee-and zee-stiffened designs at the lower frame spacings and are much heavier at the larger spacings.

Figure 145 presents the total unit weight for the upper and lower fibers. The total cross-sectional unit weight for each candidate concept of the integral tank design was defined by averaging the unit weights calculated at the upper, side and lower circumferential locations. These results are presented in Figure 146 as a function of frame spacing. A minimum weight design of approximately 3.90 lb/sq ft is indicated for the blade-stiffened panel concept at a frame spacing of approximately 40.0 inches. The corresponding minimum weight designs for both the zee-and tee-stiffened concepts occur at a frame spacing of approximately 50.0 inches. The associated average circumferential weight for both of these designs is 3.75 lb/sq ft. This affords a 0.20 lb/sq ft weight saving over the blade-stiffened design.

TABLE 62. - FRAME AND STRAP FAIL-SAFE REQUIREMENTS FOR 30.0 FRAME SPACING DESIGN, INTEGRAL TANK

Point Design Region	Frame Spacing b, (in.)	No. Straps n	Strap Spacing (in.)	Crack Length (in.)	A_e (in^2)	Strap[1] Requirement			Frame[2] Requirement	
						A_S (in^2)	ΣA_S nA_S (in^2)	$\bar{t}$ $\Sigma A_S/b$ (in.)	A_F (in^2)	$\bar{t}$ A_F/b (in.)
X = $\ell/4$ (FS 2452)	30.0	0	30.0	60.0	2.15	0	0	0	2.15	0.072
	↓	1	15.0	30.0	0.32	0.32	0.32	0.011	0.96	0.032
		2	10.0	20.0	0.18	0.18	0.36	0.012	0.54	0.018
		3	7.5	15.0	0.12	0.12	0.36	0.012	0.36	0.012
	30.0	4	6.0	12.0	0.10	0.10	0.40	0.013	0.30	0.010

1. STRAP REQUIREMENT

- Longitudinal crack arrested by hoop straps

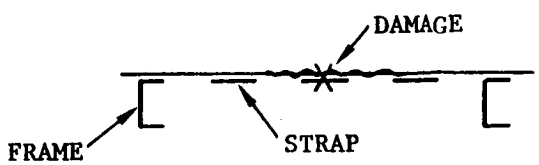

$$A_S = A_e$$

where:

A_S = Strap area, in^2

A_e = Reinforcement area, in^2

2. FRAME REQUIREMENT

- Longitudinal crack arrested by a frame

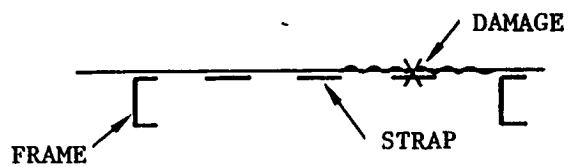

$$A_F = 3A_e$$

This assumes 1/3 of the area of the frame is effective in resisting skin cracks

TABLE 63. - FRAME AND STRAP REQUIREMENTS FOR A 30.0 INCH FRAME SPACING DESIGN, INTEGRAL DESIGN

Frame Spacing	No. Straps	Frame Equivalent Thickness (in.)					Strap Equiv. Thk. (in.)	Total Equiv. Thk. (in.)
		Stability Reqmts	Strength Reqmts	Min. Gage	Fail-Safe Reqmts	Design		
30.0	0	0.021	0.010	0.010	0.072	0.072	0	0.072
	1	0.021			0.032	0.032	0.011	0.043
	2	0.021			0.018	0.021	0.012	0.033
	3	0.021			0.012	0.021	0.012	0.033
30.0	4	0.021	0.010	0.010	0.010	0.021	0.013	0.034

TABLE 64. - SUMMARY OF MINIMUM-WEIGHT STRAP DESIGNS, INTEGRAL TANK

Frame Spacing b, (in.)	No. Straps	Strap Spacing (in.)	Strap Area A_s, (m^2)	Total Strap Area A_s, (in^2)	$\bar{t}$ (in.)
20.0	2	6.67	0.10	0.20	0.010
30.0	3	7.50	0.12	0.36	0.012
40.0	4	8.00	0.12	0.48	0.012
50.0	5	8.33	0.10	0.50	0.010

TABLE 65. - SUMMARY OF UPPER FIBER UNIT WEIGHTS AT THE QUARTER-LENGTH LOCATION, INTEGRAL DESIGN

	Unit Weight (lb./sq ft)			
Frame Spacing (in.)	20	30	40	50
Blade-Stiffened Design	(5.71)	(5.11)	(4.83)	(5.08)
Shell	4.08	4.08	4.08	4.50
Frames	0.69	0.31	0.17	0.11
Straps	0.13	0.17	0.17	0.17
NOF	0.80	0.54	0.40	0.30
Zee-Stiffened Design	(5.85)	(5.20)	(4.90)	(4.74)
Shell	4.08	4.08	4.08	4.08
Frames	0.69	0.31	0.17	0.11
Straps	0.13	0.17	0.17	0.17
NOF	0.95	0.63	0.47	0.38
Tee-Stiffened Design	(5.88)	(5.21)	(4.92)	(4.76)
Shell	4.08	4.08	4.08	4.08
Frames	0.69	0.31	0.17	0.11
Straps	0.13	0.17	0.17	0.17
NOF	0.98	0.66	0.49	0.39

7.2.3.7 Screening results: The tank weight for each candidate concept of the integral and nonintegral tanks was calculated using the results of the point design analysis. From these results the most-promising concept was selected for each basic type of tank and used as the baseline configuration for conducting the parametric studies and the investigation of the four candidate fuel containment systems.

Caution should be exercised in interpreting these results since the purpose was to screen the candidates wall concepts and not to conduct a comparison study between the two basic types of tanks.

The total tank cross-sectional weight for each candidate concept of the integral tank design was defined by using the average circumferential until weights at the two point design regions. Figure 146 presented the average circumferential unit weight as a function of frame spacing for the quarter-length location. From these data the minimum weight designs were selected and used to extrapolate the total weight of the tank cylinder.

Table 67 presents a summary of the unit weights of the upper, mid and lower fibers at each point design region. In addition, the average unit weight of the tank at the point design regions and at the ends of the tank cylinder are defined. This unit weight data was then converted to pounds per foot of

TABLE 66. - SUMMARY OF LOWER FIBER UNIT WEIGHTS AT THE QUARTER-LENGTH LOCATION, INTEGRAL DESIGN

	Unit Weight (lb/sq ft)			
Frame Spacing (in.)	20	30	40	50
Blade-Stiffened Design	(4.54	(4.01)	(4.22)	(4.65)
Shell	3.13	3.13	3.61	4.19
Frames	0.69	0.31	0.17	0.11
Straps	0.13	0.17	0.17	0.17
NOF	0.58	0.39	0.26	0.18
Zee-Stiffened Design	(4.50	(3.98)	(3.76)	(3.64)
Shell	3.13	3.13	3.13	3.13
Frames	0.69	0.31	0.17	0.11
Straps	0.13	0.17	0.17	0.17
NOF	0.55	0.37	0.27	0.22
Tee-Stiffened Design	(4.48)	(3.96)	(3.74)	(3.63)
Shell	3.13	3.13	3.13	3.13
Frames	0.69	0.31	0.17	0.11
Straps	0.13	0.17	0.17	0.17
NOF	0.52	0.35	0.26	0.21

cylinder length (average unit weight times diameter) and used to derive the weight of the tank cylinders which are shown in Figure 147.

The zee- and tee-stiffened aft tank cylinders have approximately equal weights of 5293 lb each with the blade-stiffened design weighing 5512 lb. A weight saving of approximately 220 lb is indicated for the former cylinders. Table 68 displays a tank weight for these designs which includes the weight of typical closures in addition to the cylinder weight.

The zee-stiffened design was selected as the most promising concept for the integral tank design since no appreciable variation in weight is noted between the zee- and tee-stiffened designs. In addition, the zee-stiffened tank would be slightly less complicated to manufacture, i.e., lower cost.

The unit weights for the unstiffened and stiffened concepts of nonintegral tanks are approximately equal. The unit weights of the upper and lower fibers at the quarter-length location were previously shown in Tables 60 and 61. The average unit weights were derived by the same methods described for the integral tank design. Table 69 contains the unit weights used for this analysis.

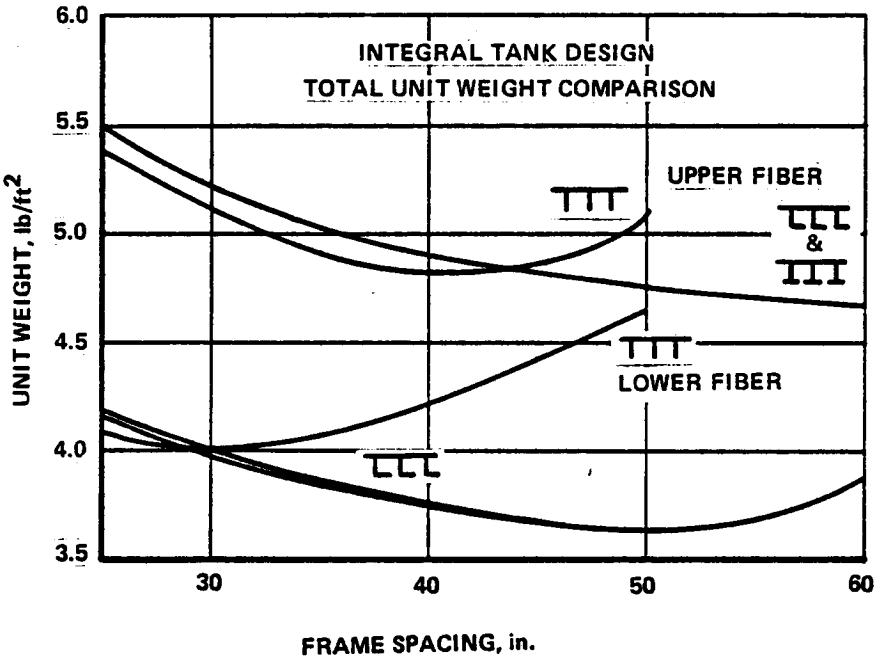

Figure 145. - Total unit weight comparison of structural candidates, integral tank design.

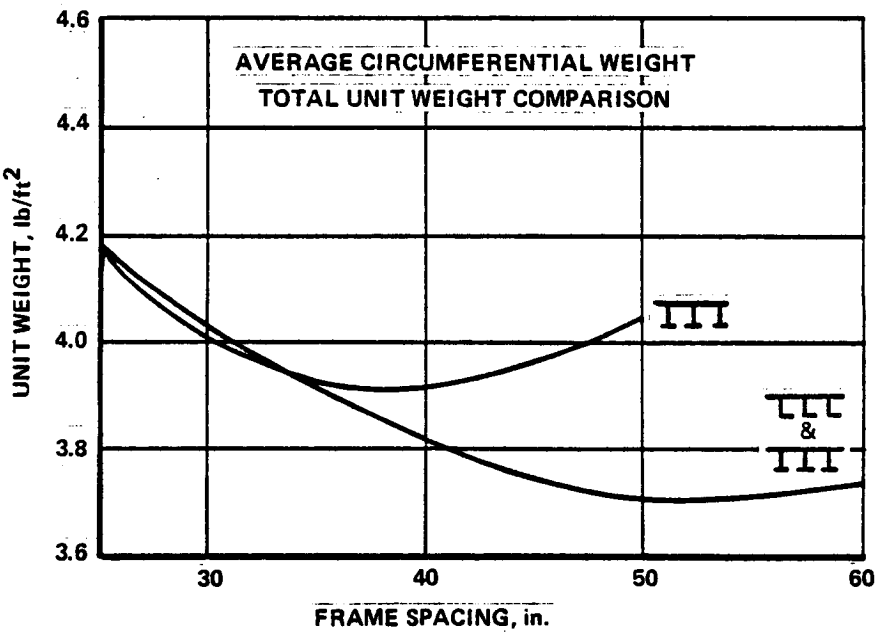

Figure 146. - Average circumferential weight comparison of structural candidates, integral tank design.

TABLE 67. SUMMARY OF UNIT WEIGHTS FOR INTEGRAL TANK DESIGN

Concept	Unit Weights (lb/sq ft)			
	X=0	X= $\ell/4$	X=3$\ell/4$	X= ℓ
Blade-Stiffened	(4.15)	(3.90)	(3.40)	(3.15)
Upper fiber	--	4.80	4.52	--
Mid fiber	--	3.30	2.70	--
Lower fiber	--	4.20	3.70	--
Zee- and Tee-Stiff.	(4.00)	(3.75)	(3.26)	(3.00)
Upper fiber	--	4.75	4.47	--
Mid fiber	--	3.30	2.70	--
Lower fiber	--	3.65	3.20	--

Figure 148 presents the development of the tank and fuselage cylinder weights for a typical aft tank. Similar to the integral design, a tank and body weight was estimated and is shown on the previously presented Table 69.

All the candidate concepts for the nonintegral tank design exhibited approximately the same weight when compared on a theoretical unit weight basis; where in reality, the tanks fabricated with the stiffened wall configuration would have a higher degree of complexity involved in the design of discrete regions, i.e., head/cylinder junctures, suspension points, tank penetrations, etc. In addition, the unstiffened wall concept has a decisive cost advantage over the stiffened concepts when the basic problem of fabrication stiffened one-piece wall designs on a conical surface are addressed. If modification of the minimum-weight proportions are attempted to ease the fabrication problems additional weight penalties are incurred for the integrally stiffened concepts.

In conclusion, the unstiffened wall concept was selected for the nonintegral tank design because of its equal or lighter weight and its lower cost.

7.2.4 Parametric studies. - Structural parametric studies were conducted to appraise various aspects related to the design of LH_2 fuel containment tanks. In general these studies encompassed basic design studies on the dome shape and suspension systems, and investigations to assess the effects of pressure (higher tank operating pressures and pressure stabilization) and a variable life on the tank design.

7.2.4.1 Dome shape study: Candidate dome configurations applicable to a constant volume liquid hydrogen tank containment system are described in this

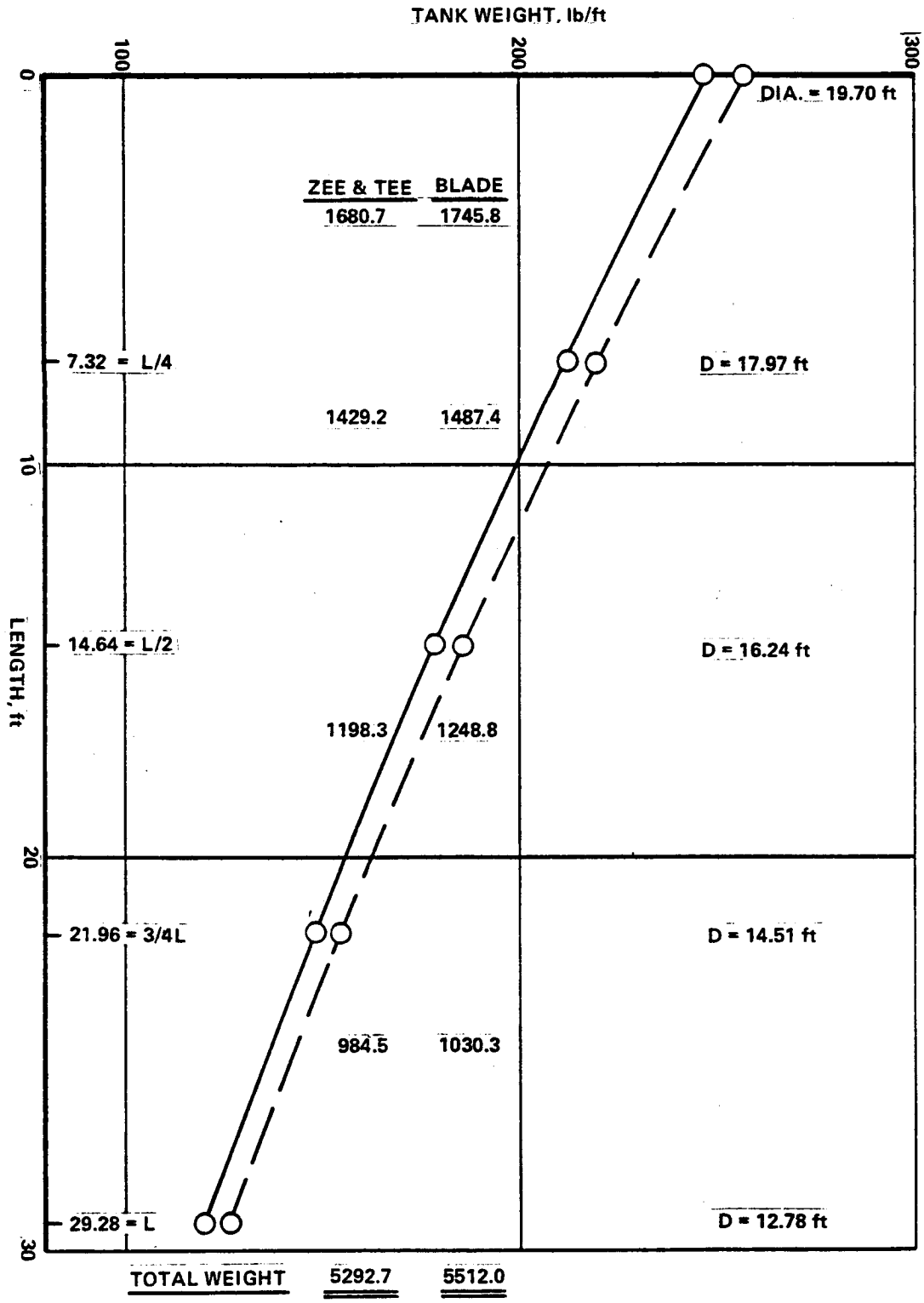

Figure 147. - Integral LH_2 tank wall, optimum weight including fail-safe straps and weld lands.

TABLE 68. - AFT TANK WEIGHT

Item	Weight (lb)		
	Nonintegral	Integral	
	All Concepts	Zee and Tee	Blade
Tank	(4968)	(6485)	(6704)
Cylindrical section	3850	5293	5512
Domes	743	817	817
Divider dome	375	375	375
Body Shell	(3342)	--	--
Total	8310	6485	6704

TABLE 69. - SUMMARY OF UNIT WEIGHTS FOR THE NONINTEGRAL TANK DESIGN

All Concepts	Unit Weight (lb/sq ft)			
	X=0	X= $\ell/4$	X=3$\ell/4$	X=ℓ
Tank	(2.86)	(2.64)	(2.19)	(1.96)
Upper fiber	2.86	2.63	2.18	1.95
Mid fiber	2.82	2.61	2.19	1.98
Lower fiber	2.94	2.69	2.19	1.94
Body	(2.11)	(1.99)	(1.75)	(1.63)
Upper fiber	2.41	2.27	1.99	1.85
Mid fiber	2.11	1.99	1.75	1.63
Lower fiber	1.81	1.71	1.51	1.41

section. Specifically, the geometric proportions and the associated weight, internal volume, and surface area of the candidate dome configuration are studied. For each dome configuration, total tank weight is calculated and evaluated with respect to airplane direct operating cost (DOC). By selecting the DOC as the objective function, the proportions of the least-costly dome-tank configuration are determined.

The nonintegrated tank design shown in Figure 149 was selected as the baseline for the study. The three candidate dome configurations as depicted in Figure 150 include a hemispherical head and the general families of ellipsoidal and torispherical heads. For the preliminary analysis of the candidate

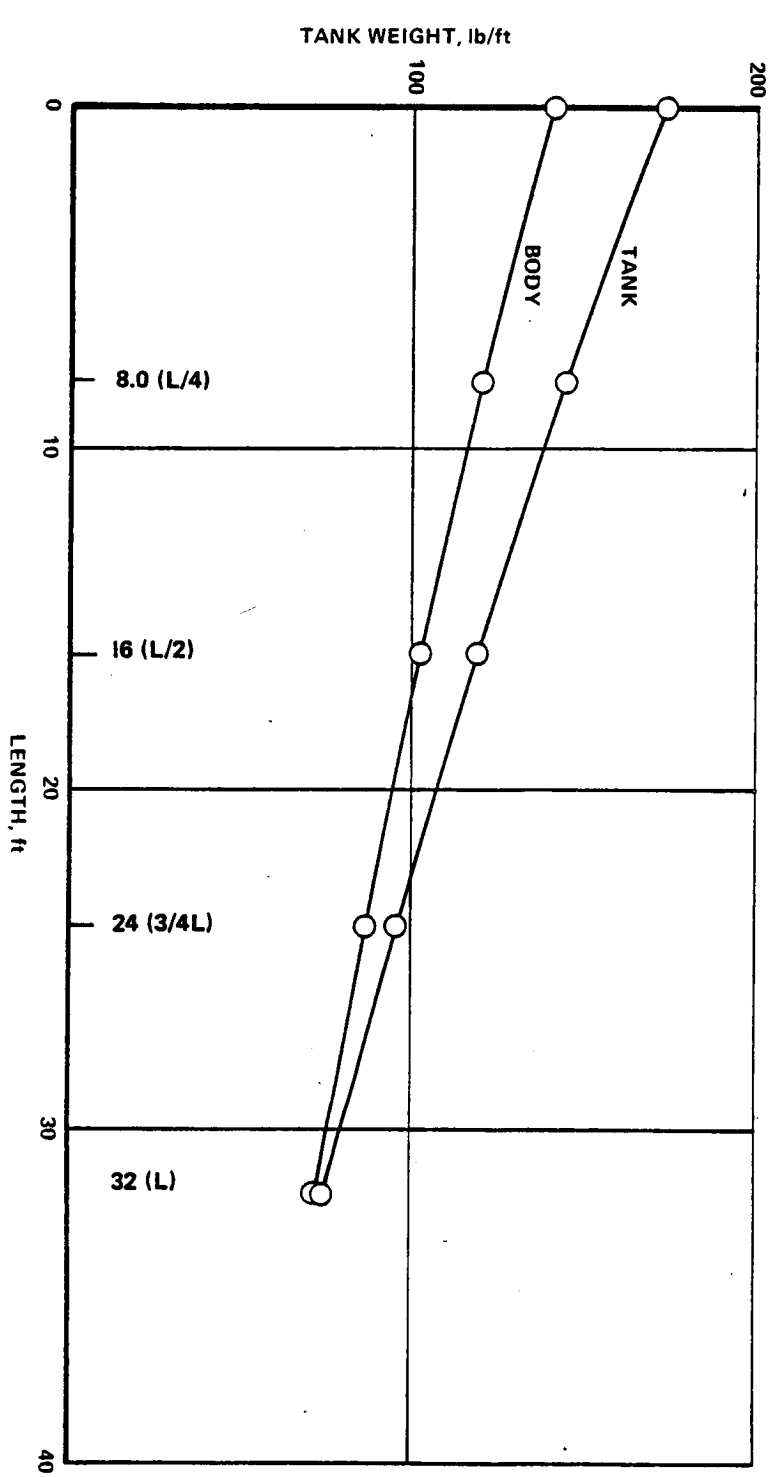

	DIAMETER, ft		WEIGHT (l/4) lb	
	BODY	TANK	BODY	TANK
	21.12	19.25		
			1066.8	1270.4
8.0 (L/4)	19.30	17.43		
			893.6	1052.0
16 (L/2)	17.48	15.61		
			754.8	853.2
24 (3/4L)	15.65	13.79		
			627.2	674.4
			(3342.4)	(3850.0)
			TOTAL	
32 (L)	13.83	11.97		

Figure 148. - Nonintegral LH_2 tank wall, optimum weight including fail-safe straps and weld lands.

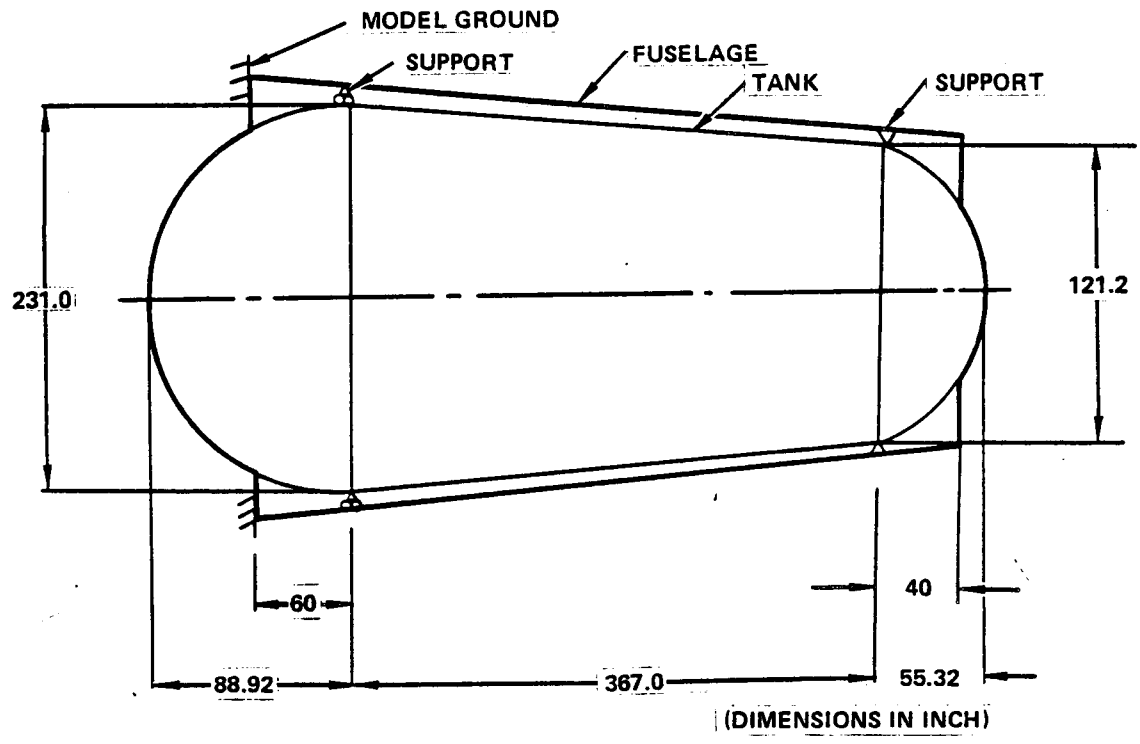

Figure 149. - Fuselage shell and tank configuration, nonintegral design.

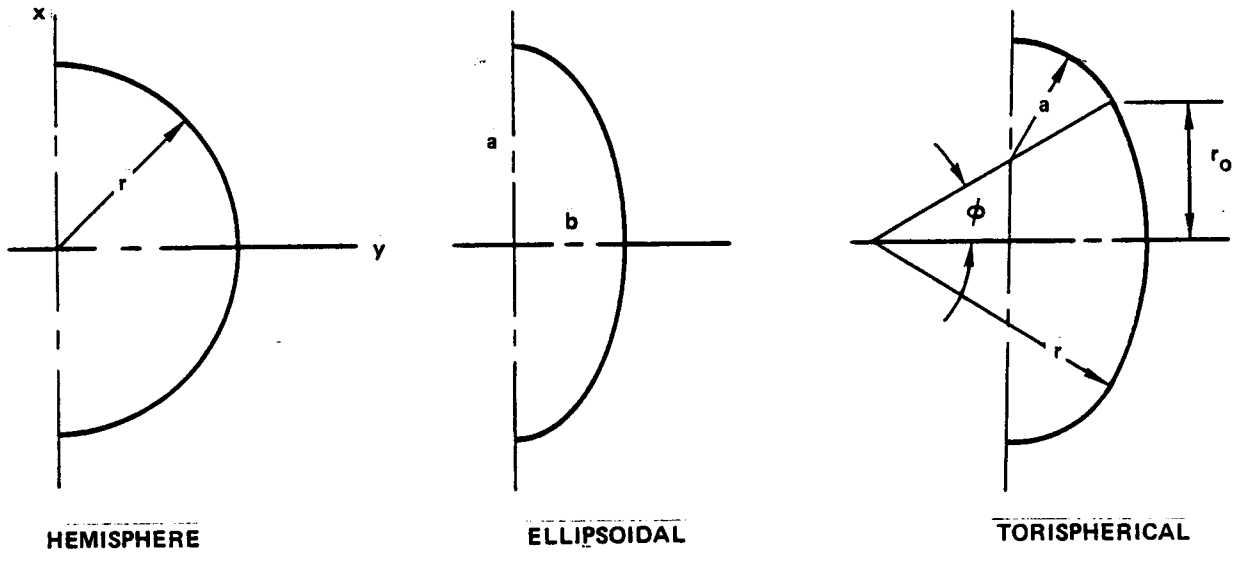

Figure 150. - Candidate configurations for dome shape study.

head configurations, thin-shell theory (membrane) was used. The dome shells were considered to be constructed of isotropic material with variable wall-thickness and subject only to internal pressurization. The operating design stress curves indicated that a fatigue allowable of 23 000 psi was most suitable for the analysis. The von-Mises failure criteria

$$\bar{\sigma}^2 = \sigma_1^2 + \sigma_2^2 - \sigma_1\sigma_2$$

was used. In this expression, σ_1 and σ_2 are the meridional and hoop stress, respectively. For axisymmetric shells of revolution subject only to internal pressure, these stresses are given by the relationships:

$$\sigma_1 = pr_2/2t$$

$$\sigma_2 = p(r_2 - r_2^2/2r_1)/_t$$

where p is the internal pressure and t is the wall thickness. The meridional radius of curvature r_1 and the hoop radius of curvature r_2 for the candidate dome configurations are given in Table 70.

Parametric studies were conducted to define the proper dome shape, considering both tank weight and volumetric efficiency. Candidate dome configurations were applied to the large diameter dome of the nonintegral tank design. Standard numerical techniques were used in the preliminary strength analysis to size the variable wall thickness requirements and obtain needed parameters such as dome radii of curvature, surface area and volume, and dome weight.

Figures 151 and 152 show the variation of surface area, volume, and weight as a function of the specific geometry parameter for the families of ellipsoidal and torispherical heads, respectively. The hemispherical dome is represented in Figure 151 by an a/b = 1.0. For the ellipsoidal configuration, minimum weight of 474 pounds is obtained at an a/b = 1.3. The torispherical design yields a minimum weight of 489 pounds at an angle ϕ of 0.95 radians. The hemispherical dome is approximately 17-percent heavier than the least-weight ellipsoidal dome.

Tank and fuselage geometric proportions were determined for a constant volume tank. The weights were calculated for these constant volume tank configurations and included the tank, fuselage shell, insulation and fuel for the nonintegral tank design. The fuel boiloff weight was accounted for as the length/surface area varied. Figure 153 shows the resultant weights of the

TABLE 70. - RADII OF CURVATURE OF CANDIDATE DOME CONFIGURATIONS

Configuration	Radii of Curvature	
	Meridional (r_1)	Hoop (r_2)
Hemispherical	r	r
Elliptical	$r_2^3(b^2/a^4)$	$((a/b)^4y^2+x^2)^{1/2}$
Torispherical (toridal segment)	a	$a(1 + b/r_o)$
See Figure 149 for geometry.		

forward and aft tanks as a function of dome parameter. Using these weights and their corresponding length and associated diameter changes, the ASSET program was used to assess the effects on aircraft L/D for a constant payload-range mission. The cost comparison data (DOC) for the resultant aircraft are shown in Figure 154 as a function of the specific dome parameters. A summary of the minimum aircraft DOC configuration for each dome shape is shown in Table 71. The aircraft utilizing ellipsoidal heads on the tanks display a minimum DOC of 1.8246 ¢/seat-nmi for a dome aspect ratio of 1.60. The associated total weight and fuselage length are 81 715 pounds and 223.0 feet, respectively. The corresponding minimum DOC for the torispherical head design is 1.8245 ¢/seat-nmi. for a $\phi = 0.36$ radian dome. A total weight of 81 355 pounds and a fuselage length of 223.7 feet are noted for this design.

Since the DOC for both the elliptical dome and torispherical dome is approximately 1.825 ¢/seat-n.mi., these designs were subject to a more detailed analysis using the BOSOR 4 computer program. This analysis included the bending as well as the membrane thickness requirements of a shell under internal pressure load. The von Mises failure criteria was also used in this analysis. Figures 155 and 156 present the undeformed shapes of the elliptical and torispherical domes, respectively.

These models were subjected to a nonlinear elastic analysis using the BOSOR program with internal pressurization being the only loading considered. As an example of the results, the stresses associated with the elliptical dome are shown in Figure 157. The arc length is measured from the apex to the equator of the dome, and along the cylinder. The upper plot reflects the hoop stress on the outer fiber (s_{20}) as a function of the meridian length; whereas, the two lower plots depict the equivalent stresses (von Mises criteria) on the inner S_{EI} and outer S_{EO} fibers, respectively. Maximum equivalent stresses of 23 000 psi and 20 000 psi are noted for the dome and cylinder, respectively.

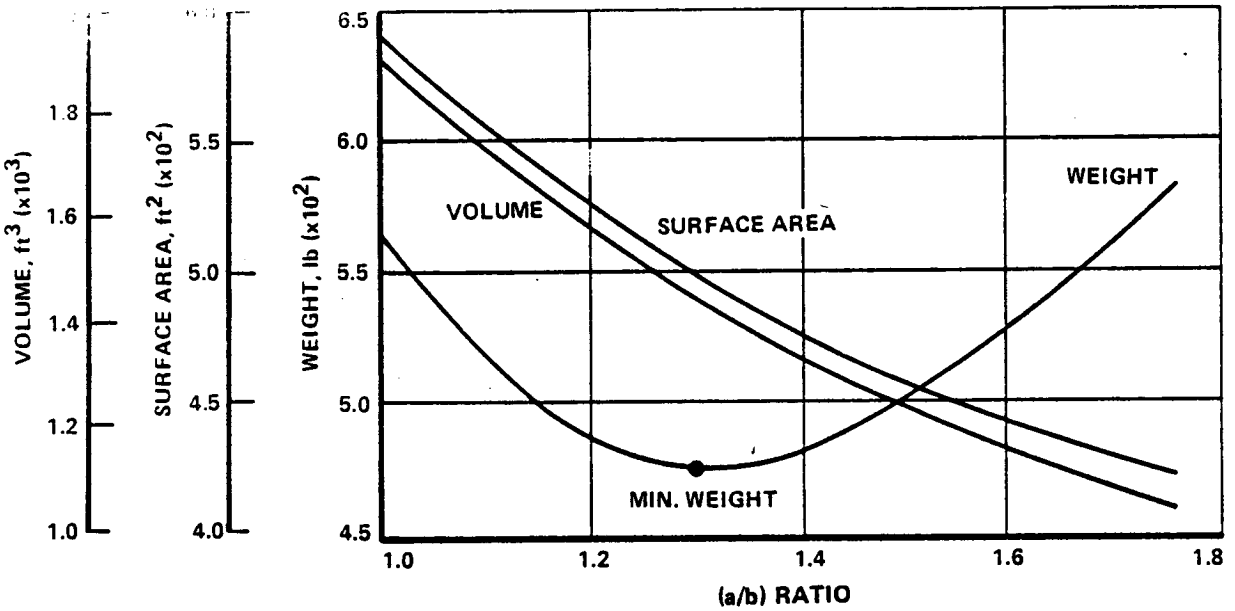

Figure 151. - Elliptical dome design data.

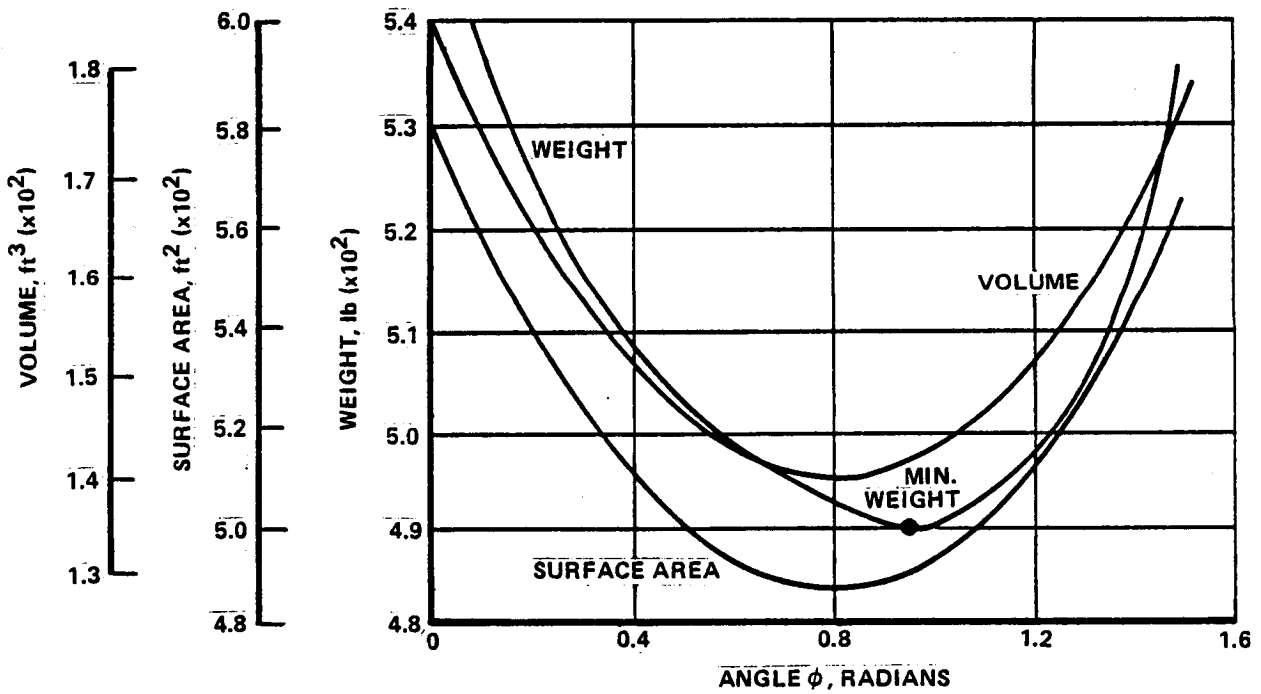

Figure 152. - Torispherical dome design data.

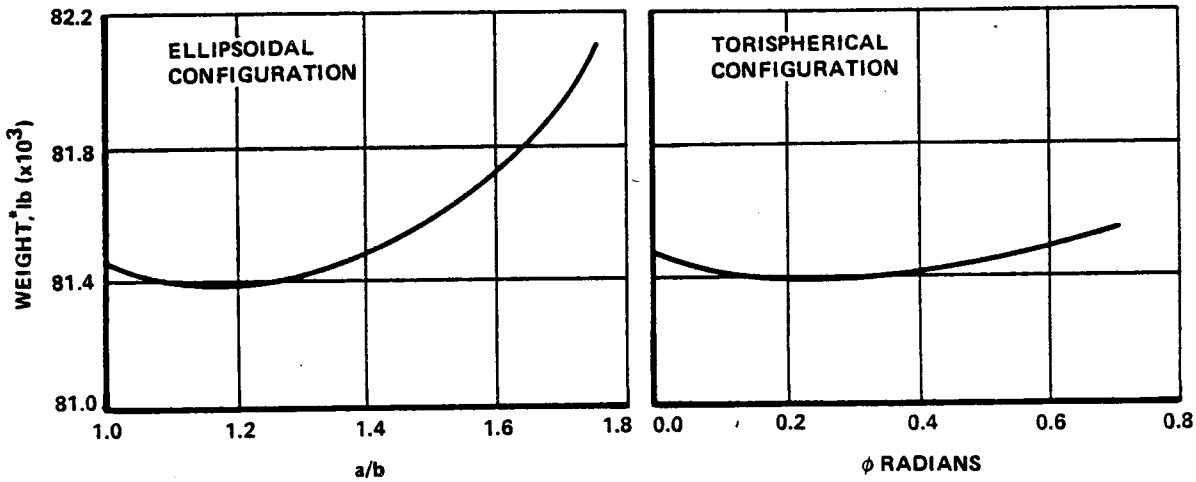

*WEIGHT IS FOR TWO TANKS AND INCLUDES THE WEIGHT OF THE TANK, FUSELAGE SHELL, INSULATION AND FUEL.

Figure 153. - Tank weight comparison dome shape study.

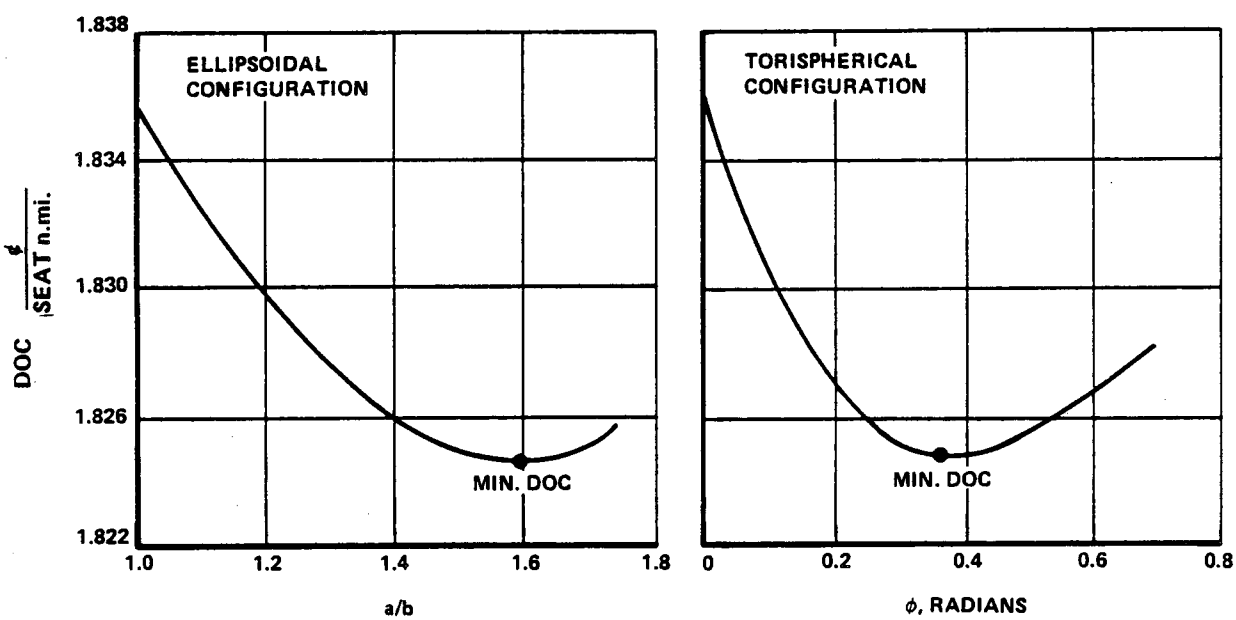

Figure 154. - Cost comparison date, dome shape study.

TABLE 71. - COMPARISON OF DATA FOR MINIMUM DOC DOMES CONFIGURATION

Item	Ellipsoidal	Torispherical
Dome Geometry		
Proportions	a/b = 1.6	ϕ = 0.36
Height (ft)	6.01	7.51
Weight (lb) (Incl- tank, shell, insul. and fuel)	81 715	81 355
Fuselage Length (ft)	223.0	223.7
DOC (¢/Seat-n.mi.)	1.8246	1.8245

The maximum equivalent stresses for the torispherical dome are 25 600 psi and 22 800 psi for the dome and cylinder, respectively. Additional evaluation indicates a weight penalty required to sustain a 23 000 psi allowable of approximately 5 lb per head or a total weight increment of approximately 20.0 lb for the combined forward and aft tanks.

A summary of the results of this study are presented in Table 72.

TABLE 72.

Concept	Evaluation Function	
	Minimum Wt.	Minimum DOC
Ellipsoidal Design		
a/b	1.30	1.60
Weight, lb	474	530
Torispherical Design		
ϕ, radians	0.95	0.36
Weight, lb	489	516

Considering minimum-weight dome designs the ellipsoidal design is the least weight design and indicates a weight saving of 15 lb (3-percent) over the equivalent torispherical design.

When DOC is the object function and the dome weight of the two designs are compared, the torispherical design is the least weight design with a weight

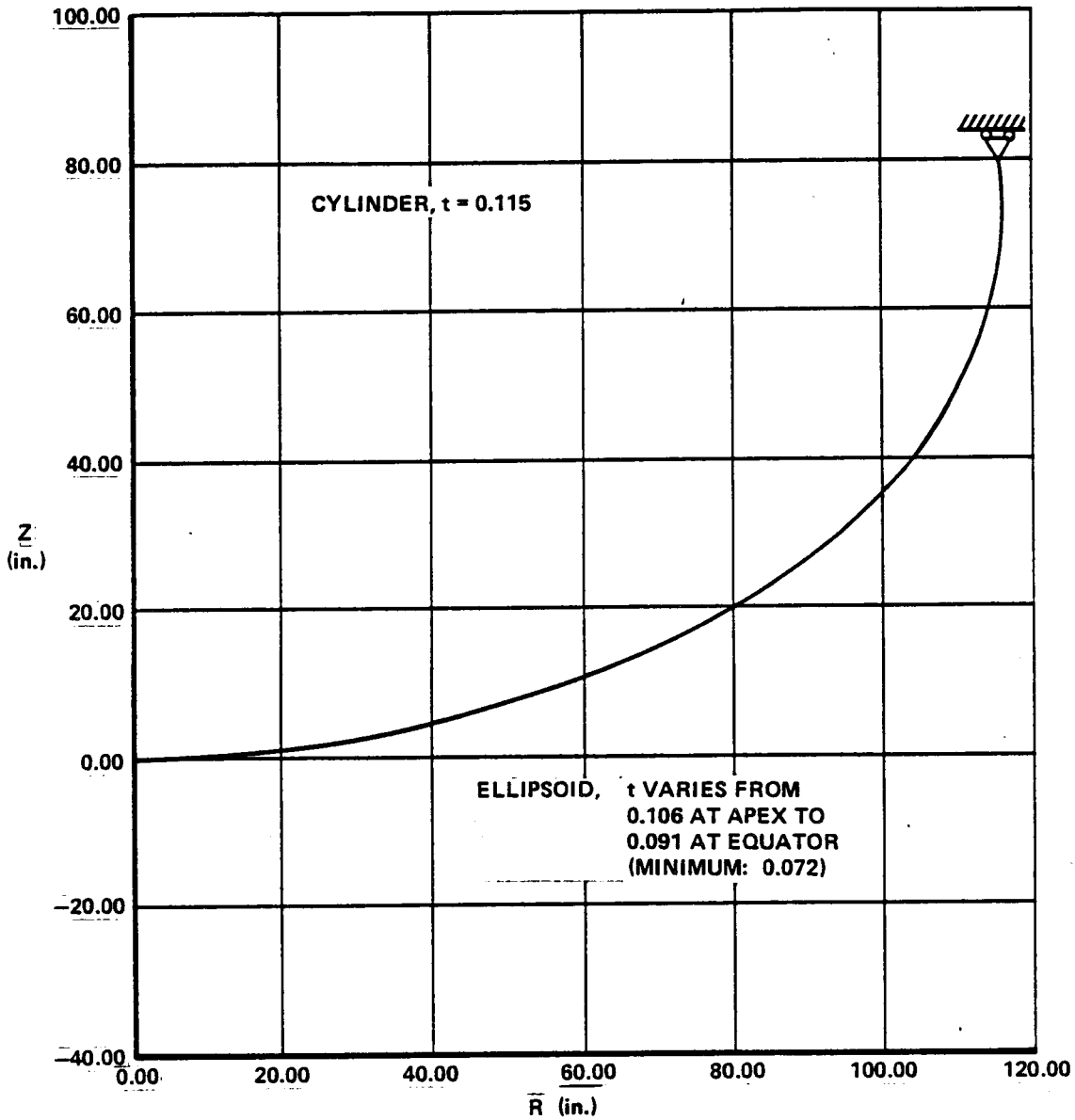

Figure 155. - Elliptic dome-nonlinear stress initial undeformed structure.

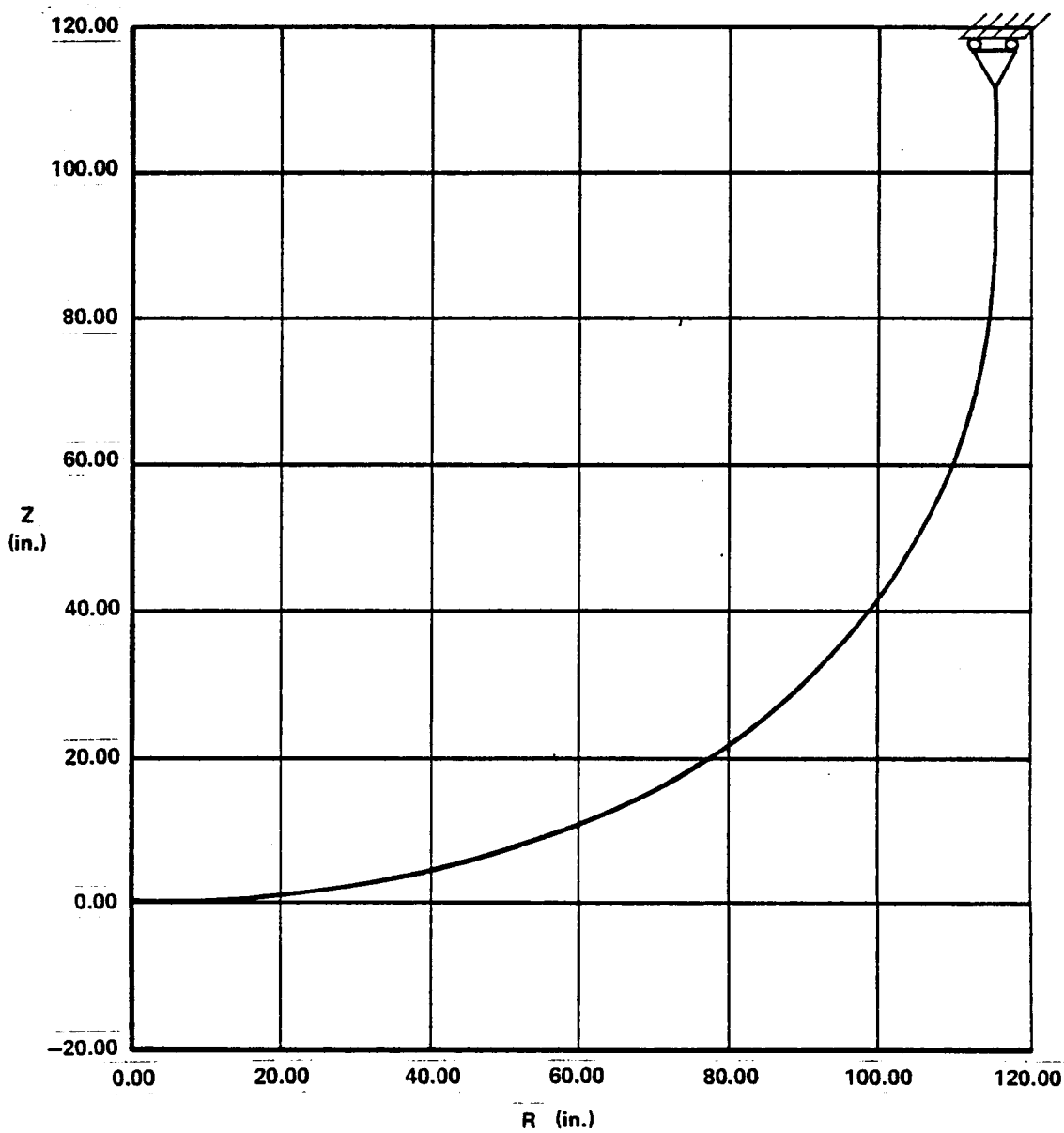

Figure 156. - Torispherical dome-nonlinear stress initial undeformed structure.

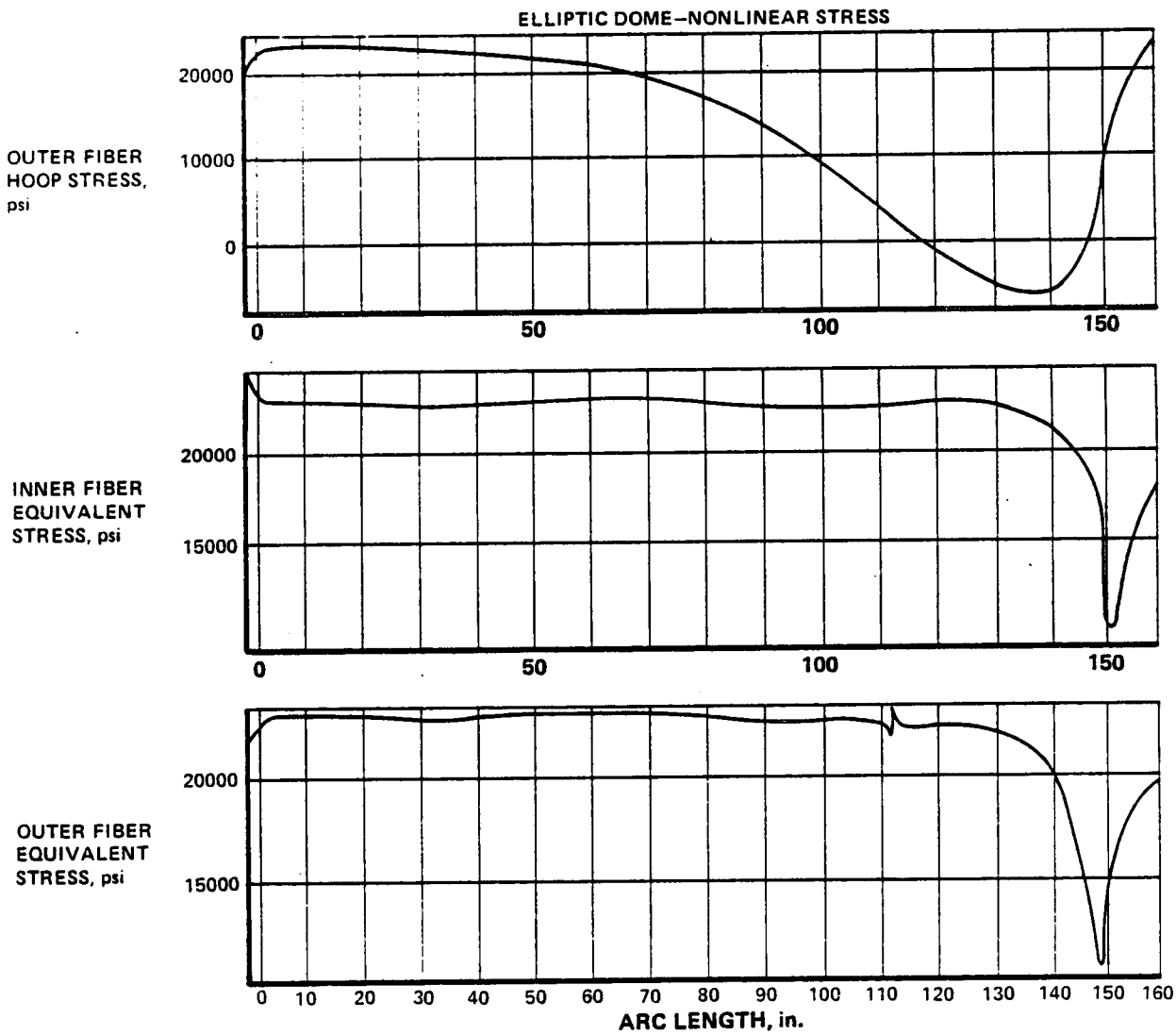

Figure 157. - Elliptical dome stresses.

savings of approximately 3-percent over ellipsoidal design. In addition no appreciable difference in the aircraft DOC is noted between the two minimum DOC designs. Both designs have a DOC of approximately 1.825 ¢/seat-n.mi.

Based on these results, neither design affords a clear cut decision as to the preferred dome configuration; hence, the elliptical dome with the minimum DOC configuration was selected as the baseline configuration for conducting further analyses.

NOTE: Sections 7.2.4.2 Tank Life Investigation, 7.2.4.3 Tank Pressurization Study, 7.2.4.4 Pressure Stabilization Study, 7.2.4.5 Tank Suspension Study will be forwarded within 2 weeks for insertion here.

7.2.4.2 Tank life investigation: A structural study was conducted to assess the mass trend associated with varying the tank design life, i.e., planning on replacing the tank during the 50 000 hours of service life required of the aircraft.

Representative tank wall and closure concepts were selected for each basic tank design (integral and nonintegral configurations) using the results of the prior concept screening analysis and dome shape study. These representative tanks were sized at selected point design regions using the applied loads and pressure schedule defined for the concept screening analysis and the design criteria specified in Section 7.2.1.

The three tank lives considered were the full aircraft life (50 000 hr), one half-life (25 000 hr) and one-third life (16 700 hr). For fatigue considerations both limit and ultimate tension design allowables were determined for each respective tank life. These allowables are presented in Figure 7-1 for baseline aluminum alloy 2219-T851. All allowables dealing with unpressurized fuselage shell structure are the same as those presented in the concept screening study.

The minimum weight tank wall designs were determined using the same methods described in the analytical methods section of the concept screening study. Using these methods, point designs were determined for a range of frame spacings for the integral tank design and as a function of the hoop fail-safe strap spacing for the nonintegral tank. The wall thicknesses of the tank closures were defined using the theory described in the dome shape study. The results of this study are presented in the following sections.

7.2.4.2.1 Integral Tank Design: As a result of the concept screening analysis, a hybrid structural approach utilizing both the zee-stiffened and unstiffened wall concepts was used for the integral tank design. Circumferentially, the stiffened wall concept was incorporated in the design at the relatively highly loaded upper and lower quadrants; while the unstiffened skin was employed at the side quadrants due to the lower loadings.

An example of the type of data obtained is summarized in Figure 7-2. This figure displays a summary of the point design data for the upper fiber at the tank quarter-length station. The upper figure shows the variation in wall thickness with life, the center figure displays the component and total unit weight for a representative life, and the lower figure depicts the total unit weight of the tank for each life investigated.

The wall thickness variations shown in the above figure incorporate longitudinal straps in the design to meet the fail-safe requirements imposed by the high tension loads. These fail-safe straps have an area of 0.2 in.^{2} and are centered between the stiffeners. The variations in the tank wall thicknesses are primarily attributable to the change in minimum skin thickness as a function of fatigue life. Dominance of the fail-safe requirements results in a constant equivalent thickness over the range of frame spacings.

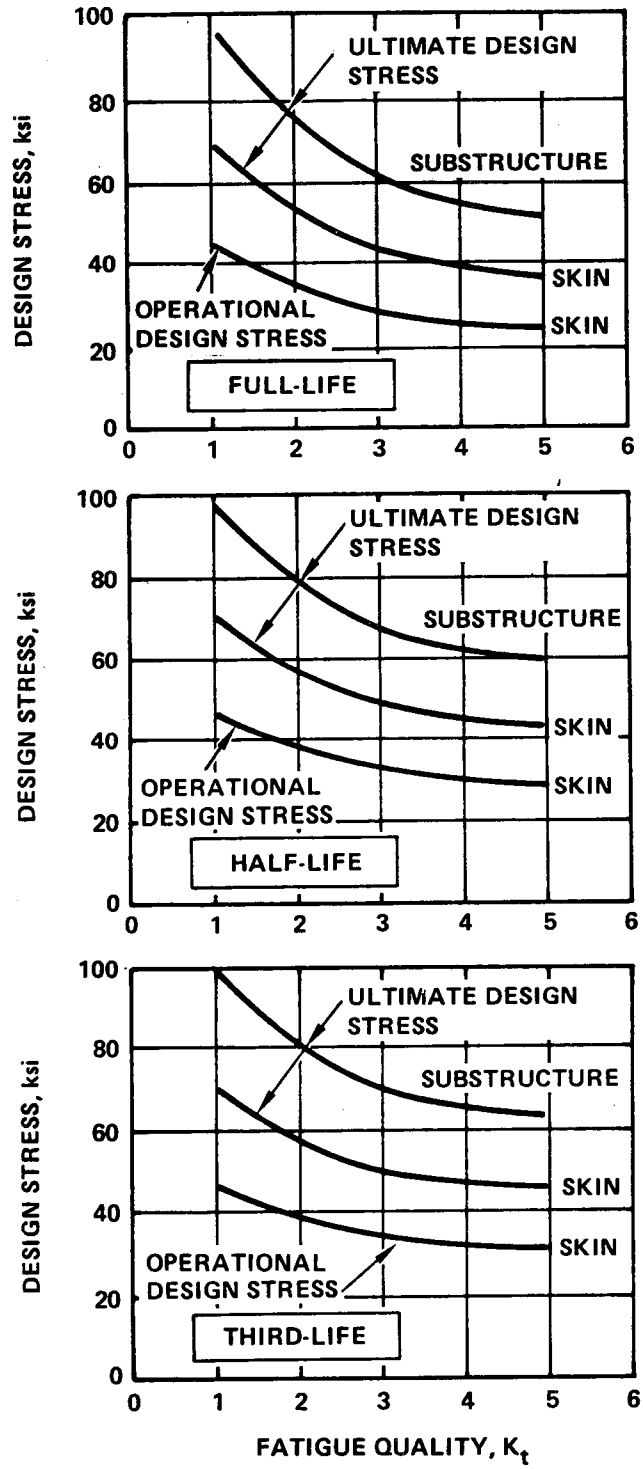

Figure 7-1. Variation in circumferential design stress with life, 2219-T851 aluminum alloy

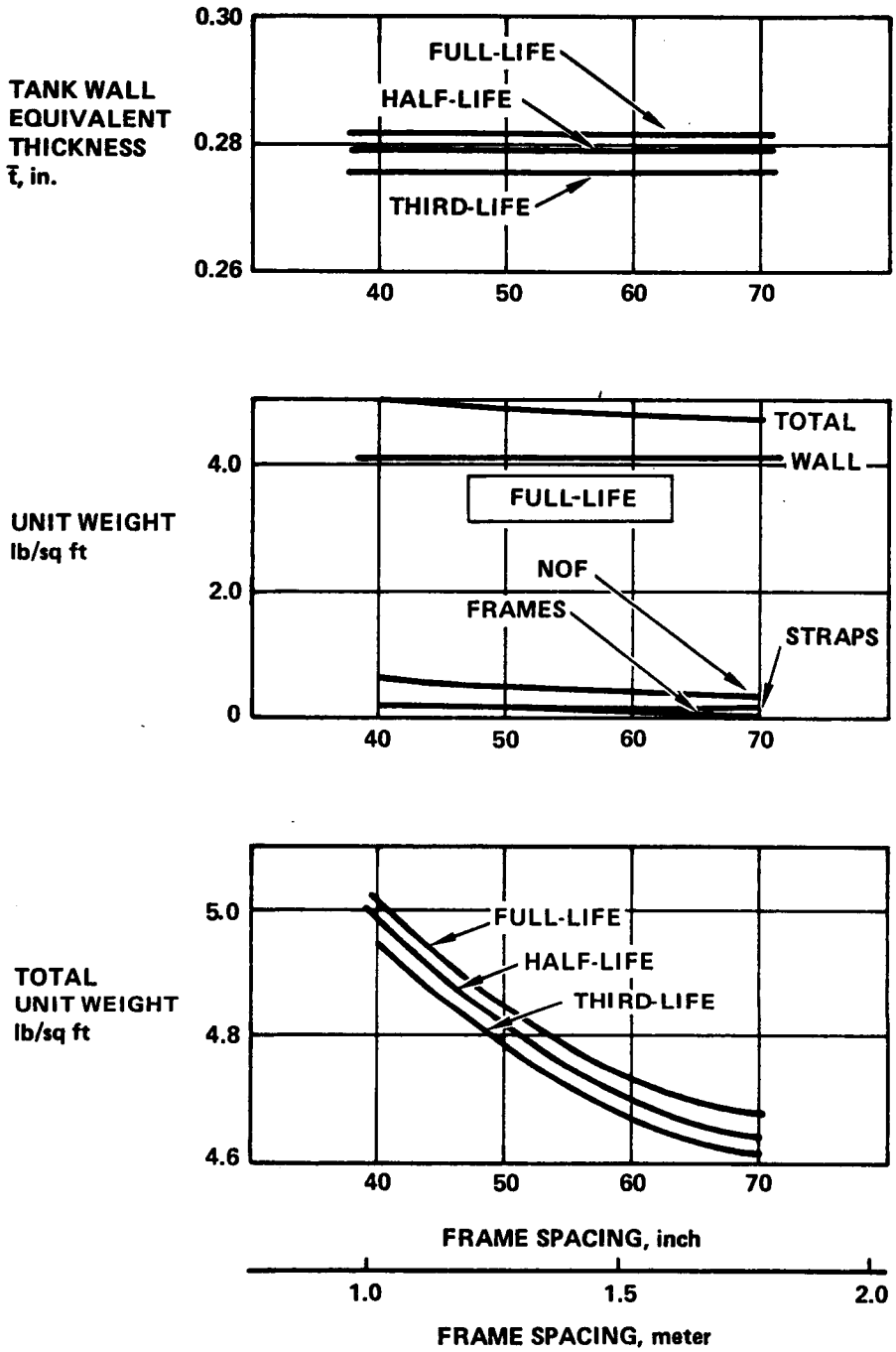

Figure 7-2. Upper fiber point design data at the quarter length station, integral tank

The equivalent panel thicknesses were then combined with the calculated thicknesses of the frames, circumferential fail-safe straps and non-optimum factors (NOF) to obtain a total panel weight. All of the subcomponents; frames, straps and NOF, vary with length of service life. A typical plot of the components and total unit weights for the full-life condition are shown in the middle plot of Figure 7-2.

The total weights for each life are shown in the lower plot of Figure 7-2 as a function of frame spacing. This plot reveals continuously decreasing values which are due to the effect of the subcomponents as the panels remain constant over the range of frame spacing. Thus, for this range of frame spacings, each life has a minimum value at a frame spacing of 70 in. with the third-life tank the lightest at 4.61 lb/ft^2, followed by the half-and full-lives at 4.63 lb/ft^2 and 4.68 lb/ft^2, respectively. Note the maximum variation in weight at this spacing is only 0.07 lb/ft^2.

An unstiffened panel design of 0.164 in. thickness was employed at midfiber location. Fail-safe considerations design these panels; hence there was no variation in thickness with life. Panel thicknesses were combined with the various applicable subcomponents to obtain both the unit and total weight for this location. As with the upper fiber location, the mid fiber location exhibits the same continuously decreasing total weight trend with tank life. Thus again, a minimum spacing of 70.0 in. provided the lightest structure with all designs weighing approximately 2.65 lb/ft^2. A weight variation of only 0.02 lb/ft^2 is noted between designs.

A summary of the results of the lower fiber point design analysis is presented in Figure 7-3. The variation in wall thickness for each tank-life (upper plot) is constant for frame spacings less than 50 in. with no variation due to change in life because of the circumferential damage fail-safe requirements. Unlike the upper fiber location, where longitudinal straps were employed, the lower fiber analysis indicated that increasing the skin thickness was a more efficient (i.e., lower weight) method of meeting the fail-safe requirements. The maximum lower fiber meridional tension load is approximately one-half of that on the upper fiber. Thus, for this region, the skin was not held to the minimum thickness dictated by fatigue for the respective life but was maintained at a level commensurate with the fail-safe requirements. The frame spacing region above 50 in. shows an increasing thickness with a variation from one life criterion to the next. Designs within these spacings are primarily controlled by local buckling with the fail-safe requirements becoming less critical as the frame spacing is increased.

Similar to the upper fiber analysis, plots of the component and total unit weights for the lower fiber were constructed for each tank life. The component unit weights for the full-life condition are presented in the center of Figure 7-3. The total weights are shown in the lower figure and indicates minimum weight designs at 50.0 in frame spacing for each of the life intervals investigated. The corresponding total unit weights for these designs are approximately the same, i.e., the heaviest weight design (full-life) has a weight of 3.78 lb/ft^2, which is only 0.01 lb/ft^2 heavier than those designed for half-and third-life intervals.

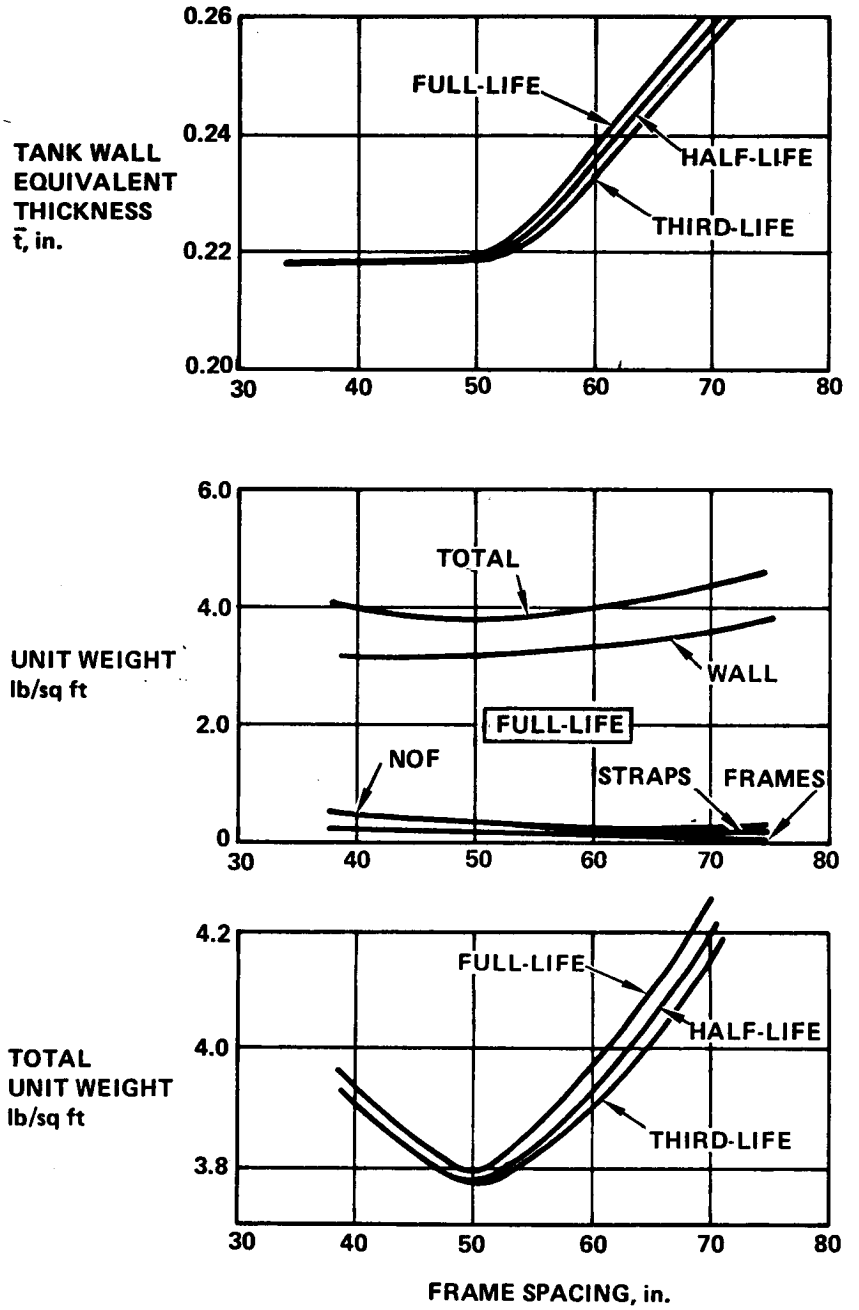

Figure 7-3. Lower Fiber point design data at quarter-length station, integral tank

An average equivalent thickness for the circumference at the quarter length station was calculated using the results of the analysis conducted on the upper, mid and lower fibers. These data were plotted as a function of frame spacing, as presented in Figure 7-4. Minimum-weight frame spacings of 53.0 in., 54.0 in and 56.0 in. are noted for the full-, half-and third-life designs, respectively. The lightest weight tank is the third-life design which weighs 3.47 lb/ft^2. It is only 0.03 lb/ft^2 lighter than the heaviest design (full-life).

The minimum weight design data at the quarter-length station were used in association with the corresponding data at the three-quarter length station to calculate the weight of the tank cylinder for each design life.

In addition to calculating the cylinder weights, the weights of ellipsoidal tank domes with an a/b ratio of 1.6 and a minimum wall thickness of 0.05 in. were estimated. Combining the cylinder weight results with the fore and aft tank dome head designs provided a total tank weight. The results are reported in section 7.2.4.2.3.

7.2.4.2.2 Nonintegral Tank Design: An unstiffened skin design, the most-promising concept resulting from the concept screening study, was used in the life study evaluation for nonintegral tanks. Due to the predominance of the fail-safe requirement, no change was found as a result of the life criterion. Subcomponents, straps, and NOF also were found to be invariant with length of service life. The fuselage shell was not considered as a replacement item; hence, it was not effected by a change in life criterion. Consequently, the non-intergral tank weight remains constant as a function of design life and is identical to the data presented in the concept screening study for all circumferential locations at both quarter point stations.

Closures similar in design to those used for the integral tank were incorporated into this design also. Ellipsoidal domes with an aspect ratio (a/b) = 1.6 were used in addition to restricting the minimum gage to 1.27 mm (0.050 in).

Thus, the only variation due to design life specification results from the change in the tank heads. Adding the tank head variation to the constant tank body weights, a total tank weight for each life is evolved and may be evaluated to find the minimum DOC life concept.

7.2.4.2.3 Conclusions: The following table presents the tank weights, excluding insulation, for the integral and nonintegral tank designs. The values shown reflect the weight of both the forward and aft tanks.

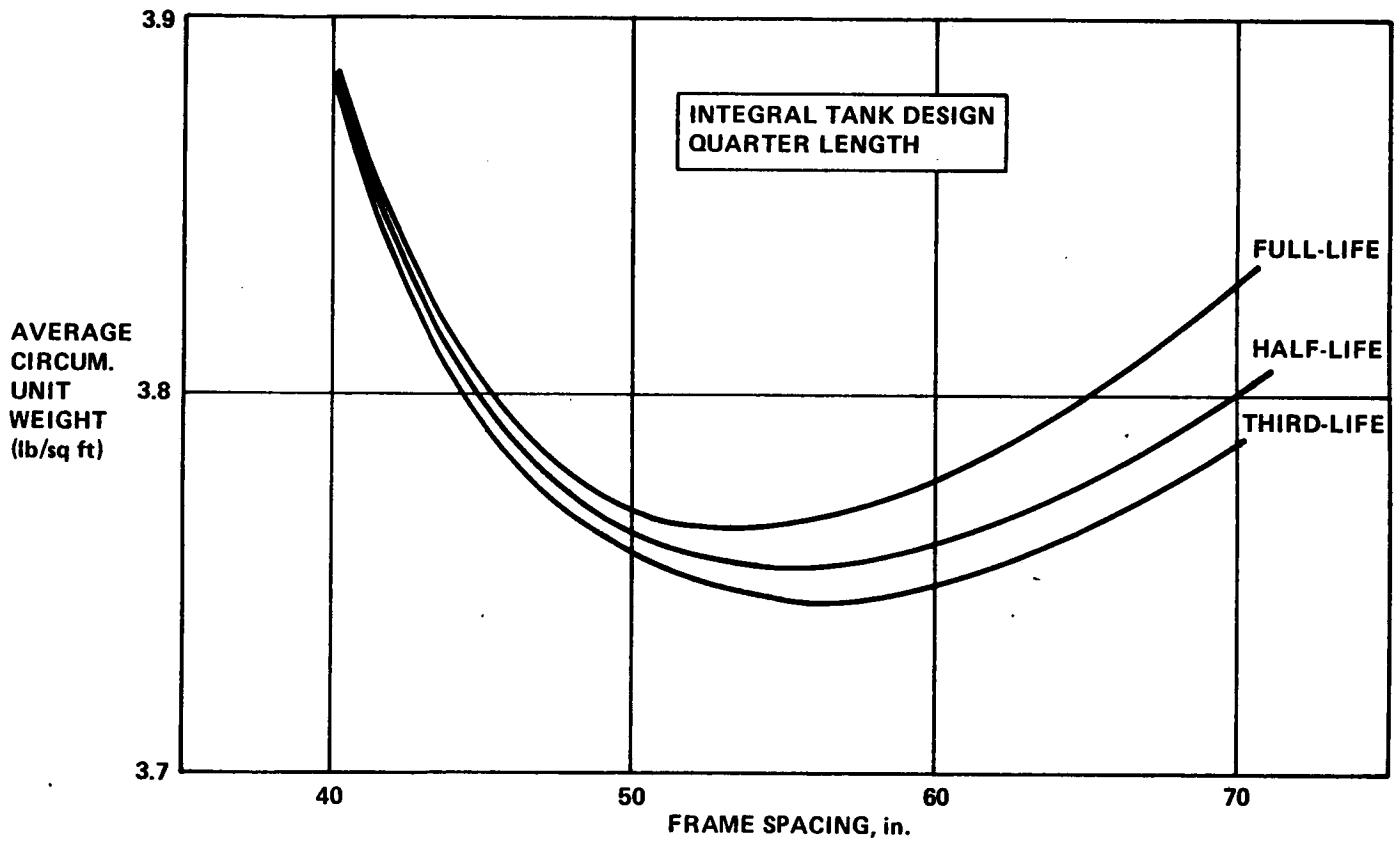

Figure 7-4. Variation in average circumferential unit weight with life, integral tank

Tank Design	Tank Weight (lb) Nonintegral Design	Integral Design
Full-Life	20 322	15 612
Half-Life	20 240	15 518
Third-Life	20 140	15 408

For both tank designs, only small changes in weight are noted as the life varies. A weight decrement of 182 lb is noted for the third-life design when compared to the full-life design for the nonintegral tank. Similarly, a weight decrement of 204 lb is noted when the same life designs are compared for the integral tank. These small weight savings offered by the reduced life tank designs translate into an insignificant decrement in aircraft DOC that would not off-set the initial investment and installation costs for replacing the tanks.

7.2.4.3 Tank Pressurization Study: This study was undertaken to assess the impact on airplane weight and DOC elicited by using higher tank pressures. Three pressures were studied, including the baseline nominal tank pressure of 21 psia. The two higher nominal tank pressures were 30 psia and 40 psia.

Both integral and nonintegral designs were investigated in this study. For the integral tank design, the one-piece zee-stiffened configuration was employed; whereas, for the nonintegral tank an unstiffened wall design was utilized. These configurations were the most-promising concepts surviving the concept screening analysis. Ellipsoidal tank domes, with their associated minimum DOC parameters, were used for both tank designs based on the results of the previously reported dome shape study. Total tank weights were thus defined for both basic types of tanks.

The tension loads corresponding to the three pressure cases are shown in Table 7-1. These loads are combined loads (airload, pressure and thermal) where only the membrane forces due to the internal pressurization are multiplied by the ratio of pressures. The criteria and analytical methods are defined in Section 7.2.1 and 7.2.3.2.

7.2.4.3.1 Integral Tank Design: At the quarter length station the zee-stiffened panel concept was evaluated at the upper fiber location with respect to frame spacing for each candidate pressure. The wall thicknesses for these designs are constant at 0.284 in., 0.336 in., and 0.408 in., for the design pressures of 21, 30, and 40 psia, respectively, regardless of frame spacing. As noted previously, all of the upper fiber designs contain longitudinal fail-safe straps centered between the stiffeners with an area of 0.20 in^2.

TABLE 7-1. MEMBRANE LOAD VARIATION WITH TANK PRESSURE, TANK PRESSURIZATION STUDY

Nominal Tank Pressure (psia)	Type of Tank	Membrane Loads (Ultimate)								
		Upper Fiber			Mid Fiber			Lower Fiber		
		Cond.	N_1 (lb/in)	N_2 (lb/in)	Cond.	N_1 (lb/in)	N_2 (lb/in)	Cond.	N_1 (lb/in)	N_2 (lb/in)
21.0	Nonintegral	Cruise	1582	3097	Cruise	1563	3145	Cruise	1615	3194
	Integral	PLA	3983	2370	Cruise	1698	2753	Neg Man	2256	2288
30.0	Nonintegral	Cruise	2356	4645	Cruise	2337	4694	Cruise	2388	4741
	Integral	PLA	4830	3755	Cruise	2524	4103	Neg Man	3105	3684
40.0	Nonintegral	Cruise	3211	6359	Cruise	3195	6406	Cruise	3244	6455
	Integral	PLA	5772	5295	Cruise	3411	5602	Neg Man	4049	5227

The dominance of the fail-safe requirements at 21 psia and the combination of fail-safe and complex stress requirements at the higher pressures, accounts for the constant equivalent thickness over the range of frame spacings. The panel equivalent thicknesses are combined with the subcomponents (straps and frames) and the nonoptimum factor to obtain the total unit weights which are shown in Figure 7-5.

The only subcomponent variation experienced was the increase of the circumferential strap equivalent thickness which was found by means of load ratios applied to the baseline case. The strength consideration in the frame design is generally not a controlling factor, especially at larger spacings, nor is the nonoptimum factor (NOF) variation of great enough magnitude to be accounted for.

The unit total weight plots display continuously decreasing curves with a decelerating rate as frame spacing increases. A drop-off of the subcomponent effect is indicated by the decreasing curves for a constant panel weight. Minimum-weight panel designs are found at the maximum frame spacing investigated, 60 inches. As expected, the panel designed for 21 psia is the lightest and the 40 psia the heaviest. Minimum-weight designs for the 21 psia, 30 psia and 40 psia are 4.66 lb/ft^2, 5.46 lb/ft^2 and 6.53 lb/ft^2, respectively.

The panel concept at the mid-fiber location is the fail-safe critical, unstiffened skin configuration with thicknesses of 0.164 in., 0.245 in. and 0.335 in. representing 21 psia., 30 psia., and 40 psia., respectively. These thicknesses are constant over the range of frame spacings. Similar to the upper fiber total weight curves, the mid-fiber location has a minimum-weight spacing of 60 in. and corresponding weights of 2.68 lb/ft^2, 3.96 lb/ft^2 and 5.38 lb/ft^2 for 21 psia., 30 psia., and 40 psia., respectively.

The variation of the panel thicknesses for the lower fiber location at the quarter length station are presented in Figure 7-6. Note that the 21 psia. case does not employ longitudinal fail-safe straps but that they are included in the 30 psia and 40 psia cases. This situation is necessitated by the added tension load brought on by the higher pressures. The straps are centered between stiffeners with an area of 0.2 in^2. The use of straps for the 21 psia. case, or the deletion of straps for the higher pressures, would result in much higher equivalent thicknesses. Although the usage indicated in Figure 7-6 does alter the one-to-one comparison, the designs represented are minimum weights.

With reference to Figure 7-6, the nonlinearities between the panel thickness curves can best be explained by describing the critical failure modes for each design. The panels designed for the baseline pressure case (21 psia) are fail-safe critical at the lower frame spacings with local buckling becoming predominate as frame spacing increases. For the 30 psia design condition, fail-safe, strength, and local buckling modes are active at various frame spacings. The fail-safe criteria are dominate at the lower frame spacings, whereas the basic strength and local buckling modes constrain the designs at higher spacings.

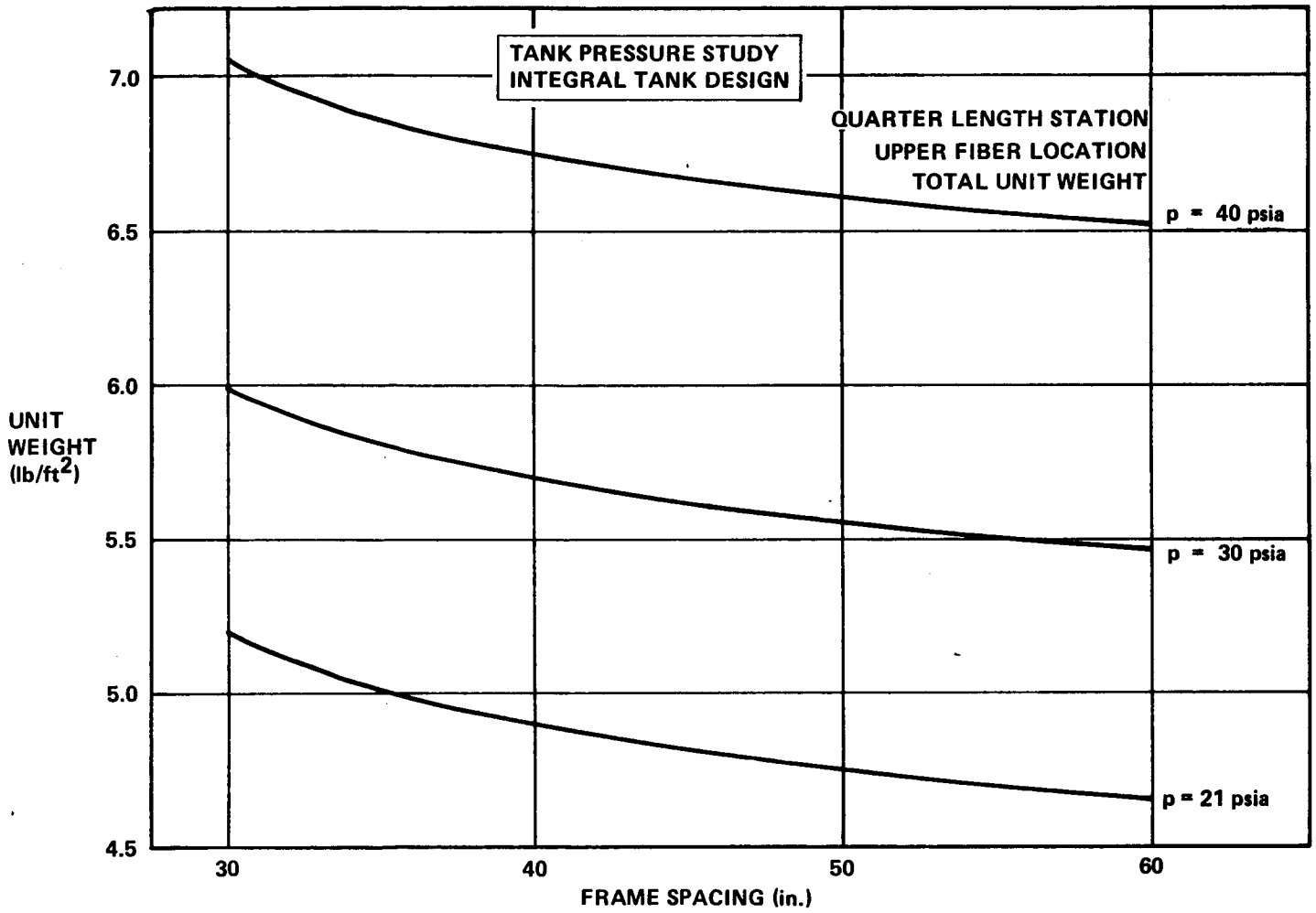

Figure 7-5. Variation in tank unit weight with internal pressure, integral design

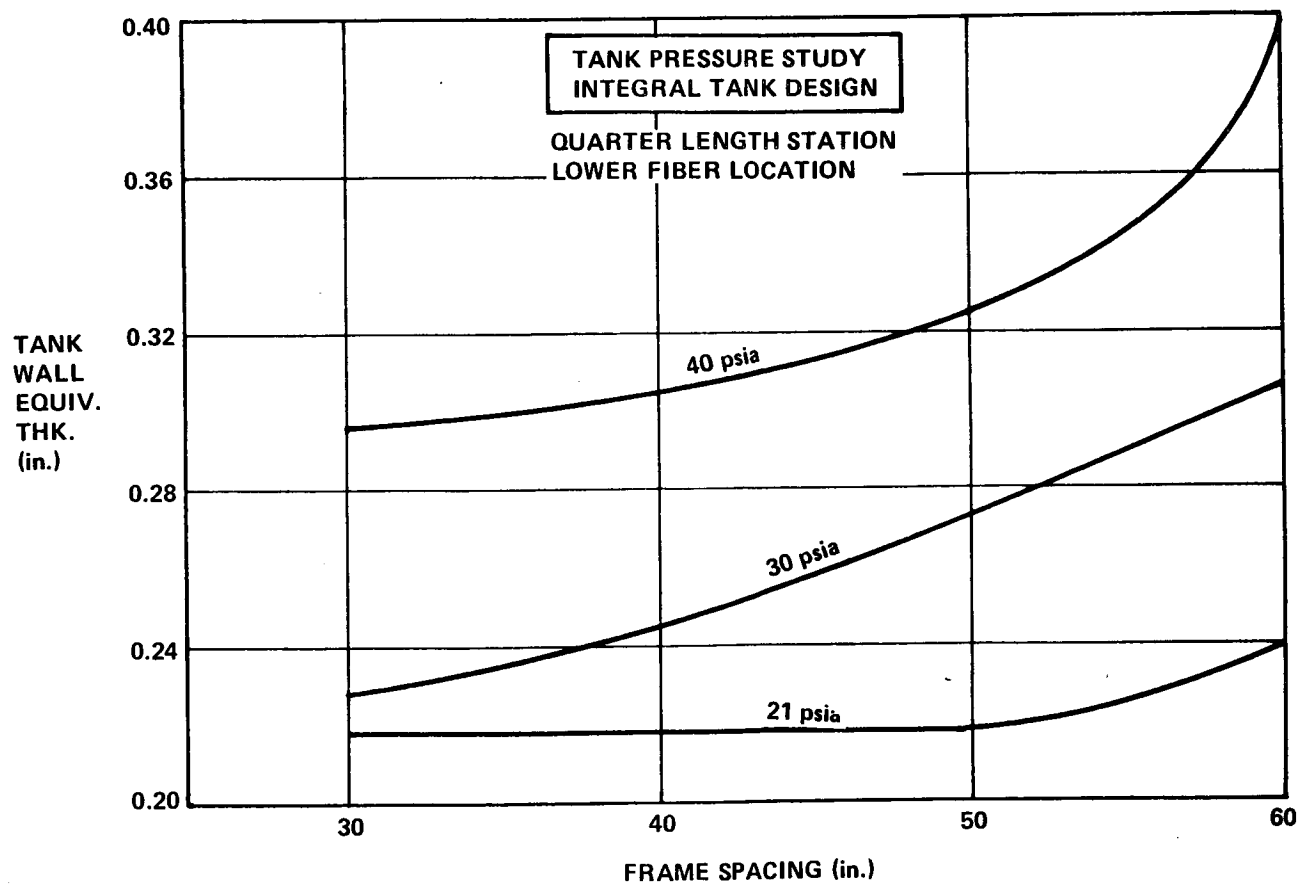

Figure 7-6. Variation in tank wall equivalent thickness with internal pressure, integral tank design

The further increase of pressure to 40 psia results in fail-safe dominance for all frame spacings. The cross-sectional geometry is proportioned by basic strength and local buckling requirements.

Plots of the total weight at the lower fiber location are presented in Figure 7-7. A minimum weight frame spacing is noted for each pressure condition. The corresponding weights for these designs are 3.64 lb/ft^2, 4.19 lb/ft^2 and 5.14 lb/ft^2 for the 21 psia., 30 psia. and 40 psia. conditions, respectively.

At the quarter-length station, the unit weights of the panel designs at the three circumferential locations are averaged to obtain a unit weight for the complete cross-section which is presented in Figure 7-8. Optimum frame spacings of 54 in., 50 in., and 50 in. are noted for the 21 psia, 30 psia and 40 psia pressures cases, respectively. The corresponding weights are 3.43 lb/ft^2, 4.49 lb/ft^2 and 5.67 lb/ft^2, respectively.

The unit weights at the three-quarter length station were obtained by extrapolating, using load ratios, the unit weights at the quarter length station. These data were then combined with the weights of the tank domes designed for the various pressure cases to calculate the total tank weights which are presented in Section 7.2.4.3.3.

7.2.4.3.2 Nonintegral Tank Design: The pressurization study conducted on the nonintegral tank design was performed using the minimum-weight design from the concept screening study, i.e., an unstiffened wall configuration for the tank with a hat-stiffened fuselage. The same panels designed for the concept screening study were used as the baseline (21 psia) tank design. A different set of panels was sized for each higher pressure case. The various wall thicknesses at the quarter length station are presented in Table 7-2. All of these designs are fail-safe critical at each circumferential location for each nominal tank pressure. As such, they are constant over the range of strap spacings. The subcomponents (straps and NOF) are increased from the baseline case by means of load ratios for each higher pressure with variations circumferentially but not longitudinally. The various components are combined to define the total unit weights. There is an insignificant variation in unit weight with strap spacing at each circumferential location. Table 7-3 presents the minimum weights for each pressure and circumferential location, all of which occur at the largest strap spacing (20.0 in.). The average circumferential weights are also shown. These average unit weights are plotted versus strap spacing in Figure 7-9. All of the nonintegral designs reveal small variations with strap spacing and minor effects of the subcomponents with the design being dominated by the weight of the panel.

The designs of the three-quarter length station were extrapolated, via load ratios applied to the one quarter length location. The weights of these two point design regions were then combined with weights of the tank domes to obtain a total tank weight for each pressure intensity.

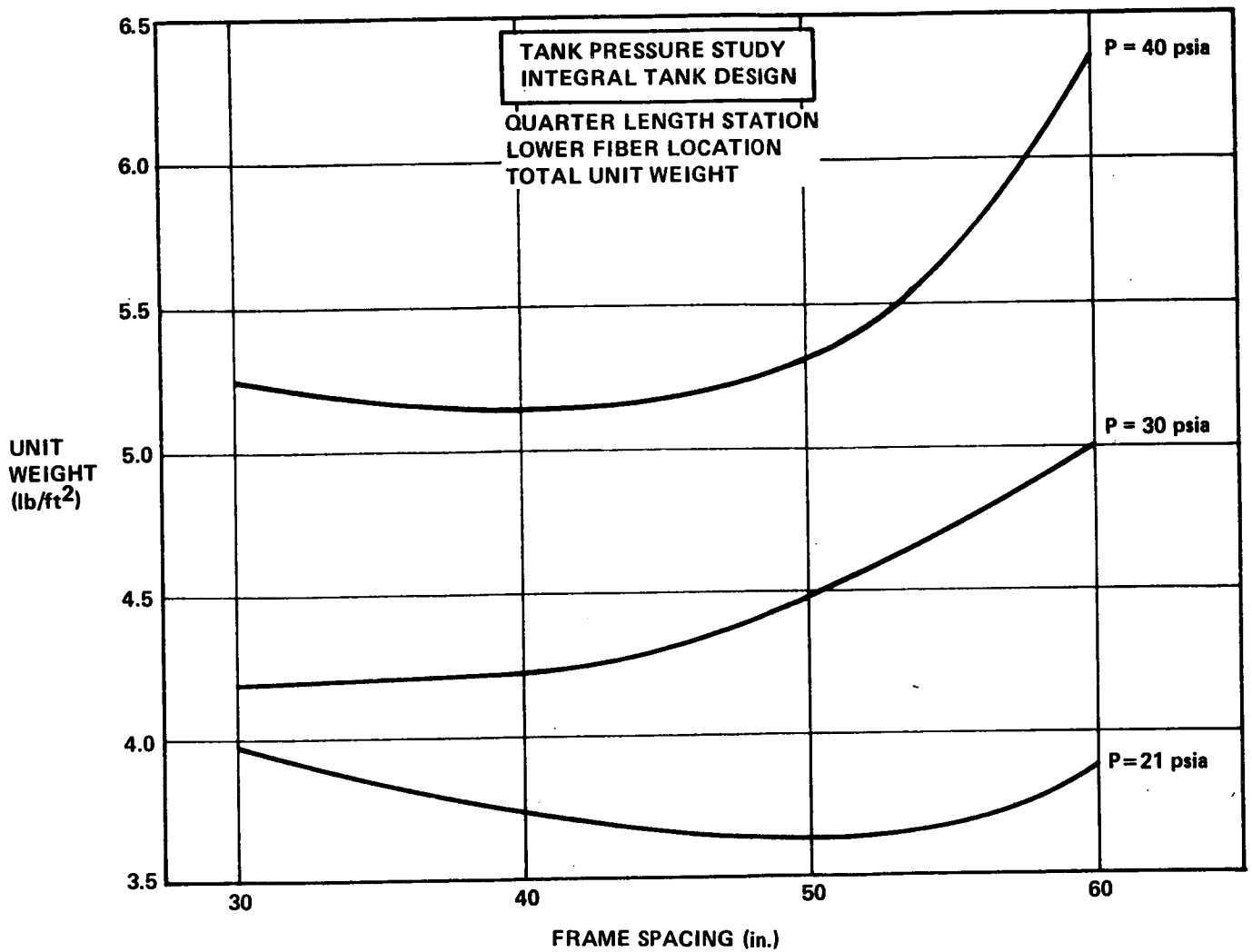

Figure 7-7. Variation in tank unit weight with internal pressure, integral design

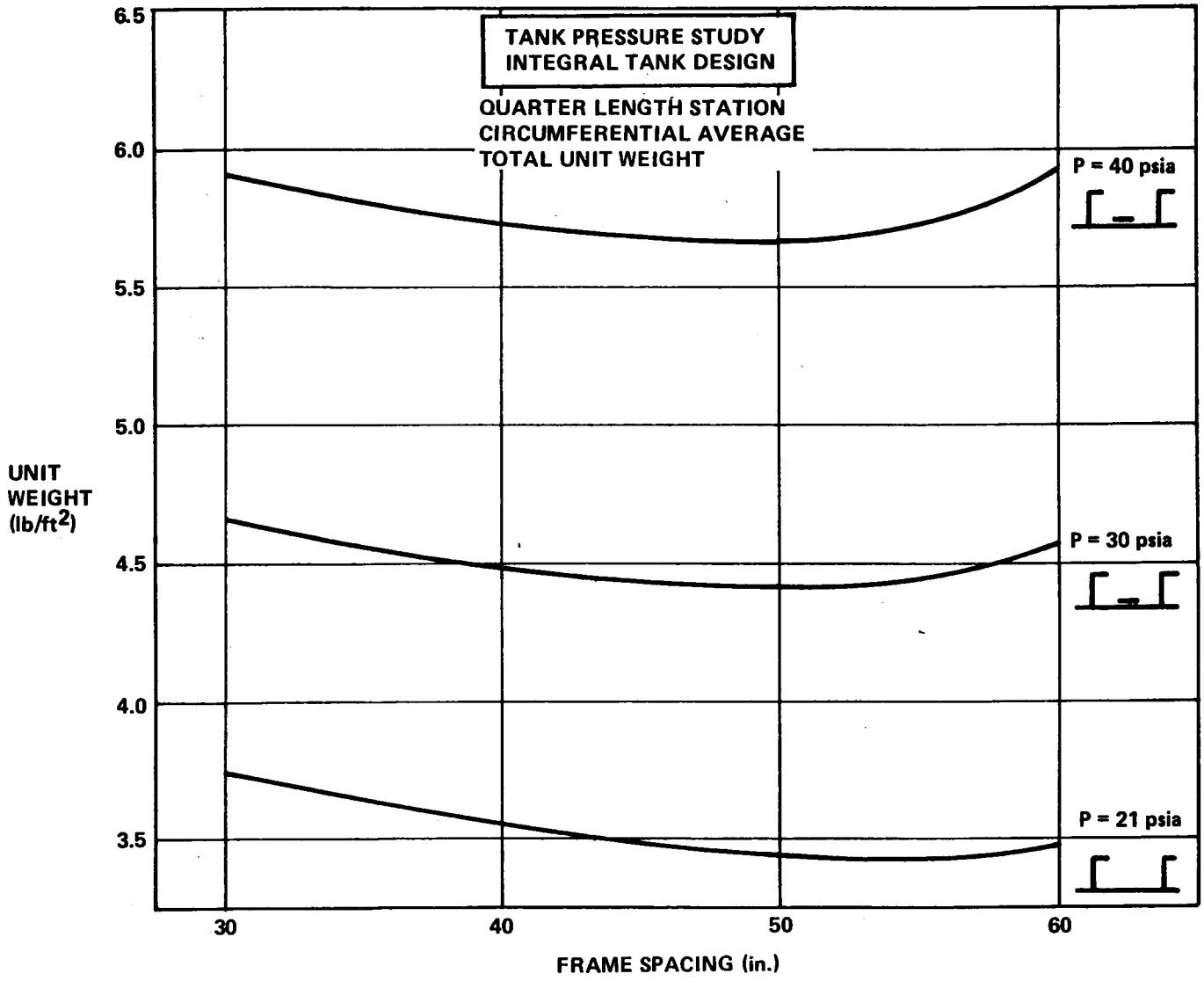

Figure 7-8. Variation in average circumferential weight with internal pressure, integral design

TABLE 7-2. VARIATION OF TANK WALL THICKNESS WITH INTERNAL PRESSURE, NONINTEGRAL DESIGN

Nominal Tank Pressure (psia)	Tank Wall Equivalent Thickness, in[1]			
	Upper Fiber	Mid Fiber	Lower Fiber	Average
21.0	0.153	0.151	0.156	0.152
30.0	0.227	0.225	0.230	0.227
40.0	0.310	0.308	0.313	0.310

[1] Quarter length point design region.

TABLE 7-3. VARIATION OF TANK UNIT WEIGHT WITH INTERNAL PRESSURE, NONINTEGRAL DESIGN

Nominal Tank Pressure (psia)	Tank Unit Weight, lb/sq ft [1][2]			
	Upper Fiber	Mid Fiber	Lower Fiber	Average
21.0	4.90	4.60	4.40	4.62
30.0	6.16	5.89	5.68	5.91
40.0	7.60	7.32	7.11	7.34

(1) Quarter length point design region

(2) All data reflects a fail-safe strap spacing of 20.0 in.

7.2.4.3.3 Conclusions: The results of the tank pressurization study are shown in Table 7-4 for both the nonintegral and integral tanks. Optimum tank weights are shown, in addition to weight of the body shell required in conjunction with nonintegral tanks over the tank conical section. As would be expected, the weight of the nonintegral tank is very nearly directly proportional to nominal design pressure. This is not the case for the integral tanks, where a significant portion of the tank cylinder is designed by body shear and bending loads in addition to tank pressure loads. The results are also plotted in Figure 7-10 and show that as tank pressure is increased the tank weights tend to converge. This is due to the reduced influence of body loads on the integral tank at higher pressures.

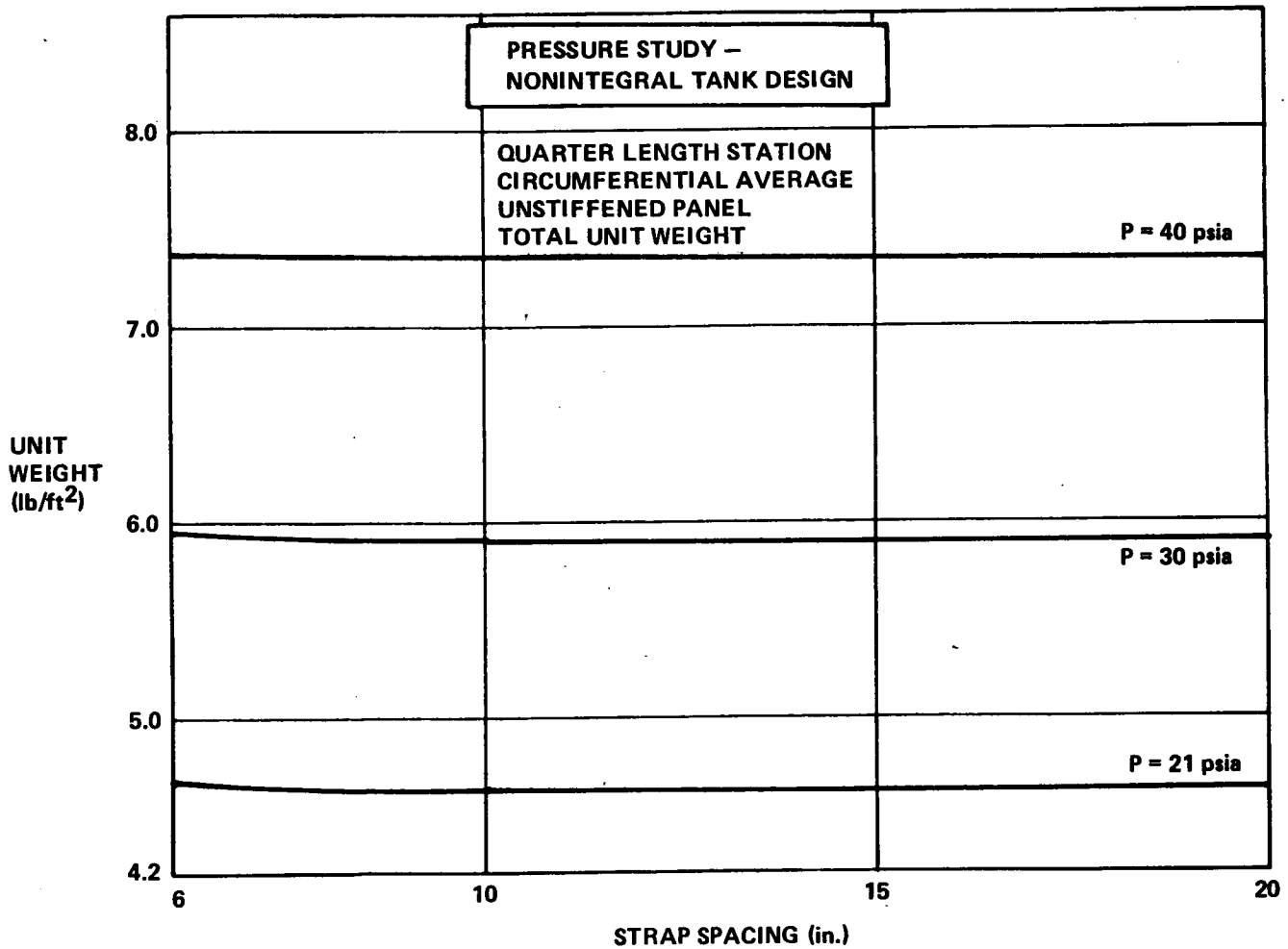

Figure 7-9. Variation in average circumferential weight with internal pressure, nonintegral tank design

TABLE 7-4. LH_2 AFT TANK PRESSURIZATION STUDY RESULTS

Item	Nonintegral			Integral		
Nominal Pressure	21	30	40	21	30	40
Tank	(4749)	(6918)	(9374)	(5884)	(7663)	(9678)
Cylindrical Section	3799	5640	7726	4852	6267	7876
Dome Ends	669	997	1367	732	1096	1502
Divider Dome	281	281	281	300	300	300
Body Shell (over tank conical section only)	2928	2928	2928	—	—	—
Total	7677	9846	12 302	5884	7663	9678

Table 7-5 shows the optimum tank and body shell thicknesses along with tank dimensions used in this study. Using the results of the concept screening study, it was found that the weight of the tank conical section could be approximated (within 1%) by the following equation:

$$W_{\text{tank cone}} = (W_{.25L} + W_{.75L}) \left(\frac{L \text{ tank cone}}{2}\right)$$

The above equation was used to calculate the weight of the tank conical section and body shell.

The effect of higher tank pressures on liquid hydrogen boiloff was reported in section 7.1.6.2.3. That analysis showed that approximately 213 kg (470 lb) of LH_2 could be saved from being vented in flight if a tank pressure of 276 kPa (40 psia) was used instead of the nominal value of 138 kPa (21 psia). A similar weight of LH_2 could be saved from being vented during the tank filling operation, however that is a less valuable saving because the vent gases are recovered and reliquefied.

In any event, design for the higher tank pressure is not a worthwhile proposition because of the tremendous weight penalty associated with the structural design.

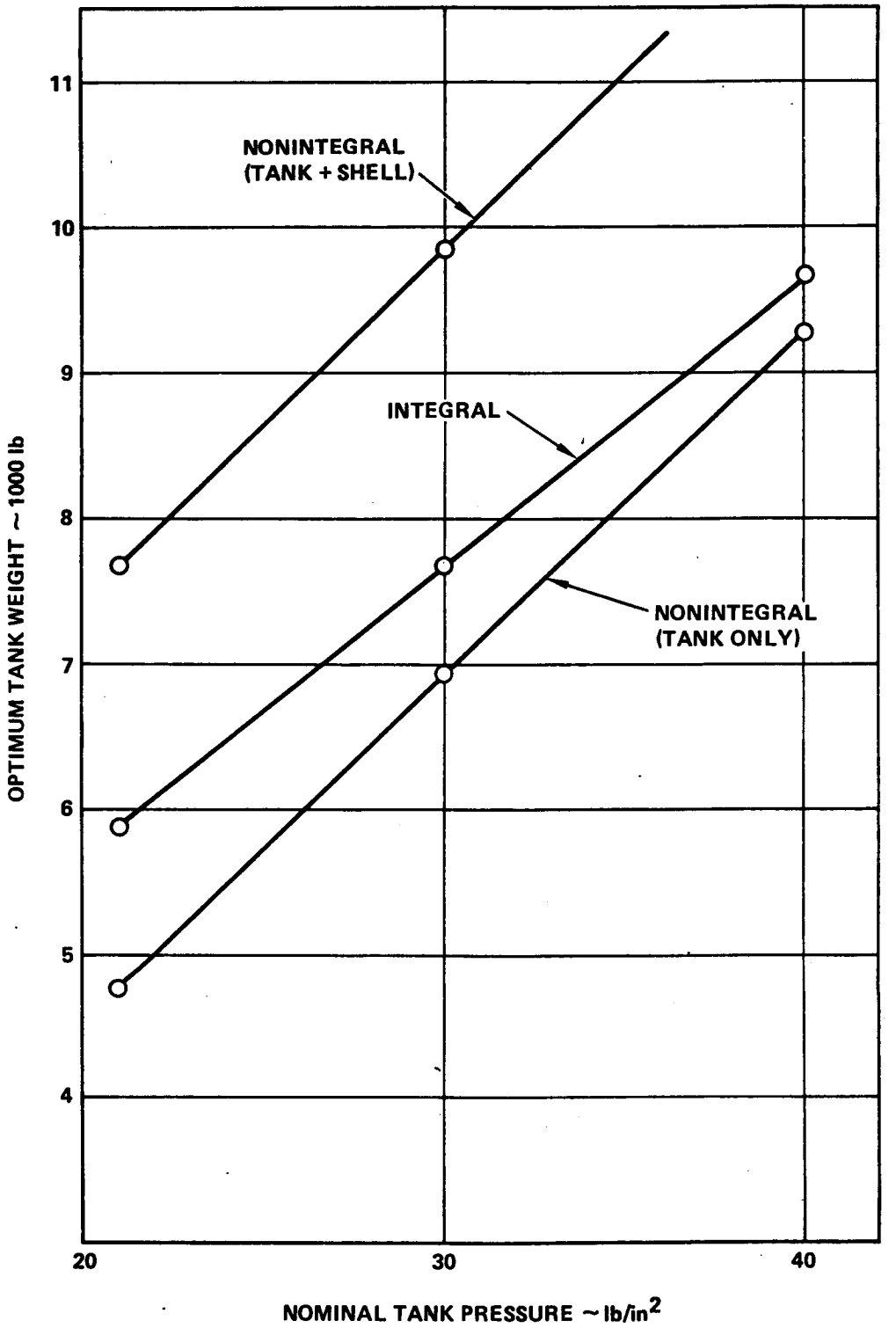

Figure 7-10. Weight vs nominal pressure for integral and nonintegral tanks

TABLE 7-5. TANK PRESSURIZATION STUDY ~ AFT TANK

NONINTEGRAL ~ Optimum $\bar{t}$ (including frames and fail-safe straps)								
Location on Tank Circumference	Body Shell		Nominal Pressure ~ psia.					
			21		30		40	
	L/4	3/4 L	L/4	3/4 L	L/4	3/4 L	L/4	3/4 L
Upper	0.157	0.141	0.183	0.145	0.270	0.215	0.371	0.296
Mid	0.104	0.091	0.181	0.145	0.271	0.215	0.370	0.296
Lower	0.119	0.106	0.187	0.145	0.276	0.215	0.375	0.296
Ave. $\bar{t}$ (in.)	0.121	0.107	0.183	0.145	0.272	0.215	0.372	0.296
$\bar{w}$ (psf)	1.74	1.54	2.64	2.09	3.92	3.10	5.36	4.26
Dia. ~ ft	19.30	15.65	17.43	13.79	17.43	13.79	17.43	13.79
Tank Unit Wt~lb/ft	105.5	75.7	144.6	90.5	214.7	134.3	293.5	184.6
Tank Cone Wt. ~ lb (L Tank Cone = 32.32')	2928.4		3799.2		5639.8		7726.1	

INTEGRAL ~ Optimum $\bar{t}$ (including frames and fail-safe straps)						
Location on Tank Circumference	Nominal Pressure ~ psia.					
	21		30		40.	
	L/4	3/4 L	L/4	3/4 L	L/4	3/4 L
Upper	0.329	0.314	0.384	0.356	0.459	0.416
Mid	0.187	0.151	0.276	0.221	0.374	0.300
Lower	0.253	0.220	0.311	0.266	0.363	0.310
Ave. (in) $\bar{t}_{AVE}$	0.239	0.209	0.312	0.266	0.394	0.332
(psf) $\bar{w}_{AVE}$	3.44	3.01	4.49	3.83	5.67	4.78
Dia. ~ ft	17.97	14.51	17.97	14.51	17.97	14.51
Tank Unit Wt. ~ lb/ft (w)	194.2	137.2	253.5	174.6	320.1	217.9
Tank Cone Wt~lb (L = 29.28')	4851.7		6267.4		7876.3	

7.2.4.4 Pressure stabilization study: The objective of the pressure stabilization study was to investigate the effect of internal tank pressurization on the buckling strength of typical LH_2 tanks. Based on the results of the concept screening analysis, the tankage for the baseline nonintegral tank design is tension designed; hence, stability is not a critical design factor. Therefore, only the integral tank design was considered for this study.

Approach: A BOSOR4 structural model was established using the baseline integral tank configuration (Section 7.2.3.3) and the tank wall data resulting from the concept screening analysis (Section 7.2.3.6). Using this model as the foundation for this study the following approach was taken, illustrated in Figure 7-11.

1. The tank was analyzed for the ultimate load condition, without internal pressurization, to ascertain if the basic design criteria is met. Point A in Figure 7-11.

2. The above step was repeated using limit loads, without internal pressurization, to assess the structural margin available in this design. Point B in Figure 7-11.

3. The stiffness of the structure was reduced so that the buckling load exactly equals the limit load. This stiffness reduction was accomplished by a reduction in the modulus of elasticity, which is approximately equivalent to a reduction in the thicknesses of the various shell components. Point C in Figure 7-11.

4. A constant internal pressure was added to the reduced stiffness configuration (step 3) until the buckling load equals 1.5 times the limit loads; i.e., the structure meets the ultimate load criteria. Curve $C\text{-}D_3$ in Figure 7-11.

5. The damage tolerance criteria was applied to the reduced stiffness tank wall configuration of step 4.

6. The amount of weight savings was assessed.

Model Definition: The geometric configuration for the selected tank (the aft tank) is shown in Figure 7-12. Fore and aft of the tank a short segment of the fuselage structure is added to the mathematical model to insure that the boundaries are properly accounted for. The forward end of the model is assumed to be clamped, the aft end is free.

The loading consists of air loads and inertia loads. At sta 2370 (see Figure 7-12) the total limit moment is 82×10^6 in lb and the limit shear 215 000 lb. At sta 2700 the moment is 32.7×10^6 in lb and the shear is 115 000 lb. The structure is assumed weightless, except for the tank, where the structure and fuel weigh 40 000 lb. With a load factor of 2.5 the inertia load of the tank is 100 000 lb which was distributed axially in proportion to the diameter of the tank. In addition to this inertia contribution, the pressure head of the tank and fuel were included in the analysis.

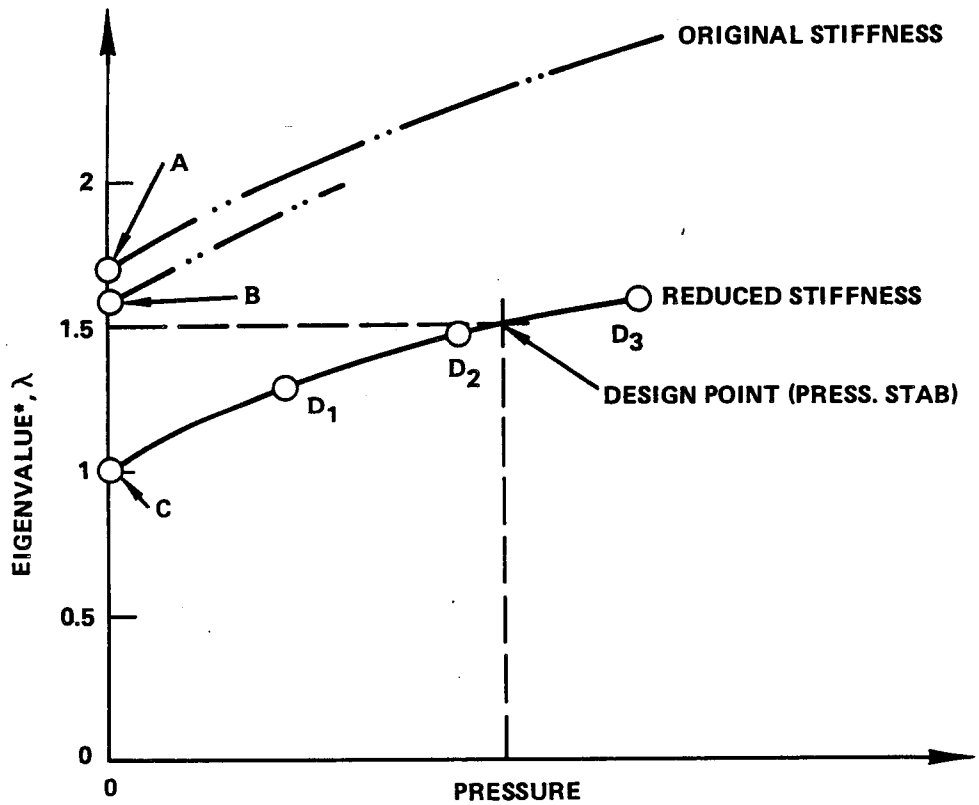

*THE EIGENVALUE BASED ON ULTIMATE LOAD IS ASSUMED TO BE MULTIPLIED BY 1.5

Figure 7-11. Analysis sequence - pressure stabilization study

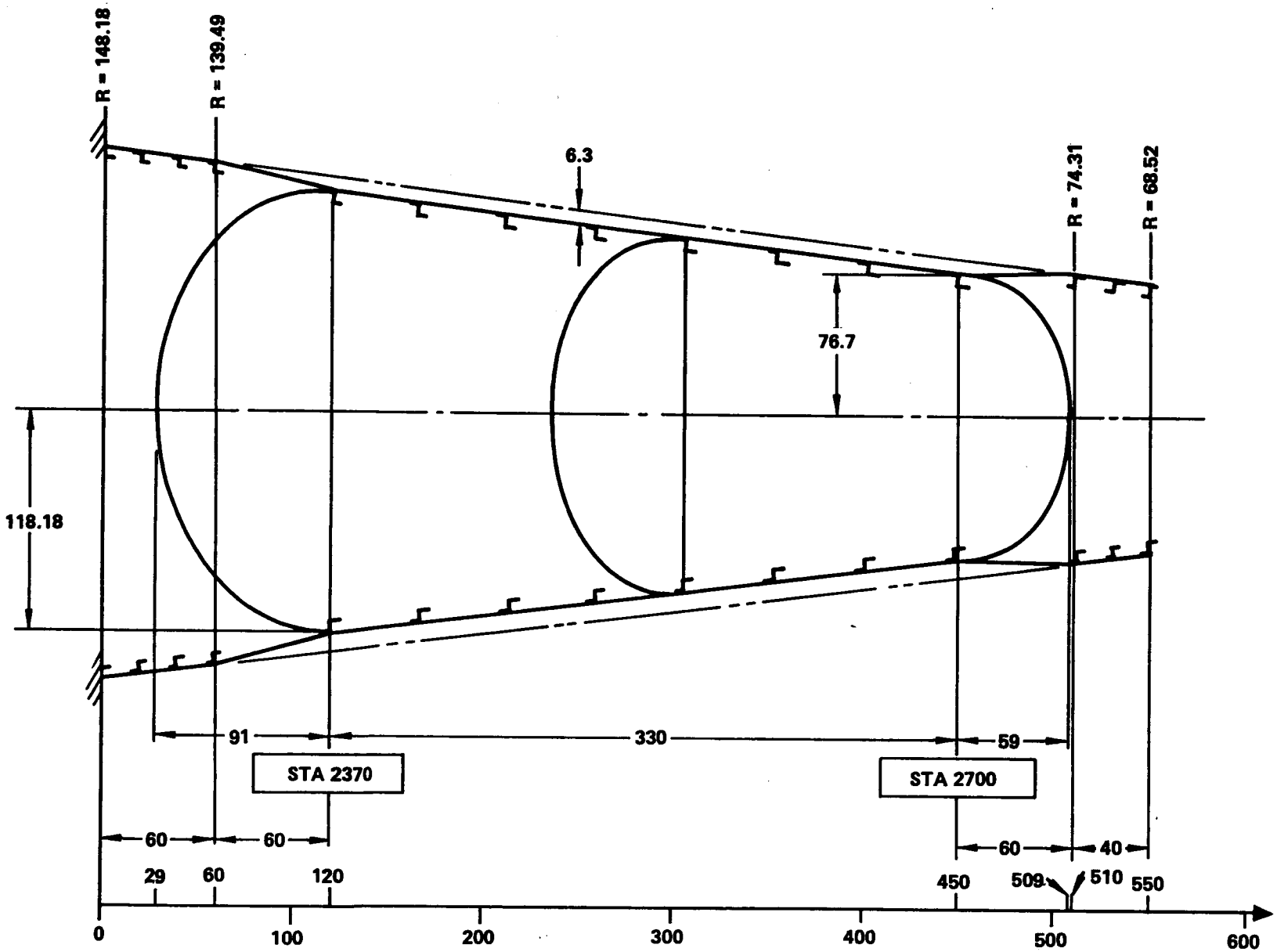

Figure 7-12. Integral tank configuration used for pressure stabilization study

Representative temperatures used on the model components were: 68°F for the fuselage, -210°F for the truss structure and -423°F for the tank.

The structure in general consists of ring- and stringer-stiffened shells. The tank-to-fuselage interface, however, consists of a tubular truss work. In the computer model the rings are modelled as discrete elements but the stringers are smeared; i.e., their various stiffnesses are added to the skin stiffness. Thus, buckling may take place between rings, but buckling between stringers is prevented. The skirts are modelled as an equivalent orthotropic shell, so that in the computer model the individual tubes cannot buckle.

The fuselage consists of a zee-stiffened 0.036 inch skin. The zee-stiffeners are approximately 1.00 in. high with an area of 0.054 in^2 and a moment of inertia of 0.079 in^4. The sheet metal frames are spaced at 20 inches, and are 4 inches deep with an area of 0.651 in^2 and a moment of inertia of 2.05 in^4. The skin and stringers are 2024-T3 aluminum, the rings of 7075-T6 aluminum.

The forward and aft interface skirts are made of tubing arranged to form a triangular truss. The angle between the tubes is approximately 20°. The tubes are made of a boron/epoxy composite with an OD of 2.25 inch and an ID of 1.50 inch. The modulus of elasticity is 18×10^6 psi. The truss members are hinged to the fuselage and to the tank, so that differential expansion or contraction of the various structures can take place without the inducement of stress.

The conical shell of the tank is made of 2219-T851 aluminum alloy with zee-stiffeners. Since BOSOR4 has the capability to handle only rotationally symmetric structures, the hoop variation of the stringer configuration was omitted. However, to compensate for the slight 3 to 8 percent deviation of the neutral axis from the center of the circular cross-section, the applied loads were adjusted to give the proper stress resultant in the critical buckling area. The section properties resulting from the concept screening analysis were used for the tank. The properties were supplied at the quarter and three-quarter length stations of the tank, and interpolated linearly between those points.

In addition to the stringers, the tank is also stiffened by frames, each with an area of 0.384 in^2, a moment of inertia of 0.560 in^4, and a depth of 3 inches. The frames are made of 2219-T851 aluminum. The three domes are of monocoque design and are made of 2219-T851 aluminum. The closures are both 0.1 inch thick, the divider 0.05 inch thick. All three domes have an a/b ratio of 1.3 because this analysis was initiated before the dome shape study, section 7.2.4.1, was completed.

Results: The lower half of the math model showing the fuselage and tank is presented in Figure 7-13. The model is broken down into nine structural segments, as shown in the figure. The directions of increasing arch lengths are indicated by the arrows in the righthand part of the figure. The deformed shape of the lower portion of the structure under the ultimate load condition, unpressurized, is shown in Figure 7-14. The deformations are exaggerated; the

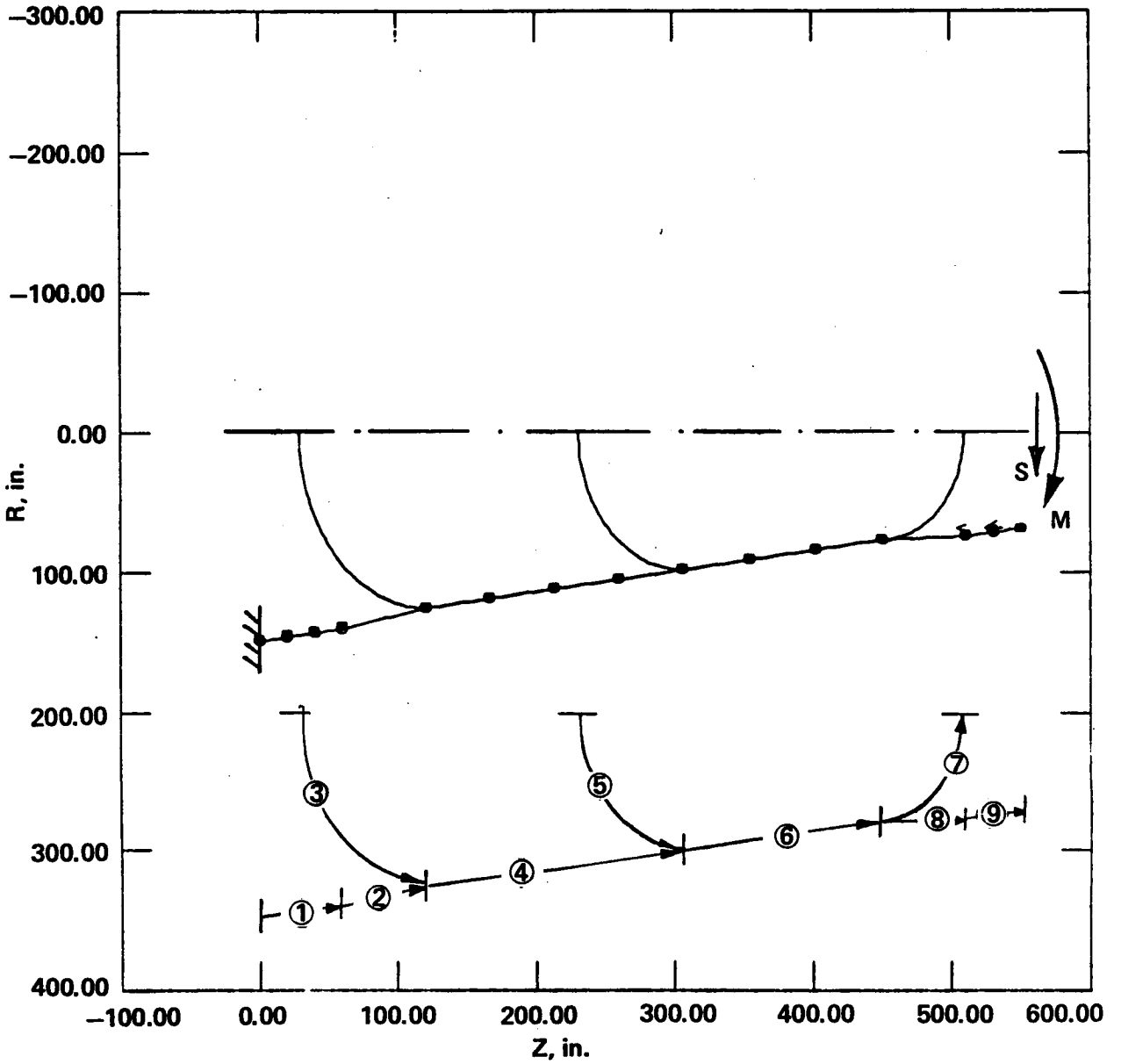

Figure 7-13. Computer model

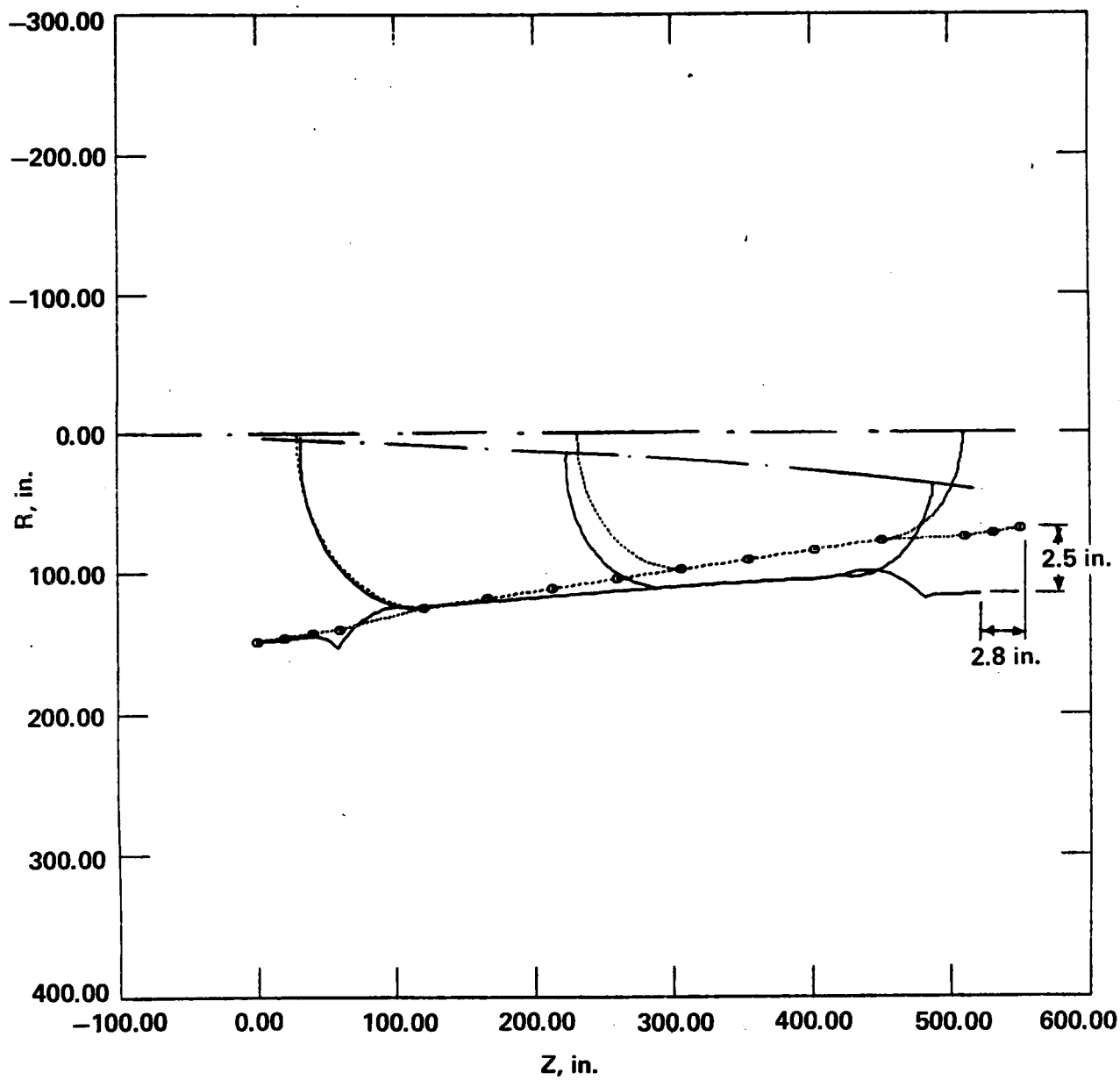

Figure 7-14. Deformed structure - ultimate load

aft dome does not penetrate the aft truss support structure. Note that the differential lateral displacement of the investigated structure is 2.5 in., and the axial shortening, caused by a combination of the temperature distribution and the inertia head of the fuel, is 2.8 in. The deformations are also plotted in Figure 7-15, where U is the meridional and W is the normal displacement.

The circumferential displacement V is zero, since the deformations are plotted for the lower extreme fiber of the structure which is a symmetry line. The stress resultants and moments, referred to the outer skin surface (not the neutral axis of the shell) are shown in Figures 7-16 and 7-17. N1 and N2 are the meridional and hoop normal stress resultants, N12 is the shear stress resultant (zero, due to symmetry); M1, M2 and MT are the meridional, hoop and shear moments.

In the BOSOR buckling analysis the number of circumferential buckles which gives a minimum buckling load is obtained. Figure 7-18 shows the buckling loads (corresponding to points A and B in Figure 7-11) as a function of the circumferential wave number. The buckling loads are represented by the eigenvalue λ, so that

$$\text{Buckling Load} = \lambda \ (\text{Applied Load Set}) + \Delta p$$

Note that the eigenvalue is multiplied by all loads, except the internal pressure Δp. Thus, the temperature is also multiplied by λ. (However, a subsequent check showed that the buckling loads are only affected in the fourth figure by the temperature, which is due to the hinged connections between the supporting structure and the tank.)

There are two minima in the buckling load: one for the fuselage ($\lambda = 1.05$ ult.) and one for the tank ($\lambda = 1.19$ ult.). The axial wave shape for the fuselage is shown in Figure 7-19 and for the tank in Figure 7-20. We note that the fuselage buckling load is smaller than the buckling load for the tank. However, the present study is only concerned with the tank, so a further investigation of the fuselage is not discussed here.

Based on the results shown in Figure 7-18, and following the approach previously outlined, the modulus of elasticity of the skin and stringers in the tank was reduced by the limit factor 1/1.78, which results in an eigenvalue of $\lambda = 1$ for the limit design condition (see Figure 7-11, Point C). A subsequent series of analyses with increasing internal pressurization, Δp, was run and is shown in Figure 7-21. With the pressure added, the number of circumferential buckles changed from 14 to 12, but the axial mode shape remained as in Figure 7-20.

The addition of the internal pressure is very effective in restoring the buckling load capability to the tank wall, with a stiffness reduction of more than 40 percent (1 - 1/1.78 = 0.438) an internal pressure of only 1.35 psi is required to increase the eigenvalue to the required value of 1.5.

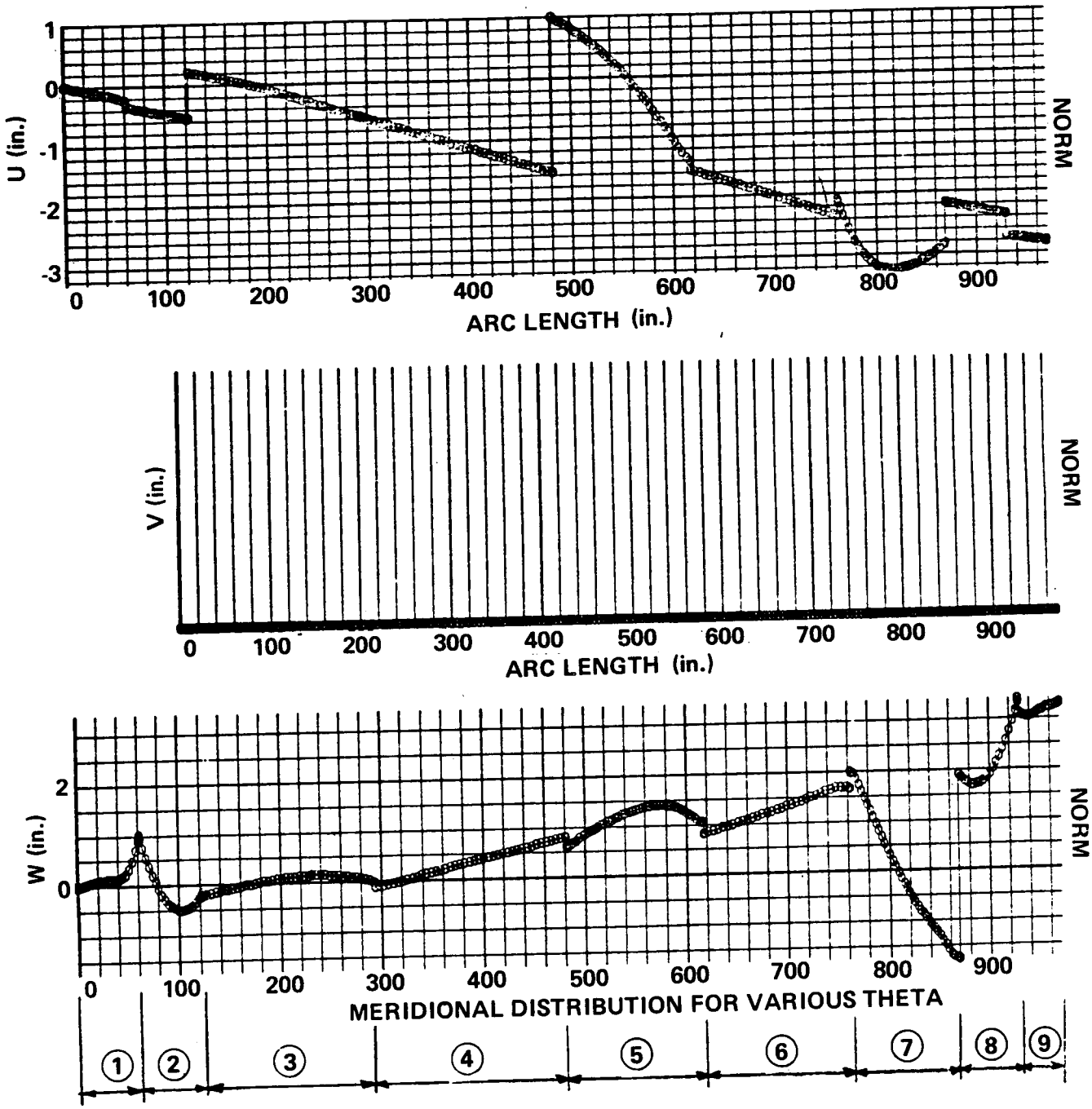

Figure 7-15. Deformations - ultimate load

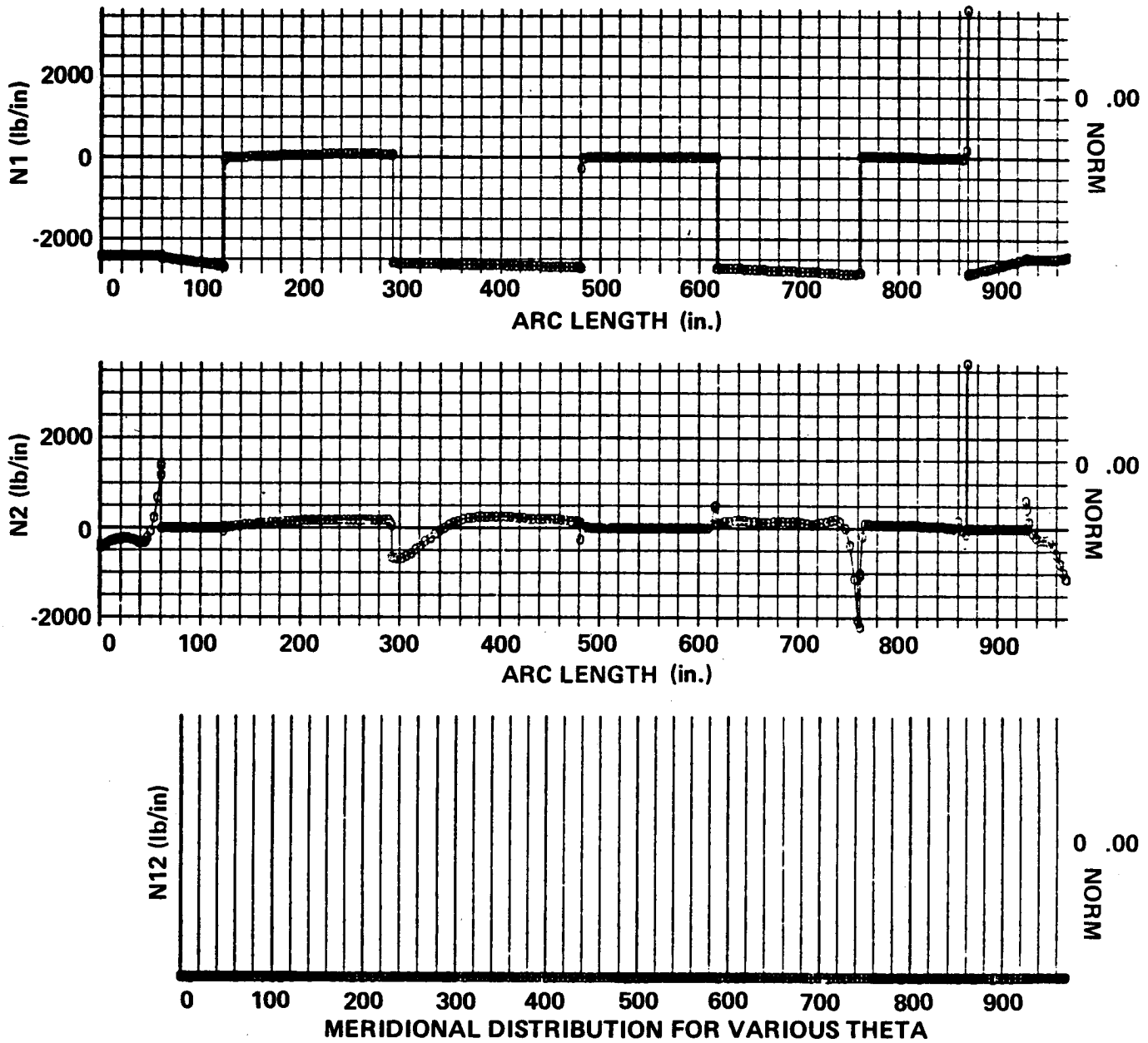

Figure 7-16. Stress resultants - ultimate load

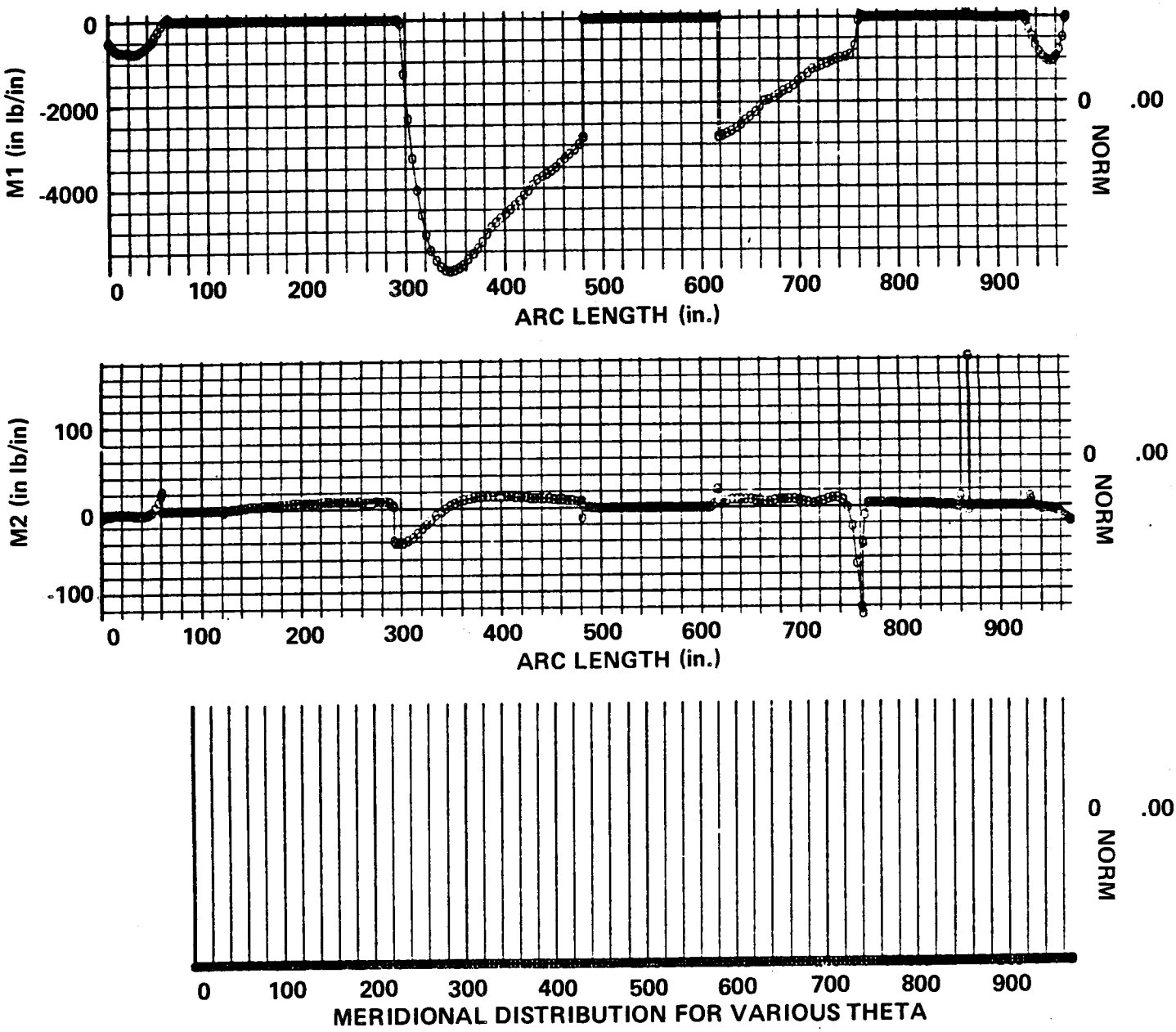

Figure 7-17. Moments - ultimate load

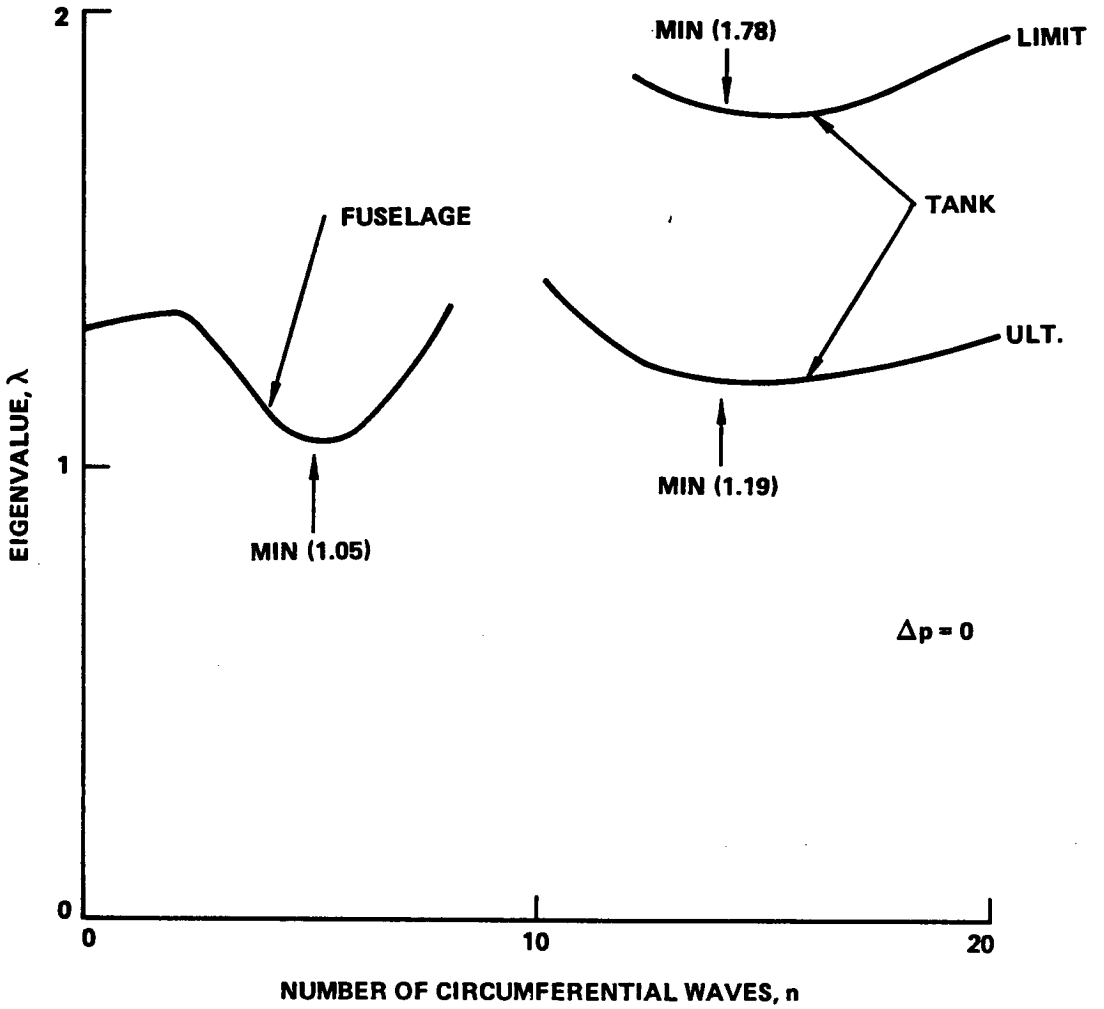

Figure 7-18. Initial buckling analysis, unpressurized

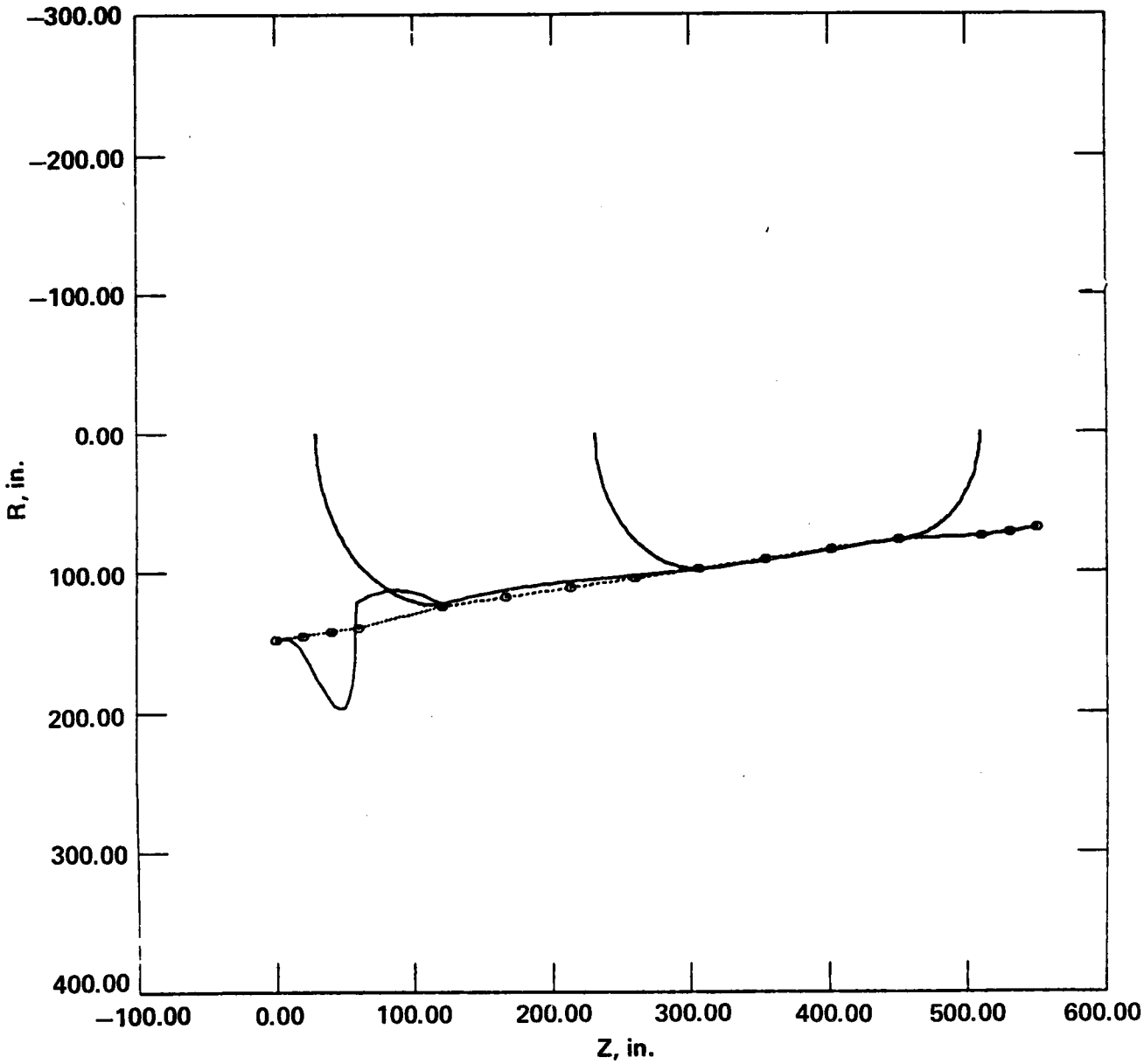

Figure 7-19. Fuselage buckling mode

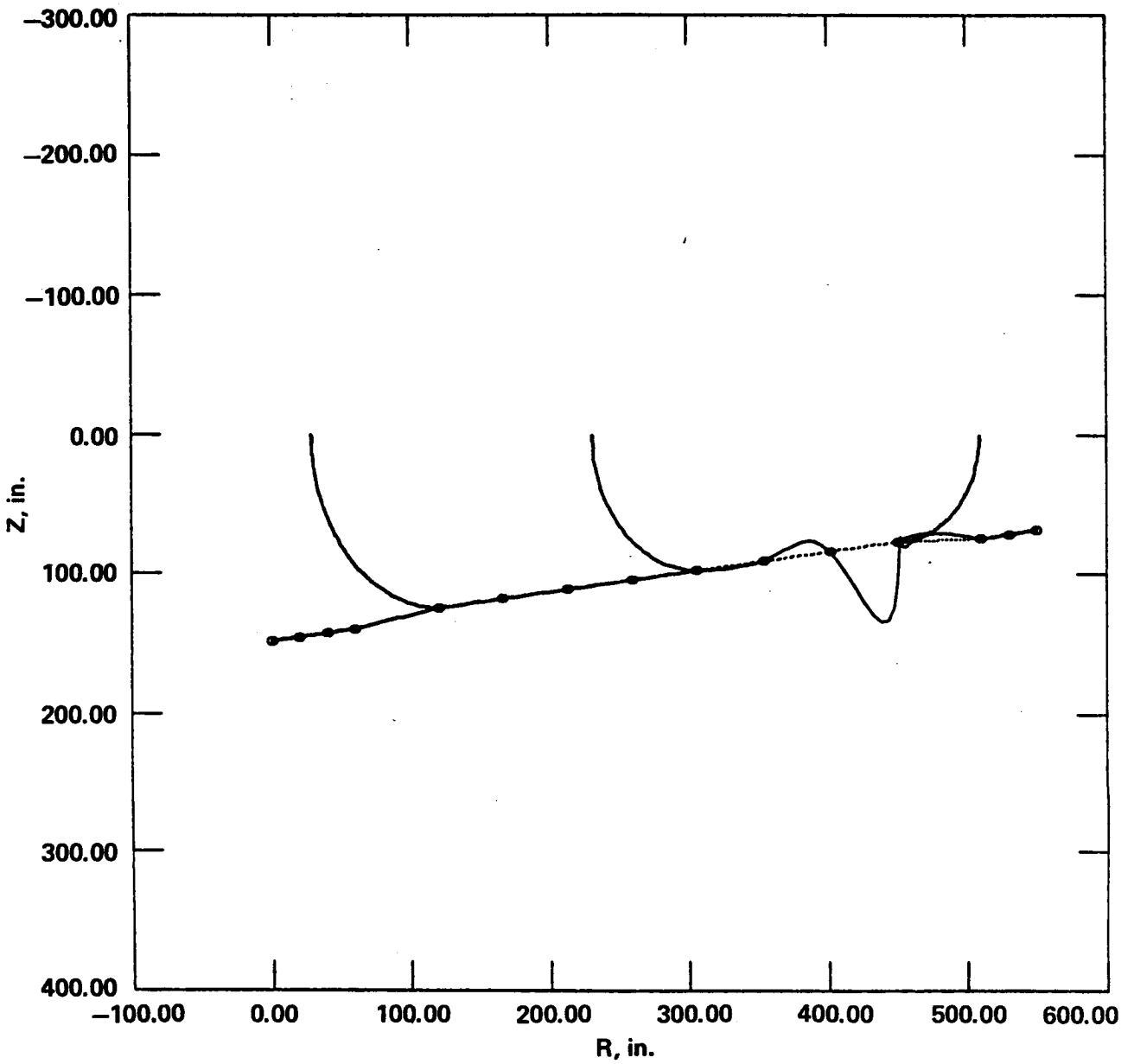

Figure 7-20. Tank buckling mode

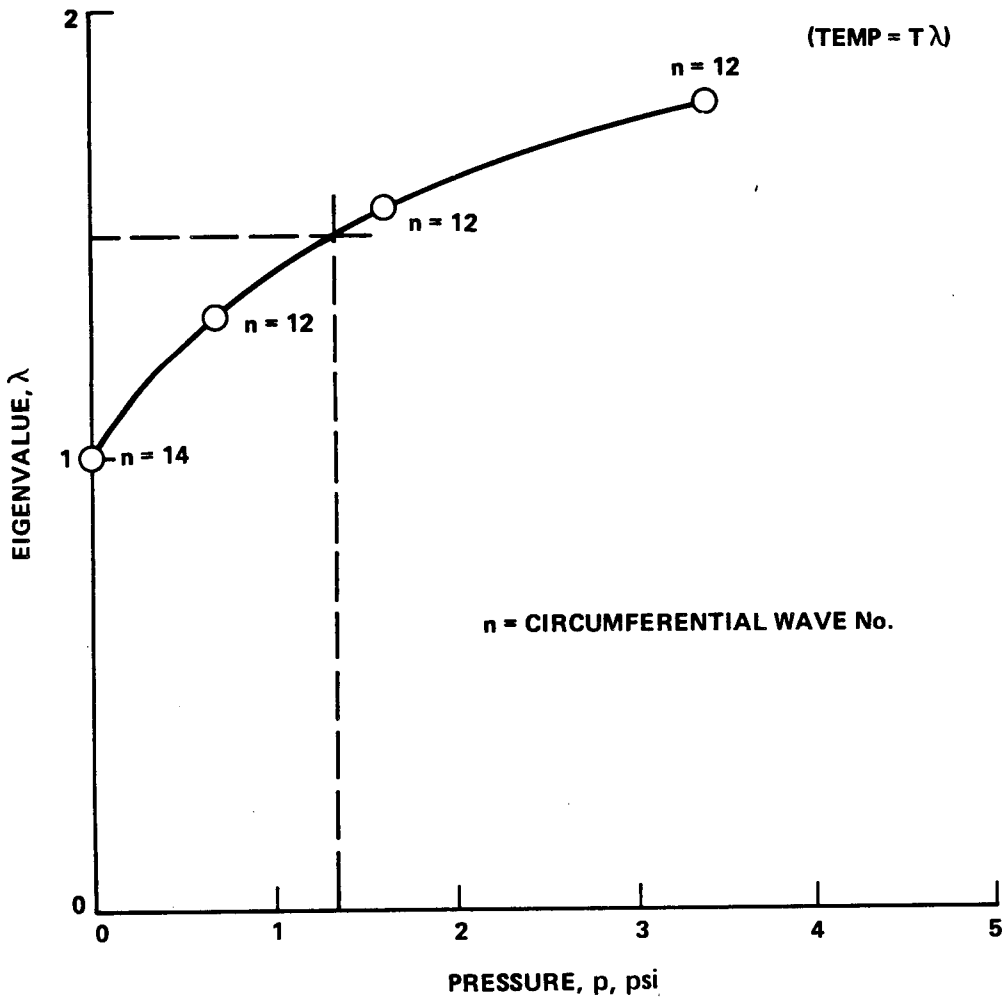

Figure 7-21. Variation in eigenvalue with pressure

The circumferential variation in wall thickness is shown in Figures 7-22 and 7-23 for the tank quarter and three-quarter length stations. These figures display the thicknesses used for the initial input to the model, the resulting reduced thicknesses when pressure stabilization is accounted for, and the thickness requirements dictated by the damage tolerance criteria.

Neglecting the damage tolerance requirements, the results of the BOSOR bifurcated buckling analysis indicates a weight savings, corresponding to a 44 percent reduction in the tank wall thickness, is possible if pressure stabilization is utilized. However, the magnitude of this weight saving (as indicated by the increment of thickness between the initial and pressure stabilized curves on Figures 7-22 and 7-23) is too high, since the wall thicknesses input into the BOSOR model reflect the maximum thickness requirements at the very localized critical buckling area at the upper fibers of the tank. Hence, the thickness corresponding to this area has to be used for the entire circumference due to BOSOR's limitation of analyzing only axisymmetric structure.

Based on the results of the concept screening analysis the cross-sectional areas dictated by the damage tolerance requirements (see Figure 7-22 and 7-23) are also adequate for any local buckling modes; therefore, little or no real weight saving is indicated since these thickness values exceed those predicated on pressure stabilizing the tank.

Based on the depth of analysis of this study no significant weight saving is indicated when the tank is pressure stabilized. In the example studied, the damage tolerance requirements are the dominant design factors with stability, in most cases, only being a secondary effect. Even if a sizable weight payoff were possible, other questions would have to be answered prior to incorporating pressure stabilized structure in commercial airframe design. Some of these are:

- The acceptance of the philosophy of pressure stabilizing structure by the FAA, airlines, and the airframe manufacturers themselves.
- The added fail-safe burden of "loss of tank pressure - possible loss of airplane."
- An assessment of the additional redundancies required in the components to accurately monitor the tank pressures.

Accordingly, it was decided that the tank design to be incorporated in the final LH_2-fueled airplane would not be pressure stabilized.

7.2.4.5 Tank Suspension Study: This study consisted of an analysis of methods proposed for supporting the integral and the nonintegral tanks.

7.2.4.5.1 Integral Tank: A tubular truss design was investigated for the structural connection to the fuselage at both ends of the integral tank design. A schematic drawing showing the location and design of this support system is presented in Figure 7.3.1.c.

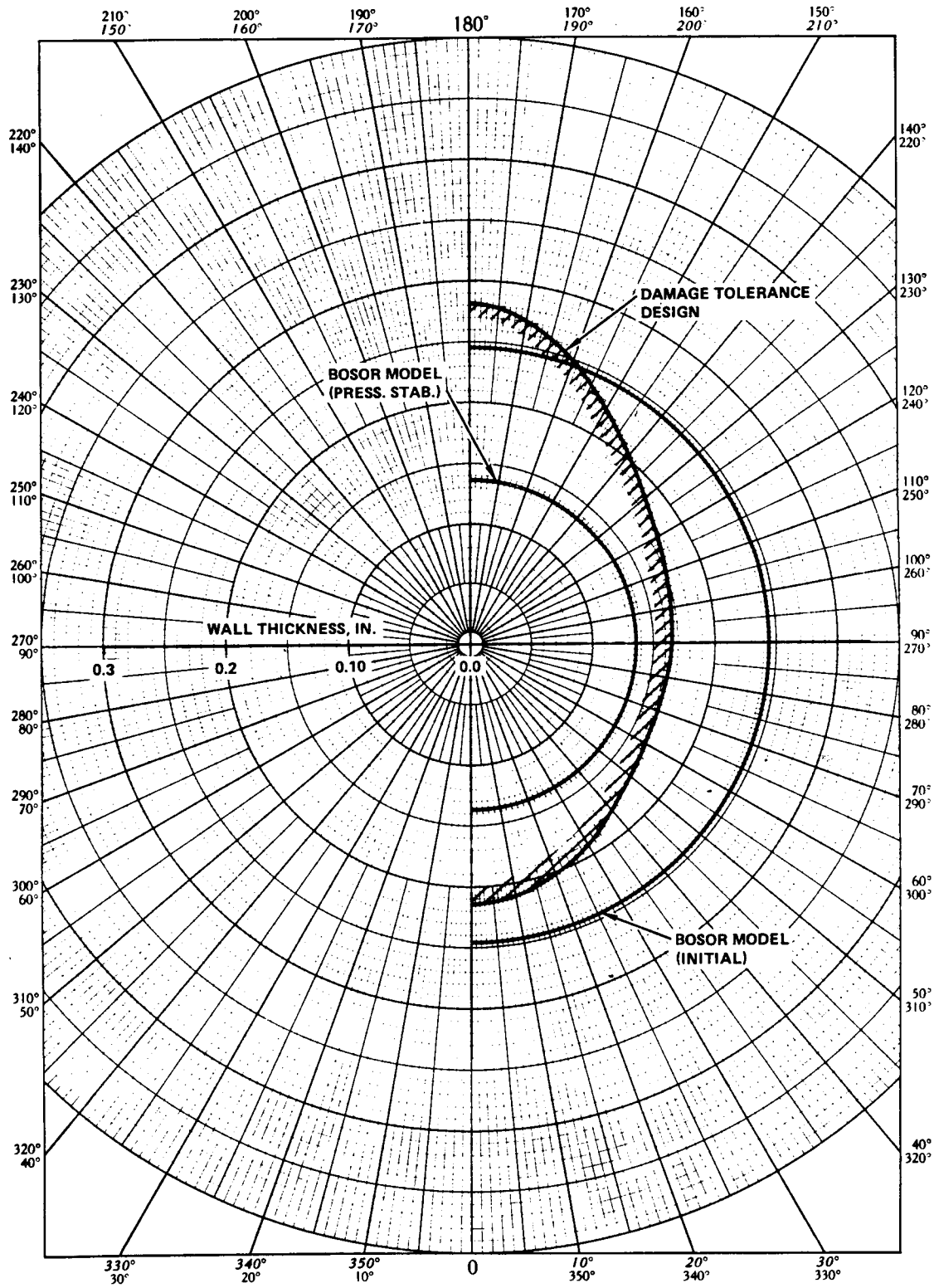

Figure 7-22. Circumferential variation in wall thickness at tank quarter length station

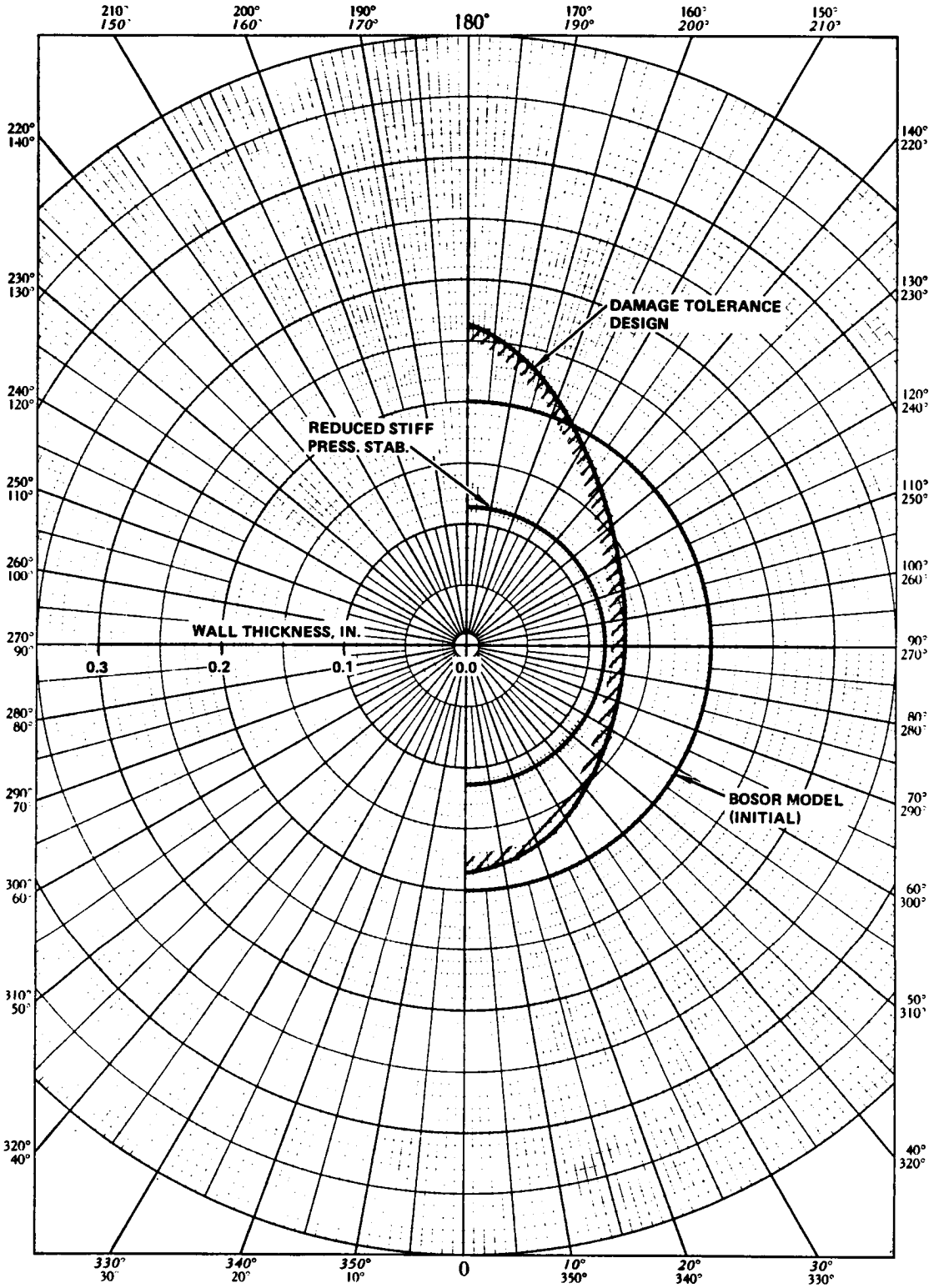

Figure 7-23. Circumferential variation in wall thickness at tank three-quarter length station

Tapered tubular Boron/epoxy struts with titanium end fittings (see Sheet 2 of above figure) were selected for the design of the truss structure. Each strut is bolted to the adjacent tank and fuselage structure to allow some relative displacement between the structural components. This helps to alleviate the thermal stresses induced in the strut and tank skirt caused by the contraction of the cryogenic tank. In addition, foamed-in-place insulation is provided over part of the length of the strut to reduce the thermal leakage from the tank, as well as to protect the adjacent structure from the cryogenic temperatures.

The Boron/epoxy diagonal elements of the truss were analyzed for the maximum loads imposed during flight. A maximum element load of ±182.4 kN (41 000 lb) and ±62.3 kN (14 000 lb) (ultimate) was defined for the forward and aft truss structure, respectively, for the 'PLA' flight condition. Euler buckling and basic material strength (tension and compression) were considered in the selection of the cross-sectional dimensions and ply orientation. In addition, a minimum value of extensional stiffness, equivalent to the stiffness of the adjacent aluminum fuselage structure was imposed on the design of the truss elements.

Using these analytical procedures and criteria, the cross-sectional dimensions and material ply orientation of the truss elements were established. An average tubular cross-section of (2.25 O.D. X 1.50 I.D.) was defined for the elements of the forward truss structure. Correspondingly, a (2.00 O.D. X 1.50 I.D.) cross-section was indicated for the elements of the aft truss structure. A Boron/epoxy strut composed of 70% 0° plies, 20% $\pm 45^{\circ}$ plies and 10% 90° plies satisfies the strength and stiffness requirements of both the forward and aft truss structure.

Transition panels are provided at the forward and aft ends of the tank, as shown in Figure 7.3.1c (sheet 2), to cover the truss structure and maintain aerodynamics smoothness. These panels are removable to allow access to the internal truss structure. A Kevlar faced sandwich with Nomex core was premised for the design of these panels. Basic strength and buckling of these panels were investigated for an external pressure condition of 5.17 k Pa (0.75 psi). The results of this evaluation defined a forward transition panel with 0.762 mm (0.030 in.) Kevlar face sheets and a 25.4 mm (1.00 in.) core thickness. The corresponding design data for the aft transition panel is 0.508 mm (0.020 in.) face sheets with 19.05 mm (0.75 in.) core thickness.

7.2.4.5.2 Nonintegral Tank: A four point support system was investigated for the nonintegral tank design. The general attachment scheme is depicted in Figure 7.3.1a, sheet 2. All points are capable of supporting the vertical forces with only the forward points used for reacting the forward/aft inertia forces.

Both circumferential and longitudinal placement of these support points were studied. For the circumferential placement study, several angular locations, included the 90° location (tank side), were investigated to define their

impact on the design of the tank and the insulation system. The results indicated that the placement of the support at other than the 90° location could result in lower applied loads on the tank but the additional linkage requires a smaller diameter tank for maintaining the proper insulation clearance. In addition, the linkage will have a longer penetration of the insulation system which could provide additional sources of heat leaks. Based on these considerations the most direct approach was taken for the design of the support system, i.e., the side location.

The longitudinal location of the support points was investigated by assuming the tank was a simple beam with overhangs at both ends. The applied vertical loads reflected a full tank with a 4.5 g load factor. Figure 7-24 presents the beam nomenclature and the magnitude and type of loads. Using this model, the location of the beam reaction points was varied until equivalent membrane forces were obtained at the maximum moment location of each beam segment. The resultant locations for the support points were approximately 1.143 m (45.0 inches) aft of the equator of the equator of the forward dome and 1.905 m (75.0 inches) forward of the equator of the aft dome.

A sketch of the components included in the design of the support system for the nonintegral tank design is shown in Figure 7.3.1. b, sheet 2, view D-D. These components were subjected to a preliminary structural sizing in order to define the material distribution for estimating the weight of the support system. In general, the critical design condition was the emergency landing condition. Section 7.2.1.6 defines the ultimate inertia load factors for this condition.

With reference to Figure 7.3.1 b, primary and secondary pins are provided for fail-safe purposes with bearings defined at the tank wall and exterior attachment point. The pin assembly is screwed into the internal threaded portion of the support cone. The structure adjacent to both the tank and fuselage support points is reinforced to provide for the redistribution of the concentrated forces. Lateral loads imposed by the tank would be resisted by suitable structure at the fuselage support points. The design shown in Figure 7.3.1. b, view J-J, uses self-aligning thrust bearings to transmit the loads to the fuselage.

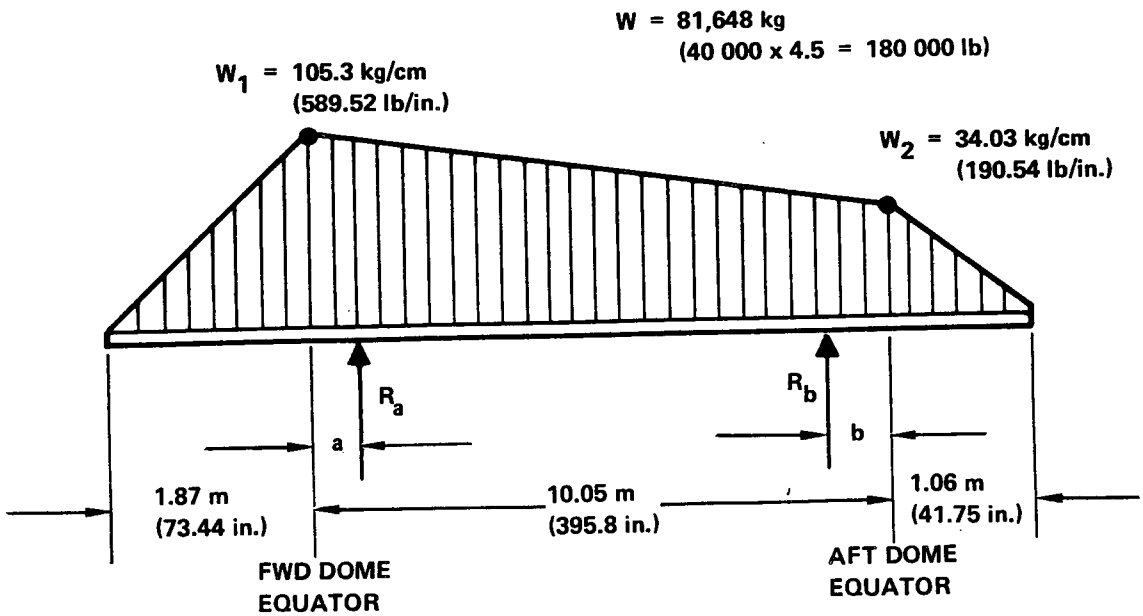

Figure 7-24. Beam Model for Longitudinal Placement Study, Nonintegral Tank

savings of approximately 3-percent over ellipsoidal design. In addition no appreciable difference in the aircraft DOC is noted between the two minimum DOC designs. Both designs have a DOC of approximately 1.825 ¢/seat-n.mi.

Based on these results, neither design affords a clear cut decision as to the preferred dome configuration; hence, the elliptical dome with the minimum DOC configuration was selected as the baseline configuration for conducting further analyses.

NOTE: Sections 7.2.4.2 Tank Life Investigation, 7.2.4.3 Tank Pressurization Study, 7.2.4.4 Pressure Stabilization Study, 7.2.4.5 Tank Suspension Study will be forwarded within 2 weeks for insertion here.

7.3 Evaluation of Preferred FCS Candidates

Evaluation of the four preferred fuel containment systems to determine which is best for application in a commercial transport aircraft was based on comparison of performance and cost characteristics of aircraft designed specifically to use each of the candidate systems. In addition, the evaluation was influenced by judgment concerning aspects such as safety, producibility, maintainability, reliability, etc.

Each of the candidate fuel containment systems (FCS) was incorporated into an aircraft design which was then subjected to the sizing routine using the ASSET computer program. The result was definition of four aircraft, one for each candidate FCS, each of which was optimized to perform the design mission at the lowest direct operating cost while still meeting all design and operational constraints such as the following:

- Maximum engine-out takeoff field length of 8 000 ft
- Minimum initial cruise altitude of 31 000 ft
- Maximum approach speed of 135 kts EAS at end of mission.

All of the aircraft designs incorporated the results of the studies and investigations reported previously herein, relative to the LH_2-fueled engine and fuel system elements. Thus, the aircraft used to evaluate the four preferred fuel containment systems represent complete, final designs (in a parametric sense and within the usual limitations of time and budget) of LH_2-fueled vehicles.

7.3.1 Weight considerations. - Evaluation of the weight of each of the candidata FCS was a critical aspect in the process of selecting a preferred design. It may be seen from Figures 158, 159, 160, and 161, scale drawings of typical cross sections of each of the candidates, that there was a wide variation in the designs which were to be considered. Figure 7.3.1a, 7.3.1b, 7.3.1c, and 7.3.1d show installation arrangements for each system.

Because of the significance of inert weight as a multiplying factor on the gross weight and cost of transport aircraft, great care was taken to assure that consistent calculation methods were used for all candidates so that the weight comparisons would be as representative as possible.

A comparison of the weights of the four preferred candidate fuel containment systems is presented in Table 73. The basic design of all structural components, such as tank, suspension system, body shell, vacuum jacket, truss and fairing, was derived from stress analyses as explained in Section 7.2. An allowance of 8 percent was added to the calculated structural weight to provide

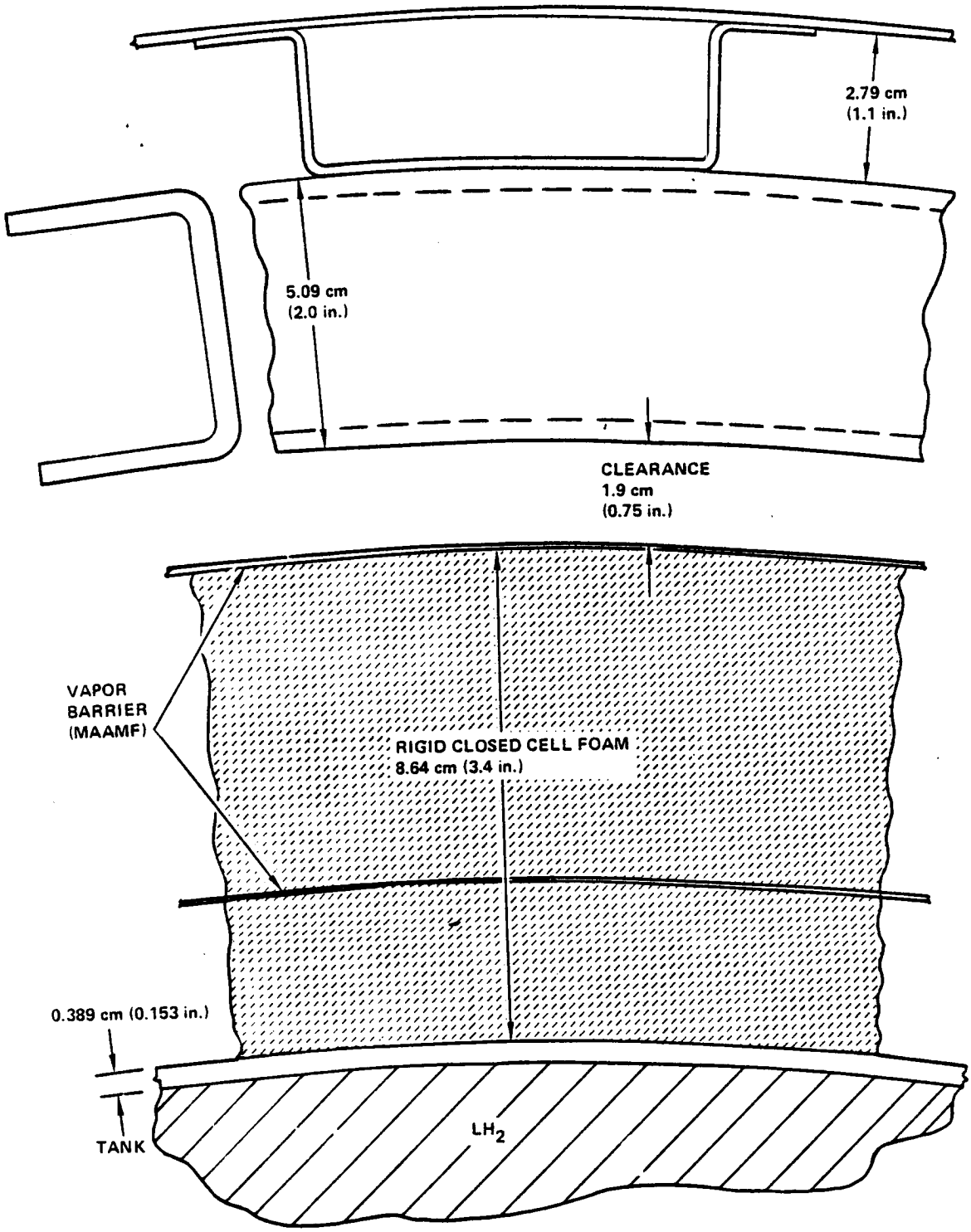

Figure 158. - Representative Cross section, FCS candidate no. 1 (nonintegral tank - external foam)

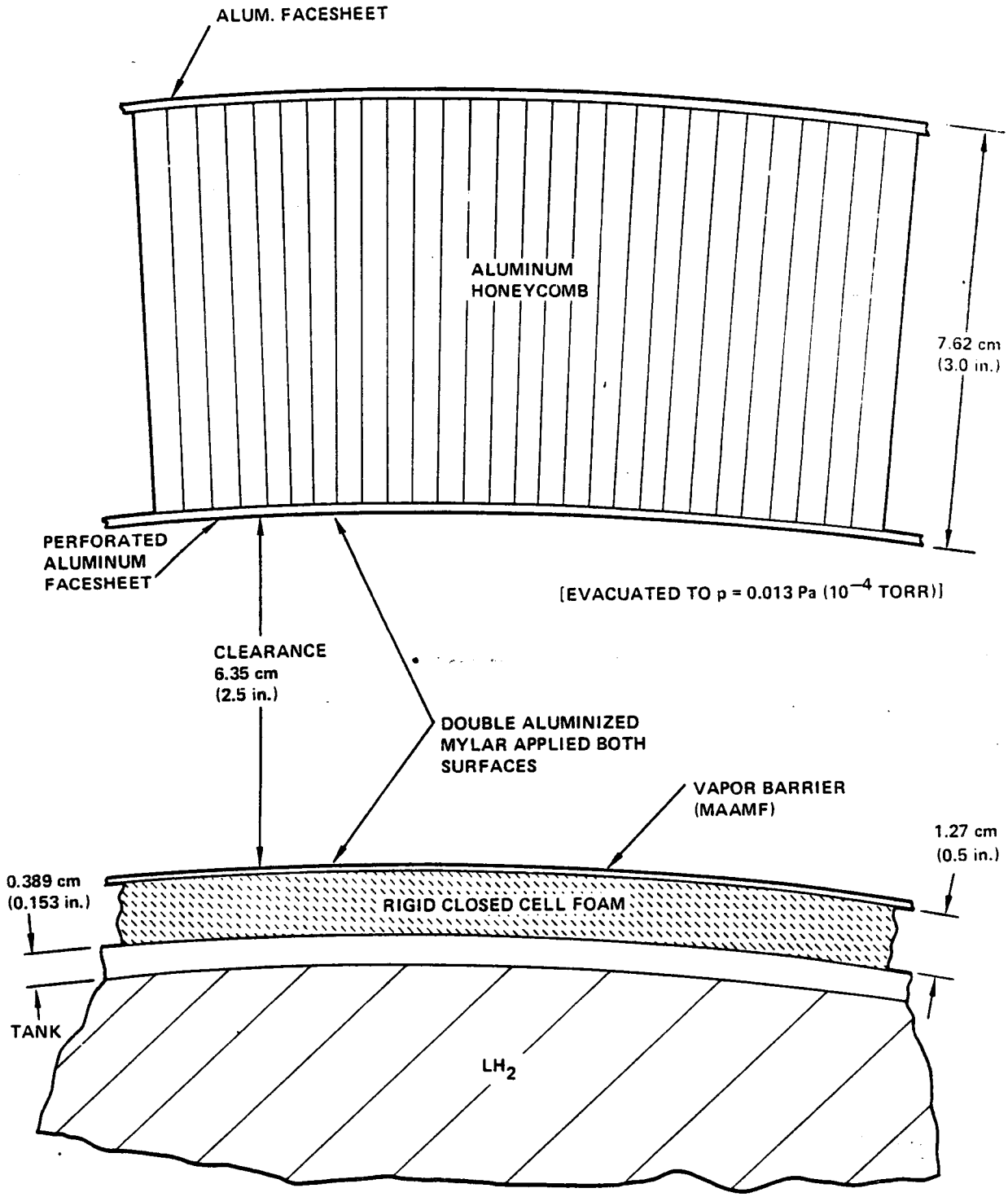

Figure 159. - Representative Cross section, FCS candidate no. 2 (nonintegral tank - hard shell vacuum)

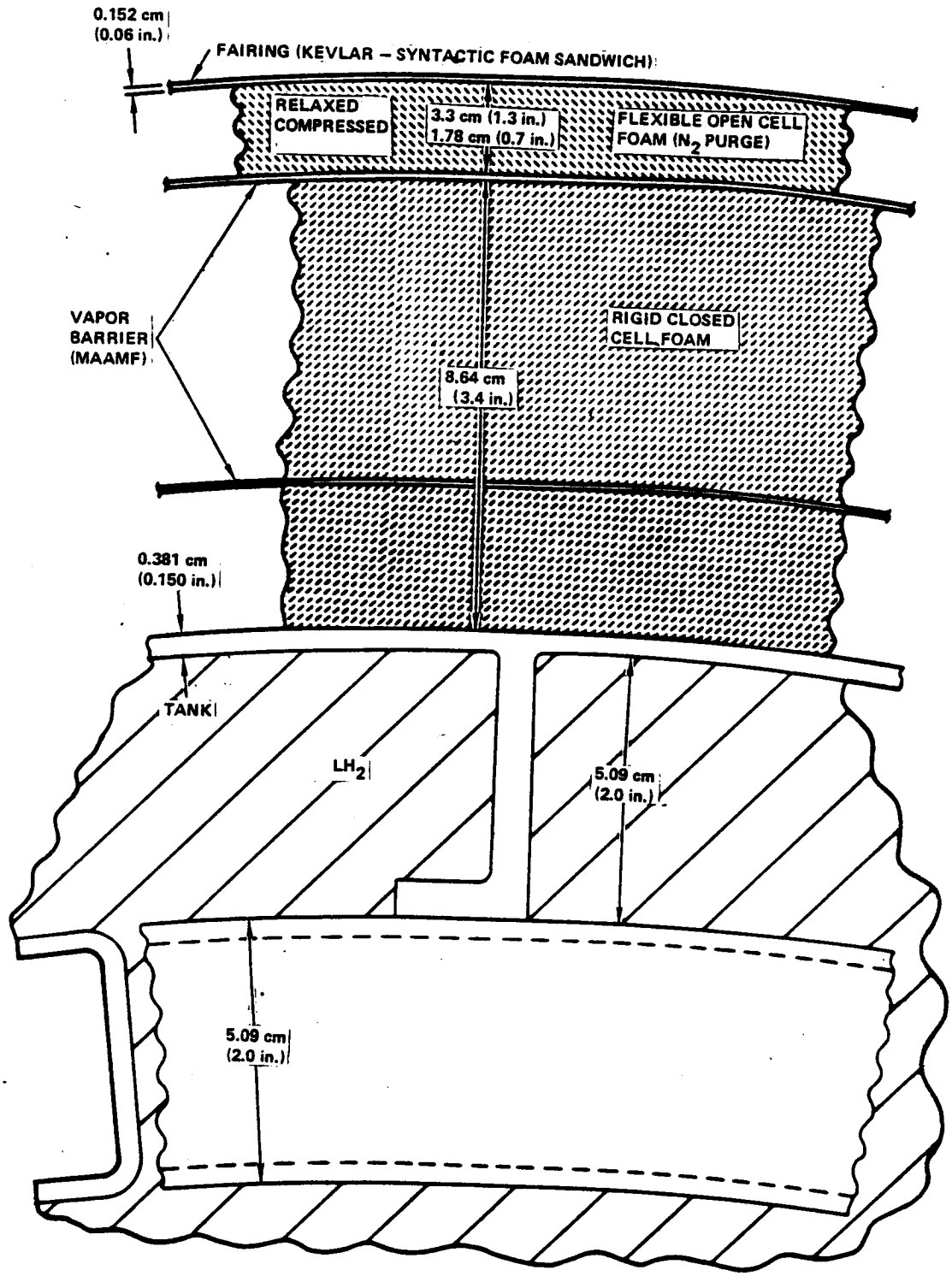

Figure 160. - Representative cross section, FCS candidate no. 3 (integral tank - external foam)

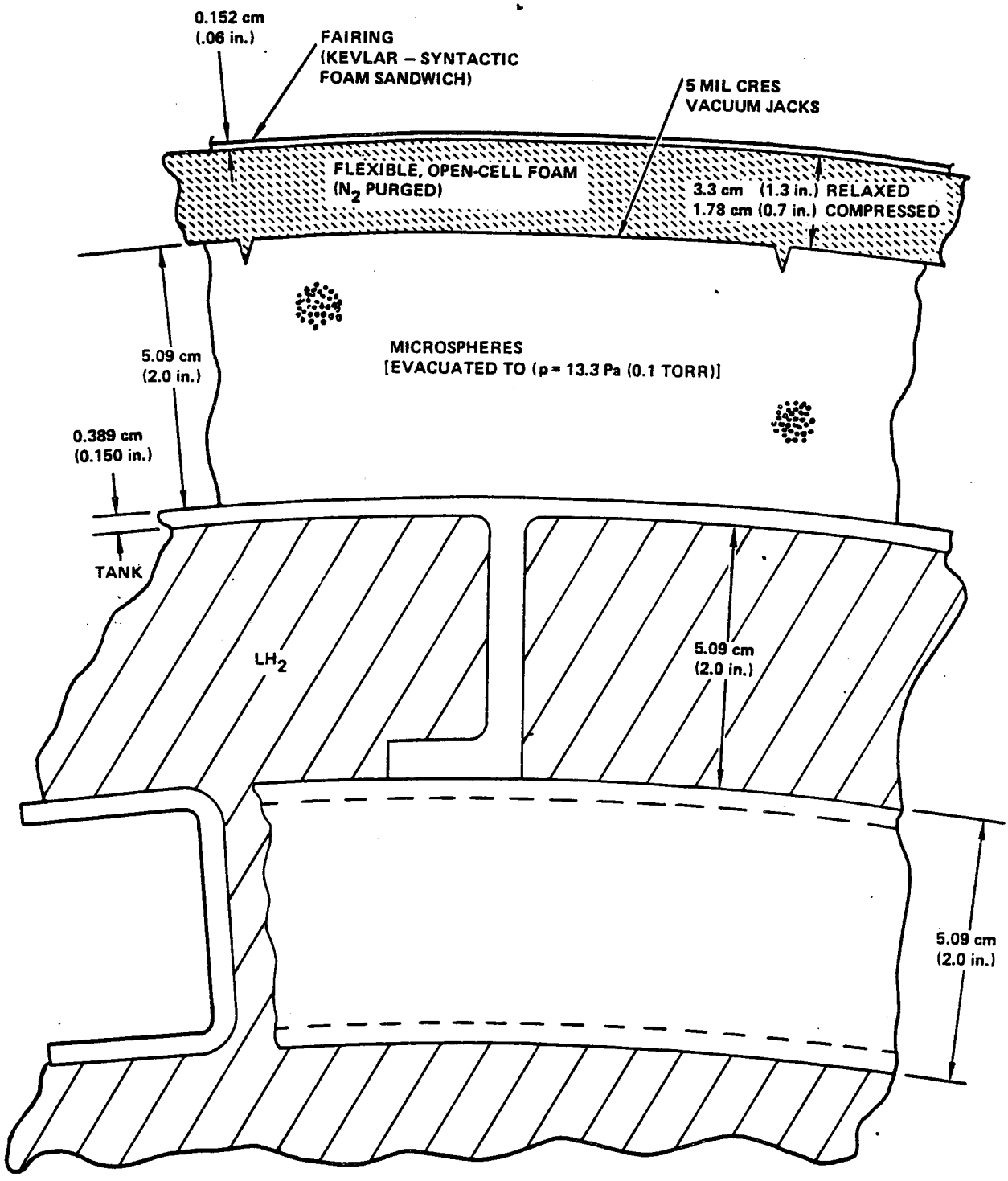

Figure 161. - Representative cross section, FCS candidate no. 4 (integral tank - microsphere insulation)

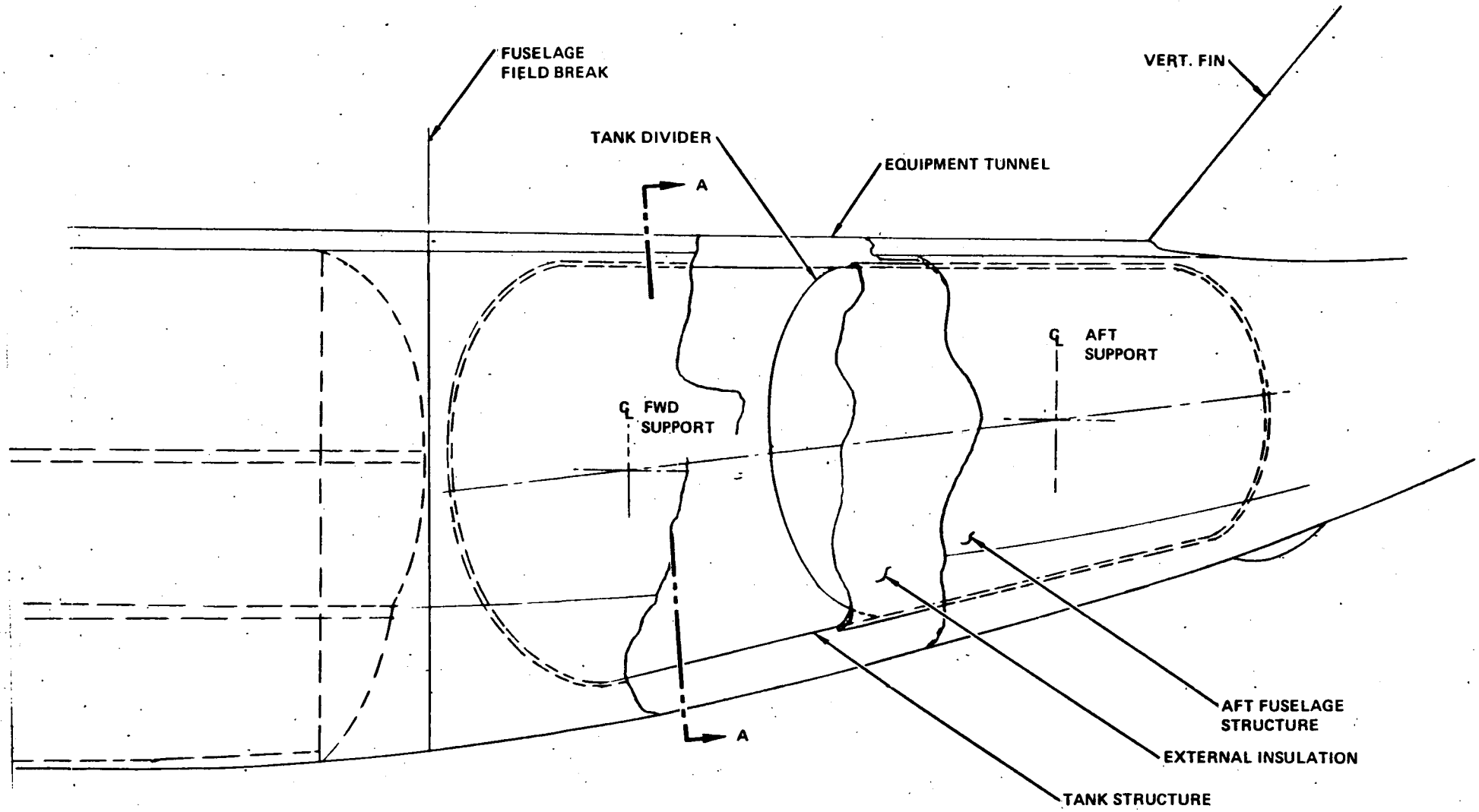

Figure 7.3.1a. - Candidate no. 1 nonintegral tank - external foam (Sheet 1 of 2)

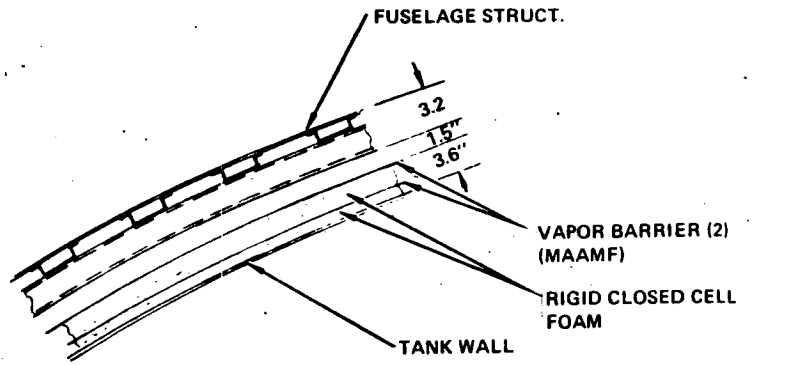

DET. B
1/10 SIZE

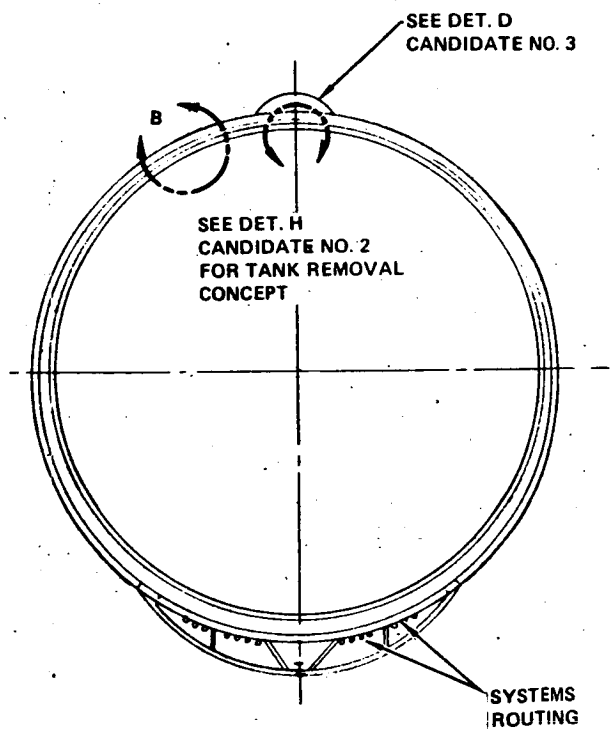

SECTION A-A

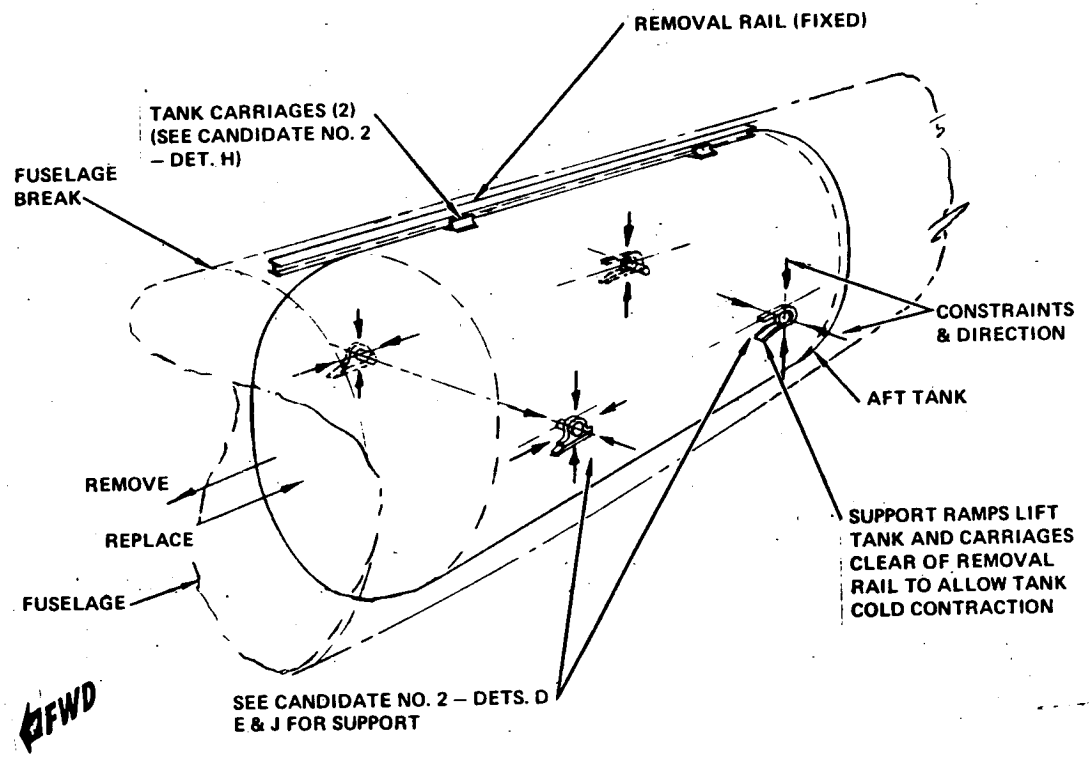

D

Figure 7.3.1a. - Concluded (Sheet 2 of 2)

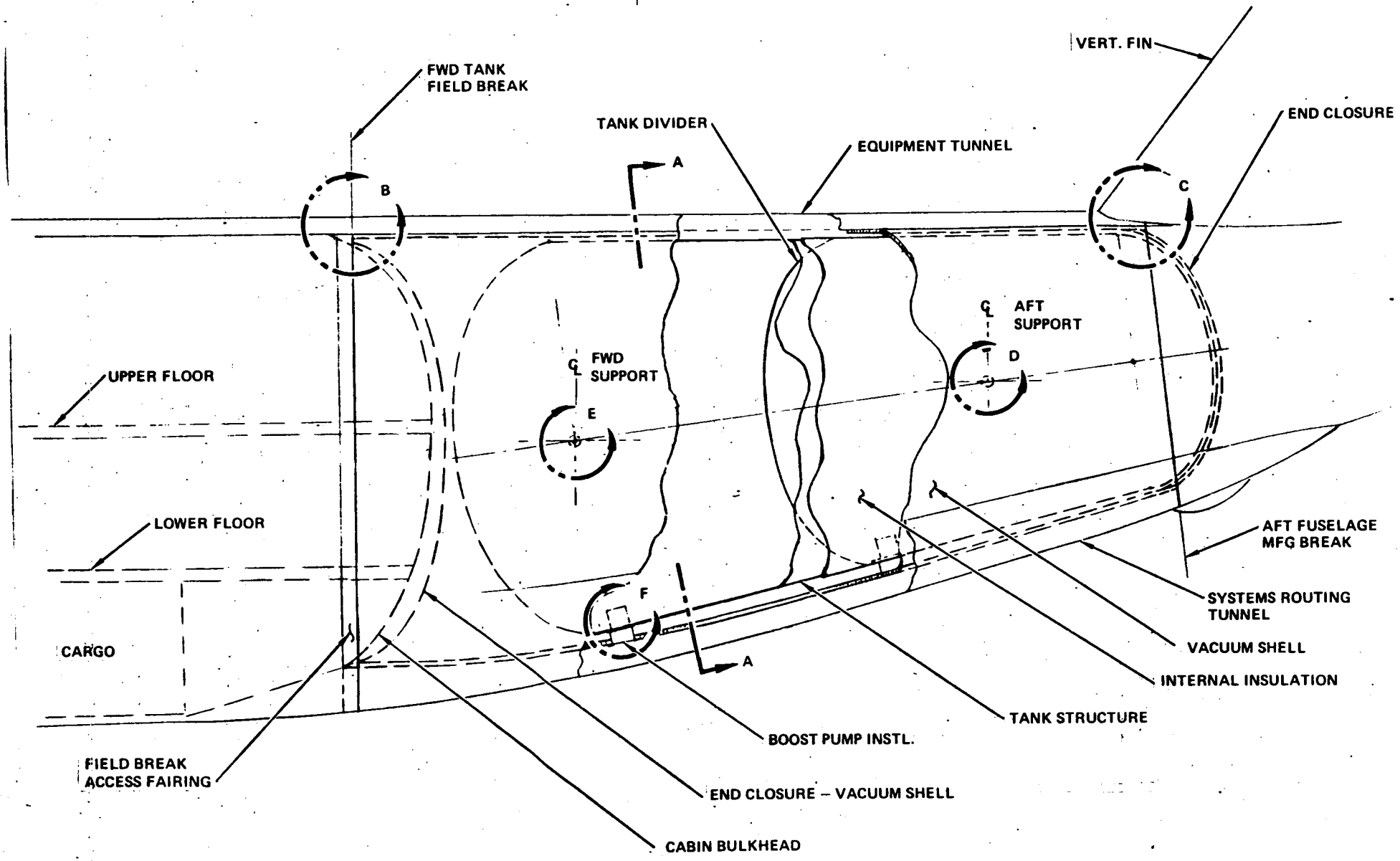

Figure 7.3.1b. - Candidate no. 2 nonintegral tank - hard shell vacuum (Sheet 1 of 2)

D

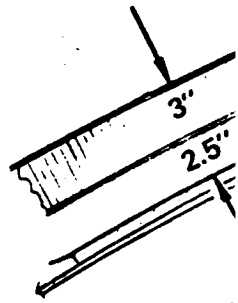
3"
2.5"

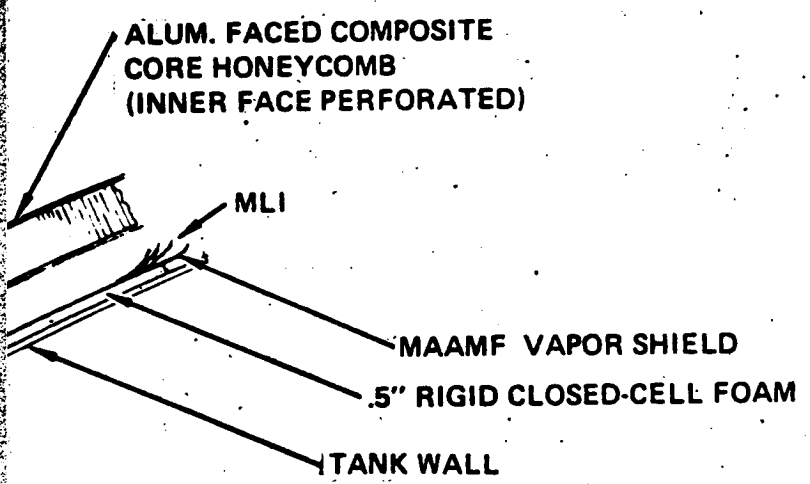

T G
0 SIZE

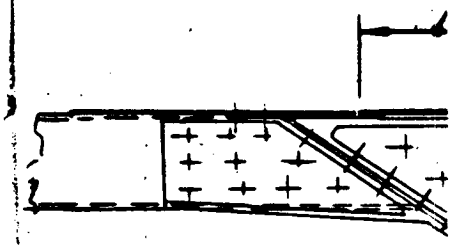

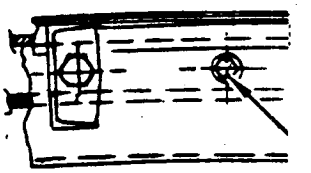

DET. B
¼ SIZE

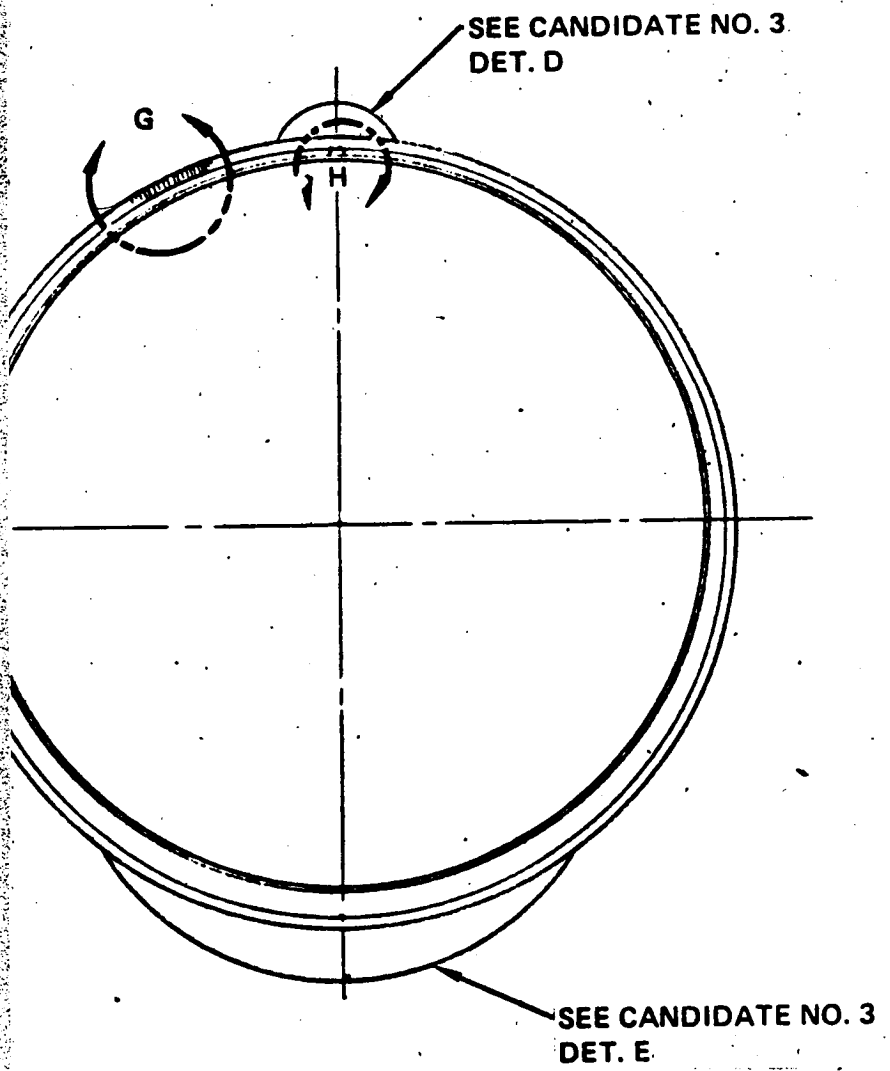

SECTION A-A

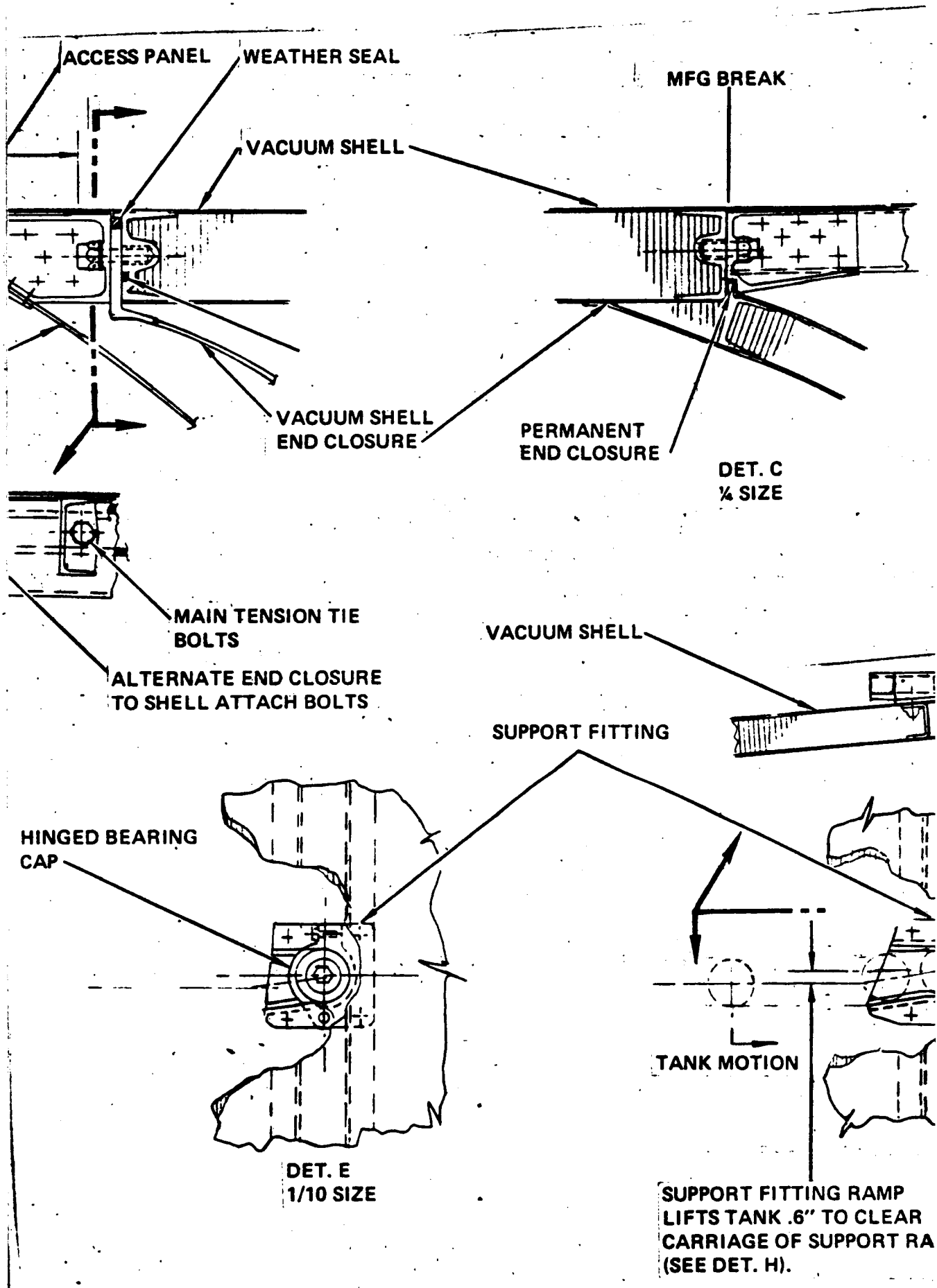
ACCESS PANEL
WEATHER SEAL
MFG BREAK
VACUUM SHELL
VACUUM SHELL
END CLOSURE
PERMANENT
END CLOSURE
DET. C
¼ SIZE
MAIN TENSION TIE
BOLTS
ALTERNATE END CLOSURE
TO SHELL ATTACH BOLTS
VACUUM SHELL
SUPPORT FITTING
HINGED BEARING
CAP
TANK MOTION
DET. E
1/10 SIZE
SUPPORT FITTING RAMP
LIFTS TANK .6" TO CLEAR
CARRIAGE OF SUPPORT RA
(SEE DET. H).

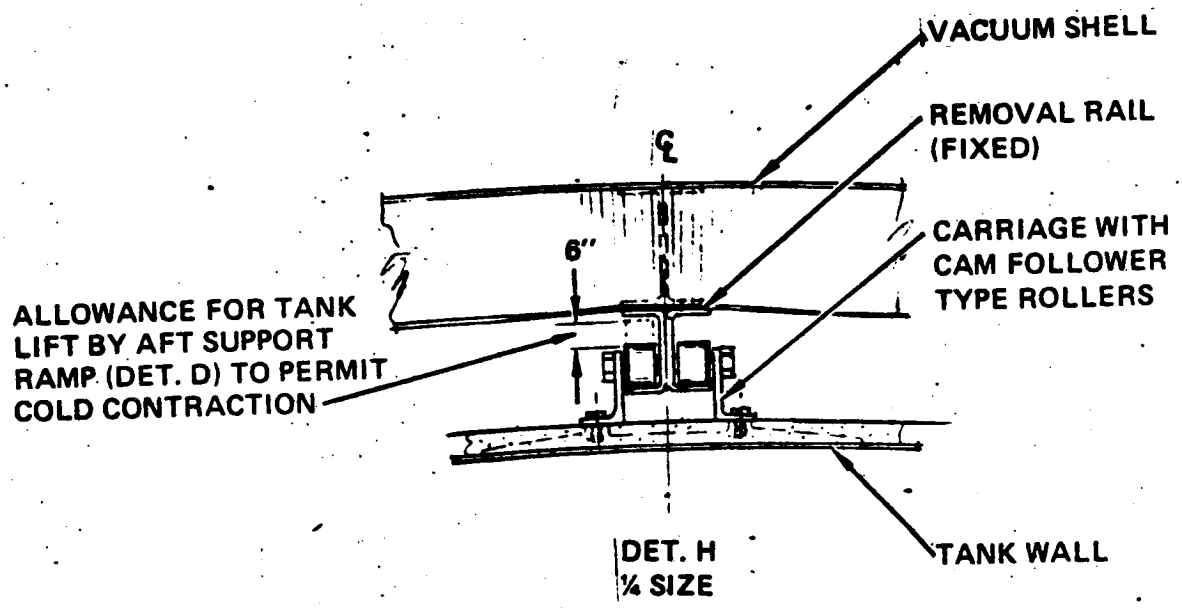

DET. H
¼ SIZE

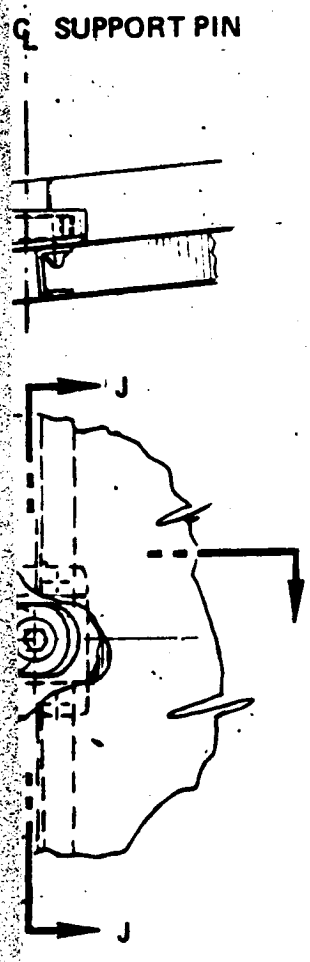

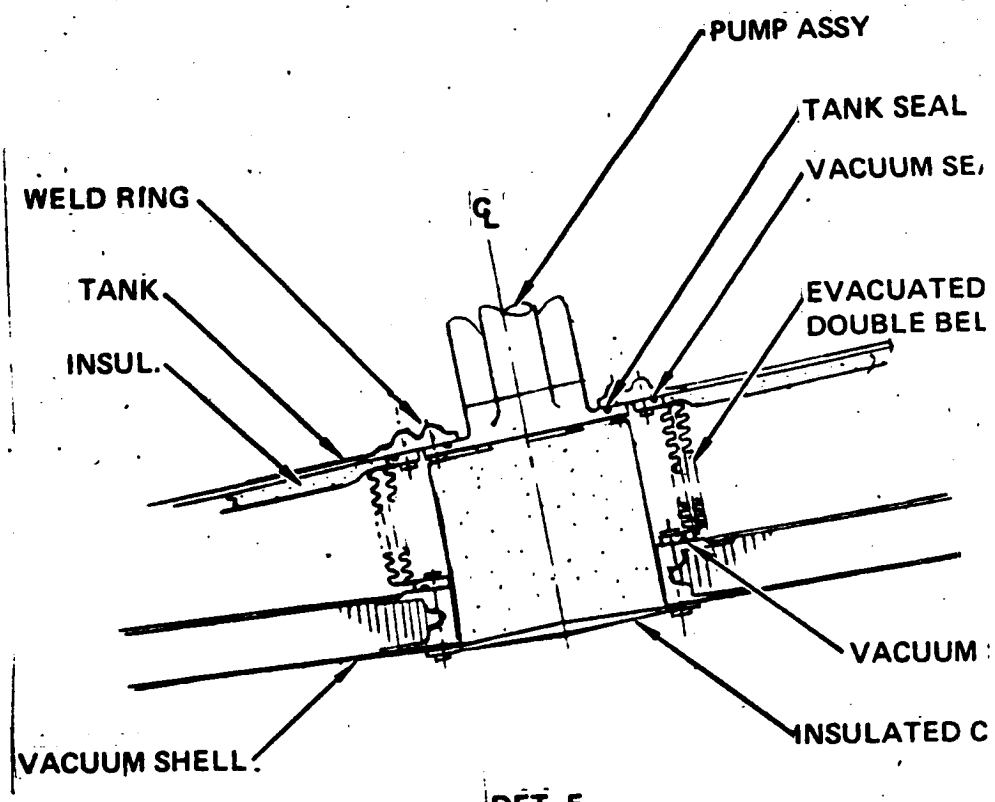

DET. F
1/10 SIZE

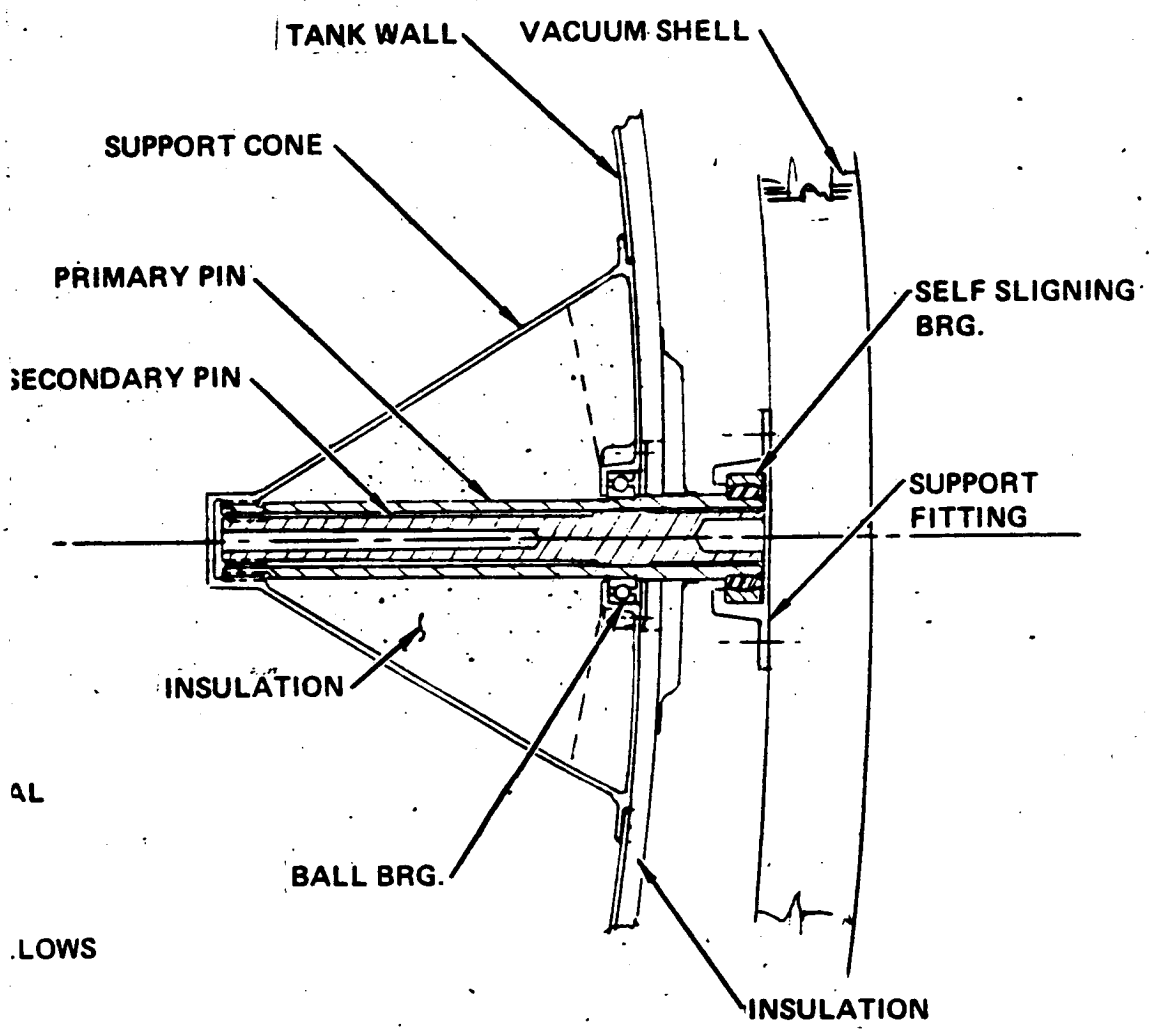

VIEW J-J
1/5 SIZE

AL

LOWS

SEAL

OVER PLATE

Figure 7.3.1b. - Concluded (Sheet 2 of 2)

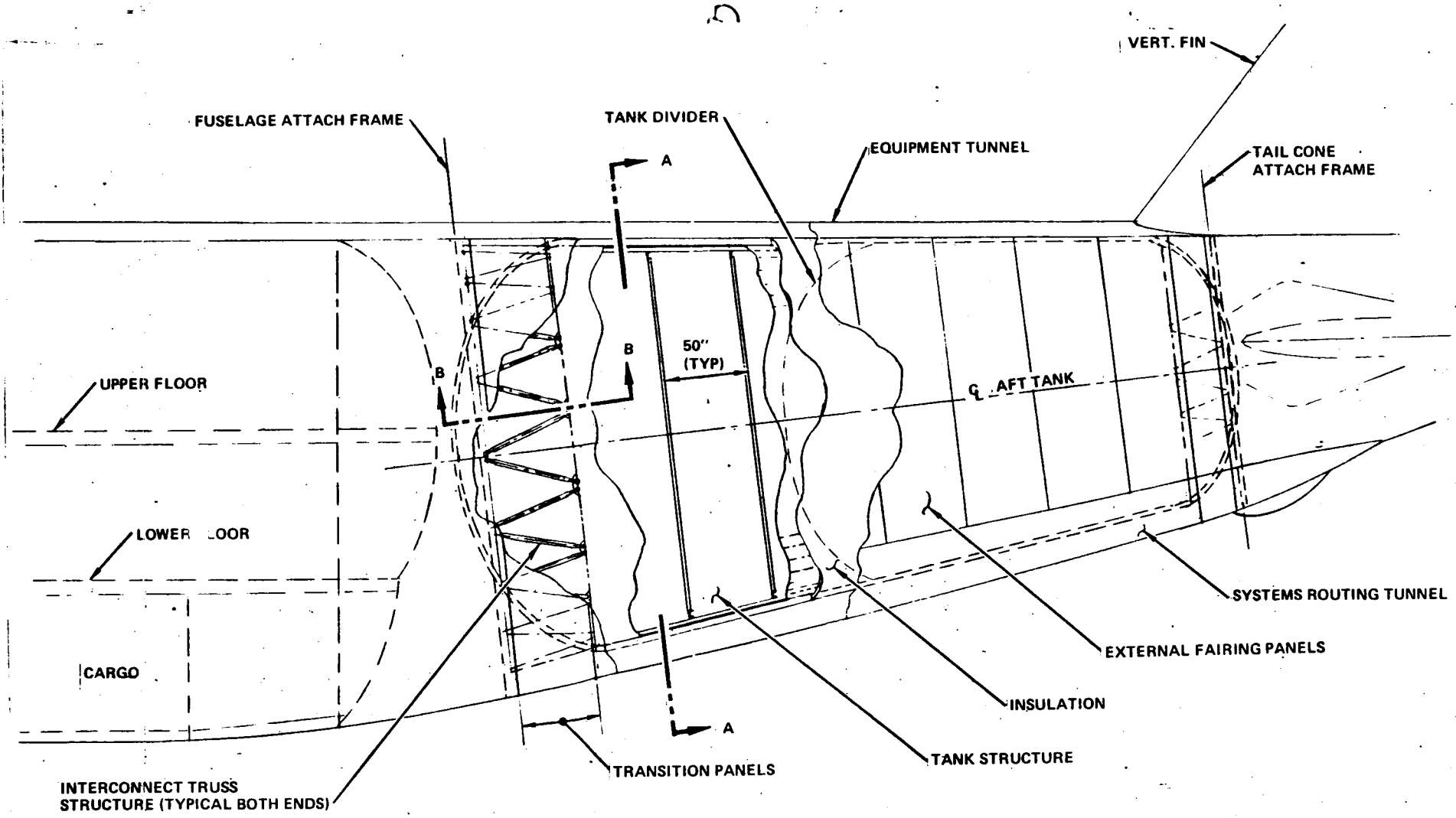

Figure 7.3.1c. - Candidate no. 3 integral tank - external foam (Sheet 1 of 2)

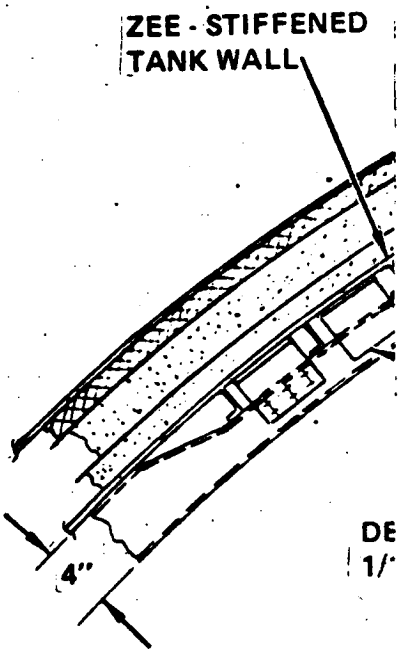

DE
1/

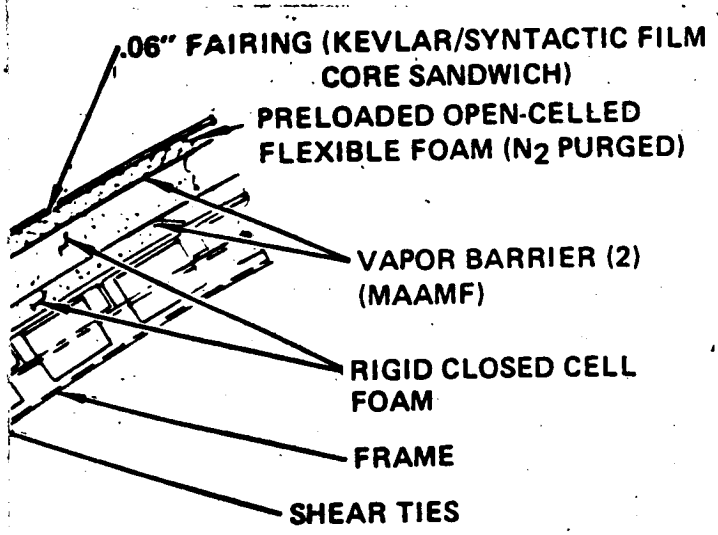
.06" FAIRING (KEVLAR/SYNTACTIC FILM CORE SANDWICH)
PRELOADED OPEN-CELLED FLEXIBLE FOAM (N_2 PURGED)
VAPOR BARRIER (2) (MAAMF)
RIGID CLOSED CELL FOAM
FRAME
SHEAR TIES

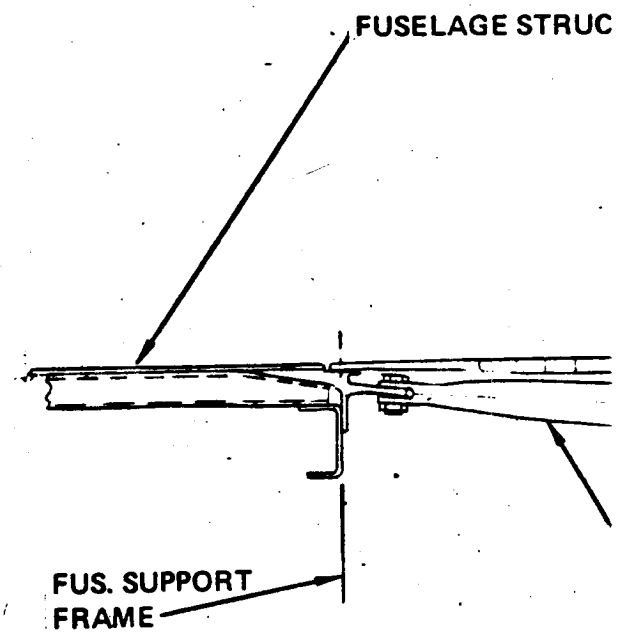
FUSELAGE STRUC
FUS. SUPPORT FRAME

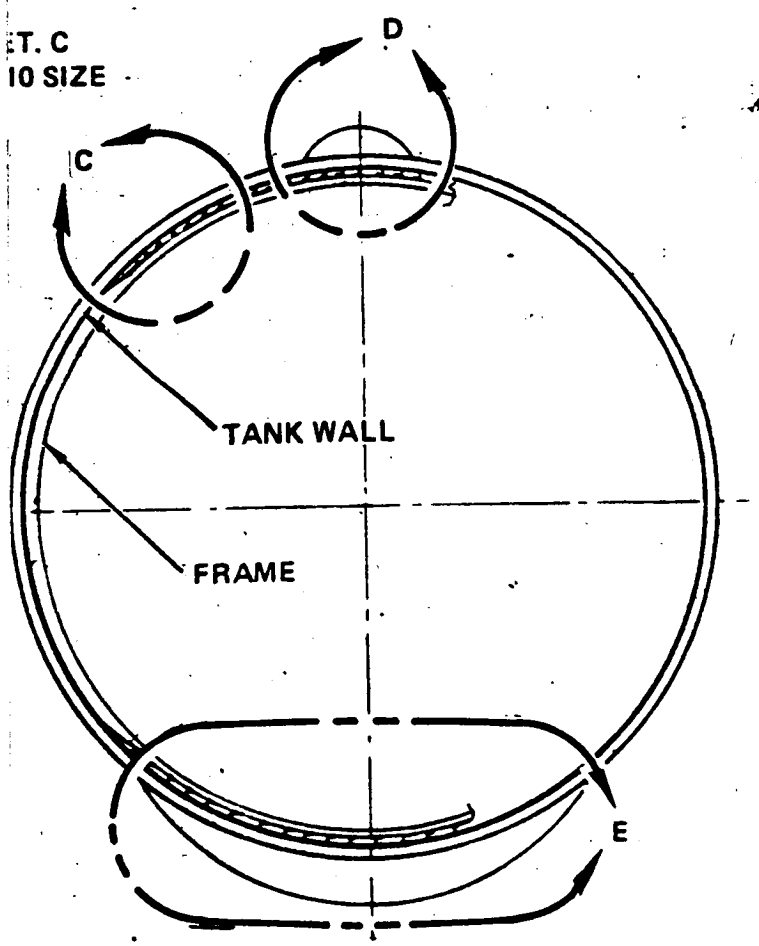
T. C
10 SIZE
D
C
TANK WALL
FRAME
E

SECTION A-A

REMOVABL
(VENTED T
DISCHARGI

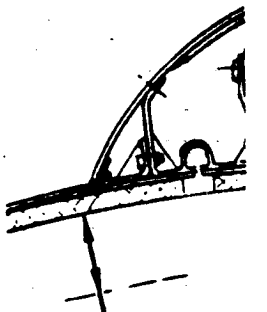

INSULAT
OMITTED

URE

TRANSITION PANELS (REMOVEABLE)
(KEVLAR FACED HONEYCOMB)

CONTRACTION JOINT

TANK
FAIRING

COMPOSITE TRUSS
(T1 END FITTINGS)

TANK
STRUCTURE

TANK SUPPORT
FRAME

INSULATION
CLOSE-OUT

OAM IN PLACE
NSULATION

VAPOR BARRIERS

SECT. B-B
1/10 SIZE

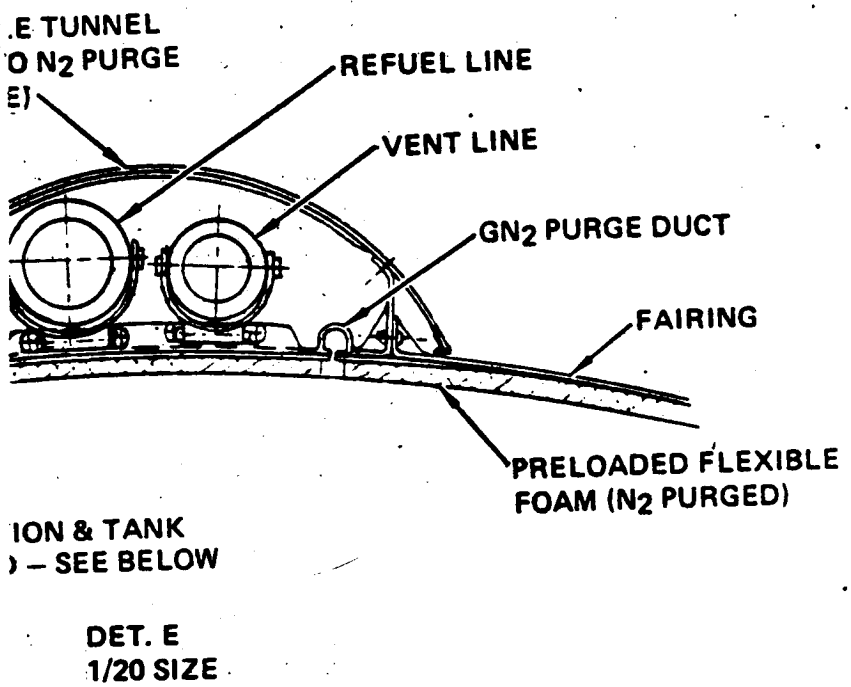

DET. E
1/20 SIZE

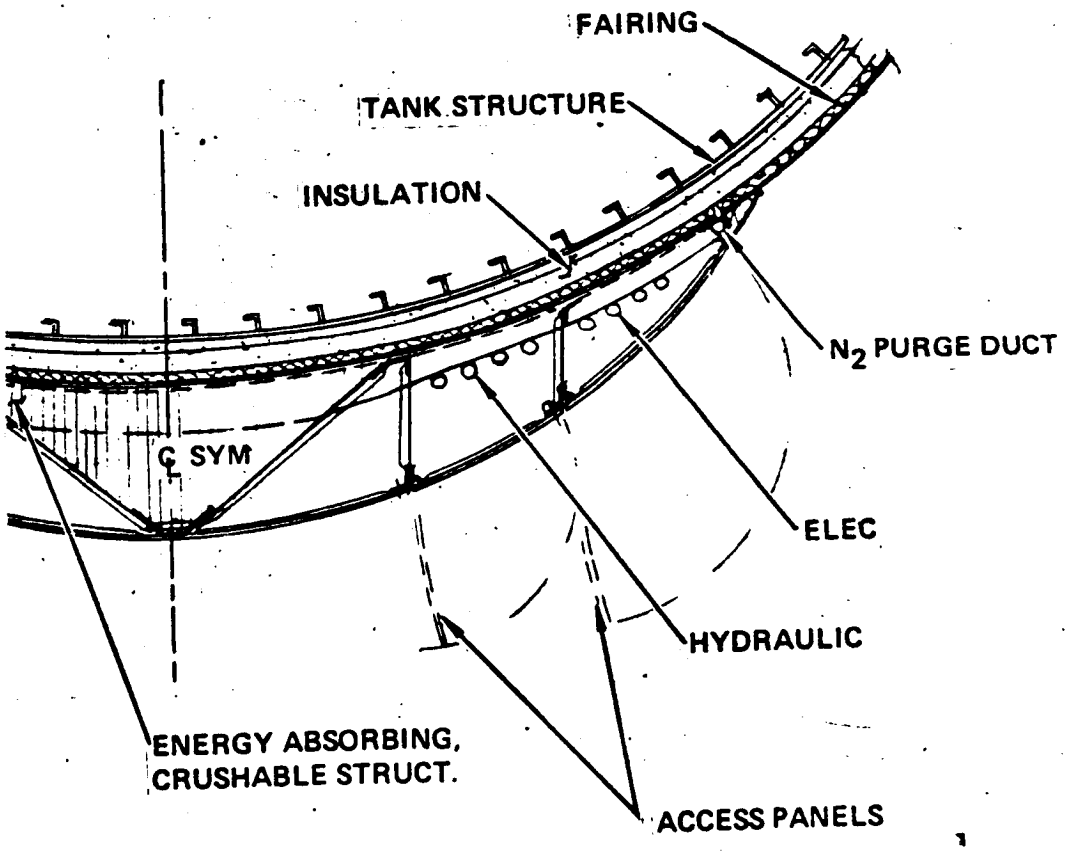

Figure 7.3.1c. - Concluded (Sheet 2 of 2)

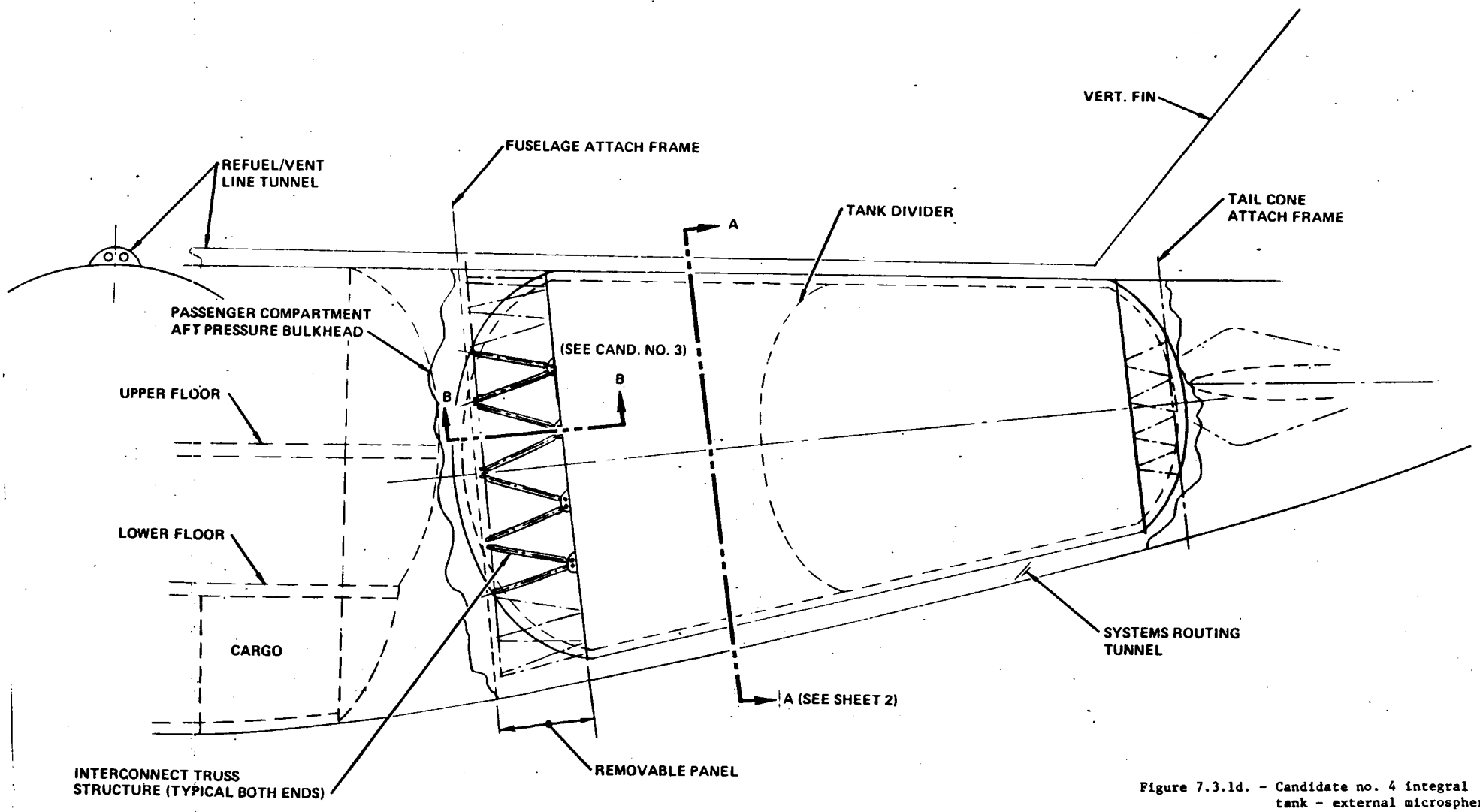

Figure 7.3.1d. - Candidate no. 4 integral tank - external microsphere insulation (Sheet 1 of 2)

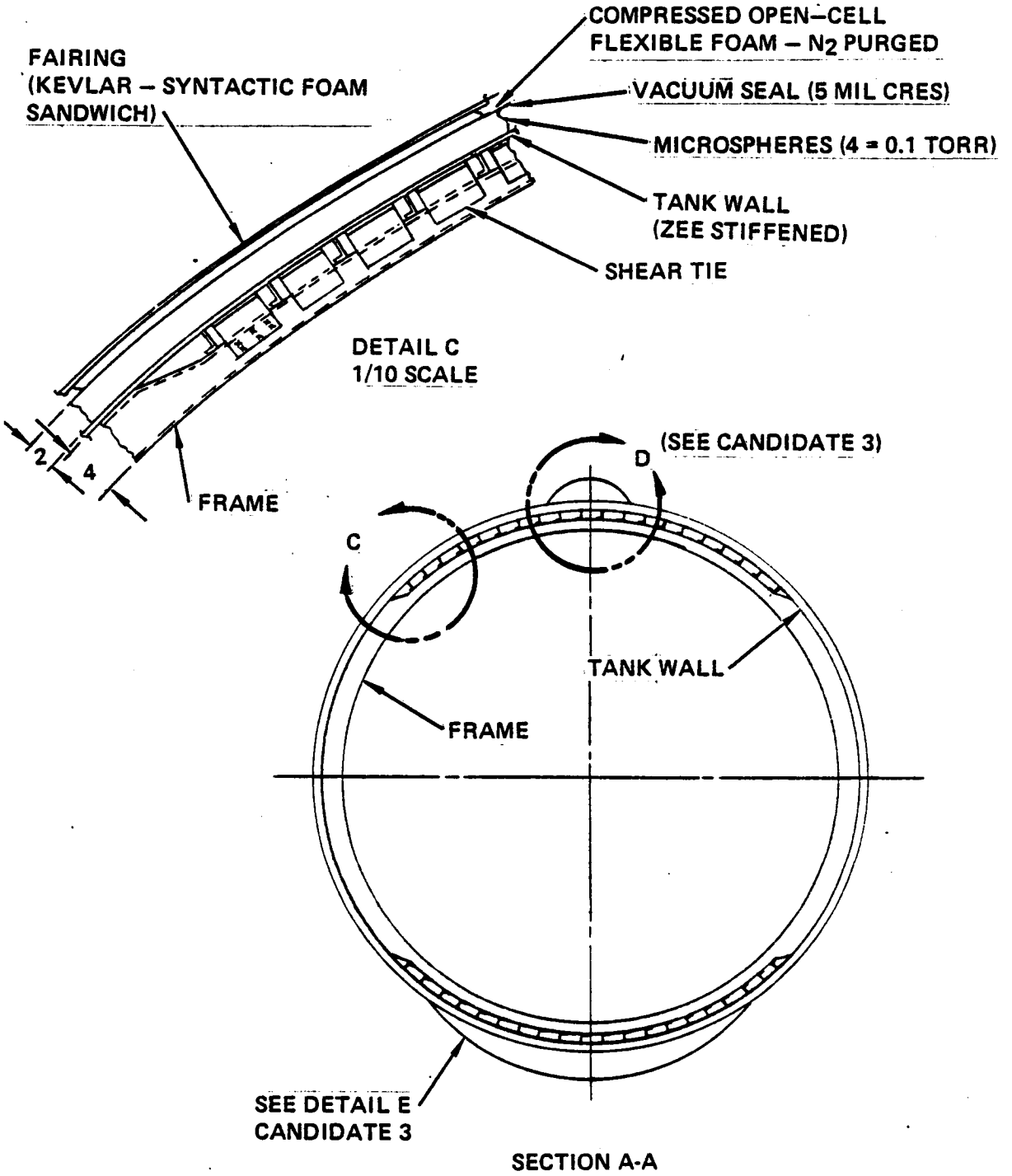

Figure 7.3.1d. - Concluded (Sheet 2 of 2)

TABLE 73. - SYSTEM WEIGHT COMPARISON OF FUEL CONTAINMENT SYSTEM CANDIDATES

Item	Candidate No. 1	2	3	4
Fuel Containment System:[a]	23 360	29 580	20 630	21 270
• Tank and Body Shell:	(20 060)	(28 030)	(16 360)	(16 160)
Dome Ends - Fwd	1 110	1 244	1 216	1 243
Dome Ends - Aft	832	932	924	955
Divider Bulkhead	690	707	732	744
Cylinder	7 556	11 927	8 471	8 192
Suspension System and Removal Rail	1 466	1 466	-	-
Truss-Tank to Body Shell	-	-	1 846	1 862
Body Shell	8 365	9 511	3 173	3 160
Vacuum Jacket Dome Ends	-	2 243	-	-
• Insulation:	(3 300)	(1 550)	(4 270)	(5 110)
Aero. Fairing	-	-	717	691
Vapor Barrier and Adhesive	1 006	517	697	203
Open Cell Foam	-	-	542	526
Closed Cell Foam	2 292	430	2 104	-
Microspheres	-	-	-	2 164
N_2 Purge System	-	-	210	210
Vacuum Pump System	-	600	-	400
Vacuum Jacket		incl. above		920
Fuel Systems:	2 307	2 325	2 260	2 250
Engine Supply	909	915	888	882
Fueling/Defuel	706	712	633	688
Pressurization/Vent	692	628	680	676
Total System Weight	25 664	31 902	22 893	23 520
Frac. of Useable Fuel Wt. - $\frac{\Sigma W_{SYS}}{W_{FUEL}}$	0.4174	0.5117	0.3804	0.3931

(a) sum of forward and aft tanks

for manufacturing tolerances, joints, weld lands, margins of safety, access, and systems provisions. A similar allowance was applied to the insulation weight for all candidates to provide for manufacturing tolerance, density variations, access and systems provisions.

Detailed stress analysis was performed for the aft tanks with only random analysis on the forward tanks to support the weight estimates. It was found that, where tank pressures were the same, the following equations could be used to accurately predict the forward tank weight:

$$W_{DOME_1} = W_{DOME_2} \left(\frac{D_1}{D_2}\right)^3$$

$$W_{CYL_1} = W_{CYL_2} \left(\frac{D_1}{D_2}\right)^2 \left(\frac{L_1}{L_2}\right)$$

where subscripts 1 and 2 refer to the forward and aft tanks, respectively, for the same candidate.

Candidate fuel containment systems 3 and 4 require nitrogen purge of the open cell foam just under the fairing cover. The total purge system requirement of 210 pounds is divided equally between the forward and aft tanks. Accordingly, the insulation system weights shown in Table 73 include 210 pounds for nitrogen purge systems for those systems. The nitrogen is assumed to be stored in liquid form in an insulated tank.

Similarly, vacuum pumping systems are required for Candidates 2 and 4. The system required for Candidate 2 weighs 300 pounds per tank. It consists of a combination of Roots blowers, fore-pumps and turbomolecular pumps. For Candidate 4 the pumping system consists of just two Roots blowers in series and the weight is 200 pounds per tank.

To assure a fair comparison between integral and nonintegral candidates, the body shell weight has been included. In the case of the forward tanks, the body shell length is measured from the tank forward end to the forward cabin pressure bulkhead frame. For the aft tanks, body shell length is measured from the aft cabin pressure bulkhead frame to the aft end of the tank. Body shell weight is greater for the nonintegral Candidate Nos. 1 and 2 since the entire tank is enclosed within the body. For Candidates 3 and 4, part of the body shell is integral with and included in the tank cylinder weight. The remaining body shell weight is for that portion covering the dome ends and the area between tank end and cabin pressure bulkhead.

7.3.2 Cost considerations. - Cost estimates were prepared for each of the candidate fuel containment systems, as well as for the basic fuel system components required for engine supply, fueling/defuel, and vent/pressurization systems. The data developed during this study were parametric cost factors to represent each design or candidate system in terms of production labor hours and material dollars per pound of total fuel system weight. The data were for use in the production cost subroutine of the Lockheed proprietary computer model, ASSET.

The production cost subroutine of ASSET contains individual cost factors for each type of material (up to five) which might be used in any of the individual structural mass groups (i.e., wing, tail, body, landing gear, nacelles, surface controls, and air induction and exhaust systems.) Labor and material cost factors are also included for the airframe and propulsion systems (including the fuel system) and avionics and engine installations. In addition, the subroutine includes provisions for learning curves, sizing factors, quality assurance, other recurring manufacturing support activities, warranty, and profit. The engine costs are estimated using modified Rand formulas and the avionics equipment are based on equipment requirements. These latter costs are estimated separately and added to that of the airframe to arrive at the total recurring cost. Production costs are used in the calculation of investment cost, DOC, IOC, and ROI.

7.3.2.1 Premises and assumptions: The basic premises and assumptions used in the cost study were as follows:

- These are engineering cost estimates for relative ranking of alternate configurations. Price quotes are neither implied or intended.
- Costs are stated in constant 1976 dollars.
- Costs include production (factory) labor and material only
- Estimated costs represent the cumulative average cost per aircraft based on a program quantity of 350 aircraft
- An 80-percent learning curve was used for labor
- A 95-percent learning curve was used for material
- Prime contractor profit is not included

7.3.2.2 Cost methodology: The first step in the cost analysis task was to define each system to the level required for estimating purposes, consistent with overall program requirements. A summary of the general characteristics, structural concepts, materials, and manufacturing methods for major items weighed individiually was prepared in matrix form. Basic parametric cost factors in terms of production labor hours and material dollars per pound of weight were selected for conventional metal skin/stringer/frame construction, as well as for composite laminated, sandwich, and hybrid structures. These basic data were suitably modified to account for individual design concepts for each applicable major item. Cost factors previously developed for wide body transports for fabrication, assembly, and installation of plumbing; and for checkout of valves, pumps, and various other components of the engine supply, fueling/defuel, and vent/pressurization systems were appropriately used. Cost of pumps required for the vacuum pumping systems were estimated by LMSC. The estimated cost of microspheres in production quantities ($2.00 per pound) was supplied informally by the 3M Corporation.

The basic cost factors in the form of labor hours and material dollars per pound were prepared so as to represent the cumulative average for 100 aircraft. The appropriate cost factors were applied to each item individually weighed, and all labor hours and material dollars were summed. Appropriate learning curves were applied, as well as labor rates, to arrive at the total cumulative average cost for 350 aircraft.

It should be noted that derivation of these cost factors required a certain amount of judgment and extrapolation of available data. Therefore, these estimates should not be construed as absolute values; however, the relative ranking of each system should be fairly consistent and representative within the framework of this study.

7.3.3 Evaluation results. - A matrix of computer runs was made with the ASSET program to determine the optimum wing loading and thrust-to-weight ratio for LH_2-fueled aircraft using each of the candidate fuel containment systems. As stated earlier, minimum DOC was the measure of merit but each aircraft was required to meet certain operational constraints while performing the design mission.

The results are shown in Table 74. The parameters whose values are listed are those considered particularly relevant to the objective of selecting a preferred FCS. On the basis of gross weight, fuel weight, OEW, fuselage length, engine size, aircraft price, DOC, and energy utilization, FCS No. 4, the integral tank design with microsphere insulation would be considered the best choice. Candidate No. 3, the integral tank design with closed cell foam insulation, would be a close second. The nonintegral tank designs are severely penalized by their greater thickness and weight. A summary of the weight of individual elements of the tank structure and insulation systems of the respective aircraft, plus the weights of their engine fuel supply systems, fueling/defuel systems, and pressurization/vent systems, was shown in Table 73.

TABLE 74. - CHARACTERISTICS OF AIRCRAFT DESIGNED FOR FOUR PREFERRED FUEL CONTAINMENT SYSTEMS

LH_2 fuel; 400 passengers; 10 190 km (5 500 n.mi.); M = 0.85

		FCS Candidate No.			
		1	2	3	4
Tank Type Insulation Concept		Nonintegral Closed Cell Foam	Nonintegral Hard Vacuum	Integral Closed Cell Foam	Integral Microspheres
Gross weight	lb	387 800	395 600	379 500	377 800
Fuel weight (total)	lb	61 480	62 350	60 190	59 820
Payload weight	lb	88 000	88 000	88 000	88 000
Operating empty weight	lb	238 320	245 250	231 310	229 280
Fuel Containment System					
Weight	lb	23 360	29 580	20 630	21 270
Thickness*	in.	7.9	6.0	3.5	2.45
System Wt.	(W_{FCS}/W_f)	.380	.474	.343	.356
Fuel Systems weight	lb	2 307	2 325	2 261	2 246
Fuselage length	ft	224.2	222.9	218.5	215.6
Thrust per engine	lb	2472.0	25 220	24 190	24 080
Lift/Drag (cruise)	-	16.42	16.53	16.41	16.43
Specific Fuel Consump. (cruise)	$\frac{lb}{hr}/lb$	0.202	0.202	0.202	0.202
Aircraft Price	$\$10^6$	39.1	40.0	38.3	38.1
LH_2 Systems Cost	$\$10^6$	0.95	1.43	0.86	0.89
Block DOC	¢/S n.mi.	1.626	1.650	1.598	1.591
Total DOC (incl ground boiloff	¢/S n.mi.	1.638	1.656	1.609	1.600
Energy Utilization	Btu/S n.mi.	1 222	1 238	1 196	1 189

*From inside surface of tank skin to external surface of aircraft

However, as obvious as it may seem that the integral tank candidates are the superior choice on the basis of these aircraft parameters, there are other considerations which need to be taken into account. These include such items as safety, producibility, maintainability, reliability, and operational considerations. These factors are subjective in nature and therefore are not amenable to being quantified.

Accordingly, an evaluation scheme was established wherein each of the significant parameters could be considered on a relative basis. Three items which were considered especially significant to the objective were selected from Table 74. They were the following:

	Candidate Fuel Containment System			
	1	2	3	4
Direct Operating Cost (¢/seat n.mi.)	1.6378	1.6563	1.6089	1.5998
Energy Utilization (BTu/seat n.mi.)	1222	1238	1198	1189
Aircraft Price ($\$10^6$)	39.06	39.99	38.27	38.09

By limiting the number of quantified parameters in the evaluation scheme to only three, they could not overbalance the importance of the subjective considerations.

An evaluation scale running from 1 to 10 was used, with 10 being best. To encourage a wide spread between the candidate FCS in the final total, the system which was preferred for each parameter being evaluated was awarded the maximum rating of 10. It was not necessary that the lowest rated system be given a 1, this was a matter of judgment concerning the significance of the difference between the best and the worst systems.

The fuel containment systems were evaluated on the subjective items on the basis of considerations which were discussed throughout Section 7 and in Appendix E and F.

The result of the weighted judgment evaluation of the candidate fuel containment systems is presented in Table 75. Candidates 3 and 4 are again the obvious winners with the difference between them being too small to be meaningful. Accordingly, although Candidate No. 4, the integral tank with the microsphere insulation system, is designated the preferred fuel containment system, it is emphasized that further development of both Candidate No. 3 and Candidate No. 4 is strongly recommended.

TABLE 75. - EVALUATION OF PREFERRED FCS CANDIDATES

(uses scale of 1 to 10, 10 being best)

	Candidate No.			
	1	2	3	4
DOC	3	1	8	10
Energy utilization	4	1	9	10
Aircraft price	7	5	9	10
Safety	6	8	6	10
Producibility	8	2	10	9
Maintenance				
Inspection	7	10	7	10
Repair	3	1	10	7
Replacement	3	1	10	7
Reliability	10	3	10	7
Operations	8	8	8	10
Total	59	40	87	90

It would be a serious mistake if future development of LH_2-fueled aircraft was tied exclusively to only one FCS concept when a) there is so little actual experience with the microsphere system, b) the evaluation procedure involved so much subjective judgment and resulted in so little difference between the first and second choices, and c) the fuel containment system is such an important element in the design of a satisfactory aircraft.

The fundamental risk involved with Candidate No. 3, an integral tank with closed cell foam applied on the external surfaces, pertains to the useful life which might be realizable with the foam and its vapor barrier. With Candidate No. 4, it is a question of the degree of difficulty which will be encountered in fabrication and maintenance of the flexible stainless steel vacuum jacket, and questions of safety concerning the effect of a major fracture or penetration of the vacuum jacket during service. These questions can only be resolved by further development of both concepts.

8. LH_2 FUELED AIRCRAFT CHARACTERISTICS

The results of all the analyses and studies described in foregoing sections were put together into the design of a final liquid hydrogen fueled aircraft which conforms to all the guidelines and meets all the requirements established at the beginning of the program.

In this section, the airplane and its operational characteristics are described; and the implications of its fuel system with regard to malfunctions, reliability, safety and fire protection, and FAR and industry standards are discussed

8.1 LH_2 Aircraft Description

The final airplane design is the one described in Section 7 which uses fuel containment system No. 4, the integral tank design with microsphere insulation system. It also incorporates the LH_2-fueled turbofan engine discussed in Section 4.3.3; the design of engine fuel supply system with its boost pumps, feed lines, engine pump, and fuel control system as selected in Section 5; and the fuel subsystems defined in Section 6.

Significant characteristics of the aircraft are listed in Table 76. Its general description is fundamentally the same as that of the baseline aircraft from Reference 1. The general arrangement shown in Figure 2 (Section 3) is an accurate representation of the configuration; however, the overall dimensions are different. As listed in Table 1, the wing span is now 52.07 m (170.84 ft) and the body length is 65.73 m (215.64 ft). Internally, the 400 passengers are located in the central portion of the fuselage in a double-deck arrangement with the fuel tanks located forward and aft. The fuselage is basically circular in cross-section with a lower lobe attached which contains cargo and baggage.

The wing has a supercritical section and incorporates high lift devices including 15 percent leading edge slats and 35 percent double-slotted Fowler flaps out to the outboard engines. Conventional ailerons are attached to the outboard wing panel. Spoilers are provided for direct lift control in flight and for deceleration during landing ground run. Active controls are employed to minimize gust loading, provide a smoother ride and minimize tail size. The wing and body structure incorporates nearly 50 percent by weight of advanced composite materials.

The differences in performance and weight of the present design, relative to the Reference 1 aircraft, are due to small changes in specific fuel consumption in various engine settings and flight conditions resulting from the work reported herein to define a more realistic LH_2-fueled engine, and

TABLE 76. - CHARACTERISTICS OF FINAL DESIGN, LH_2 - FUELED TRANSPORT AIRCRAFT [400 PAX; 10 190 km (5500 n.mi.); MACH 0.85]

	SI Units		U.S. Units	
Gross Wt	kg		lb	377 800
Total Fuel Wt	kg		lb	59 820
Block Fuel Wt	kg		lb	50 710
Operating Empty Wt	kg		lb	230 000
Aspect Ratio	-	9	-	9
Wing Area	m^2		ft^2	3242.9
Sweep	deg		deg	30
Span	m		ft	170.84
Fuselage Length	m		ft	215.64
L/D - Cruise	-		-	16.43
SFC - Cruise	$\frac{kg}{hr}$ / daN		$\frac{lb}{hr}$ / lb	0.202
Initial Cruise Altitude	m		ft	37 000
Wing Loading	kg/m^2		lb/ft^2	116.5
Thrust/Weight	N/kg		-	0.25
No. Engines		4		4
Thrust Per Engine	N		lb	24 080
FAR T.O. Distance	m		ft	7945
FAR Ldg. Distance	m	1770	ft	5810
2nd Seg Climb Grad. (Eng Out)		0.0571		0.0571
Approach Speed	m/s	69.5	KEAS	135
Weight Fractions	percent		percent	
Fuel		15.83		
Payload		23.29		
Structure		33.03		
Propulsion (Includes Tanks & Fuel System)		9.73		
Price	$\$10^6$	38.09	$\$10^6$	38.09
DOC (a)	$\frac{¢}{\text{seat km}}$		$\frac{¢}{\text{seat n.mi.}}$	1.599
Energy Utilization	$\frac{kJ}{\text{seat km}}$		$\frac{Btu}{\text{seat n.mi.}}$	1189

(a) DOC based on LH_2 cost = \$5.69 per GJ (\$6/10^6 Btu = 31¢/lb) (includes ground boiloff losses)

to changes in weight of various components of the LH_2 fuel system and the engine.

The engine used in the previous study (Reference 1) was flat rated to provide the same takeoff thrust under hot day (32.6°C) conditions as at standard day conditions. The engine was sized by the requirement to provide an aircraft thrust-to-weight ratio (T/W) that would meet the initial cruise altitude specification of 9449 m (31 000 ft).

The engine from the present study is not flat rated. In addition, it has a lower thrust lapse with altitude than did the original engine. For example; at 35 000 ft Mach 0.85, the original engine produced 21.3 percent of its hot day, sea level static thrust while the present engine produces 28.7 percent, or in other words, 34.7 percent more thrust at altitude. The net effect of this is that while the reference aircraft required a 0.293 sea level static thrust-to-weight ratio to meet the minimum cruise altitude, the present engine can meet this with ease at a lower T/W. As a result, the engine-out takeoff field length requirement became critical in the present study in determining the thrust-to-weight ratio of 0.255 which was selected as optimum for the final aircraft design.

8.2 Weight Estimating Relationships

Weight estimating relationships normally used for conventional subsonic passenger transport aircraft were employed in the present study, except as it was found necessary to modify them to account for features associated with use of LH_2 fuel. The changes included the following:

- Body - The body weight estimating equation was modified to account for the large volume required for the low density LH_2 which is equally distributed in tanks forward and aft of the passenger cabin. This distribution causes greater shear and bending loads in the body shell than for a conventional passenger transport which carries its Jet A fuel in the wing box. Although the wing equation was not modified for this study, the absence of fuel in the wing for bending relief would cause the wing specific weight to be somewhat heavier for an LH_2 design than for a conventional Jet-fueled aircraft.

- Fuel Tanks - The weight of the fuel containment system was calculated as described in Section 7.3.1. For the subject, final design aircraft, the weight of the integral tank design with microspheres contained in a soft vacuum annulus for insulation was represented.

- Engine Fuel Supply System - The engine fuel supply system weight was based on use of 2.54 cm diameter x 0.406 mm thick (1.0 in dia. x 0.016 in thick) stainless steel lines wrapped with 3.81 cm (1.5 in) of closed cell foam. A 10.16 cm diameter x 0.406 mm thick (4.0 in dia. x 0.016 in. thick) aluminum tube enclosed the foam insulation to provide a vapor seal and mechanical protection. The weight of the complete engine fuel supply system including boost pumps, lines, valves, engine pump, and engine fuel control system was calculated as outlined in Section 5.6. Similarly, the aircraft fuel subsystems weights were taken from Section 6.

- Propulsion - The LH_2 fueled turbofan engine weight was scaled from the baseline engine described in Section 4.3 which weighs 2082 kg (4589 pounds) and delivers 114.4 kN (25 724 pounds) of thrust at sea level static, standard day conditions.

  The engine weight includes

  - Engine accessories and gearbox
  - Engine mounts and pylon splitter fairing
  - Gas generator cowl and tailpipe
  - Fan duct acoustic ring

  Installed engine weight per aircraft is expressed in pounds as:

$$WENG = (0.17839)\ (NENG)\ (TSLS)$$

  where

$$NENG = \text{Total number of engines}$$

$$TSLS = \text{Installed sea level static thrust/engine}$$

  Nacelle and pylon weight per aircraft, before applying a weight reduction factor for advanced composite usage, is equal to 31.66 percent of the total installed engine weight. On the same basis, the air inlets are 16.12 percent of the engine weight. The remaining propulsion group items, including fan thrust reversers, engine controls, and starting and oil systems weigh approximately 10 percent of the installed engine weight.

- Advanced Composites - Weight reduction factors were applied to the estimating equations to reflect the benefits expected from advanced composites usage in the 1990-1995 time period. These weight reduction factors were taken from the Advanced Technology Transport Study (Reference 39), performed by the Lockheed - Georgia Company, and are based on the intermediate technology level discussed therein. Table 77 lists the weight reduction factors as well as the estimated materials distribution for each group.

8.3 Operational Requirements of LH_2 Fuel System

A detailed accounting of all of the flight and maintenance crew operational requirements for the airplane is beyond the scope of this program; however, some of the requirements which can be addressed in this conceptual phase of the airplane design are discussed in the following paragraphs.

8.3.1 Fueling and defueling - Because it is cyrogenic and is also very easily ignitable, hydrogen must be handled in a different manner than practices which have been developed for hydrocarbon fueled aircraft during fueling operations.

TABLE 77. - ADVANCED TECHNOLOGY WEIGHT REDUCTION FACTORS AND ESTIMATED MATERIALS DISTRIBUTION

Group	Weight Reduction Factors	Materials Distribution (% of Total Wt.)				
		ALUM.	TI.	STEEL	COMPOS.	OTHER
Wing	0.635	44	4	2	48	2
Tail	0.730	49	15	2	32	2
Body	0.664	38	4	2	50	6
Landing Gear	0.848	8	15	20	20	37
Nacelles, pylon	0.787	5	30	30	35	0
Air Ind.	0.787	45	5	4	41	5
Flight Controls	0.950	20	5	20	5	50

8.3.1.1 Recommended practices for fueling procedure:

1. Operating personnel should be suitably attired in protective apparel including thermally insulated gauntlet type gloves, head and body splash protective clothing, and nonconductive footwear.

2. Bond the airplane and ground fueling equipment to each other and to a permanently installed airport grounding terminal. (It is assumed that all parts of the airframe are bonded together electrostatically so that no unbonded components can cause a static discharge in the presence of a combustible mixture of hydrogen and air.)

3. Determine the total quantity of fuel required to accomplish the intended flight including normal reserve.

4. Set the "bug" on each fuel quantity indicator on the refuel panel (see Figure 162) at one fourth of the total fuel load required.

5. Insert the vapor recovery nozzle into the vapor recovery adaptor making sure that no contaminants are on the mating surfaces at the interfaces of the nozzle and adaptor.

6. Insert the fueling nozzle into the fueling adaptor taking the same precautions as in (5).

7. Place the actuating linkage for the vapor recovery nozzle in the open position.

8. Place the refueling valve switches on the fueling panel in the open position.

9. Initiate fueling by placing the actuating linkage of the fueling nozzle in the open position. (The fueling time for a full load of fuel starting from a 15 percent reserve quantity remaining from a previous flight should be approximately 20 minutes).

10. Close the actuating linkage of the fueling nozzle.

11. Place the refueling valve switches in the refuel panel in the closed position.

12. Remove the fueling nozzle.

13. Remove the dust cover.

14. Close the actuating linkage of the vapor recovery nozzle.

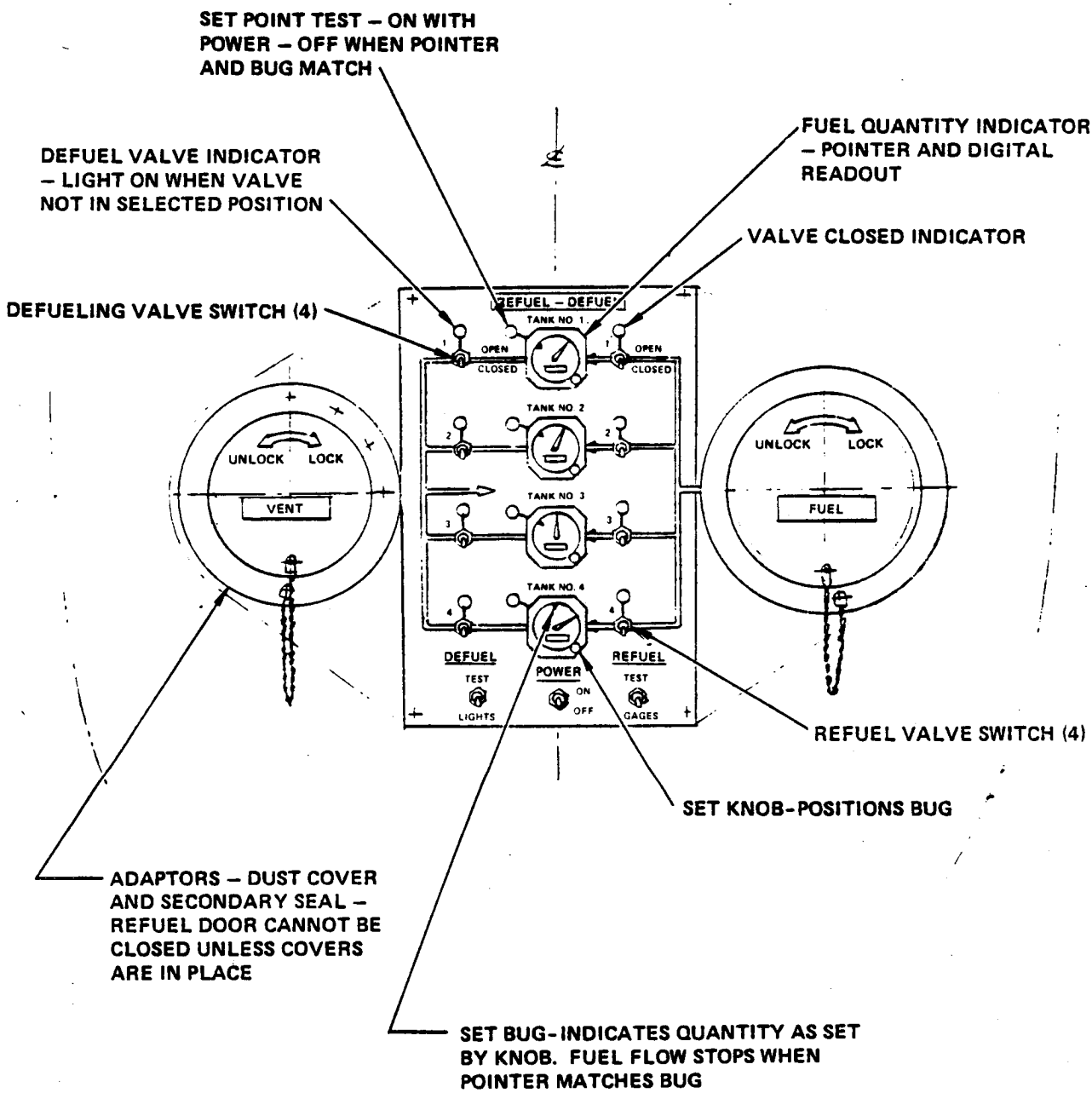

Figure 162. - Refuel panel.

15. Remove the vapor recovery nozzle.

16. Replace the dust cover.

8.3.1.2 Defueling procedure: Defueling is not a normal operation since it usually results from the need for maintenance activities. This usually involves emptying the tanks completely which is a specialized activity requiring special procedures to ensure that no impurities get into the tanks while the tanks are being:

1. emptied,

2. warmed to ambient temperature,

3. purged of hydrogen gas,

4. purged of air after maintenance activities are complete,

5. cooled to cryogenic temperatures, and

6. refueled.

These specialized procedures are discussed in some detail in Section 4.5.5 of Reference 2 and will not be discussed herein.

8.3.2 Flight engineer's panel. - Figure 163 shows the flight engineer's panel arranged in a functional manner to permit visualization of the essential features of the system. The diagram is self explanatory with the exception of the "press-relief" and "vent" push-to-test buttons. When depressed, these close the primary tank and vent line (back pressure) valves respectively. Continued depression will allow the tank (or vent line) pressure to rise to the higher setting of the secondary valves at which time the pressures should stabilize at the higher pressure. In this manner, it can be determined that both primary and secondary tank pressure and vent line valves are functional.

Fuel quantity gauges are backed by fuel totalizers which indicate the total quantity of fuel used by each engine by means of integration of the engine mounted fuel flowmeter.

The optional fuel jettison valves are also shown. To jettison fuel, all 12 pumps should be turned on, the jettison chute or boom extended and the jettison valve opened.

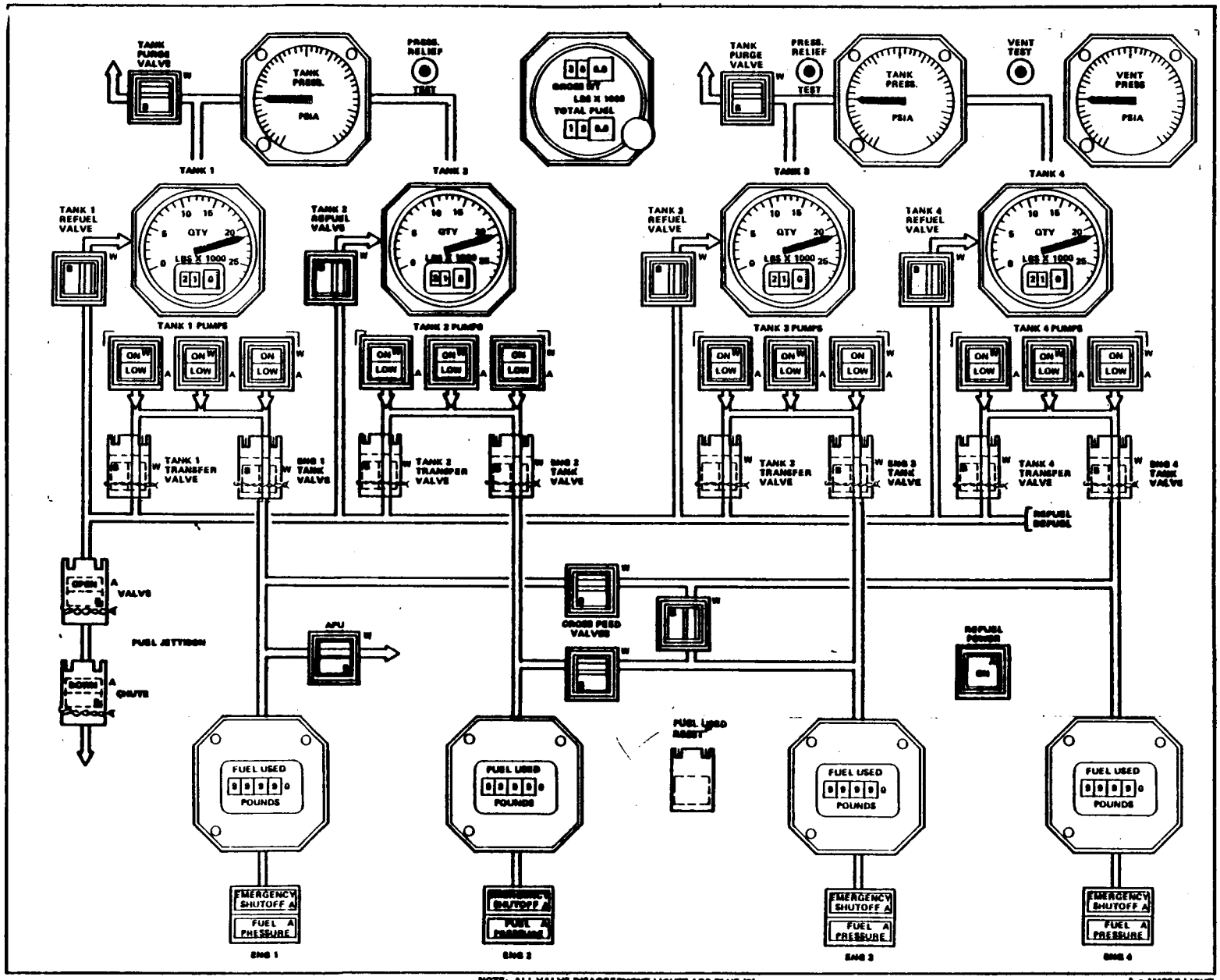

Figure 163. - Fuel system control panel - flight engineer.

8.3.3 Fuel management. - Installation of fuel tanks at the forward and aft locations in the fuselage could potentially lead to a situation which would involve excessive c.g. movement as fuel is consumed. In normal operation, balance is maintaned by having equal tank capacities with approximately equal moment arms for the forward and aft tanks. To illustrate this point, Figure 164 was prepared to show c.g. travel based on a typical weight and balance sheet. At gross takeoff weight, the aircraft c.g. is at 41.5 percent MAC, well within the limits of 30 to 47 percent MAC at that weight. For normal fuel usage, the c.g. moves forward to 36.8 percent MAC at zero fuel weight creating a minimum requirement for aircraft trim adjustment. However, a failure of the fuel line tank isolation valve in any one tank to the closed position could make fuel trapped in that tank unavailable for engine consumption if an alternate path for fuel to be removed from the tank were not provided. The consequences of such a condition, illustrated on the figure for fuel trapped in either Tank 1 or Tank 4, are not tolerable.

To preclude the above possibility, the fuel transfer system described in Section 6.5 and illustrated in Figure 77 was incorporated in the fuel system design. An example of the effectiveness of the system can be illustrated by the following example. If the fuel valve in Tank No. 1 fails in the closed position the corrective action is to open the fuel transfer valve in Tank 1 and close its refuel control valve (see Fig. 77). Fuel immediately begins to flow from Tank 1 to Tank 2 through the Tank 2 fueling manifold. This does entail some nominal shift in c.g., but the amount is less than 2 percent as can be seen in Figure 164. In the other extreme situation, where the feed line from Tank 4 is blocked, requiring transfer to Tank 3, the forward c.g. shift is still less than 2 percent and entails an aircraft trim adjustment no greater than encountered in normal operation.

8.3.4 Maintenance. - The cryogenic nature of hydrogen fuel will require major changes in the methods used to maintain and repair the aircraft fuel system. These changes are exemplified in the way fuel tank pumps are replaced and in the preparation for repair of fuel system insulation leaks.

A major objective of the design study was to locate all equipment possible external to the fuel tanks so that the time consuming process of entering the tanks for fuel system maintenance could be avoided. This has been accomplished and only the necessary plumbing lines are located in the tank.

Another important objective was to devise a method by which the fuel pumps could be replaced quickly and safely, without requiring that the liquid-hydrogen fuel tank be drained. The design solution to this problem is described in Section 5.3.6. Included are drawings and a description of the physical configuration of the pump mounting, the method of changing the

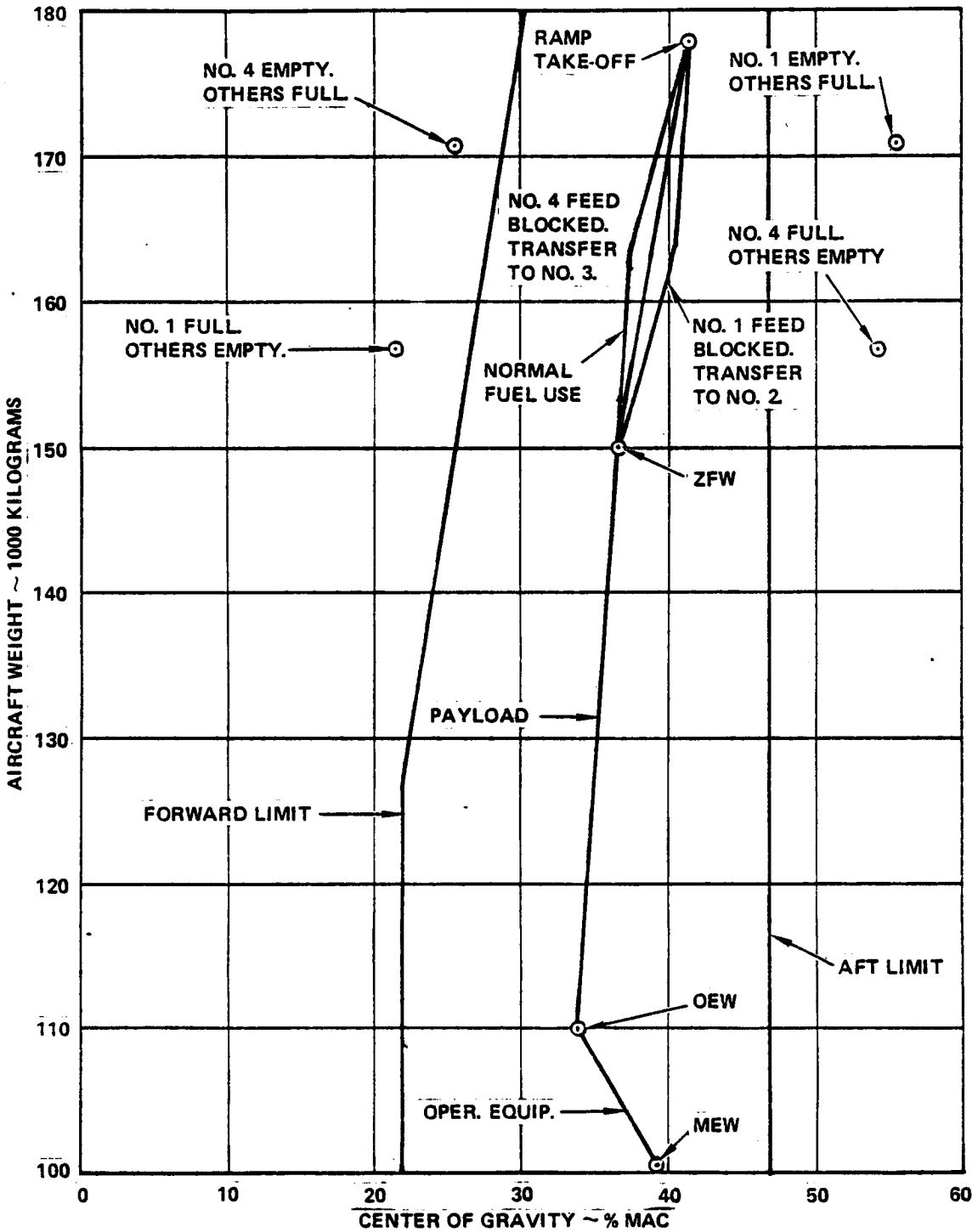

Figure 164. - C.G. travel with blocked feed line.

pump without draining the fuel tank, and a tool designed to accomplish the changing of the pump. Particular consideration was given to ensuring the safety of the personnel involved in the operation and the integrity of the equipment on the airplane.

8.4 Fuel System Malfunction Analysis

Table 79 provides results of an analysis of possible malfunctions which can occur with critical LH_2 fuel system components. The components which were analyzed are used in the engine fuel supply system, the refuel/defuel system, and the pressurization/vent system.

Under each of the system headings the table lists the component, its normal function, possible malfunctions and their cause, and how the existence of the malfunction would be detected. The result of the failure on operation of the system is then described, proper corrective action indicated, and some remarks offered which explain the consequences of the malfunction.

8.5 Reliability Analysis

The following reliability analysis provides an assessment of the probability of loss relative to the function of the two primary critical subsystems of the LH_2 fuel system. The design concept for the two critical functions, fuel pumping and fuel venting, employ redundancy, thus enhancing the functional reliability. In developing the probability expressions, Trans World Airline Boeing 747 statistics for average flight duration of 6.1 hours and an average daily utilization of 12.2 hours were used as the time base for the equations. Thus, in the nominal case, the aircraft is expected to fly two flights per day. Component failure rates which are estimated to be realistic and were assumed to be allowable for an initial evaluation of the systems are listed in Table 80. Where two numbers are listed the number in parenthesis represents the allowable failure rate in the specified mode.

8.5.1 Pumping and distribution system. - The reliability logic employed in the following analysis is conventional using the binomial expansion to evaluate the active/parallel redundant systems. The porposed design concept employs four pumping sources, each source using a 3 pump cluster. Each pump cluster has been allocated to a separate tank/engine feed circuit. Successful completion of a prescribed daily flight schedule requires operation of one of the three pumps in each cluster. Crossfeed between pumping sources is provided thus allowing the continuous operation of all engines should a failure of one complete pumping cluster occur during the flight. The probability (P_1) of partial loss of the pumping system for the typical 6.1 hour flight is illustrated and expressed as follows:

TABLE 79. - FUEL SYSTEM MALFUNCTION ANALYSIS

Item No.	System and Component	Function	Malfunction	Cause of Malfunction	Detection of Malfunction	Result of Malfunction	Corrective Action	Remarks
				ENGINE FEED				
1	Fuel boost pump (3 pumps per tank)	Supplies fuel for: a) engine b) defueling c) jettison	Low flow Low press. or No flow or press.	Mechanical or electrical failure	Low press. light on fit. engrs. panel	Loss of pump	Turn pump off	Loss of 1 pump is not dispatch item. At least one pump should ne kept on at all times since engine will not run with all pumps out. Fuel in tank will not be available if 3rd pump fails.
2	Fuel boost pump outlet check valve (1 per pump)	Prevents reverse flow into pump when not running	Fails closed	Mechanical	None	No fuel flow	See remarks	Cannot be detected if at least 2 pumps are running. If valve is in the only pump running flow will stop. Engine can still be supplied from 1 pump. Can be checked on ground by testing each pump for flow and engine pump inlet pressure (engine idling)
			Fails open	Mechanical	None	None		Some reverse flow will occur. Sufficient flow provided for engine.
3	Tank shutoff valve (D.C.) Tanks 1,2,3, and 4	Isolate fuel supply from line when fire handle is pulled. Also controlled from flight engrs. panel (Normally open)	Fails open	Mechanical or electrical failure	Disagreement light goes on if valve is in any position other than selected	None unless emergency exists	None	Pumps should be turned off to stop fuel flow from tank in case line ruptures.
			Fails shut	Mechanical or electrical failure	Disagreement light goes on if valve is in any position other than selected	No flow from tank	Open fuel transfer valve.	Fuel in tank with failed valve can be transferred by pump to any or all tanks by opening the desired refuel valves and made available to the engines. Cross-feed valves must be used to equalize fuel consumption from the remaining tanks.
4	Firewall shutoff valve (D.C.) Engs. 1,2,3 and 4	To shutoff fuel flow to engine when emergency handle is pulled (Normally closed)	Fails open	Mechanical or electrical failure	Disagreement light goes on if valve is in any position other than selected	None unless emergency exists	None	Tank shutoff valve (above) will shutoff flow to engine. Fuel in line will be contained unless line ruptures.
			Fails closed	Mechanical or electrical failure	Disagreement light goes on if valve is in any position other than selected	Loss of engine if valve closes in flight	Shut off engine	Use cross feed to use fuel in tank normally feeding shutdown engine.

TABLE 79. - FUEL SYSTEM MALFUNCTION ANALYSIS (Continued)

Item No.	System and Component	Function	Malfunction	Cause of Malfunction	Detection of Malfunction	Result of Malfunction	Corrective Action	Remarks
5	Cross feed valves (D.C.) (3 valves)	Permits feeding any any eng. from any tank	Open or closed	Mechanical or electrical failure	Disagreement light goes on if valve is in any position other than selected	See remarks	See remarks	By the proper fuel management and using the intertank transfer capability, all fuel can be made available to all engines in the event of any combination of cross feed valve.
				REFUEL/DEFUEL				
6	Fueling adapter	Provides connection for ground refueling nozzle	Poppet fails closed	Damage or abuse	Nozzle cannot be opened	Aircraft cannot be refueled	Replace	A very unlikely failure. When not in use the poppet is protected by an adapter cap.
			Poppet fails open	Damage or abuse	When nozzle is removed fuel is released. Also visual indication.	Fuel release	Replace	Very unlikely since it is only used on ground. Dual springs are provided for return of poppet in case one fails.
7	Fueling shutoff valve (D.C.)	Shuts off refueling flow. Also allows intertank transfer and level control in flight.	Fails open	Mechanical or electrical failure	Disagreement light goes on when valve is not in position selected.	None	Replace	This valve is prechecked both during and at the end of refueling. Even if valve fails to shut during refueling, tank cannot be overpressurizer since fueling and pressure is 35 psia and tank can take up to 41 psia limit load. Fuel overflow is returned to liquefaction facility via vent line. During defuel, open valve will allow fuel from other tanks to enter. This fuel can be removed by pressure transfer after the other tanks have been defueled.
			Fails shut	Mechanical or electrical failure	Disagreement light goes on when valve is not in position selected.	Tank cannot refueled	Replace	Fuel already in tank can be used. In-flight transfer into tank cannot be done however.

TABLE 79. - FUEL SYSTEM MALFUNCTION ANALYSIS (Continued)

Item No.	System and Component	Function	Malfunction	Cause of Malfunction	Detection of Malfunction	Result of Malfunction	Corrective Action	Remarks
PRESSURIZATION/VENTING								
8	Tank pressure control valve (2)	a. Primary valve regulates tank pressure to 21 psia	Fails closed	Mechanical failure	Tank press. risers to 23 psia.	Tank press. rises to 23	Replace	Tank protected by secondary regulator (b).
			Fails open	Mechanical failure	Loss in tank press.	See remarks	Replace	Fuel will flash in tank until equilibrium temperature corresponding to vent back pressure valve setting is reached. Approximately 9-10% of fuel will be lost. Rest of fuel is usable.
		b. Secondary valve regulates tank to 23 psia if (a) above fails closed	Fails closed	Mechanical failure	Close override solenoid of (a) above. Tank press. will rise above 23 psia.	None	Replace	If tank pressure rises above 23 psia override solenoid actuated by "push to test" button must be released to prevent overpressure. (See Fig.)
			Fails open	Mechanical failure	← Same as item (a) above (all open mode) →			
		c. Purge valve permits ground purging of tanks at reduced pressure	Fails closed	Mechanical or electrical failure	Tank press. rises to 21 psia when purge gas is introduced.	None	Replace	Ground operation only. Tank pressure cannot exceed 21 psia.
			Fails open	Mechanical or electrical failure	← Same as item (a) above (fail open mode) →			
9	Vent back pressure valve (primary)	Prevents air from entering vent line (Servo operated)	Fails closed	Icing or mechanical failure	Vent line pressure rises to 3.5 psig	Alternate vent is used	Icing will clear. Replace if machanical.	This is a flight dispatch item. Flight precheck should include using primary vent valve override solenoid to determine if vent line pressure rises to 3.5 psig, indicating alternate vent is operating.
			Fails open	Mechanical failure or foreign object.	Vent line press. falls to zero	See remarks	Replace	If failure occurs in flight, vent scoop airflow should prevent air backflowing into line. On ground tank venting should maintain vent exit pressure higher than ambient. This should be extremely rare due to valve design.

TABLE 79. - FUEL SYSTEM MALFUNCTION ANALYSIS (Continued)

Item No.	System and Component	Function	Malfunction	Cause of Malfunction	Detection of Malfunction	Result of Malfunction	Corrective Action	Remarks
10	Vent back pressure valve (alternate)	Prevents air from entering vent. Operates if primary vent fails shut (servo operated)	Fails closed	Mechanical or electrical failure	Press. rises above 3.5 psig on precheck	See remarks	Replace	Flight dispatch item. Flight precheck by closing primary vent override solenoid. If pressure rises above 3.5 psig alternate is failed close.
			Fails open	Mechanical or electrical failure	Press. will not rise to 3.5 psig or vent fails to close on refuel	See remarks	Replace	See remarks in item 9 (fail open)
11	Vent adapter	a. Provide connection for ground vent nozzle	Fails closed	Damage or abuse	Nozzle can not be opened	Aircraft cannot be refueled	Replace	Unlidely failure. Protected by an adapter cap when not in use.
		b. Closes fail (primary) vent to allow return of vent gases for liquefaction	Fails open	Damage or abuse	When nozzle is removed vent gases are released. Also visual indication.	Vent gas release	Replace	Very unlikely. Used only on ground. Dual springs provided for return of poppet.

TABLE 80. - ALLOWABLE FAILURE RATES FOR LH_2 PUMPING AND VENTING SYSTEM COMPONENTS

Component (Critical Failure Mode)	MTBF (HRS)	Failure Rate (λ) Per Flight Hour
1. Pump - Fuel Boost (Failure to operate)	2 500	.000400
2. Control valve - Vent pressure and regulation.	9 350	.000107
• Primary regulator - (Failure in closed mode)	50 000	.000020 (.000015)
• Secondary regulator - (Failure in closed mode)	50 000	.000020 (.000015)
• Vent valve & motor - (Failure to open)	15 000	.000067 (.000033)
• Solenoid by pass valve - (Failed in closed mode)	100 000	.000010 (.000001)
• Manual over-ride - press. regulator - (Failure to operate when required)	100 000	.000010 (.000010)
3. Vent valve - Primary (Failure in closed mode)	50 000	.000020 (.000015)
4. Vent valve - Auxiliary (Failure in closed mode)	50 000	.000020 (.000015)

RELIABILITY SERIES/PARALLEL DIAGRAM FOR P_1

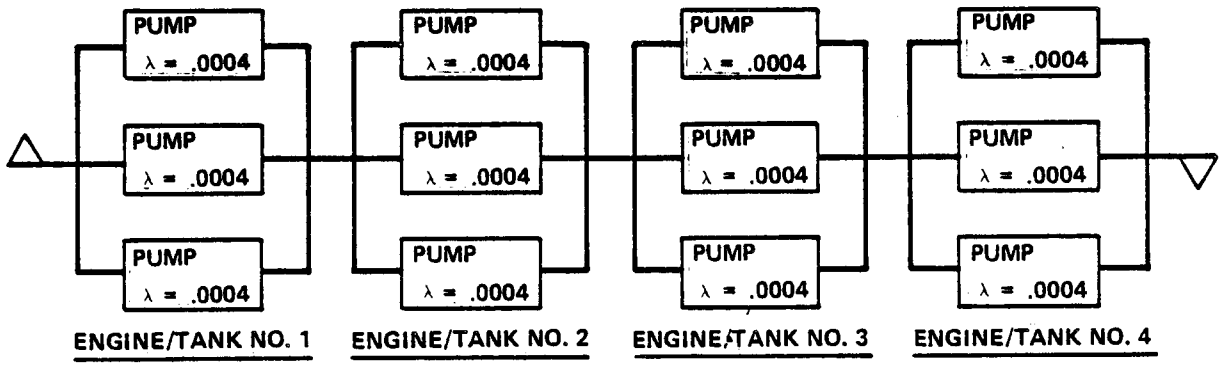

Reliability expression:

$$P_1 = 4\left[1 - (R^3 + 3R^2Q + 3RQ^2)\right]$$

$$R = e^{-\lambda t}$$

$$Q = 1-R = \text{probabiility of failure}$$

where

λ = Failure rate/hour = .0004

t = Flight time = 6.1 hours

e = Exponential reliability function

$$P_1 = 4(1 - .99999984) = 6.4 \times 10^{-7}$$

or, conversely, the probability of one operational pump remaining in each of the four pump clusters.

To provide a basis for evaluating whether a given probability of failure is acceptable or not, current practice with commercial aircraft is as follows. In cases where failure of a component or system would result in loss of life or aircraft, Q must have a value not greater than 1×10^{-9}. Where failure would result in no hazard to life or aircraft but might require cancellation

or diversion of a flight, Q is usually required to be not greater than 1×10^{-6} or 1×10^{-7}. Accordingly, the value of 6.4×10^{-7} calculated for this instance is acceptable and the assumed failure rate for boost pumps shown in Table 80 is valid as a design target.

P_2 = Probability of loss of one of the four pump clusters during 2nd flight of the day (6.1 hours), assuming one pump in each of the four pump clusters has already failed.

RELIABILITY SERIES/PARALLEL DIAGRAM FOR P_2

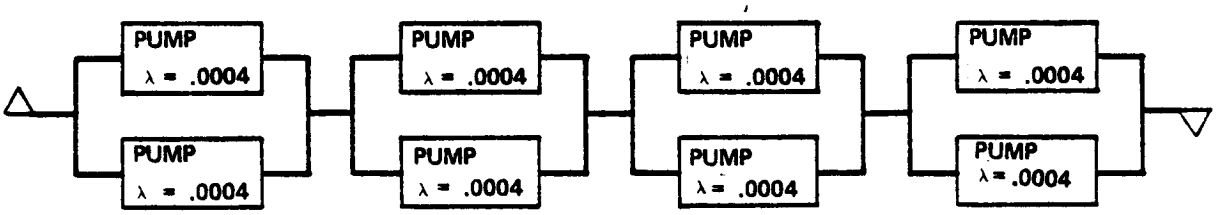

Reliability expression:

$$P_2 = 4(Q^2)$$

$$Q = 1 - R = \text{Probability of Failure}$$

$$R = e^{-\lambda t}$$

where

λ = Failure rate/hour = .0004

t = Flight time = 6.1 hours

e = Exponential reliability function

$$P_2 = 2.3 \times 10^{-5}$$

This proability of failure is marginal for acceptance as a non-hazardous occurrance. A logical conclusion is that the conventional requirement be adhered to, namely, that an aircraft not be dispatched if more than two pumps are failed.

P_3 = Probability of flight diverting to an alternate landing site due to the loss of one pump cluster which would dictate crossfeed control to the affected engine.

RELIABILITY SERIES/PARALLEL DIAGRAM FOR P_3

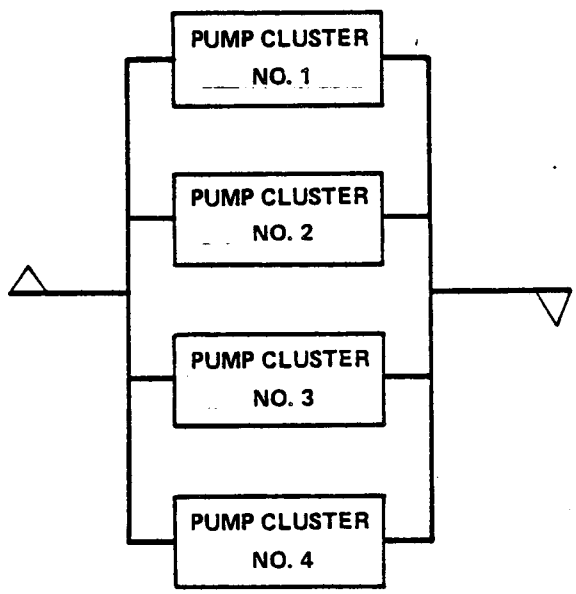

Reliability expression:

$$P_3 = R_1^4 + 4R_1^3Q$$

$$R_1 = \text{Reliability of Pump Cluster} = 1 - Q^3$$

$$Q = 1 - R = \text{Probability of Failure}$$

$$P_2 = e^{-\lambda t}$$

where

λ = Failure rate/hour/pump = .0004

t = Flight time = 6.1 hours

e = Exponential reliability function

$$P_3 = 5 \times 10^{-16}$$

8.5.2 Fuel venting regulation and control system. - Similar to the pumping/distribution system, the reliability logic employed in this system uses the conventional binomial expansion equation to evaluate the probability of success. The design concept employs redundant control valve logic and redundant vent valve logic. Within the control valve the design uses redundant control for pressure regulating with different regulator pressure settings. This concept provides the flight engineer the capability of monitor/indication of a faulty primary regulator. A manual override function to the pressure control valve is provided thus affording a third level of control for venting. The vent valves are single regulating valves, i.e., the auxiliary valve in a reliability diagram parallel to the primary vent valve. Probability of the loss of the venting system is illustrated and expressed numerically as follows:

P_4 = Probability of the loss of the Venting System during a 6.1 hour flight.

RELIABILITY SERIES/PARALLEL DIAGRAM FOR P_4

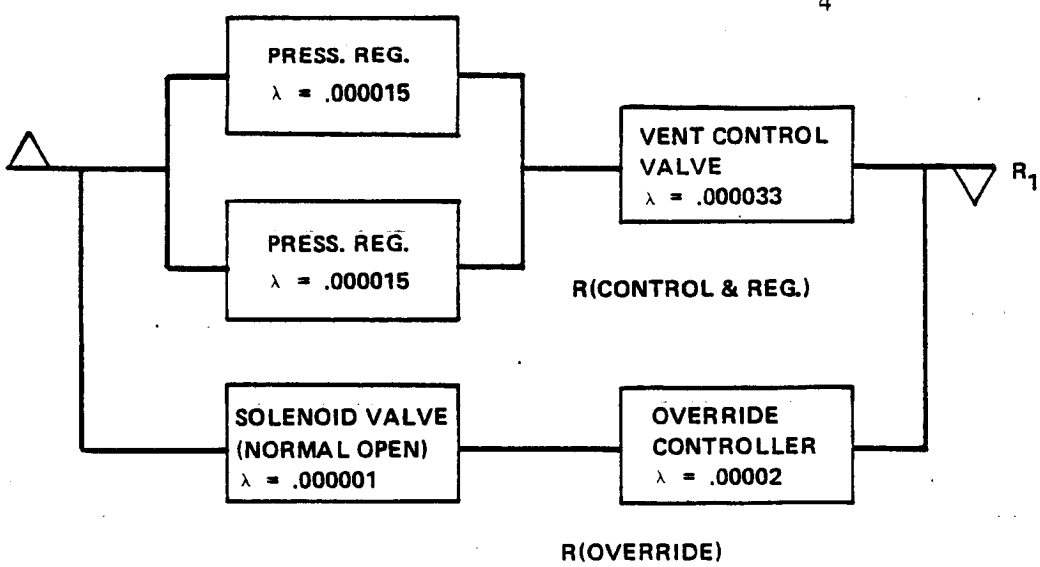

PRESSURE CONTROL AND VENT SYSTEM LOGIC

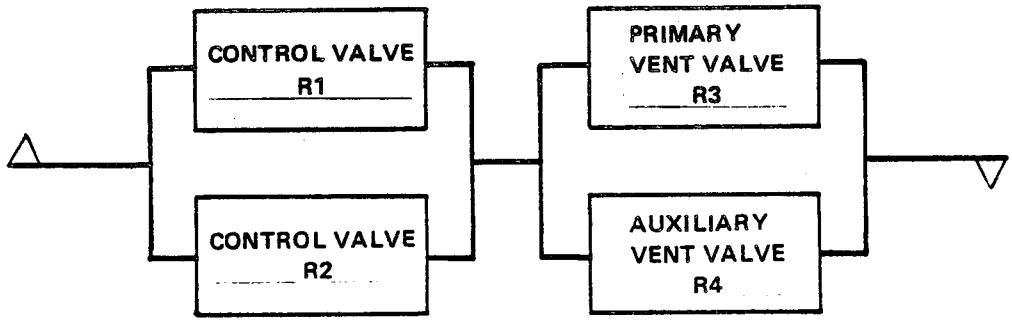

RELIABILITY EXPRESSION FOR TYPICAL CONTROL VALVE LOGIC.

$$R_1 = R_2$$

$$R_1 = 1 - \left(1 - R_{(\text{control \& reg.})}\right)\left(1 - R_{(\text{override})}\right)$$

$$R = e^{-\lambda t}$$

where

λ = Failure rate for the failure mode defined in table R1.

t = 6.1 hour flight

e = Exponential reliability function

$$R_1 = 1 - (.000033008 \times .000021)$$

$$R_1 = 1 - 6.9(10^{-10})$$

Since Q is 6.9×10^{-10} the probability of failure is well within the acceptable range

RELIABILITY EXPRESSION FOR PRESSURE CONTROL AND VENT SYSTEM LOGIC

$$P_4 = \left(6.9(10)^{-10}\right)^2 + \left(6.1(10)^{-5}\right)^2$$

$$P_4 = 3.6 \times 10^{-9}$$

It is concluded that the LH_2 fuel system arrangements as specified herein will meet operational requirements at least as rigorous as those of current transport aircraft. The only recommendation is that dispatch regulations require that not more than two pumps can be failed.

8.6 Safety and Fire Protection

The usual precautions taken to minimize fire and explosion hazards in hydrocarbon fueled systems, such as separation of combustibles from ignition sources, compartmentization, compartment draining and purging must also be observed in the LH_2 airplane. However, the characteristics of cryogenic hydrogen require unique precautions in all of these areas.

Because of the low spark energy required to ignite gaseous hydrogen, electrical and electrostatic discharge levels which are acceptable in hydrocarbon/air mixtures will have to be reevaluated for acceptability in the presence of hydrogen/air mixtures. On the other hand, the combustible limit of H_2 - Air (4 percent by volume) is considerably higher than that of gasoline-air (1 percent). These effects may require a redefinition of what constitutes an explosion proof component. In this regard, it is probable that flame arrestors, as now conceived, will not be effective for hydrogen/air mixtures.

8.6.1 Compartment purging. - Compartmentation, to localize and minimize the effects of fire as well as to separate sources of potential fuel leaks from areas containing potential ignition sources, will be used extensively. Each compartment can be drained and vented, or protected by fire detecting and extinguishing systems effectively. Because of the low density of gaseous hydrogen, each compartment in which hydrogen can be released must have vent outlets at the top of the compartment as well as at the bottom. Each compartment will incorporate ram scoops for inflight air purging. Those compartments having a high probability of hydrogen leaks under ground static conditions will incorporate an active venting system using fans for forced circulation when a leak is detected. Compartment drainage will be used where the hydrogen leak can be large enough for some of it to accumulate as a liquid. Hydrogen detectors (sniffers) will be placed at vent exits to detect and locate gaseous H_2 leakage. Leakage will be indicated in the flight station.

The extremely low temperature of the stored hydrogen can create an environmental hazard for personnel in and around the airplane. Hence, it is essential that all points of discharge for liquid or gaseous hydrogen be remote to areas normally occupied by people.

8.6.2 Nitrogen inerting. - Both of the preferred fuel containment systems, Nos. 3 and 4, use a N_2 purge system to prevent moisture accumulation and freezing in the flexible open cell foam insulation layer beneath the outer protective cover. This has the added advantage of inerting the space surrounding the fuel tanks in the event of H_2 leakage since the GN_2 purge gas is vented overboard. The system is functionally the same as that described in Section 6.8..

The volume requirements for N_2 are very small and the total system weight is estimated to be 210 lbs per aircraft, including the N_2 purge gas. Spaces surrounding the tank ends and lines for these systems will be purged as described above in 8.5.1.

8.6.3 Preparation for repair of insulation leaks. - Insulation leaks do not normally constitute a critical safety item. However, certain precautions must be observed when emptying the fuel system or tanks of liquid hydrogen in preparation for repair of the insulation. The effect of a hydrogen leak will almost always cause condensation and solidification of air by the process of cryopumping in the vicinity of the leak. As the liquid hydrogen is removed from the tank or line where the leak occurs, the system temperature will rise, warmed by the surrounding atmosphere. If this process is too rapid, the rate of air vaporization may be so high that large sections of insulation may be damaged, or even blown off, by the rapidly expanding air. Hence, the rate of heating should be controlled by monitoring the rate of removal of the hydrogen fuel.

8.7 Adjustments Required in FAR or Industry Standards

The use of hydrogen as a fuel for aircraft instead of a hydrocarbon fuel will affect many of the standards currently used in the industry. The standards most directly affected are the Federal Airworthiness Standards for Transport Category Airplanes (FAR Part 25), Airworthiness Standards for Aircraft Engines (FAR Part 33), and the National Fire Protection Association documents for Aircraft Fuel Servicing (NFPA No. 407) and Aircraft Fuel System Maintenance (NFPA No. 410C). In the following paragraphs, affected parts of the standards are listed, as well as the effects that must be considered when liquid hydrogen is used as a fuel.

FAR Part 25

25.801(d) - In ditching operations where structural damage can result in the removal of large sections of fuel tank insulation, a jettison system may be required to preclude excessive tank pressures being developed by the rapid vaporization of liquid hydrogen.

25.951 General

(a) ok

(b) and (c) - The effects on engine operation of the introduction of air or water in the fuel does not apply to a hydrogen fueled airplane because contaminants of this type cannot be tolerated in liquid hydrogen fuel tanks.

(b) Revise - "Each fuel system must be designed so as to prevent vapor being introduced to the engine pump, if such should momentarily occur, it shall not result in an engine flameout."

(c) Revise - "Each fuel system must be capable of sustained operation throughout the aircraft operating envelope - including air start - with the liquid fuel in an initially saturated state."

25.953 Fuel system independence - ok

25.954 Fuel system lightning protection - ok

25.955 Fuel flow

(a) ok

(b) ok

(c) Add - "No flameout or interruption of engine thrust shall occur when switching from one tank to another."

25.957 Flow between interconnected tanks - ok

25.959 Unusable fuel supply - ok

25.961 Fuel system hot weather operation.

(a) 1, 2, 3, 4 - ok

(a) 5 - Delete. For hydrogen fueled airplanes, the fuel system must perform satisfactorily with the tank ullage pressure equal to the vapor pressure of the fuel.

(b) Delete last sentence.

25.965(a) (1) and (2) Hydrogen fuel tanks are closed systems in which the pressure is a function of the liquid fuel temperature.

(c) For hydrogen tanks, the fuel temperature during the fuel tank test must be determined by the maximum vapor pressure to be encountered during actual operation.

25.967(b) For hydrogen tanks, spaces adjacent to the tank wall cannot be ventilated because the air would be liquified. Ventilation external to the tank insulation may be advisable but the insulation must be sealed to prevent introduction of air to areas adjacent to the tank wall.

25.969 Fuel tank expansion space

Revise as follows:

Each fuel tank must provide a positive expansion space beyond that required by consideration of the following:

(1) Contraction of the tank from the normal ambient to the cryogenic condition and expansion resulting from pressurization.

(2) Expansion of the fuel when warming from the as-loaded density to that corresponding to a saturated liquid at the tank design pressure

(3) Space occupied by structure, lines and equipment

It must be impossible to fill this total expansion space inadvertently with the airplane in a normal ground attitude.

25.971 Fuel tank sump - delete

25.973 Fuel tank filler connection - delete

25.975 Fuel tank vents and carburetor vapor vents

Revise as follows:

25.975 Fuel tank pressurization and venting

The fuel tank pressurization and venting system shall:

(a) Maintain tank pressures within the design values during all normal and emergency ground and flight conditions.

(b) Prevent overpressurization beyond the limit pressure in the event of any single or probable combination of failures during refueling, ground hold, and all flight conditions.

(c) Prevent air ingestion into the tank and vent lines.

(d) Avoid vent stoppage by dirt or ice formation.

(e) The vent(s) shall discharge in an area clear of the aircraft and potential ignition sources both on the ground and in flight.

25.977 Fuel tank outlet

(a) ok

(b) (c) (d) (e) - delete

25.979 Pressure fueling system

(a) Revise "Each pressure fueling (and vent) connection to ground equipment must have means to prevent the escape of hazardous quantities of liquid or vapor, both upon initial connection and disconnect.

(b) (1) (2), ok

(c) ok

(d) Add - "Means must be provided to prevent excessive pressure rise in the fueling manifold due to vaporization of trapped liquid."

25.981 Fuel tank temperature. Delete

25.991 Fuel pumps

(a) ok

(b) ok

25.993 Fuel system lines and fittings

A paragraph must be added to this section to indicate that no materials which would be adversely affected when exposed to liquid hydrogen can be in the fuel system.

(a) (b) (c) (d) (e) (f) - ok

Add (g) "All lines connected by a means of positive shutoff must be provided with a means of preventing excess pressures due to vaporization of the trapped liquid fuel"

25.994 Fuel system components - ok

25.997 Fuel strainer or filter - delete

25.999 Fuel system drains - delete

25.1001 Fuel jettisoning system - ok

25.1305 Fuel tank pressure indicators must be added at the flight station.

FAR Part 33

3.3.67(a) For a hydrogen fueled engine, operation with water in the fuel is not required.

NFPA

No. 407 Aircraft Fuel Servicing - A section must be added specifying methods of servicing a hydrogen fueled airplane.

No. 410C Aircraft Fuel System Maintenance - A section must be added specifying methods of maintaining a hydrogen fueled airplane.

9. EQUIVALENT JET A-FUELED AIRCRAFT

The characteristics of a conventionally fueled aircraft designed to perform the identical mission using equivalent technology and design requirements as the LH_2-fueled aircraft of Section 8 were developed in order to be able to compare the two on an equitable basis.

The first requirement was that the characteristics of a Jet A-fueled engine be developed which would have performance and weight based on the same technology as was used to represent the LH_2-fueled engine discussed in Section 4.3. It was then possible to parametrically generate an airplane design using the same guidelines and operational requirements as were used in the LH_2 aircraft design study.

The results of this work are reported in this section, together with a comparison of characteristics and performance of the two aircraft.

9.1 Jet A Engine Definition

The objective of this effort was to provide definition of a Jet A-fueled engine which would be directly comparable in technology to that of the LH_2-fueled design previously discussed. The hydrocarbon fueled engine which was used as a basis for the earlier, equivalent aircraft studies reported in Reference 1, could not be used because of changes made in assessment of component performance and efficiencies which could be available for initial operational capability in 1990-1995, which were incorporated into the LH_2 engine design.

Accordingly, a new design of Jet A engine was developed in which all characteristics matched those of the LH_2 engine developed by AiResearch - Arizona Division; see Section 4.3. Basic component efficiencies and performance were matched and the only changes made were due to differences in properties of the two fuels. The only modifications made to the AiResearch hydrogen fueled engine's thermodynamic cycle in order to develop the Jet A engine thermodynamic cycle were those due to the change in high pressure turbine cooling air temperature. In the hydrogen engine, the turbine cooling air is cooled by the fuel. Since this heat sink is not available for the Jet A engine, the turbine cooling airflow was increased from 3.5 percent to 7 percent. This increase maintains the same level of turbine cooling on both engines but decreases the high pressure turbine efficiency by 0.5 percent.

The aerothermodynamic changes that were required to make a hydrogen fueled engine into a Jet A fueled engine involved modification of the fuel lower heating value to 18 400 Btu/lb, compared to 51 590 Btu/lb for hydrogen, and modification of the thermodynamic properties of the combustion products from the combustor to the nozzle.

The thermodynamic cycle properties listed in Table 81 were used in the gas turbine synthesis computer program, (Reference 40), with the supplied combustion products subroutine for hydrocarbon fuel and air to calculate off-design performance of the Jet A engine. The resulting installed engine performance of the Jet A engine is given in Appendix G.

In order to have a valid comparison, the Jet A fueled engine was designed to be physically identical to the AiResearch hydrogen engine with the exception of the fuel system and the heat exchangers. Accordingly, both the physical dimensions and the weight of the Jet A engine are identical with those of the AiResearch hydrogen engine, except for allowances for the fuel system and the heat exchangers. The weight difference amounts to 210 lb for the baseline case. The same scaling relationships are valid for both engines.

TABLE 81. - THERMODYNAMIC DESIGN PARAMETERS

Inlet recovery	0.991
Fan efficiency	0.892
Fan pressure drop $\Delta P/P$	0.015
Compressor efficiency	0.862
Turbine cooling air	7.0%
Combustor efficiency	1.0
High pressure turbine efficiency	0.895
Low pressure turbine efficiency	0.900
Fan nozzle thrust coefficient	0.991
Core nozzle thrust coefficient	0.988
Horsepower extracted	125
Horsepower, accessories	21

9.2 Comparison: LH_2 vs Jet A Equivalent Aircraft

The design of a conventionally fueled transport sized to carry 400 passengers, 10 190 km (5 500 n.mi.) at a cruise speed of Mach 0.85 was accomplished using the ASSET computer program. The parametric optimization process was carried out in the same manner as previously described for the LH_2 aircraft.

The characteristics of the resulting Jet A-fueled airplane are listed in Table 82, along with corresponding data on the LH_2 counterpart. The LH_2 airplane data are a repeat of that listed previously in Table 76. They are shown here for convenience in comparing.

The Jet A-fueled design is identical in configuration to the Jet A aircraft reported in Reference 1 except that it is heavier and has a larger wing. The larger wing stems from the more conservative engine component performance postulated for the new engine designs (both LH_2 and Jet A) in the present study, which in turn leads to greater fuel weight because specific fuel consumption is increased. The result is that, although both the previous (Reference 1) and the present Jet A designs were found to be optimum with a wing loading of 125 lb/ft^2, the greater fuel weight required an increase of nearly 10 000 lb, in gross weight.

The LH_2 engine performance did not suffer such a decrease, relative to the Reference 1 work, because ways were found to exploit the heat capacity of hydrogen to compensate for the effects of the reduction in component efficiencies and performance.

Comparing the aircraft designs shown in Table 82, the LH_2 version is seen to offer quite significant advantages in nearly all parameters. The only parameter in which the Jet A airplane shows an advantage is L/D. This is because its fuselage is smaller in diameter [5.84 m (230 in.) vs 6.63 m (261 in.)] and also shorter [60.05 m (197 ft) vs 65.72 m (215.64 ft)] relative to the LH_2 aircraft. In addition, the Jet A design has a larger wing. The combination of the large wing with a smaller fuselage, compared with the small wing and a larger fuselage on the LH_2 design leads to the 11 percent advantage in L/D for the Jet A airplane.

However, this advantage is completely nullified by the almost 300 percent disadvantage the Jet A design suffers in cruise SFC. This leads to the tremendous difference in fuel weights between the two designs and accounts for the advantage the LH_2 aircraft enjoys in price, DOC, and energy utilization.

The direct operating costs shown in Table 82 were calculated on the basis of the respective fuel prices shown at the bottom of the table. Figure 165 shows the effect variation in fuel price would have on DOC for both aircraft. The baseline prices of \$4.74 per GJ (\$5/10^6 Btu) for Jet A and \$5.69 per GJ (\$6/10^6 Btu) for LH_2 were specified to represent reasonable costs assuming both fuels are manufactured from coal and water. As a point of reference, U.S. domestic air carriers today are paying an average of about 40¢/gal for Jet A produced from petroleum.

TABLE 82. - COMPARISON: LH_2 vs JET A SUBSONIC TRANSPORT AIRCRAFT

(400 Passengers; 10 190 km (5 500 m.mi.); Mach 0.85)

		LH_2	Jet A	Ratio $\left(\frac{\text{Jet A}}{LH_2}\right)$
Gross Wt	lb	377 800	532 420	1.41
Total Fuel Wt	lb	59 820	201 020	3.36
Block Fuel Wt	lb	50 710	172 720	3.41
Operating Empty Wt	lb	230 000	243 400	1.06
Aspect Ratio	-	9	9	
Wing Area	ft^2	3 242.9	4 259	1.31
Sweep	deg	30	30	
Span	ft	170.84	195.8	1.17
Fuselage Length	ft	215.64	197.0	0.91
L/D - Cruise	-	16.43	18.18	1.11
SFC - Cruise	$\frac{lb}{hr}/lb$	0.202	0.603	2.99
Initial Cruise Altitude	ft	37 000	37 000	
Wing Loading	lb/ft^2	116.5	125.0	1.07
Thrust/Weight	-	0.255	0.27	1.06
No. Engines		4	4	
Thrust Per Engine	lb	24 080	35 940	1.49
FAR T.O. Distance	ft	7 945	7 967	
FAR Ldg. Distance	ft	5 810	5 210	
2nd Seg Climb Grad. (Eng Out)		0.0571	0.0695	
Approach Speed	KEAS	135	124	
Weight Fractions	percent			
Fuel		15.83	37.75	
Payload		23.29	16.53	
Structure		33.03	26.71	
Propulsion (Includes Tanks & Fuel Sys)		9.73	6.09	
Price	$\$10^6$	38.09	40.94	1.07
DOC[a]	$\frac{¢}{\text{seat n.mi.}}$	1.599	1.699	1.07
Energy Utilization	$\frac{\text{Btu}}{\text{seat n.mi.}}$	1 189	1 445	1.22

(a) DOC based on LH_2 cost = \$5.69 per GJ (\$6/10^6 Btu = 31¢/lb)
Jet A cost = \$4.74 per GJ (5/10^6 Btu = 62.2¢/gal)

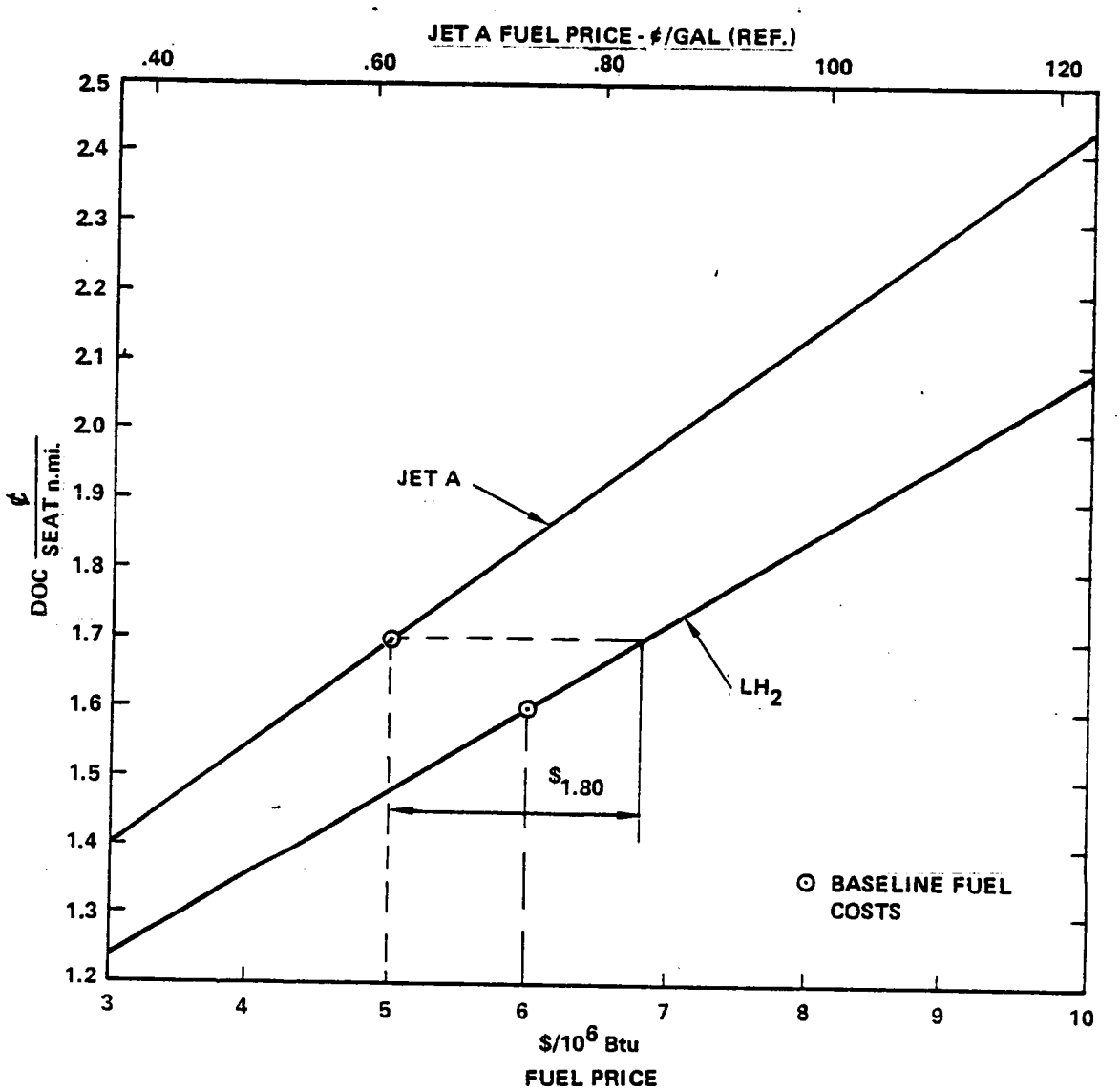

Figure 165. - Sensitivity of DOC to fuel price for both LH_2 and Jet A aircraft.

The direct operating costs calculated for the LH_2 airplane include consideration of the increment due to fuel losses from all ground boiloff.

Two things are significant to note regarding Figure 165. One is the spread of \$1.80 per 10^6 Btu measured from the baseline price of Jet A to a value which can be paid for LH_2 and still provide the operator with equal DOC. The other is the divergence of the two lines, indicating that as fuel prices continue to climb, the advantage for LH_2 will steadily increase.

10. TECHNOLOGY DEVELOPMENT

Throughout this report, at the end of most major sections, research and technology development items pertinent to the subject are listed. Each of these items is considered significant and necessary for the ultimate development of LH_2-fueled aircraft. In this section a development program is presented which is the result of consideration and evaluation of these individual items. The items are listed in order of perceived priority, 1 through 5, to indicate recommended scheduling. The priority rating is not intended to designate relative signficance or importance.

10.1 First Priority

Item 1) Large Model Tank Fabrication and Test. - Design, fabricate, and test a sizeable model of an aircraft tank, large enough that minimum gage considerations will not seriously distort the heat transfer properties of the structural attachments and the insulation system. A half scale (approximately 10 ft dia) model of either of the subject aircraft tanks is suggested to provide valid experimental data at a reasonable program cost.

Such a tank would serve a number of useful functions:

A. Focus design attention on detail problems which tend to be overlooked or glossed-over in conceptual studies, e.g.,

- specific fabrication methods
- attachment of appendages
- structural support provisions
- inspection and repair provisions.

B. Provide experience in fabricating, maintaining, and operating a sizeable flightweight tank insulated to meet aircraft requirements.

C. Permit experimental determination of the heat transfer mechanism in a large, horizontally inclined, insulated tank containing LH_2. Nusselt Number, tank wall temperatures, vapor volume temperatures, and the temperature and quantity of the GH_2 vented from the tank can all be determined as functions of the following conditions within the tanks, and for various liquid levels:

- stratified (liquid and vapor)
- turbulent (liquid and/or vapor)
- simulated aircraft motions.

D. Investigate aircraft tank filling procedures. Experimentally determine the preferred design of plumbing system and operational procedure which will permit refueling of aircraft tanks within specified time limits.

E. Test various quantity sensor devices to determine which provides most reliable data for an aircraft tank application. Conduct tests with tank in motion to simulate aircraft ride quality with resultant agitation of liquid surface.

F. In conjunction with Items 4 and 7 (following), conduct flow tests of a representation of an engine fuel supply and control system to determine:

- system chill-down time
- transient response characteristics
- delivery conditions of the LH_2 at the engine-end of the feed system
- other characteristics as described under Items 4 and 7.

These flow tests could be performed with the entire feed system functioning except that the output from the engine-mounted pump would be valved to simulate engine consumption vs throttle setting. Flow delivery from the feed system could be captured in a ground storage tank for return and reuse in the experimental equipment.

Item 2.) Pump Development. - Design and development of LH_2 pumps for the aircraft application is recognized as a major requirement. The following characteristics must be provided by both the boost pumps and the high pressure, engine-mounted pumps:

- Long life
- Reliable
- Maintainable
- Efficient over a wide range of flow rates and pressures
- Qualify as line replaceable units.

The proposed effort would include design, fabrication, and experimental development to achieve these objectives.

An initial step would be preliminary design of pumps for both applications in sufficient depth to establish the bearing requirements. Design, fabrication, and feasibility testing of bearing systems would then be carried

out to demonstrate that these requirements can be met. The bearing feasibility tests would be conducted in a bearing test rig. It is necessary that both the boost pump and the high pressure engine pump be designed, built, and tested because of the difference in their design requirements and their potential bearing designs.

Item 3.) Systems Analysis of Ways to Initiate LH_2 Fuel Service in Airline Operations. - Analyze airline route structures, traffic densities, and aircraft usage throughout the United States as projected for the 1990-2000 time period. In addition, include consideration of connecting international routes, with special attention to routes to those countries most likely to require early relief from use of hydrocarbon fuel.

Objectives:

A. Determine feasible ways to initiate use of LH_2 fuel in commercial transport aircraft, for example,

- by airline
- by city-pair, e.g., L.A to Washington
- by region, e.g., West Coast

B. Project the fuel changeover from U.S. domestic airlines to international carriers.

C. Establish a feasible schedule for installation of LH_2 facilities at airports and determine costs and fuel requirements vs years.

D. Define principal problems, costs, and possible methods of funding.

E. Justify early use of hydrogen for air transportation industry, rather than other possible candidates, e.g., utilities, industry, etc.

10.2 Second Priority

Item 4.) Engine Fuel Supply System Experiments. - Design, fabricate, and test a complete engine fuel supply system including boost pumps, valves, and line. Duplicate a feed line to an outboard engine with equivalent turns, joints, and length to represent the aircraft installation. Mount on tank (Item No. 1) per aircraft installation. Experimentally determine:

- operational characteristics
  - chill-down time
  - flow response transients
  - temperature rise vs flow rate

- vent requirements vs time after simulated engine shutdown
- requirements to maintain insulation properties
- structural support requirments.

Two types of fuel lines are viable candidates. One uses a vacuum annulus between concentric tubes to provide the insulation. The other also uses concentric tubes but has closed cell foam in the annulus. Experimental work is required on both types of designs to determine a preference on the basis of

- fabricability
- maintenance
- operational characteristics
- susceptibility to mechanical damage.

Item 5.) Advanced Engine Design Study. - The engine conceptual design study conducted in the present program was a very abbreviated effort. It was not intended to be an investigation which would provide final answers to all questions about LH_2 engine design. Rather, it served as a guide, primarily in determining the potential of several possible ways to use the heat capacity of hydrogen to good advantage. Accordingly, it is proposed that a comprehensive design study be made which would involve investigation of more of the design potential of LH_2-fueled turbofan engines on both a broader and a more in-depth basis. The objectives would be as follows:

- Establish design and performance characteristics of an advanced design, quiet, cleanburning LH_2-fueled engine to match requirements of a selected airplane design. Provide size, weight, cycle characteristics, performance, and cost estimates.
- Establish requirements for major components, e.g., high pressure pump, heat exchangers, combustor design, noise suppression devices, engine control system, compressor, fan, turbines, and cooling system.
- Provide input for Item 8.

Item 6.) Aircraft Vent System Design and Test. - The vent which must be provided on an aircraft fueled with LH_2 presents problems which are unique.

- The vent must be capable of releasing cryogenic gaseous hydrogen at any time the pressure in the aircraft fuel tanks exceeds a set upper limit. The release can be into cold moist air which can cause the vent valve to freeze when venting stops. Methods must be devised to avoid the consequences of this happening.

- The vented gas can catch fire. Surrounding aircraft structure must be protected so as to be invulnerable to this occurrence.

- The vent must be provided with the capability of preventing external flame from propagating upstream into the vent system tubes leading to the fuel tanks. Conventional flame suppressors used on hydrocarbon fueled aircraft will not be effective with hydrogen vapor fires because the very high flame speed and short quenching distance of hydrogen appears to make the system mechanically infeasible.

- The vent exit must be protected from the effects of lightning strikes.

The proposed technology development would involve design and fabrication of a vent system mounted in representative aircraft structures, and tests conducted under typical exposure conditions.

10.3 Third Priority

Item 7.) Engine Fuel Control System Testing. - This item is contingent upon Items 1, 2, 4, and 8A, having been successfully completed and the hardware being available for additional flow testing with LH_2. The objective would be to determine transient response characteristics of the entire fuel supply system (to one engine) including the control network. The program would consist of both an analytical and an experimental effort. An analysis and an analog simulation of the engine fuel delivery and control system would be made to determine performance capability, including the effect of transients. The experimental effort would involve fabrication of a representative system and testing to simulate the following operations and verify the analysis:

- start

- shutdown

- control representing flow variation to satisfy design flight conditions.

Use of the 270 Vdc system to control boost pump output with brushless dc motor drives, a high temperature sensor in the engine, and microelectronics in an advanced design of fuel control system will make this development item particularly desirable because of the great flexibility offered by the system.

Item 8.) Engine Technology Development. - The results from the advanced engine design study, Item No. 5, will provide the basis for this task. It involves design, fabrication and test of components of an advanced design of LH_2-fueled engine, including:

- Heat exchanger
- Combustor
- Cooled turbine vanes and blades

The objective is to develop component technology required to build a liquid hydrogen fueled engine incorporating features to capitalize on advantages available with the fuel.

Task 8A) Heat Exchanger Development

Design and develop heat exchangers as required by the engine concept, e.g., to cool engine oil, compressor bleed air for cabin air conditioning and turbine cooling, and to heat the fuel with the core engine exhaust. Experimental testing is required to demonstrate:

- anti-icing protection
- heat exchanger effectiveness
- transient fuel flow response characteristics
- compliance with design requirements

Task 8B) Combustor Experiments

Very little experimental development work has been performed on combustors for aircraft gas turbines where the components were designed to use hydrogen as the fuel. Work performed at NASA-Lewis starting in the late 1950's used fuel injectors and combustor cans taken from existing hydrocarbon fueled engines, modified only as required. The work proposed here involves design of injection systems and combustor configurations specifically for hydrogen fuel, and experimental determination of the temperature profile and NO_x concentrations as functions of various design parameters. The objectives would be to determine:

- a preferred geometry and design of injectors and combustor for hydrogen/air
- the practical limits of NO_x generation at the design combustion temperature
- the variation of NO_x as a function of design combustion temperature
- temperature profile characteristics as a function of injector design and combustor configuration.

Task 8C) Cooled Turbine Vanes and Blades

The present study showed the desirability of cooling the turbine cooling air to reduce the bleed air requirement and to gain HP turbine efficiency. An existing engine could be used as a test article to develop a satisfactory design of HP turbine stage utilizing refrigerated air as a coolant. The testing could be done in conjunction with the appropriate heat exchanger developed in Task (A). Experiments would show:

- the effectiveness of blade and vane cooling as a function of air quantity and temperature for various designs.
- the effect of cooling air flow rate on turbine efficiency.

Item 9.) Materials Development. -

Activity:

Conduct literature searches, obtain manufacturer's data, and perform laboratory experiments.

Objectives:

A. Determine materials preferred for use as

- Cryogenic insulation for fuel tank
- Impermeable barrier to either GH_2 or air
- Tank bladder/structural material
- Structural connection between cryogenic tank and ambient temperature aircraft structure
- Cryogenic fuel line/bellows/support structure
- Sealing surfaces for valves

B. Begin determination of effects of long-term exposure to hydrogen of selected structural and component materials.

Item 10.) Hazard Studies and Tests. - Use of LH_2 poses different problems related to safety, compared to conventional aircraft procedures and requirements. The following tasks are suggested to explore those differences and to develop appropriate preventive and combative measures for the hazards which exist with LH_2. This item is considered especially important because of the widespread misapprehension which exists regarding safety of hydrogen. It is felt that studies and demonstrations such as are proposed will provide a basis for dispelling and quieting these fears which are largely based on lack of knowledge.

Task 10A.) Study of Relative Hazards of LH_2 vs Jet A Fuel in Commercial Aircraft

Activity:

Study representative designs of a selected size of commercial transport aircraft; one fueled with LH_2, the other with conventional Jet A. Analyze the designs for probable failure modes, both in-flight and on the ground. Where appropriate, supplement the study with analysis of accident reports.

Objectives:

A. By analysis of probabilities of various kinds of accidents, both in-flight and on the ground, estimate probable failure modes and results which can be expected with both fuel systems.

B. Provide input for Item 10C.

Task 10B.) Hazard Posed by Fire: LH_2 vs Jet A Fuel

Activity:

Expose instrumented fuselage sections of surplus transport aircraft to fire from equal-energy quantities of LH_2 and Jet A fuel.

Objective:

Determine effect of fire from burning fuel adjacent to passenger compartment and compare relative hazards to crew and passengers.

Task 10C.) Safety in Nonfatal Crashes

Activity:

Simulate nonfatal crashes with surplus aircraft components containing residual fuel in typical tank structures. Perform duplicate tests with surplus aircraft having fuel tanks designed for LH_2 and for Jet A.

Objective:

Determine effect of simulated crash using each fuel system and compare relative hazard to crew and passengers.

10.4 Fourth Priority

Item 11.) Aircraft Fuel System Test. - Before an LH_2-fueled aircraft is committed to flight test a replica or model of its fuel system should be tested on the ground. With equipment from all the foregoing tests, the major

portion of the aircraft fuel system will be available for this purpose. Equipment from Items 1, 4, 6, 7, and 8, respectively, will provide the following:

- A half scale model of one tank of the fuel containment system with vapor return and fueling adapters
- Engine fuel supply system
- Aircraft vent system
- Engine fuel control system
- Heat exchangers

This will leave just the following items to be obtained in order to conduct meaningful tests of a replica of a complete aircraft fuel system:

- Parts of the fueling/defuel system
- Parts of the vent and pressurization system
- Leak detection system.

With the entire aircraft fuel system assembled, tests could be conducted which would permit accomplishing the following objectives:

- Determine operational characteristics of an integrated design of an aircraft fuel system.
- Provide a basis for writing design specifications for LH_2 fuel systems and components suitable for aircraft service.
- Determine procedures for performing inspection and repair of LH_2 system components.
- Determine effect of repeated flight cycles and fueling/defueling cycles on tank structure, insulation system, and fuel feed system.

10.5 Fifth Priority

Item 12.) Flight Demonstration Program. - Following the ground tests of the LH_2 fuel system, the next logical step would be a flight demonstration program. This would involve building a complete fuel system for an existing airplane and flying the airplane using the LH_2 fuel system in a routine, operational manner for a significant length of time, e.g., a year or more.

Selection of the airplane should be given very careful consideration. The aircraft needs to be big enough to contain at least one LH_2 tank in the fuselage, with sufficient volume to provide for a range of at least km (2500 nmi). This would permit the converted aircraft to be used operationally during the test period, thus imposing a need to meet schedules and offering a chance to show whether the LH_2 fuel system can be competitive in terms of maintenance, reliability, and operational requirements. On the other hand, the selected aircraft should not be too big because of cost aspects.

The objectives of a flight demonstration program would be:

- Learn how to handle LH_2 as an aircraft fuel in an operational manner.
- Determine the practicability of the cryogenic fuel system in terms of inspection, maintenance, durability, and performance.
- Provide a basis for writing design and operational specifications for hydrogen-related equipment and procedures.
- Establish confidence that hydrogen can be used safety in airline-type operations.

REFERENCES

1. Brewer, G. D.; Morris, R. E.; Lange, R. H.; and Moore, J. W.: Study of the Application of Hydrogen Fuel to Long-Range Subsonic Transport Aircraft. NASA CR-132559, prepared by Lockheed-California Company and Lockheed-Georgia Company under Contract NAS1-12972, January 1975.

2. Brewer, G. D.: LH_2 Airport Requirements Study. NASA CR-2700, prepared by Lockheed-California Company under Contract NAS1-14137, March 1976.

3. Anon: An Exploratory Study to Determine the Integrated Technological Air Transportation System Ground Requirements of Liquid-Hydrogen-Fueled Subsonic, Long-Haul Civil Air Transports. NASA CR-2699, prepared by The Boeing Commercial Airplane Company under Contract NAS1-14159, May 1976.

4. Anon: Survey Study of the Efficiency and Economics of Hydrogen Liquefaction. NASA CR-132621, prepared by Linde Division of Union Carbide Corp. under Contract NAS1-13395, April 8, 1975.

5. Biermann, A. E.; and Kohl, R. C.: Preliminary Study of a Piston Pump for Cryogenic Fluids, NASA Memorandum 3-6-59E, March 1959.

6. Biermann, A. E.; and Shinko, W. G.: Performance of a Piston Type Pump for Liquid Hydrogen, NASA Technical Note D-276, March 1960.

7. Goldsmith, J. S. and Bennett, G. W.: Hydrogen-Methane Fuel Control Systems for Turbojet Engines, General Electric Co., NASA-CR-121247.

8. Schalla, C. A.: Hydrogen Liquid Level Influence on Aircraft Tank Insulation. Advances in Cryogenic Engineering, Vol 12, Plenum Press, New York (1967) pp 255-264.

9. Keller, C. W.: Handbook of Physical and Thermal Property Data for Hydrogen. LMSC K-11-67-1, Contract NAS 8-20342, Lockheed Missiles and Space Company, Inc. (June 1967).

10. Parmley, R. T.: Handbook of Thermal Design Data for Multilayer Insulation Systems. LMSC A847882, Vol II, Contract NAS8-20353, Lockheed Missiles and Space Company, Inc. (June 1967).

11. Childs, G. E.; et al: Thermal Conductivity of Solids at Room Temperature and Below. NBS Monograph 131, National Bureau of Standards, U.S. Department of Commerce (Sept 1973).

12. Johnson, V. J., ed.: A Compendium of the Properties of Materials at Low Temperature. WADD Technical Report 60-56 Part II, Wright Air Development Division, Wright-Patterson Air Force Base (Oct 1960).

13. Barker, H. H.; et al: Internal Insulation Systems for LH_2 Tanks - Gas Layer and Reinforced Foam. Proceedings Space Transportation System Propulsion Technology Conference, Vol IV, NASA George C. Marshall Space Flight Center (April 1971) pp 1455-1480.

14. Yates, G. B.; and Tatro, R. E.: PPO Foam Internal Insulation. Proceedings Space Transportation System Propulsion Technology Conference, Vol IV, NASA George C. Marshall Space Flight Center (April 1971) pp 1439-1452.

15. Barber, J. R.: Cryogenic Insulation Technology Review for the Space Shuttle. NASA TMX-52876, Vol V (July 1974) pp 146-166.

16. Cunnington, G. R.; and Tien, C. L.: Advances in Cryogenic Engineering Vol 22, Plenum Press, New York (1975) pp 263-

17. ---: Development and Design Application of Rigidized Surface Insulation Thermal Protection Systems. LMSC D282673, Vol I, Contract NAS9-12856, Lockheed Missiles and Space Company, Inc. (Dec 1972).

18. Lindquist, C. R.; and Nies, G. E.: Lightweight Multilayer Insulation System. NASA CR-72363, Final Report Contract NAS3-7953, Union Carbide Corporation.

19. Burkley, R. A.; et al: Development of Materials and Materials Application Concepts for Joint Use for Cryogenic Insulations and Micrometeroid Bumpers. Annual Summary Report GER 11676S/24, Contract NAS8-11747, Goodyear Aerospace Corporation (June 1967).

20. Ruccia, F. E.: Final report for Contract NAS1-14157 (data taken from Progress Reports 13 and 14, Jan 1976).

21. Tye, R. P.: Measurements of Heat Transmission in Thermal Insulations at Cryogenic Temperatures Using a Guarded Hot Plate Method. Proceedings XIIIth International Congress of Refrigeration, Vol 1, Washington DC (1971) pp 371-378.

22. --- Hexcell TSB 120, "Mechanical Properties of Hexcell Honeycomb Materials" (Jan 1966).

23. Elam, B. F.: Heat Transfer in Honeycomb-Core Sandwich Panels. Paper 65-HT-13, AIChE-ASME Heat Transfer Conference (Aug 1965).

24. Dunkle; et al: The Thermal Conductivity of Aluminum Honeycomb Material Near Room Temperature. Paper ASME 58-SA-1, ASME Semiannual Meeting, Detroit, Michigan (June 1958).

25. ---: ICAO Standard Atmosphere, NACA TN-3182

26. Harper, E. Y.; et al: Analytical and Experimental Study of Stratification and Liquid-Ullage Coupling. LMSC 2-05-65-1, Contract NAS8-11525, Lockheed Missiles and Space Company, Inc. (Aug 1965).

27. Louthan, M. R.; Caskey, G. R.: Hydrogen Transport and Embrittlement in Structural Metals, 1st World Hydrogen Energy Conference, Miami Beach, Florida, Paper DP-MS-75-54X, Volume 1, March 1976.

28. Gray, H. R.; Nelson, H. G.; Johnson, R. E.; McPherson, W. B.; Howard, F. S.: and Swisher, J. H.: Potential Structural Material Problems in a Hydrogen Energy System, 1st World, Hydrogen Energy Conference, Miami Beach, Florida, Volume 1, March 1976.

29. Bushnell, David: Stress, Stability, and Vibration of Complex Branched Shells of Revolutions, User's Manual for BOSOR 4; Lockheed Missiles and Space Co., LMSC-D457038, May 1975.

30. Almroth, R. O.; Brogan, F. A.; and Stanley, G. M.: Structural Analyses of General Shells, Volume III, User's Instructions for STAGS; Lockheed Missiles and Space Co., LMSC-D502227, December 1975.

31. Plank, P. P.; Sakata, I. F.; Davis G. W.; and Richie, C. C.: Substantiation Data for Hypersonic Cruise Vehicle Structure Evaluation. NASA CR-66897-3, 1970.

32. Flood, M. M.; Leon, A.: A Universal Adaptive Code for Optimization (GROPE); IWP No. 1-9 Space Science Laboratory, University of California, Berkeley, 1964.

33. Shanely, F. R.: Weight-Strength Analysis of Aircraft Structures, Second Edition, Dover Publications, Inc., New York, N.Y., 1960.

34. Ekvall, J. C.; Brussat, T. R.; Liu, A. F.; and Creager, M.: Engineering Criteria and Analysis Methodology for the Appraisal of Potential Fracture Resistant Primary Aircraft Structure, AFFDL-TR-72-80, Sept. 1972.

35. Anon, "Standard Method of Estimating Comparative Direct Operating Costs of Turbine Powered Transport Airplanes," Air Transport Association of America, December 1967.

36. R. E. Neitzel, R. Hirskron, and R. P. Johnston," Study of Turbofan Engine Designed for Low Energy Consumption," NASA CR-135053, Aug 1976.

37. D. E. Gray, "Study of Turbofan Engines Designed for Low Energy Consumption," NASA CR-135002, April 1976.

38. D. E. Gray, "Study of Unconventional Aircraft Engines Designed for Low Energy Consumption," NASA CR-135065, June 1976.

39. Lange, R. H., et al.; "Study of the Application of Advanced Technologies to Long-Range Transport Aircraft," NASA CR-112088, prepared by the Lockheed-Georgia Company under Contract No. NAS1-10701, May 1972, CONFIDENTIAL.

40. D. W. Hutchinson, "Syntha II-GT, The Gas Turbine Performance Computer Program," The Syntha Corporation.

41. Tsaros, C. L., Arora, J. L., and Burnham, K. B., "A Study of the Conversion of Coal to Hydrogen, Methane, and Liquid Fuels for Aircraft," Technology, NASA CR-145028, June 1976.

APPENDIX A

PRELIMINARY MISSION FUEL FLOW SCHEDULE

For use during the early stages of the study it was necessary to establish a representative fuel flow schedule for the design mission. The following data were derived using the ASSET computer program and the characteristics of the 400 passenger, 5 500 n. mi. range, M 0.85 LH_2-fueled aircraft from Reference 1. These data served as a basis for initial sizing of pumps, lines, valves, etc., until the characteristics of the LH_2 engine discussed in Section 4, herein, were determined and the aircraft resized, Section 8.

TABLE A-1. - DESIGN MISSION FUEL FLOW SCHEDULE

(LH_2, M 0.85, 400 PAX, 5 500 n.mi.)

CL 1317-1
ASSET RUN DATED 9-14-76

Segment	Initial Altitude (ft)	Initial Mach	Incremental			Segment			Total		
			Fuel (lb)	Time (min)	Avg $\dot{w}$ (lb/hr)	Fuel (lb)	Time (min)	Avg. SFC $\left(\frac{lb}{hr}/lb\right)$	Fuel (lb)	Time (min)	Distance (n.mi.)
Taxi	0	0	-	-	669	156	14.0	0.117	156	14.0	0
Takeoff	0	0	-	-	10 800	180	1.0	0.094	336	15.0	0
Climb	0	0.378	-	-	10 011	584	3.5	0.152	920	18.5	16
	1,000	0.385	57	0.31	11 032						
	2 000	0.392	58	0.32	10 875						
	3 000	0.399	57	0.32	10 688						
	4 000	0.407	58	0.33	10 545						
	5 000	0.414	57	0.34	10 059						
	6 000	0.422	58	0.35	9 943						
	7 000	0.430	59	0.35	10 114						
	8 000	0.438	59	0.37	9 566						
	9 000	0.447	60	0.39	9 231						
	10 000	0.456	61	0.40	9 150						
Accelerate	10 000	0.456	-	-	9 000	210	1.4	0.173	1,130	19.8	24
	10 000	0.476	18	0.12	9 000						
	10 000	0.496	20	0.13	9 120						
	10 000	0.516	20	0.13	9 158						

TABLE A-1. - DESIGN MISSION FUEL FLOW SCHEDULE (Continued)

(LH_2, M 0.85, 400 PAX, 5 500 n.mi.)

CL 1317-1
ASSET RUN DATED 9-14-76

Segment	Initial Altitude (ft)	Initial Mach	Incremental			Segment			Total		
			Fuel (lb)	Time (min)	Avg $\dot{w}$ (lb/hr)	Fuel (lb)	Time (min)	Avg. SFC $\left(\frac{lb}{hr}/lb\right)$	Fuel (lb)	(min)	Distance (n.mi.)
Accelerate (Cont'd)	10 000	0.536	21	0.14	9 115						
	10 000	0.556	22	0.14	9 182						
	10 000	0.576	24	0.15	9 259						
	10 000	0.596	25	0.16	9 278						
	10 000	0.616	28	0.18	9 287						
	10 000	0.636	29	0.18	9 338						
	10 000	0.638	3	0.02	9 333						
Climb	10 000	0.638	-	-	6 441	4 788	44.6	0.200	5 918	64.5	388
	11 000	0.651	85	0.54	9 444						
	12 000	0.663	87	0.56	9 321						
	13 000	0.677	91	0.60	9 100						
	14 000	0.690	94	0.63	8 952						
	15 000	0.705	100	0.68	8 824						
	16 000	0.719	104	0.72	8 667						
	17 000	0.734	107	0.76	8 447						
	18 000	0.749	112	0.81	8 296						
	19 000	0.764	120	0.89	8 090						

TABLE A-1. - DESIGN MISSION FUEL FLOW SCHEDULE (Continued)

(LH_2, M 0.85, 400 PAX, 5 500 n.mi.)

CL 1317-1
ASSET RUN DATED 9-14-76

Segment	Initial Altitude (ft)	Initial Mach	Incremental			Segment			Total		
			Fuel (lb)	Time (min)	Avg $\dot{w}$ (lb/hr)	Fuel (lb)	Time (min)	Avg. SFC $\left(\frac{lb}{hr}/lb\right)$	Fuel (lb)	Time (min)	Distance (n.mi.)
Climb (Cont'd.)	20 000	0.780	126	0.95	7 958						
	21 000	0.797	138	1.06	7 811						
	22 000	0.814	152	1.19	7 664						
	23 000	0.832	179	1.43	7 510						
	24 000	0.849	228	1.86	7 355						
	25 000	0.850	184	1.54	7 169						
	26 000	0.850	184	1.58	6 987						
	27 000	0.850	186	1.65	6 764						
	28 000	0.850	191	1.74	6 586						
	29 000	0.850	196	1.85	6 357						
	30 000	0.850	203	1.97	6 183						
	31 000	0.850	220	2.21	5 973						
	32 000	0.850	251	2.62	5 748						
	33 000	0.850	306	3.34	5 497						
	34 000	0.850	417	4.75	5 267						
	35 000	0.850	727	8.70	5 014						

TABLE A-1. - DESIGN MISSION FUEL FLOW SCHEDULE (Continued)

(LH_2, M 0.85, 400 PAX, 5 500 n.mi.)

CL 1317-1
ASSET RUN DATED 9-14-76

Segment	Initial Altitude (ft)	Initial Mach	Incremental			Segment			Total		
			Fuel (lb)	Time (min)	Avg $\dot{w}$ (lb/hr)	Fuel (lb)	Time (min)	Avg. SFC $\left(\frac{lb}{hr}/lb\right)$	Fuel (lb)	Time (min)	Distance (n.mi.)
Cruise	35 000 to 38,000	0.850	-	-	4 492	46 145	616.4	0.199	52 063	680.8	5 398
Descent	35 000	0.850	-	-	1 310	155	7.1	-1.654	52 218	687.9	5 454
	34 000	0.850	3	0.26	692						
	33 000	0.850	4	0.26	923						
	32 000	0.850	4	0.25	960						
	31 000	0.850	3	0.24	750						
	30 000	0.850	4	0.23	1 043						
	29 000	0.850	3	0.23	783						
	28 000	0.850	4	0.22	1 091						
	27 000	0.850	4	0.21	1 143						
	26 000	0.850	3	0.21	857						
	25 000	0.850	4	0.20	1 200						
	24 000	0.849	4	0.19	1 263						
	23 000	0.832	6	0.30	1 200						
	22 000	0.814	6	0.31	1 161						
	21 000	0 797	7	0.31	1 355						

TABLE A-1. - DESIGN MISSION FUEL FLOW SCHEDULE (Continued)

(LH_2, M 0.85, 400 PAX, 5 500 n.mi.)

CL 1317-1
ASSET RUN DATED 9-14-76

Segment	Initial Altitude (ft)	Initial Mach	Incremental			Segment			Total		
			Fuel (lb)	Time (min)	Avg $\dot{w}$ (lb/hr)	Fuel (lb)	Time (min)	Avg. SFC $\left(\frac{lb}{hr}/lb\right)$	Fuel (lb)	Time (min)	Distance (n.mi.)
Descent (Cont'd.)	20 000	0.780	7	0.32	1 312						
	19 000	0.764	7	0.32	1 312						
	18 000	0.749	8	0.33	1 455						
	17 000	0.734	8	0.32	1 500						
	16 000	0.719	8	0.33	1 455						
	15 000	0.705	9	0.34	1 588						
	14 000	0.677	9	0.34	1 588						
	13 000	0.677	9	0.34	1 588						
	12 000	0.663	10	0.35	1 714						
	11 000	0.651	10	0.36	1 667						
	10 000	0.638	11	0.36	1 833						
Decelerate	10 000	0.638	-	-	1 763	47	1.6	-	52 265	689.5	5 463
	10 000	0.618	4	0.14	1 714						
	10 000	0.598	5	0.14	2 143						
	10 000	0.578	4	0.16	1 500						
	10 000	0.558	5	0.16	1 875						
	10 000	0.538	5	0.17	1 765						

TABLE A-1. - DESIGN MISSION FUEL FLOW SCHEDULE (Continued)

(LH_2, M 0.85, 400 PAX, 5 500 n.mi.)

CL 1317-1
ASSET RUN DATED 9-14-76

Segment	Initial Altitude (ft)	Initial Mach	Incremental			Segment			Total		
			Fuel (lb)	Time (min)	Avg $\dot{w}$ (lb/hr)	Fuel (lb)	Time (min)	Avg. SFC $\left(\frac{lb}{hr}/lb\right)$	Fuel (lb)	Time (min)	Distance (n.mi.)
Decelerate (Cont'd.)	10 000	0.518	6	0.19	1 895						
	10 000	0.498	6	0.19	1 895						
	10 000	0.478	5	0.20	1 500						
	10 000	0.458	7	0.21	2 000						
	10 000	0.456	0	0.02	-						
Descent	10 000	0.456	-	-	2 111	292	8.3	-	52 557	698.8	5 500
	9 000	0.447	22	0.75	1 760						
	8 000	0.438	24	0.76	1 895						
	7 000	0.430	24	0.78	1 846						
	6 000	0.422	27	0.80	2 025						
	5 000	0.414	28	0.82	2 049						
	4 000	0.407	29	0.84	2 071						
	3 000	0.399	32	0.86	2 233						
	2 000	0.392	33	0.89	2 225						
	1 000	0.385	35	0.91	2 308						
	0	0.378	38	0.93	2 452						
Loiter	1 500	0.286	-	-	2 920	292	6	-	52 849	703.9	5 500

TABLE A-1. - DESIGN MISSION FUEL FLOW SCHEDULE (Continued)

RESERVE FUEL FLOW SCHEDULE (LH_2, M 0.85, 400 PAX, 5 500 n.mi.)

CL 1317-1
ASSET RUN DATED 9-14-76

Segment	Initial Altitude (ft)	Initial Mach	Incremental			Segment			Total		
			Fuel (lb)	Time (min)	Avg w (lb/hr)	Fuel (lb)	Time (min)	Avg. SFC $\left(\frac{lb}{hr}/lb\right)$	Fuel (lb)	Time (min)	Distance (n.mi.)
Cruise	38 000	0.85			4 198	4 898	70.0	0.199	57 747	70	0
Climb	0	0.378			10 157	474	2.8	0.152	58 221	72.8	13
Accelerate	10 000	0.456			8 880	74	0.5	0.165	58 295	73.3	15
Climb	10 000	0.547			7 265	1 223	10.1	0.182	59 518	83.4	83
Cruise	30 000	0.695			3 630	236	3.9	0.185	59 754	87.3	110
Descent	30 000	0.700			1 346	184	8.2	-	59 938	95.5	164
Decelerate	10 000	0.547			1 733	26	0.9	-	59 964	96.4	169
Descent	10 000	0.456			2 043	235	6.9	-	60 199	103.3	200
Loiter	1 500	0.284			2 848	1 424	30.0	0.148	61 623	133.3	200

APPENDIX B

DESIGN CONCEPTS OF SELECTED LH_2 FUEL SYSTEM COMPONENTS

Five fuel system components having critical operational requirements or technically challenging design requirements were selected for conceptual design study. The components studied were:

- Fuel level control shutoff valve
- Ground fueling quick disconnect
- Vapor recovery quick disconnect
- Absolute tank pressure relief and vent valve
- Absolute tank pressure regulator.

B1.1 Component Requirements

Operational and performance requirements were established for each selected component based upon the preliminary fuel system analysis. These requirements were used as the starting point for the component conceptual designs and, in some instances, iteration of the requirements was performed to assure or improve development feasibility.

In addition, some general design requirements were established which applied to all components. These requirements had to do with materials compatibility with GH_2 and LH_2, materials corrosion resistance, avoidance of dissimilar metals in contact, accessibility of the component for installation and adjustment and, in some cases, means for indicating satisfactory functioning or failure. These general requirements were also considered in the analysis and selection of the individual component design concepts.

B1.1.1 Fuel level control shutoff valve. - The fuel level control shutoff valve was an electric motor operated valve, having the purpose of admitting and stopping the flow of fuel to a LH_2 fuel tank. In addition, it had the special requirement for a pressure relief valve set at 1.25 times the maximum stabilized blocked fueling line pressure to provide for thermal pressure relief of the fueling line after valve closure.

Significant parameters of the selected design were:

Rated flow	4.99 kg/sec (11.0 lb/sec)
Pressure drop	23.2 kPa (3.36 psid)
Operating pressure range	241 to 193 kPa (35 to 28 psia)
Operating temperature range	20.6° K to 328° K (37°R to 590°R)
Duct diameter	7.34 cm (2.90 in)
Weight	4.94 kg (10.90 lb)
Estimated MTBF	15 000 hours.

A schematic diagram, and description of the valve design and operation are presented in drawing P398726-1.

For this valve and the following selected components to be discussed, the conceptual design, and estimates of performance, weight, and MTBF were based upon experience with similarly designed equipment.

Also, for this valve and the following selected components to be discussed, the non-recurring design and development costs, and the production costs in the quantity of 350 ship sets plus 20 percent spares were estimated, and the results used as an input to the ASSET evaluation of aircraft costs.

B1.1.2 Ground fueling quick disconnect. - The ground fueling quick disconnect was a manually operated, aircraft fueling quick disconnect and shutoff valve assembly, intended for use in the aircraft LH_2 fueling operation. The unit consisted of an airborne adapter mounted in the aircraft at the fueling interface, and a ground hose adapter mounted at the end of the ground fueling line. Each unit included an internal valve which was normally seated, preventing flow thru the valve, and which was automatically unseated when the two mating units were joined and secured to each other.

It was a design requirement that no hazard to personnel or equipment occur if ice formed on the units prior to, during, or after the fueling operation, and that the presence of ice on either mating unit not interfere with the mating process. In addition, it was required that the design of the mating units not permit ingestion of ice, water, or other contaminants into the system during the filling process.

It was required that the adapter in the aircraft be easily replaceable and designed to break away without damage to the aircraft if the supply truck pulled away from the aircraft without disconnecting the supply hose, and that the part of the adapter remaining in the aircraft automatically close in the event of a break, to preclude the loss of hydrogen from the aircraft.

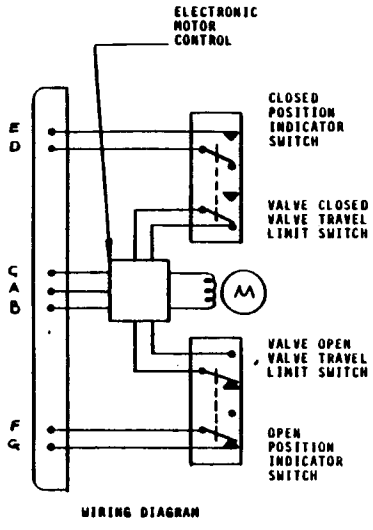

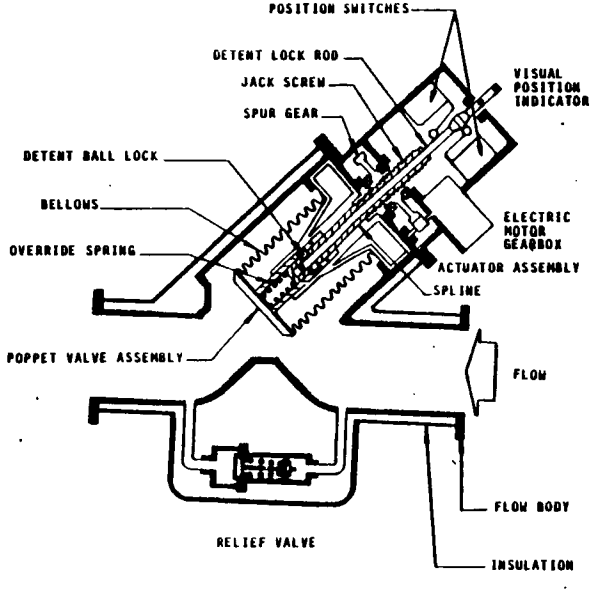

Description:

This is an electric motor operated poppet-type shutoff valve designed for cryogenic operation.

The valve has an insulated flow body to reduce heat transfer to the cryogenic flow media. The flow body has an integral bellows-sealed poppet assembly which eliminates the need for any sliding seals.

The valve is operated by a reversible brushless electric motor driven actuator assembly. The actuator assembly is replaceable without opening the cryogenic line. After removing the detent lock rod, the balls are free to de-couple from the poppet assembly, allowing complete removal of the jack screw and actuator assembly. The detent lock rod has a tapered end to allow re-coupling of the jack screw rod when re-installing a new actuator assembly.

All electrical components are located outside of the flow media area.

Operation:

With the motor appropriately energized, the motor torque is transmitted to the spur gear which is threaded to the jack screw. The jack screw is splined to the flow body and coupled to the poppet assembly through the detent ball lock. As the spur gear rotates, the jack screw moves the poppet assembly to the full open or full closed position, as desired.

An override spring is incorporated in the poppet assembly to limit the valve sealing force.

A visual position indicator is provided to indicate poppet position. Open and closed position switches are incorporated to limit the valve travel and to provide a remote indication when the valve is in the open or closed position.

A pressure relief valve is provided to prevent excessive pressure build-up due to thermal expansion of the flow media when the valve is in the closed position.

Electrical Operation:

Energize Pins C & A to close the valve.
Energize Pins C & B to open the valve.
Continuity between Pins E & D valve closed.
Continuity between Pins F & G valve open.

Figure B-1. - Liquid hydrogen fuel level control shutoff valve.

It was a design requirement that the quick disconnect be suitable for manual handling, installation, and control, by personnel wearing the necessary protective gloves and clothing, and that the required manual force of installation and actuation not exceed 22.2 daN (50 lb).

From the safety viewpoint, it was required that the ground fueling adapter be designed to preclude inadvertent mating with the vapor recovery nozzle. It was further required that complete electrical contact be established between the two adapters before they were connected, and that the contact resistance not exceed 10 ohms.

Significant parameters of the selected design were:

Rated flow	19.26 kg/sec (44.0 lb/sec)
Pressure drop	49.3 kPa (7.15 psid)
Operating pressure	110.3 kPa (16.0 psia)
Duct diameter	12.40 cm (4.88 in)
Weight	
Airborne adapter	2.90 kg (6.40 lb)
Ground adapter	6.45 kg (14.21 lb)

A schematic diagram, and description of the quick disconnect design and operation are presented in drawing P3224622-1 and -2.

B1.1.3 Vapor recovery quick disconnect. - The vapor recovery quick disconnect was a manually operated quick disconnect and shutoff valve assembly, intended for use in GH_2 vapor recovery during the aircraft fueling operation. The unit consisted of an airborne adapter mounted in the aircraft at the fueling interface, and a ground hose adapter mounted at the end of the ground vapor recovery line. Each unit included an internal valve which was normally seated, preventing flow thru the valve, and which was automatically unseated when the two mating units were joined and secured to each other.

It was a design requirement that no hazard to personnel or equipment occur if ice formed on the units prior to, during, or after the fueling operation, and that the presence of ice on either mating unit not interfere with the mating process. In addition, it was required that the design of the mating units not permit ingestion of ice, water, or other contaminants into the system during the filling process.

It was required that the adapter in the aircraft be easily replaceable and designed to break away without damage to the aircraft if the supply truck pulled away from the aircraft without disconnecting the supply hose, and that the part of the adapter remaining in the aircraft automatically

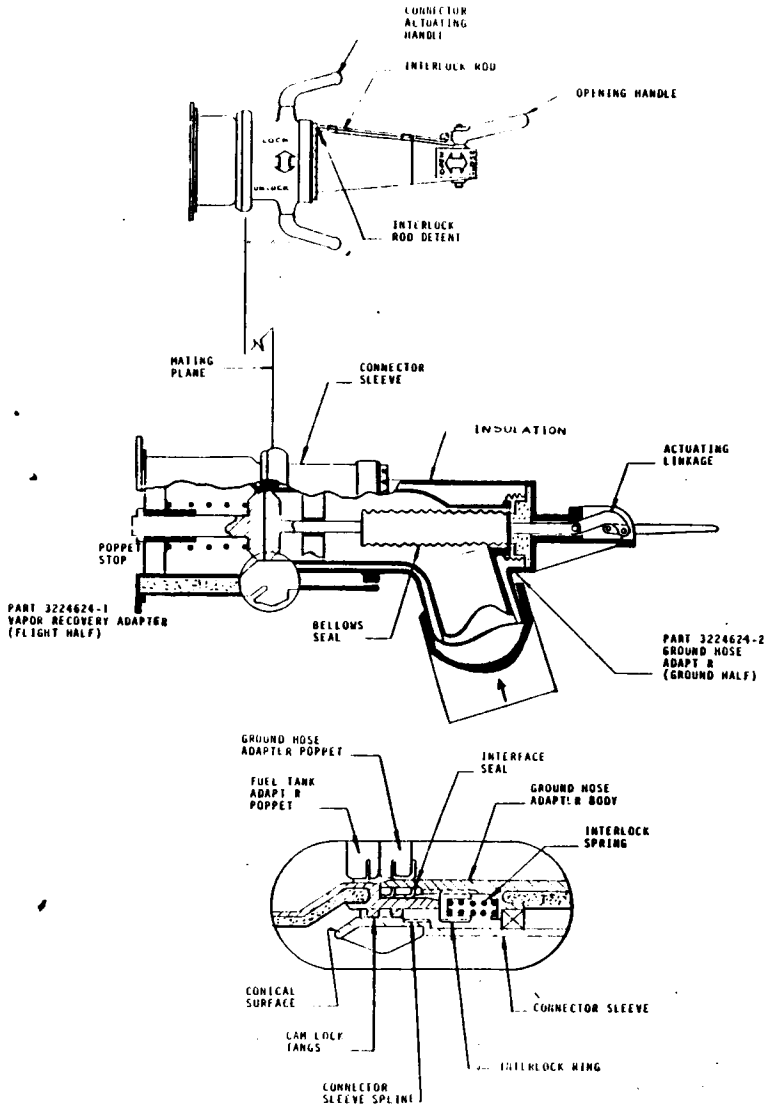

Description:

This unit is a manually operated, vapor recovery, quick disconnect shutoff valve, designed for cryogenic service. The unit consists of an airborne-vapor recovery adapter and a ground hose adapter.

Both components are insulated to minimize the heat transfer to the flow media. The evacuated double wall bellows seals in the ground hose adapter also contributes to isolate the ambient temperature from the flow media and in addition eliminates the requirement for a sliding shaft seal.

The unit is shown in the closed position, with the ground hose adapter fully mated to the airborne fuel tank vapor adapter. Dust caps are provided for use when the two elements are disconnected. Unit tolerances are such that any airborne fuel tank vapor recovery adapter can be mated to any ground hose adapter. The vapor recovery disconnect components cannot be interchanged with the aircraft fueling quick disconnect components shown in schematic P 3224622.

The design of the unit provides a minimum duct volume between the two halves to eliminate the need to purge the connection prior to opening the valve.

Operation:

To connect the two adapters, the ground hose adapter is manually positioned to the fuel tank vapor recovery adapter. The conical surface on the connector sleeve guides the two halves together so that the cam lock tangs are aligned and the interlock ring displaced unlocking the connector sleeve from the ground hose adapter body. With the interlock ring in the position shown, the connector sleeve can be rotated in the direction shown. This action advances the cam lock tangs which fully mates the two halves, placing the poppets face to face and seating the interface seal.

When the connector sleeve is rotated to the fully locked position, the interlock rod detent aligns with the interlock rod.

To open the unit, the opening handle is rotated in the direction shown which advances the interlock rod into the detent and through the actuating linkage, displacing the two poppets to the full open position.

To disconnect the unit, the opening handle is first rotated back to the closed position, which closes both poppets (as shown) and withdraws the interlock rod from the detent on the connector sleeve. The connector sleeve can then be rotated to the unlocked position to decouple the unit. As the two halves are separated, the interlock ring is spring loaded back into the connector sleeve spline preventing rotation of the connector sleeve.

The interlock ring prevents inadvertent rotation of the connector sleeve and subsequent opening of the ground hose adapter (by opening handle rotation) when not properly mated to the fuel tank vapor recovery adapter. The interlock rod prevents accidental de-coupling of the unit when the valve is in the open position.

Figure B-2. - Ground fueling quick disconnect.

close in the event of a break, to preclude the loss of hydrogen from the aircraft.

It was a design requirement that the quick disconnect be suitable for manual handling, installation, and control, by personnel wearing the necessary protective gloves and clothing, and that the required manual force of installation and actuation not exceed 22.2 daN (50 lb).

From the safety viewpoint, it was required that the ground vapor recovery adapter be designed to preclude inadvertent mating with the LH_2 fueling nozzle. It was further required that complete electrical contact be established between the two adapters before they were connected, and that the contact resistance not exceed 10 ohms.

Significant parameters of the selected design were:

Rated flow	0.39 kg/sec (0.87 lb/sec)
Pressure drop	3.31 kPa (0.48 psid)
Operating pressure	110.3 kPa (16.0 psia)
Duct diameter	9.86 cm (3.88 in.)
Weight	
Airborne adapter	2.32 kg (5.11 lb)
Ground adapter	5.15 kg (11.36 lb)

A schematic diagram, and description of the quick disconnect design and operation are presented in drawing P3224624-1 and -2.

B1.1.4 Absolute tank pressure relief and vent valve: The absolute tank pressure relief and vent valve was an assembly consisting of two tank pressure relief valves and an electric motor driven shutoff valve. One tank pressure relief valve was designated the primary relief valve and was designed to maintain an absolute tank pressure of 141.3 kPa (20.5 psia) and the other tank pressure relief valve was designated the secondary relief valve and was designed to maintain an absolute tank pressure of 155.1 kPa (22.5 psia). In the event of failure of the primary valve, the secondary valve would maintain tank pressure at the value slightly higher than normal, thus revealing the fact of the primary valve malfunction. The electric motor shutoff valve was required for use as a purge gas vent valve when initially filling the system.

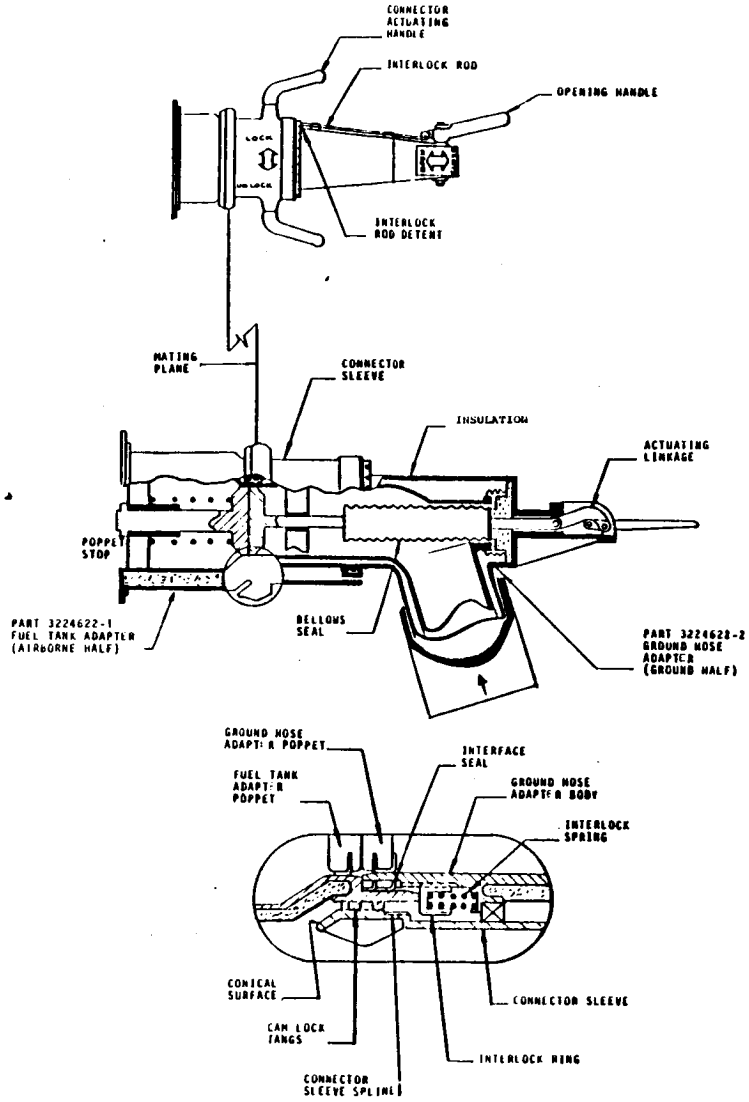

Description:

This unit is a manually operated, aircraft fueling, quick disconnect shutoff valve, designed for cryogenic service. The unit consists of an airborne fuel tank adapter and a ground hose adapter.

Both components are insulated to minimize the heat transfer to the flow media. The evacuated double wall bellows seals in the ground hose adapter also contributes to isolate the ambient temperature from the flow media and in addition eliminates the requirement for a sliding shaft seal.

The unit is shown in the closed position, with ground hose adapter fully mated to the airborne fuel tank adapter. Dust caps are provided for use when the two elements are disconnected. Unit tolerances are such that any airborne fuel tank adapter can be mated to any ground hose adapter. The fueling quick disconnect components cannot be interchanged with the vapor recovery quick disconnect components shown in schematic P 1224624.

The design of the unit provides a minimum duct volume between the two halves to eliminate the need to purge the connection prior to opening the valve.

Operation:

To connect the two adapters, the ground hose adapter is manually positioned to the fuel tank adapter. The conical surface on the connector sleeve guides the two halves together so that the cam lock tangs are aligned and the interlock ring is displaced unlocking the connector sleeve from the ground hose adapter body. With the interlock ring in the position shown, the connector sleeve can be rotated in the direction shown. This action advances the cam lock tangs which fully mates the two halves, placing the poppets face to face and seating the interface seal.

When the connector sleeve is rotated to the fully locked position, the interlock rod detent aligns with the interlock rod.

To open the unit, the opening handle is rotated in the direction shown which advances the interlock rod into the detent and through the actuating linkage, displacing the two poppets to the full open position.

To disconnect the unit, the opening handle is first rotated back to the closed position which closes both poppets (as shown) and withdraws the detent on the connector sleeve interlock rod from the detent of the connector sleeve. The connector sleeve can then be rotated to the unlocked position to decouple the unit. As the two halves are separated, the interlock ring is spring loaded back into the connector sleeve spline preventing rotation of the connector sleeve.

The interlock ring prevents inadvertent rotation of the connector sleeve and subsequent opening of the ground hose adapter (by opening handle rotation) when not properly mated to the fuel tank adapter. The interlock rod prevents accidental decoupling of the unit when the valve is in the open position.

Figure B-3. - Vapor recovery quick disconnect.

Significant parameters of the selected design were:

	Primary Pressure Relief Valve	Secondary Pressure Relief Valve
Rated flow	0.02 kg/sec (0.05 lb/sec)	0.02 kg/sec (0.05 lb/sec)
Relief pressure	141.3 kPa (20.5 psia)	155.1 kPa (22.5 psia)
Pressure drop	0.025 kPa (0.1 in H_2O)	0.025 Kpa (0.1 in H_2O)
Duct diameter	9.86 cm (3.88 in)	9.86 cm (3.88 in)
Weight for complete valve assembly	7.03 kg (15.5 lb)	
Estimated MTBF		
Primary pressure relief valve	50 000 hours	
Secondard pressure relief valve	50 000 hours	
Vent valve	15 000 hours	

A schematic diagram, and description of the valve design and operation are presented in drawing P3224620-1.

Referring to the schematic drawings for the pressure relief valves, the operation may be understood as follows: Vapor from the tank bleeds thru the poppet orifice into the reference pressure chamber and incurs a pressure drop thru the orifice. The pilot valve and partially evacuated bellows bleed vapor from the reference pressure chamber as required to maintain the chamber absolute pressure at a preselected value. The resulting chamber pressure is determined by the design of the pilot valve and partially evacuated bellows, and by the position setting of the adjustment screw. The value of chamber absolute pressure is selected to be such that the resulting pressure force on the main poppet, plus the force of the poppet actuation bellows, is just equal to the desired tank pressure times the main poppet area. If the tank pressure slightly exceeds the desired value, the main poppet will open to a modulated position, thus venting vapor from the tank and thereby limiting further increase in tank pressure.

B1.1.5 Absolute tank pressure regulator. - The absolute tank pressure regulator was required to sense the LH_2 tank absolute pressure, and supply LH_2 as required to a vaporizing heat exchanger (boiler) to generate vapor for

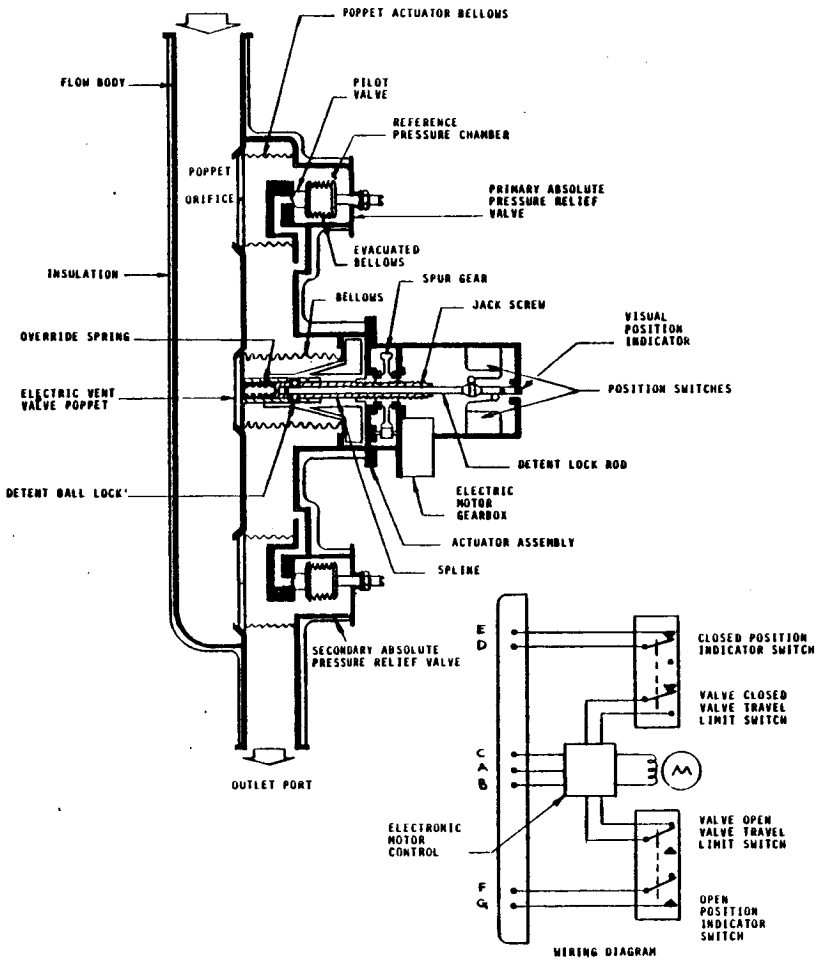

Description:

This unit is composed of a primary and secondary absolute pressure relief valve and an electric motor driven poppet type shutoff valve.

The unit functions to automatically maintain a fixed maximum absolute pressure in an aircraft cryogenic fuel system. The secondary absolute pressure regulator is calibrated above that of the primary to provide back up operation and greater flow capacity in the event of unusual upstream pressure transients. The remotely controlled electrically driven poppet valve can be actuated to bypass both absolute pressure relief valves to provide full venting of the fuel system.

The valve housing is insulated to reduce the heat transfer to the cryogenic flow media. All dynamic seals employ metal bellows to eliminate the need for any sliding seals.

The electric shutoff valve is operated by a reversible brushless electric motor driven actuator assembly. The actuator assembly is replaceable without opening the line. After removing the detent lock rod, the balls are free to decouple from the poppet assembly, allowing complete removal of the jack screw and actuator assembly. The detent lock rod has a tapered end to allow recoupling of the jack screw when reinstalling a new actuator assembly.

All electrical components are located outside of the flow media area.

Pressure Relief Valve Operation:

The primary absolute pressure relief valve poppet is held closed by the preload force in the poppet actuator bellows. When inlet pressure is applied, the orifice admits pressure to the reference pressure chamber and to the evacuated bellows. The evacuated bellows is calibrated so that when the inlet pressure is below the desired actuation point of the primary absolute pressure relief valve, the pilot valve is closed. This results in fluid pressure equalization across the poppet thus keeping the valve closed. As the inlet pressure increases to the desired actuation pressure, the evacuated bellows compresses slightly which moves the pilot valve to vent the reference pressure chamber to the outlet port. The resulting pressure differential acosss the orifice allows the inlet pressure force to overcome the poppet actuator bellows load to open the poppet and allow inlet pressure to vent to the outlet port. The evacuated bellows will respond to increases or decreases in upstream pressure, sensed through the orifice, to modulate the reference pressure chamber and thus the position of the primary relief valve poppet to maintain a fixed maximum upstream absolute pressure.

The secondary absolute pressure relief valve operates identically to the primary device. The evacuated bellows preload of the secondary system is greater than that of the primary device so as to increase the inlet pressure setting at which the device operates. In this way, the secondary valve provides a backup of the primary relief valve in case the primary pressure relief valve malfunctions or cannot accommodate the necessary flow.

Shutoff Valve Operation:

With the motor appropriately energized, the motor torque is transmitted to the spur gear which is threaded to the jack screw. The jack screw is splined to the flow body and coupled to the poppet assembly through the detent ball lock. As the spur gear rotates, the jack screw moves the poppet assembly to the full open or full closed position as desired.

An override spring is incorporated in the poppet assembly to limit the valve sealing force.

A visual position indicator is provided to indicate poppet position. Open and closed position switches are incorporated to limit valve travel and to provide remote position indication.

Electrical Operation:

Energize Pins C & A to close the valve.
Energize Pins C & B to open the valve.
Continuity between Pins E & D valve closed.
Continuity between Pins F & G valve open.

Figure B-4. - Absolute tank pressure regulator (relief valve and vent valve).

tank pressurization, if normal tank boil-off was not sufficient to maintain tank pressure at the primary relief valve absolute pressure level.

Significant parameters of the selected design were:

	Liquid Side	Gas Side
Rated flow	0.02 kg/sec (0.050 lb/sec)	0.02 kg/sec (0.050 lb/sec)
Pressure drop	1.77 kPa (0.256 psid)	77.33 kPa (11.22 psid)
Operating pressure	272.3 kPa (39.5 psia)	262.0 kPa (38.0 psia)
Duct diameter	0.960 cm (0.378 in)	0.960 cm (0.378 in)
Weight	2.33 kg (5.13 lb)	
Estimated MTBF	40 000 hours	

A schematic diagram, and description of the valve design and operation, are presented in drawing P3214134-1.

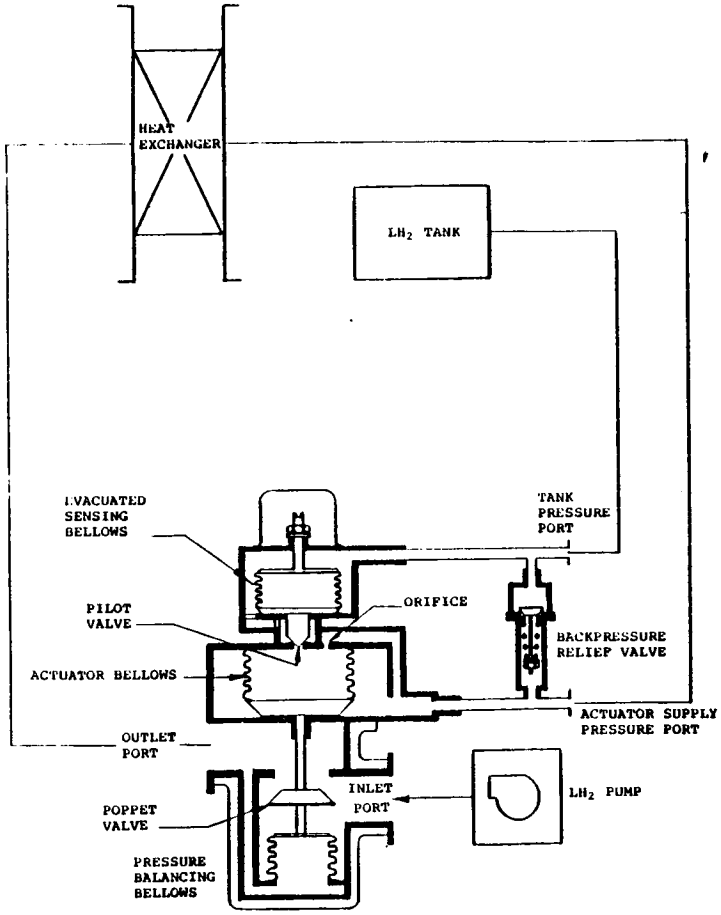

Description:

This unit is a poppet type absolute pressure regulator valve designed for cryogenic service. The valve regulates the pressure in a remotely located liquid hydrogen (LH_2) tank by controlling the amount of fluid passing through the unit. The flow passes through the unit twice, once in the form of liquid and the second time in the form of gas.

Operation:

The liquid hydrogen is routed from the inlet port through the normally open poppet valve to the outlet port. The outlet port is directed to a heat exchanger where the liquid is gasified. The gaseous hydrogen is directed back to the unit to the actuator supply pressure port to a normally closed backpressure relief valve, to the external side of the actuator bellows, through an orifice to the internal side of the actuator bellows, and to a normally closed pilot valve.

As the pressure to the actuator supply pressure port continues to rise, the backpressure relief valve opens and bleeds off flow to the tank pressure port. The backpressure relief valve maintains the pressure at a predetermined value above the tank pressure port. Since the tank pressure port is connected to the LH_2 tank it also provides a means of sensing the LH_2 tank pressure to the evacuated sensing bellows.

As the LH_2 tank pressure rises to calibrated setting of the evacuated sensing bellows, the evacuated sensing bellows moves to open the pilot valve which bleeds off the internal pressure of the actuator bellows. The flow into the actuator bellows is restricted by an orifice which creates a pressure differential across the actuator bellows, causing the poppet valve to modulate towards the closed position. This reduces the liquid H_2 flow through the heat exchanger, and reduces the pressure to the actuator supply pressure port. In turn, this action reduces the flow into the LH_2 tank, to limit the tank pressure to the desired absolute value.

The poppet is inlet pressure balanced by a bellows of identical area of the poppet valve and is exposed to the same differential pressure as the poppet but with a force reaction in the opposite direction. The exterior of the unit is insulated to limit the heat transfer into the flow media.

Figure B-5. - Absolute tank pressure regulator.

APPENDIX C

CONCEPT SCREENING ANALYSIS THERMAL MODEL DEVELOPMENT

The LH_2 airplane tank screening model was developed considering an elemental length of a horizontal cylinder filled with LH_2. Both the liquid and vapor volumes can be expected to stratify, with rather high temperature walls possible opposite the ullage volume. Temperature distribution of the tank walls is needed to determine the heat leak into the tank through the insulation system, and also for structural analysis of the tank. Only two temperatures are fixed in this problem, the liquid surface temperature T_S which corresponds to the vent pressure, and the ambient temperature T_A surrounding the tank. A complicating feature is the need to consider the variable thermal properties of the tank wall and insulation system, and the liquid and vapor phases under the ranges of temperature expected for these components.

Solution for the temperature distribution of the tank wall (Figure C-1) as a function of the heat transfer coefficients to the wall is obtained with an analysis similar to Jakob [A-1]. Figure C-1 assumes that the liquid vapor interface is at $X = 0$, with the liquid at $X < 0$ and the vapor at $X > 0$ along the tank wall. As the temperature distribution solutions of the tank wall will be similar for the regions opposite the liquid and vapor, we solve for the temperature distribution opposite the vapor, where $X \geq 0$. For a steady state energy balance on the differential element dx; of unit width:

$$k\bar{t}\,\frac{d^2 T}{dx^2} = \left(h_I + h_V\right)\left(T - T_{DOV}\right) \qquad \text{(C1)}$$

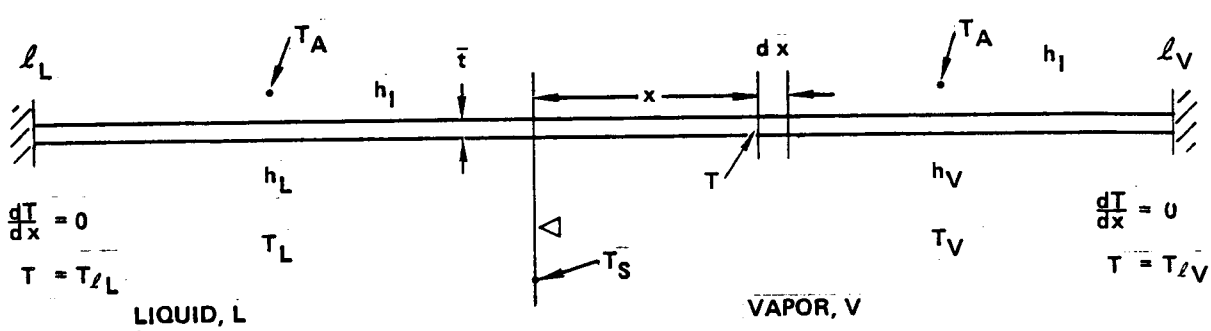

Figure C-1. - Tank wall model.

where

$$T_{\infty V} = \frac{h_I T_A + h_V T_V}{(h_I + h_V)} = \text{the wall temp that would occur if } X \rightarrow \infty.$$

Based upon Carslaw and Jaeger[A-2] solutions for constant thermal conductivity can be converted to variable conductivity solutions by making use of thermal conductivity integrals, providing the boundary conditions are specified only as temperature or the temperature slope. Starting with a constant thermal property solution of equation (C1), which can be rearranged as:

$$\frac{d^2 T}{dx^2} = \frac{(h_I + h_V)}{k\bar{t}} (T - T_{\infty V}) \tag{C2}$$

Letting

$$m_V = \sqrt{\frac{(h_I + h_V)}{k\bar{t}}} \quad , \quad \text{so that}$$

$$\frac{d^2 T}{dx^2} = m_V^2 (T - T_{\infty V}) \tag{C3}$$

The solution to this differential equation is:

$$T = T_{\infty V} + M_V e^{-m_V X} + N_V e^{+m_V X}$$

The integration constants M_V and N_V are evaluated from two boundary conditions. The slope is $dT/dx = 0$ at $x = \ell_V$, but neither the magnitude or slope of the temperature is known at $x = 0$. Applying this one boundary condition to the equation (C3) yields:

$$\frac{dT}{dx} = - M_V M_V e^{-m_V X} + m_V N_V e^{+m_V X} \tag{C4}$$

$$\left.\frac{dT}{dx}\right]_{X=\ell_V} = m_V \left(- M_V \, e^{-m_V \ell_V} + N_V \, e^{+m_V \ell_V} \right) = 0$$

$$N_V = M_V \frac{e^{-m_V \ell_V}}{e^{+m_V \ell_V}} = M_V \, e^{-2m_V \ell_V} \tag{C5}$$

Substituting for N_v, the solution then becomes

$$T = T_{\infty V} + M_V \left(e^{-m_V X} + e^{m_V (X - 2\ell'_V)} \right), \quad \text{for} \quad x \geq 0. \tag{C6}$$

The solution for the region opposite the liquid, where $x \leq 0$, is found from a similar differential equation, which yields:

$$T = T_{\infty L} + M_L \, e^{-m_L X} + N_L \, e^{+m_L X}$$

where

$$T_{\infty L} = \frac{h_I \, T_A + h_L \, T_L}{(h_I + h_L)}$$

$$m_L = \sqrt{\frac{(h_I + h_L)}{k\bar{t}}}$$

One integration constant, M_L, can be solved based upon the boundary condition that $dT/dx = 0$ at $x = -\ell_L$.

$$\frac{dT}{dx} = - m_L \, M_L \, e^{-m_L X} + m_L \, N_L \, e^{+m_L X} \tag{C7}$$

$$\left.\frac{dT}{dx}\right]_{X=-\ell_L} = m_L\left(-M_L\, e^{-m_L(-\ell_L)} + N_L\, e^{+m_L(-\ell_L)}\right) = 0$$

$$M_L = N_L \cdot \frac{e^{-m_L\ell_L}}{e^{+m_L\ell_L}} = N_L \cdot e^{-2m_L\ell_L} \qquad \text{(C8)}$$

Substituting for M_L, the solution opposite the liquid becomes:

$$T = T_{\infty L} + N_L\left(e^{-m_L(X+2\ell_L)} + e^{+m_L X}\right), \quad \text{for } x = 0. \qquad \text{(C9)}$$

Equations (C6) and (C9) contain 2 unknowns, N_L and M_V, which can be found from the condition at $x = 0$, where T and the slope of T must be equal for both of these solutions. Setting the temperature $T_{x \geq 0} = T_{x \leq 0}$ at $x = 0$, then

$$T_{\infty V} + M_V\left(1 + e^{-2m_V\ell_V}\right) = T_{\infty L} + N_L\left(e^{-2m_L\ell_L} + 1\right) \qquad \text{(C10)}$$

Setting the slopes $\left(dT/dx\right)_{x\geq 0} = \left(dT/dx\right)_{x\leq 0}$ at $x = 0$ yields:

$$-m_V M_V + m_V M_V e^{-2m_V\ell_V} = -m_L N_L e^{-2m_L\ell_L} + m_L N_L \qquad \text{(C11)}$$

Solving equation (C11) for N_L, and then substituting N_L into equation (C10) yields:

$$M_V = \frac{T_{\infty V} - T_{\infty L}}{\left[\frac{m_V}{m_L} \cdot \frac{\left(e^{-2m_V\ell_V} - 1\right)}{\left(1 - e^{-2m_L\ell_L}\right)} \cdot \left(1 + e^{-2m_L\ell_L}\right) - \left(1 + e^{-2m_V\ell_V}\right)\right]} \qquad \text{(C12)}$$

The expression for N_L yields the other constant, which is positive:

$$N_L = \frac{\dfrac{m_V}{m_L} \cdot \dfrac{\left(e^{-2m_V \ell_V} - 1\right)}{\left(1 - e^{-2m_L \ell_L}\right)} \cdot (T_{\infty V} - T_{\infty L})}{\left[\dfrac{m_V}{m_L} \cdot \dfrac{\left(e^{-2m_V \ell_V} - 1\right.}{\left(1 - e^{-2m_L \ell_L}\right.} \cdot \left(1 + e^{-2m_L \ell_L}\right) - \left(1 + e^{-2m_V \ell_V}\right)\right]} \tag{C13}$$

Hence, the complete solution, using the above values of M_V and N_L is:

$$T = T_{\infty L} + N_L \quad e^{-m_L (X + 2\ell_L)} + e^{+m_L X} \quad , \text{ for } x \le 0. \tag{C14}$$

$$T = T_{\infty V} + M_V \quad e^{-m_V X} + e^{m_V (X - 2\ell_V)} \quad , \text{ for } x \ge 0. \tag{C15}$$

where

$$m_L = \sqrt{\frac{h_I + h_L}{kt}}$$

$$m_V = \sqrt{\frac{h_I + h_V}{kt}}$$

The tank wall temperature solution for the case of variable conductivity in the wall, insulation, and fluids is determined by assuming all of the thermal conductivities are proportional to temperature. The thermal conductivity integral then will have the form

$$\int_0^T k dT = \int_0^T k'T dT = \frac{k'}{2} \cdot T^2$$

where k' = slope of thermal conductivity curve.

From Reference (A-2) the variable properties solution may be obtained from the constant k solution by replacing the temperature by the thermal conducitivity integral. The original steady state differential equation expressed in terms of variable conductivity is

$$\bar{t} \frac{d}{dx} \left(k \frac{dT}{dx}\right) = q_I'' + q_V'' ,$$

for the wall opposite the vapor phase.

Since $$k = k'T$$

and

$$U = \int_0^T k dT = \int_0^T k'T dT - k' \int_0^T T dT = \frac{k'}{2} \cdot T^2$$

$$\frac{dU}{dT} = \frac{k'}{2} \cdot 2T \frac{dT}{dx} = k'T \frac{dT}{dx} = k \frac{dT}{dx}$$

$$\frac{d^2U}{dx^2} = \frac{d}{dx} \left(\frac{dU}{dx}\right) = \frac{d}{dx} k \left(\frac{dT}{dx}\right)$$

Hence, the differential equation can be expressed by:

$$\bar{t} \cdot \frac{d^2U}{dx^2} = q_I'' + q_V'' \qquad \text{(C16)}$$

For the case of variable conductivities in the insulation and vapor

$$q''_I = \frac{1}{t_I}\left[\int_o^T k_I dT - \int_o^{T_A} k_I dT\right] = \left[\frac{k'_T}{D_{hV}} \quad T^2 - T_A{}^2\right]$$

$$q''_V = \frac{N_{uV}}{D_{hV}}\left[\int_o^T k_V dT - \int_o^{T_V} k_V dT\right] = \left[\frac{N_{uV}k'_V}{D_{hV}} \quad T^2 = T_V{}^2\right]$$

Hence, the differential equation becomes

$$\bar{t} \cdot \frac{d^2U}{dx^2} = \frac{k'_I}{2t_I}\left(T^2 - T_A{}^2\right) + \frac{N_{uV}\ k'_V}{2\ D_{hV}}\left(T^2 - T_V{}^2\right) \qquad \text{(C17)}$$

Since U is defined in terms of the wall conductivity k, then the above differential equation can be put into the form:

$$\bar{t} \cdot \frac{d^2U}{dx^2} = \frac{k'_I}{t_I k'}\left(\frac{k'}{2}\ T^2 - \frac{k'}{2}\ T_A{}^2\right) + \frac{Nu_V k'_V}{D_{h_V}\ k'}\left(\frac{k'}{2}\ T^2 - \frac{k'}{2}\ T_V{}^2\right) \qquad \text{(C18)}$$

$$\bar{t} \cdot \frac{d^2U}{dx^2} = \frac{k'_I}{t_I k'}\left(U - U_A\right) + \frac{Nu_V k'_V}{D_{h_V}\ k'}\left(U - U_V\right)$$

Since

$$U_i = \frac{k'}{2}\ T_i{}^2$$

From the above equation, solve for the value of U at $x \to \infty$, when $d^2U/dx^2 = 0$. Defining that value of the wall conductivity integral as u_{∞_V}, then:

$$u_{\infty_V} = \frac{\frac{k'_I}{t_I} U_A + \frac{Nu_V k'_V}{D_{h_V}} U_V}{\frac{k'_I}{t_I} + \frac{Nu_V k'_V}{D_{h_V}}}$$

Substitution of u_{∞_V} into the differential equation then yields:

$$\frac{d^2U}{dx^2} = \frac{1}{k't}\left(\frac{k'_I}{t_I} + \frac{Nu_V k'_V}{D_{h_V}}\right)\left(U - U_\infty\right) = m^2_V \left(U - U_{\infty_V}\right) \qquad \text{(C19)}$$

This equation for variable conductivity has exactly the same form as the constant k differential equation at equation (C3), with U substituted for T. The total solution for the wall temperature opposite the liquid and vapor regions can then be taken from the total constant k solutions completed with the new definitions of m_V and m_L which yields

$$M_V = \frac{\left(U_{\infty V} - U_{\infty L}\right)}{\left[\frac{m_V}{m_L} \cdot \frac{\left(e^{-2m_V \ell_V} - 1\right)}{\left(1 - e^{-2m_L \ell_L}\right)} \cdot \left(1 + e^{-2m_L \ell_L}\right) - \left(1 + E^{-2m_V \ell_V}\right)\right]} \qquad \text{(C20)}$$

$$N_L = \frac{\frac{m_V}{m_L} \cdot \frac{\left(e^{-2m_V \ell_V} - 1\right)}{\left(1 - e^{-2m_L L}\right)} \cdot \left(U_{\infty_V} - U_{\infty_L}\right)}{\left[\frac{m_V}{m_L} \cdot \frac{\left(e^{-2m_V \ell_V} - 1\right)}{\left(1 - e^{-2m_L \ell_L}\right)} \cdot \left(1 + e^{-2m_L L}\right) - \left(1 + e^{-2m_V \ell_V}\right)\right]} \qquad \text{(C21)}$$

$$U = \frac{k'}{2} \cdot T^2, \quad T^2 = \frac{2U}{k'} \quad \text{and} \quad T = \sqrt{\frac{2U}{A'}}$$

These solutions are then used to compute the heat transfer into the fluid. Assuming that there is no gross vapor motion in the ullage space, $R_a < 10\ 000$, vapor conduction will be the principal mode of heat transfer to a mean vapor temperature, T_v, with the vapor heat transfer coefficient, k_v, defined by a constant Nusselt number, Nu_v, and hydraulic diameter, D_{kv}, of the ullage volume. For steady state heat transfer and venting, not considering LH_2 withdrawal from the tank, the liquid boiloff rate is equal to the heat transfer directly occurring to the liquid phase. The vapor will be formed at temperature, T_s, and then be heated by the dry tank ullage and finally vented from the top of the tank. This vent temperature, T_{v_o}, will be a function of the boiloff rate, heat transfer from the ullage surfaces and vent pressures.

Initially, assume the mean vapor temperature is equal to the average temperature of the walls and liquid surface base of the ullage vapor volume. An iterative solution can then be performed to set the initial assumed T_v equal to the final computed mean T_v based upon the computed wall temperature variation.

The liquid heat transfer coefficient, h_L, is computed based upon free convection along a vertical plate of the same height L as the liquid depth in the tank. Using the Vliet and Liu [A-3] correlation for constant heat flux, which closely simulates the heat flux into the liquid, the average liquid Nusselt Number is given by the following relations:

$$Nu_L = \frac{h_L L}{k_L} = 0.25\ (Gr^*_L\ Pr)^{0.24} \qquad R_{a_L} \geq 4.2535 \times 10^{12}$$

$$Nu_L = 0.80\ (Gr^*_L\ Pr)^{0.20} \qquad 10^4 \leq R_{a^*_L} \leq 4.2535 \times 10^{12}$$

$$Nu_L = 5.0476 \qquad R_{a^*_L} \leq 10^4$$

where

$$R_{a^*_L}\ L^* = Gr^*_L\ Pr$$

$$Gr^*_L = \frac{g\beta q''\ L^4}{B\nu^2} = \frac{g\beta\rho^2}{B\mu^2} \cdot q''\ L^4 = Z_L \cdot q''\ L^4$$

$$Pr = \frac{ucs}{k}$$

For the ullage vapor, the average conduction Nusselt number, Nu_v, is a constant based upon hydraulic diameter D_{k_v} of the volume, $Nu_v = h_v D_{kv}/k_v = 4.386$.

Having defined temperature distributions and the heat transfer coefficients an energy balance can now be performed to calculate the mass of liquid evaporated and the sensible heat in the vapor.

APPENDIX D

"THERM" PROGRAM

A modification of the basic THERM program is used for the fuel tank analysis program. This program is structured to allow the maximum flexibility in describing energy transport phenomena in a cryogenic storage tank. Calculations during the energy balance can be performed in any of 24 dummy subroutines that are called automatically at various points in the basic integration algorithms. This permits modification or updating of any aspect of the model by simply replacing the appropriate dummy routines with subroutines containing the desired operations. The fluid stratification problem, liquid-ullage coupling through mass and energy exchanges associated with evaporation, bulk boiling and condensation, the geometrical calculations required in the node definition and the various Nusselt number correlations needed for characterization of several energy transport mechanisms are all modeled as subroutines that modify and update the basic heat balance calculation.

The program was developed specifically for operation on the UNIVAC 1100 series system. Structurally, it is divided into three major subprograms, THERM, CYCLE, and OUTPUT, and a number of lesser routines.

THERM is the name of the main program as well as the system. It reads in and stores the network description from cards, tape or disk, saves the network data on disks, if necessary, for restart, and calls CYCLE. (The term "restart" in this context refers to the running of two or more cases on the same run. It does not involve taking the job off the machine.) On return from CYCLE, THERM retrieves the original network from disk, reads in network changes from cards, updates the network, and again calls CYCLE. After the last restart, THERM terminates the run.

CYCLE performs the heat balance calculations. It includes two independent iterative procedures: one for converging (i.e., relaxing the network at a specific time to obtain steady-state conditions at that time) and the other for the usual thermal analyzer transient calculations. In order to increase the speed and efficiency of the program, several routines that are called many times, such as the calculation of $\sum$ (I/R) and $\sum$ (T/R) for each node, are written as assembly language subroutines.

OUTPUT is called from CYCLE at prescribed times during transient calculations and after a prescribed number of iterations during converge. It causes the status of the parameters prescribed in the "O" block (see below) to be listed.

Input consists of nine blocks of data, labeled T, C, Q, R, K, D, O, G, and P. The initial temperature, capacitance, and heat input (internal plus external) of each node are input in the "T", "C", and "Q" blocks,

respectively. The "R" block contains the values and connections of the resistors, except the radiation resistors. The "K" block contains the values and connections of the radiation resistors (RADK's). Tabular data are input in the "D" block - the data may consist of periodic or non-periodic tables or of groups of unrelated constants. The "O" block specifies the quantities to be listed during each normal output. These may include temperatures in any desired units, capacitances, resistors RADK's, tabular data, problem variables, heat rates, $\sum$ (1/R), and $\sum$ (T/R). Comments describing the output may also be written. The "P" block contains the values of the problem variables such as initial time, final time, print interval, fractions of the minimum RC to be used in computing the time step, etc. The "G" block specifies the portion of the output that is to be plotted. The data for each case are ended by an "M" card (put data for restart on disk), an "S" card (save restart data from preceding case), or an "F" card (final case).

The user has the option of performing calculations during input through 15 ENTRIES and during the heat balance calculations through 24 MODES. These are provided in THERM in the form of dummy routines of the form SUBROUTINE NAME, RETURN, END and are called automatically at various points during input and during the heat balance. The entry B4D, for example, is called just before the first data input in the "D" block' B4HB is called just before CYCLE is called; the MODES similarly provide entry to CYCLE before and after each significant calculation during the heat balance calculations. If the user wants to perform calculations or modify the model at any of these points, he simply replaces the dummy routine with a hand-coded routine containing the desired operations.

Direct access to all of the parameters of the model is provided through THERM's FIND and STORE routines. The function FINDTF(N), for example, produces the current temperature in ^{o}F of node N; FINDD (N,I) produces the value of the I-th location in table N; CALL FINDRH (N,I,J) give the ID's, I and J, of the nodes to which resistor N is connected: FPTIM(N) finds the present time (N is a dummy variable required by the system). Similarly, CALL STORTF (N,V) stores V in absolute units as the temperature of node N; CALL STORD (N,I,V) stores V in the I-th location of table N; CALL STORRH(N, I,J) destroys the previous connections of resistor N and connects it to nodes I and J; CALL SPTIM(V) changes the present time to V. Other routines find and store the values of the other parameters.

All of the data, except the problem variables and the locations and ID's of the data tables, is stored in one variably-dimensioned array. The number of cells needed for a given program are five times the maximum node ID, plus two times the maximum resistor ID, plus two times the maximum RADK ID, plus one cell for each data item, plus, basically, three cells for each quantity specified in the output (this varies as to the specific type of output). The maximum allowable table ID is 300.

The simplest form of plot output presents the transient temperatures of up to eight nodes per plot. Considerably more complex graphic output, including three-dimensional plots, can be achieved by linking THERM with the DISSPLA plot program that is resident on the computer.

APPENDIX E

SAFETY ANALYSIS

The safety analysis was a four step process. First, a preliminary malfunction analysis was performed to determine if any of the systems had failure modes dangerous to life or aircraft. Secondly, requirements for hydrogen detectors were established, third, an assessment of flammability and toxicity was made, and fourth, the ability to inspect barriers and the tank was evaluated.

The screening malfunction analysis used a standardized format as shown in the following tables. For each system, the type of failure was postulated with the normal resulting condition, the effect of the failure on the flight and the aircraft and existing protective measures. Table E-1 summarizes the results of the analysis for each concept.

TABLE E-1

POTENTIAL MALFUNCTION SCREENING ANALYSIS

Concept	Type of Failure	Normal Resulting Condition	Effect on Flight	Effect on Aircraft	Protective Measures
1. GHe Purge	Jacket leakage	Loss of helium	N (unless excessive)		Carry extra helium on board, monitor press decay rate (with He flow off) prior to flight.
		Buckling of jacket, air liquefaction.	A	D	
	Jacket over pressure	Loss of He through relief valve	A	D	Redundant pressure transducers, dual stage regulator, shut off valves relief valve.
	He flow stopped	Possible jacket buckling during aircraft descent	A	D	Might require parallel redundancy in shut off valves or dual operator on single valve.
	GH_2 tank leakage	None if leakage rate is not excessive	N		H_2 vented with He purge, burst disc/relief valve.
	He bottle over-pressure during loading	Loss of He through burst disc/relief valve	A		Burst disc/relief valve, conservative margins of safety.
2. Dual GHe/GN_2 Purge	He jacket leakage	Loss of He, increased heat rate, possible N_2 liquefaction, N_2 jacket buckling.	A	D	Carry extra He and LH_2 on board, monitor press decay rate (with He flow off) prior to flight
	N_2 jacket leakage	Loss of N_2, buckling of jacket if N_2 supply runs out.	N (unless excessive)		Carry extra N_2 on board. Monitor press decay rate (with N_2 flow off) prior to flight
			A	D	

N - None
A - Potential Abort
D - Potential Aircraft Damage
L - Potential Aircraft Loss
NA - Not Applicable

TABLE E-1 (Continued)

Concept	Type of Failure	Normal Resulting Condition	Effect on Flight	Effect on Aircraft	Protective Measures
3. & 4. External foam	Effect of 350 thermal cycles/yr				
	o Bond line delamination	Possible local loss of insulation, increased heat rates, buildup of cryodeposits (moisture, air)	A	D	Inspect insulation for frosting, monitor tank boiloff, periodically replace or repair insulation if required
	o Foam breakup	May cause vapor barrier leakage, increased heat rates	A	D	
	o Vapor barrier leakage	Increased heat rates, buildup of cryodeposits, further damage to vapor barrier as tank warms up each flt.	A	D	
	GH_2 tank leakage into foam	Increased heat rates, possible safety hazard	A	D	Periodically check tank pressure integrity, frosting of foam, tank boiloff, monitor space outside insulation for GH_2
5. Internal Foam	Liquid seal, foam breakup due to thermal cycling 350 times/yr	Increased heat rate, potential LH_2 pump damage	A	D	Screens over tank outlets, monitor tank for frost, monitor tank boiloff
	Tank leakage	Possible safety hazard	A	D	Periodically check tank pressure integrity, monitor space outside tank for GH_2

N - None
A - Potential Abort
D - Potential Aircraft Damage
L - Potential Aircraft Loss
NA - Not Applicable

TABLE E-1 (Continued)

Concept	Type of Failure	Normal Resulting Condition	Effect on Flight	Effect on Aircraft	Protective Measures
6. Internal/External Foam System	Internal foam breakup	Increased heat rate, potential pump damage	A	D	Screens over tank outlets
	Internal bond line delamination	Same as above, potential decrease in LH_2 flow to pumps	A	D	Same as above
	External bond line delamination	Possible local loss of insulation, increased heat rates, buildup of moisture, cryodeposits	A	D	Inspect insulation for frosting, monitor tank boiloff, periodically replace or repair insulation
	External foam breakup	May cause vapor barrier leakage, increased heat rates	A	D	
	External vapor barrier leakage	Cryopump moisture, damage barrier further with each thermal cycle	A	D	
	Tank leakage	Increased heat rates, possible safety hazard	A	D	Periodically check tank pressure integrity, frost formation on insulation, tank boiloff, monitor space outside insulation for GH_2

N - None
A - Potential Abort
D - Potential Aircraft Damage
L - Potential Aircraft Loss
NA - Not Applicable

TABLE E-1 (Continued)

Concept	Type of Failure	Normal Resulting Condition	Effect on Flight	Effect on Aircraft	Protective Measures
	He jacket overpressure	Loss of He through relief valve, tank buckling if tank pressure is exceeded	A	L	Redundant pressure transducers, dual stage regulator shutoff valves, relief valve
	N_2 jacket overpressure	Loss of N_2 through relief valve. Buckling of He jacket if He pressure is exceeded	A	D	Same as above
	He flow stopped	Potential inward buckling of He jacket during descent, N_2 cryopumping	A	D	Might require parallel redundancy in shutoff valves or dual operator on single valve
	N_2 flow stopped	Potential inward buckling of N_2 jacket during descent	A	D	Same as above
	GH_2 tank leakage	None if leakage rate is not excessive	N		H_2 vented with He purge burst disc/relief valve
	He or N_2 bottle overpressure during loading	Loss of gas through burst disc/relief valve	A		Burst disc/relief valve, conservative margins of safety

N - None
A - Potential Abort
D - Potential Aircraft Damage
L - Potential Aircraft Loss
NA - Not Applicable

TABLE E-1 (Continued)

Concept	Type of Failure	Normal Resulting Condition	Effect on Flight	Effect on Aircraft	Protective Measures
7. PPO	Tank leakage	Possible safety hazard	A	D	Periodically check tank integrity, monitor space outside tank for GH_2
	Foam breakup	Increased heat rates, possible LH_2 pump damage	A		Inspect tank for frosting, monitor tank boiloff, screens over tank outlets
8. Honeycomb/ Perforated Face Sheet	Delamination of face sheet	Sharp rise in heat rate, possible reduction in LH_2 flow to engines, air liquefaction on outside of tank.	A	D	Screens over tank outlets, check tank for frost, monitor boiloff
	Debonding of honeycomb	Minimal effect if localized	N		Screens over tank outlets, check tank for frost, monitor boiloff
	Tank leakage	Possible safety hazard	A	D	Periodically check tank integrity, monitor space outside tank for GH_2
9. Hard Shell Vacuum	Shell leakage	No effect if pressure does not exceed 10^{-5} Torr. Heat rate increases above 10^{-5} Torr	N ($< 10^{-5}$ Torr) A ($> 10^{-5}$ Torr)		Active pumping system, cryopumping at LH_2 surface of 10,800 l/sec/ft^2

N - None
A - Potential Abort
D - Potential Aircraft Damage
L - Potential Aircraft Loss
NA - Not Applicable

TABLE E-1 (Continued)

Concept	Type of Failure	Normal Resulting Condition	Effect on Flight	Effect on Aircraft	Protective Measures
	Tank leakage	No effect if pressure does not exceed 10^{-5} Torr. Heat rate increases up to conductivity of GH_2 at that pressure if 10^{-5} Torr is exceeded, possible air liquefaction on jacket exterior.	N (< 10^{-5} Torr) A (> 10^{-5} Torr)		Active pumping system, relief valve, vent in tail
	Turbomolecular pump shutdown	Pressure in insulation may rise slowly as will heat rate	A		Cryopumping at LH_2 surface of 10,800 l/sec/ft^2, redundant components, getters if required, relief valve
	Blower pump shutdown	No effect if no leakage occurs	N		Same as above
10. External Microspheres, Flexible Vacuum Jacket	Air leakage	No effect if pressure does not exceed .1 Torr. Heat rate increases above .1 Torr pressure	N (≤ .1 Torr) A (> .1 Torr)		Active pumps, cryopumping at LH_2 surface of 10,800 l/sec/ft^2

N - None
A - Potential Abort
D - Potential Aircraft Damage
L - Potential Aircraft Loss
NA - Not Applicable

TABLE E-1 (Continued)

Concept	Type of Failure	Normal Resulting Condition	Effect on Flight	Effect on Aircraft	Protective Measures
	Tank leakage	No effect if pressure does not exceed .1 Torr. Heat rate increases up to 1/3 conductivity of GH_2 at that pressure if .1 Torr is exceeded. Over expansion of jacket if insulation pressure exceeds ambient pressure	N (<.1 Torr) A (>.1 Torr)	D	Active pumps, insulation relief valves, vent in tail
	Blower shutdown	Slow rise in insulation pressure may occur accompanied by heat rate increase above .1 Torr pressure	A		Cryopumping at LH_2 tank surface of 10,800 l/sec/ft^2, relief valves, redundant components
11. Internal Microspheres, Invar Liner, Evacuated	Liner leakage	No effect if pressure does not exceed .1 Torr, heat rate increases up to 1/3 conductivity of GH_2 at that pressure if .1 Torr is exceeded. Liner reversal if insulation pressure exceeds tank pressure	N (<.1 Torr) A (>.1 Torr)	D	Monitor insulation pressure, presence of GH_2 in insulation active pumps, tank pressurization system, insulation relief valves Insulation prevents LH_2 from striking the warm tank wall and vaporizing, exceeding the tank pressure.

N - None
A - Potential Abort
D - Potential Aircraft Damage
L - Potential Aircraft Loss
NA - Not Applicable

TABLE E-1 (Continued)

Concept	Type of Failure	Normal Resulting Condition	Effect on Flight	Effect on Aircraft	Protective Measures
	Tank leakage	None if pressure does not exceed .1 Torr. Increased heat rate if pressure exceeds .1 Torr	N (<.1 Torr) A (>.1 Torr)		Active pumps, tank cryopumps at LH_2 temp, 10,800 l/sec/ft^2
	Blower shutdown	Slow rise in insulation pressure may occur accompanied by heat rate increase above .1 Torr pressure	A		Cryopumping at LH_2 tank surface of 10,800 l/sec/ft^2, relief valves, redundant components
12. Internal SiO_2 Insulation, Invar Liner, Evacuated	Liner leakage	No effect if pressure does not exceed .1 Torr. Heat rate increases up to ~ conductivity of GH_2 at that pressure if .1 Torr is exceeded. Liner reversal if insulation pressure exceeds tank pressure.	N (<.1 Torr) A (>.1 Torr)	D	Monitor insulation pressure, presence of GH_2 in insulation, active pumps, tank pressurization system, insulation relief valves. Insulation prevents LH_2 from striking the warm tank wall and vaporizing, exceeding the tank pressure.
	Tank leakage	None if pressure does not exceed .1 Torr. Increased heat rate if pressure exceeds .1 Torr	N (<.1 Torr) A (>.1 Torr)		Active pumps, tank cryopumps at LH_2 temp, 10,800 l/sec/ft^2

N - None
A - Potential Abort
D - Potential Aircraft Damage
L - Potential Aircraft Loss
NA - Not Applicable

TABLE E-1 (Continued)

Concept	Type of Failure	Normal Resulting Condition	Effect on Flight	Effect on Aircraft	Protective Measures
	Blower shutdown	Slow rise in insulation pressure may occur accompanied by heat rate increase above .1 Torr pressure	A		Cryopumping at LH_2 tank surface of 10,800 l/sec/ft^2, relief valves, redundant components
13. Self Evacuating Shingles	Vapor barrier leakage	Increased heat rates, buildup of cryodeposits, potential further damage to vapor barrier as tank drains (and cryodeposits vaporize) each flight	A	D	Inspect insulation for frost, monitor tank boiloff, periodically repair vapor barrier if required
	Tank leakage	Potential safety hazard, increased heat rates	A	D	Periodically check tank pressure integrity, frosting of vapor barrier, tank boiloff, monitor space outside insulation for GH_2
14. Self Evacuating Honeycomb/ Foam	External vapor barrier leakage	Cryopumping of moisture, increased heat rate	A	D	Inspect insulation for frost, monitor tank boiloff, periodically repair vapor barrier if required

N - None
A - Potential Abort
D - Potential Aircraft Damage
L - Potential Aircraft Loss
NA - Not Applicable

TABLE E-1 (Continued)

Concept	Type of Failure	Normal Resulting Condition	Effect on Flight	Effect on Aircraft	Protective Measures
	Honeycomb vapor barrier leakage	Local cryopumping of gas from foam into the honeycomb, increased leakage of vapor barrier probable after thermal cycling	N (unless extensive)		
	GH_2 tank leakage	Increased heat rate, possible safety hazard	A	D	Periodically check tank pressure integrity, inspect insulation for frost, monitor tank boiloff, space outside insulation for GH_2
15. Self Evacuating Honeycomb/ GN_2 Fiberglass	External vapor barrier leakage	Loss of nitrogen	N (unless excessive)		Carry extra nitrogen onboard. Monitor press decay rate prior to flight
		Buckling of Jacket if N_2 supply is exhausted, air liquefaction.	A	D	
	Honeycomb vapor barrier leakage	Local cryopumping of nitrogen into honeycomb, increased heat rate, potential rupture of honeycomb barrier upon tank warm-up.	A	D	

N - None
A - Potential Abort
D - Potential Aircraft Damage
L - Potential Aircraft Loss
NA - Not Applicable

TABLE E-1 (Continued)

ncept	Type of Failure	Normal Resulting Condition	Effect on		Protective Measures
			Flight	Aircraft	
	GH_2 tank leakage	Increased heat rate, possible rupture of honeycomb vapor barrier.	A	D	Periodically check tank pressure integrity, inspect insulation for frost, monitor tank boiloff, nitrogen purge gas for hydrogen

N - None
A - Potential Abort
D - Potential Aircraft Damage
L - Potential Aircraft Loss
NA - Not Applicable

TABLE F-1 PRELIMINARY PRODUCIBILITY ANALYSIS

Concept	Fab & Assembly	Inspection	Servicing & Maintenance	Areas that May Require Development
1. He Purge	Fab and install fiberglass batting panels and purge jacket standoffs on tank, fab fiberglass/resin purge jacket on mandrel in two parts, leak check, assemble over the insulation. Assemble plumbing, controls, leak check.	Dimensional check, pressure decay leak check, functional check including loading LH_2, temperature measurements and boiloff measurement.	Load helium each flight and perform pressure decay check; periodically service plumbing components, hydrogen detectors, pressure monitoring and control system. Bond repair patches if required.	Purge jacket to tank standoffs to allow differential movement during tank fill.
2. He/N_2 Double Purge	Fab and install fiberglass batting panels and purge jacket standoffs on tank, fab two fiberglass/resin purge jackets on mandrels in two parts, leak check, install first jacket, leak check, install fiberglass batting panels, install second purge jacket with standoffs, leak check, assemble plumbing, controls, leak check.	Same as above for both He and N_2.	Same as above for both He and N_2.	Purge jacket to tank and purge jacket to purge jacket standoffs to allow differential movement during tank fill.
3. & 4. External Closed Cell Foam	Prime tank exterior with adhesive spray on foam in multiple phases, machine, spray on sealer and adhesive, lay on MAAMF and bond.	Visual inspection and dimensional check, LH_2 boiloff test with temperature measurements.	Examine insulation for frosting, monitor boiloff and temperatures in service, repair or replace insulation as required, service external hydrogen detectors.	No direct way to check integrity of seal coat other than by temperature measurements and frost formation. Frost and other cryopumped gases can build up in insulation. Life cycle testing required.
5. Internal Polyurethane Foam, Liquid Seal	Prime tank interior, fab and trim 3-D foam blocks, bond, install fiberglass/resin.	Same as above.	Same as above.	Insulation this thick has not not been installed in tanks before.

TABLE F-1 PRELIMINARY PRODUCIBILITY ANALYSIS (CONTINUED)

Concept	Fab & Assembly	Inspection	Servicing & Maintenance	Areas that May Require Development
6. Internal PPO Foam/External Polyurethane Foam	Prime tank interior, fab and trim foam blocks, bond. Prime tank exterior, spray on foam, machine, spray on sealer.	Same as above.	Same as above.	PPO in the thicknesses required is not currently available. No direct way to check integrity of seal coat other than by frost formation and temperature measurements. Life cycle testing required.
7. & 8. Internal PPO Foam	See comments on System 6 regarding PPO foam			
Internal Honeycomb Gas Barrier Layer	Prime tank interior, blow fiberglass batting into honeycomb, bond perforated barrier to honeycomb panels, bond panels to tank, bond seal strips.	Visual inspection and dimensional check, LH_2 boil-off test and temperatures.	Examine tank for frosting in service, monitor boiloff and temperatures in service. Service hydrogen detectors.	This thickness of honeycomb will require a special order; blowing fiberglass batting into the honeycomb cells may require development. Life cycle testing may be required.
9. Rigid Vacuum Shell with Fiberglass Batting	Form, trim, weld outer face sheets. Leak check. Bond honeycomb to outer face sheets. Bond perforated inner face sheets. Fab, install insulation panels. Install vacuum jacket, weld final closure. Leak check. Pumpdown.	Visual inspection and dimensional check, pump down to 10^{-5} torr, pressure decay test.	Monitor vacuum pressure and hydrogen detectors, service pumping and pressure measuring system. Service hydrogen detectors.	Life cycle testing of jacket to insure structural and pressure integrity. Development of high vacuum pumping system and controls suitable for use in aircraft.
10. Microspheres with Flexibles External Jacket	Stretch form stainless steel gores, trim, resistance seam weld together, leak check, form wedges, bond spring standoffs to tank, install jacket, weld final closure, leak check, fill with microspheres, evacuate to $< .1$ Torr.	Visual, dimensional check, pressure check, pressure decay test, functional check of blowers and pressure monitoring equipment.	Monitor vacuum pressure and hydrogen detectors, service blowers and pressure measuring system.	Forming wedges after gores have been welded, final closure joint, leak-checking jacket. Demonstration of pumping system and controls suitable for aircraft use.

TABLE F-1 PRELIMINARY PRODUCIBILITY ANALYSIS (CONTINUED)

Concept	Fab & Assembly	Inspection	Servicing & Maintenance	Areas that May Require Development
11. Microspheres with Internal Invar Liner	Stretch form Invar gores, trim, weld, leak check on mandrel, install spring assemblies and layer of PPO foam, install liner into tank cone section supported on mandrel, bond springs with anerobic adhesive, remove mandrel, install end of tank with Invar liner already installed, weld Invar liner, weld tank, leak check, fill with microspheres, evacuate to <.1 torr.	Same as above.	Same as above.	Installation of liner into the tank and final closure welds. Demonstration of pumping system and controls suitable for aircraft use.
12. Silica Insulation with Internal Invar Liner	Fab, trim insulation blocks, bond to tank interior. Fab, install liner as described for system 8b (minus PPO foam). Evacuate.	Visual; dimensional check, pressure check, pressure decay test, functional check of blowers and pressure monitoring equipment.	Monitor vacuum pressure and hydrogen detectors, service blowers and pressure measuring equipment.	Installation of liner into the tank and final closure welds. Demonstration of pumping system and controls suitable for aircraft use.
13. Self-evacuating Shingles	Fab, trim, layup foam and radiation shield layers, assemble with buttons, bag, leak check, purge with CO_2, bond to tank, bond sealing strips.	Visual, dimensional check, LH_2 boiloff test, temperature measurements.	Examine insulation for frosting, monitor boiloff and temperatures in service. Service external hydrogen monitors.	It is doubtful this system can be made vacuum leak tight since metal barriers can't be used due to heat leak considerations.

TABLE F-1 PRELIMINARY PRODUCIBILITY ANALYSIS (CONTINUED)

Concept	Fab & Assembly	Inspection	Servicing & Maintenance	Areas that May Require Development
14. Self-evacuating Honeycomb/ Foam	Foam vapor barrier, bond to honeycomb panels, prime tank exterior, bond panels, bond seal strips, spray foam, machine, spray sealer.	Visual inspection, dimensional check, LH_2 boiloff test with temperature measurements.	Examine insulation for frosting, monitor boiloff and temperatures in service, repair or replace insulation as required. Service external hydrogen monitors.	No direct way to check integrity of seals other than temperature measurements and frost formation. Repair of honeycomb seal difficult. Life cycle testing required.
15. Self-evacuating Honeycomb/N_2 Purge	Fab and install honeycomb as described for system 14. Fab and install fiberglass batting panels and purge jacket as described for the system 2 nitrogen purge.	Same as above. Run pressure decay leak check on purge jacket.	Same as above. Load N_2 each flight, service plumbing components, pressure monitoring, temperature and control systems. Service external hydrogen monitors.	No direct way to check integrity of honeycomb seal other than temperature measurements and frost formation.

Table F-2 EXAMPLE OF INSPECTION, MAINTENANCE AND OPERATIONAL REQUIREMENTS

	TIME INTERVAL[1]			
	PER FLT	WEEKLY	MONTHLY	QUARTERLY
1. He Purge				
o Load Helium	X			
o Visual Check			X	
o Pressure Decay Check	X			
o Plumbing Functional Check		X		
o Hydrogen Leak Detector Check		X		
o Pressure Monitoring and Control System Check		X		
o Boiloff Measurement	X			
o Complete System Servicing				X
o Weigh Aircraft			X	
2. He/N_2 Double Purge				
o Load He and N_2	X			
o Visual Check			X	
o Pressure Decay Check	X			
o Plumbing Functional Check		X		
o Hydrogen Leak Detector Check		X		
o Pressure Monitoring and Control System Check		X		
o Boiloff Measurement	X			
o Complete System Servicing				X
o Weigh Aircraft			X	

[1] These intervals would probably increase as experience is gained with system.

TABLE F-2 - (CONTINUED)

	TIME INTERVAL[1]			
	PER FLT	WEEKLY	MONTHLY	QUARTERLY
3. & 4. External Closed Cell Foam				
o Visual Check for Frost		X		
o Weigh Aircraft		X		
o Boiloff Measurement	X			
o Temp. Measurement	X			
o Service Hydrogen Detectors		X		
o Service Sensors				
5. Internal Polyurethane Foam, Liquid Seal				
o Visual Check for Frost		X		
o Weigh Aircraft			X	
o Boiloff Measurement	X			
o Temp. Measurement	X			
o Service Hydrogen Detectors		X		
o Examine Foam, Service Sensors				X

[1] These intervals would probably increase as experience is gained with system.

TABLE F-2. (CONTINUED)

	TIME INTERVAL[1]			
	PER FLT	WEEKLY	MONTHLY	QUARTERLY
6. Internal PPO Foam/External Polyurethane Foam				
o Visual Check for Frost		X		
o Weigh Aircraft		X		
o Boiloff Measurement	X			
o Temp. Measurement	X			
o Service Hydrogen Detectors		X		
o Examine Internal Foam, Service Sensors				X
7. Internal PPO Foam	Same as System 5			
8. Internal Honeycomb Gas Barrier Layer	Same as System 5			
9. Rigid Vacuum Shell with Fiberglass Batting				
o Visual Check			X	
o Vacuum Decay Check	X			
o Vacuum Monitoring and Control System Check		X		
o Pump Servicing				X
o Weigh Aircraft			X	

[1] These intervals would probably increase as experience is gained with system.

TABLE F-2 - (CONTINUED)

	TIME INTERVAL[1]			
	PER FLT	WEEKLY	MONTHLY	QUARTERLY
10. Microspheres with External Flexible Jacket				
o Visual Check			X	
o Vacuum Decay Check	X			
o Vacuum Monitoring and Control System Check		X		
o Pump Servicing				X
o Weigh Aircraft			X	
11. Microspheres with Internal Invar Liner	See System 10	for other items.		
o Examine Liner				X
12. Silica Insulation with Internal Invar Liner	See System 10	for other items.		
o Examine Liner				X
13. Self-Evacuating Shingles				
o Visual Check for Frost		X		
o Weigh Aircraft		X		
o Boiloff Measurement	X			
o Temp. Measurement	X			

[1] These intervals would probably increase as experience is gained with system.

TABLE F-2 - (CONTINUED)

	TIME INTERVAL[1]			
	PER FLT	WEEKLY	MONTHLY	QUARTERLY
13. Continued				
o Service Hydrogen Detectors		X		
o Service Sensors				
14. Self-Evacuating Honeycomb Foam	Same as System 3			
15. Self-Evacuating Honeycomb/N_2 Purge	Same as System 1			

[1] These intervals would probably increase as experience is gained with system.

TABLE F-3. - FACTORS INFLUENCING THE CANDIDATE INSULATION SYSTEM'S LIFE EXPECTANCY

Ranking	System No.	Vapor Barrier					Insulation				No. of LH_2 Thermal Cycle Tests Which Have Been Conducted to Date on Similar Systems
		Type	Max. Barrier Temp Change °F	ΔP (PSI)	Flex Desirable ?	Designed to Flex	Type	Press. Loaded	Max. Bond Line Temp Change °F	Structural Integrity	
1*	1	Epoxy/ Glass/ Teflon	180	2	No	No	Fiber-glass Batt	No	N.A.	Excellent	100
1	2	He Epoxy/ Glass Teflon	390	2	No	No	"	No	N.A.	Excellent	1
		N_2 Epoxy/ Glass Teflon	180	2	No	No	"	No	N.A.	Excellent	
3	3&4	Poly-urethane Seal Coat	180	15	Yes	No	Closed Cell Poly-urethane Foam	Yes	530	Fair	6
2	3&4	MAAMF	180	15	Yes	No	"	Yes	530	Fair	--
2	5	Glass/ Poly-urethane Seal	530	20 (Initially)	Yes	No	Glass-Fiber Reinforced Foam	Yes (Initially)	180	Good	135
3	6	Poly-urethane Seal Coat	180	~2	Yes	No	Closed Cell Poly-urethane Foam	Yes	390	Fair	--
		None	--	--	--	--	Open Cell PPO Foam	No	390	Excellent	100

*Longest Life Systems

TABLE F-3. - FACTORS INFLUENCING THE CANDIDATE INSULATION SYSTEM'S LIFE EXPECTANCY (CONT'D)

Ranking	System No.	Vapor Barrier					Insulation				No. of LH_2 Thermal Cycle Tests Which Have Been Conducted to Date on Similar Systems
		Type	Max. Barrier Temp Change °F	ΔP (PSI)	Flex Desirable ?	Designed to Flex	Type	Press. Loaded	Max. Bond Line Temp Change °F	Structural Integrity	
1	7	None	--	--	--	--	Open Cell PPO Foam	No	180	Excellent	100
1	8	Perforated Mylar	530	0	Yes	No	Mylar Honeycomb	No	180	Excellent	?
2	9	Aluminum	180	15	No	No	Fiberglass Batt & Radiation Shields	No	N.A.	Excellent	29
1	10	Stainless Steel	180	15	Yes	Yes	Glass Microspheres	Yes	N.A.	Excellent	Test program started Jan. 1977
1	11	Invar	530	20	No	No	Glass Microspheres	Yes	N.A.	Excellent	--
1	12	Invar	530	20	No	No	Rigidized Silica Fiber	Yes	180	Excellent	--
3	13	Mylar	180	15	Yes	Partially	Foam/Radiation Shield Layers	Yes	530	Foam layers Questionable	4 (Panels leaked)

*Longest Life Systems

TABLE F-3. - FACTORS INFLUENCING THE CANDIDATE INSULATION SYSTEM'S LIFE EXPECTANCY (CONT'D)

Ranking	System No.	Vapor Barrier					Insulation				No. of LH_2 Thermal Cycle Tests Which Have Been Conducted to Date on Similar Systems
		Type	Max. Barrier Temp Change ^oF	ΔP (PSI)	Flex Desirable ?	Designed to Flex	Type	Press. Loaded	Max. Bond Line Temp Change ^oF	Structural Integrity	
2	14	MAAMF Film	390	13	Yes	No	Mylar Honeycomb	Yes	530	Excellent	14 (Leaked)
		Polyurethane Seal Coat	180	2	Yes	No	Closed Cell Polyurethane Foam	Yes	390	Fair	--
2	15	MAAMF Film	390	17	Yes	No	Mylar Honeycomb	Yes	530	Excellent	14 (Leaked)
		Polyurethane Seal Coat	180	2	No	No	Fiberglass Batt	No	N.A.	Excellent	--

*Longest Life Systems

APPENDIX G

ENGINE PERFORMANCE CHARTS

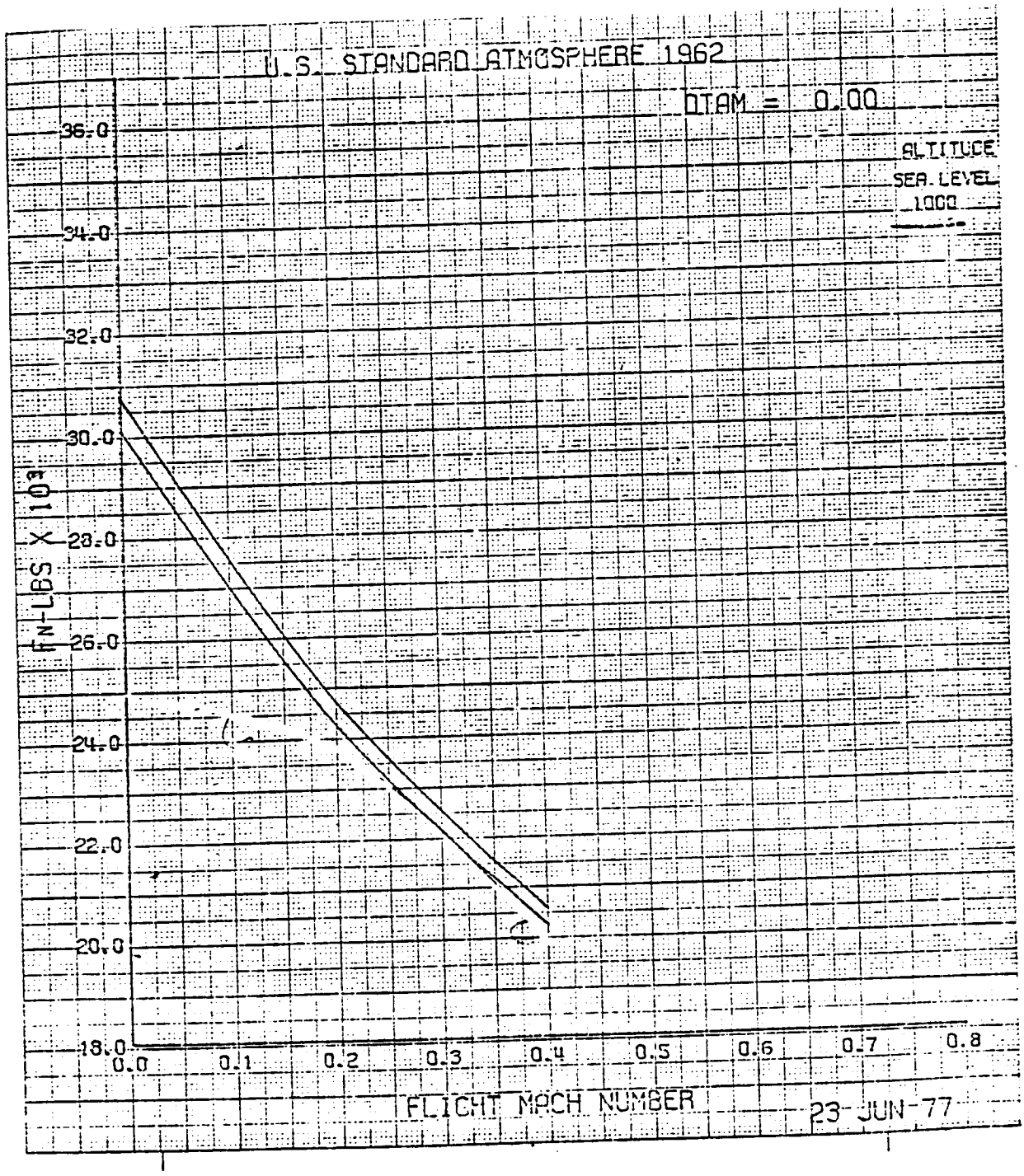

Figure G-1. - AiResearch LH_2 engine takeoff power - thrust.

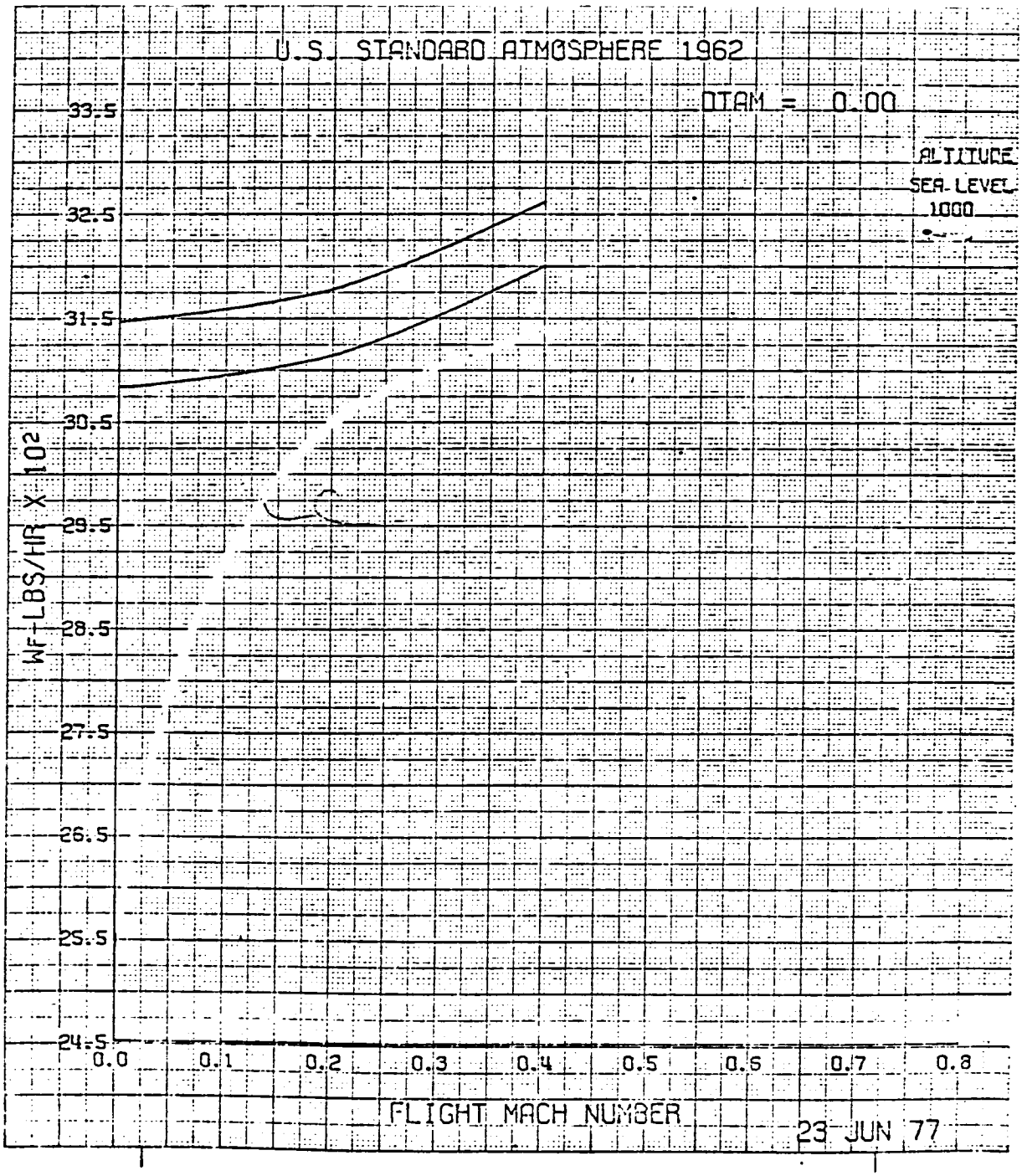

Figure G-2. - AiResearch LH_2 engine takeoff power - fuel flow.

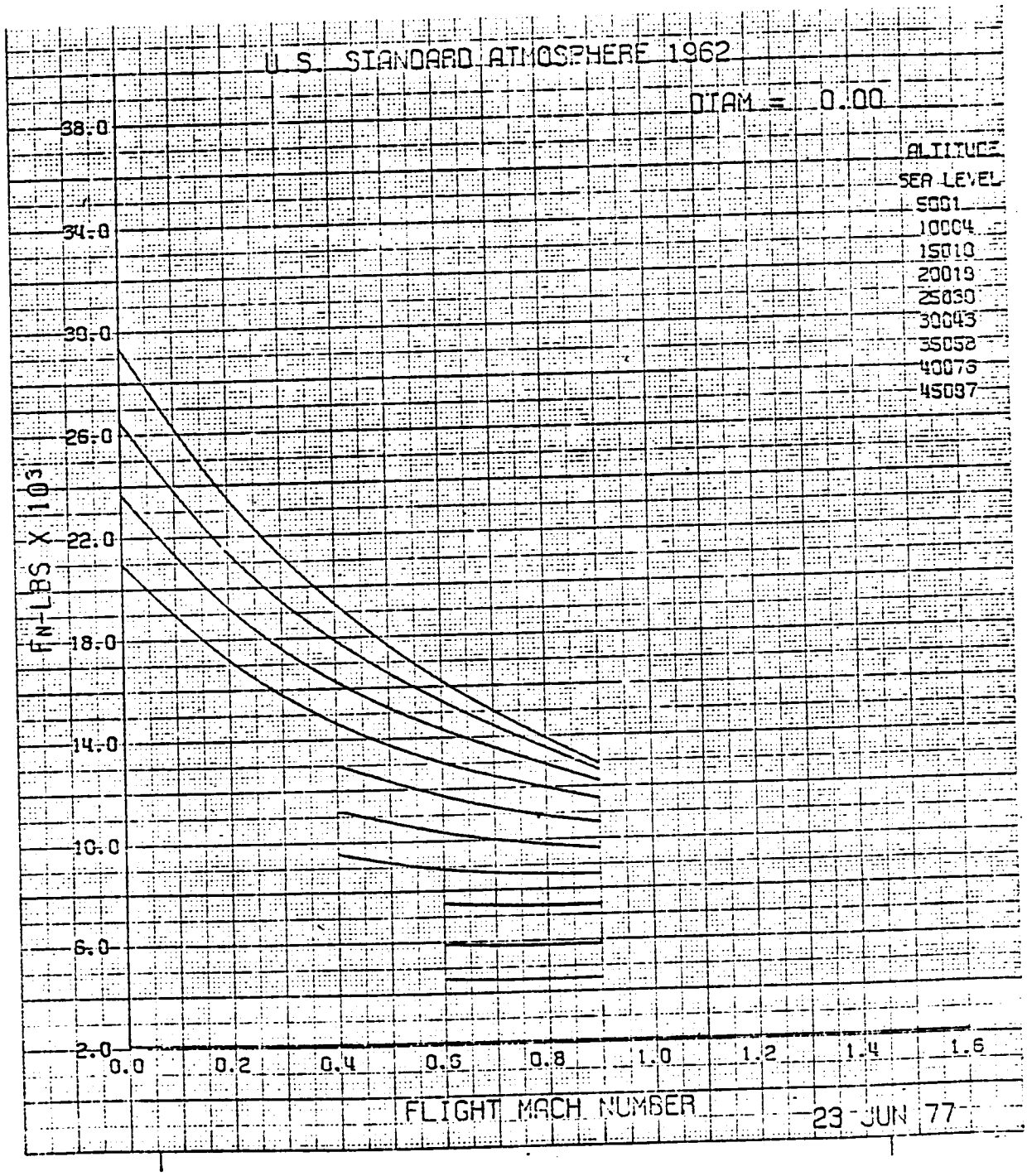

Figure G-3. - AiResearch LH_2 engine maximum climb - thrust.

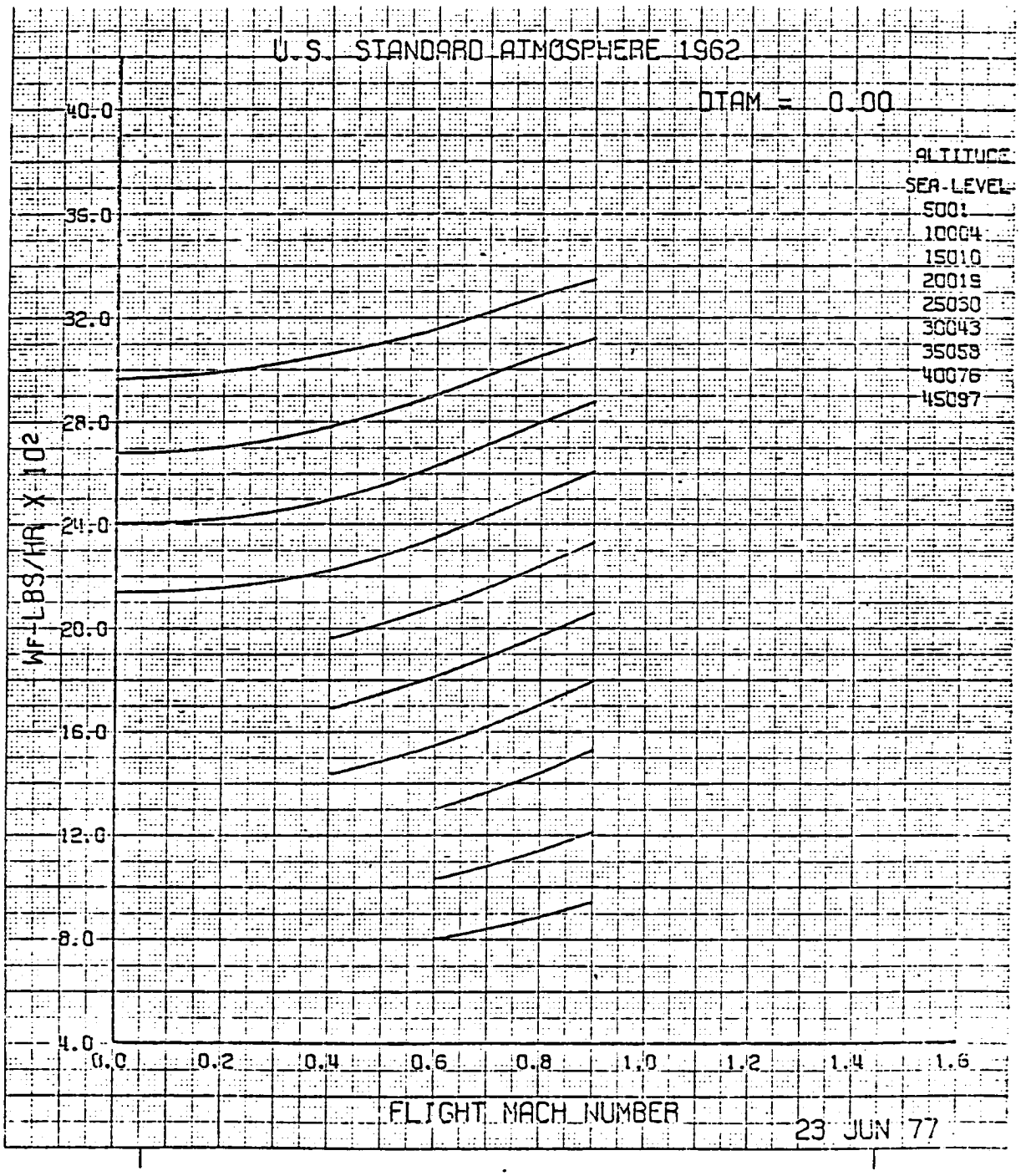

Figure G-4. - AiResearch LH_2 engine maximum climb - fuel flow.

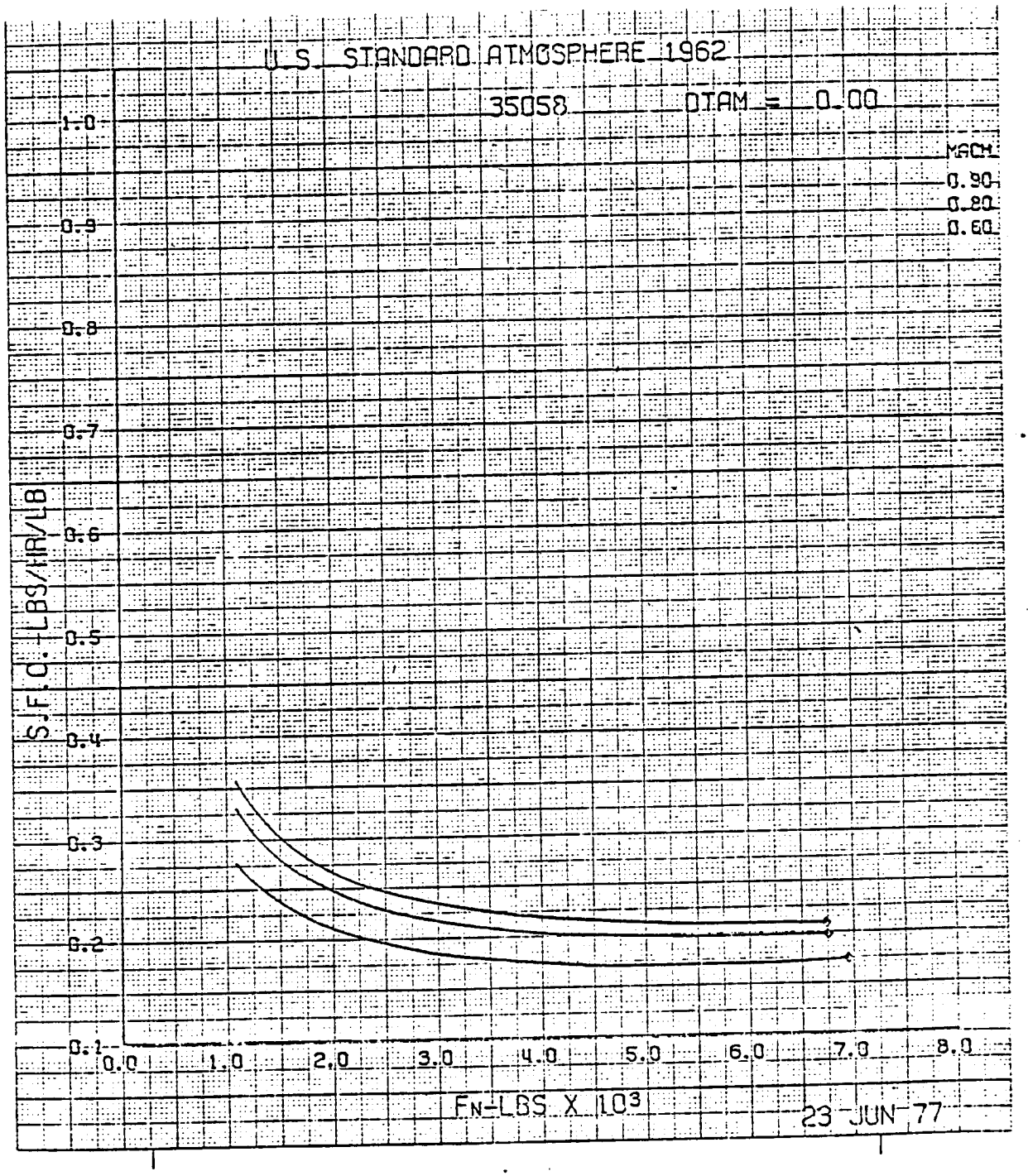

Figure G-5. - AiResearch LH_2 engine part power - cruise.

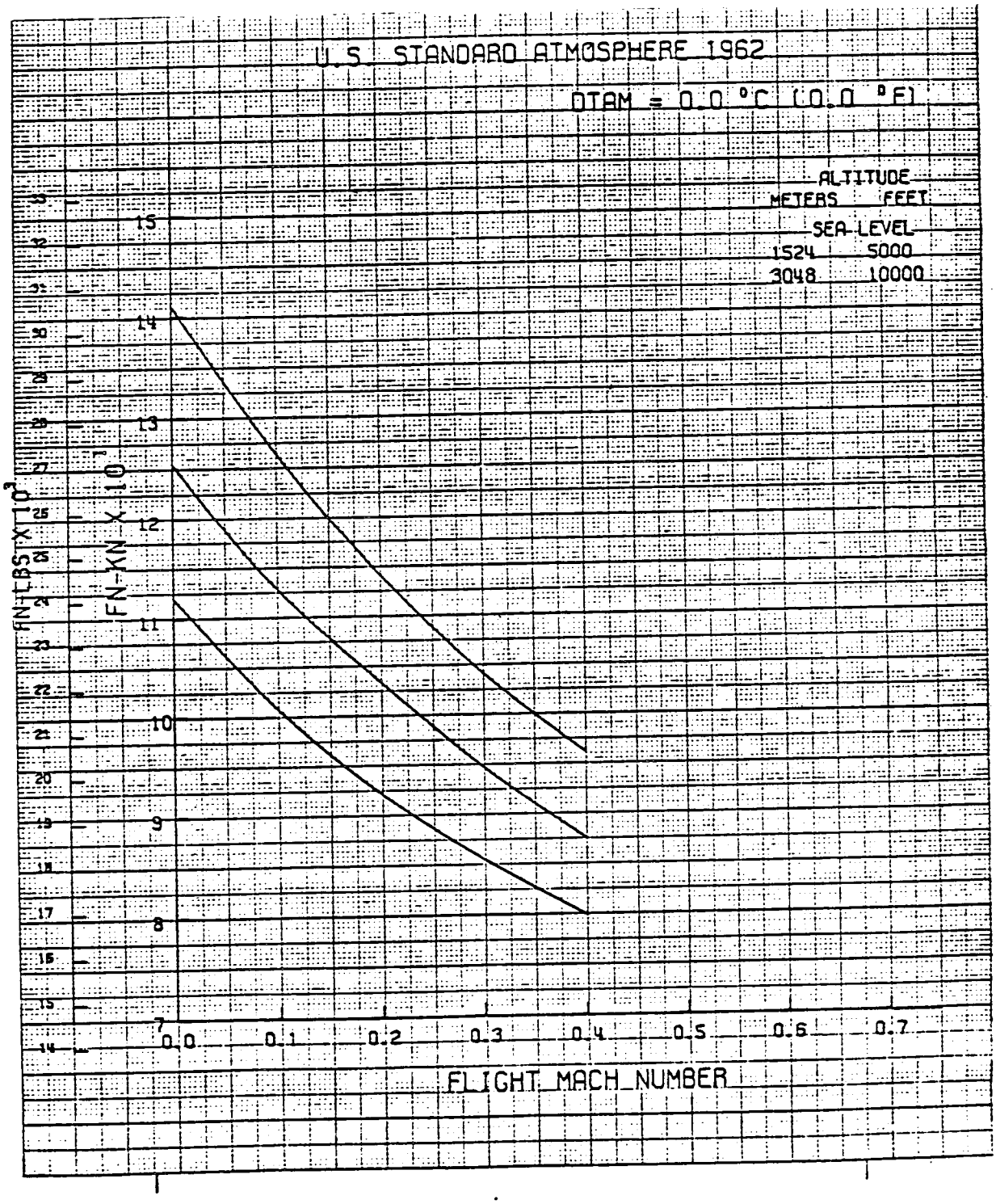

Figure G-6. - Jet A engine takeoff power - thrust.

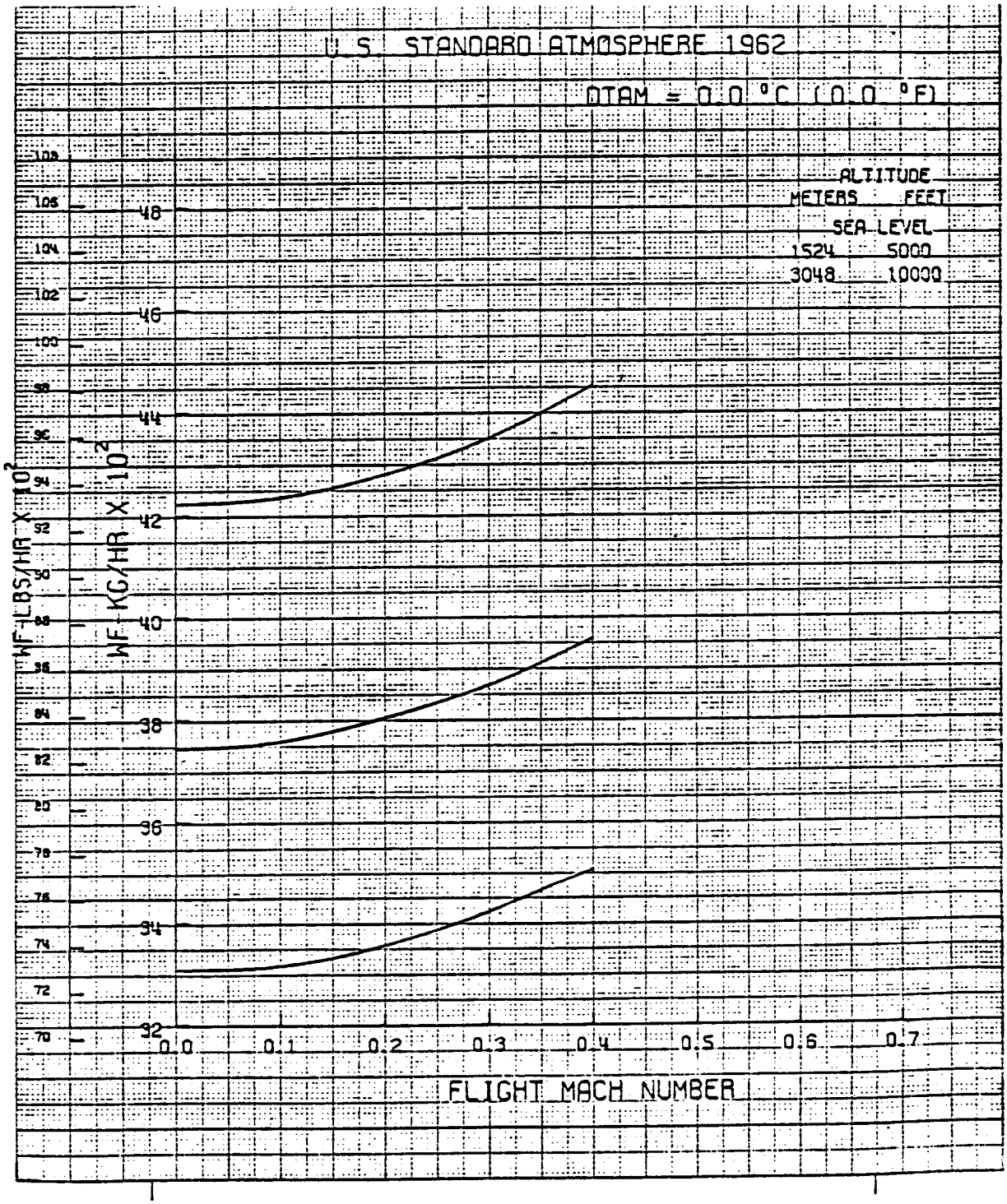

Figure G-7. - Jet A engine takeoff power - fuel flow.

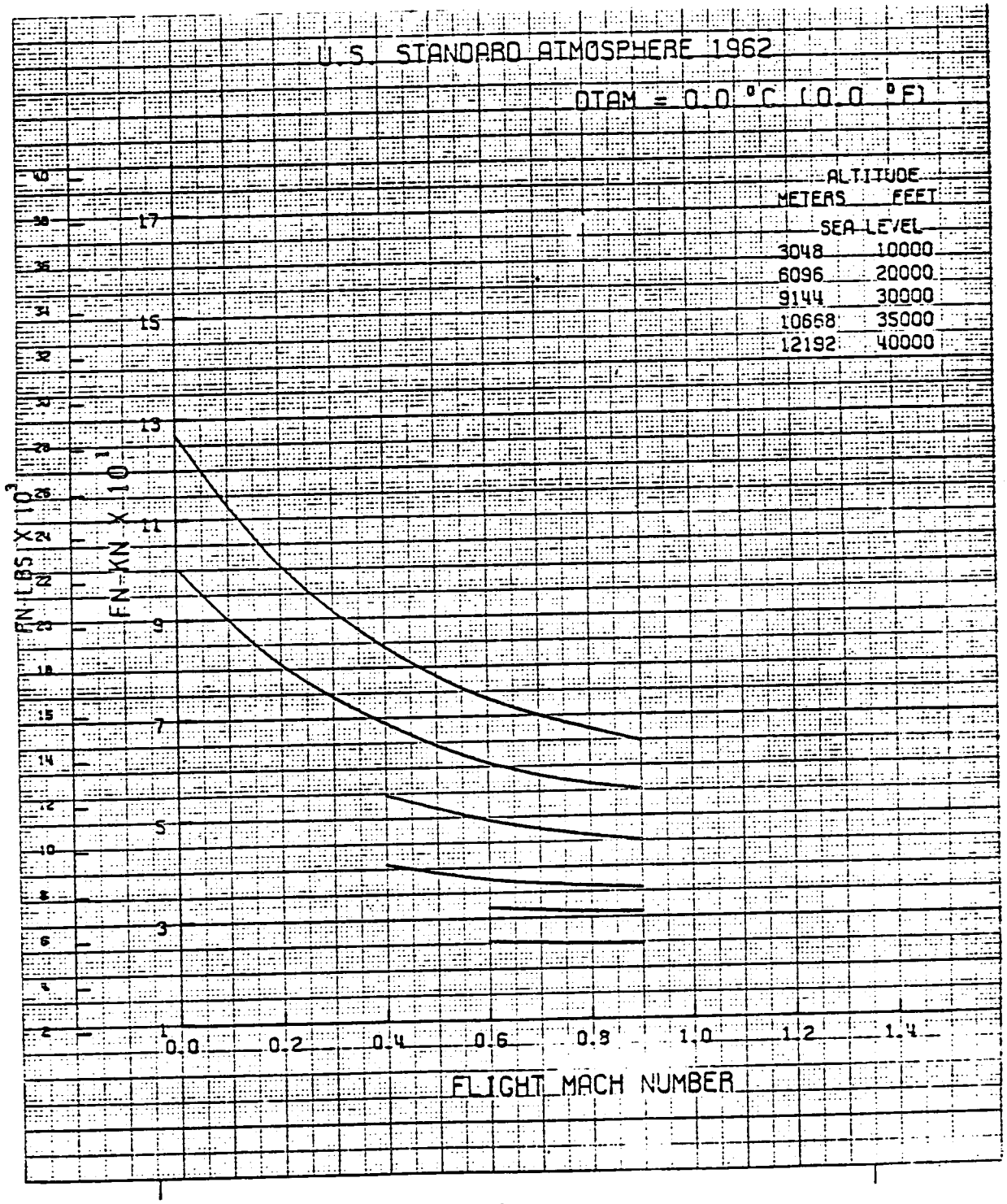

Figure G-8. - Jet A engine maximum climb - thrust.

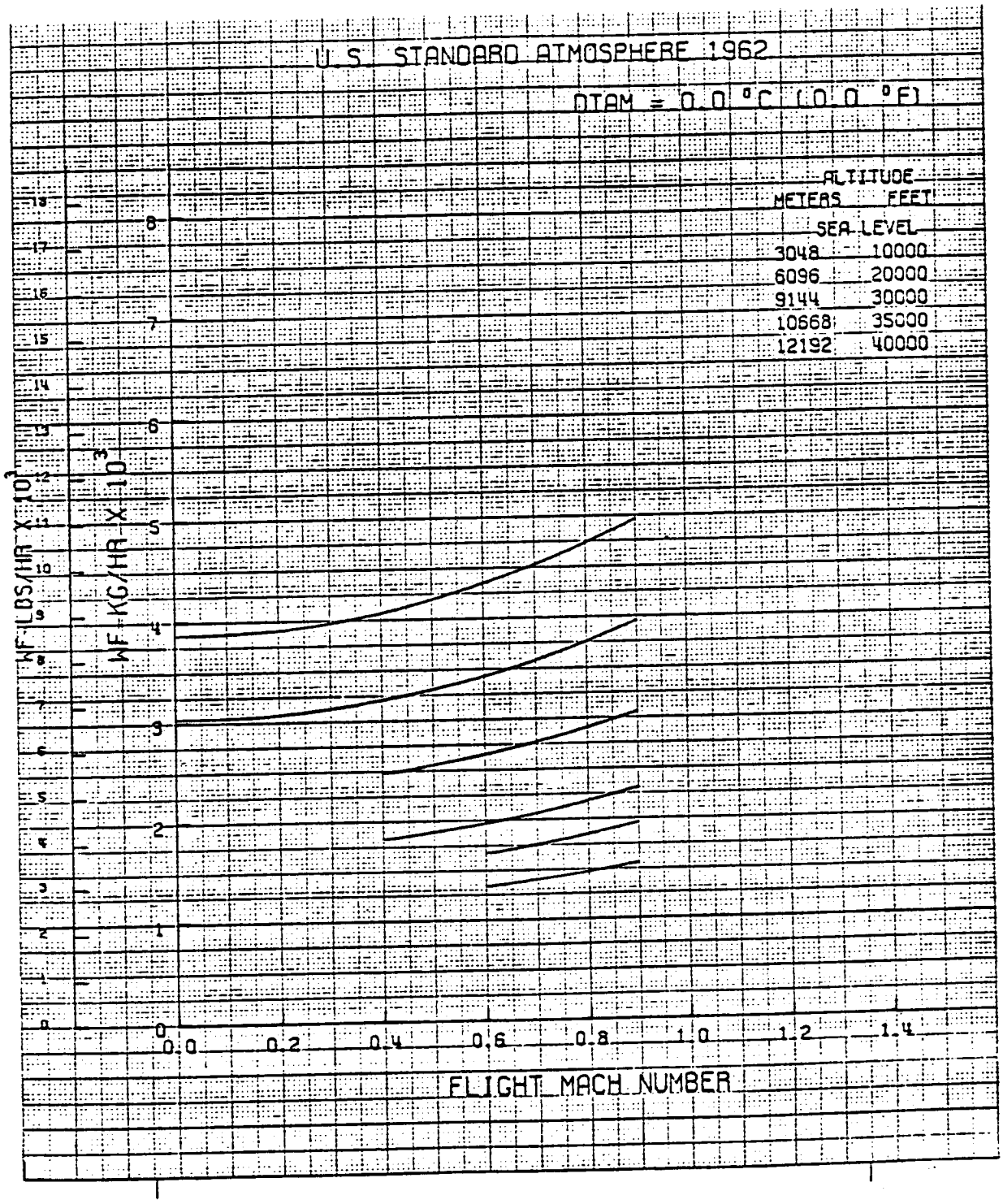

Figure G-9. - Jet A engine maximum climb - fuel flow.

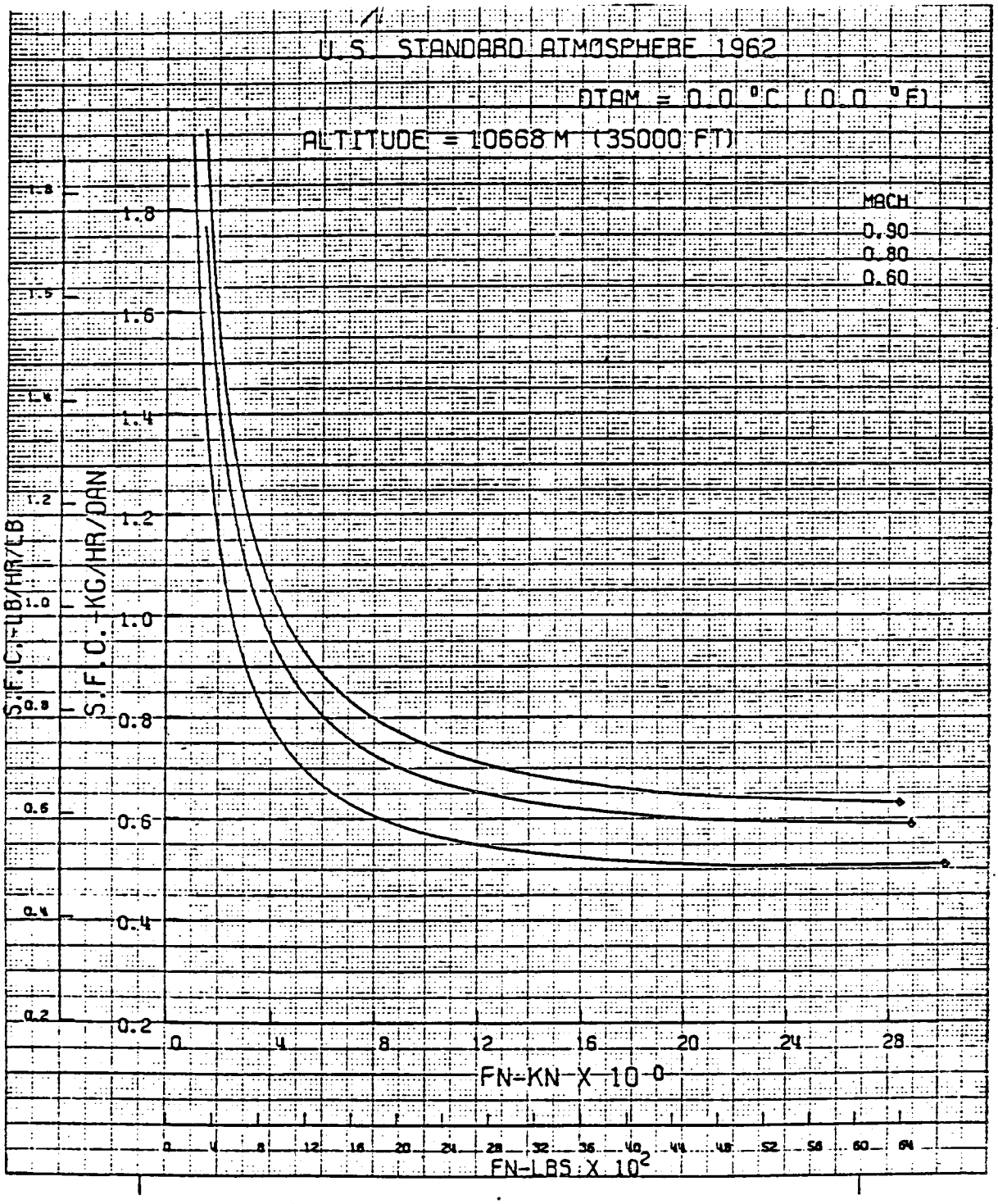

Figure G-10. - Jet A engine part power - cruise.

1. REPORT NO.	2. GOVERNMENT ACCESSION NO.	3. RECIPIENT'S CATALOG NO.
NASA CR -		

4. TITLE AND SUBTITLE	5. REPORT DATE
FINAL REPORT: STUDY OF FUEL SYSTEMS FOR LH_2 - FUELED SUBSONIC TRANSPORT AIRCRAFT	Dec 1977
	6. PERFORMING ORG CODE
7. AUTHOR(S) G.D. Brewer, R.E. Morris, G.W. Davis, E.F. Versaw, G.R. Cunnington, Jr., J.C. Riple, C.F. Baerst, G. Garmong	8. PERFORMING ORG REPORT NO. LR 28384
9. PERFORMING ORGANIZATION NAME AND ADDRESS LOCKHEED-CALIFORNIA COMPANY P.O. BOX 551 BURBANK, CALIFORNIA 91520	10. WORK UNIT NO.
	11. CONTRACT OR GRANT NO. NAS 1-14614
12. SPONSORING AGENCY NAME AND ADDRESS National Aeronautics and Space Administration Langley Research Center Hampton, Virginia 23665	13. TYPE OF REPORT AND PERIOD COVERED CONTRACTOR FINAL REPT.: SEPT. 1976 – DEC. 1977
	14. SPONSORING AGENCY CODE

15. SUPPLEMENTARY NOTES

16. ABSTRACT

This study was performed to define the characteristics of an efficient fuel system for a LH_2-fueled subsonic transport aircraft. Several engine concepts were examined to determine a preferred design which most effectively exploits the characteristics of hydrogen. The problems related to efficient containment of the liquid hydrogen fuel in aircraft tanks received major emphasis. Many candidate designs of tank structure and cryogenic insulation systems were evaluated. Designs of all major elements of the aircraft fuel system including pumps, lines, valves, regulators, and heat exchangers received attention. Selected designs of boost pumps to be mounted in the LH_2 tanks, and of a high pressure pump to be mounted on the engine were defined. A final design of LH_2-fueled transport aircraft was established which incorporates a preferred design of fuel system. That aircraft was then compared with a conventionally fueled counterpart designed to equivalent technology standards.

17. KEY WORDS (SUGGESTED BY AUTHOR(S))	18. DISTRIBUTION STATEMENT
Hydrogen, Aircraft fuel system, Fuel containment, Engine concepts, Cryogenic insulation, LH_2 pumps, Tank structure, Aircraft comparison	

19. SECURITY CLASSIF. (OF THIS REPORT)	20. SECURITY CLASSIF. (OF THIS PAGE)	21. NO. OF PAGES	22. PRICE*
Unclassified	Unclassified		